MASARYK UNIVERSITY
Faculty of Medicine

HABILITATION THESIS

Homologous recombination and its quality control

Mgr. Lumír Krejčí, PhD

Brno, March 2012

Acknowledgement

ABSTRACT

DNA is under constant toxic stress from both endogenous and exogenous sources. To avoid deleterious mutations, blockage of replication and transcription, and chromosomal breakage resulting DNA lesions need to be repaired. DNA double-strand breaks (DSBs) represent one of the most serious kinds of DNA lesions, which, if left unrepaired, could lead to aneuploidy, genetic aberrations or cell death. This is further underlined by the fact that many human syndromes, such as neurodegenerative diseases and cancer, are linked to the defects in DSB repair. Homologous recombination (HR) represents one of the major repair pathways that repairs a variety of DNA lesions, including double-strand DNA breaks (DSBs), single-strand DNA gaps, and interstrandcrosslinks. Repair of DSBs is essential for the first meiotic division where it is required for proper pairing and segregation of homologous chromosomes, and the generation of genetic diversity.

During last years I have focused on genetic and biochemical characterization of several yeast and human proteins involved in process of DSB repair. I have isolated and genetically characterized a large number of *RAD51* alleles that are differentially inactivated for interaction with various recombination factors (p.50). Furthermore, I have examined the functional significance of the Rad51/Rad52 interaction and identified minimal region on C-terminus required for this interaction (p.51). Additional experiments demonstrate that C-terminal portion of Rad52 is responsible not only for interaction with Rad51, but is also able to mediate Rad51 loading on RPA-coated ssDNA, and contains novel DNA binding region (p.52).

Under certain circumstances, however, recombination is not a preferred pathway to repair damaged DNA and we speculated that Rad51 filament could be a regulatory point of the recombination. Indeed, using biochemical approach we have demonstrated that Srs2 helicase can disrupt Rad51 nucleoprotein filament (p.53) and helicase activity is indispensable of this function (p.54). The protein interaction between Srs2 and Rad51 serves two purposes: one is to localize Srs2 protein to site of Rad51 filament formation, and the other is to trigger ATP hydrolysis within the Rad51 filament, causing a weakening of the Rad51-DNA interaction, thus allowing more efficient clearing of the nucleoprotein filament by Srs2 (p.55). Importantly, mediator proteins (*i.e.* Rad52) can suppress the action of Srs2 anti-recombinase, indicating that the relative strength of the two types of regulation determines the fate of presynaptic filaments (p.56). Rad52 and Srs2 thus form parts of a quality control mechanism that seems to be regulated through post-translational modification (p.57). We have identified residues that are being modified, and analyzed *in vivo* and *in vitro* effect of these mutations together with their biological characterization (p.58).

Very recently, we have turned our focus to reconstitution of downstream events during repair of DSB including DNA repair synthesis, and processing of recombination and replication intermediates by structure-specific nucleases (p.59 and 60). These research activities should help us to understand selected biological problems in molecular details but also to uncover possible regulatory circuitries that could be used for therapy.

ABSTRAKT

DNA je pod neustálým toxickým vlivem jak z endogenních, tak z exogenních zdrojů. Vznikající poškození DNA musí být opravena, aby nedocházelo ke vzniku mutací, zablokování replikace a chromozomálním zlomům. Jedno z nejzávažnějších typů poškození DNA představují dvouřetězcové zlomy (double-strand breaks, DSBs), které, pokud zůstanou neopraveny, mohou vést k aneuploiditě, genetickým aberacím nebo buněčné smrti. Tento fakt je navíc zdůrazněn skutečností, že s chybami v opravě dvouřetězcových zlomů jsou spojeny mnohé syndromy vyskytující se u lidí, např. neurodegenerativní a nádorová onemocnění. Jednu z hlavních opravných cest představuje homologní rekombinace (HR), kterou jsou opraveny různá poškození DNA, včetně jedno- a dvouřetězcových zlomů a mezitřetězcových crosslinků. Oprava DSBs homologní rekombinací je navíc zásadní pro první meiotické dělení, kde umožňuje správné párování a segregaci homologních chromozomů a podílí se tak na vzniku genetické rozmanitosti.

Během minulých let jsem se zaměřil na genetickou a biochemickou charakterizaci několika kvasinkových a lidských proteinů podílejících se na opravě DSBs. Izoloval a geneticky charakterizoval jsem velké množství alel *RAD51*, které jsou různě inaktivovány pro interakci s rozličnými rekombinačními faktory (str.50). Dále jsem studoval funkční význam interakce Rad51/Rad52 a identifikoval nejmenší oblast na C-konci, která je pro tuto inerakci nezbytná (str.51). Další experimenty ukázaly, že C-konec Rad52 je nejen zodpovědný za interakci s Rad51, ale je také schopen zprostředkovat nasedání Rad51 na ss-DNA pokrytou RPA a navíc obsahuje nově objevenou DNA vazebnou oblast (str.52).

Za určitých podmínek ovšem rekombinace není správnou cestou pro opravu DNA a proto jsme předpověděli, že tvorba Rad51 filamenta je místem, ve kterém dochází k regulaci rekombinace. Pomocí biochemického přístupu jsme ukázali, že helikáza Srs2 může rozrušit nukleoproteinové filamento Rad51 (str.53), přičemž helikázová aktivita je pro tuto funkci nezbytná. (str.54). Proteinová interakce mezi Srs2 a Rad51 slouží dvěma účelům: jedním z nich je lokalizace Srs2 proteinu do oblasti, kde dochází k tvorbě Rad51 filamenta, druhým je spuštění hydrolýzy ATP v rámci Rad51 filamenta, čímž dojde k oslabení interakce Rad51-DNA a následnému snazšímu odstranění nukleoproteinového filamenta pomocí Srs2 (str.55). Důležitá je skutečnost, že mediátorové proteiny (např. Rad52) mohou působení Srs2 anti-rekombinázy potlačit, což naznačuje, že relativní síla těchto dvou typů regulací determinuje osud presynaptického filamenta (str.56). Rad52 a Srs2 tak tvoří části kontrolního mechanismu, který je pravděpodobně regulován post-translační modifikací (str.57). Identifikovali jsme rezidua, kde dochází k modifikaci a analyzovali jsme *in vivo* a *in vitro* vliv těchto mutací společně s jejich biologickou charakterizací (str.58).

V poslední době jsme náš zájem upřeli také na rekonstituci dějů v další fázi opravy DSBs, včetně DNA opravné syntézy a zpracování rekombinačních a replikačních meziproduktů pomocí struktrurně-specifických nukleáz (str.59 a 60). Tento výzkum by nám měl pomoci nejen detailně porozumět vybraným biologickým problémům, ale i odhalit možné regulační cesty, které by měly terapeutické využití.

Table of Contents

Introduction - Rad51 nucleofilaments and HR pathways

Cells are under constant genotoxic pressure from both endogenous and exogenous sources. It has been estimated that more than tens of thousands of DNA lesions occur in a single human cell every day(1). These lesions need to be repaired to avoid deleterious mutations, blockage of replication and transcription, and chromosomal breakage. The importance of DNA repair to human health is highlighted by the fact that failure to repair damaged DNA increases the likelihood of developing tumours and other diseases. In this review, we focus on HR, a repair mechanism that repairs a variety of DNA lesions, including double-strand DNA breaks (DSBs), single-strand DNA gaps, and interstrandcrosslinks. Among these lesions, DSBs are highly toxic as a single unrepaired DSB can lead to aneuploidy, genetic aberrations, or cell death. DSBs can be generated by a number of sources, including treatment with genotoxic chemicals and ionizing radiation, collapsed replication forks, and other endogenous DNA breaks. On the other hand, Repair of DSBs is essential for the first meiotic division where it contributes to the formation of chiasmata, required for proper pairing and segregation of homologous chromosomes, and the generation of genetic diversity in most organisms (2).

A central player of HR is the strand exchange protein, called Rad51 in eukaryotic cells (RecA in *E. coli*). Rad51 functions in all three phases of HR: pre-synapsis, synapsis and post-synapsis (Figure 1A;(3). In the pre-synaptic phase, Rad51 is loaded onto single-strand DNA (ssDNA) that either is generated by degrading 5' strands at DSBs or arises from replication perturbation. The resulting Rad51-ssDNA filament (presynaptic filament) is right-handed and comprises six Rad51 molecules and eighteen nucleotides per helical turn. The ssDNA within the filament is stretched as much as half the length of B-form dsDNA (4). The stretching of the filament is essential for fast and efficient homology search(5,6). During synapsis, Rad51 facilitates the formation of a physical connection between the invading DNA substrate and homologous duplex DNA template, leading to the generation of heteroduplex DNA (D-loop). Here, Rad51-dsDNA filaments are formed by accommodating both the invading and donor ssDNA strands within the filament. Finally, during post-synapsis when DNA is synthesized using the invading 3' end as a primer, Rad51 dissociates from dsDNA to expose the 3' OH required for DNA synthesis.

At least three different routes can be used once DNA synthesis is initiated (Figure 1B-1D). First, as envisioned in the double-strand break repair model (DSBR), the second end of DSB is engaged to stabilize the D-loop structure (2nd end capture), leading to the generation of a double-Holliday Junction (dHJ) ((7), reviewed in (8); Figure 1B). A dHJ is then resolved to produce crossover or non-crossover products (Figure 1B), or dissolved to exclusively generate non-crossover products. Second, the invading strand is displaced from D-loop and anneals either with its complementary strand as seen in gap repair or with the complementary strand associating with the other end of the DSB. This represents the synthesis-dependent strand-annealing mode of HR (SDSA) ((9); Figure 1C). SDSA mechanism is preferred over DSBR during mitosis. During meiosis, crossover is formed by resolution of dHJ via DSBR mechanism, while non-crossover is primarily produced via SDSA mechanism (10,11). In the third
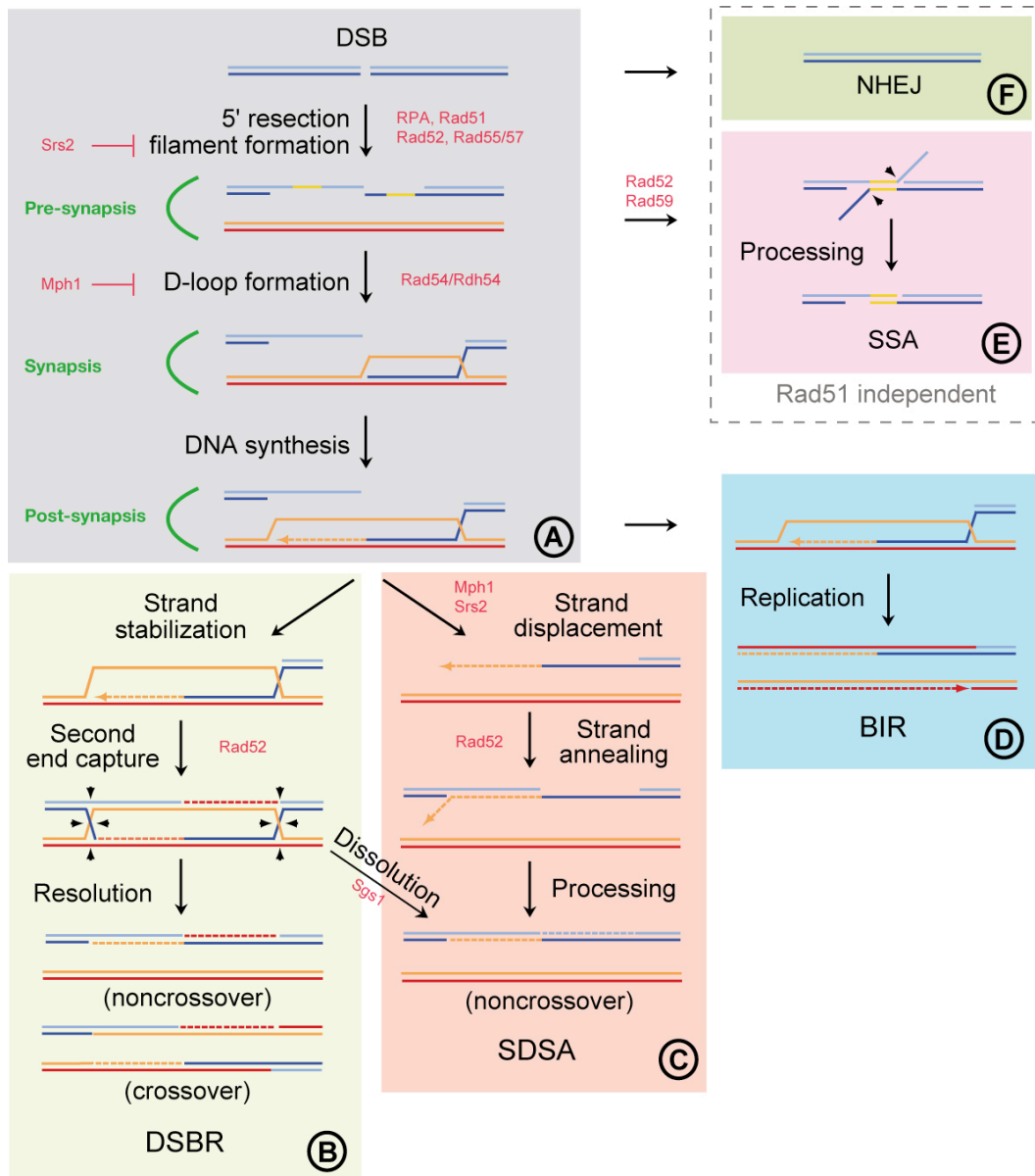
Figure 1: Models for the repair of DNA double-strand breaks. DNA DSBs are resected to generate 3' protruding end followed by formation of a Rad51 filament that invades into homologous template to form a D-loop structure (**A**). After priming DNA synthesis, three pathways can take place. In the DSBR pathway, the second end is captured and a double Holliday junction intermediate is formed (**B**). Resolution of dHJs can occur in either plane to generate crossover or noncrossover products. Alternatively, dHJs can be dissolved by the action of Sgs1-Top1-Rmi1 complex to generate only non-crossovers. In the SDSA pathway (**C**), the extended nascent strand is displaced, followed by pairing with the other 3' single-stranded tail, and DNA synthesis completes repair. Nucleolytic trimming might be also required. In the third pathway of BIR (**D**), which can act when the second end is absent, the D-loop intermediate turns into a replication fork capable of both lagging and leading strand synthesis**.** Two other Rad51-independent recombinational repair pathways are also depicted. In SSA (**E**), extensive resection can reveal complementary sequences at two repeats, allowing annealing. The 3' tails are removed nucleolytically and the nicks are ligated. SSA leads to the deletion of one of the repeats and the intervening DNA Finally, the ends of DSB can be directly ligated resulting in non-homologous end joining, NHEJ (**F**). Newly synthesized DNA is represented by dashed lines.

mode, the D-loop structure can assemble into a replication fork and copy the entire chromosome arm in a process called break-induced replication (BIR) ((12); Figure 1D). This mechanism is evoked more often when there is only one DNA end, either due to the loss of the other end or in the process of lengthening telomeres in telomerase-deficient cells.

All the above pathways require Rad51, with the exception that some forms of BIR may not. However, DSBs can also be sealed by pathways independent of Rad51 (Figure 1E-1F). One of these pathways is the single-strand annealing pathway (SSA). In SSA, ssDNA sequences generated during DSB processing contain regions of homology at both sides of DSB and can be annealed and ligated(13); Figure 1E). SSA does not require Rad51 but requires other HR proteins that mediate annealing. Another Rad51-independent pathway that operates at DSBs is non-homologous end joining (NHEJ), which ligates ends of DSBs with little or no requirement for homology (reviewed in (8); Figure 1F).

The many facets of HR regulation

The presence of multiple Rad51-dependent pathways and other alternative pathways suggests the existence of regulatory mechanisms that determine which pathway is to be used and how a particular process can be performed. Many important decisions need to be made that determine the outcome of repair of different types of lesions. For example, whether both ends of DSBs are used for repair, how DNA synthesis is initiated and terminated, whether SSA and BIR pathways are used only when other repair attempts fail. Considering the central role of Rad51 in HR, it is only logical that many of the regulations impinge on this protein and its regulators. Here, we provide a comprehensive and up-to-date overview of how this multi-layered regulation affects the formation, maintenance, and disassembly of Rad51 nucleofilaments. There are both positive and negative regulators of Rad51 function, some of which play a general role in both mitotic and meiotic cells, whereas others are specific to one of these types of cells (Table 1). In addition, HR regulation employs protein modifications, such as phosphorylation and sumoylation, to provide the required flexibility and dynamics.

We also envision that coordination and hierarchies exist among the large number of Rad51 regulation modules. In a sense, the system of HR regulation may be considered as a "quality control" scheme in which an optimal output requires specific interplay between all regulatory modules (Figure 2). An understanding of such an "HR quality control" system requires better characterization of each regulation module, their relationships, and how the dynamics of the system is achieved. As many facets of this regulation are best studied in the model organism budding yeast, examples in this system are often used to illustrate the principles of HR regulation. Additional regulation in mammalian cells and occasionally in other organisms is described in the later part of the text, though some are mentioned early on where they can be helpful to illustrate the point. While this review presents HR regulation from a Rad51-centric view, additional information on HR mechanisms can be found in several reviews (3,8,14-16).
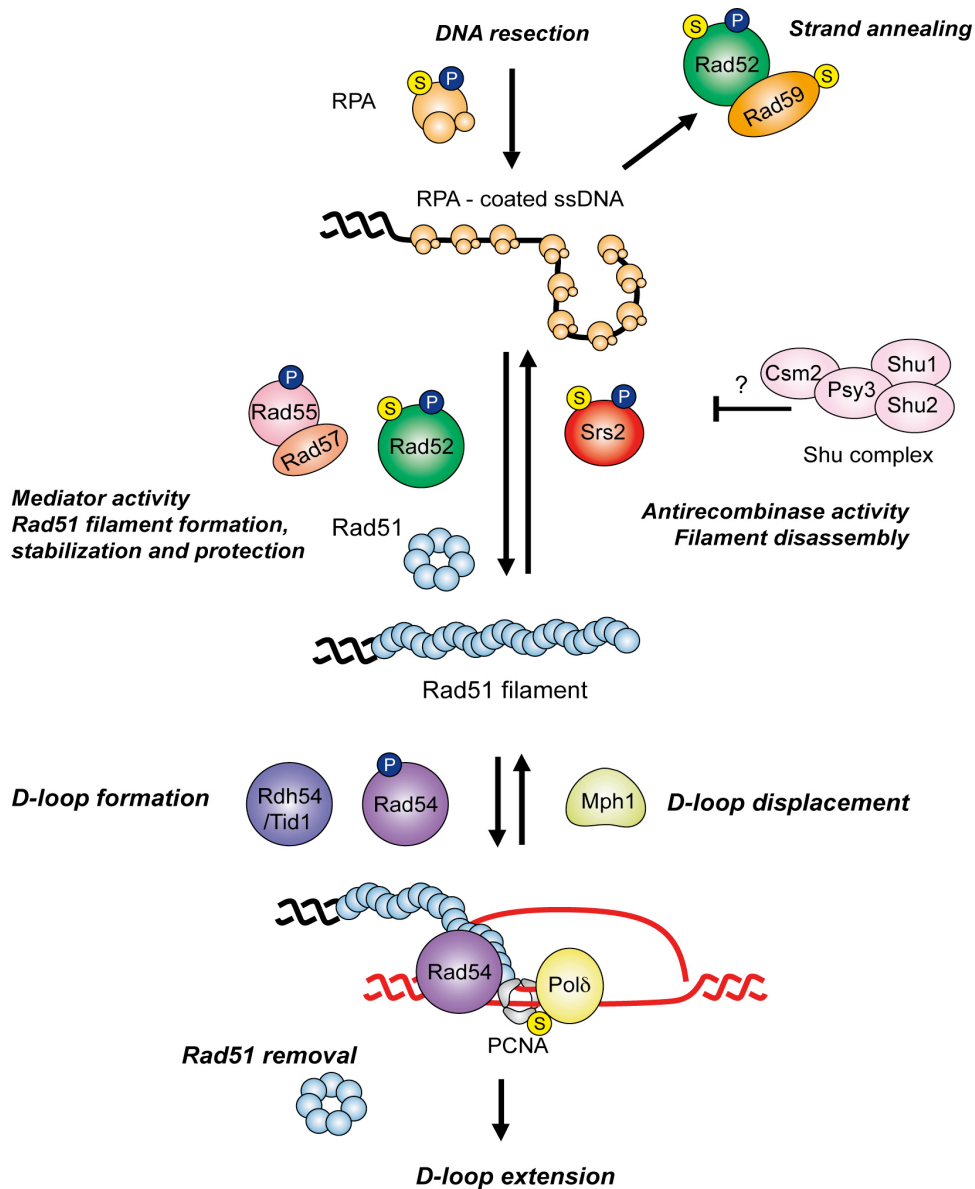
Figure 2: Rad51 filament formation and regulation, RPA can be replaced by Rad51 from ssDNA with the help of recombination mediators, including Rad52 and Rad55/57. These proteins can promote both the formation and stability of Rad51 presynaptic filaments and they themselves also bind DNA during this process (not drawn here for simplicity). Rad51 presynaptic filaments perform homology search with the help from Rad54 and Rhd54. Mph1 can promote the SDSA pathway by unwinding the D-loop intermediate. Srs2 is capable of dismantling the Rad51 filament in ATP-dependent manner leading to displacement of Rad51 by RPA. This prevents untimely or unwanted recombination. However, Rad52 and Rad55/57 can antagonize the Srs2 activity. The Shu complex promotes Rad51 functions during replication-associated repair but may also function by antagonizing Srs2. RPA-ssDNA complex can also lead to Rad51-independent repair where Rad52 and Rad59 replace RPA from DNA and anneal complementary strands. The balancing act of proteins with antagonistic roles as depicted here determines the fate of Rad51 nucleofilament and the recombination outcome. Most proteins regulating Rad51 are modified by phosphorylation (P) and/or sumoylation (S). The modifications are depicted on one form of the protein for simplicity; future works are needed to determine when the modification takes place. These modifications can dynamically change in response to DNA damaging agents and regulate the functions of the target proteins

Competition and collaboration betweeen Rad51 and RPA

One level of HR regulation occurs at the interplay between Rad51 and the ssDNA binding factor, Replication Protein A (RPA) complex. RPA has higher affinity for ssDNA than Rad51 and the presence of RPA on ssDNA prevents Rad51 from binding *in vitro*, suggesting that RPA-ssDNA formation precedes Rad51 presynaptic filament formation(17,18). In line with this, RPA was found to arrive at DSB sites prior to Rad51 based on both cytology data and ChIP analysis (19-22). For recombination to proceed, it is critical that RPA is subsequently replaced by Rad51 with the help of other proteins known as mediators (Figure 2). Mutations in RPA can impair HR by slowing this replacement step. For example, the recombination-deficient RPA mutant *rfa1-t11* is displaced more slowly from ssDNA by Rad51 than wild-type RPA, and consequently inhibits Rad51 protein-mediated DNA strand exchange (23).

On the other hand, RPA also promotes recombination by removing secondary structures formed on ssDNA that could impede Rad51 filament formation (3). In addition, RPA can aid Rad51 by preventing the reversal reaction of Rad51-mediated D-loop formation. This is mediated by the sequestration and scavenging of free ssDNA, thereby preventing DNA from entering the second DNA binding site of Rad51 (24,25). RPA's contributions to HR extend beyond its interplay with Rad51. For example, it promotes DSB resection by stimulating the Sgs1 helicase, directing Dna2 nucleolytic activity towards the 5' terminus and protecting the 3' end from degradation (26,27). In addition, the amount of RPA-ssDNA is sensed by checkpoint kinases, to elicit cell cycle arrest, allowing sufficient time for repair (28-30).

Recombination mediators: Positive Rad51 regulators

The proteins that can overcome the inhibitory effect of RPA on Rad51 nucleofilament formation are referred to as recombination mediators. In yeast, these include at least two types of proteins: Rad52, and the Rad51 paralogues, Rad55 and Rad57 that share the RecA core sequences with Rad51 (Figure 2). They can facilitate Rad51 loading on ssDNA, increase intrinsic stability of Rad51 presynapticfilament, and protect Rad51 from removal by factors such as helicases. The roles of mediator proteins in mammals and other eukaryotes will be described later in the text.

Rad52

Rad52 interacts with Rad51, and can also bind RPA once the latter coats ssDNA (31,32). The Rad51-Rad52 interaction is required to recruit and nucleate Rad51 onto RPA-coated DNA (33,34). Only catalytic amounts of Rad52 are needed for presynaptic filament formation (3), suggesting that RPA is not displaced from DNA directly by Rad52, but rather as a consequence of filament extension by the polymerization of nucleated Rad51 molecules (35,36). The mediator function of Rad52 is largely attributable to its C-terminus where the Rad51 and DNA interacting domains are located. However, other Rad52 domains also contribute to recombination (31). The middle part of Rad52 interacts with RPA and is essential for the localization of Rad52 to repair centres (31,37). The N-terminal part of the protein possesses several activities, including oligomerization, DNA binding and annealing, and binding to a homologous protein Rad59 (34,38,39).

The DNA annealing function of yeast Rad52 protein can promote second-end DNA capture in the DSBR pathway, as well as in SSA and possibly other forms of HR (40,41). Similar functions were found for mammalian Rad52 (more in a later section) (40,41). The importance of this function is supported by the observation that most defective *rad52* mutations are found in the N-terminal part of the protein. For example, *rad52-R70A* is defective in DNA binding and annealing, but is proficient for mediator functions and does not affect the recruitment of Rad51 and itself to DSBs. Since *rad52-R70A* cells areγ-radiation sensitive, Rad52's roles in the steps of HR that do not entail Rad51-loading play important roles in DSBs repair (42,43).

The Rad55-Rad57 heterodimer
Like Rad51, the Rad55 and Rad57 heterodimer exhibits ATPase activity and binds ssDNA; but unlike Rad51, it cannot catalyze strand-exchange reaction (44-46). It is noteworthy that while a Rad57 ATPase deficient mutant confers little sensitivity to irradiation, the corresponding mutation in Rad55 has much stronger effect(45), indicating that the role of the two proteins is not equivalent. The Rad55-Rad57 heterodimer directly interacts with Rad51 and can load Rad51 onto RPA-coated ssDNA (Figure 2). It can also form co-filaments with Rad51 and the resulting nucleofilament is more resistant to Srs2 anti-recombinase activity (47). These functions are in line with previous data suggesting a role for this complex in the stabilization or protection of Rad51 nucleofilament that is required for downstream HR steps. For example, Rad51 overexpression, gain-of-function Rad51 mutations, or Srs2 removal can rescue the DSB repair defects and DNA damage sensitivity of *rad57Δ* or *rad55Δ* (48-50). However, Rad55 and Rad57 may have other roles besides being Rad51 mediators. For example, spontaneous sister chromatid recombination (SCR) is more defective in *rad51Δ rad57Δ* double mutant than *rad51Δ*, and this phenotype cannot be suppressed by *RAD51*overexpression or deletion of *SRS2* (51). This suggests a specialized role for Rad55/Rad57 in SCR that is distinct from its role in modulating Rad51 function.

A less understood positive regulators of Rad51- The Shu complex
The Shu complex is composed of Shu1, Psy3, Shu2, and Csm2 proteins, with Shu1 and Psy3 being Rad51 paralogues. This complex is conserved in *S. pombe* and likely so in humans (52,53). The precise role of the Shu complex is not well understood, but available data indicate that it functions as a positive regulator of Rad51 (Figure 2). Like *rad51Δ*, mutants of Shu subunits suppress the DNA damage sensitivity and defects in dissolution of recombination structures associated with mutants such as *sgs1Δ* and *top3Δ*, suggesting that the complex can facilitate Rad51 function (54,55). However, lack of this complex leads to sensitivity only to replication blocking agents and not DSB-inducing agents, indicating a specialized role in dealing with HR during damaged replication, such as the facilitation of Rad51 loading onto DNA containing lesions, or a function in ssDNA gap (54-58). Another suggestion is that the Shu complex, like Rad55 and Rad57, may promote recombination by inhibiting Srs2, since *shu1Δ* results in the accumulation of Srs2 foci (59).

Multifaceted regulators of Rad51 - the Snf2/Swi2 family members

Two members of the Snf2/Swi2 family of DNA-dependent ATPases, Rad54 and Rdh54/Tid1, play multiple roles in regulating Rad51. They serve as positive regulators of Rad51 at early stages of recombination by stabilizing presynaptic filaments, stimulating Rad51-mediated strand invasion, and promoting migration of the branch point of D-loops/HJs, with the later activity not yet demonstrated for Rdh54/Tid1 (Figure 2, reviewed in (3,60)). Furthermore, these activities promote Rad51-mediated homology search within the chromatin context (61-64). However, they both also work as negative regulators of Rad51 at later stages of recombination by preventing nonspecific binding of Rad51 to dsDNA or by removing Rad51 from dsDNA to expose a free 3'-OH primer terminus for DNA synthesis (65-68) (Figure 2). Mutants lacking Rad54 or Rdh54 accumulate Rad51 foci, with *rad54Δ* more defective in the removal of the DNA damage-associated Rad51 foci and *rdh54Δ* in spontaneous ones (69). The sequential execution of positive and negative regulation by Rad54 or Rdh54 is important for efficient recombination.

More recently, another member of this family, Uls1 in budding yeast and Rfp1/2 in fission yeast, was found to genetically interact with recombination factors, such as mediator proteins and Sgs1, and to be required for efficient replication of damaged genomes (70). Since mutants lacking Rad54, Rdh54 and Uls1 exhibit more severe defects in Rad51 foci accumulation, slow growth and chromosome loss than any single mutant, these homologues may partially substitute for each other in removing Rad51-DNA complexes (69). Unlike Rad54 and Rdh54, Uls1 was also proposed to be a SUMO-targeted ubiquitinligase (STUbL) (71). It will be interesting to determine how this and the ATPase functions of Uls1 contribute to HR.

Negative regulators of Rad51

There are at least three reasons to remove Rad51 from DNA or block its action. First, recombination can be harmful in certain situations such as stalled replication forks, which may be more safely restored using translesion synthesis. Also, nucleoprotein intermediates generated by the HR machinery can trigger cell-cycle arrest and even cause cell death in certain genetic backgrounds (72-74). This means that recombination events that can interfere with replication progression and DNA repair need to be prevented at an early step, such as presynaptic filament formation. Second, it is important to choose the right forms of HR in different types of cells and at specific times of the cell cycle. For example, SDSA should be preferentially used during mitosis to avoid potentially harmful events such as loss of heterozygosity. To achieve this, Rad51-ssDNA filaments need to be efficiently displaced from D-loops. Third, Rad51 needs to be removed from postsynaptic filaments to allow subsequent DNA synthesis, resolution and chromatin assembly. These three types of regulation at three different stages of HR require several helicases and translocases each with properties attuned to a special task.

1) Srs2, an anti-recombinase that disassembles Rad51 presynaptic filaments
The Srs2 protein belongs to the superfamily I of DNA helicases with strongest homology to the *E.coli* protein UvrD. Genetic studies suggest that the Srs2 protein can counteract Rad51 function. For example, *srs2Δ* leads to hyper-recombination and sensitizes other helicase mutations, and these defects are suppressed by removal of recombination proteins or mutation of the active site of Rad51 (reviewed in (75)). Direct evidence for an anti-Rad51 function came from biochemical studies showing that catalytic amounts of Srs2 efficiently dismantle Rad51 presynaptic filaments (76,77) (Figure 2). The disassembly of Rad51 presynaptic filament by Srs2 requires both its translocase activity and interaction with Rad51, and is enhanced in the presence of RPA that prevents re-nucleation of Rad51 (76-80). The protein interaction between Srs2 and Rad51 serves two purposes, one to target Srs2 to Rad51, and the other to trigger ATP hydrolysis within the Rad51 filament, causing a weakening of the Rad51-DNA interaction, thus allowing more efficient clearing of the nucleoprotein filament by Srs2 (81). Importantly and as described above, mediator proteins can suppress the action of Srs2 anti-recombinase, indicating that the relative strength of the two types of regulation determines the fate of presynaptic filaments (47,76). Although Srs2 is often referred to as an anti-recombinase due to its ability to disassemble presynaptic filaments, it also plays a pro-recombination role to promote SDSA. The mechanisms underlying this latter function are not well understood, though three non-mutually exclusive possibilities can be proposed. Srs2 may remove Rad51 filaments from D-loops, prevent second end capture, or collaborate with nucleases to cleave DNA tails or other intermediates after annealing.

Although no mammalian homologue of Srs2 has been identified, several helicases appear to have acquired a similar function. For example, RecQ5, BLM and FANCJ were reported to disrupt unstable RAD51-ssDNA filaments (82-84). In addition, the human FBH1 protein, which has both helicase and SCF ubiquitinligase domains, can carry out a subset of the Srs2 functions in yeast, suggesting that it could represent functional Srs2 homologue in human cells (85). Functional studies of human and *S. pombe* are in agreement with this prediction (86,87). Finally, another human protein, PARI, which lacks ATPase activity, can also suppress inappropriate recombination via its interaction with sumoylated PCNA and Rad51 (88). Notably, both Srs2 and an FBH1-like protein are present in *U. maydis* and *S. pombe*, and the *fbh1 srs2* double mutant shows more then additive reduction in growth due to unrestrained recombination in *S. pombe*, indicating that overlapping systems could exist in some organisms to keep recombination under control (89,90).

2) Translocases that unwind D-loop intermediates
Mph1 and its homologues, Fml proteins in fission yeast and FANCM in humans, are translocases. They share several activities, including disrupting Rad51-coated D-loops and catalyzing branch migration (91-94). Mph1 can also displace the extended primer in D-loop-based DNA synthesis (95) (Figure 2). These functions underlie the role of Mph1, and likely its homologues, in favouring SDSA over DSBR, thereby suppressing crossover in mitotic cells (92). The function of these helicases appears to be regulated by accessory proteins. For example, the histone-fold proteins Mhf1 and Mhf2 appear to cooperate with Mph1 in DNA

damage and replication fork repair and are suggested to facilitate Mph1 activity (96).

It is likely that similar mechanisms can be used to disrupt telomere specific D-loops (also called T-loops) to facilitate telomere maintenance (97). Indeed, the human RTEL1 protein was shown to efficiently disassemble D-loops (98). Correspondingly, *RTEL1*-deficient cells undergo DSBR at telomeres, resulting in telomere loss, chromosomal rearrangements and formation of telomere circles (99).

3) Helicases that dissolve dHJs and channel D-loops into SDSA

Sgs1, a RecQ family helicase, forms a complex with Top3 and Rmi1 proteins in yeast (100,101). Sgs1 has five orthologues in humans, including the cancer syndrome-associated proteins BLM, WRN and RTS, with BLM being the functional Sgs1 homolog. Sgs1 and its homologues have several roles in regulating Rad51 nucleofilaments. Since *sgs1Δ*, like *srs2Δ*, shows hyper-recombination and Sgs1 overexpression can rescue *srs2Δ* recombination defects, Sgs1 may directly dismantle presynaptic filaments, an activity that has been observed for BLM (82,102,103). Additional mechanisms include elimination of aberrant invasion events and resolution of recombination intermediates. This is supported by the ability of Sgs1 to prevent the formation of multi-chromatid joint molecules (104,105). In addition, Sgs1-Top3-Rmi1 can dissolve dHJs in a non-crossover configuration; both Sgs1 and BLM promote the formation of hemicatenanestructures by branch migrating two HJs between paired duplexes and this is followed by dissolution using topoisomerase III to produce non-crossover products (106,107).Finally, Sgs1 and similar proteins may also prevent the channeling of D-loop intermediates into the crossover-forming DSBR pathway (Figure 1B). For example, genetic studies in *Drosophila melanogaster*suggest that the BLM orthologue, MUS-309, can free the invading ssDNA tail from D-loops, thereby channeling it into the strand-annealing step of SDSA (108,109). Combination of these functions likely underlies the increased crossover levels in cells lacking Sgs1 (102,110,111). We note that Sgs1 can also indirectly promote Rad51 filament formation by generation of 3'overhang during end processing (102,112). For more details about Sgs1 and its homologues, see review by Ashton (113).

4) Removal of Rad51 from dsDNA

Several studies suggest that removal of Rad51 from dsDNA is required to promote downstream recombination events. This may occur in multiple steps with the initial ejection of Rad51 from the 3' end of the invading strand to promote extension of the D-loop by DNA repair synthesis (Figure 2). But complete removal of Rad51 from dsDNA may be required for the resolution of recombination intermediates and chromatin assembly. A function in Rad51 removal from dsDNA was first reported for yeast Rad54 protein as described above. Recently, *C. elegans* proteins ceHELQ-1 and ceRFS-1 were also shown to promote postsynaptic Rad51 filament disassembly from strand invasion intermediates (114). This is in agreement with the persistence of ceRad51 foci at meiotic DSBs in *helq-1 rfs-1* mutants*,* and the biochemical evidence that these proteins can remove ceRad51 from dsDNA but not ssDNA. The disruption activity of the ceRFS-1 peptide requires ceRad51 ATP hydrolysis, as dsDNA-

ceRad51 filaments formed in the presence of AMP-PMP are resistant to disruption. Since ceRFS-1 is a ceRad51 paralogue, it might integrate into and stabilize the ceRad51 filament on ssDNA, but lead to removal of ceRad51 from dsDNA (114).

Regulating Rad51 and its regulators by post-translational modifications

The regulatory mechanisms governing HR involve not only the aforementioned positive and negative regulator proteins, but also an intricate network of post-translational modifications (PTMs) (Table 1). Genetic studies provide the first clues for the important roles of PTMs, particularly phosphorylation and sumoylation, in HR regulation. For example, lack of CDK and DNA damage checkpoint severely diminishes HR in yeast and higher eukaryotic cells (reviewed in (72)). In addition, mutating the sumoylation or desumoylation enzymes in yeast leads to a range of phenotypes indicative of HR defects, such as hypersensitivity to DNA damaging agents and accumulation of recombination intermediates (115-118). Recent advances in this field provide some degree of detailed understanding of how CDK and checkpoint-mediated phosphorylation and sumoylation affect the functions of Rad51 and its regulators.

Modifications of RPA, Rad51, and Rad55

The large subunit of RPA in both budding yeast and humans is sumoylated upon genotoxic treatment (119,120). Genetic data in yeast suggest that RPA sumoylation may disfavour Rad51-independent pathways, such as SSA and BIR. In human cells, DNA damage triggers the dissociation of the RPA subunit, RPA70, from the desumoylating enzyme SENP6, resulting in RPA modification by SUMO-2/3. Sumoylated RPA70 facilitates Rad51 foci formation, and promotes HR and DNA damage resistance (120). Depletion of PIAS1 or PIAS4, the human SUMO E3 ligases, impairs human RPA accumulation at damage sites and causes a decrease in HR levels, indicating that sumoylation is also important for RPA recruitment to DSB sites (121,122).

RPA is phosphorylated both by checkpoint kinases, ATM/Mec1, and by cell cycle kinasesCDKs. Phosphorylation of RPA by these kinases is critical for Rad51 recruitment to DSB sites or for HR during replication stress (30,123). *In vitro* studies provide some mechanistic understanding of this modification. Phosphorylation of RPA increases the binding affinity of Rad52 for ssDNA, thus promoting the mediator function of Rad52 (124). In line with this idea, Rad52 recruitment is dependent upon RPA during S and G2/M phases, and CDK1 activity (20,125). The role of CDK1 in this case may be both to generate ssDNA by enabling resection and to modify RPA to facilitate Rad52 recruitment (126). Dephosphorylation of RPA is also important, as depletion of PP4C or PP4R2, components of the heterodimericphosphatase that controls dephosphorylation of RPA, also impairs HR (127).

Table 1. The effect of post-translational modifications (PTMs) on Rad51 and its regulators

	Human	*S. cerevisiae*	Function	PTM	Effect of the PTM modification
Recombinase	RAD51	Rad51	Homology search and DNA strand exchange	P	Mec1-mediated phosphorylation of Rad51 at S192 is required for ATPase and DNA binding activities (133) Phosphorylation of RAD51 T309 by Chk1 is essential for Rad51 foci formation (320) RAD51 is phosphorylated on Y54 and Y315 in c-Abl dependent manner (321) BCR-ABL1-mediated phosphorylation of RAD51 at Y315 promotes error-prone HR in leukemia cells (131,132) Plk1- and CK2-dependent phosphorylation facilitates RAD51 recruitment to damage sites and its binding to NBS1 (134)
Positive regulators	RAD52	Rad52	Recombination mediator, SSA	SUMO	SUMOylation of Rad52 at K43,44,253 promotes protein stability, disfavors nucleolar localization, and inhibits DNA binding and annealing activity (138,141,142) SUMOylation of RAD52 alters its subcellular localization (143)
				P	Phosphorylation of RAD52 mediated by c-ABL enhances RAD52 annealing activity (146)
	BRCA2		Recombination mediator	P	CDK-dependent phosphorylation at S3291 of BRCA2 regulates its interaction with RAD51 (322)
				Ub	Ubiquitylation of BRCA2 after MMC treatment leads to its proteasomal degradation (323)
	RAD51B-RAD51C RAD51D-XRCC2 RAD51C-XRCC3	Rad55-Rad57	Recombination mediator	P	Phosphorylation of Rad55 at S2,8,14 is required for efficient recombination after replication fork stalling (136)
	Psy3=RAD51D, Shu2=SWS1 Shu1=XRCC2 Csm2=not identified	Shu1-Psy3-Shu2-Csm2	Regulation of Srs2 activity, stabilization Rad51 filament	P	XRCC2 is phosphorylated upon DNA damage, probably by ATM or ATR (324)
		Rad59	ssDNA annealing, Rad51 filament stability	SUMO	Deletion of *SLX5/8* decreases Rad59 sumoylation and increases SSA and BIR (119)
	RAD54	Rad54	ATP-dependent dsDNA translocase, stabilization of Rad51 filament	P	Mek1-mediated phosphorylation of Rad54 down-regulates Rad51 recombinase activity (157)
				Ub	APC/C-dependent ubiquitylation of *S.pombe* Rdh54 in G1 phase is required for efficient HR (156)
	RAD54B	Rdh54/Tid1	ATP-dependent dsDNA translocase, stabilization of Dmc1 filament		
		Tid4/Uls1	SUMO-dependent ubiquitin ligase, stabilization of Rad51 filament		
	RAD51AP1		Stabilization of D-loop formation		
	SWI5-MEI5	Mei5-Sae3*	Mediator activity		
	MND1-HOP2*	Mnd1-Hop2*	Stabilization of Rad51- and Dmc1-presynaptic filaments		
Negative regulators		Srs2	Helicase activity, disruption of Rad51 presynaptic filament, promotes SDSA	SUMO	Srs2 SUMOylation at K1081,1089,1142 is responsible for toxicity seen in cells lacking Cdk1-mediated phosphorylation of Srs2 (147)
				P	Cdk1-dependent phosphorylation of Srs2 promotes accurate DSB repair (147)
		Hed1*	Inhibition of Rad54 recruitment to Rad51 presynaptic filament		
	FANCM	Mph1	Helicase and branch migration activity, dissociation of D-loops formed by Rad51, promotes SDSA	P	FANCM is phosphorylated after DNA damage (325)
	BLM	Sgs1	RecQ-like DNA helicase, multiple roles in HR and DNA replication (resolution dHJ)	SUMO	BLM SUMOylation promotes RAD51 function (153) Sgs1 sumoylation promotes telomere recombination (152)
				P	Sgs1 is phosphorylated *in vivo* (326) BLM phosphorylation at T99 causes its dissociation from Top3a (327) MPS1-dependent BLM phosphorylation is essential for accurate chromosome segregation (328)
	RTEL1		ATP-dependent DNA helicase, inhibition of D-loop formation, promoting SDSA		
	PARI		Inhibition of HR, binds PCNA and Rad51		
Other regulators	RPA	RPA	Binding to resected ssDNA ends (competition with Rad51)	SUMO	SUMOylation of RPA70 facilitates RAD51 foci formation and promotes HR (120) Deletion of *SLX5/8* decreases sumoylation of Rfa1 and Rfa2 and affects SSA and BIR (119)
				P	Hyperphosphorylated RPA2 is required for RAD51 recruitment to DSB sites (123)

* meiosis specific proteins, PTM –post-translational modifications: P – phosphorylation, Ub – ubiquitylation, SUMO – sumoylation

Rad51 was identified as a SUMO and Ubc9 interactor (128,129). A further support of the connection between Rad51 and sumoylation is the observation that mislocalization of UBC9 or depletion of SUMO E3 MMS21 disrupts RAD51 trafficking, resulting in marked inhibition of DNA damage-induced RAD51 nuclear foci formation (130). However it is not clear whether this is mediated by a direct effect on RAD51. Rad51 isphosphorylated by several kinases (Table 1). Phosphorylation of Tyr-315 by BCR/ABL appears to be essential for enhanced DSB repair and drug resistance, and phosphorylation of Tyr-54 by c-Abl inhibits the binding of Rad51 to DNA and its ATP-dependent DNA strand exchange reaction (131,132). Recent work also uncovered the phosphorylation of Ser-192 in a Mec1-dependent manner in response to DNA damage (133). This residue is required for Rad51 ATPase and DNA-binding activity *in vitro*, suggesting that the modification can affect Rad51 activity (133). Moreover, human RAD51 isphosphorylated at Ser-14 by Plk1 in a cell cycle- and DNA-damage-responsive manner. Ser-14 phosphorylation triggers subsequent phosphorylation at Tyr-13 by casein kinase (CK2) leading to direct binding to MRN component, Nbs1. This process helps RAD51 to recruit to DNA damage sites thus allowing accurate HR (134). Phosphorylation also affects the formation of Rad51 nucleofilaments by modifying the mediator Rad55 (135). Rad55 is phosphorylated by DNA damage checkpoint kinases at three residues (Serine 2,8, and 14), and the unphosphorylable mutant displays increased sensitivity to genotoxic stress and replication fork stalling, indicating that this modification promotes Rad51 function (136).

Rad52 and its modifications

Rad52 proteins in fission yeast, budding yeast, and human cells are all sumoylated (137,138). In budding yeast, Rad52 sumoylation is induced after DSB generation in meiotic cells or genotoxic treatment of S phase cells (139,140). Sumoylation of Rad52 likely precedes Rad51 filament formation based on the observations that RPA-bound ssDNA enhances Rad52 sumoylation and that sumoylation inhibits Rad52 DNA binding and strand-annealing activity (141). Since *rad51Δ* leads to the accumulation of Rad52 foci, it is likely that Rad52 sumoylation can be attenuated once Rad51 filaments are formed. Studies using mutants affecting the three sumoylation sites Rad52 (lysines 10, 11, and 220) suggest that the role of Rad52 sumoylation can be diverse depending on the state of the DNA substrates. First, this modification can shelter Rad52 from proteasome-mediated degradation when recombination intermediates accumulate in *sgs1Δ srs2Δ* background (138). It was extrapolated that sumoylation may serve to protect the active forms of Rad52 from degradation (138). Second, sumoylation of Rad52 is important for damage-induced interchromosomal recombination and for recombination pathway choices, with a bias toward gene conversion and against BIR and SSA (139,141). Furthermore, Rad52 sumoylation appears to facilitate the exclusion of Rad52 foci from the rDNA locus thereby inhibiting rDNA recombination (142). It will be interesting to determine whether the different effects seen for Rad52 sumoylation are mediated by the same or different molecular mechanisms.

In contrast to yeast Rad52, sumoylation does not seem to affect the biochemical activities of human Rad52 nor is it induced by DNA damage. Rather sumoylation alters RAD52 subcellular localization (143). In addition to

sumoylation, Rad52 also undergoes phosphorylation. While phosphorylation of yeast Rad52 occurs constitutively, that of RAD52 at tyrosine 104 is mediated by c-ABL and is activated upon exposure to various types of DNA damage (144,145). The phosphotyrosine analogue of Y104 of RAD52 enhances ssDNA annealing activity by attenuating dsDNA binding by the protein, suggesting that this modification can direct RAD52 to DNA repair intermediates that undergo annealing (146).

Modifications of translocases in HR regulation

The dual functions of Srs2, both as a negative regulator of HR by dismantling presynaptic filaments and as a positive regulator by processing recombination intermediates in favour of the SDSA pathway, suggest that the protein may be regulated by different modifications to serve different functional purposes. Indeed, Srs2 is regulated both by Cdk1-dependent phosphorylation and sumoylation in response to DNA damage. Cdk1-mediated phosphorylation of Srs2 appears to promote the SDSA pathway (147). A pro-SDSA function may provide an explanation for the requirement of this phosphorylation in HR-dependent recovery after chronic exposure to low doses of UV irradiation (148). Additionally, Srs2 is sumoylated near the C-terminus of the protein ((147)and our unpublished data), a region that interacts with both SUMO and PCNA and is required to prevent unscheduled recombination events at replication forks (149,150). The function of Srs2 sumoylation is less clear, but genetic data suggest an important role for this modification. In particular, inhibition of Srs2 phosphorylation results in the accumulation of sumoylated Srs2. In addition, sumoylation of Srs2 is responsible for the DSB repair defects associated with non-phosphorylable Srs2, as eliminating its sumoylation is able to rescue the phenotype of the latter. Understanding how sumoylation can cause toxicity to cells when Srs2 is not phosphorylated will provide important clues about the function of Srs2 sumoylation.

Additionally, both Sgs1 and BLM proteins are sumoylated (115,151). While sumoylation of yeast Sgs1 appears to specifically promote recombination at telomeres, that of BLM was shown to increase its binding to RAD51 and promote HR at stalled replication forks (152,153). Cells expressing a SUMO-deficient mutant of BLM display defects in RAD51 localization to stalled replication forks and failure to induce sister chromatid exchanges (SCEs), indicating that sumoylation of BLM controls the recruitment and/or retention of RAD51 at damaged replication forks (153). Additionally, sumoylation of another RecQ-like helicase, WRN, was suggested to be involved in multiple processes, such as co-localization with RAD51, stabilization of stalled replication forks, and telomere maintenance (154,155). It remains to be determined whether these functions reflect a more fundamental effect of sumoylation of WRN that is manifested in different cell lines or conditions.

The function of Rad54 is also regulated by at least two types of PTMs. Its activity during the G1 phase of the cell cycle in *S. pombe* seems to be regulated by ubiquitin-mediated proteolysis (156). In meiosis, Rad54 undergoes Mek1-dependent phosphorylation that abrogates its interaction with Rad51, thus preventing inter-sister recombination (157). Recently, the Rad53 kinase was also shown to target Rad54 for phosphorylation at the same site, suggesting that

Rad54 may also be under checkpoint control in the mitotic DNA damage response (158).

In summary, available data suggest that post-translational modifications regulate HR at different levels. Just recently, it has been shown that DNA damage-induced sumoylation could function alongside checkpoint signalling as an integral part of DNA damage response (DDR) (159). A better understanding of how these modifications affect HR proteins will require the integration of biochemical examination of the modified forms of the protein and *in vivo* genetic studies. In addition, it is important to understand the interplay between the different forms of modifications: when they can work in a concerted manner and when they can be antagonistic. Moreover, given the existence of STUbL proteins such as Uls1 and the Slx5/8 complex that have been implicated in HR, it will not be surprising if the interplay between sumoylation and ubiquitylation is also an important aspect of HR regulation.

Functions of Rad51 and its regulators in mammalian cells

The function of Rad51 appears to be largely conserved in higher eukaryotic cells, however its regulators and their functions are more complex (Table 1). Multiple homologues of the yeast proteins are evolved to affect different aspects of DSB repair or in different tissues, or to link repair with other cellular processes such as checkpoint control and apoptosis. In addition, new mediators and regulators have also appeared. Here, we focus on the core proteins that directly interact with Rad51, including ssDNA binding proteins, mediators and their regulators, and the Rad54 proteins. Understanding of other translocases and helicase homologues in higher eukaryotic cells can be found in several recent reviews (160-165).

RAD51 and ssDNA binding proteins

Although the biochemical activities of RAD51 mimic those of yeast Rad51 and bacterial RecA, RAD51 in higher eukaryotic cells is essential for cell survival as demonstrated in both mouse and chicken DT40 cells (166-169). The essentiality of RAD51 in these organisms is likely due to the increased burden of repair associated with the higher number of lesions in larger genomes (166). Another intriguing function of RAD51 and its paralogues is that they are implicated in the oxidative stress response in mitochondria (170). Further developments on this front will help answer the long-standing question of recombination in mitochondrial genomes.

While RPA is highly conserved between yeast and humans, human cells have two other ssDNA binding proteins, human SSB1 and SSB2, that bear a greater resemblance to bacterial SSB than RPA. SSB1 deficiency does not affect replication and S-phase progression, but exhibit checkpoint activation defects, increased IR sensitivity, and impaired HR, implying a role in the DSB response (171). Indeed, SSB1 and SSB2 are part of the sensor ssDNA complex that binds to DSB ends and is required for ATM checkpoint signalling and efficient HR repair (172,173). An additional function was assigned to SSB1 in DSB processing, during which it can recruit and stimulate the activity of MRN complex via its interaction with the NBS1 subunit (174,175).

BRCA2 - the main mediator

While the requirement for mediators is universally conserved, the specific proteins can be different among organisms. Despite the presence of human RAD52 protein, the central RAD51 mediator function in humans is carried out by another protein, BRCA2. Although BRCA2 has no homology with yeast Rad52, BRCA2 is its functional equivalent, since it controls the assembly of human RAD51 into nucleoprotein filaments as demonstrated both *in vivo* and *in vitro* (15,176). Especially, the structural characterization of the C-terminal part of BRCA2 and its mediator activity was essential in this regard (177). For example, both BRCA2 and RAD52 specifically interact with the corresponding Rad51 proteins, show preferential binding affinity towards ssDNA, have the ability to overcome RPA inhibition, and promote RAD51-mediated strand exchange.

As BRCA2 orthologues in various organisms appear to function as mediators, yeast may be an exception that uses Rad52 as the mediator. They differ greatly in size and domain structures, suggesting evolutionary flexibility and explaining the ability of the ssDNA binding region from RPA or RAD52 proteins to substitute for the BRCA2 DNA binding domain (DBD domain) to efficiently suppress the cellular defects of BRCA2-mutant cells (178). The understanding of the role of BRCA2 in HR benefits greatly from studies of its *U. maydis* homolog Brh2, which is much smaller than BRCA2 (179,180). The recent breakthrough with the purification of full length BRCA2 confirmed previous results seen by using truncated protein, as well as provides new insights into the biochemical functions of BRAC2, such as its possible dimerization, its capacity to bind approximately six RAD51 proteins, and its stimulation of RAD51 activities without direct interaction with RPA (181-183).

Recent studies have also provided more insight into how BRCA2 interacts with and affects RAD51 function. BRCA2 can interact with RAD51 through two types of domains. The first type includes various conserved BRC repeats that exhibit different capacities for RAD51 interaction. One category of BRC domain performs the mediator function by targeting RAD51 to ssDNA to form a nucleoprotein filament, and by stabilizing this nucleofilament in active form via down-regulation of RAD51 ATP hydrolysis. The other category of BRC domainscan prevent the nucleation of RAD51 on dsDNA (184-187). Besides BRC domains, BRCA2 also interacts with RAD51 through its C-terminal part that is encoded by exon 27 of the human BRCT gene. Unlike BRC domains, this region can interact with the RAD51 only in the nucleoprotein filament form in a cell cycle-dependent fashion (188,189). Two recent studies suggest that this domain stabilizes RAD51 filament or replication forks. In the first study, mutations within the BRCA2 C-terminus that block its interaction with RAD51 was shown to not affect Rad51 foci formation or HR repair, but instead result in rapid foci disassembly and mitotic entry (190). In another case, the C-terminal domain of BRCA2 is essential for fork protection by stabilizing RAD51 filament and preventing MRE11-mediated degradation (191). Altogether, the multiple RAD51 interaction domains meet the different demands for BRCA2 function as both a mediator and a scaffold protein that links HR with replication and mitosis. It is noteworthy that inside cells, the interaction between BRCA2 and RAD51 is also subject to regulation by localization, as DNA damage can induce a redistribution of soluble nucleoplasmic BRCA2 available for RAD51 binding (192). In addition, it will be interesting to understand whether the BRCA2-RAD51 interaction is

critical for the newly described role of BRCA2 in preventing the degradation of newly synthesized DNA when replication is interrupted (191).

DSS1- a binding partner of BRCA2

DSS1 interacts with the C-terminal DNA binding domain of BRCA2 (177). In *Ustilagomaydis,dss1Δ* mutants are phenotypically similar to *rad51Δ* and *brh2Δ.* DSS1 confers allosteric regulation of the Brh2-DNA interaction and prevents the formation of Brh2 homo-oligomers, thereby maintaining it in an active state (193,194). No such effect was observed for the human protein, but rather thehuman DSS1 facilitates BRCA2 in RAD51-ssDNA filament formation (168). Strangely, the yeast DSS1 homologue, Sem1, is a subunit of the regulatory component of the proteasome as well as signalosome, which is involved in de-neddylation and activation of some types of ubiquitin E3s, respectively. This indicates that the Sem1/DSS1 family proteins are versatile proteins regulating the integrity and function of several protein complexes involved in diverse pathways (195). Depletion of DSS1, like BRCA2 depletion, greatly reduces HR efficiency, and this is not via an ubiquitin-proteasome system, suggesting that DSS1 regulates BRCA2 by means other than regulating protein stability (196).

PALB2 and other BRCA2 regulators

Another important regulator of BRCA2 is PALB2. PALB2 interacts with the N-terminus of BRCA2 and plays several roles in HR by regulating BRCA2 and possibly by directly affecting RAD51 function. Several germline BRCA2 mutations identified in breast cancer patients lead to loss of PALB2 binding and BRCA2 function in HR, suggesting that PALB2 is a key regulator of BRCA2's biochemical and tumour suppression function (197). In addition, a germline mutation of PALB2 itself was also identified in breast cancer patients (198). The structure of the PALB2 C-terminus in complex with BRCA2-peptide identifies molecular determinants for protein-protein interaction and helps to explain the effects of cancer-associated truncations of both proteins (199).

PALB2 colocalizes with BRCA2 in nuclear foci and stabilizes BRCA2 by promoting its chromatin association. In addition, PALB2 and its oligomerization promote the delivery and stabilization of RAD51 to the site of DNA damage (197,200). While this effect likely involves its regulation of BRCA2, PALB2 may also directly affect RAD51 function. PALB2 was recently shown to bind DNA, directly associate with RAD51, and promote RAD51-mediated D-loop formation. Additionally, it also binds to and cooperates with RAD51AP1 (described below) to enhance RAD51-mediated recombination activities, supporting its role after the assembly of presynaptic filaments (201,202). Both PALB2 and BRCA2 influence cell cycle checkpoints, as depletion of either prematurely abrogates checkpoint signalling and activate the checkpoint-recovery pathway (203). In addition, p53 interacts with multiple regions of BRCA2 and suppresses HR in a transactivation-independent fashion, whereas overexpression of BRCA2 attenuates p53-mediated apoptosis, suggesting that BRCA2 also connects HR with apoptosis (204).

MCPH1 (microcephalin) is another BRCA2-interacting partner that can reduce the levels of both BRCA2 and RAD51 at damage sites and interfere with BRCA2-dependent HR (205). Similar results were observed for the mouse

homologue of microcephalin, BRIT1 (206), suggesting that these proteins provide a means to attenuate RAD51 function.

RAD52 with non-conserved functions

While human RAD52 shares structural and some biochemical similarity with yeast Rad52, it has not been shown to possess recombination mediator activity. This could explain both the minor role of RAD52 in vertebrate HR and its replacement by BRCA2 for loading RAD51 on ssDNA (207). Despite its high homology to yeast Rad52, the human RAD52 protein is functionally more similar to the yeast Rad59 protein, which acts with Rad52 and has both a minor role in Rad51-dependent recombination and a critical role in SSA between direct repeats. Like Rad59, human RAD52 lacks the C-terminal part of the yeast Rad52 that contains Rad51- and RPA-interaction domains, as well as the region responsible for mediator activity (31). Similarly, RAD52 also possesses strand annealing activity and acts in parallel to BRCA2, and its inactivation is lethal in BRCA2 deficient cells (208-210). However, RAD52 may be able to compensate for BRCA2 under certain circumstances as observed in *U. maydis*(211). RAD52 also has a function in the late stages of DSB repair at stalled or collapsed replication forks that does not appear to be shared by BRCA2 (212). These observations argue that RAD52 has a unique role in catalyzing ssDNA annealing in homology-directed DNA repair. These activities may be toxic in certain genetic background since RAD52 deletion can partially rescue the T cell development and reduce T-cell lymphomas in ATM-deficient mice (213).

Rad51 paralogues and other Rad51 binding factors

The RAD51 paralogues, including RAD51B, RAD51C, RAD51D, XRCC2 and XRCC3, share 20-30% sequence identity with RAD51. Several lines of evidence suggest that they function as mediators or promote and/or stabilize RAD51 nucleofilaments. For example, depletion of these proteins block IR-induced RAD51 foci formation, and the defects in each of these RAD51 paralogues is partially suppressed by overproduction of RAD51 in chicken DT40 cell lines (214-216). Two complexes can be formed by RAD51 paralogues, including the RAD51B-RAD51C-RAD51D-XRCC2 complex and the RAD51C-XRCC3 complex (217). The first complex has the highest affinity for branched DNA substrates, which is consistent with a function in formation or stabilization of RAD51 filaments during repair of damaged replication forks (218-221). In addition, this complex can stimulate homologous DNA pairing, likely due to the ability of RAD51C to promote the melting of dsDNA. The second complex likely plays a role in the later steps of recombination, as suggested by the association of RAD51C-XRCC3 complex with HJ resolution activity in human cell extracts and that RAD51C-deficient cells show phenotype associated with defects in HJ resolution activity (222,223). The RAD51 paralogues may function in parallel to BRCA2 in RAD51 loading, as RAD51C foci are not affected in BRCA2-deficient cell lines (218). While mutations in any of these paralogues in chicken or hamster cells lead to increased sensitivity to DNA damaging agents (224), disruption of RAD51B, RAD51D, and XRCC2 in mice leads to embryonic lethality, indicating an increased dependency of these proteins in larger genomes (225-227). Further elucidation of the molecular mechanisms of how RAD51 paralogues function in different steps of HR will illuminate the complex regulation of RAD51.

RAD51AP1

Additional factors are also involved in regulating RAD51. Most noticeably, RAD51AP1 (Rad51 associated protein 1) represents a vertebrate-specific protein that interacts with human RAD51 (228). It enhances RAD51 recombination activity by stabilizing D-loops formed by RAD51, but plays little or no role in the assembly of DNA damage-induced RAD51 foci (229,230). This suggests that the function of RAD51AP1 is limited to the DNA strand invasion step of HR. Meiosis-specific roles of RAD51AP1 are described below.

Human Snf2/Swi2 members involved in HR

Human cells possess two Rad54 homologues, RAD54 and RAD54B, which share similar biochemical activities (231). However, in contrast to what is seen in yeast, knockouts of either RAD54 or RAD54B show modest to no defects in HR in vertebrates, though the RAD54RAD54B double knockout displays stronger defects (232). One possible explanation for the different effects of lack of Rad54 in yeast and in vertebrates is that yet other members of the Snf2/Swi2 family in the latter case may be able to carry out similar functions, though these factors are yet to be identified.

Meiosis-specific regulation of recombination nucleofilaments

Recombination in meiosis shares similarities with mitotic recombination, but also exhibits many unique features. Unlike mitotic recombination, meiotic recombination is genetically programmed with DNA breaks being endogenously induced by Spo11 (233). The repair of Spo11-generated breaks is essential for homolog pairing in some organisms and also for generation of genetic diversity. Recombination also mediates crossing-over between homologues leading to the formation of chiasmata, which are required for proper segregation of homologous chromosomes at meiosis I. In addition, the process of HR in meiosis needs to be tightly integrated with other DNA-protein structures uniquely required for meiosis such as the synaptonemal complex. Finally, to allow homologous chromosomal pairing and the generation of genetic diversity, the DSBR mode of recombination is more favoured in meiosis than in mitosis by several mechanisms. These specific requirements during meiosis are fulfilled both by a specialized strand exchange proteins and several meiosis-specific regulators.

Meiosis-specific strand exchange proteins

Most eukaryotes contain a meiosis-specific Rad51 paralogue, Dmc1. Unlike *rad51Δ,* which leads to severe defects in both mitotic and meiotic recombination, *dmc1Δ* is deficient only in meiotic recombination (8,233,234). The essential role of Dmc1 in this process is demonstrated by the spore inviability, the absence of recombination intermediates and dramatic reduction of crossover products in *dmc1* mutants (235-237). A conserved role of Dmc1 is seen in mouse cells, as lack of the mouse Dmc1 results in the same phenotype as that of yeast *dmc1* mutants (238,239). However several organisms, such as fission yeast and plants, lack the Dmc1 protein, suggesting alternative mechanisms are being utilized there (233).

There are several similarities and differences between Rad51 and Dmc1.

In the absence of DNA, both exist as rings consisting of several protomers. In the presence of DNA, Dmc1 forms a helical filament as well as stacked rings (240-243). However, only the filament similar to that formed by Rad51 shows the ability to catalyze DNA pairing and strand exchange (242,244). Several papers have described the differences in the properties of Dmc1 and Rad51. For example, Rad51 and Dmc1 proteins localize differently on meiotic chromosome (245,246). In addition, D-loops formed by DMC1 are more resistant to dissociation by branch-migration proteins such as RAD54 than the ones formed by RAD51 (247). It needs to be noted that interpretations of these observations should consider the different methodologies as well as conditions employed (243,248).

The interplay between Rad51 and Dmc1 is still not yet fully understood, and several nonexclusive models have been put forward. The cooperative model suggests the formation of co-filaments composed of both proteins, whereas other models prefer the formation of asymmetric filaments or the assembly of different types of nucleofilaments leading to different HR subpathways(249). However, it does not seem that Rad51 and Dmc1 can form different filament structures with intrinsically distinct biochemical activities. This means that the different effects of the two proteins have to be also influenced by the distinct sets of specific accessory proteins that can differently interact with these proteins.

The Mei5-Sae3 complex - a meiosis-specific mediator only in budding yeast

Mei5 and Sae3 likely represent meiosis-specific recombination mediator required for Dmc1 recruitment and loading, with no effect on Rad51 filament formation in budding yeast (250). As a typical recombination mediator, the Mei5-Sae3 heterodimer interacts with Dmc1, RPA, and both ssDNA and dsDNA, and is able to overcome the inhibitory effect of RPA on the Dmc1-mediated strand exchange reaction (251,252). In addition, similar to other recombination mediators, such as Rad55/Rad57, mutations in the *SAE3* gene result in hyper-resection of DSB (253). Sae3-Mei5 localization is dependent on Dmc1, suggesting mutually dependency. This is reminiscent of the relationship between the Rad55-Rad57 complex and Rad51 (20,49,254). The roles of these proteins appear to be conserved, but may exhibit some variation regarding whether they facilitate Rad51 and/or Dmc1.

The Mei5-Sae3complex also functionsin mitosis in other organisms.The fission yeast homologues (Swi5-Sfr1) function in both mitotic and meiotic cells, and exhibit mediator activity in both Dmc1- and Rad51-mediated strand exchange reactions (255-258). Recently, the human and mouse homologues of the Swi5-Mei5 complex have been identified and were shown to interact with Rad51. Accordingly, their depletion leads to defects in Rad51 foci formation and increased sensitivity to DNA damaging agents (259,260). It appears that this complex functions in both mitosis and meiosis and the budding yeast situation is the exception.

The Hop2-Mnd1 complex and its multiple roles in promoting meiotic recombination

The Hop2-Mnd1 complex is another meiosis-specific factor identified in all organisms expressing Dmc1. The absence of both proteins results in non-homologous synapsis and persistence of meiotic DSB (261). This complex likely

performs two functions. First, it can stabilize Rad51- and Dmc1-presynaptic filaments (262,263). However this activity is different from a recombination mediator role, as both Rad51 and Dmc1 foci form normally in *mnd1* and *hop2* mutants, and unlike mediators, Mnd1 is not recruited to DSB sites (261,264,265). Second, the Hop2-Mnd1 complex facilitates strand invasion and stimulates D-loop formation by promoting the capture of dsDNA by Dmc1 or Rad51 nucleoprotein filaments (262,263). This function is suggested by the observation that *mnd1* mutants exhibit normal initiation of recombination but fail to form heteroduplex DNA or dHJs(266). A likely mechanism for this function is the reversible dsDNA condensation that allows efficient capture of homologous dsDNA(265,267). This represents a mechanism distinct from Rad54 stimulated synapsis, where dsDNA capture follows ATP hydrolysis-coupled dsDNA translocation (268). Further work is needed to understand how the various biochemical functions of Hop2-Mnd1 contribute to meiotic recombination.

Rad54 and Rdh54/Tid1 and their different roles in meiosis
Rad54 and Rdh54/Tid1 are also important for recombination during meiosis. Their double mutant almost eliminates meiotic HR, whereas each single mutant results in partial defects in both sporulation and spore viability(269,270). Rdh54 seems to be more critical during meiosis than mitosis, likely due to its role in promoting Dmc1-mediated interhomologue recombination (269-271). Indeed, Dmc1 interacts with Rdh54/Tid1, but not Rad54, although Rad51 interacts with both (271-273).In addition, Rdh54 prevents the accumulation of Dmc1 on chromatin in the absence of DSBs in an ATPase-dependent manner, suggesting that Rdh54 can dissociate dead-end Dmc1 complexes (274). These activities have also been demonstrated biochemically: purified SpRdh54 that can both stimulate Dmc1 reaction and remove Dmc1 from dsDNA in an ATP-dependent manner (275).

In contrast to an active role of Rdh54/Tid1 in regulating Dmc1, Rad54 fails to disassociate Dmc1-mediated D-loops (247). This may provide a better opportunity for second end capture of Dmc1 D-loops and promote DSBR. In addition, Rad54 is regulated by Mek1-mediated phosphorylation that inhibits the Rad51-Rad54 interaction, providing another means to favour Dmc1-mediated recombination (157). However, Rad54 does contribute to meiotic progression likely by promoting sister chromatid or interhomologue recombination (276).

Hed1- a meiotic Rad51 inhibitor
Hed1 mediates another mechanism in favour of Dmc1-mediated recombination in meiosis in budding yeast. Hed1 interacts with Rad51 in yeast two-hybrid assays and colocalizes with Rad51 at meiotic DSBs in a Rad51-dependent manner (277). Hed1 does not affect Rad51 presynaptic filament formation, rather it interferes with the Rad51-Rad54 interaction thereby restricts Rad54 recruitment to site-specific DSBs(278). In agreement with this, overexpression of both Rad51 and Rad54 in *dmc1* cells can suppress Hed1-mediated inhibition of Rad51 function (279,280). As no apparent Hed1 homologue is found in other higher eukaryotic cells, how Rad51 is inhibited in these systems remain to be elucidated.

Other meiotic recombination factors
Two mammalian Rad51 interacting proteins, RAD51AP1 and RAD51AP2, also

regulate meiotic HR. hDmc1-mediated D-loop formation is enhanced by RAD51AP1 and the function synergy of the two proteins requires their physical interaction (281). RAD51AP2 is a meiosis-specific Rad51 interacting protein as suggested by yeast 2-hybrid results, but the possible regulatory role of this protein remains unclear (282).

Besides a critical role in mitotic recombination, BRCA2 is also implicated in meiosis and binds both Rad51 and Dmc1 in *A. thaliana* and humans (283,284). Distinct interaction domains could allow coordinated interactions of the two strand exchange proteins with BRCA2 during meiosis. Genetic data from several organisms also support a role of BRCA2 in meiosis. First, silencing of plant BRCA2 results in meiotic defects and sterility, which could also be related to its role in oocyte nuclear architecture and gametogenesis(285,286). Second, deletion of *Drosophila* BRCA2 leads to recombination defects and checkpoint activation during meiosis (287). Finally, BRCA2-deficient zebrafish and mice cell lines reveal a role for BRCA2 in ovarian development, and in tumorigenesis of reproductive tissues and impairment of mammalian gametogenesis, respectively (288,289). Similarly, Brh2 and Dss1 proteins together with Rad51 are required during meiotic HR in *U. maydis*(180).

Recombination defects in human diseases

Given the important roles of RAD51 and its regulators in repairing DNA lesions and preventing inappropriate recombination, it is not surprising that mutations of these proteins can lead to predisposition to a variety of cancers (Table 2) (290-292). Among the RAD51 regulators, heterozygous mutations in BRCA2 increase susceptibility to breast and ovarian cancers (293). While heterozygous mutations in several HR genes involved in Rad51 filament assembly, including BRCA2, PALB2, and RAD51C increase the risk of breast, pancreatic and ovarian cancer, homozygous mutations cause Fanconi anaemia (FA), a cancer predisposition syndrome characterized by a defect in the repair of DNA interstrandcrosslinks(197,198,294-298). Mutations of other RAD51 regulators were also found in cancer cells. For example, translocation of RAD51B was found in uterine leiomyoma and several mutations of RAD54B that reduce or eliminate its activity *in vitro* have been found in primary colon carcinomas and lymphomas (299-301). Inappropriate HR during meiosis due to mutation of RAD51 regulators, results in abnormal numbers of homologous chromosomes, developmental abnormalities, and/or embryonic death (288,302). In addition, mutations in BLM and WRN helicases, are associated with cancer predispose syndromes, genomic instability and premature aging (160,163).

Although mutations in RAD51 have not been linked to any disease, many cancer cell lines show elevated levels of the protein. It has been proposed that high levels of RAD51 may lead to uncontrolled HR and destabilization of the genome in the early events in carcinogenesis (303). Another view is that higher levels of RAD51 help to maintain the genome during tumorigenesis when it experiences some levels of instability (224). Accordingly, it was shown that p53 plays an important role in suppressing RAD51 expression and activity (for review see (304)). In addition, constitutive activation of c-ABL due to the BCR–ABL fusion, a key event in the pathogenesis of chronic myeloid leukaemia and other myelo-proliferative diseases, results in higher expression and

phosphorylation of RAD51, promoting unfaithful HR events and contributing to secondary aberrations or drug resistance (131). Another example is that c-ABL activation enhances nuclear localization of RAD52 (305), accompanied by upregulation of SSA (306). This suggests that the BCR/ABL kinase may shift the balance from error-free HR to mutagenic recombination. Finally, mutation in other strand exchange protein, DMC1, has been associated with infertility (307).

Diagnosis and Therapeutic strategies

Due to the important roles of HR proteins in tumour progression and their involvement of resistance to some therapeutic agents, they represent potential targets for diagnosis and therapy. One main concept in devising these strategies is that HR-deficient tumours are more sensitive to killing by DNA damaging agents or by chemicals that inhibit other repair pathways or checkpoint mechanisms (208,308,309). For example, tumour cells that are mutated for the FA repair pathway show hypersensitivity to inhibitors of a main checkpoint kinase CHK1 (310). Another example is the selective killing of RAD54B-deficient colorectal cancers by down-regulation of FEN1 a nuclease involved in replication and excision repair (311). A third promising strategy uses PARP inhibitors. PARP is an enzyme involved in the repair of SSBs, and its inhibition leads to the persistence of DNA lesions normally repaired by homologous recombination. As a result, inhibition of PARP in HR-deficient cells confers strong lethality. Since PARP inhibition selectively targets HR-defective cells, they have shown good effects in cancers associated with BRCA1 or BRCA2 mutations (308,312).

Diagnosis tools can also be generated based on the interplay between PARP and HR proteins. Since PARP inhibitors can result in RAD51 foci formation only in HR-proficient cells, a diagnostic tool using PARP inhibitors has been developed in primary cell cultures to identify HR-deficient tumours (313). Similarly, since PARP is hyperactivated in HR-defective cells, including RAD54, RAD52, BLM, WRN, and XRCC3 (314), a strategy can be devised which uses this feature as predictive biomarkers for PARP inhibition.

More complex therapy strategies that use multiple agents to impair HR and other repair pathways have shown some promise. For example, preclinical and preliminary clinical evidence suggest a potentially broad scope of PARP inhibitors in combination with DNA-damaging agents (for review see (315,316)). In addition, *in vitro* studies on BRCA2-deficient cells showed synergistic effects for combinations of olaparib with alkylating agents (317). However, as the DNA-damaging agents used to target rapidly dividing cancer cells also affect other proliferating cells, the therapeutic window of the drug cocktail needs to be regulated to minimize toxicity in healthy cells. In addition, BRCA2-deficient cells were shown to gain resistance to PARP inhibitors due to acquired mutations in BRCA2 that restore its activity (318,319). These observations have implications for understanding drug resistance in BRCA mutation carriers (318). The recently observed synthetic lethality of RAD52 and BRCA2 deficient cells could provide a treatment strategy not only in BRCA2-defective tumours, but also in BRCA2 revertants that become treatment-resistant (208,318,319). It is clear that further research in this area will contribute to a better understanding of the processes underlying the maintenance of genomic integrity in eukaryotes, with implications for design of innovative treatment strategies.

Table 2 List of diseases linked or associated to either recombination mediators or its interacting partners, synthetic lethality interaction are also shown(291,292).

Gene	Syndrome/Disorder	Cancers	Synthetic lethality
BRCA1	-	Breast, prostate, ovarian cancer	PARP1
BRCA2	Fanconianemia (FANCD1)	Breast prostate, ovarian cancer	PARP1, RAD52
RAD54B	-	Colon cancer, Non-Hodgkin Lymphoma	PARP1, FEN1
RAD51B	-	Lipoma, uterine leiomyoma	PARP1
RAD51C	Fanconianemia (FANCO)	Breast, ovarian cancer	-
BLM	Bloom	-	-
WRN	Werner	-	-
RECQL4	Rothmund-Thomson	-	-
p53	Li-Fraumeni	Breast, pancreatic, lung cancer	-
FANCM	Fanconianemia (FANCM)	-	-
PALB2	Fanconianemia (FANCN)	Breast, pancreatic cancer	
Potential associations with diseases			
RAD51	-	Breast cancer in BRCA1 and BRCA2 carriers	-
DMC1	infertility		
XRCC2	-	Breast cancer	-
XRCC3	-	Basal cell carcinoma, Malignant melanoma, Bladder cancer, breast cancer	RAD52
RAD51D	-	Breast cancer	-
DSS1	Split hand/split foot malformation	Skin squamous cell carcinoma	-

References

1.   Jackson, S.P. and Bartek, J. (2009) The DNA-damage response in human biology and disease. *Nature*, **461**, 1071-1078.
2.   Paques, F. and Haber, J.E. (1999) Multiple pathways of recombination induced by double-strand breaks in Saccharomyces cerevisiae. *Microbiol Mol Biol Rev*, **63**, 349-404.
3.   Sung, P., Krejci, L., Van Komen, S. and Sehorn, M.G. (2003) Rad51 recombinase and recombination mediators. *J Biol Chem*, **278**, 42729-42732.
4.   Ogawa, T., Yu, X., Shinohara, A. and Egelman, E.H. (1993) Similarity of the yeast RAD51 filament to the bacterial RecA filament. *Science*, **259**, 1896-1899.
5.   Chen, Z., Yang, H. and Pavletich, N.P. (2008) Mechanism of homologous recombination from the RecA-ssDNA/dsDNA structures. *Nature*, **453**, 489-484.
6.   Klapstein, K., Chou, T. and Bruinsma, R. (2004) Physics of RecA-mediated homologous recognition. *Biophys J*, **87**, 1466-1477.
7.   Szostak, J.W., Orr-Weaver, T.L., Rothstein, R.J. and Stahl, F.W. (1983) The double-strand-break repair model for recombination. *Cell*, **33**, 25-35.
8.   Krogh, B.O. and Symington, L.S. (2004) Recombination proteins in yeast. *Annu Rev Genet*, **38**, 233-271.
9.   Nassif, N., Penney, J., Pal, S., Engels, W.R. and Gloor, G.B. (1994) Efficient copying of nonhomologous sequences from ectopic sites via P-element-induced gap repair. *Mol Cell Biol*, **14**, 1613-1625.
10.   Allers, T. and Lichten, M. (2001) Differential timing and control of noncrossover and crossover recombination during meiosis. *Cell*, **106**, 47-57.
11.   Hunter, N. and Kleckner, N. (2001) The single-end invasion: an asymmetric intermediate at the double-strand break to double-holliday junction transition of meiotic recombination. *Cell*, **106**, 59-70.
12.   Malkova, A., Ivanov, E.L. and Haber, J.E. (1996) Double-strand break repair in the absence of RAD51 in yeast: a possible role for break-induced DNA replication. *Proc Natl Acad Sci U S A*, **93**, 7131-7136.
13.   Lin, F.L., Sperle, K. and Sternberg, N. (1984) Model for homologous recombination during transfer of DNA into mouse L cells: role for DNA ends in the recombination process. *Mol Cell Biol*, **4**, 1020-1034.
14.   Heyer, W.D., Ehmsen, K.T. and Liu, J. (2010) Regulation of homologous recombination in eukaryotes. *Annu Rev Genet*, **44**, 113-139.
15.   San Filippo, J., Sung, P. and Klein, H. (2008) Mechanism of eukaryotic homologous recombination. *Annu Rev Biochem*, **77**, 229-257.
16.   Sung, P. and Klein, H. (2006) Mechanism of homologous recombination: mediators and helicases take on regulatory functions. *Nat Rev Mol Cell Biol*, **7**, 739-750.
17.   Sugiyama, T., Zaitseva, E.M. and Kowalczykowski, S.C. (1997) A single-stranded DNA-binding protein is needed for efficient presynaptic complex formation by the Saccharomyces cerevisiae Rad51 protein. *J Biol Chem*, **272**, 7940-7945.
18.   Sung, P. (1997) Function of yeast Rad52 protein as a mediator between replication protein A and the Rad51 recombinase. *J Biol Chem*, **272**, 28194-28197.
19.   Gasior, S.L., Wong, A.K., Kora, Y., Shinohara, A. and Bishop, D.K. (1998) Rad52 associates with RPA and functions with rad55 and rad57 to assemble meiotic recombination complexes. *Genes Dev*, **12**, 2208-2221.
20.   Lisby, M., Barlow, J.H., Burgess, R.C. and Rothstein, R. (2004) Choreography of the DNA damage response: spatiotemporal relationships among checkpoint and repair proteins. *Cell*, **118**, 699-713.
21.   Sugawara, N., Wang, X. and Haber, J.E. (2003) In vivo roles of Rad52, Rad54, and Rad55 proteins in Rad51-mediated recombination. *Mol Cell*, **12**, 209-219.

22. Wolner, B., van Komen, S., Sung, P. and Peterson, C.L. (2003) Recruitment of the recombinational repair machinery to a DNA double-strand break in yeast. *Mol Cell*, **12**, 221-232.
23. Kantake, N., Sugiyama, T., Kolodner, R.D. and Kowalczykowski, S.C. (2003) The recombination-deficient mutant RPA (rfa1-t11) is displaced slowly from single-stranded DNA by Rad51 protein. *J Biol Chem*, **278**, 23410-23417.
24. Eggler, A.L., Inman, R.B. and Cox, M.M. (2002) The Rad51-dependent pairing of long DNA substrates is stabilized by replication protein A. *J Biol Chem*, **277**, 39280-39288.
25. Van Komen, S., Petukhova, G., Sigurdsson, S. and Sung, P. (2002) Functional cross-talk among Rad51, Rad54, and replication protein A in heteroduplex DNA joint formation. *J Biol Chem*, **277**, 43578-43587.
26. Cejka, P., Cannavo, E., Polaczek, P., Masuda-Sasa, T., Pokharel, S., Campbell, J.L. and Kowalczykowski, S.C. (2010) DNA end resection by Dna2-Sgs1-RPA and its stimulation by Top3-Rmi1 and Mre11-Rad50-Xrs2. *Nature*, **467**, 112-116.
27. Niu, H., Chung, W.H., Zhu, Z., Kwon, Y., Zhao, W., Chi, P., Prakash, R., Seong, C., Liu, D., Lu, L. *et al.* (2010) Mechanism of the ATP-dependent DNA end-resection machinery from Saccharomyces cerevisiae. *Nature*, **467**, 108-111.
28. Ball, H.L., Ehrhardt, M.R., Mordes, D.A., Glick, G.G., Chazin, W.J. and Cortez, D. (2007) Function of a conserved checkpoint recruitment domain in ATRIP proteins. *Mol Cell Biol*, **27**, 3367-3377.
29. Choi, J.H., Lindsey-Boltz, L.A., Kemp, M., Mason, A.C., Wold, M.S. and Sancar, A. (2010) Reconstitution of RPA-covered single-stranded DNA-activated ATR-Chk1 signaling. *Proc Natl Acad Sci U S A*, **107**, 13660-13665.
30. Zou, L. and Elledge, S.J. (2003) Sensing DNA damage through ATRIP recognition of RPA-ssDNA complexes. *Science*, **300**, 1542-1548.
31. Seong, C., Sehorn, M.G., Plate, I., Shi, I., Song, B., Chi, P., Mortensen, U., Sung, P. and Krejci, L. (2008) Molecular anatomy of the recombination mediator function of Saccharomyces cerevisiae Rad52. *J Biol Chem*, **283**, 12166-12174.
32. Shinohara, A., Ogawa, H. and Ogawa, T. (1992) Rad51 protein involved in repair and recombination in S. cerevisiae is a RecA-like protein. *Cell*, **69**, 457-470.
33. Krejci, L., Song, B., Bussen, W., Rothstein, R., Mortensen, U.H. and Sung, P. (2002) Interaction with Rad51 is indispensable for recombination mediator function of Rad52. *J Biol Chem*, **277**, 40132-40141.
34. Shinohara, A. and Ogawa, T. (1998) Stimulation by Rad52 of yeast Rad51-mediated recombination. *Nature*, **391**, 404-407.
35. Song, B. and Sung, P. (2000) Functional interactions among yeast Rad51 recombinase, Rad52 mediator, and replication protein A in DNA strand exchange. *J Biol Chem*, **275**, 15895-15904.
36. Sugiyama, T., New, J.H. and Kowalczykowski, S.C. (1998) DNA annealing by RAD52 protein is stimulated by specific interaction with the complex of replication protein A and single-stranded DNA. *Proc Natl Acad Sci U S A*, **95**, 6049-6054.
37. Plate, I., Hallwyl, S.C., Shi, I., Krejci, L., Müller, C., Albertsen, L., Sung, P. and Mortensen, U.H. (2008) Interaction with RPA is necessary for Rad52 repair center formation and for its mediator activity. *J Biol Chem*, **283**, 29077-29085.
38. Davis, A.P. and Symington, L.S. (2001) The yeast recombinational repair protein Rad59 interacts with Rad52 and stimulates single-strand annealing. *Genetics*, **159**, 515-525.
39. Mortensen, U.H., Bendixen, C., Sunjevaric, I. and Rothstein, R. (1996) DNA strand annealing is promoted by the yeast Rad52 protein. *Proc Natl Acad Sci U S A*, **93**, 10729-10734.
40. McIlwraith, M.J. and West, S.C. (2008) DNA repair synthesis facilitates RAD52-mediated second-end capture during DSB repair. *Mol Cell*, **29**, 510-516.

41. Nimonkar, A.V., Sica, R.A. and Kowalczykowski, S.C. (2009) Rad52 promotes second-end DNA capture in double-stranded break repair to form complement-stabilized joint molecules. *Proc Natl Acad Sci U S A*, **106**, 3077-3082.
42. Mortensen, U.H., Erdeniz, N., Feng, Q. and Rothstein, R. (2002) A molecular genetic dissection of the evolutionarily conserved N terminus of yeast Rad52. *Genetics*, **161**, 549-562.
43. Shi, I., Hallwyl, S.C., Seong, C., Mortensen, U., Rothstein, R. and Sung, P. (2009) Role of the Rad52 amino-terminal DNA binding activity in DNA strand capture in homologous recombination. *J Biol Chem*, **284**, 33275-33284.
44. Hays, S.L., Firmenich, A.A. and Berg, P. (1995) Complex formation in yeast double-strand break repair: participation of Rad51, Rad52, Rad55, and Rad57 proteins. *Proc Natl Acad Sci U S A*, **92**, 6925-6929.
45. Johnson, R.D. and Symington, L.S. (1995) Functional differences and interactions among the putative RecA homologs Rad51, Rad55, and Rad57. *Mol Cell Biol*, **15**, 4843-4850.
46. Sung, P. (1997) Yeast Rad55 and Rad57 proteins form a heterodimer that functions with replication protein A to promote DNA strand exchange by Rad51 recombinase. *Genes Dev*, **11**, 1111-1121.
47. Liu, J., Renault, L., Veaute, X., Fabre, F., Stahlberg, H. and Heyer, W.D. (2011) Rad51 paralogues Rad55-Rad57 balance the antirecombinase Srs2 in Rad51 filament formation. *Nature*, **479**, 245-248.
48. Fortin, G.S. and Symington, L.S. (2002) Mutations in yeast Rad51 that partially bypass the requirement for Rad55 and Rad57 in DNA repair by increasing the stability of Rad51-DNA complexes. *EMBO J*, **21**, 3160-3170.
49. Fung, C.W., Mozlin, A.M. and Symington, L.S. (2009) Suppression of the double-strand-break-repair defect of the Saccharomyces cerevisiae rad57 mutant. *Genetics*, **181**, 1195-1206.
50. Malik, P.S. and Symington, L.S. (2008) Rad51 gain-of-function mutants that exhibit high affinity DNA binding cause DNA damage sensitivity in the absence of Srs2. *Nucleic Acids Res*, **36**, 6504-6510.
51. Mozlin, A.M., Fung, C.W. and Symington, L.S. (2008) Role of the Saccharomyces cerevisiae Rad51 paralogs in sister chromatid recombination. *Genetics*, **178**, 113-126.
52. Braybrooke, J.P., Spink, K.G., Thacker, J. and Hickson, I.D. (2000) The RAD51 family member, RAD51L3, is a DNA-stimulated ATPase that forms a complex with XRCC2. *J Biol Chem*, **275**, 29100-29106.
53. Martín, V., Chahwan, C., Gao, H., Blais, V., Wohlschlegel, J., Yates, J.R., McGowan, C.H. and Russell, P. (2006) Sws1 is a conserved regulator of homologous recombination in eukaryotic cells. *EMBO J*, **25**, 2564-2574.
54. Mankouri, H.W., Ngo, H.P. and Hickson, I.D. (2007) Shu proteins promote the formation of homologous recombination intermediates that are processed by Sgs1-Rmi1-Top3. *Mol Biol Cell*, **18**, 4062-4073.
55. Shor, E., Weinstein, J. and Rothstein, R. (2005) A genetic screen for top3 suppressors in Saccharomyces cerevisiae identifies SHU1, SHU2, PSY3 and CSM2: four genes involved in error-free DNA repair. *Genetics*, **169**, 1275-1289.
56. Ball, L.G., Zhang, K., Cobb, J.A., Boone, C. and Xiao, W. (2009) The yeast Shu complex couples error-free post-replication repair to homologous recombination. *Mol Microbiol*, **73**, 89-102.
57. Choi, K., Szakal, B., Chen, Y.H., Branzei, D. and Zhao, X. (2010) The Smc5/6 complex and Esc2 influence multiple replication-associated recombination processes in Saccharomyces cerevisiae. *Mol Biol Cell*, **21**, 2306-2314.
58. Huang, M.E., Rio, A.G., Nicolas, A. and Kolodner, R.D. (2003) A genomewide screen in Saccharomyces cerevisiae for genes that suppress the accumulation of mutations. *Proc Natl Acad Sci U S A*, **100**, 11529-11534.

59. Bernstein, K.A., Reid, R.J., Sunjevaric, I., Demuth, K., Burgess, R.C. and Rothstein, R. (2011) The Shu complex, which contains Rad51 paralogues, promotes DNA repair through inhibition of the Srs2 anti-recombinase. *Mol Biol Cell*, **22**, 1599-1607.

60. Mazin, A.V., Mazina, O.M., Bugreev, D.V. and Rossi, M.J. (2010) Rad54, the motor of homologous recombination. *DNA Repair (Amst)*, **9**, 286-302.

61. Alexeev, A., Mazin, A. and Kowalczykowski, S.C. (2003) Rad54 protein possesses chromatin-remodeling activity stimulated by the Rad51-ssDNA nucleoprotein filament. *Nat Struct Biol*, **10**, 182-186.

62. Alexiadis, V. and Kadonaga, J.T. (2002) Strand pairing by Rad54 and Rad51 is enhanced by chromatin. *Genes Dev*, **16**, 2767-2771.

63. Jaskelioff, M., Van Komen, S., Krebs, J.E., Sung, P. and Peterson, C.L. (2003) Rad54p is a chromatin remodeling enzyme required for heteroduplex DNA joint formation with chromatin. *J Biol Chem*, **278**, 9212-9218.

64. Kwon, Y., Seong, C., Chi, P., Greene, E.C., Klein, H. and Sung, P. (2008) ATP-dependent chromatin remodeling by the Saccharomyces cerevisiae homologous recombination factor Rdh54. *J Biol Chem*, **283**, 10445-10452.

65. Chi, P., Kwon, Y., Seong, C., Epshtein, A., Lam, I., Sung, P. and Klein, H.L. (2006) Yeast recombination factor Rdh54 functionally interacts with the Rad51 recombinase and catalyzes Rad51 removal from DNA. *J Biol Chem*, **281**, 26268-26279.

66. Heyer, W.D., Li, X., Rolfsmeier, M. and Zhang, X.P. (2006) Rad54: the Swiss Army knife of homologous recombination? *Nucleic Acids Res*, **34**, 4115-4125.

67. Li, X. and Heyer, W.D. (2009) RAD54 controls access to the invading 3'-OH end after RAD51-mediated DNA strand invasion in homologous recombination in Saccharomyces cerevisiae. *Nucleic Acids Res*, **37**, 638-646.

68. Solinger, J.A., Kiianitsa, K. and Heyer, W.D. (2002) Rad54, a Swi2/Snf2-like recombinational repair protein, disassembles Rad51:dsDNA filaments. *Mol Cell*, **10**, 1175-1188.

69. Shah, P.P., Zheng, X., Epshtein, A., Carey, J.N., Bishop, D.K. and Klein, H.L. (2010) Swi2/Snf2-related translocases prevent accumulation of toxic Rad51 complexes during mitotic growth. *Mol Cell*, **39**, 862-872.

70. Cal-Bakowska, M., Litwin, I., Bocer, T., Wysocki, R. and Dziadkowiec, D. (2011) The Swi2-Snf2-like protein Uls1 is involved in replication stress response. *Nucleic Acids Res*.

71. Uzunova, K., Göttsche, K., Miteva, M., Weisshaar, S.R., Glanemann, C., Schnellhardt, M., Niessen, M., Scheel, H., Hofmann, K., Johnson, E.S. *et al.* (2007) Ubiquitin-dependent proteolytic control of SUMO conjugates. *J Biol Chem*, **282**, 34167-34175.

72. Branzei, D. and Foiani, M. (2009) The checkpoint response to replication stress. *DNA Repair (Amst)*, **8**, 1038-1046.

73. Gangloff, S., Soustelle, C. and Fabre, F. (2000) Homologous recombination is responsible for cell death in the absence of the Sgs1 and Srs2 helicases. *Nat Genet*, **25**, 192-194.

74. Pellicioli, A., Lee, S.E., Lucca, C., Foiani, M. and Haber, J.E. (2001) Regulation of Saccharomyces Rad53 checkpoint kinase during adaptation from DNA damage-induced G2/M arrest. *Mol Cell*, **7**, 293-300.

75. Marini, V. and Krejci, L. (2010) Srs2: the "Odd-Job Man" in DNA repair. *DNA Repair (Amst)*, **9**, 268-275.

76. Krejci, L., Van Komen, S., Li, Y., Villemain, J., Reddy, M.S., Klein, H., Ellenberger, T. and Sung, P. (2003) DNA helicase Srs2 disrupts the Rad51 presynaptic filament. *Nature*, **423**, 305-309.

77. Veaute, X., Jeusset, J., Soustelle, C., Kowalczykowski, S.C., Le Cam, E. and Fabre, F. (2003) The Srs2 helicase prevents recombination by disrupting Rad51 nucleoprotein filaments. *Nature*, **423**, 309-312.

78. Colavito, S., Macris-Kiss, M., Seong, C., Gleeson, O., Greene, E.C., Klein, H.L., Krejci, L. and Sung, P. (2009) Functional significance of the Rad51-Srs2 complex in Rad51 presynaptic filament disruption. *Nucleic Acids Res*, **37**, 6754-6764.

79. Krejci, L., Macris, M., Li, Y., Van Komen, S., Villemain, J., Ellenberger, T., Klein, H. and Sung, P. (2004) Role of ATP hydrolysis in the antirecombinase function of Saccharomyces cerevisiae Srs2 protein. *J Biol Chem*, **279**, 23193-23199.

80. Seong, C., Colavito, S., Kwon, Y., Sung, P. and Krejci, L. (2009) Regulation of Rad51 recombinase presynaptic filament assembly via interactions with the Rad52 mediator and the Srs2 anti-recombinase. *J Biol Chem*, **284**, 24363-24371.

81. Antony, E., Tomko, E.J., Xiao, Q., Krejci, L., Lohman, T.M. and Ellenberger, T. (2009) Srs2 disassembles Rad51 filaments by a protein-protein interaction triggering ATP turnover and dissociation of Rad51 from DNA. *Mol Cell*, **35**, 105-115.

82. Bugreev, D.V., Yu, X., Egelman, E.H. and Mazin, A.V. (2007) Novel pro- and anti-recombination activities of the Bloom's syndrome helicase. *Genes Dev*, **21**, 3085-3094.

83. Hu, Y., Raynard, S., Sehorn, M.G., Lu, X., Bussen, W., Zheng, L., Stark, J.M., Barnes, E.L., Chi, P., Janscak, P. *et al.* (2007) RECQL5/Recql5 helicase regulates homologous recombination and suppresses tumor formation via disruption of Rad51 presynaptic filaments. *Genes Dev*, **21**, 3073-3084.

84. Sommers, J.A., Rawtani, N., Gupta, R., Bugreev, D.V., Mazin, A.V., Cantor, S.B. and Brosh, R.M. (2009) FANCJ uses its motor ATPase to destabilize protein-DNA complexes, unwind triplexes, and inhibit RAD51 strand exchange. *J Biol Chem*, **284**, 7505-7517.

85. Chiolo, I., Saponaro, M., Baryshnikova, A., Kim, J.H., Seo, Y.S. and Liberi, G. (2007) The human F-Box DNA helicase FBH1 faces Saccharomyces cerevisiae Srs2 and postreplication repair pathway roles. *Mol Cell Biol*, **27**, 7439-7450.

86. Fugger, K., Mistrik, M., Danielsen, J.R., Dinant, C., Falck, J., Bartek, J., Lukas, J. and Mailand, N. (2009) Human Fbh1 helicase contributes to genome maintenance via pro- and anti-recombinase activities. *J Cell Biol*, **186**, 655-663.

87. Lorenz, A., Osman, F., Folkyte, V., Sofueva, S. and Whitby, M.C. (2009) Fbh1 limits Rad51-dependent recombination at blocked replication forks. *Mol Cell Biol*, **29**, 4742-4756.

88. Moldovan, G.L., Dejsuphong, D., Petalcorin, M.I., Hofmann, K., Takeda, S., Boulton, S.J. and D'Andrea, A.D. (2011) Inhibition of Homologous Recombination by the PCNA-Interacting Protein PARI. *Mol Cell*.

89. Morishita, T., Furukawa, F., Sakaguchi, C., Toda, T., Carr, A.M., Iwasaki, H. and Shinagawa, H. (2005) Role of the Schizosaccharomyces pombe F-Box DNA helicase in processing recombination intermediates. *Mol Cell Biol*, **25**, 8074-8083.

90. Osman, F., Dixon, J., Barr, A.R. and Whitby, M.C. (2005) The F-Box DNA helicase Fbh1 prevents Rhp51-dependent recombination without mediator proteins. *Mol Cell Biol*, **25**, 8084-8096.

91. Gari, K., Decaillet, C., Stasiak, A.Z., Stasiak, A. and Constantinou, A. (2008) The Fanconi anemia protein FANCM can promote branch migration of Holliday junctions and replication forks. *Mol Cell*, **29**, 141-148.

92. Prakash, R., Satory, D., Dray, E., Papusha, A., Scheller, J., Kramer, W., Krejci, L., Klein, H., Haber, J.E., Sung, P. *et al.* (2009) Yeast Mph1 helicase dissociates Rad51-made D-loops: implications for crossover control in mitotic recombination. *Genes Dev*, **23**, 67-79.

93. Sun, W., Nandi, S., Osman, F., Ahn, J.S., Jakovleska, J., Lorenz, A. and Whitby, M.C. (2008) The FANCM ortholog Fml1 promotes recombination at stalled replication forks and limits crossing over during DNA double-strand break repair. *Mol Cell*, **32**, 118-128.

94. Zheng, X.F., Prakash, R., Saro, D., Longerich, S., Niu, H. and Sung, P. (2011) Processing of DNA structures via DNA unwinding and branch migration by the S. cerevisiae Mph1 protein. *DNA Repair (Amst)*, **10**, 1034-1043.

95. Sebesta, M., Burkovics, P., Haracska, L. and Krejci, L. (2011) Reconstitution of DNA repair synthesis in vitro and the role of polymerase and helicase activities. *DNA Repair (Amst)*, **10**, 567-576.

96. Singh, T.R., Saro, D., Ali, A.M., Zheng, X.F., Du, C.H., Killen, M.W., Sachpatzidis, A., Wahengbam, K., Pierce, A.J., Xiong, Y. *et al.* (2010) MHF1-MHF2, a histone-fold-containing protein complex, participates in the Fanconi anemia pathway via FANCM. *Mol Cell*, **37**, 879-886.

97. Wang, R.C., Smogorzewska, A. and de Lange, T. (2004) Homologous recombination generates T-loop-sized deletions at human telomeres. *Cell*, **119**, 355-368.

98. Barber, L.J., Youds, J.L., Ward, J.D., McIlwraith, M.J., O'Neil, N.J., Petalcorin, M.I., Martin, J.S., Collis, S.J., Cantor, S.B., Auclair, M. *et al.* (2008) RTEL1 maintains genomic stability by suppressing homologous recombination. *Cell*, **135**, 261-271.

99. Uringa, E.J., Youds, J.L., Lisaingo, K., Lansdorp, P.M. and Boulton, S.J. (2011) RTEL1: an essential helicase for telomere maintenance and the regulation of homologous recombination. *Nucleic Acids Res*, **39**, 1647-1655.

100. Ahmad, F. and Stewart, E. (2005) The N-terminal region of the Schizosaccharomyces pombe RecQ helicase, Rqh1p, physically interacts with Topoisomerase III and is required for Rqh1p function. *Mol Genet Genomics*, **273**, 102-114.

101. Chang, M., Bellaoui, M., Zhang, C., Desai, R., Morozov, P., Delgado-Cruzata, L., Rothstein, R., Freyer, G.A., Boone, C. and Brown, G.W. (2005) RMI1/NCE4, a suppressor of genome instability, encodes a member of the RecQ helicase/Topo III complex. *EMBO J*, **24**, 2024-2033.

102. Ira, G., Malkova, A., Liberi, G., Foiani, M. and Haber, J.E. (2003) Srs2 and Sgs1-Top3 suppress crossovers during double-strand break repair in yeast. *Cell*, **115**, 401-411.

103. Mankouri, H.W., Craig, T.J. and Morgan, A. (2002) SGS1 is a multicopy suppressor of srs2: functional overlap between DNA helicases. *Nucleic Acids Res*, **30**, 1103-1113.

104. Oh, S.D., Lao, J.P., Hwang, P.Y., Taylor, A.F., Smith, G.R. and Hunter, N. (2007) BLM ortholog, Sgs1, prevents aberrant crossing-over by suppressing formation of multichromatid joint molecules. *Cell*, **130**, 259-272.

105. Oh, S.D., Lao, J.P., Taylor, A.F., Smith, G.R. and Hunter, N. (2008) RecQ helicase, Sgs1, and XPF family endonuclease, Mus81-Mms4, resolve aberrant joint molecules during meiotic recombination. *Mol Cell*, **31**, 324-336.

106. Cejka, P., Plank, J.L., Bachrati, C.Z., Hickson, I.D. and Kowalczykowski, S.C. (2010) Rmi1 stimulates decatenation of double Holliday junctions during dissolution by Sgs1-Top3. *Nat Struct Mol Biol*, **17**, 1377-1382.

107. Wu, L. and Hickson, I.D. (2003) The Bloom's syndrome helicase suppresses crossing over during homologous recombination. *Nature*, **426**, 870-874.

108. Adams, M.D., McVey, M. and Sekelsky, J.J. (2003) Drosophila BLM in double-strand break repair by synthesis-dependent strand annealing. *Science*, **299**, 265-267.

109. McVey, M., Larocque, J.R., Adams, M.D. and Sekelsky, J.J. (2004) Formation of deletions during double-strand break repair in Drosophila DmBlm mutants occurs after strand invasion. *Proc Natl Acad Sci U S A*, **101**, 15694-15699.

110. Liberi, G., Maffioletti, G., Lucca, C., Chiolo, I., Baryshnikova, A., Cotta-Ramusino, C., Lopes, M., Pellicioli, A., Haber, J.E. and Foiani, M. (2005) Rad51-dependent DNA structures accumulate at damaged replication forks in sgs1 mutants defective in the yeast ortholog of BLM RecQ helicase. *Genes Dev*, **19**, 339-350.

111. Rockmill, B., Fung, J.C., Branda, S.S. and Roeder, G.S. (2003) The Sgs1 helicase regulates chromosome synapsis and meiotic crossing over. *Curr Biol*, **13**, 1954-1962.
112. Mimitou, E.P. and Symington, L.S. (2008) Sae2, Exo1 and Sgs1 collaborate in DNA double-strand break processing. *Nature*, **455**, 770-774.
113. Ashton, T.M. and Hickson, I.D. (2010) Yeast as a model system to study RecQ helicase function. *DNA Repair (Amst)*, **9**, 303-314.
114. Ward, J.D., Muzzini, D.M., Petalcorin, M.I., Martinez-Perez, E., Martin, J.S., Plevani, P., Cassata, G., Marini, F. and Boulton, S.J. (2010) Overlapping mechanisms promote postsynaptic RAD-51 filament disassembly during meiotic double-strand break repair. *Mol Cell*, **37**, 259-272.
115. Branzei, D., Sollier, J., Liberi, G., Zhao, X., Maeda, D., Seki, M., Enomoto, T., Ohta, K. and Foiani, M. (2006) Ubc9- and mms21-mediated sumoylation counteracts recombinogenic events at damaged replication forks. *Cell*, **127**, 509-522.
116. Maeda, D., Seki, M., Onoda, F., Branzei, D., Kawabe, Y. and Enomoto, T. (2004) Ubc9 is required for damage-tolerance and damage-induced interchromosomal homologous recombination in S. cerevisiae. *DNA Repair (Amst)*, **3**, 335-341.
117. Soustelle, C., Vernis, L., Fréon, K., Reynaud-Angelin, A., Chanet, R., Fabre, F. and Heude, M. (2004) A new Saccharomyces cerevisiae strain with a mutant Smt3-deconjugating Ulp1 protein is affected in DNA replication and requires Srs2 and homologous recombination for its viability. *Mol Cell Biol*, **24**, 5130-5143.
118. Zhao, X. and Blobel, G. (2005) A SUMO ligase is part of a nuclear multiprotein complex that affects DNA repair and chromosomal organization. *Proc Natl Acad Sci U S A*, **102**, 4777-4782.
119. Burgess, R.C., Rahman, S., Lisby, M., Rothstein, R. and Zhao, X. (2007) The Slx5-Slx8 complex affects sumoylation of DNA repair proteins and negatively regulates recombination. *Mol Cell Biol*, **27**, 6153-6162.
120. Dou, H., Huang, C., Singh, M., Carpenter, P.B. and Yeh, E.T. (2010) Regulation of DNA repair through deSUMOylation and SUMOylation of replication protein A complex. *Mol Cell*, **39**, 333-345.
121. Galanty, Y., Belotserkovskaya, R., Coates, J., Polo, S., Miller, K.M. and Jackson, S.P. (2009) Mammalian SUMO E3-ligases PIAS1 and PIAS4 promote responses to DNA double-strand breaks. *Nature*, **462**, 935-939.
122. Morris, J.R., Boutell, C., Keppler, M., Densham, R., Weekes, D., Alamshah, A., Butler, L., Galanty, Y., Pangon, L., Kiuchi, T. *et al.* (2009) The SUMO modification pathway is involved in the BRCA1 response to genotoxic stress. *Nature*, **462**, 886-890.
123. Shi, W., Feng, Z., Zhang, J., Gonzalez-Suarez, I., Vanderwaal, R.P., Wu, X., Powell, S.N., Roti Roti, J.L. and Gonzalo, S. (2010) The role of RPA2 phosphorylation in homologous recombination in response to replication arrest. *Carcinogenesis*, **31**, 994-1002.
124. Deng, X., Prakash, A., Dhar, K., Baia, G.S., Kolar, C., Oakley, G.G. and Borgstahl, G.E. (2009) Human replication protein A-Rad52-single-stranded DNA complex: stoichiometry and evidence for strand transfer regulation by phosphorylation. *Biochemistry*, **48**, 6633-6643.
125. Barlow, J.H. and Rothstein, R. (2009) Rad52 recruitment is DNA replication independent and regulated by Cdc28 and the Mec1 kinase. *EMBO J*, **28**, 1121-1130.
126. Barlow, J.H. and Rothstein, R. (2010) Timing is everything: cell cycle control of Rad52. *Cell Div*, **5**, 7.
127. Lee, D.H., Pan, Y., Kanner, S., Sung, P., Borowiec, J.A. and Chowdhury, D. (2010) A PP4 phosphatase complex dephosphorylates RPA2 to facilitate DNA repair via homologous recombination. *Nat Struct Mol Biol*, **17**, 365-372.
128. Kovalenko, O.V., Plug, A.W., Haaf, T., Gonda, D.K., Ashley, T., Ward, D.C., Radding, C.M. and Golub, E.I. (1996) Mammalian ubiquitin-conjugating enzyme Ubc9

interacts with Rad51 recombination protein and localizes in synaptonemal complexes. *Proc Natl Acad Sci U S A*, **93**, 2958-2963.

129. Shen, Z., Pardington-Purtymun, P.E., Comeaux, J.C., Moyzis, R.K. and Chen, D.J. (1996) UBL1, a human ubiquitin-like protein associating with human RAD51/RAD52 proteins. *Genomics*, **36**, 271-279.

130. Saitoh, H., Pizzi, M.D. and Wang, J. (2002) Perturbation of SUMOlation enzyme Ubc9 by distinct domain within nucleoporin RanBP2/Nup358. *J Biol Chem*, **277**, 4755-4763.

131. Slupianek, A., Dasgupta, Y., Ren, S.Y., Gurdek, E., Donlin, M., Nieborowska-Skorska, M., Fleury, F. and Skorski, T. (2011) Targeting RAD51 phosphotyrosine-315 to prevent unfaithful recombination repair in BCR-ABL1 leukemia. *Blood*.

132. Yuan, Z.M., Huang, Y., Ishiko, T., Nakada, S., Utsugisawa, T., Kharbanda, S., Wang, R., Sung, P., Shinohara, A., Weichselbaum, R. *et al.* (1998) Regulation of Rad51 function by c-Abl in response to DNA damage. *J Biol Chem*, **273**, 3799-3802.

133. Flott, S., Kwon, Y., Pigli, Y.Z., Rice, P.A., Sung, P. and Jackson, S.P. (2011) Regulation of Rad51 function by phosphorylation. *EMBO Rep*, **12**, 833-839.

134. Yata, K., Lloyd, J., Maslen, S., Bleuyard, J.Y., Skehel, M., Smerdon, S.J. and Esashi, F. (2012) Plk1 and CK2 Act in Concert to Regulate Rad51 during DNA Double Strand Break Repair. *Mol Cell*, **45**, 371-383.

135. Bashkirov, V.I., King, J.S., Bashkirova, E.V., Schmuckli-Maurer, J. and Heyer, W.D. (2000) DNA repair protein Rad55 is a terminal substrate of the DNA damage checkpoints. *Mol Cell Biol*, **20**, 4393-4404.

136. Herzberg, K., Bashkirov, V.I., Rolfsmeier, M., Haghnazari, E., McDonald, W.H., Anderson, S., Bashkirova, E.V., Yates, J.R. and Heyer, W.D. (2006) Phosphorylation of Rad55 on serines 2, 8, and 14 is required for efficient homologous recombination in the recovery of stalled replication forks. *Mol Cell Biol*, **26**, 8396-8409.

137. Ho, J.C., Warr, N.J., Shimizu, H. and Watts, F.Z. (2001) SUMO modification of Rad22, the Schizosaccharomyces pombe homologue of the recombination protein Rad52. *Nucleic Acids Res*, **29**, 4179-4186.

138. Sacher, M., Pfander, B., Hoege, C. and Jentsch, S. (2006) Control of Rad52 recombination activity by double-strand break-induced SUMO modification. *Nat Cell Biol*, **8**, 1284-1290.

139. Ohuchi, T., Seki, M., Branzei, D., Maeda, D., Ui, A., Ogiwara, H., Tada, S. and Enomoto, T. (2008) Rad52 sumoylation and its involvement in the efficient induction of homologous recombination. *DNA Repair (Amst)*, **7**, 879-889.

140. Ohuchi, T., Seki, M., Kugou, K., Tada, S., Ohta, K. and Enomoto, T. (2009) Accumulation of sumoylated Rad52 in checkpoint mutants perturbed in DNA replication. *DNA Repair (Amst)*, **8**, 690-696.

141. Altmannova, V., Eckert-Boulet, N., Arneric, M., Kolesar, P., Chaloupkova, R., Damborsky, J., Sung, P., Zhao, X., Lisby, M. and Krejci, L. (2010) Rad52 SUMOylation affects the efficiency of the DNA repair. *Nucleic Acids Res*, **38**, 4708-4721.

142. Torres-Rosell, J., Sunjevaric, I., De Piccoli, G., Sacher, M., Eckert-Boulet, N., Reid, R., Jentsch, S., Rothstein, R., Aragón, L. and Lisby, M. (2007) The Smc5-Smc6 complex and SUMO modification of Rad52 regulates recombinational repair at the ribosomal gene locus. *Nat Cell Biol*, **9**, 923-931.

143. Saito, K., Kagawa, W., Suzuki, T., Suzuki, H., Yokoyama, S., Saitoh, H., Tashiro, S., Dohmae, N. and Kurumizaka, H. (2010) The putative nuclear localization signal of the human RAD52 protein is a potential sumoylation site. *J Biochem*, **147**, 833-842.

144. Antúnez de Mayolo, A., Lisby, M., Erdeniz, N., Thybo, T., Mortensen, U.H. and Rothstein, R. (2006) Multiple start codons and phosphorylation result in discrete Rad52 protein species. *Nucleic Acids Res*, **34**, 2587-2597.

145. Kitao, H. and Yuan, Z.M. (2002) Regulation of ionizing radiation-induced Rad52 nuclear foci formation by c-Abl-mediated phosphorylation. *J Biol Chem*, **277**, 48944-48948.

146. Honda, M., Okuno, Y., Yoo, J., Ha, T. and Spies, M. (2011) Tyrosine phosphorylation enhances RAD52-mediated annealing by modulating its DNA binding. *EMBO J*, **30**, 3368-3382.

147. Saponaro, M., Callahan, D., Zheng, X., Krejci, L., Haber, J.E., Klein, H.L. and Liberi, G. (2010) Cdk1 targets Srs2 to complete synthesis-dependent strand annealing and to promote recombinational repair. *PLoS Genet*, **6**, e1000858.

148. Hishida, T., Hirade, Y., Haruta, N., Kubota, Y. and Iwasaki, H. (2010) Srs2 plays a critical role in reversible G2 arrest upon chronic and low doses of UV irradiation via two distinct homologous recombination-dependent mechanisms in postreplication repair-deficient cells. *Mol Cell Biol*, **30**, 4840-4850.

149. Papouli, E., Chen, S., Davies, A.A., Huttner, D., Krejci, L., Sung, P. and Ulrich, H.D. (2005) Crosstalk between SUMO and ubiquitin on PCNA is mediated by recruitment of the helicase Srs2p. *Mol Cell*, **19**, 123-133.

150. Pfander, B., Moldovan, G.L., Sacher, M., Hoege, C. and Jentsch, S. (2005) SUMO-modified PCNA recruits Srs2 to prevent recombination during S phase. *Nature*, **436**, 428-433.

151. Eladad, S., Ye, T.Z., Hu, P., Leversha, M., Beresten, S., Matunis, M.J. and Ellis, N.A. (2005) Intra-nuclear trafficking of the BLM helicase to DNA damage-induced foci is regulated by SUMO modification. *Hum Mol Genet*, **14**, 1351-1365.

152. Lu, C.Y., Tsai, C.H., Brill, S.J. and Teng, S.C. (2010) Sumoylation of the BLM ortholog, Sgs1, promotes telomere-telomere recombination in budding yeast. *Nucleic Acids Res*, **38**, 488-498.

153. Ouyang, K.J., Woo, L.L., Zhu, J., Huo, D., Matunis, M.J. and Ellis, N.A. (2009) SUMO modification regulates BLM and RAD51 interaction at damaged replication forks. *PLoS Biol*, **7**, e1000252.

154. Kawabe, Y., Seki, M., Seki, T., Wang, W.S., Imamura, O., Furuichi, Y., Saitoh, H. and Enomoto, T. (2000) Covalent modification of the Werner's syndrome gene product with the ubiquitin-related protein, SUMO-1. *J Biol Chem*, **275**, 20963-20966.

155. Woods, Y.L., Xirodimas, D.P., Prescott, A.R., Sparks, A., Lane, D.P. and Saville, M.K. (2004) p14 Arf promotes small ubiquitin-like modifier conjugation of Werners helicase. *J Biol Chem*, **279**, 50157-50166.

156. Trickey, M., Grimaldi, M. and Yamano, H. (2008) The anaphase-promoting complex/cyclosome controls repair and recombination by ubiquitylating Rhp54 in fission yeast. *Mol Cell Biol*, **28**, 3905-3916.

157. Niu, H., Wan, L., Busygina, V., Kwon, Y., Allen, J.A., Li, X., Kunz, R.C., Kubota, K., Wang, B., Sung, P. *et al.* (2009) Regulation of meiotic recombination via Mek1-mediated Rad54 phosphorylation. *Mol Cell*, **36**, 393-404.

158. Chen, S.H., Albuquerque, C.P., Liang, J., Suhandynata, R.T. and Zhou, H. (2010) A proteome-wide analysis of kinase-substrate network in the DNA damage response. *J Biol Chem*, **285**, 12803-12812.

159. Cremona, C.A., Sarangi, P., Yang, Y., Hang, L.E., Rahman, S. and Zhao, X. (2012) Extensive DNA Damage-Induced Sumoylation Contributes to Replication and Repair and Acts in Addition to the Mec1 Checkpoint. *Mol Cell*.

160. Chu, W.K. and Hickson, I.D. (2009) RecQ helicases: multifunctional genome caretakers. *Nat Rev Cancer*, **9**, 644-654.

161. Knoll, A. and Puchta, H. (2011) The role of DNA helicases and their interaction partners in genome stability and meiotic recombination in plants. *J Exp Bot*, **62**, 1565-1579.

162. Lu, X., Lou, H. and Luo, G. (2011) A Blm-Recql5 partnership in replication stress response. *J Mol Cell Biol*, **3**, 31-38.

163. Rossi, M.L., Ghosh, A.K. and Bohr, V.A. (2010) Roles of Werner syndrome protein in protection of genome integrity. *DNA Repair (Amst)*, **9**, 331-344.
164. Unk, I., Hajdú, I., Blastyák, A. and Haracska, L. (2010) Role of yeast Rad5 and its human orthologs, HLTF and SHPRH in DNA damage tolerance. *DNA Repair (Amst)*, **9**, 257-267.
165. Whitby, M.C. (2010) The FANCM family of DNA helicases/translocases. *DNA Repair (Amst)*, **9**, 224-236.
166. Dudás, A. and Chovanec, M. (2004) DNA double-strand break repair by homologous recombination. *Mutat Res*, **566**, 131-167.
167. Lim, D.S. and Hasty, P. (1996) A mutation in mouse rad51 results in an early embryonic lethal that is suppressed by a mutation in p53. *Mol Cell Biol*, **16**, 7133-7143.
168. Sonoda, E., Sasaki, M.S., Buerstedde, J.M., Bezzubova, O., Shinohara, A., Ogawa, H., Takata, M., Yamaguchi-Iwai, Y. and Takeda, S. (1998) Rad51-deficient vertebrate cells accumulate chromosomal breaks prior to cell death. *EMBO J*, **17**, 598-608.
169. Tsuzuki, T., Fujii, Y., Sakumi, K., Tominaga, Y., Nakao, K., Sekiguchi, M., Matsushiro, A., Yoshimura, Y. and MoritaT. (1996) Targeted disruption of the Rad51 gene leads to lethality in embryonic mice. *Proc Natl Acad Sci U S A*, **93**, 6236-6240.
170. Sage, J.M., Gildemeister, O.S. and Knight, K.L. (2010) Discovery of a novel function for human Rad51: maintenance of the mitochondrial genome. *J Biol Chem*, **285**, 18984-18990.
171. Richard, D.J., Bolderson, E., Cubeddu, L., Wadsworth, R.I., Savage, K., Sharma, G.G., Nicolette, M.L., Tsvetanov, S., McIlwraith, M.J., Pandita, R.K. *et al.* (2008) Single-stranded DNA-binding protein hSSB1 is critical for genomic stability. *Nature*, **453**, 677-681.
172. Huang, J., Gong, Z., Ghosal, G. and Chen, J. (2009) SOSS complexes participate in the maintenance of genomic stability. *Mol Cell*, **35**, 384-393.
173. Li, Y., Bolderson, E., Kumar, R., Muniandy, P.A., Xue, Y., Richard, D.J., Seidman, M., Pandita, T.K., Khanna, K.K. and Wang, W. (2009) HSSB1 and hSSB2 form similar multiprotein complexes that participate in DNA damage response. *J Biol Chem*, **284**, 23525-23531.
174. Richard, D.J., Cubeddu, L., Urquhart, A.J., Bain, A., Bolderson, E., Menon, D., White, M.F. and Khanna, K.K. (2011) hSSB1 interacts directly with the MRN complex stimulating its recruitment to DNA double-strand breaks and its endo-nuclease activity. *Nucleic Acids Res*, **39**, 3643-3651.
175. Richard, D.J., Savage, K., Bolderson, E., Cubeddu, L., So, S., Ghita, M., Chen, D.J., White, M.F., Richard, K., Prise, K.M. *et al.* (2011) hSSB1 rapidly binds at the sites of DNA double-strand breaks and is required for the efficient recruitment of the MRN complex. *Nucleic Acids Res*, **39**, 1692-1702.
176. Thorslund, T. and West, S.C. (2007) BRCA2: a universal recombinase regulator. *Oncogene*, **26**, 7720-7730.
177. Yang, H., Jeffrey, P.D., Miller, J., Kinnucan, E., Sun, Y., Thoma, N.H., Zheng, N., Chen, P.L., Lee, W.H. and Pavletich, N.P. (2002) BRCA2 function in DNA binding and recombination from a BRCA2-DSS1-ssDNA structure. *Science*, **297**, 1837-1848.
178. Saeki, H., Siaud, N., Christ, N., Wiegant, W.W., van Buul, P.P., Han, M., Zdzienicka, M.Z., Stark, J.M. and Jasin, M. (2006) Suppression of the DNA repair defects of BRCA2-deficient cells with heterologous protein fusions. *Proc Natl Acad Sci U S A*, **103**, 8768-8773.
179. Holloman, W.K. (2011) Unraveling the mechanism of BRCA2 in homologous recombination. *Nat Struct Mol Biol*, **18**, 748-754.
180. Holloman, W.K., Schirawski, J. and Holliday, R. (2008) The homologous recombination system of Ustilago maydis. *Fungal Genet Biol*, **45 Suppl 1**, S31-39.
181. Jensen, R.B., Carreira, A. and Kowalczykowski, S.C. (2010) Purified human BRCA2 stimulates RAD51-mediated recombination. *Nature*, **467**, 678-683.

182. Liu, J., Doty, T., Gibson, B. and Heyer, W.D. (2010) Human BRCA2 protein promotes RAD51 filament formation on RPA-covered single-stranded DNA. *Nat Struct Mol Biol*, **17**, 1260-1262.

183. Thorslund, T., McIlwraith, M.J., Compton, S.A., Lekomtsev, S., Petronczki, M., Griffith, J.D. and West, S.C. (2010) The breast cancer tumor suppressor BRCA2 promotes the specific targeting of RAD51 to single-stranded DNA. *Nat Struct Mol Biol*, **17**, 1263-1265.

184. Carreira, A., Hilario, J., Amitani, I., Baskin, R.J., Shivji, M.K., Venkitaraman, A.R. and Kowalczykowski, S.C. (2009) The BRC repeats of BRCA2 modulate the DNA-binding selectivity of RAD51. *Cell*, **136**, 1032-1043.

185. Carreira, A. and Kowalczykowski, S.C. (2011) Two classes of BRC repeats in BRCA2 promote RAD51 nucleoprotein filament function by distinct mechanisms. *Proc Natl Acad Sci U S A*, **108**, 10448-10453.

186. Pellegrini, L., Yu, D.S., Lo, T., Anand, S., Lee, M., Blundell, T.L. and Venkitaraman, A.R. (2002) Insights into DNA recombination from the structure of a RAD51-BRCA2 complex. *Nature*, **420**, 287-293.

187. Shivji, M.K., Mukund, S.R., Rajendra, E., Chen, S., Short, J.M., Savill, J., Klenerman, D. and Venkitaraman, A.R. (2009) The BRC repeats of human BRCA2 differentially regulate RAD51 binding on single- versus double-stranded DNA to stimulate strand exchange. *Proc Natl Acad Sci U S A*, **106**, 13254-13259.

188. Davies, O.R. and Pellegrini, L. (2007) Interaction with the BRCA2 C terminus protects RAD51-DNA filaments from disassembly by BRC repeats. *Nat Struct Mol Biol*, **14**, 475-483.

189. Esashi, F., Galkin, V.E., Yu, X., Egelman, E.H. and West, S.C. (2007) Stabilization of RAD51 nucleoprotein filaments by the C-terminal region of BRCA2. *Nat Struct Mol Biol*, **14**, 468-474.

190. Ayoub, N., Rajendra, E., Su, X., Jeyasekharan, A.D., Mahen, R. and Venkitaraman, A.R. (2009) The carboxyl terminus of Brca2 links the disassembly of Rad51 complexes to mitotic entry. *Curr Biol*, **19**, 1075-1085.

191. Schlacher, K., Christ, N., Siaud, N., Egashira, A., Wu, H. and Jasin, M. (2011) Double-strand break repair-independent role for BRCA2 in blocking stalled replication fork degradation by MRE11. *Cell*, **145**, 529-542.

192. Jeyasekharan, A.D., Ayoub, N., Mahen, R., Ries, J., Esposito, A., Rajendra, E., Hattori, H., Kulkarni, R.P. and Venkitaraman, A.R. (2010) DNA damage regulates the mobility of Brca2 within the nucleoplasm of living cells. *Proc Natl Acad Sci U S A*, **107**, 21937-21942.

193. Zhou, Q., Kojic, M., Cao, Z., Lisby, M., Mazloum, N.A. and Holloman, W.K. (2007) Dss1 interaction with Brh2 as a regulatory mechanism for recombinational repair. *Mol Cell Biol*, **27**, 2512-2526.

194. Zhou, Q., Mazloum, N., Mao, N., Kojic, M. and Holloman, W.K. (2009) Dss1 regulates interaction of Brh2 with DNA. *Biochemistry*, **48**, 11929-11938.

195. Faza, M.B., Kemmler, S. and Panse, V.G. (2010) Sem1: A versatile "molecular glue"? *Nucleus*, **1**, 12-17.

196. Kristensen, C.N., Bystol, K.M., Li, B., Serrano, L. and Brenneman, M.A. (2010) Depletion of DSS1 protein disables homologous recombinational repair in human cells. *Mutat Res*, **694**, 60-64.

197. Xia, B., Sheng, Q., Nakanishi, K., Ohashi, A., Wu, J., Christ, N., Liu, X., Jasin, M., Couch, F.J. and Livingston, D.M. (2006) Control of BRCA2 cellular and clinical functions by a nuclear partner, PALB2. *Mol Cell*, **22**, 719-729.

198. Rahman, N., Seal, S., Thompson, D., Kelly, P., Renwick, A., Elliott, A., Reid, S., Spanova, K., Barfoot, R., Chagtai, T. *et al.* (2007) PALB2, which encodes a BRCA2-interacting protein, is a breast cancer susceptibility gene. *Nat Genet*, **39**, 165-167.

199. Oliver, A.W., Swift, S., Lord, C.J., Ashworth, A. and Pearl, L.H. (2009) Structural basis for recruitment of BRCA2 by PALB2. *EMBO Rep*, **10**, 990-996.

200. Sy, S.M., Huen, M.S., Zhu, Y. and Chen, J. (2009) PALB2 regulates recombinational repair through chromatin association and oligomerization. *J Biol Chem*, **284**, 18302-18310.
201. Buisson, R., Dion-Cote, A.M., Coulombe, Y., Launay, H., Cai, H., Stasiak, A.Z., Stasiak, A., Xia, B. and Masson, J.Y. (2010) Cooperation of breast cancer proteins PALB2 and piccolo BRCA2 in stimulating homologous recombination. *Nat Struct Mol Biol*, **17**, 1247-1254.
202. Dray, E., Etchin, J., Wiese, C., Saro, D., Williams, G.J., Hammel, M., Yu, X., Galkin, V.E., Liu, D., Tsai, M.S. *et al.* (2010) Enhancement of RAD51 recombinase activity by the tumor suppressor PALB2. *Nat Struct Mol Biol*, **17**, 1255-1259.
203. Menzel, T., Nahse-Kumpf, V., Kousholt, A.N., Klein, D.K., Lund-Andersen, C., Lees, M., Johansen, J.V., Syljuasen, R.G. and Sorensen, C.S. (2011) A genetic screen identifies BRCA2 and PALB2 as key regulators of G2 checkpoint maintenance. *EMBO Rep*, **12**, 705-712.
204. Rajagopalan, S., Andreeva, A., Rutherford, T.J. and Fersht, A.R. (2010) Mapping the physical and functional interactions between the tumor suppressors p53 and BRCA2. *Proc Natl Acad Sci U S A*, **107**, 8587-8592.
205. Wu, X., Mondal, G., Wang, X., Wu, J., Yang, L., Pankratz, V.S., Rowley, M. and Couch, F.J. (2009) Microcephalin regulates BRCA2 and Rad51-associated DNA double-strand break repair. *Cancer Res*, **69**, 5531-5536.
206. Liang, Y., Gao, H., Lin, S.Y., Peng, G., Huang, X., Zhang, P., Goss, J.A., Brunicardi, F.C., Multani, A.S., Chang, S. *et al.* (2010) BRIT1/MCPH1 is essential for mitotic and meiotic recombination DNA repair and maintaining genomic stability in mice. *PLoS Genet*, **6**, e1000826.
207. Fujimori, A., Tachiiri, S., Sonoda, E., Thompson, L.H., Dhar, P.K., Hiraoka, M., Takeda, S., Zhang, Y., Reth, M. and Takata, M. (2001) Rad52 partially substitutes for the Rad51 paralog XRCC3 in maintaining chromosomal integrity in vertebrate cells. *EMBO J*, **20**, 5513-5520.
208. Feng, Z., Scott, S.P., Bussen, W., Sharma, G.G., Guo, G., Pandita, T.K. and Powell, S.N. (2011) Rad52 inactivation is synthetically lethal with BRCA2 deficiency. *Proc Natl Acad Sci U S A*, **108**, 686-691.
209. Singleton, M.R., Wentzell, L.M., Liu, Y., West, S.C. and Wigley, D.B. (2002) Structure of the single-strand annealing domain of human RAD52 protein. *Proc Natl Acad Sci U S A*, **99**, 13492-13497.
210. Van Dyck, E., Stasiak, A.Z., Stasiak, A. and West, S.C. (2001) Visualization of recombination intermediates produced by RAD52-mediated single-strand annealing. *EMBO Rep*, **2**, 905-909.
211. Kojic, M., Zhou, Q., Fan, J. and Holloman, W.K. (2011) Mutational analysis of Brh2 reveals requirements for compensating mediator functions. *Mol Microbiol*, **79**, 180-191.
212. Wray, J., Liu, J., Nickoloff, J.A. and Shen, Z. (2008) Distinct RAD51 associations with RAD52 and BCCIP in response to DNA damage and replication stress. *Cancer Res*, **68**, 2699-2707.
213. Treuner, K., Helton, R. and Barlow, C. (2004) Loss of Rad52 partially rescues tumorigenesis and T-cell maturation in Atm-deficient mice. *Oncogene*, **23**, 4655-4661.
214. Takata, M., Sasaki, M.S., Sonoda, E., Fukushima, T., Morrison, C., Albala, J.S., Swagemakers, S.M., Kanaar, R., Thompson, L.H. and Takeda, S. (2000) The Rad51 paralog Rad51B promotes homologous recombinational repair. *Mol Cell Biol*, **20**, 6476-6482.
215. Takata, M., Sasaki, M.S., Tachiiri, S., Fukushima, T., Sonoda, E., Schild, D., Thompson, L.H. and Takeda, S. (2001) Chromosome instability and defective recombinational repair in knockout mutants of the five Rad51 paralogs. *Mol Cell Biol*, **21**, 2858-2866.

216. Thacker, J. (2005) The RAD51 gene family, genetic instability and cancer. *Cancer Lett*, **219**, 125-135.

217. Masson, J.Y., Tarsounas, M.C., Stasiak, A.Z., Stasiak, A., Shah, R., McIlwraith, M.J., Benson, F.E. and West, S.C. (2001) Identification and purification of two distinct complexes containing the five RAD51 paralogs. *Genes Dev*, **15**, 3296-3307.

218. Badie, S., Liao, C., Thanasoula, M., Barber, P., Hill, M.A. and Tarsounas, M. (2009) RAD51C facilitates checkpoint signaling by promoting CHK2 phosphorylation. *J Cell Biol*, **185**, 587-600.

219. Henry-Mowatt, J., Jackson, D., Masson, J.Y., Johnson, P.A., Clements, P.M., Benson, F.E., Thompson, L.H., Takeda, S., West, S.C. and Caldecott, K.W. (2003) XRCC3 and Rad51 modulate replication fork progression on damaged vertebrate chromosomes. *Mol Cell*, **11**, 1109-1117.

220. Petermann, E., Orta, M.L., Issaeva, N., Schultz, N. and Helleday, T. (2010) Hydroxyurea-stalled replication forks become progressively inactivated and require two different RAD51-mediated pathways for restart and repair. *Mol Cell*, **37**, 492-502.

221. Yokoyama, H., Sarai, N., Kagawa, W., Enomoto, R., Shibata, T., Kurumizaka, H. and Yokoyama, S. (2004) Preferential binding to branched DNA strands and strand-annealing activity of the human Rad51B, Rad51C, Rad51D and Xrcc2 protein complex. *Nucleic Acids Res*, **32**, 2556-2565.

222. Kuznetsov, S., Pellegrini, M., Shuda, K., Fernandez-Capetillo, O., Liu, Y., Martin, B.K., Burkett, S., Southon, E., Pati, D., Tessarollo, L. *et al.* (2007) RAD51C deficiency in mice results in early prophase I arrest in males and sister chromatid separation at metaphase II in females. *J Cell Biol*, **176**, 581-592.

223. Liu, Y., Tarsounas, M., O'regan, P. and West, S.C. (2007) Role of RAD51C and XRCC3 in genetic recombination and DNA repair. *J Biol Chem*, **282**, 1973-1979.

224. Schild, D. and Wiese, C. (2010) Overexpression of RAD51 suppresses recombination defects: a possible mechanism to reverse genomic instability. *Nucleic Acids Res*, **38**, 1061-1070.

225. Deans, B., Griffin, C.S., O'Regan, P., Jasin, M. and Thacker, J. (2003) Homologous recombination deficiency leads to profound genetic instability in cells derived from Xrcc2-knockout mice. *Cancer Res*, **63**, 8181-8187.

226. Pittman, D.L. and Schimenti, J.C. (2000) Midgestation lethality in mice deficient for the RecA-related gene, Rad51d/Rad51l3. *Genesis*, **26**, 167-173.

227. Shu, Z., Smith, S., Wang, L., Rice, M.C. and Kmiec, E.B. (1999) Disruption of muREC2/RAD51L1 in mice results in early embryonic lethality which can Be partially rescued in a p53(-/-) background. *Mol Cell Biol*, **19**, 8686-8693.

228. Kovalenko, O.V., Golub, E.I., Bray-Ward, P., Ward, D.C. and Radding, C.M. (1997) A novel nucleic acid-binding protein that interacts with human rad51 recombinase. *Nucleic Acids Res*, **25**, 4946-4953.

229. Modesti, M., Budzowska, M., Baldeyron, C., Demmers, J.A., Ghirlando, R. and Kanaar, R. (2007) RAD51AP1 is a structure-specific DNA binding protein that stimulates joint molecule formation during RAD51-mediated homologous recombination. *Mol Cell*, **28**, 468-481.

230. Wiese, C., Dray, E., Groesser, T., San Filippo, J., Shi, I., Collins, D.W., Tsai, M.S., Williams, G.J., Rydberg, B., Sung, P. *et al.* (2007) Promotion of homologous recombination and genomic stability by RAD51AP1 via RAD51 recombinase enhancement. *Mol Cell*, **28**, 482-490.

231. Ceballos, S.J. and Heyer, W.D. (2011) Functions of the Snf2/Swi2 family Rad54 motor protein in homologous recombination. *Biochim Biophys Acta*.

232. Wesoly, J., Agarwal, S., Sigurdsson, S., Bussen, W., Van Komen, S., Qin, J., van Steeg, H., van Benthem, J., Wassenaar, E., Baarends, W.M. *et al.* (2006) Differential contributions of mammalian Rad54 paralogs to recombination, DNA damage repair, and meiosis. *Mol Cell Biol*, **26**, 976-989.

233. Neale, M.J. and Keeney, S. (2006) Clarifying the mechanics of DNA strand exchange in meiotic recombination. *Nature*, **442**, 153-158.
234. Hunter, N. (2007). Springer, Berlin Heidelberg New York, pp. 381-441.
235. Bishop, D.K., Park, D., Xu, L. and Kleckner, N. (1992) DMC1: a meiosis-specific yeast homolog of E. coli recA required for recombination, synaptonemal complex formation, and cell cycle progression. *Cell*, **69**, 439-456.
236. Rockmill, B., Sym, M., Scherthan, H. and Roeder, G.S. (1995) Roles for two RecA homologs in promoting meiotic chromosome synapsis. *Genes Dev*, **9**, 2684-2695.
237. Schwacha, A. and Kleckner, N. (1997) Interhomolog bias during meiotic recombination: meiotic functions promote a highly differentiated interhomolog-only pathway. *Cell*, **90**, 1123-1135.
238. Pittman, D.L., Cobb, J., Schimenti, K.J., Wilson, L.A., Cooper, D.M., Brignull, E., Handel, M.A. and Schimenti, J.C. (1998) Meiotic prophase arrest with failure of chromosome synapsis in mice deficient for Dmc1, a germline-specific RecA homolog. *Mol Cell*, **1**, 697-705.
239. Yoshida, K., Kondoh, G., Matsuda, Y., Habu, T., Nishimune, Y. and Morita, T. (1998) The mouse RecA-like gene Dmc1 is required for homologous chromosome synapsis during meiosis. *Mol Cell*, **1**, 707-718.
240. Benson, F.E., Stasiak, A. and West, S.C. (1994) Purification and characterization of the human Rad51 protein, an analogue of E. coli RecA. *EMBO J*, **13**, 5764-5771.
241. Passy, S.I., Yu, X., Li, Z., Radding, C.M., Masson, J.Y., West, S.C. and Egelman, E.H. (1999) Human Dmc1 protein binds DNA as an octameric ring. *Proc Natl Acad Sci U S A*, **96**, 10684-10688.
242. Sehorn, M.G., Sigurdsson, S., Bussen, W., Unger, V.M. and Sung, P. (2004) Human meiotic recombinase Dmc1 promotes ATP-dependent homologous DNA strand exchange. *Nature*, **429**, 433-437.
243. Sheridan, S.D., Yu, X., Roth, R., Heuser, J.E., Sehorn, M.G., Sung, P., Egelman, E.H. and Bishop, D.K. (2008) A comparative analysis of Dmc1 and Rad51 nucleoprotein filaments. *Nucleic Acids Res*, **36**, 4057-4066.
244. Bugreev, D.V., Golub, E.I., Stasiak, A.Z., Stasiak, A. and Mazin, A.V. (2005) Activation of human meiosis-specific recombinase Dmc1 by Ca2+. *J Biol Chem*, **280**, 26886-26895.
245. Sheridan, S. and Bishop, D.K. (2006) Red-Hed regulation: recombinase Rad51, though capable of playing the leading role, may be relegated to supporting Dmc1 in budding yeast meiosis. *Genes Dev*, **20**, 1685-1691.
246. Shinohara, M., Gasior, S.L., Bishop, D.K. and Shinohara, A. (2000) Tid1/Rdh54 promotes colocalization of rad51 and dmc1 during meiotic recombination. *Proc Natl Acad Sci U S A*, **97**, 10814-10819.
247. Bugreev, D.V., Pezza, R.J., Mazina, O.M., Voloshin, O.N., Camerini-Otero, R.D. and Mazin, A.V. (2011) The resistance of DMC1 D-loops to dissociation may account for the DMC1 requirement in meiosis. *Nat Struct Mol Biol*, **18**, 56-60.
248. Kagawa, W. and Kurumizaka, H. (2010) From meiosis to postmeiotic events: uncovering the molecular roles of the meiosis-specific recombinase Dmc1. *FEBS J*, **277**, 590-598.
249. Ehmsen, K.T. and Heyer, W.D. (2008) Biochemistry of Meiotic Recombination: Formation, Processing, and Resolution of Recombination Intermediates. *Genome Dyn Stab*, **3**, 91.
250. Hayase, A., Takagi, M., Miyazaki, T., Oshiumi, H., Shinohara, M. and Shinohara, A. (2004) A protein complex containing Mei5 and Sae3 promotes the assembly of the meiosis-specific RecA homolog Dmc1. *Cell*, **119**, 927-940.
251. Ferrari, S.R., Grubb, J. and Bishop, D.K. (2009) The Mei5-Sae3 protein complex mediates Dmc1 activity in Saccharomyces cerevisiae. *J Biol Chem*, **284**, 11766-11770.

252. Say, A.F., Ledford, L.L., Sharma, D., Singh, A.K., Leung, W.K., Sehorn, H.A., Tsubouchi, H., Sung, P. and Sehorn, M.G. (2011) The budding yeast Mei5-Sae3 complex interacts with Rad51 and preferentially binds a DNA fork structure. *DNA Repair (Amst)*, **10**, 586-594.

253. Schwacha, A. and Kleckner, N. (1997) Interhomolog bias during meiotic recombination: meiotic functions promote a highly differentiated interhomolog-only pathway. *Cell*, **90**, 1123-1135.

254. Tsubouchi, H. and Roeder, G.S. (2004) The budding yeast mei5 and sae3 proteins act together with dmc1 during meiotic recombination. *Genetics*, **168**, 1219-1230.

255. Akamatsu, Y., Dziadkowiec, D., Ikeguchi, M., Shinagawa, H. and Iwasaki, H. (2003) Two different Swi5-containing protein complexes are involved in mating-type switching and recombination repair in fission yeast. *Proc Natl Acad Sci U S A*, **100**, 15770-15775.

256. Akamatsu, Y., Tsutsui, Y., Morishita, T., Siddique, M.S., Kurokawa, Y., Ikeguchi, M., Yamao, F., Arcangioli, B. and Iwasaki, H. (2007) Fission yeast Swi5/Sfr1 and Rhp55/Rhp57 differentially regulate Rhp51-dependent recombination outcomes. *EMBO J*, **26**, 1352-1362.

257. Ellermeier, C., Schmidt, H. and Smith, G.R. (2004) Swi5 acts in meiotic DNA joint molecule formation in Schizosaccharomyces pombe. *Genetics*, **168**, 1891-1898.

258. Haruta, N., Kurokawa, Y., Murayama, Y., Akamatsu, Y., Unzai, S., Tsutsui, Y. and Iwasaki, H. (2006) The Swi5-Sfr1 complex stimulates Rhp51/Rad51- and Dmc1-mediated DNA strand exchange in vitro. *Nat Struct Mol Biol*, **13**, 823-830.

259. Akamatsu, Y. and Jasin, M. (2010) Role for the mammalian Swi5-Sfr1 complex in DNA strand break repair through homologous recombination. *PLoS Genet*, **6**, e1001160.

260. Yuan, J. and Chen, J. (2011) The role of the human SWI5-MEI5 complex in homologous recombination repair. *J Biol Chem*, **286**, 9888-9893.

261. Leu, J.Y., Chua, P.R. and Roeder, G.S. (1998) The meiosis-specific Hop2 protein of S. cerevisiae ensures synapsis between homologous chromosomes. *Cell*, **94**, 375-386.

262. Chi, P., San Filippo, J., Sehorn, M.G., Petukhova, G.V. and Sung, P. (2007) Bipartite stimulatory action of the Hop2-Mnd1 complex on the Rad51 recombinase. *Genes Dev*, **21**, 1747-1757.

263. Pezza, R.J., Voloshin, O.N., Vanevski, F. and Camerini-Otero, R.D. (2007) Hop2/Mnd1 acts on two critical steps in Dmc1-promoted homologous pairing. *Genes Dev*, **21**, 1758-1766.

264. Henry, J.M., Camahort, R., Rice, D.A., Florens, L., Swanson, S.K., Washburn, M.P. and Gerton, J.L. (2006) Mnd1/Hop2 facilitates Dmc1-dependent interhomolog crossover formation in meiosis of budding yeast. *Mol Cell Biol*, **26**, 2913-2923.

265. Zierhut, C., Berlinger, M., Rupp, C., Shinohara, A. and Klein, F. (2004) Mnd1 is required for meiotic interhomolog repair. *Curr Biol*, **14**, 752-762.

266. Gerton, J.L. and DeRisi, J.L. (2002) Mnd1p: an evolutionarily conserved protein required for meiotic recombination. *Proc Natl Acad Sci U S A*, **99**, 6895-6900.

267. Pezza, R.J., Camerini-Otero, R.D. and Bianco, P.R. (2010) Hop2-Mnd1 condenses DNA to stimulate the synapsis phase of DNA strand exchange. *Biophys J*, **99**, 3763-3772.

268. Van Komen, S., Petukhova, G., Sigurdsson, S., Stratton, S. and Sung, P. (2000) Superhelicity-driven homologous DNA pairing by yeast recombination factors Rad51 and Rad54. *Mol Cell*, **6**, 563-572.

269. Klein, H.L. (1997) RDH54, a RAD54 homologue in Saccharomyces cerevisiae, is required for mitotic diploid-specific recombination and repair and for meiosis. *Genetics*, **147**, 1533-1543.

270. Shinohara, M., Shita-Yamaguchi, E., Buerstedde, J.M., Shinagawa, H., Ogawa, H. and Shinohara, A. (1997) Characterization of the roles of the Saccharomyces cerevisiae

RAD54 gene and a homologue of RAD54, RDH54/TID1, in mitosis and meiosis. *Genetics*, **147**, 1545-1556.

271. Dresser, M.E., Ewing, D.J., Conrad, M.N., Dominguez, A.M., Barstead, R., Jiang, H. and Kodadek, T. (1997) DMC1 functions in a Saccharomyces cerevisiae meiotic pathway that is largely independent of the RAD51 pathway. *Genetics*, **147**, 533-544.

272. Clever, B., Interthal, H., Schmuckli-Maurer, J., King, J., Sigrist, M. and Heyer, W.D. (1997) Recombinational repair in yeast: functional interactions between Rad51 and Rad54 proteins. *EMBO J*, **16**, 2535-2544.

273. Jiang, H., Xie, Y., Houston, P., Stemke-Hale, K., Mortensen, U.H., Rothstein, R. and Kodadek, T. (1996) Direct association between the yeast Rad51 and Rad54 recombination proteins. *J Biol Chem*, **271**, 33181-33186.

274. Holzen, T.M., Shah, P.P., Olivares, H.A. and Bishop, D.K. (2006) Tid1/Rdh54 promotes dissociation of Dmc1 from nonrecombinogenic sites on meiotic chromatin. *Genes Dev*, **20**, 2593-2604.

275. Chi, P., Kwon, Y., Moses, D.N., Seong, C., Sehorn, M.G., Singh, A.K., Tsubouchi, H., Greene, E.C., Klein, H.L. and Sung, P. (2009) Functional interactions of meiotic recombination factors Rdh54 and Dmc1. *DNA Repair (Amst)*, **8**, 279-284.

276. Arbel, A., Zenvirth, D. and Simchen, G. (1999) Sister chromatid-based DNA repair is mediated by RAD54, not by DMC1 or TID1. *EMBO J*, **18**, 2648-2658.

277. Tsubouchi, H. and Roeder, G.S. (2006) Budding yeast Hed1 down-regulates the mitotic recombination machinery when meiotic recombination is impaired. *Genes Dev*, **20**, 1766-1775.

278. Busygina, V., Sehorn, M.G., Shi, I.Y., Tsubouchi, H., Roeder, G.S. and Sung, P. (2008) Hed1 regulates Rad51-mediated recombination via a novel mechanism. *Genes Dev*, **22**, 786-795.

279. Shinohara, M., Sakai, K., Shinohara, A. and Bishop, D.K. (2003) Crossover interference in Saccharomyces cerevisiae requires a TID1/RDH54- and DMC1-dependent pathway. *Genetics*, **163**, 1273-1286.

280. Tsubouchi, H. and Roeder, G.S. (2003) The importance of genetic recombination for fidelity of chromosome pairing in meiosis. *Dev Cell*, **5**, 915-925.

281. Dray, E., Dunlop, M.H., Kauppi, L., San Filippo, J., Wiese, C., Tsai, M.S., Begovic, S., Schild, D., Jasin, M., Keeney, S. *et al.* (2011) Molecular basis for enhancement of the meiotic DMC1 recombinase by RAD51 associated protein 1 (RAD51AP1). *Proc Natl Acad Sci U S A*, **108**, 3560-3565.

282. Kovalenko, O.V., Wiese, C. and Schild, D. (2006) RAD51AP2, a novel vertebrate- and meiotic-specific protein, shares a conserved RAD51-interacting C-terminal domain with RAD51AP1/PIR51. *Nucleic Acids Res*, **34**, 5081-5092.

283. Dray, E., Siaud, N., Dubois, E. and Doutriaux, M.P. (2006) Interaction between Arabidopsis Brca2 and its partners Rad51, Dmc1, and Dss1. *Plant Physiol*, **140**, 1059-1069.

284. Thorslund, T., Esashi, F. and West, S.C. (2007) Interactions between human BRCA2 protein and the meiosis-specific recombinase DMC1. *EMBO J*, **26**, 2915-2922.

285. Rodríguez-Marí, A., Wilson, C., Titus, T.A., Cañestro, C., BreMiller, R.A., Yan, Y.L., Nanda, I., Johnston, A., Kanki, J.P., Gray, E.M. *et al.* (2011) Roles of brca2 (fancd1) in oocyte nuclear architecture, gametogenesis, gonad tumors, and genome stability in zebrafish. *PLoS Genet*, **7**, e1001357.

286. Siaud, N., Dray, E., Gy, I., Gérard, E., Takvorian, N. and Doutriaux, M.P. (2004) Brca2 is involved in meiosis in Arabidopsis thaliana as suggested by its interaction with Dmc1. *EMBO J*, **23**, 1392-1401.

287. Klovstad, M., Abdu, U. and Schüpbach, T. (2008) Drosophila brca2 is required for mitotic and meiotic DNA repair and efficient activation of the meiotic recombination checkpoint. *PLoS Genet*, **4**, e31.

288. Sharan, S.K., Pyle, A., Coppola, V., Babus, J., Swaminathan, S., Benedict, J., Swing, D., Martin, B.K., Tessarollo, L., Evans, J.P. *et al.* (2004) BRCA2 deficiency in mice leads to meiotic impairment and infertility. *Development*, **131**, 131-142.

289. Shive, H.R., West, R.R., Embree, L.J., Azuma, M., Sood, R., Liu, P. and Hickstein, D.D. (2010) brca2 in zebrafish ovarian development, spermatogenesis, and tumorigenesis. *Proc Natl Acad Sci U S A*, **107**, 19350-19355.

290. Branzei, D. and Foiani, M. (2010) Maintaining genome stability at the replication fork. *Nat Rev Mol Cell Biol*, **11**, 208-219.

291. Halazonetis, T.D., Gorgoulis, V.G. and Bartek, J. (2008) An oncogene-induced DNA damage model for cancer development. *Science*, **319**, 1352-1355.

292. Spry, M., Scott, T., Pierce, H. and D'Orazio, J.A. (2007) DNA repair pathways and hereditary cancer susceptibility syndromes. *Front Biosci*, **12**, 4191-4207.

293. Narod, S.A. and Foulkes, W.D. (2004) BRCA1 and BRCA2: 1994 and beyond. *Nat Rev Cancer*, **4**, 665-676.

294. Howlett, N.G., Taniguchi, T., Olson, S., Cox, B., Waisfisz, Q., De Die-Smulders, C., Persky, N., Grompe, M., Joenje, H., Pals, G. *et al.* (2002) Biallelic inactivation of BRCA2 in Fanconi anemia. *Science*, **297**, 606-609.

295. Jones, P., Altamura, S., Boueres, J., Ferrigno, F., Fonsi, M., Giomini, C., Lamartina, S., Monteagudo, E., Ontoria, J.M., Orsale, M.V. *et al.* (2009) Discovery of 2-{4-[(3S)-piperidin-3-yl]phenyl}-2H-indazole-7-carboxamide (MK-4827): a novel oral poly(ADP-ribose)polymerase (PARP) inhibitor efficacious in BRCA-1 and -2 mutant tumors. *J Med Chem*, **52**, 7170-7185.

296. Meindl, A., Hellebrand, H., Wiek, C., Erven, V., Wappenschmidt, B., Niederacher, D., Freund, M., Lichtner, P., Hartmann, L., Schaal, H. *et al.* (2010) Germline mutations in breast and ovarian cancer pedigrees establish RAD51C as a human cancer susceptibility gene. *Nat Genet*, **42**, 410-414.

297. Reid, S., Schindler, D., Hanenberg, H., Barker, K., Hanks, S., Kalb, R., Neveling, K., Kelly, P., Seal, S., Freund, M. *et al.* (2007) Biallelic mutations in PALB2 cause Fanconi anemia subtype FA-N and predispose to childhood cancer. *Nat Genet*, **39**, 162-164.

298. Vaz, F., Hanenberg, H., Schuster, B., Barker, K., Wiek, C., Erven, V., Neveling, K., Endt, D., Kesterton, I., Autore, F. *et al.* (2010) Mutation of the RAD51C gene in a Fanconi anemia-like disorder. *Nat Genet*, **42**, 406-409.

299. Hiramoto, T., Nakanishi, T., Sumiyoshi, T., Fukuda, T., Matsuura, S., Tauchi, H., Komatsu, K., Shibasaki, Y., Inui, H., Watatani, M. *et al.* (1999) Mutations of a novel human RAD54 homologue, RAD54B, in primary cancer. *Oncogene*, **18**, 3422-3426.

300. Schoenmakers, E.F., Huysmans, C. and Van de Ven, W.J. (1999) Allelic knockout of novel splice variants of human recombination repair gene RAD51B in t(12;14) uterine leiomyomas. *Cancer Res*, **59**, 19-23.

301. Smirnova, M., Van Komen, S., Sung, P. and Klein, H.L. (2004) Effects of tumor-associated mutations on Rad54 functions. *J Biol Chem*, **279**, 24081-24088.

302. Martinez-Perez, E. and Colaiacovo, M.P. (2009) Distribution of meiotic recombination events: talking to your neighbors. *Curr Opin Genet Dev*, **19**, 105-112.

303. Richardson, C., Stark, J.M., Ommundsen, M. and Jasin, M. (2004) Rad51 overexpression promotes alternative double-strand break repair pathways and genome instability. *Oncogene*, **23**, 546-553.

304. Klein, H.L. (2008) The consequences of Rad51 overexpression for normal and tumor cells. *DNA Repair (Amst)*, **7**, 686-693.

305. Cramer, K., Nieborowska-Skorska, M., Koptyra, M., Slupianek, A., Penserga, E.T., Eaves, C.J., Aulitzky, W. and Skorski, T. (2008) BCR/ABL and other kinases from chronic myeloproliferative disorders stimulate single-strand annealing, an unfaithful DNA double-strand break repair. *Cancer Res*, **68**, 6884-6888.

306. Fernandes, M.S., Reddy, M.M., Gonneville, J.R., DeRoo, S.C., Podar, K., Griffin, J.D., Weinstock, D.M. and Sattler, M. (2009) BCR-ABL promotes the frequency of mutagenic single-strand annealing DNA repair. *Blood*, **114**, 1813-1819.

307. Mandon-Pepin, B., Touraine, P., Kuttenn, F., Derbois, C., Rouxel, A., Matsuda, F., Nicolas, A., Cotinot, C. and Fellous, M. (2008) Genetic investigation of four meiotic genes in women with premature ovarian failure. *European journal of endocrinology / European Federation of Endocrine Societies*, **158**, 107-115.

308. Farmer, H., McCabe, N., Lord, C.J., Tutt, A.N., Johnson, D.A., Richardson, T.B., Santarosa, M., Dillon, K.J., Hickson, I., Knights, C. *et al.* (2005) Targeting the DNA repair defect in BRCA mutant cells as a therapeutic strategy. *Nature*, **434**, 917-921.

309. Kaelin, W.G. (2005) The concept of synthetic lethality in the context of anticancer therapy. *Nat Rev Cancer*, **5**, 689-698.

310. Chen, C.C., Kennedy, R.D., Sidi, S., Look, A.T. and D'Andrea, A. (2009) CHK1 inhibition as a strategy for targeting Fanconi Anemia (FA) DNA repair pathway deficient tumors. *Mol Cancer*, **8**, 24.

311. McManus, K.J., Barrett, I.J., Nouhi, Y. and Hieter, P. (2009) Specific synthetic lethal killing of RAD54B-deficient human colorectal cancer cells by FEN1 silencing. *Proc Natl Acad Sci U S A*, **106**, 3276-3281.

312. Bryant, H.E., Schultz, N., Thomas, H.D., Parker, K.M., Flower, D., Lopez, E., Kyle, S., Meuth, M., Curtin, N.J. and Helleday, T. (2005) Specific killing of BRCA2-deficient tumours with inhibitors of poly(ADP-ribose) polymerase. *Nature*, **434**, 913-917.

313. Mukhopadhyay, A., Elattar, A., Cerbinskaite, A., Wilkinson, S.J., Drew, Y., Kyle, S., Los, G., Hostomsky, Z., Edmondson, R.J. and Curtin, N.J. (2010) Development of a functional assay for homologous recombination status in primary cultures of epithelial ovarian tumor and correlation with sensitivity to poly(ADP-ribose) polymerase inhibitors. *Clin Cancer Res*, **16**, 2344-2351.

314. Gottipati, P., Vischioni, B., Schultz, N., Solomons, J., Bryant, H.E., Djureinovic, T., Issaeva, N., Sleeth, K., Sharma, R.A. and Helleday, T. (2010) Poly(ADP-ribose) polymerase is hyperactivated in homologous recombination-defective cells. *Cancer Res*, **70**, 5389-5398.

315. Banerjee, S., Kaye, S.B. and Ashworth, A. (2010) Making the best of PARP inhibitors in ovarian cancer. *Nat Rev Clin Oncol*, **7**, 508-519.

316. Evers, B., Drost, R., Schut, E., de Bruin, M., van der Burg, E., Derksen, P.W., Holstege, H., Liu, X., van Drunen, E., Beverloo, H.B. *et al.* (2008) Selective inhibition of BRCA2-deficient mammary tumor cell growth by AZD2281 and cisplatin. *Clin Cancer Res*, **14**, 3916-3925.

317. Evers, B., Helleday, T. and Jonkers, J. (2010) Targeting homologous recombination repair defects in cancer. *Trends Pharmacol Sci*, **31**, 372-380.

318. Edwards, S.L., Brough, R., Lord, C.J., Natrajan, R., Vatcheva, R., Levine, D.A., Boyd, J., Reis-Filho, J.S. and Ashworth, A. (2008) Resistance to therapy caused by intragenic deletion in BRCA2. *Nature*, **451**, 1111-1115.

319. Sakai, W., Swisher, E.M., Karlan, B.Y., Agarwal, M.K., Higgins, J., Friedman, C., Villegas, E., Jacquemont, C., Farrugia, D.J., Couch, F.J. *et al.* (2008) Secondary mutations as a mechanism of cisplatin resistance in BRCA2-mutated cancers. *Nature*, **451**, 1116-1120.

320. Sorensen, C.S., Hansen, L.T., Dziegielewski, J., Syljuasen, R.G., Lundin, C., Bartek, J. and Helleday, T. (2005) The cell-cycle checkpoint kinase Chk1 is required for mammalian homologous recombination repair. *Nat Cell Biol*, **7**, 195-201.

321. Popova, M., Shimizu, H., Yamamoto, K., Lebechec, M., Takahashi, M. and Fleury, F. (2009) Detection of c-Abl kinase-promoted phosphorylation of Rad51 by specific antibodies reveals that Y54 phosphorylation is dependent on that of Y315. *FEBS Lett*, **583**, 1867-1872.

322. Esashi, F., Christ, N., Gannon, J., Liu, Y., Hunt, T., Jasin, M. and West, S.C. (2005) CDK-dependent phosphorylation of BRCA2 as a regulatory mechanism for recombinational repair. *Nature*, **434**, 598-604.

323. Schoenfeld, A.R., Apgar, S., Dolios, G., Wang, R. and Aaronson, S.A. (2004) BRCA2 is ubiquitinated in vivo and interacts with USP11, a deubiquitinating enzyme that exhibits prosurvival function in the cellular response to DNA damage. *Mol Cell Biol*, **24**, 7444-7455.

324. Matsuoka, S., Ballif, B.A., Smogorzewska, A., McDonald, E.R., 3rd, Hurov, K.E., Luo, J., Bakalarski, C.E., Zhao, Z., Solimini, N., Lerenthal, Y. *et al.* (2007) ATM and ATR substrate analysis reveals extensive protein networks responsive to DNA damage. *Science*, **316**, 1160-1166.

325. Kim, J.M., Kee, Y., Gurtan, A. and D'Andrea, A.D. (2008) Cell cycle-dependent chromatin loading of the Fanconi anemia core complex by FANCM/FAAP24. *Blood*, **111**, 5215-5222.

326. Fricke, W.M., Kaliraman, V. and Brill, S.J. (2001) Mapping the DNA topoisomerase III binding domain of the Sgs1 DNA helicase. *J Biol Chem*, **276**, 8848-8855.

327. Rao, V.A., Fan, A.M., Meng, L., Doe, C.F., North, P.S., Hickson, I.D. and Pommier, Y. (2005) Phosphorylation of BLM, dissociation from topoisomerase IIIalpha, and colocalization with gamma-H2AX after topoisomerase I-induced replication damage. *Mol Cell Biol*, **25**, 8925-8937.

328. Leng, M., Chan, D.W., Luo, H., Zhu, C., Qin, J. and Wang, Y. (2006) MPS1-dependent mitotic BLM phosphorylation is important for chromosome stability. *Proc Natl Acad Sci U S A*, **103**, 11485-11490.

This part of Habilitation Thesis will be included in review article submitted to Nucleic Acid Research (Krejci L.,Altmannova V., Spirek M. and Zhao X, Homologous recombination and its regulation)

List of publications as an attachment

1. **Krejci, L.**, Damborsky, J., Thomsen, C., Duno, M., and Bendixen, C. (2001) Molecular dissection of interactions between Rad51 and members of the recombination-repair group. *Mol. Cell. Biol.* 21:966-976.
2. **Krejci, L.***, Song, B., Bussen, W., Rothstein, R., Mortensen, U., and Sung, P. (2002) Interaction with Rad51 is indispensable for recombination mediator function of Rad52. *J. Biol. Chem.* 277:40132-41.
3. Seong, C., Sehorn, M.G., Plate, I., Shi, I., Song, B., Chi, P., Mortensen, U., Sung, P., and **Krejci, L.*** (2008). Molecular anatomy of the recombination mediator function of Saccharomyces cerevisiae Rad52. The Journal of biological chemistry. **J Biol Chem. 2**83(18):12166-74.
4. **Krejci, L.*,** Van Komen, S., Li, Y., Villemain, J., Reddy, M. S., Klein, H., Ellenberger, T., Sung, P. (2003) DNA helicase Srs2 disrupts the Rad51 presynaptic filament. *Nature* 423:305-9.
5. **Krejci L,** Macris M, Li Y, Van Komen S, Villemain J, Ellenberger T, Klein H, Sung P. (2004) Role of ATP hydrolysis in the antirecombinase function of *S. cerevisiae* Srs2 protein. *J Biol Chem.*, 279(22): 23193-9.
6. Colavito S, Macris-Kiss M, Seong C, Gleeson O, Greene EC, Klein HL, **Krejci L***, Sung P (2009) Functional significance of the Rad51-Srs2 complex in Rad51 presynaptic filament disruption.*Nucleic Acids Res.* 37 (20): 6754-64.
7. Antony E, Tomko EJ, Xiao Q, **Krejci L**, Lohman TM, Ellenberger T. (2009) Srs2 disassembles Rad51 filaments by a protein-protein interaction triggeringATP turnover and dissociation of Rad51 from DNA.*Mol Cell.* 10;35(1):105-15.
8. Burgess RC, Lisby M, Altmannova V, **Krejci L**, Sung P, Rothstein R (2009) Localization of recombination proteins and Srs2 reveals anti-recombinase function in vivo. *J Cell Biol.* 185(6):969-81.
9. Seong C, Colavito S, Kwon Y, Sung P, **Krejci L*.** (2009) Regulation of Rad51 Recombinase Presynaptic Filament Assembly via Interactions with the Rad52 Mediator and the Srs2 Anti-recombinase.*J Biol Chem.* 284(36):24363-71.
10. Marini, V, and **Krejci, L*,** (2010), Srs2: the "Odd-Job Man", *DNA Repair*, 9(3):268-75.
11. Altmannova V, Eckert-Boulet N, Arneric M, Kolesar P, Chaloupkova R, Damborsky J, Sung P, Zhao X, Lisby M and **Krejci L***(2010)Rad52 SUMOylation affects the efficiency of the DNA repair. *Nucleic Acids Res.* 38 (14): 4708-21.
12. Matulova P, Marini V, Burgess RC, Sisakova A, Kwon Y, Rothstein R, Sung P, **Krejci L.*** (2009) Co-operativity of Mus81-Mms4 with Rad54 in the resolution of recombination and replication intermediates. *J Biol Chem.* 284 (12):7733-7745.
13. Sebesta M, Burkovics P, Haracska L and **Krejci L. *** (2011) Reconstitution of DNA repair synthesis in vitro and the role of polymerase and helicase activities. *DNA Repair (Amst).* 10(6):567-76.

* corresponding author

Attachment 1

Krejci, L., Damborsky, J., Thomsen, C., Duno, M., and Bendixen, C.

Molecular dissection of interactions between Rad51 and members of the recombination-repair group.

Mol. Cell. Biol. 21:966-976. 2001

Molecular Dissection of Interactions between Rad51 and Members of the Recombination-Repair Group

LUMIR KREJCI,[1,2] JIRI DAMBORSKY,[3] BO THOMSEN,[2] MORTEN DUNO,[2]
AND CHRISTIAN BENDIXEN[2]*

*Department of Analysis of Biologically Important Molecular Complexes, Masaryk University, 612 65 Brno,[1]
and Laboratory of Biomolecular Structure and Dynamics, Masaryk University, 611 37 Brno,[3]
Czech Republic, and Department of Breeding and Genetics, Section of Molecular
Genetics, Research Center Foulum, DK-8830 Tjele, Denmark[2]*

Recombination is important for the repair of DNA damage and for chromosome segregation during meiosis; it has also been shown to participate in the regulation of cell proliferation. In the yeast *Saccharomyces cerevisiae*, recombination requires products of the *RAD52* epistasis group. The Rad51 protein associates with the Rad51, Rad52, Rad54, and Rad55 proteins to form a dynamic complex. We describe a new strategy to screen for mutations which cause specific disruption of the interaction between certain proteins in the complex, leaving other interactions intact. This approach defines distinct protein interaction domains and protein relationships within the Rad51 complex. Alignment of the mutations onto the constructed three-dimensional model of the Rad51 protein reveal possible partially overlapping interfaces for the Rad51-Rad52 and the Rad51-Rad54 interactions. Rad51-Rad55 and Rad51-Rad51 interactions are affected by the same spectrum of mutations, indicating similarity between the two modes of binding. Finally, the detection of a subset of mutations within Rad51 which disrupt the interaction with mutant Rad52 protein but activate the interaction with Rad54 suggests that dynamic changes within the Rad51 protein may contribute to an ordered reaction process.

In the yeast *Saccharomyces cerevisiae*, genes of the *RAD52* epistasis group are required for both homologous recombination and the repair of double strand-breaks (DSBs) (10). Mutations in these genes result in severe cellular sensitivity to ionizing radiation and alkylating agents (e.g., methyl methanesulfonate [MMS]), reduced spontaneous and DNA damage-induced mitotic recombination, and the production of inviable spores in meiotic recombination (36).

Biochemical data suggest that some products of the *RAD52* epistasis group (Rad51, Rad52, Rad54, Rad55, Rad57, and replication protein A [RPA]) assemble-disassemble on DNA. The Rad51 protein is a key component of this complex. It has significant sequence and functional similarity to *Escherichia coli* RecA protein, the crystal structure of which has been determined (47). The two proteins share a region of 30% identity, comprising amino acid residues 154 to 374 of Rad51 and 33 to 240 of RecA, corresponding to a large middle domain essential for recombination. Indeed, Rad51 protein also possesses some of the RecA functional activities, e.g., binding of single-stranded DNA (ssDNA) and double-stranded DNA, ATP hydrolysis, formation of nucleoprotein filaments, and formation of heteroduplex DNA (51, 54).

Rad51 interacts with itself, with Rad52 (9, 43), with Rad54 (7, 17), and with Rad55, which in turn associates with Rad57 (15, 18). In accordance with the biochemical and two-hybrid data obtained for these interactions, there are also many genetic data supporting their cellular relevance (7, 11, 41). The

importance of the N-terminal part of Rad51 has been demonstrated in Rad51 self-association and in the interaction with Rad52 (31). The details of these two interactions have not been explored further.

Recently, much attention has been paid to the biochemical function of Rad51 and its associated proteins, Rad51, Rad52, Rad54, and the Rad55-Rad57 heterodimer. Rad52 shows annealing activities (32, 50) and promotes the exchange of RPA for Rad51 protein on ssDNA (28, 52), and human Rad52 binds double-strand breaks (56). Rad54 belongs to a SWI2/SNF2 protein family, whose members modulate chromatin structure (57). Biochemical studies show that Rad54 forms a dimer or oligomer on DNA and promotes Rad51-dependent homologous DNA pairing through changes in DNA double-helix conformation (37). Both *RAD55* and *RAD57* are sequence homologs of *RAD51*, and they form heterodimers that assist Rad51 in interacting with the ssDNA. The heterodimer may be involved in overcoming an inhibition of strand exchange by RPA (52).

The sequence of the *RAD* genes is conserved in a wide variety of eukaryotic organisms, suggesting their importance to eukaryotic cellular function in general. An interesting feature of Rad51p is its crucial role in the mouse, where the *rad51* mutant displays early embryonic lethality (24) but also impairs spontaneous and DSB-induced conservative recombination without affecting cell viability (22). The physical interaction of HsRad51 with several tumor suppressor genes, namely, p53, BRCA1, and BRCA2, implies its possible role(s) in tumorigenesis (26, 48).

Here we describe a new approach to dissect protein interactions within the multiprotein complex and the application of this technique to the yeast recombination-repair complex. By

---

* Corresponding author. Mailing address: Department of Breeding and Genetics, Section of Molecular Genetics, Research Center Foulum, P.O. Box 50, DK-8830 Tjele, Denmark. Phone: 45 89991360. Fax: 45 89991300. E-mail: Christian.Bendixen@agrsci.dk.

TABLE 1. Primers used in this study

Oligonucleotide	Sequence (5′ to 3′)
scRAD51-FOR	CGGGGATTCGTATGTCTCAAGTTCAAGAACAA
scRAD51-REV	ACGCGTCGACCTACTCGTCTTCTTCTCTGG
scRAD52-FOR	GGAGAATTCATGGCGTTTTTAAGCTATTT
scRAD52-REV	ACGCGTCGACTCAAGTAGGCTTGCGTG
scRAD54-FOR	GGAGAATTCATGGCAGACGCAGATTACC
scRAD54-REV	AAACTGCAGTCAATGTGAAATATATTGAA
scRAD51-crev	GGATCCGAAATGATAAGATCTTTATATCCC
scRAD51-393D	TGTTCGCGATCTATGAAGATGGTGTTGATG
scRAD51-393S	TGTTCGCGATCTATGAAGATGGTGTTAGTG
scRAD51-R2	GTAGCTCACGTAACGGTTTG
disrup51-FOR	AGCGACAAAGAGCAGACGTAGTTATTTTTTAAAGGCCTACTAATTTGT TATCGTCATATGTCGCAAGTTCAAGAACAAC

this strategy, mutations introduced into one component of a two-hybrid interaction pair can be readily and simultaneously screened for effects on interactions with each of several desired partner proteins, thus directly revealing different patterns of effects and defining the residues involved. We have used this approach to investigate the interactions of yeast Rad51 with Rad52, Rad54, Rad55, and Rad51 itself by isolating *rad51* mutants which abolish specific interactions within the Rad51 complex without affecting others. Such analysis was not possible using the conventional two-hybrid system. Localization of these mutations in a homology model of the Rad51 protein and the Rad51 filament reveals possible interaction interfaces. The mutants defective in specific interactions also show a decrease in MMS-induced DSB repair, revealing new data on the importance of protein-protein interactions in recombination and repair. Possible compensatory mutations that activate protein interactions were also identified. This mutagenic two-hybrid strategy can be used to dissect other multiprotein complexes or mechanisms and can help us understand the evolution of compensatory mutations as well as define interaction regions de novo.

MATERIALS AND METHODS

Media and plasmids. Yeast and bacterial media, as well as all the standard yeast genetic methods, were used as described previously (2). 5-Fluoroorotic acid medium was prepared by the method of Boeke et al. (5). The vectors pGBT9 and pGAD10 have been described elsewhere (6). Coding sequences of *RAD51*, *RAD52*, and *RAD54* were amplified from genomic clones by PCR using the primers scRAD51-FOR plus scRAD51-REV, scRAD52-FOR plus scRAD52-REV, and scRAD54-FOR plus scRAD54-REV, respectively (Table 1). The PCR products were digested with *Bam*HI-*Sal*I, *Eco*RI-*Sal*I, and *Eco*RI-*Pst*I, respectively, and cloned into the same site within pGBT9 to generate pGBT9-RAD51, pGBT9-RAD52, and pGBT9-RAD54, respectively. pGBT9-RAD55 and pGAD10-RAD51 were kindly provided by R. Rothstein (Columbia University). Plasmids pRS413-rad51x, carrying different *rad51* mutations, were constructed by inserting the *Bst*EII-*Bsu*36I fragment from pGAD-rad51x into the *Bst*EII-*Bsu*36I site of pRS413-RAD51 (kindly provided by L. Symington, Columbia University). Plasmid pRS413-rad51A27V was constructed by ligating the *Stu*I-*Bsu*36I fragment produced by PCR using disrup51-FOR and scRAD51-R2 primers, with pGAD10-rad51A27V as template. pRS413-G393S and pRS413-G393D were produced by site-directed mutagenesis using primers scRAD51-393S and scRAD51-393D as forward primers and scRAD51-crev as a reverse primer. The resulting fragments were digested with *Nru*I-*Sty*I and cloned into the pRS413-RAD51 vector. All PCR products were isolated from agarose gels by Gene Clean II (Bio 101, Inc.), and the final constructs were verified by DNA sequencing.

Yeast strains. The yeast strains used to study two-hybrid interactions were CBY14.1**a** and CBY14.1α (*ade2 his3 leu2 trp1 URA3::UAS_{GAL1}-HIS3 gal4Δ gal80Δ LYS::UAS_{GAL1}-lacZ*) (4) and PJ69-4**a** and PJ69-4α (*trp1 leu2 ura3 his3 gal4Δ gal80Δ LYS::GAL1-HIS3 GAL2-ADE2 met2::GAL7-lacZ*) (16). The LM1

strain used for *rad51* complementation studies is a derivative of W303 (*rad51:: URA3 ade2 can1 his3 leu2 trp1 ura3*) (55). The *RAD51* gene was replaced with the *URA3* gene by transformation of yeast cells with the PCR fragment of the *URA3* gene with 60 bp of the *RAD51* sequence at the 3′ and 5′ ends of the fragment, compatible to the sequence outside the open reading frame. Yeast strains were transformed by the method of Gietz et al. (12).

Detection of two-hybrid interactions. Individual interactions were examined using isogenic CBY14.1**a** plus CBY14.1α and PJ69-4**a** plus PJ69-4α yeast two-hybrid strains. The diploids were selected on synthetic complete medium lacking Trp and Leu (SC-Trp-Leu) plates and replica plated to SC-Trp-Leu-His plates supplemented with 30 mM 3-amino-1,2,4-triazole. The cells were incubated at 30°C for 3 to 4 days and then subjected to a β-galactosidase assay (2). The β-galactosidase activity was quantified by the method of Guarente (14). Additional selection on SC-Trp-Leu-Ade was performed on the PJ69-4**a**/α diploid strain, since it carries the *ADE2* reporter gene (16). To investigate the temperature sensitivity of the protein interactions, the same studies were done at two additional temperatures, 25 and 34°C.

Mutational screen. Mutations in the *RAD51* gene were introduced by propagating the two-hybrid plasmid pGAD10-RAD51 through an *Escherichia coli mutD5* mutator strain, GM4708 (35). Mutagenesis was induced by cultivation for different periods (16, 19, 21, and 24 h) in Luria-Bertani (LB) medium containing ampicillin (75 μg/ml). The mutation rate followed the Gaussian distribution, with an optimum at 20 h of incubation, and was determined by loss of function of the *LEU2* plasmid to complement the *leuB* mutation in *E. coli* strain HB101. The mutated plasmid (pGAD10-rad51x) was used to transform the yeast strain CBY14.1**a**. Around 10,000 transformants were then manually patched on selective media so that each colony would be easily identified by its position, with its row and column numbers in a chess-like pattern. Eighty plates (140 mm), containing 131 individual colonies, were then replica plated onto four lawns with the CBY14.1α strain containing pGBT9-RAD51, pGBT9-RAD52, pGBT9-RAD54 or pGBT9-RAD55 fusion plasmids. Diploids were recovered on SC-Trp-Leu plates and afterwards replica plated on SC-Trp-Leu-His triple-dropout plates supplemented with 30 mM 3-amino-1,2,4-triazole and placed at 30°C. The cells were then subjected to a β-galactosidase filter assay, and pGAD10-rad51x plasmids were isolated from candidate colonies and subsequently sequenced. Due to the organized pattern of the colonies, each transformant was compared for its ability to interact with the Rad51, Rad52, Rad54, or Rad55 proteins, respectively. Thus, colonies where specific interactions were disrupted while others remained intact could be isolated.

MMS sensitivity. Transformants of each clone were grown to stationary phase in yeast extract-peptone-dextrose medium (YPD) and subjected to titer determination in four 10-fold serial dilutions with sterile water. Aliquots of each dilution were plated in duplicate on SC-His plates in the presence and absence of various concentrations of MMS. After preparation, the plates were immediately wrapped in foil to prevent evaporation, and they were used within 12 h. The cells were incubated in the dark at 30°C, and colonies were counted daily for 6 days.

Rad51 modeling. A theoretical model of Rad51 was constructed using the homology modeling approach as implemented in the program Modeller 3.0 (39). The crystal structure of the RecA protein (47) obtained from Brookhaven Protein Database served as a template (accession code 2reb). The template and the target sequence were aligned manually using the program Cameleon 3.14a (Oxford Molecular). An effort has been made to align the secondary elements and to avoid the gaps in the regions of known secondary elements of RecA. The

secondary structure of Rad51 was predicted using the JPred server (8). The constructed models were refined by the molecular dynamic "refine3" option of Modeller 3.0. The protein structures were visualized and manipulated in the modeling package InsightII (MSI/Biosym). The reliability of the models was tested by analyzing their stereochemical accuracy, folding reliability, and packing quality. The stereochemical quality was checked by PROCHECK 3.0 (23). The folding reliability was determined by calculation of the three-dimensional–one-dimensional profile (25), and the total energy of the amino acid profile was determined using PROSAII 3.0 software (46). The packing quality was confirmed by performing bump checks and by visual inspection of the distribution of the hydrophobic and hydrophilic residues within the protein.

RESULTS

Delineation of the two-hybrid interactions between members of the RAD52 epistasis group. Since the yeast two-hybrid system was capable of detecting at least some Rad51 interactions, we examined systematically which regions of Rad51 protein are required for these protein interactions. First, full-length versions of Rad51, Rad52, Rad54, or Rad55 protein (each fused to the binding domain of Gal4p) were transformed into a haploid strain of one mating type. Full-length Rad51 (fused to the activation part of Gal4p) was transformed into a haploid strain of the opposite mating type. Thereafter, the two haploid strains were mated and the diploids were examined for Rad51 interaction with each of the other constructs (Fig. 1B, lanes wt). In addition, several N- and C-terminal deletion mutants of Rad51 were assayed, and it was found that N-terminal deletion of 93 amino acids from Rad51 (residues 93 to 400) did not affect interaction with its partners (data not shown) with the exception of Rad54, whose interaction was substantially reduced (data not shown). In contrast, Rad51 constructs with larger N-terminal (residues 151 to 400) or C-terminal (residues 1 to 285) deletions failed to interact with any of its full-length partners.

Screen for interaction mutants. Since the truncation studies did not provide satisfactory detailed information about the interactive regions of the Rad51 protein, we modified the basic protocol of the two-hybrid screen. In this revised protocol, random mutations are introduced into the Rad51 protein, and each mutant is simultaneously tested for specific interaction with the Rad51-associated proteins. The Rad51 construct was mutagenized by passage through a *mutD* strain (35) and screened for mutations that disrupt specific interaction (see Materials and Methods). Thirty-seven diploid colonies showed detectable loss of Rad51 interaction with one or more partner proteins. To avoid the interference of mutations elsewhere in the plasmid, mutants were recloned into a new pGAD10 vector and the interaction assay was repeated; this left 35 mutants for further characterization. Sequence analysis of these clones identified 19 different mutants containing 22 mutational changes, 19 of which were transitions and 3 of which were transversions. Sixteen mutants represent multiple isolation of the same mutations, probably reflecting the clonal origin. No frameshift mutations were found, confirming the results from truncation studies (see above), which showed that even a small C-terminal deletion disrupted individual Rad51 interactions. Two or more mutations in a single mutant were separately cloned into the pGAD10 vector to find which mutation caused the selected phenotype (data not shown). Finally, Western blots revealed no significant difference in the level of expression from two-hybrid vectors among any of the 19 *rad51* mu-

tants in the final set, with the exception of the G211S and A27V mutants, which are expressed at low levels or are proteolytically unstable (data not shown).

Individual mutants were grouped into seven classes, based on their ability to interact with wild-type Rad51 partner proteins or with the Rad52-K353E mutant protein (Fig. 1A). The K353E allele of the *RAD52* gene was independently isolated in a screen for mutants with reduced affinity for wild-type Rad51 protein and can be suppressed by co-overexpression of *RAD51* (data not shown). Three classes of mutations identified affect interactions of Rad51 with Rad52 and/or Rad54 (classes I to III). Mutants with class I and II mutations disrupt interactions with Rad52 (class I) and Rad54 (class II), respectively. Mutants with Class III mutations show disruption of the interaction with both Rad52 and Rad54 proteins. A fourth class of mutants disrupts the interaction of Rad51 with both Rad55 and Rad54. Class V mutants include those which activate the Rad51-Rad54 interaction. The last two classes include separately isolated mutants that either increase (class VI) or decrease (class VII) the interaction of Rad51 with the Rad52-K353E protein.

MMS sensitivity of *rad51* mutants. To determine the effect of disruption of a specific protein-protein interaction on survival after DNA damage in vivo, we examined the sensitivity of all mutants to MMS. A single-copy vector containing different *rad51* mutants (pRS413-rad51x) or the *scRAD51* gene (pRS413-RAD51) was transformed into the *rad51Δ* strain, LM1. Cells transformed with *scRAD51* were fully complemented, since an equal number of colonies appeared in the presence and absence of MMS (Fig. 2). Two of the three mutations (G210C and A248T) that disrupt the interaction of the Rad51 protein with both Rad52 and Rad54 (class III) conferred the highest sensitivity to MMS, indistinguishable from that of the *rad51Δ* strain (Fig. 2). The third mutant with the same phenotype (class III, G211S) showed higher resistance to MMS, probably reflecting an incomplete interaction deficiency, since some residual interaction is still observed (Fig. 1B, lane G211S). *rad51* cells expressing the rest of the mutants conferred various degrees of sensitivity to MMS but did not complement the loss of Rad51. None of the mutants could fully complement the *rad51Δ* strain, suggesting the importance of both the Rad51-Rad52 and Rad51-Rad54 interactions for the DNA repair process.

Temperature sensitivity of Rad51 interactions. The interaction assays described above were all carried out at 30°C. We also examined wild-type Rad51 interactions and all interactions of mutant proteins with wild-type partner proteins at lower and higher temperatures, 23 and 34°C, respectively (Fig. 1A). None of the wild-type Rad51 interactions were as robust at 34°C as at the lower temperature, but the Rad51 self-association and the interaction of Rad51 with Rad55 were especially compromised. The mutants of class IV (L86P, L99P, and L104P), which abolish Rad51-Rad55 interaction, also disrupt Rad51 self-association at higher temperatures (Fig. 1A). Interestingly, all three mutations involve a change from leucine to proline, in close proximity to each other, suggesting severe structural changes within the Rad51 protein. This could also explain the isolation of the interaction-disrupting mutant (L86P) despite the inability to detect such a disruption when 93 residues from the N-terminus of Rad51 are deleted.

A

Class	rad51 mutant	Two-hybrid interaction with				
		Rad51	Rad52	Rad54	Rad55	Rad52-K
	wt	+ (597)	+ (149)	+ (95)	+ (654)	+ (45)
I	A320V	+ (548)	↓ (<1)	+ (85)	+ (702)	↓ (<1)
	Y388H	+ (562)	↓ (<1)	+ (111)	+ (682)	↓ (<1)
	G393S	+ (521)	↓ (<1)	+ (142)	+ (564)	↓ (<1)
	G393D	+ (612)	↓ (<1)	+ (89)	+ (598)	↓ (<1)
II	L310S	+ (521)	+ (139)	↓ (9.2)	+ (784)	+ (42)
	M269V	+ (573)	+ (132)	↓ (<1)	+ (695)	↓ (<1)
	S231P	+ (725)	+ (125)	↓ (5.3)	+ (532)	↓ (<1)
	G103E	+ (453)	+ (146)	↓ (<1)	+ (589)	↑ (110)
	T146A	+ (586)	+ (129)	↓ (<1)	+ (612)	↑ (96)
	C377Y	+ (486)	+ (156)	↓ (<1)	+ (685)	↑ (132)
	A27V	ts↓ (421)	+ (151)	↓ (<1)	ts↓ (595)	+ (38)
III	A248T	+ (681)	↓ (<1)	↓ (<1)	+ (586)	↓ (<1)
	G210C	ts↓ (598)	↓ (<1)	↓ (<1)	ts↓ (508)	↓ (<1)
	G211S	ts↓ (502)	↓ (2.5)	↓ (7.1)	ts↓ (257)	↓ (<1)
IV	L86P	ts↓ (315)	+ (132)	↓ (<1)	↓ (<1)	↑ (95)
	L99P	ts↓ (75)	+ (151)	↓ (<1)	↓ (<1)	↑ (118)
	L104P	ts↓ (421)	+ (146)	↓ (<1)	↓ (<1)	↑ (108)
V	E186K	ts↓ (513)	+ (115)	↑ (414)	ts↓ (538)	↓ (<1)
	K342E	+ (498)	+ (152)	↑ (324)	+ (621)	↓ (<1)
VI	C366T	+ (456)	+ (147)	+ (121)	+ (664)	↑ (136)
	V81M	+ (602)	+ (141)	+ (45)	+ (546)	↑ (123)
VII	I208T	+ (582)	+ (139)	+ (102)	+ (523)	↓ (<1)
	A264T	+ (451)	+ (140)	+ (95)	+ (638)	↓ (<1)

B
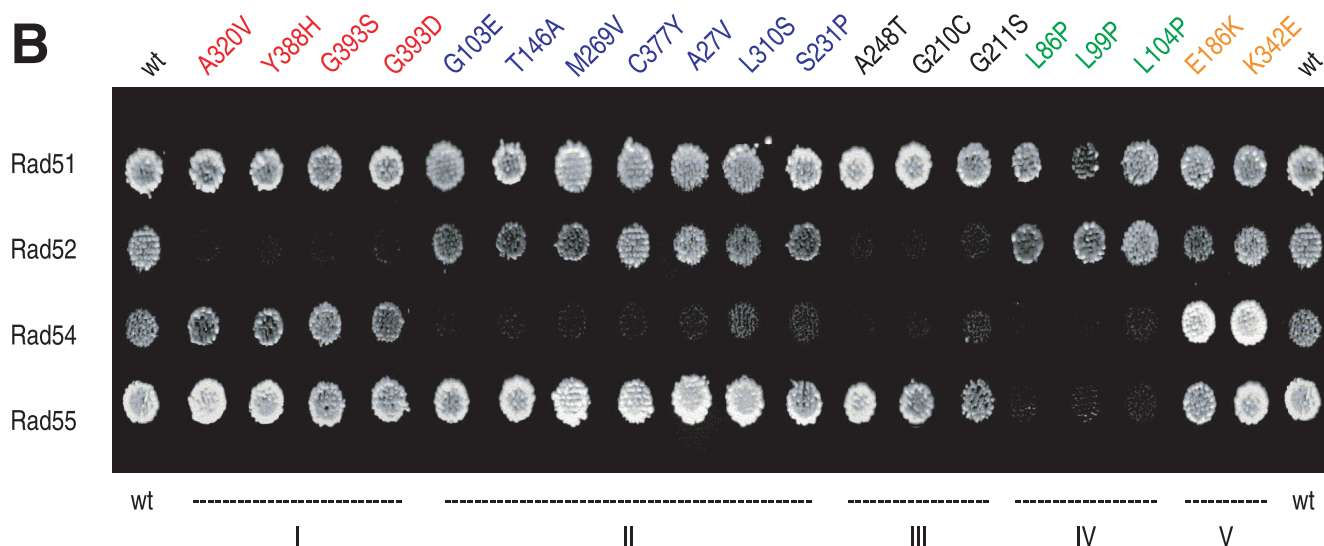
FIG. 1. (A) Classification of *rad51* mutants based on their two-hybrid interaction with Rad51-associated partners. The plus signs indicate the two-hybrid interaction of *rad51* mutant indistinguishable from wild-type Rad51. Black and red arrows depict disruption or activation of the corresponding interaction. Numbers in parentheses represent the average β-galactosidase activity (in Miller units) of three independent experiments. The ts superscript indicates the temperature-sensitive phenotype, where individual interaction is disrupted at 34°C. Rad52-K corresponds to the Rad52-K353E mutant protein. The colors representing individual classes are also used in other figures for easier identification. (B) The two-hybrid assay between individual Rad51 mutant proteins and wild-type Rad51, Rad52, Rad54, and Rad55 proteins. The mutants are grouped into classes according to disruption of the appropriate interaction as follows: class I, Rad52 disruption; class II, Rad54 disruption; class III, Rad52 and Rad54 disruption; class IV, Rad54 and Rad55 disruption; and class V, mutants that activate the interaction to Rad54. The cells were grown on selective medium (SC-Trp-Leu-Ade); two other reporter genes (*HIS3* and *lacZ*) were used as additional controls of the appropriate interactions. wt, wild type.

969
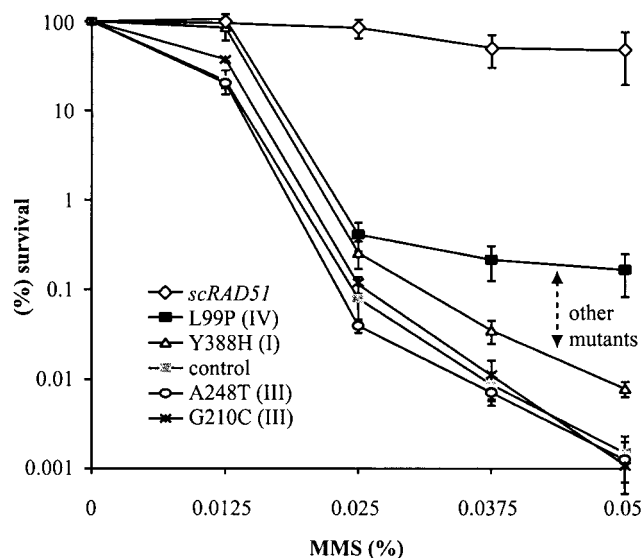
FIG. 2. MMS sensitivity of the *rad51Δ* strain transformed with the different *rad51* mutants. Two mutants (G210C and A248T) showed the highest sensitivity to MMS, indistinguishable from that of the *rad51Δ* strain. The sensitivity of all other mutants (not shown, for clarity) fall in the area indicated by the arrow and demarcated by mutants Y388H and L99P. Data in the figure are displayed as the fraction of colonies viable in the presence of MMS relative to the non-MMS control plates. At least three independent experiments were carried out, and the values obtained from each experiment were averaged. Control, pRS413; *scRAD51*, pRS413-RAD51.

Furthermore, four additional mutants showed weaker interactions with both wild-type Rad51 and Rad55 while having no additional effect on other interactions (mutants A27V, E186K, G210C and G211S in Fig. 1A). These mutants probably exacerbate the already intrinsically thermolabile interactions that occur between the wild-type proteins. The remaining 12 mutants exhibited no variation in the efficiency of any interaction as a function of temperature, except for partial reactivation of Rad51-Rad54 interactions at 25°C in a few cases (data not shown).

Distribution of mutations. MMS sensitivity could result either from malfunction of appropriate protein-protein interactions or from mutation of a functional residue in Rad51. To address this possibility, the 19 newly isolated *rad51* mutations were mapped onto a sequence alignment between Rad51 and bacterial RecA (Fig. 3B). None of the mutations affect residues conserved between Rad51 and RecA. Since these two proteins share important basic functional determinants but interact with entirely unrelated partner proteins, this is the pattern expected if the MMS sensitivity observed in the mutant strain reflects absence of protein-protein interactions.

The 19 mutations were also mapped onto an alignment of known eukaryotic Rad51 proteins (data not shown). About 16 of the 19 mutations affect residues that are identical from yeasts to humans, suggesting the importance of these residues for Rad51 protein interactions in eukaryotes. Furthermore, only a subset of these residues is conserved among yeast Rad51 homologs (4 of 19 for Rad57, and 0 of 19 for Rad55), suggesting that the homologs lack the ability to accomplish some Rad51 interactions.

Molecular modeling of the Rad51 protein. The positions of the 19 Rad51 mutations exhibit no obvious clustering along the linear sequence of the protein that might point to an interaction domain, with two exceptions (Fig. 3A). First, all three mutations that disrupt the Rad51-Rad55 interaction (class IV) are located within 20 residues in the N-terminal part of the protein, revealing a possible interaction domain or somewhat improper folding, since all three mutations involve conversions to proline residues. Second, all mutations that disrupt the interaction of Rad51 with Rad52 (class I and class II) are located in the C-terminal half of the protein.

A three-dimensional (3D) model of the Rad51 protein was constructed to reveal additional information about the possible interaction surfaces of the protein. Since Rad51 is 30% identical to RecA, we chose a structural model of the RecA protein as a template for our predictions. To find how well conserved the individual residues are in the RecA protein, all 64 members of the RecA family were aligned; this revealed that only the core of the RecA protein is conserved throughout the family (data not shown). Furthermore, homologous residues from the Rad51-RecA alignment also match the core region of the RecA protein (data not shown), allowing us to use the RecA structure as a template. The 3D model of the core of the Rad51 protein was generated by homology modeling (Fig. 4). Comparison of the template structure with the homology model in terms of charge distribution and location of hydrophilic and hydrophobic residues revealed a very similar pattern (data not shown). There are N-terminal and C-terminal regions where no structure could be predicted, and there are a few insertions where the predicted geometry has low reliability. These regions were excluded from the analysis.

Rad52 binding domain. The identification of *rad51* mutants that specifically disrupt Rad51-Rad52 and Rad51-Rad54 protein interactions, while other Rad51 interactions remain intact, indicates possible separate domains for these interactions. To address this theory, individual mutations were localized onto a 3D model of the Rad51 protein. Four of the mutations that disrupt the interaction with Rad52 (G210C, G211S, A248T, and A320V) can be aligned into this model, and they localize in a single region at the top of the model (Fig. 4A). Magnification of this domain (Fig. 4B) reveals the accessibility of this region for protein interaction, with the substitutions G210C and G211S possibly localized on a binding epitope. Three other class I mutations, affecting Rad52 specifically, lie at the C-terminal part of the Rad51 protein, whose structure could not be predicted in our model. We suggest that the C-terminal part might fold close to the predicted domain or, alternatively, that there might be two regions for interaction with Rad52p.

Rad54 binding domain. Of the 13 *rad51* mutations which disrupt interaction with Rad54, 6 can be localized to a possible interacting region with an orientation similar to that of the Rad52 interaction domain (Fig. 4A and C). Among the seven mutations that disrupt interaction with Rad54 alone (Fig. 1, class II) and the three mutations that disrupt interaction with Rad54 and Rad52 (class III), five residues constitute a domain (G210C, G211S, S231P, A248T, and M269V). Residue L310S is possibly buried in the structure, and so its effect on the interaction might be rather indirect. For instance, a serine residue has quite a low propensity for inclusion in an α-helix
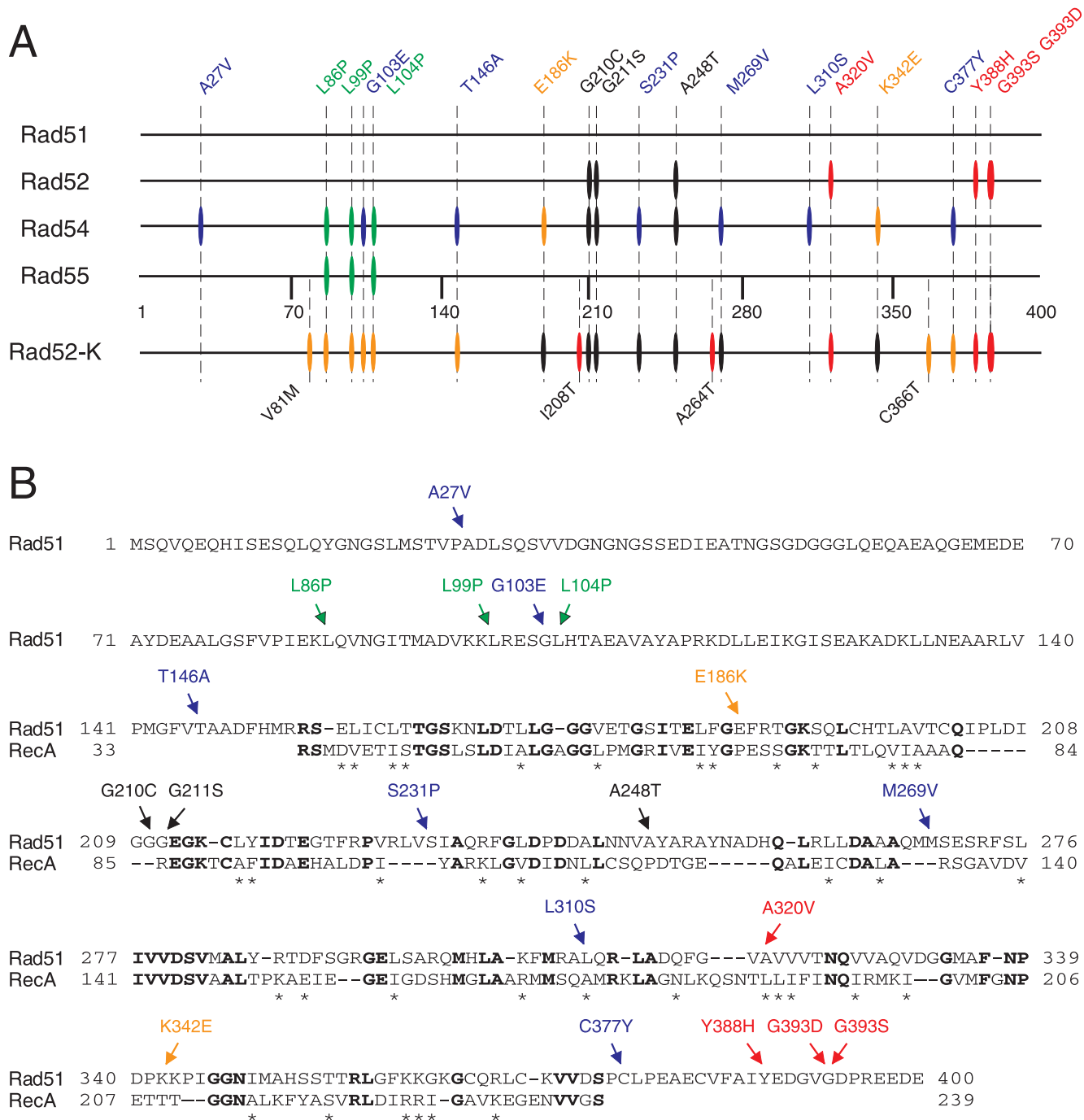
FIG. 3. (A) Linear representation of mutations within Rad51 protein that affect interactions with the Rad51, Rad52, Rad54, and Rad55 proteins. Horizontal lines illustrate the amino acid sequence of the Rad51 protein. Vertical bars represent the mutations defective in the interactions with individual Rad51 partners. The blue and red bars indicate the mutations that disrupt the interaction with only Rad54 or Rad52, respectively. The black bars correspond to the mutations disrupting interaction with both Rad52 and Rad54 proteins. Mutations affecting Rad51-Rad54 as well as Rad51-Rad55 association are depicted by green bars. The yellow bars indicate the mutations that significantly increase the interaction with Rad51. The same Rad51 mutated residues were used to examine the interaction between the Rad51 and Rad52 mutant protein (Rad52-K353E). This mutant protein has lower overall affinity to the Rad51 protein and shows additional phenotypes with the *rad51* mutants compared to wild-type Rad52. (B) Amino acid sequence of *S. cerevisiae* Rad51 protein (residues 1 to 400) aligned with the corresponding homologous part of the *E. coli* RecA protein (residues 33 to 239). Mutations affecting protein-protein interactions are shown above the Rad51 sequence with the same color coding as in panel A. Bold letters and stars indicate identical and similar amino acids, respectively.
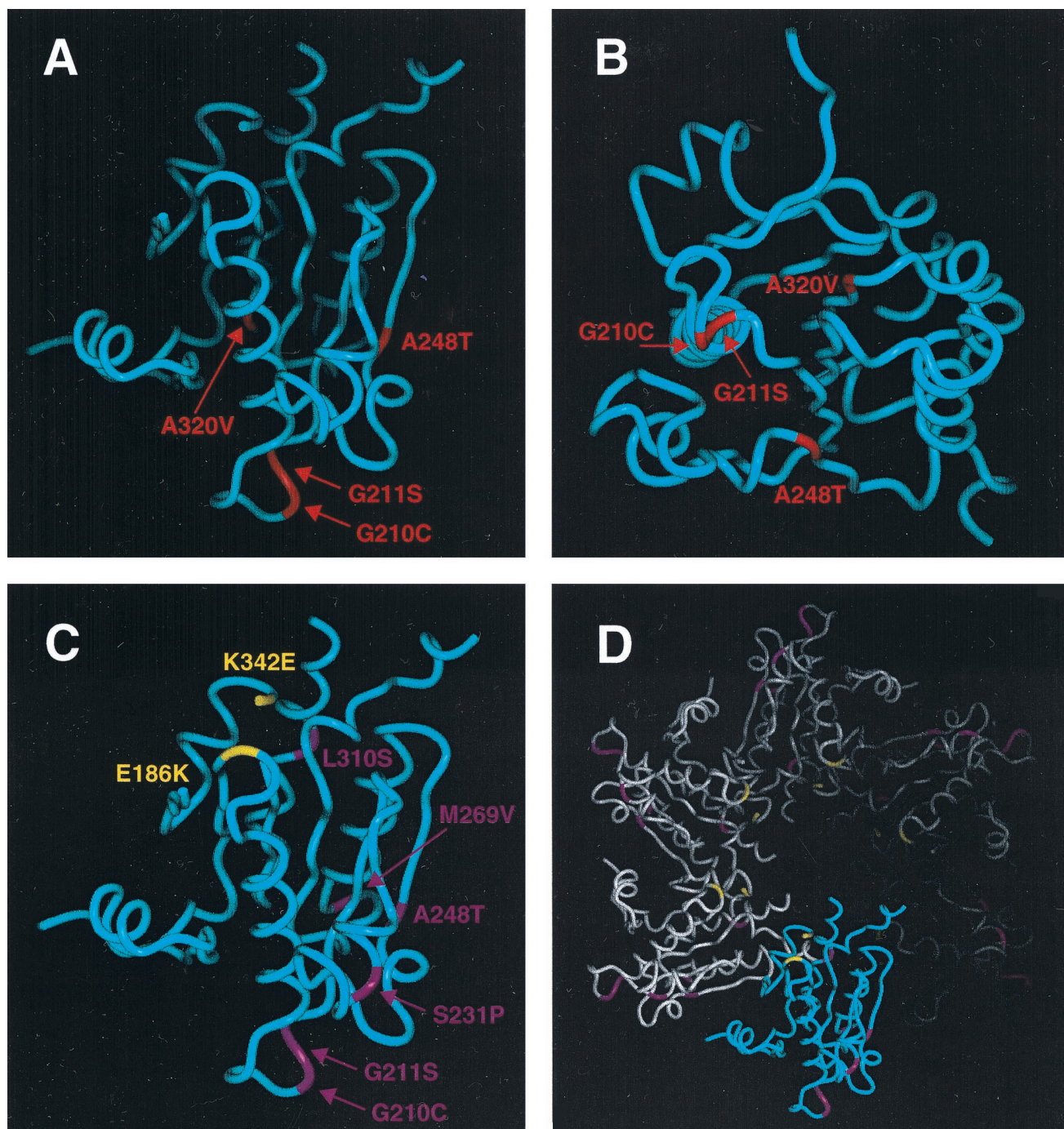
FIG. 4. Model of the Rad51 protein with the proposed Rad52 interaction domain. (A) This model represents the core of Rad51 protein (residues 154 to 375), with localized mutations affecting the Rad51-Rad52 interaction shown in red. Mutations that could be localized within this model constitute the surface region accessible for the Rad52 protein. (B) The same Rad52 interaction domain viewed from the bottom. For this view, the Rad51 protein model in panel A was rotated 90° backward with respect to the viewer. (C) Location of the Rad54p interaction domain within the structural model of Rad51 protein. The Rad51 monomers with localized mutations that disrupt the interaction with Rad54 are indicated in purple. Residues in yellow indicate two mutations that increase the efficiency of Rad51-Rad54 interaction. (D) Model of one turn of a Rad51 filament, showing a highlighted monomer with the suggested Rad54 interaction domain. Note the opposite orientation of mutations disrupting and activating this interaction.

and could significantly change the structure of the protein. The other seven mutations affecting the interaction to Rad54 cannot be localized in the Rad51 model. Six of these mutations are located at the N terminus, thus perhaps creating an additional

binding site for this protein (Fig. 3A). Alternatively, the mutations could influence the conformation of this domain since they introduce proline residues into the Rad51 sequence (Fig. 1, class IV). Furthermore, the T146A mutation is located at a

possible linker between the core and the N-terminal domain and A27V maps to the N-terminal domain, which does not have any effect on Rad51 interaction when deleted.

Activation of the Rad51-Rad54 interaction. Class V represents two mutants that activate the interaction with the Rad54 protein (Fig. 1B). Interestingly, both mutations cause a dramatic charge change, since residue E186 mutates to K and residue K342 mutates to E. Mutated residues in Rad51 are located very close to each other (distance, 12 Å), at a site close to the polymer axis, contrasting with the suggested Rad54 interaction domain (Fig. 4D). This axis region has been proposed to be involved in the binding of DNA (47) and ATP (40), suggesting that their binding could have similar effects.

Since electron microscopy also suggests an overall structural similarity of Rad51 and RecA protein filaments (34), a 3D model of the Rad51 polymer was constructed (Fig. 4D). Since RecA packs in the P6$_1$ crystals to form a polymer, the individual monomers of Rad51 protein were packed to form a continuous spiral of protein. Within the proposed polymer structure, the putative Rad54 binding domain is located at the outer accessible site of the polymer, opposite the mutations that activate the Rad54 interaction and the proposed DNA binding regions corresponding to the L1 and L2 disorder loops of RecA protein.

Rad52 mutant protein affects interaction with Rad51. A mutant of the Rad52 protein, with reduced affinity to wild-type Rad51 (Rad52-K353E), has also been combined with the above-described *rad51* mutants (Fig. 1A and 3A). All mutations disrupting the interaction with wild-type Rad52 also affect the interaction with Rad52-K353E. In addition, four *rad51* mutants that interact with wild-type Rad52 are defective in their interaction with this mutant protein (Fig. 1A, classes II and V). Other Rad51 mutations, A264T and I208T, isolated after the initial screen, also exhibit this property (Fig. 1A, class VII). The mutations all colocalize near the predicted Rad52 interaction domain, in the core of Rad51 protein, and probably further sensitize the already weakened Rad51–Rad52-K353E interaction.

A total of six Rad51 mutations exhibit enhanced interaction with Rad52-K353E (Fig. 1A, classes II and IV). Five of these mutations (L86P, L99P, G103E, L104P, and T146A) map to the N-terminal region, while one (C377Y) is located at the C-terminal end of the Rad51 protein (Fig. 3A). A second screen carried out to identify additional mutations of this type yielded two other alleles, V81M and C366T (class VI). Both mutations specifically activated Rad52 interaction, while other Rad51 interactions were not affected. The data suggest two possible interaction-enhancing and -stabilizing regions, one at the N terminus (spanning residues 81 to 146) and the other at the C terminus (spanning residues 366 to 377) (Fig. 3A). Interestingly, all mutations activating the Rad52-K353E interaction also inhibit Rad51 interaction with Rad54 and vice versa, suggesting opposite binding modes toward Rad51. These regions thus might stabilize Rad52 or Rad54 interactions and perhaps block the binding of the other protein.

DISCUSSION

The modified strategy of the two-hybrid system described above has allowed us to isolate *rad51* mutations which specif-

ically disrupt interactions between Rad51 and its associated proteins, including Rad51 itself. All of the Rad51 mutant proteins identified in this screen exhibit a reduced ability for DNA repair. In addition, most of the mutations are positioned close to or in the regions where the above proteins differ by deletion or insertion of residues. These regions, in turn, correspond to the turns and loops predicted in the structural model of Rad51p. This further indicates that the mutations probably do not disturb the whole structure but, rather, affect domains with some flexibility that are important for protein-protein interactions.

The MMS sensitivity is often partial compared to that of the *rad51*Δ strain, suggesting that some interaction remains. An alternative explanation may be that loss of the interaction can be compensated by the activity of another protein; the yeast Rad52 and Rad54 homologs could play such a role (3, 19, 45). In addition, the two alleles conferring the most severe MMS sensitivity disrupt the interaction with both Rad52 and Rad54, indicating that in these cases, cell survival is as low as in the *rad51*Δ strain. This clearly illustrates the importance of the identified protein-protein interactions in vivo, although some mutants may not have a direct effect on DSB repair, recombination, meiosis, etc.

Comparison of different Rad51 proteins from higher eukaryotes suggests that the same interaction mechanism might have been conserved throughout evolution. Indeed, there are reports describing some of these interactions in higher eukaryotes (13, 42). Intriguingly, the A320V mutation, resulting in disrupted interaction with Rad52, as well as a defect in DSB repair, is located only 3 amino acids away from the aligned human Rad51 F259V mutation, which was recently reported to impair binding with human Rad52 and to decrease homologous pairing (21). This comparison further supports the evolutionary conservation of Rad51 protein-protein interactions.

In contrast, all the mutated residues in Rad51 are only poorly conserved within the yeast Rad51-homologous proteins, Rad55 and Rad57. The absence of these residues may reveal a basic difference between the Rad51, Rad55, and Rad57 proteins, indicating that Rad55 and Rad57 have retained only part of the biological function of Rad51. Both are required in the presynaptic formation of the Rad51 nucleoprotein filament (53) and to gain access to otherwise inaccessible regions of chromatin (49). Furthermore, the Rad55 interaction was more temperature sensitive, being lost at 30°C, while the Rad51 interaction required higher temperatures (34°C) before disruption was apparent (Fig. 1A, class IV). This suggests a higher binding affinity of the Rad51 protein to itself than to Rad55. The fact that we were not able to isolate mutations that specifically disrupt only the process of self-association indicates the presence of a quite flexible binding surface, which might allow Rad51 to compensate for mutated residues. Intriguingly, at high temperatures, disruption of the Rad51-Rad51 interaction was always associated with disruption of the Rad51-Rad55 interaction, demonstrating their close relationship and suggesting that these interactions might be integral to the RecA-like filament of Rad51. We conclude that the Rad51 and Rad55 proteins share a similar but quite complex Rad51 interaction domain consisting of several flexible regions. The N-terminal part of Rad51 seems to be important for these interactions but

could reflect interfilament rather than direct subunit-subunit contacts.

To reveal individual interaction domains within the Rad51 protein, we constructed a 3D model based on structural data from the RecA protein. Mutations localized in this model indicate a possible core binding domain for both Rad52 and Rad54 proteins, situated on the outer face of the filament at a site accessible for protein interactions. The proteins may compete for this binding site, since the two domains partially overlap (compare Fig. 4A and C) on each side of a potential interaction "epitope" containing residues G210 and G211, while N- and C-terminal regions play a role in stabilization of individual interactions. We cannot confirm the localization of the Rad52 interaction domain at the N-terminal part of the protein, suggested by Donovan et al. (9), since not a single mutation disrupting the interaction with the Rad52 protein was found in this region. This is in agreement with recent data from Kurumizaka et al. (21), showing that the N-terminal part of human Rad51 protein also does not exhibit binding to the human Rad52 protein.

Apart from the suggested binding domains, there are also other regions that might affect these interactions. In the Rad52 and Rad54 interactions with Rad51, there are other mutations in the C- and N-terminal regions, respectively, that might be directly involved in the binding process or stabilize these interactions. In particular, the N terminus constitutes a separate domain (1), and we suggest that mutations here alter conformation, resulting in blocked access of the Rad54 protein to the binding site. Surprising results were found for the Rad51-Rad54 interaction, where two interaction-activating mutations were isolated (E186K and K342E). Both activators reverse the charge of the wild-type residues and localize to the inner part of the filament. Interestingly, the E186K mutation corresponds to residue P67 in the P-loop of RecA (Fig. 3B), a region responsible for the binding of ATP (40), and specific substitution of this residue results in separation of RecA functions (20). In addition, the K342E mutation corresponds to residue T210 of RecA located between the L2-loop, which is proposed to be a DNA binding domain (47), and α-helix G, which is proposed to be involved in conformational change following ATP hydrolysis (38). Therefore, the effects of mutated residues on the efficiency of the interaction might mimic the transition between alternative conformations as a part of a chain of events, in this case represented by the binding of ATP (29, 30), affecting the binding efficiency of the Rad54 protein. Determining the conformation of interacting amino acids may be a common strategy by which distal elements influence specific affinity.

In the Rad51 interaction with Rad52-K353E, compensatory mutations were found. These suppressor mutations, which increase the efficiency of interaction with Rad52-K353E, are located within residues 86 to 104 and 366 to 377 at the N- and C-terminal regions of Rad51, respectively. Interestingly, the mutations activating the Rad51 interaction with either Rad52-K353E or Rad54 proteins are often antagonistic; e.g., mutations increasing the affinity to Rad54 disrupt the association of Rad51 with Rad52-K353E, and Rad51 activators of the Rad52-K353E interaction often disrupt the Rad54 interaction. The presence of these activating mutations strongly argues for com-

petition between Rad52 and Rad54 for their overlapping binding sites, suggested by the 3D model superposition.

In summary, the data indicate that the assembly of the whole complex and/or cycle of Rad51 reaction might be sequential with competitive binding sites. Binding of a substrate, ATP, or the protein components of the recombination-repair complex might alternate conformations within the Rad51 protein that could play a role in stabilization of the complex and/or in the accessibility of Rad51 to other proteins. Rad51 is much less active than RecA protein in its reactions (43, 54), indicating that an additional cofactor(s) alters Rad51 activity. Indeed, Rad52 probably stimulates the action of Rad51 by displacing the RPA from ssDNA during the formation of the Rad51 nucleoprotein filament (33, 44), the Rad55-Rad57 heterodimer promotes strand exchange activity (53), and Rad54 promotes Rad51-mediated homologous DNA pairing (37). Therefore, protein-protein interaction seems to be essential for nucleation as well as for the proper functioning of Rad51. The basis for a model of Rad51 assembly might be as follows: (i) RPA binds to the resected ssDNA tails; (ii) Rad52 nucleates Rad51 to this site, together with the Rad55-Rad57 heterodimer; (iii) the Rad51 filament is assembled in a cooperative manner, displacing the RPA from binding sites on ssDNA; (iv) after assembly, the Rad51 nucleoprotein filament permits Rad54 to bind, which stimulates Rad54-mediated ATP hydrolysis and DNA strand separation (27); and (v) consequently, Rad54 stimulates Rad51 to overcome kinetic impediments limiting homologous pairing. This highlights the fact that to comprehend the mechanism of homologous recombination, one needs to study both the single reactions performed by individual proteins and the multistage reactions catalyzed by a set of collaborating proteins. Finally, the above-described mutants could facilitate dissection of the individual steps in the assembly of recombination-repair proteins and permit detection of intermediate stages in the process of homologous recombination. In particular, they will permit assessment of the function or temporal order of specific interactions. It is clear that other biochemical and/or genetic studies will confirm or specify the role of individual Rad51-mediated protein interactions and result in additional insight into these reactions.

This novel strategy of selecting the mutants based on interaction phenotype rather than loss of function provides an important tool for the dissection of other complex multiprotein structures. The strategy allows a determination of the interaction regions and an identification of the effects of individual components on the biochemistry of the process. Furthermore, the activation of the interaction between Rad52 and Rad54 with Rad51 suggests the possibility of isolation of compensatory mutations within these two proteins. This work can be further developed, and preliminary results indicate that the interactions could be switched off and on as desired.

REFERENCES

1. **Aihara, H., Y. Ito, H. Kurumizaka, S. Yokoyama, and T. Shibata.** 1999. The N-terminal domain of the human Rad51 protein binds DNA: structure and a DNA binding surface as revealed by NMR. J. Mol. Biol. **290:**495–504.
2. **Ausubel, F. M., R. Brent, R. Kingston, D. Morre, J. Seidman, A. Smith, and K. Struhl.** 1994. Current protocols in molecular biology. John Wiley & Sons, Inc., New York, N.Y.
3. **Bai, Y., and L. S. Symington.** 1996. A Rad52 homolog is required for *RAD51*-independent mitotic recombination in *Saccharomyces cerevisiae.* Genes Dev. **10:**2025–2037.
4. **Bendixen, C., S. Gangloff, and R. Rothstein.** 1994. A yeast mating-selection scheme for detection of protein-protein interactions. Nucleic Acids Res. **22:**1778–1779.
5. **Boeke, J. D., F. LaCroute, and G. R. Fink.** 1984. A positive selection for mutants lacking orotidine-5′-phosphate decarboxylase activity in yeast: 5-fluoro-orotic acid resistance. Mol. Gen. Genet. **197:**345–346.
6. **Chien, C. T., P. L. Bartel, R. Sternglanz, and S. Fields.** 1991. The two-hybrid system: a method to identify and clone genes for proteins that interact with a protein of interest. Proc. Natl. Acad. Sci. USA **88:**9578–9582.
7. **Clever, B., H. Interthal, J. Schmuckli-Maurer, J. King, M. Sigrist, and W. D. Heyer.** 1997. Recombinational repair in yeast: functional interactions between Rad51 and Rad54 proteins. EMBO J. **16:**2535–2544.
8. **Cuff, J. A., M. E. Clamp, A. S. Siddiqui, M. Finlay, and G. J. Barton.** 1998. JPred: a consensus secondary structure prediction server. Bioinformatics **14:**892–893.
9. **Donovan, J. W., G. T. Milne, and D. T. Weaver.** 1994. Homotypic and heterotypic protein associations control Rad51 function in double-strand break repair. Genes Dev. **8:**2552–2562.
10. **Game, J. C.** 1983. Radiation-sensitive mutants and repair in yeast, p. 105–137. *In* J. F. T. Spencer, D. Spencer, and A. R. W. Smith (ed.), Yeast genetics: fundamental and applied aspects. Springer-Verlag, New York, N.Y.
11. **Gasior, S. L., A. K. Wong, Y. Kora, A. Shinohara, and D. K. Bishop.** 1998. Rad52 associates with RPA and functions with Rad55 and Rad57 to assemble meiotic recombination complexes. Genes Dev. **12:**2208–2221.
12. **Gietz, R. D., R. H. Schiestl, A. R. Willems, and R. A. Woods.** 1995. Studies on the transformation of intact yeast cells by the LiAc/SS-DNA/PEG procedure. Yeast **11:**355–360.
13. **Golub, E. I., O. V. Kovalenko, R. C. Gupta, D. C. Ward, and C. M. Radding.** 1997. Interaction of human recombination proteins Rad51 and Rad54. Nucleic Acids Res. **25:**4106–4110.
14. **Guarente, L.** 1983. Yeast promoters and *lacZ* fusions designed to study expression of cloned genes in yeast. Methods Enzymol. **101:**181–191.
15. **Hays, S. L., A. A. Firmenich, and P. Berg.** 1995. Complex formation in yeast double-strand break repair: participation of Rad51, Rad52, Rad55, and Rad57 proteins. Proc. Natl. Acad. Sci. USA **92:**6925–6929.
16. **James, P., J. Halladay, and E. A. Craig.** 1996. Genomic libraries and a host strain designed for highly efficient two-hybrid selection in yeast. Genetics **144:**1425–1436.
17. **Jiang, H., Y. Xie, P. Houston, K. Stemke-Hale, U. H. Mortensen, R. Rothstein, and T. Kodadek.** 1996. Direct association between the yeast Rad51 and Rad54 recombination proteins. J. Biol. Chem. **271:**33181–33186.
18. **Johnson, R. D., and L. S. Symington.** 1995. Functional differences and interactions among the putative RecA homologs Rad51, Rad55, and Rad57. Mol. Cell. Biol. **15:**4843–4850.
19. **Klein, H. L.** 1997. RDH54, a *RAD54* homologue in *Saccharomyces cerevisiae*, is required for mitotic diploid-specific recombination and repair and for meiosis. Genetics **147:**1533–1543.
20. **Konola, J. T., H. G. Nastri, K. M. Logan, and K. L. Knight.** 1995. Mutations at Pro67 in the RecA protein P-loop motif differentially modify coprotease function and separate coprotease from recombination activities. J. Biol. Chem. **270:**8411–8419.
21. **Kurumizaka, H., H. Aihara, W. Kagawa, T. Shibata, and S. Yokoyama.** 1999. Human Rad51 amino acid residues required for Rad52 binding. J. Mol. Biol. **291:**537–548.
22. **Lambert, S., and B. S. Lopez.** 2000. Characterization of mammalian RAD51 double strand break repair using non-lethal dominant-negative forms. EMBO J. **19:**3090–3099.
23. **Laskowski, R. A., M. W. McArthur, D. S. Moss, and J. M. Thornton.** 1993. PROCHECK: a program to check the stereochemical quality of protein structures. J. Appl. Crystallogr. **26:**283–291.
24. **Lim, D. S., and P. Hasty.** 1996. A mutation in mouse rad51 results in an early embryonic lethal that is suppressed by a mutation in p53. Mol. Cell. Biol. **16:**7133–7143.
25. **Luthy, R., J. U. Bowie, and D. Eisenberg.** 1992. Assessment of protein models with three-dimensional profiles. Nature **356:**83–85.
26. **Marmorstein, L. Y., T. Ouchi, and S. A. Aaronson.** 1998. The BRCA2 gene product functionally interacts with p53 and RAD51. Proc. Natl. Acad. Sci. USA **95:**13869–13874.
27. **Mazin, A. V., C. J. Bornarth, J. A. Solinger, W. Heyer, and S. C. Kowalczykowski.** 2000. Rad54 protein is targeted to pairing loci by the Rad51 nucleoprotein filament. Mol. Cell **6:**1–20.
28. **Mazin, A. V., E. Zaitseva, P. Sung, and S. C. Kowalczykowski.** 2000. Tailed duplex DNA is the preferred substrate for Rad51 protein-mediated homologous pairing. EMBO J. **19:**1148–1156.
29. **Menetski, J. P., and S. C. Kowalczykowski.** 1985. Interaction of recA protein with single-stranded DNA. Quantitative aspects of binding affinity modulation by nucleotide cofactors. J. Mol. Biol. **181:**281–295.
30. **Menetski, J. P., A. Varghese, and S. C. Kowalczykowski.** 1988. Properties of the high-affinity single-stranded DNA binding state of the *Escherichia coli* recA protein. Biochemistry **27:**1205–1212.
31. **Milne, G. T., and D. T. Weaver.** 1993. Dominant negative alleles of *RAD52* reveal a DNA repair/recombination complex including Rad51 and Rad52. Genes Dev. **7:**1755–1765.
32. **Mortensen, U. H., C. Bendixen, I. Sunjevaric, and R. Rothstein.** 1996. DNA strand annealing is promoted by the yeast Rad52 protein. Proc. Natl. Acad. Sci. USA **93:**10729–10734.
33. **New, J. H., T. Sugiyama, E. Zaitseva, and S. C. Kowalczykowski.** 1998. Rad52 protein stimulates DNA strand exchange by Rad51 and replication protein A. Nature **391:**407–410.
34. **Ogawa, T., X. Yu, A. Shinohara, and E. H. Egelman.** 1993. Similarity of the yeast RAD51 filament to the bacterial RecA filament. Science **259:**1896–1899.
35. **Palmer, B. R., and M. G. Marinus.** 1991. DNA methylation alters the pattern of spontaneous mutation in *Escherichia coli* cells (mutD) defective in DNA polymerase III proofreading. Mutat. Res. **264:**15–23.
36. **Petes, T. D., R. E. Malone, and L. S. Symington.** 1991. Recombination in yeast, p. 407–521. *In* J. R. Broach, J. R. Pringle, and E. W. Jones (ed.), The molecular and cellular biology of the yeast *Saccharomyces*: genome dynamics, protein synthesis, and energetics. Cold Spring Harbor Laboratory Press, Cold Spring Harbor, N.Y.
37. **Petukhova, G., S. Van Komen, S. Vergano, H. Klein, and P. Sung.** 1999. Yeast Rad54 promotes Rad51-dependent homologous DNA pairing via ATP hydrolysis-driven change in DNA double helix conformation. J. Biol. Chem. **274:**29453–29462.
38. **Roca, A. I., and M. M. Cox.** 1997. RecA protein: structure, function, and role in recombinational DNA repair. Prog. Nucleic Acid Res. Mol. Biol. **56:**129–223.
39. **Sali, A., and T. L. Blundell.** 1993. Comparative protein modelling by satisfaction of spatial restraints. J. Mol. Biol. **234:**779–815.
40. **Saraste, M., P. R. Sibbald, and A. Wittinghofer.** 1990. The P-loop–a common motif in ATP- and GTP-binding proteins. Trends Biochem. Sci. **15:**430–434.
41. **Schild, D.** 1995. Suppression of a new allele of the yeast *RAD52* gene by overexpression of *RAD51*, mutations in *srs2* and *ccr4*, or mating-type heterozygosity. Genetics **140:**115–127.
42. **Shen, Z., K. G. Cloud, D. J. Chen, and M. S. Park.** 1996. Specific interactions between the human RAD51 and RAD52 proteins. J. Biol. Chem. **271:**148–152.
43. **Shinohara, A., H. Ogawa, and T. Ogawa.** 1992. Rad51 protein involved in repair and recombination in S. cerevisiae is a RecA-like protein. Cell **69:**457–470.
44. **Shinohara, A., and T. Ogawa.** 1998. Stimulation by Rad52 of yeast Rad51-mediated recombination. Nature **391:**404–407.
45. **Shinohara, M., E. Shita-Yamaguchi, J. M. Buerstedde, H. Shinagawa, H. Ogawa, and A. Shinohara.** 1997. Characterization of the roles of the *Saccharomyces cerevisiae RAD54* gene and a homologue of *RAD54, RDH54/TID1*, in mitosis and meiosis. Genetics **147:**1545–1556.
46. **Sippl, M. J.** 1993. Recognition of errors in three-dimensional structures of proteins. Proteins **17:**355–362.
47. **Story, R. M., I. T. Weber, and T. A. Steitz.** 1992. The structure of the *E. coli* recA protein monomer and polymer. Nature **355:**318–325.
48. **Sturzbecher, H. W., B. Donzelmann, W. Henning, U. Knippschild, and S. Buchhop.** 1996. p53 is linked directly to homologous recombination processes via RAD51/RecA protein interaction. EMBO J. **15:**1992–2002.
49. **Sugawara, N., E. L. Ivanov, J. Fishman-Lobell, B. L. Ray, X. Wu, and J. E. Haber.** 1995. DNA structure-dependent requirements for yeast RAD genes in gene conversion. Nature **373:**84–86.
50. **Sugiyama, T., J. H. New, and S. C. Kowalczykowski.** 1998. DNA annealing by Rad52 protein is stimulated by specific interaction with the complex of replication protein A and single-stranded DNA. Proc. Natl. Acad. Sci. USA **95:**6049–6054.
51. **Sugiyama, T., E. M. Zaitseva, and S. C. Kowalczykowski.** 1997. A single-stranded DNA-binding protein is needed for efficient presynaptic complex formation by the *Saccharomyces cerevisiae* Rad51 protein. J. Biol. Chem. **272:**7940–7945.
52. **Sung, P.** 1997. Function of yeast Rad52 protein as a mediator between replication protein A and the Rad51 recombinase. J. Biol. Chem. **272:**28194–28197.
53. **Sung, P.** 1997. Yeast Rad55 and Rad57 proteins form a heterodimer that

functions with replication protein A to promote DNA strand exchange by Rad51 recombinase. Genes Dev. **11:**1111–1121.

54. **Sung, P., and D. L. Robberson.** 1995. DNA strand exchange mediated by a Rad51-ssDNA nucleoprotein filament with polarity opposite to that of RecA. Cell **82:**453–461.

55. **Thomas, B. J., and R. Rothstein.** 1989. The genetic control of direct-repeat recombination in Saccharomyces: the effect of rad52 and rad1 on mitotic recombination at GAL10, a transcriptionally regulated gene. Genetics **123:** 725–738.

56. **Van Dyck, E., A. Z. Stasiak, A. Stasiak, and S. C. West.** 1999. Binding of double-strand breaks in DNA by human Rad52 protein. Nature **398:**728–731.

57. **Whitehouse, I., A. Flaus, B. R. Cairns, M. F. White, J. L. Workman, and T. Owen-Hughes.** 1999. Nucleosome mobilization catalysed by the yeast SWI/ SNF complex. Nature **400:**784–787.

Attachment 2

Krejci, L., Song, B., Bussen, W., Rothstein, R., Mortensen, U., and Sung, P.

Interaction with Rad51 is indispensable for recombination mediator function of Rad52.

J. Biol. Chem. 277:40132-41. 2002

Interaction with Rad51 Is Indispensable for Recombination Mediator Function of Rad52*

Lumir Krejci‡, Binwei Song§, Wendy Bussen, Rodney Rothstein¶, Uffe H. Mortensen‡‖**, and Patrick Sung

From the Department of Molecular Medicine/Institute of Biotechnology, University of Texas Health Science Center at San Antonio, San Antonio, Texas 78245-3207, the ¶Department of Genetics and Development, Columbia University College of Physician and Surgeons, New York, New York 10032-2704, and ‖BioCentrum-DTU, Technical University of Denmark, 2800 Lyngby, Denmark

In the yeast *Saccharomyces cerevisiae*, the *RAD52* gene is indispensable for homologous recombination and DNA repair. Rad52 protein binds DNA, anneals complementary ssDNA strands, and self-associates to form multimeric complexes. Moreover, Rad52 physically interacts with the Rad51 recombinase and serves as a mediator in the Rad51-catalyzed DNA strand exchange reaction. Here, we examine the functional significance of the Rad51/Rad52 interaction. Through a series of deletions, we have identified residues 409–420 of Rad52 as being indispensable and likely sufficient for its interaction with Rad51. We have constructed a four-amino acid deletion mutation within this region of Rad52 to ablate its interaction with Rad51. We show that the rad52Δ409–412 mutant protein is defective in the mediator function *in vitro* even though none of the other Rad52 activities, namely, DNA binding, ssDNA annealing, and protein oligomerization, are affected. We also show that the sensitivity of the *rad52Δ409–412* mutant to ionizing radiation can be complemented by overexpression of Rad51. These results thus demonstrate the significance of the Rad51-Rad52 interaction in homologous recombination.

Homologous recombination in eukaryotic organisms is conserved in mechanism and mediated by a group of genes known as the *RAD52* epistasis group. The *RAD52* group members were first identified in the baker's yeast, *Saccharomyces cerevisiae*, and include *RAD50, RAD51, RAD52, RAD54, RAD55, RAD57, RAD59, RDH54/TID1, MRE11,* and *XRS2* (1–4). In *S. cerevisiae* and in other eukaryotes, homologous recombination is also an important means of eliminating DNA double-stranded breaks induced by ionizing radiation and other lesions that arise during the normal course of DNA replication (4). In mammals, homologous recombination also appears to be indispensable for cell viability and tumor suppression (1, 4).

A DNA double strand break can be repaired by pathways that are based on either end-joining or homologous recombination. In the latter case, the ends of the break are processed by a nuclease to yield 3′ ssDNA tails. These ssDNA[1] tails attract recombination proteins, and the resulting nucleoprotein complex conducts a search for a homologous DNA sequence. Next, one of the ssDNA tails invades the homologous DNA target to form a DNA joint where *de novo* DNA synthesis can take place, eventually leading to an exchange of genetic information between the recombining chromosomes and to restoration of the integrity of the broken chromosome (2, 3).

The enzymatic process responsible for the formation of heteroduplex DNA joints in recombination is called homologous DNA pairing and strand exchange (2). The *RAD51* encoded product, the equivalent of the *Escherichia coli* recombinase RecA, mediates the homologous DNA pairing and strand exchange reaction (5). Electron microscopic analyses have indicated that Rad51, like *E. coli* RecA protein, forms a highly ordered nucleoprotein filament on DNA (6). Biochemical studies have suggested that pairing and exchange of DNA strands in recombination processes occur within the confines of the Rad51-ssDNA nucleoprotein filament. The reaction phase in which the Rad51-ssDNA nucleoprotein filament is assembled is commonly referred to as the presynaptic phase, and the nucleoprotein filament as the presynaptic filament (2, 6, 7).

Formation of the presynaptic filament requires ATP binding by Rad51 (2). When plasmid length ssDNA substrates are used, presynaptic filament assembly is facilitated by the heterotrimeric single-stranded DNA binding factor, replication protein A (RPA), which functions to remove secondary structure in the ssDNA (5, 8, 9). The beneficial effect of RPA is seen most clearly when it is incorporated after Rad51 has been given an opportunity to nucleate onto the ssDNA template. In contrast, if RPA is added together with Rad51, it interferes with the filament assembly process by competing for binding sites on the ssDNA molecule. However, the inhibitory behavior of RPA can be alleviated by the addition of either of two recombination mediators (10), Rad52 or the Rad55-Rad57 heterodimer (11–14).

We are interested in the molecular basis of the mediator function of Rad52 and the Rad55-Rad57 heterodimer in the above mentioned reaction. Both Rad52 and the Rad55-Rad57 complex bind ssDNA and physically interact with Rad51 (15).[2] In the present study, we have performed a fine mapping of the domain in Rad52 that is responsible for the interaction with

¹ The abbreviations used are: ssDNA, single-stranded DNA; RPA, replication protein A; ScRPA, *Saccharomyces cerevisiae* RPA; DTT, dithiothreitol; GST, glutathione *S*-transferase; Oligo, oligonucleotide; aa, amino acid; MOPS, 4-morpholinepropanesulfonic acid.
² L. Krejci and P. Song, unpublished observation.

Rad51. Furthermore, we have used this information to introduce a small deletion mutation into Rad52 to ascertain the significance of Rad51-interaction in Rad52 mediator function. The combination of genetic and biochemical analyses of the mutant rad52 protein unequivocally demonstrate the requirement for a physical association of Rad52 with Rad51 to effect its mediator function.

MATERIALS AND METHODS

Yeast Media and Strains—Yeast extract-peptone-dextrose (YPD) medium, synthetic complete (SC) medium, and synthetic complete medium without leucine (SC−Leu) and without uracil (SC−Ura) were prepared as described previously (16) except that the synthetic media contained twice the amount of leucine (60 mg/liter). Yeast extract-peptone-acetate (YEPA) contained 10 g/liter yeast extract, 20 g/liter peptone, and 20 g/liter potassium acetate. Sporulation medium contained 2.5 g/liter yeast extract and 15 g/liter potassium acetate supplemented with 62 mg/liter Leu and 20.6 mg/liter each of adenine, His, Trp, and uracil. All strains are derivatives of Trp-303 (17) except that they are wild type for *RAD5* (18, 19). Standard genetic techniques were used to manipulate yeast strains (20). The *rad52Δ409–412* allele was integrated into the yeast genome at the *RAD52* locus by a cloning-free PCR-based allele replacement method (21). Specifically, gene-targeting substrates were made by amplifying a region of the *rad52* allele, which comprises the *Δ409–412* mutation, from the vector pR52Δ409–412.1 by PCR using the primers and Pr-Rad52-C-Adap-B (5′-GATCCCCGGGAATTGCCAT-GTGGTCTTCCAACTTCTCTTCG-3′) and Pr-C-adap-A (5′-AATTC-CAGCTGACCACCATGAAGGATCCCGTTGTAGCTAAG-3′). The underlined sections of the primers correspond to unique tags that match sequences upstream and downstream of *Kluyveromyces lactis URA3*, respectively. Next, two PCR fragments containing the upstream and the downstream two-thirds of the *K. lactis URA3* gene were fused individually to the *rad52Δ409–412* PCR fragment as described in Erdeniz *et al.* (21).

Plasmids for Protein Expression—GST fusion fragments of Rad52 were constructed as follows: GST-Rad52N (aa 1–168), GST-Rad52 M (aa 169–327), and GST-Rad52C (aa 328–504), encoded within the *Hpa*II/*Bgl*II, *Bgl*II/*Bam*HI, and *Bam*HI/*Dra*I fragments from the *RAD52* open reading frame were subcloned into *Sma*I-digested pGEX-3X, *Bam*HI-digested pGEX-2T, and *Sma*I-digested pGEX-3X vector, respectively. For the expression of other GST fusion proteins, specific primers with *Eco*RI sites were used for the PCR reactions. The PCR products were digested with *Eco*RI, purified by phenol extraction and ethanol precipitation, and then ligated into *Eco*RI-linearized pGEX-3X vector to fuse the Rad52 fragments to the GST protein. The ligation products were transformed into *E. coli* strain BL21(DE3) for protein expression.

DNA Substrates—The φX 174 viral (+) strand was purchased from New England Biolabs, and the replicative form (about 90% supercoiled form and 10% nicked circular form) was from Invitrogen. Oligonucleotide 1 used in the ssDNA annealing and DNA binding experiments had the sequence 5′-AAATGAACATAAAGTAAATAAGTATAAGGATAATA-CAAAATAAGTAAATGAATAAACATAGAAAATAAAGTAAAGGATAT-AAA-3′. Oligonucleotide 2 is the exact complement of oligonucleotide 1. These oligonucleotides were purified from a 15% polyacrylamide gel as described previously (22). The two oligonucleotides were labeled with [γ-^{32}P]ATP and T4 polynucleotide kinase for use in DNA binding and single strand annealing experiments.

DNA Binding Assays—Varying amounts of Rad52 or rad52 Δ409–412 protein was incubated with ^{32}P-labeled Oligo-1 (1.36 μM nucleotides) at 37 °C in 10 μl of buffer D (40 mM Tris-HCl, pH 7.8, 50 mM KCl, 1 mM DTT, and 100 μg/ml bovine serum albumin) for 10 min. After the addition of gel loading buffer (50% glycerol, 20 mM Tris-HCl, pH 7.4, 2 mM EDTA, 0.05% orange G), the reaction mixtures were resolved in 12% native polyacrylamide gels at 4 °C in TAE buffer (40 mM Tris-HCl, pH 7.4, 0.5 mM EDTA) and dried, and the DNA species were quantified using Quantity One software in the phosphorimaging device (Personal Molecular Imager FX from Bio-Rad). To release the bound DNA, the reaction mixture was deproteinized with 0.5% SDS and 500 μg/ml proteinase K at 37 °C for 10 min before being loading onto the polyacrylamide gel.

Single-stranded DNA Annealing Assays—Oligo-1 (3.6 μM nucleotides) and radiolabeled Oligo-2 (3.6 μM nucleotides) were incubated in separate tubes at 37 °C for 2 min in the absence or presence of RPA (0.55 μM) in 24 μl of buffer D. Rad52 or rad52 Δ409–412 (0.36 μM) was added in 2 μl to the tube containing Oligo-1 and then mixed with Oligo-2. The completed reactions (50 μl) were incubated at 25 °C, and at

the indicated times, 9 μl of the annealing reactions was removed and treated with 0.5% SDS, 500 μg/ml proteinase K, and an excess of unlabeled Oligo-2 (20 μM) at 25 °C for 5 min in a total volume of 15 μl. The various samples (6 μl) were resolved in 12% native polyacrylamide gels run in TAE buffer. DNA annealing was quantified as the portion of the ^{32}P-labeled Oligo-2 that had been converted into the double-stranded form.

Purification of Proteins—All of the GST fusion proteins were expressed in *E. coli* strain BL21(DE3), and all of the protein purification steps were carried out at 4 °C. For the purification of the GST fusion proteins, lysate was prepared from *E. coli* cell paste using a French press in buffer G (20 mM NaH$_2$PO$_4$, pH 7.4, 0.5 mM EDTA, 1 mM DTT, and 150 mM NaCl that also contained the protease inhibitors aprotinin, chymostatin, leupeptin, and pepstatin A at 5 μg/ml each, as well as 1 mM phenylmethylsulfonyl fluoride). The crude lysate was clarified by centrifugation (100,000 ×*g*, 90 min), and the supernatant (20 ml) from the centrifugation step was mixed with 1 ml of glutathione-Sepharose 4B (Amersham Biosciences) for 3 h at 4 °C. The beads were washed three times with 20 ml of buffer G containing 150 mM KCl. The bound GST fusion protein was eluted with 5 ml of 10 mM reduced glutathione in buffer G. The eluate was dialyzed against buffer G and concentrated to 10 mg/ml in a Centricon-30 microconcentrator.

Plasmids encoding untagged versions of Rad52 protein (pR52.2) and rad52Δ409–412 mutant protein (pR52Δ409–412.1) under the control of the *GAL-PGK* promoter were introduced into yeast strain BJ5464-6B. For the purification of these proteins, extract was prepared from 300 g of cell paste from 100 liters of culture in high salt buffer (23). The extract was clarified by centrifugation and then subjected to the chromatographic fractionation procedure described before (12) except that Sephacryl 400 was used instead of Sepharose 6B in the gel filtration step.

GST Pull-down Assay—The purified GST fusion proteins (0.4 μM) were incubated with purified Rad51 (0.2 μM) in 30 μl buffer G and incubated at 4 °C for 1 h before the reaction mixture was mixed with 10 μl of glutathione-Sepharose-4B beads in 150 μl of buffer K (20 mM KH$_2$PO$_4$, pH 7.4, 150 mM KCl, 10% glycerol, 0.01% Nonidet P-40) at 4 °C for an additional hour. The beads were then washed twice with 150 μl of buffer K with 300 mM KCl, and the bound proteins were eluted with 30 μl of 3% SDS. The supernatant that contained unbound protein, the KCl wash (10 μl each), and also the SDS eluate (3 μl) were subjected to immunoblotting analysis with anti-Rad51 antibodies to determine their Rad51 content. Coomassie Blue staining of the SDS eluates revealed that ∼70% of GST and all of the GST fusion proteins were immobilized on glutathione-Sepharose.

Binding of Rad52 to Rad51 Immobilized on Affi-gels—Affi-gel 15 beads containing Rad51 (Affi-Rad51; 5 mg/ml) and bovine serum albumin (Affi-BSA, 12 mg/ml) were prepared as described previously (24). Purified Rad52 or rad52 Δ409–412 (5 μg) was mixed with 5 μl of Affi-Rad51 or Affi-BSA in 50 μl of buffer K for 30 min at 4 °C. The beads were washed once with 150 μl of buffer K before being treated with 50 μl of 2% SDS to elute-bound proteins. The starting material, supernatant that contained unbound Rad52 or rad52 protein, and the SDS eluate (10 μl each) were analyzed by SDS-PAGE in a 10% gel.

Gel Filtration—A Sephacryl S400 column (1 × 30 cm, 20 ml total) was used to monitor the migration of Rad51 (30 μg), Rad52 (40 μg) and rad52Δ409–412 (40 μg) and to examine complex formation between Rad51 (30 μg) and Rad52 (40 μg). The mixtures of Rad51/Rad52 and Rad51/rad52Δ409–412 were incubated on ice for 1 h in 100 μl of buffer K and then filtered through the sizing column at 0.1 ml/min in the same buffer, collecting 0.5 ml fractions. The indicated column fractions were separated by SDS-PAGE electrophoresis to determine their content of the Rad51, Rad52, or rad52Δ409–412 proteins, respectively. For calibration of the column, thyroglobulin (669 kDa), catalase (232 kDa), and dextran blue (>2000 kDa) were used.

DNA Strand Exchange Reactions—All steps were carried out at 37 °C unless stated otherwise. The standard DNA strand exchange reaction was performed as described previously (23). Briefly, Rad51 (10 μM) was incubated with ssDNA (30 μM nucleotides) in 10 μl of buffer R (35 mM K-MOPS, pH 7.2, 1 mM DTT, 50 mM KCl, 2.5 mM ATP, and 3 mM MgCl$_2$) for 5 min. After the addition of the indicated amounts of RPA in 0.5 μl, the reaction mixtures were incubated for another 5 min before the incorporation of 1 μl of double-stranded DNA (25 μM nucleotides) and 1 μl of 50 mM spermidine hydrochloride. At the indicated times, a 4.5-μl portion of the reaction mixtures was withdrawn, deproteinized, and then analyzed in 0.9% agarose gels in TAE buffer. The gels were treated with eithidium bromide to stain the DNA species. Gel images were recorded in a NucleoTech gel documentation system and analyzed with GelExpert software. To examine the Rad52 mediator function,

Dissection of Rad52-Rad51 Interaction
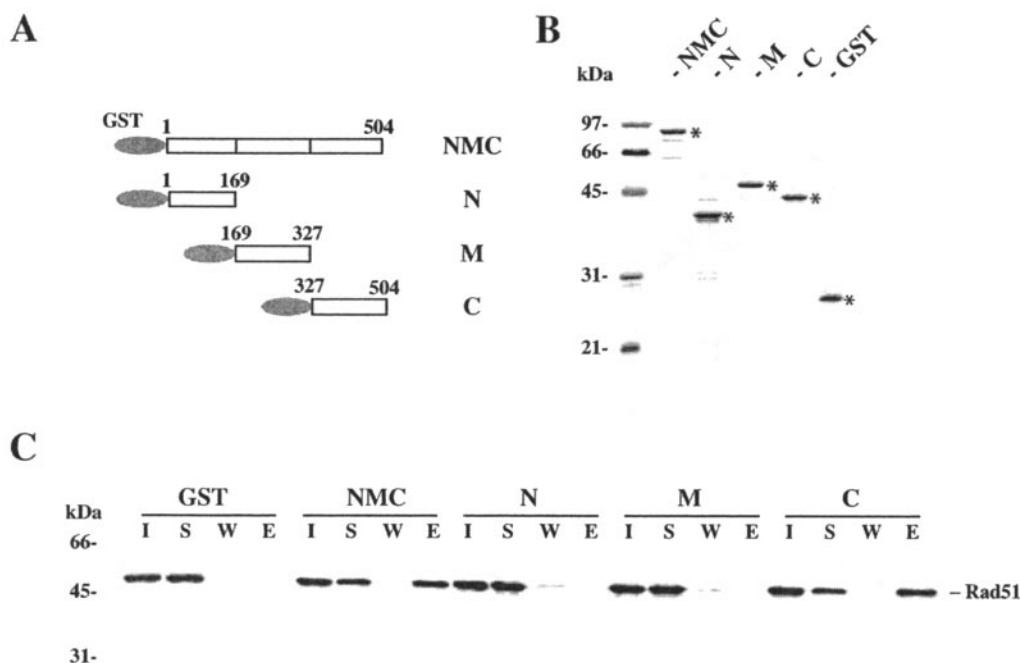
FIG. 1. **The carboxyl terminus of Rad52 is responsible for interaction with Rad51.** *A*, schematic representation of GST fusion proteins consisting of near full-length Rad52 (*NMC*) as well as the amino-terminal (*GST-N*), the middle (*GST-M*), and the carboxyl-terminal (*GST-C*) portions of Rad52. *B*, purified GST, GST-NMC, GST-M, and GST-C, 1 μg each and designated by an *asterisk*, were run in a 10% denaturing polyacrylamide gel and stained with Coomassie Blue. *C*, GST pull-down assay. Purified GST fusion proteins were incubated individually with Rad51 and then mixed with glutathione-Sepharose beads. The beads were washed twice with buffer containing 300 mM KCl before being treated with SDS to elute bound proteins. The input material (*I*), the supernatant after mixing with glutathione-Sepharose (*S*), the KCl wash (*W*), and the SDS eluate (*E*) from these binding reactions were subjected to electrophoresis in a 10% denaturing polyacrylamide gel followed by immunoblot analysis with anti-Rad51 antibodies to determine their Rad51 content.

reaction mixtures (12.5 μl, final volume) containing the indicated amounts of Rad51, Rad52, and RPA were incubated on ice for 45 min in 10.5 μl of buffer R followed by the addition of ssDNA and a 10-min incubation. After the incorporation of linear duplex and spermidine, the completed reactions were incubated and analyzed as described for the standard reaction. For the time course experiments in Fig. 7, the reactions were scaled up four times to 50 μl but were otherwise assembled in the same fashion.

Cellular Sensitivity to γ-Irradiation—Three independent haploid spores from each strain were picked and analyzed for their sensitivity to γ-irradiation, and the average values were reported. Yeast cultures were grown in YPD at 30 °C to the mid-log phase. At this point, the cultures were sonicated using a W-385 device (Heat Systems-Ultrasonics, Farmingdale, NY), and the appropriate number of cells were plated on YPD plates and irradiated in a Gammacell-220 ^{60}Co irradiator (Atomic Energy of Canada). In Fig. 8*B*, cells transformed with pYESS10-Rad51 (*2μ, RAD51*) and with the empty vector pRS426 (25) were grown on selective medium (SC−Ura) containing galactose as the sole carbon source at all stages of the experiment. The yeast cultures were analyzed as described above, except that for each strain, serial 10-fold dilutions were made and 5 μl of the diluted cell suspensions were spotted in duplicate on solid media prior to irradiation.

Determination of Mitotic Recombination Rates, Sporulation Efficiency, and Meiotic Recombination Frequencies—Mitotic rates of interchromosomal heteroallelic recombination were determined as described previously (26). For each strain, nine independent trials were performed. The meiotic interchromosomal heteroallelic recombination frequency, sporulation efficiency, and spore viability were determined as described in Lisby *et al.* (27) except that strains were grown at 30 °C. Three trials were performed for each strain.

RESULTS

Location of the Rad51 Interaction Domain—Rad52 possesses 504 amino acid residues (28). Results from yeast two-hybrid analyses have suggested that the carboxyl terminus of Rad52 encompassing residues 328 to 504 can interact with Rad51 (29). Exploiting this information, we divided Rad52 into three fragments: Rad52N (aa 34–168), Rad52 M (aa 169–327), and Rad52C (aa 328–504), which were fused individually to gluta-

thione-*S*-transferase (GST) as depicted in Fig. 1*A*. These GST fusion proteins were expressed in *E. coli* and purified using affinity chromatography on glutathione-Sepharose (Fig. 1*B*). We also expressed and purified a GST fusion protein, termed GST-NMC, which contain the Rad52 protein sequence starting from the third ATG codon (aa 34); the region corresponding to amino acid 1–34 is not required for *in vivo* Rad52 function.[3] To determine which portion of Rad52 contains the Rad51 binding domain, the purified GST fusion proteins were mixed with Rad51 and then immobilized on the glutathione-Sepharose beads. After washing with high salt buffer, the GST fusion proteins and associated Rad51 were eluted from the glutathione beads by treatment with SDS and then analyzed by immunoblotting with anti-Rad51 antibodies (Fig. 1*C*). The results show that Rad51 binds GST-NMC and GST-C, but not GST-N, GST-M, or GST alone. We then asked whether the purified GST fusions could be retained on Affi-gel 15 beads that contained covalently coupled Rad51 protein (24). As expected, the Affi-Rad51 beads were able to bind GST-NMC and GST-C but not GST-M, GST-N, or GST (data not shown). None of the GST-Rad52 fusion proteins was retained on Affi-gel 15 beads containing bovine serum albumin (data not shown). Thus, in agreement with yeast two-hybrid studies (29), the results from our *in vitro* analyses with purified Rad52 protein fragments revealed that the Rad51 interaction domain is located within the last 177 amino acid residues of Rad52 protein.

Fine Mapping of Rad51 Interaction Domain and Construction of a Rad51 Interaction-defective Mutant—To delimit the region in Rad52 required for interaction with Rad51, additional GST-tagged fragments of Rad52 derived from the carboxyl-terminal residues were generated (Fig 2*A*). These GST fusions were again purified by affinity chromatography and tested for

---

[3] R. Rothstein and U. H. Mortensen, unpublished observation.
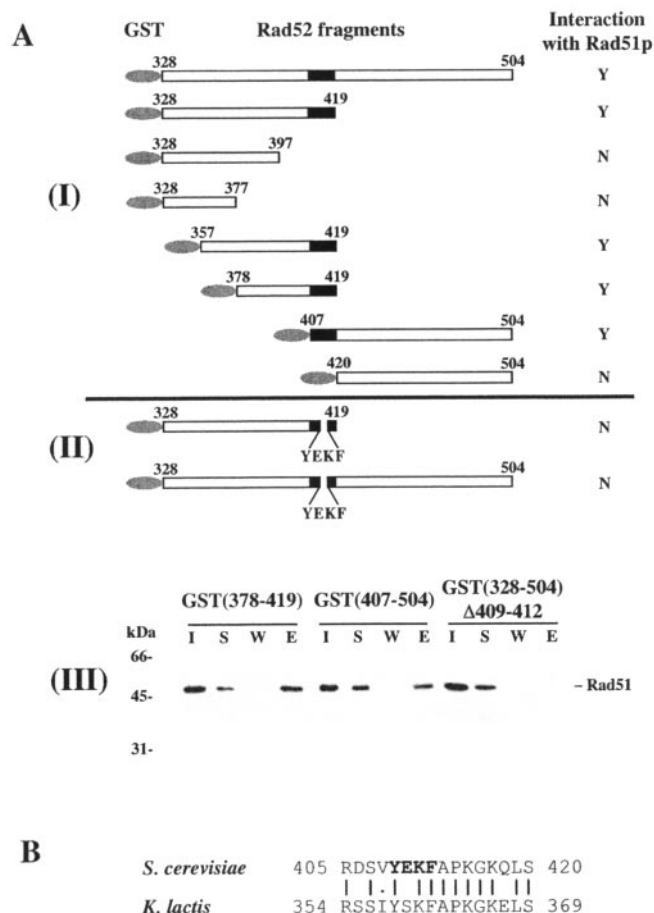
FIG. 2. **Minimal region required for Rad51-Rad52 association.** *A*, *panel I*, summary of domain mapping results from pull-down experiments with GST fusion proteins containing different segments of the Rad52 carboxyl terminus, done as described for Fig. 1*C*. The *numbers* indicate the amino acid residues in Rad52 protein. The ability (*Y*) or inability (*N*) of individual Rad52 fragments to bind Rad51 is indicated. The region (residues 407–419) common to all of the Rad52 fragments capable of Rad51 binding is shown in *black*. *Panel II* shows the two GST-Rad52 fusion proteins deleted for four amino acids (*YEKF*) in the putative Rad51 binding domain. This deletion mutation (Δ409–412) ablates the ability to bind Rad51. *Panel III* shows the GST pull-down assay with three Rad52 carboxyl-terminal fragments. Purified GST-(378–419), GST-(407–504), and GST-(328–504), with deletion of residues 409–412, were mixed with glutathione-Sepharose beads. The input mixture (*I*), the unbound protein in the supernatant (*S*), the wash (*W*), and the SDS eluate (*E*) were analyzed by SDS-PAGE. The amount of Rad51 protein was determined by immunoblot analysis. *B*, comparison of *S. cerevisiae* and *K. lactis* Rad52 sequences that contain the likely Rad51 binding domain. The four amino acids deleted in the ScRad52 protein are in *boldface type*.

Rad51 interaction by pull-down using glutathione-Sepharose beads as described before (Fig. 1*C*). The binding of the various GST-Rad52 fusions to Affi-gel-Rad51 beads was also examined. The results from these combined analyses, as summarized in Fig. 2, revealed that amino acids 407–419 of the Rad52 protein are likely involved in binding Rad51.

Overexpression of the Rad52 protein from another yeast, *K. lactis*, confers a dominant negative phenotype in *S. cerevisiae* that can be overcome by overexpression of the *S. cerevisiae* Rad51 (29). The authors of this study (29) suggested that the negative dominance of the *K. lactis* Rad52 in *S. cerevisiae* cells is due to the formation of a biologically inactive complex between KlRad52 and ScRad51. Even though the carboxyl terminus of the *S. cerevisiae* and *K. lactis* Rad52 counterparts display only a low level of identity (29%), the KlRad52 protein contains a sequence that is highly similar to the one in

ScRad52 protein found here to be involved in Rad51 binding (Fig 2*B*). Consistent with the suggestion that the sequence encoded within amino acid residues 407–419 of Rad52 is critical for Rad51 binding, we found that a small deletion spanning amino acid residues 409–412 within this region completely ablates the ability of Rad52 to interact with Rad51 (Fig. 2*A*, *panel II*), as determined by the GST pull-down assay, binding of the GST fusion proteins to Affi-Rad51 beads, and other criteria (see below).

Purification and Biochemical Characterization of a Rad51 Interaction-deficient Rad52 Mutant—The results presented above show that amino acid residues 409–412 are likely to be required for Rad51 binding. To further demonstrate the importance of these four amino acid residues, we introduced the same deletion mutation (Δ409–412) into the untagged Rad52 protein. For biochemical analyses, we overexpressed both the rad52Δ409–412 mutant and the wild-type protein by using the *GAL-PGK* promoter and galactose induction in the protease-deficient yeast strain BJ5464-6B. The level of expression of the wild-type and mutant proteins was very similar (data not shown), and they could be purified to near homogeneity by the same chromatographic procedure (see "Materials and Methods"; Fig. 3*A*). Approximately 1 mg of each of the wild-type and mutant proteins was obtained from 300 g of starting yeast paste. This represents a 5–10-fold improvement compared with protein yield obtained when the *PGK* promoter is used for protein expression, as described in our previously published study (12).

Unlike wild-type Rad52 protein, the purified rad52Δ409–412 mutant protein did not bind Affi-Rad51 beads (Fig. 3*B*), indicating that the four-amino acid deletion indeed eliminates the ability of Rad52 to associate with Rad51. Both Rad51 and Rad52 self-associate to form oligomeric molecules (14, 23, 30). A very large complex of these two proteins can be isolated in a sizing column (23). Accordingly, we subjected the purified rad52Δ409–412 mutant protein to sizing analysis in Sephacryl 400 to obtain independent verification that it does not associate with Rad51 and also to determine whether the Δ409–412 mutation affects self-association. When a mixture of Rad51 and wild-type Rad52 was analyzed, they formed a complex that emerged from the gel filtration column at an earlier position than either Rad51 or Rad52 alone (Fig. 4, compare *panel IV* with *panels I* and *III*). In contrast, when the rad52Δ409–412 mutant was mixed with Rad51, no apparent shift of the elution profile of either protein was observed (Fig. 4, compare *panel V* with *panels II* and *III*). Importantly, the peak of the rad52Δ409–412 mutant protein migrated at the same position as wild-type Rad52 (Fig. 4, compare *panels I* and *II*), strongly suggesting that the mutant rad52 protein has the same oligomeric composition as the wild-type protein. Thus, the results from the gel filtration analyses demonstrated that the rad52Δ409–412 mutant is defective in Rad51 interaction but maintains the ability to self-associate.

As first reported by Mortensen *et al.* (15) and later confirmed by others (13, 14, 23), Rad52 possesses an ssDNA binding function. We therefore addressed the possibility that the four-amino acid deletion affects the DNA binding activity of the rad52Δ409–412 mutant protein. To do this, increasing amounts of Rad52 and rad52Δ409–412 proteins were incubated with a ^{32}P-labeled 83-mer oligonucleotide. Subsequently, the capacity of these proteins to bind DNA was evaluated by gel mobility shift of the radiolabeled DNA substrate. The results presented in Fig. 5*A* show that rad52Δ409–412 shifts the DNA fragment just as efficiently as the wild-type protein. We also used φX ssDNA as substrate to test the DNA binding capacity of the protein species. As in the previous experiment, no differ-

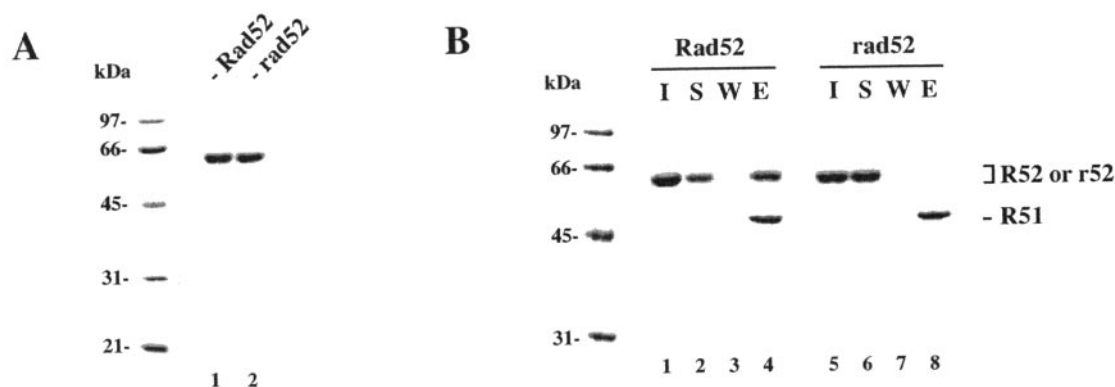FIG. 3. **Mutation in Rad52 that abrogates interaction with Rad51.** *A*, SDS-PAGE analysis of Rad52 (2 μg, *lane 1*) and rad52Δ409−412 (2 μg, *lane 2*) proteins. *B*, purified wild type and rad52Δ409−412 were mixed with Affi-Rad51 beads. The beads were washed with buffer and then treated with SDS to elute bound Rad52 and rad52Δ409−412. The input mixture (*I*), the supernatant containing unbound Rad52 or rad52Δ409−412 (*S*), the wash (*W*), and the SDS eluate (*E*) were run on 10% SDS-PAGE followed by staining with Coomassie Blue. Given the oligomeric nature of Rad51 (23, 30), some of the Rad51 molecules were tethered to the Affi-beads through other covalently conjugated molecules and therefore were readily eluted by SDS treatment (*lanes 4* and *8*). The rad52Δ409−412 mutant protein is designated as *rad52*.
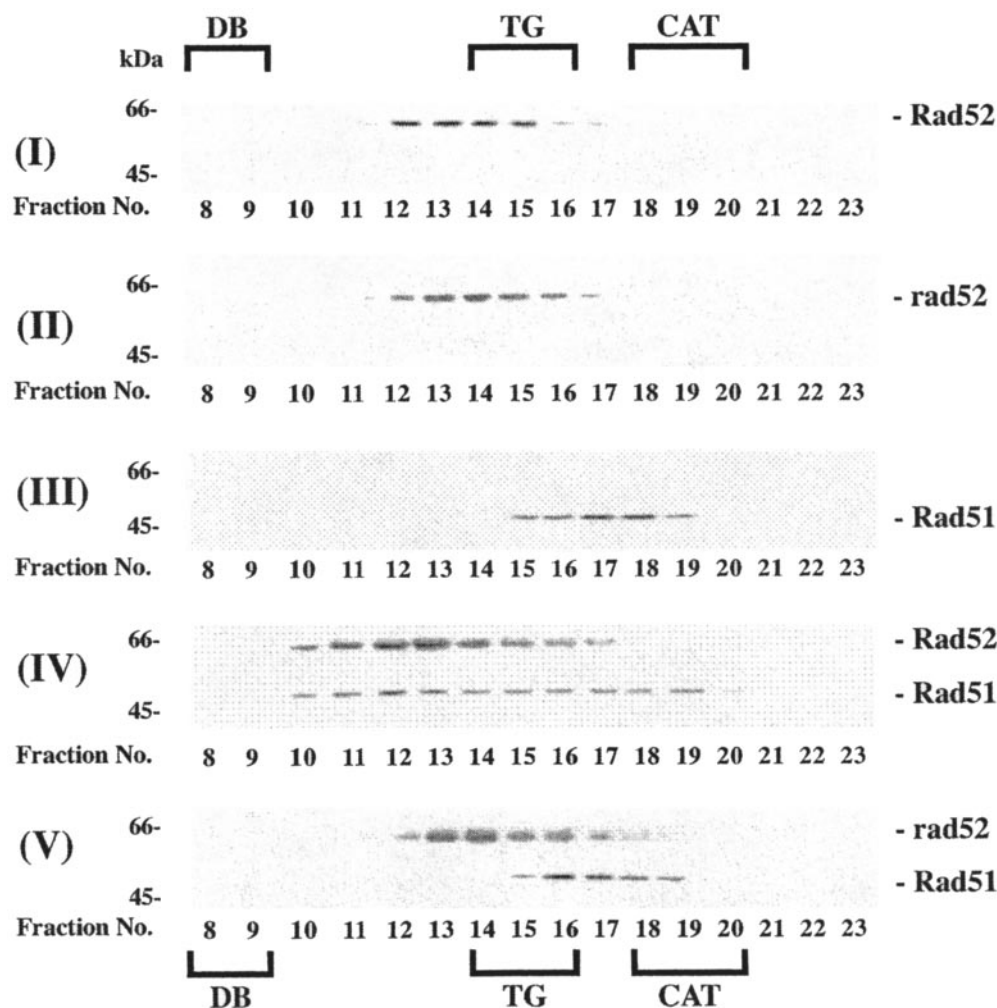
FIG. 4. **Oligomeric structure of Rad52 is unaffected by the Δ409−412 mutation.** Rad52 protein (*panel I*), rad52Δ409−412 protein (*panel II*), and Rad51 protein (*panel III*) were filtered through a Sephacryl S400 column. In *panels IV* and *V*, Rad51 and either Rad52 (*IV*) or rad52Δ409−412 (*V*) were mixed, incubated on ice for 1 h, and then filtered. The indicated fractions were run on 10% SDS-PAGE followed by staining with Coomassie Blue. The elution positions of the size markers are indicated: *DB*, dextran blue (>2,000 kDa); *TG*, thyroglobulin (669 kDa); *CAT*, catalase (223 kDa).

ence in DNA binding activity was observed between wild-type and mutant proteins (data not shown).

In addition to DNA binding, Rad52 also anneals complementary DNA strands (15). Interestingly, the Rad52-mediated DNA annealing reaction occurs efficiently with RPA-coated DNA strands (8, 14), whereas RPA alone slows the spontaneous rate of DNA annealing (8, 14). This annealing reaction is likely to involve a specific interaction between Rad52 and RPA, as the heterologous *E. coli* SSB and human RPA strongly inhibit the Rad52-ssDNA annealing activity (8). We examined the
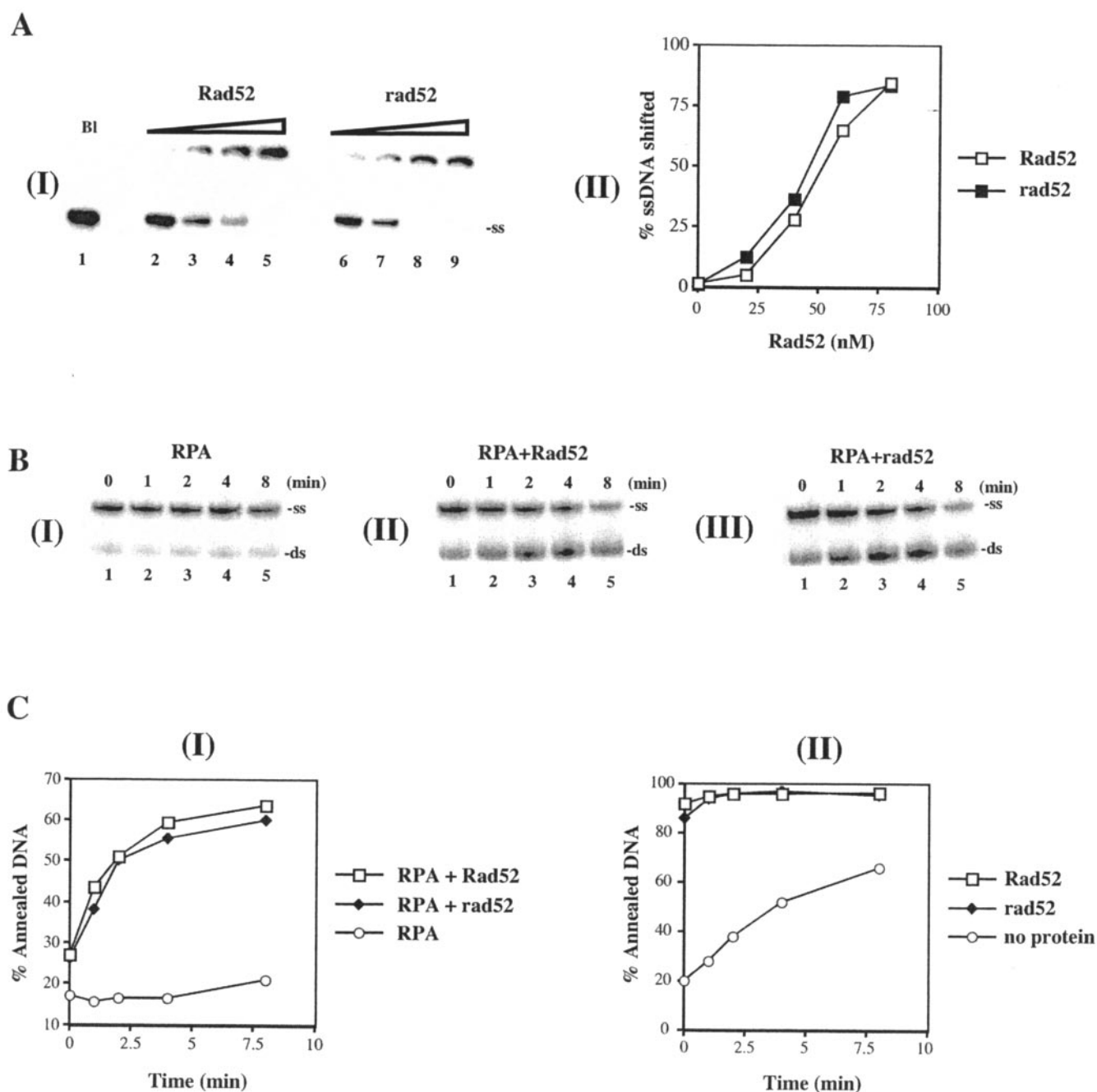
FIG. 5. **DNA binding and strand annealing activities of rad52Δ409–412.** *A*, in *panel I*, ^{32}P-labeled Oligo-1 (1.4 μM nucleotides), designated as *ss*, was incubated without protein (*Bl*; *lane 1*) and with Rad52 (35, 70, 105, and 140 nM in *lanes 2–5*, respectively) or rad52Δ409–412 (35, 70, 105, and 140 nM in *lanes 6–9*, respectively). The reaction mixtures were analyzed on a nondenaturing polyacrylamide gel, which was dried and subjected to phosphorimaging analysis to quantify the results (*panel II*). The rad52Δ409–412 mutant is designated as *rad52*. *B*, unlabeled Oligo-1 (3.6 μM nucleotides) and radiolabeled Oligo-2 (3.6 μM nucleotides) were incubated separately with RPA (0.55 μM; *panels I, II,* and *III*) for 2 min. The annealing reactions were initiated by mixing the RPA-coated oligonucleotides and Rad52 (0.36 μM; *panel II*) or rad52Δ409–412 (0.3 μM; *panel III*) in a final volume of 50 μl. At the indicated times, 9 μl of each reaction was removed and treated with 0.5% SDS, 500 μg/ml proteinase K, and an excess of unlabeled Oligo-2 (20 μM nucleotides) at room temperature for 5 min. The reaction mixtures were resolved in 12% native polyacrylamide gels. *Panel I* displays results from the reaction in which no Rad52 or rad52Δ409–412 was added. *C*, in *panel I*, the results from *B* are graphed. Another set of strand annealing experiments using the same amounts of RPA-free DNA substrates and Rad52 or rad52Δ409–412 were carried out as in *B*, and the results are graphed in *panel II*. Consistent with previously published work (8), a higher spontaneous rate of DNA annealing was seen in the absence of RPA (compare the RPA curve in *panel I* with the no protein curve in *panel II*).

rad52Δ409–412 mutant protein for its ability to anneal ScRPA-coated complementary single strands. The results from this experiment indicate that the rate and extent of the annealing reaction obtained in the presence of either Rad52 or rad52Δ409–412 are essentially identical for both (Fig. 5*B* and Fig. 5*C*, *panel I*). With DNA substrates free of ScRPA, the rad52Δ409–412 mutant protein was again as proficient as wild-type Rad52 in its annealing reaction (Fig. 5*C*, *panel II*).

This observation shows that rad52Δ409–412 likely retains the ability to physically interact with RPA.

Taken together, the biochemical analyses documented here allowed us to conclude that rad52Δ409–412 mutant has the wild-type level of ssDNA binding and DNA annealing activities and also possesses the same oligomeric state as the wild-type protein. In addition, the ability of the rad52Δ409–412 mutant to anneal RPA-coated single strands like the wild-type protein
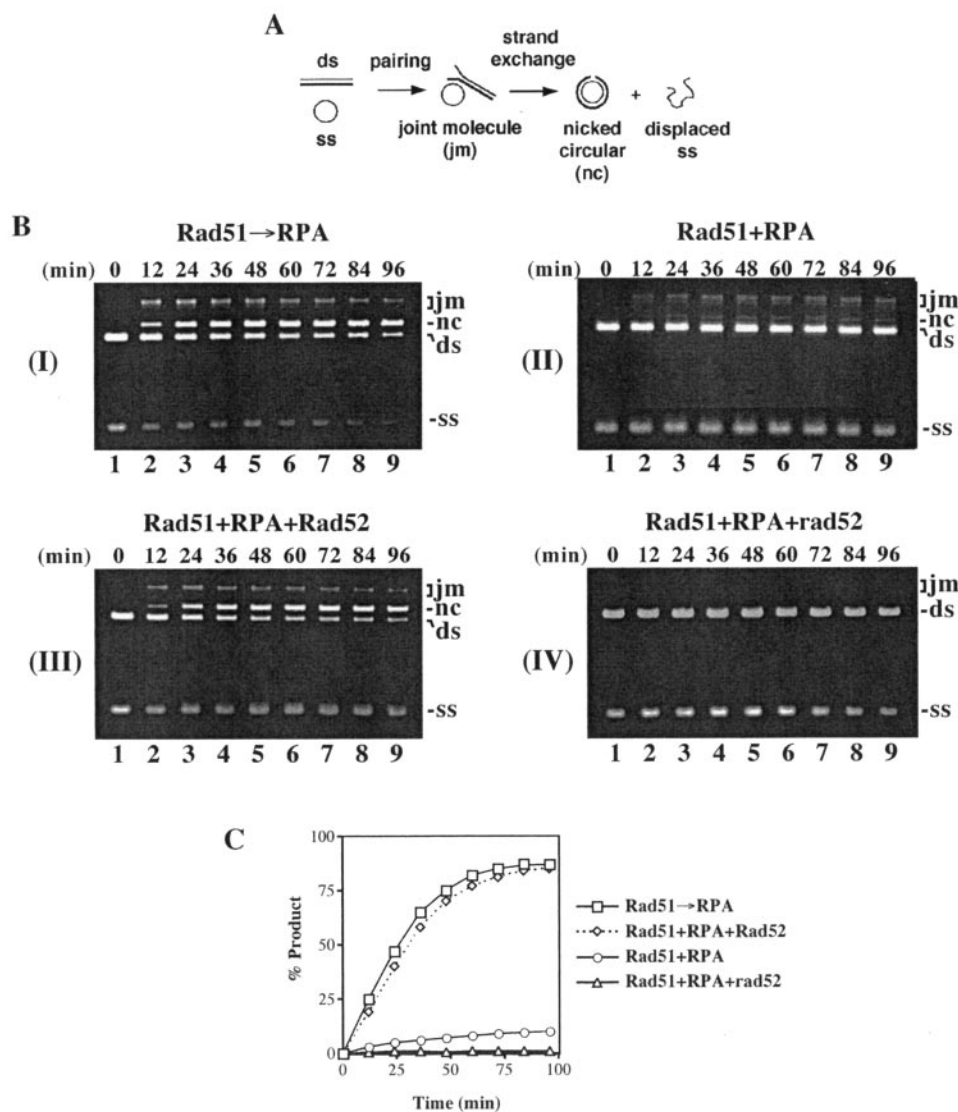
FIG. 6. **The rad52Δ409–412 mutant lacks recombination mediator activity.** *A*, schematic representation of the homologous DNA pairing and strand exchange reaction. Homologous pairing between the ssDNA (*ss*) and linear duplex (*ds*) substrates yields a DNA joint molecule (*jm*), which is converted into a nicked circular duplex molecule (*nc*) by strand exchange. *B*, in *panel I*, the φX174 ssDNA (30 μM nucleotides) was first incubated with Rad51 (10 μM) for 5 min before RPA (2 μM) was added. Following another 5-min incubation, the linear duplex (25 μM nucleotides) was incorporated to complete the reaction. The reaction in *panel II* contained the same amount of DNA substrates and proteins as *panel I* except that the ssDNA was incubated with both Rad51 and RPA for 10 min before the duplex was added. The reactions in *panels III* and *IV* were assembled as in *panel II* except that either Rad52 (1.2 μM) or rad52Δ409–412 (1.2 μM; designated as rad52) was also present during the incubation of ssDNA with Rad51 and RPA. *C*, graphical representation of the results in *B*.

is consistent with the premise that it retains the ability to interact with RPA.

rad52Δ409–412 Mutant Is Specifically Defective in Mediator Function—The above data have demonstrated that the rad52Δ409–412 mutant protein does not interact with Rad51 but that it otherwise behaves like the wild-type protein in various biochemical attributes. We next tested whether the rad52Δ409–412 mutant protein retains the recombination mediator activity of wild-type Rad52.

We and others have shown that, with plasmid length DNA substrates, the efficiency of the Rad51-mediated DNA strand exchange reaction is greatly enhanced by RPA (8, 12). However, the order of addition of RPA relative to Rad51 is critical for efficient DNA strand exchange. Specifically, if RPA is added after Rad51 has already nucleated onto the ssDNA, a robust strand exchange reaction is observed. In contrast, if RPA is added to the ssDNA at the same time as Rad51, the level of DNA strand exchange diminishes greatly (11–14) (Fig. 6*B*, *panels I* and *II*). As shown before and repeated here (Fig. 6*B*,

panel III), the inhibitory effect of RPA in the latter experiment can be alleviated by adding a substoichiometric amount of Rad52 (10 μM Rad51 and 1.2 μM Rad52). In contrast, when the same experiment was performed with the equivalent amount of rad52Δ409–412 mutant protein, the suppressed level of DNA strand exchange caused by RPA was not relieved. In fact, the presence of the rad52Δ409–412 protein further reduced the already low level of DNA strand exchange caused by RPA co-addition. Because of this result, we also examined lower amounts of rad52Δ409–412 (0.4 to 1.0 μM) for a possible mediator effect but found that it is devoid of such activity at any of these concentrations (Fig. 7, *lanes 8–12*). On the other hand, the addition of rad52Δ409–412 (0.4–1.2 μM) and RPA to a preformed Rad51-ssDNA complex did not affect the efficiency of DNA strand exchange (data not shown). Taken together, the results establish a direct linkage between the Rad51-interacting activity of Rad52 and its mediator function in the DNA strand exchange reaction.

Repair and Recombination Defects of rad52Δ409–412—The

FIG. 7. **Mediator activity as a function of concentration of Rad52 or rad52Δ409–412.** *A*, increasing amounts of either Rad52 (0.4, 0.6, 0.8, 1.0, and 1.2 μM in *lanes 3–6*, respectively) or rad52Δ409–412 (0.4, 0.6, 0.8, 1.0, and 1.2 μM in *lanes 8–12*, respectively), Rad51 (10 μM; *lanes 2–12*), or RPA (2 μM; *lanes 2–12*) were incubated with ssDNA (30 μM nucleotides) for 10 min followed by the incorporation of the linear duplex (25 μM nucleotides) to complete the reactions; the reaction in *lane 2* (*Inh*) did not contain Rad52 or rad52Δ409–412. In *lane 1* (*Std*), ssDNA (30 μM) was incubated with Rad51 (10 μM) for 5 min followed by the addition of RPA (2 μM) and a 5-min incubation before the duplex substrate (25 μM nucleotides) was incorporated to complete the reaction. Aliquots of the reactions were withdrawn at 30 and 60 min and processed for electrophoresis. The results from the 30-min time point are shown. *B*, the results from *A* and from analyzing the gel containing the 60-min time point samples are graphed.
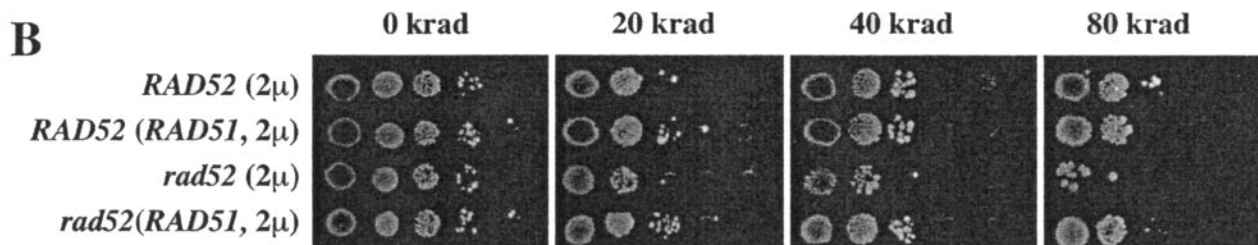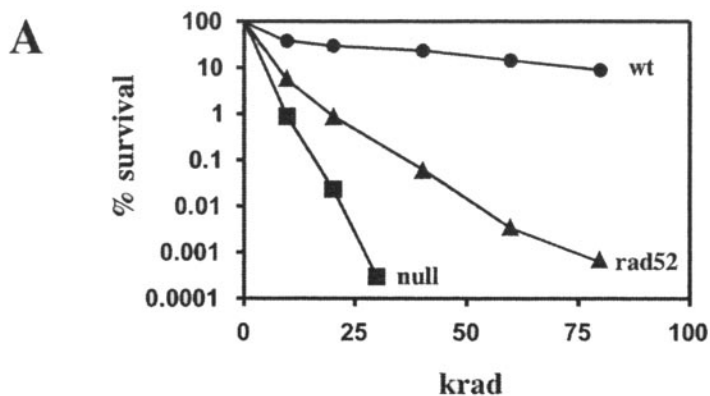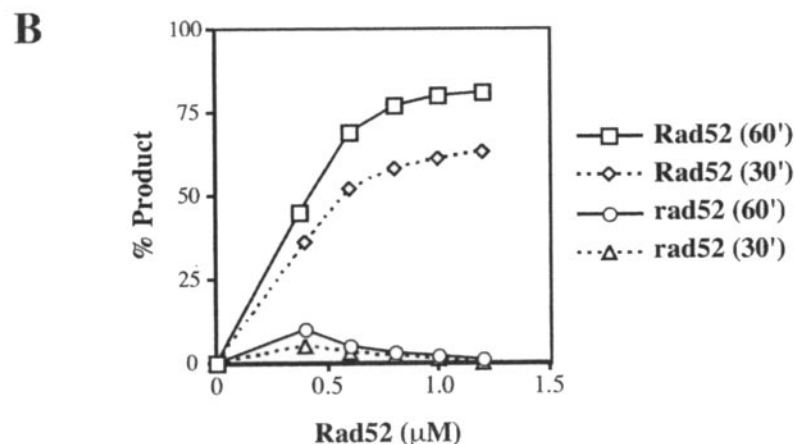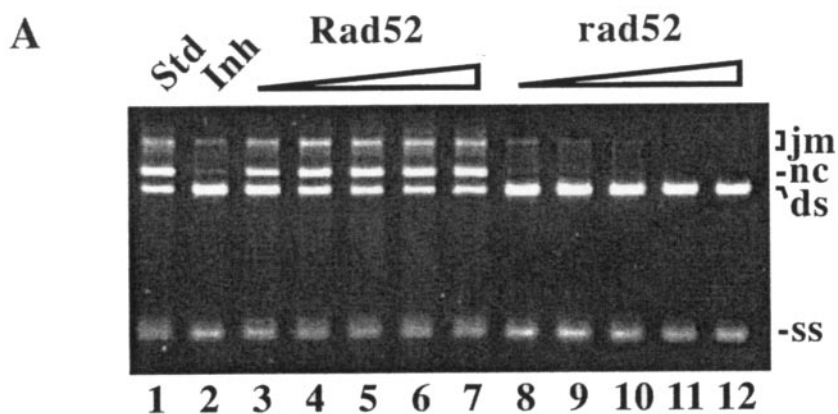
FIG. 8. **γ-Ray sensitivity of the *rad52Δ409–412* mutant.** *A*, the log fraction of surviving cells (*% survival*) after exposure to the indicated doses of γ-radiation (*krad*) of yeast strains with the following genetic backgrounds: wild-type *RAD52* (*wt*), rad52Δ409–412 (*rad52*), and rad52Δ (*null*). *B*, effect of *RAD51* overexpression. *RAD52* or rad52Δ409–412 cells were spotted in serial 10-fold dilutions and irradiated as indicated (0, 20, 40, and 80 kilorads). The same set of strains was also transformed with a *2μ* vector or the same vector containing the *RAD51* gene and then analyzed. The *rad52Δ409–412* allele is designated *rad52*.

biochemical experiments described above demonstrated a specific defect in the rad52Δ409–412 mutant protein, namely, that it fails to interact with Rad51 and is devoid of recombination mediator function. To establish the role of the Rad52 mediator activity *in vivo*, we replaced the chromosomal *RAD52* gene with the *rad52Δ409–412* allele in the Trp-303 background (see "Material and Methods") and then tested the mutant strain for its γ-ray sensitivity. The *rad52Δ409–412* mutant strains show a marked increase in sensitivity to ionizing radiation although not to the same extent as isogenic *rad52* deletion strain (Fig. 8*A*). This result indicates that the interaction with Rad51 is indeed important for the full biological activity of Rad52 protein in double strand break repair *in vivo*. Interestingly, the γ-ray sensitivity of the *rad52Δ409–412* mutant can be complemented fully by the overexpression of the Rad51 protein on a *2μ* plasmid (Fig. 8*B*). Similar complementation by Rad51 overexpression has been observed by Livingston and Kaytor (31) for a *rad52* allele (*rad52Δ327*) that lacks the carboxyl-terminal 177 residues.

We also compared the frequencies of meiotic interchromosomal heteroallelic recombination and spore viability of wild-type *RAD52* and *rad52Δ409–412* strains (data not shown). In both cases, no significant differences were observed, indicating that the Rad51-Rad52 interaction is not essential for successful completion of meiosis. In contrast, the mitotic interchromosomal heteroallelic recombination is reduced 4-fold in the *rad52Δ409–412* strain (data not shown). Thus, the overall phenotype of the *rad52Δ409–412* strain is very similar to that obtained with the *rad52Δ327* strain except that the spore viability of the latter strain is somewhat impaired (32).

DISCUSSION

The Rad51 interaction domain was first shown to reside within the carboxyl-terminal 177 amino acids residues of Rad52 by a yeast two-hybrid analysis (29). Here we have verified the two-hybrid result by showing biochemically that the carboxyl terminus, but not the amino-terminal and middle portions, of Rad52 has the ability to bind Rad51 in the absence of another protein factor or DNA. Next, we finely mapped the Rad51 interaction domain and used this information to conduct a variety of biochemical and genetic experiments to firmly establish the biological and functional significance of the Rad51-Rad52 association.

First we examined a series of deletion fragments derived from the carboxyl terminus of Rad52 for complex formation with Rad51. The results strongly suggest that a short sequence encompassing residues 407–419 is involved in mediating interaction with Rad51. This mapping information and a sequence comparison to *K. lactis* Rad52 prompted us to introduce a short deletion in the region spanning residues 409–412 into the full-length Rad52 protein. We find that the rad52Δ409–412 mutant protein can be stably expressed in yeast cells and that it behaves like wild-type Rad52 during column chromatography, allowing us to use the same procedure to purify both wild-type and mutant proteins to near homogeneity for biochemical experiments. Here we have shown, by several criteria, that the rad52Δ409–412 mutant protein lacks the ability to interact with Rad51. In contrast, its ability to bind DNA and mediate DNA annealing, as well as its oligomerizing properties, are indistinguishable from those of the wild-type protein. These results demonstrated that the short sequence (*i.e.* aa residues 407–419) in Rad52 identified in our mapping work is likely to be indispensable to and is possibly responsible for Rad51 binding. Furthermore, the biochemical results have verified that the Rad51 interaction-defective rad52Δ409–412 mutant is normal in all other known biochemical attributes of Rad52.

In DNA strand exchange experiments, the rad52Δ409–412 mutant protein over a wide range of concentrations is devoid of the mediator function seen in the Rad52 protein. Consistent with the biochemical result, the *rad52Δ409–412* mutation renders cells sensitive to ionizing radiation and confers a 4-fold decrease in mitotic recombination. It has been suggested from yeast two-hybrid and *in vitro* studies that Rad52 physically interacts with RPA and that this interaction is important for its mediator activity and biological function (8, 13, 14, 33). It could be argued that the lack of mediator function in the rad52Δ409–412 mutant protein is due to an inability to recognize RPA. We have attempted to demonstrate a direct interaction between purified Rad52 and RPA but have thus far been unable to find the conditions to detect such an interaction in the absence of DNA. However, it remains quite possible that the interaction between Rad52 and RPA occurs only when these factors are bound to DNA. Consistent with this premise, it has been demonstrated that Rad52 effectively anneals DNA strands coated with ScRPA (8, 14) but not with heterologous ssDNA-binding proteins (8), implying a direct interaction between Rad52 and RPA as the likely reason for this observed specificity. We have demonstrated that the rad52Δ409–412 mutant is perfectly capable of mediating ssDNA annealing with an ScRPA-coated template. This result strongly suggests that the mutant protein also retains the ability to interact with RPA (14). Given this consideration, our data provide evidence that the lack of recombination mediator function in rad52Δ409–412 is specifically due to its inability to form a complex with Rad51 protein.

The DNA repair deficiency of the *rad52Δ409–412* mutant strain can be complemented by Rad51 overproduction. It seems possible that a substantial increase in the intracellular pool of Rad51 may accelerate the assembly of the presynaptic Rad51 filament, thus rendering this process less prone to the competitive effect of RPA even when the Rad52 mediator function has been disabled, as in the case of the *rad52Δ409–412* mutant. However, a more attractive explanation is that the elevated Rad51 levels facilitate complex formation between Rad51 and other mediator proteins. This could conceivably lead to more effective loading of Rad51 onto ssDNA via the other recombination mediators. In fact, our observation that Rad51 shows only a weak interaction with the Rad55-Rad57 complex[4] (11) is congruent with the latter view. Mutants of the *RAD59* gene show some deficiency in Rad51-dependent recombination events (34, 35). It remains to be seen whether Rad59 also functions as a mediator in Rad51-catalyzed homologous DNA pairing and strand exchange and, if so, whether the mediator activity of Rad59 will require complex formation with Rad51 that is enhanced by increased intracellular Rad51 levels.

The *rad52* null mutation renders cells highly defective in recombination, and overexpression of Rad51 does not compensate for the loss of Rad52 (36). Thus, Rad52 must have a function in recombination/repair pathways independent of Rad51 interaction. It is possible that in the cellular setting, Rad52 renders the RPA-coated ssDNA template more accessible to Rad51 even in the absence of a specific interaction with Rad51. Alternatively, or additionally, the Rad51 interaction-defective rad52 variant may enhance the interaction between Rad51 and other recombination mediators without directly contacting Rad51. Also, it seems possible that the severe phenotype associated with *RAD52* deletion may be related to the ability of Rad52 to promote the assembly of DNA repair centers as revealed in recent cytological studies (27).

---

[4] L. Krejci and P. Song, unpublished observation.

REFERENCES

1. Pierce, A. J., Stark, J. M., Araujo, F. D., Moynahan, M. E., Berwick, M., and Jasin, M. (2001) *Trends Cell Biol.* **11,** S52–59
2. Sung, P., Trujillo, K. M., and Van Komen, S. (2000) *Mutat. Res.* **451,** 257–275
3. Paques, F., and Haber, J. E. (1999) *Microbiol. Mol. Biol. Rev.* **63,** 349–404
4. Cox, M. M. (2001) *Annu. Rev. Genet.* **35,** 53–82
5. Sung, P. (1994) *Science* **265,** 1241–1243
6. Bianco, P. R., Tracy, R. B., and Kowalczykowski, S. C. (1998) *Front. Biosci.* **3,** D570–603
7. Roca, A. I., and Cox, M. M. (1997) *Prog. Nucleic Acids Res. Mol. Biol.* **56,** 129–223
8. Sugiyama, T., New, J. H., and Kowalczykowski, S. C. (1998) *Proc. Natl. Acad. Sci. U. S. A.* **95,** 6049–6054
9. Sigurdsson, S., Trujillo, K., Song, B., Stratton, S., and Sung, P. (2001) *J. Biol. Chem.* **276,** 8798–8806
10. Beernink, H. T., and Morrical, S. W. (1999) *Trends Biochem. Sci.* **24,** 385–389
11. Sung, P. (1997) *Genes Dev.* **11,** 1111–1121
12. Sung, P. (1997) *J. Biol. Chem.* **272,** 28194–28197
13. New, J. H., Sugiyama, T., Zaitseva, E., and Kowalczykowski, S. C. (1998) *Nature* **391,** 407–410
14. Shinohara, A., Shinohara, M., Ohta, T., Matsuda, S., and Ogawa, T. (1998) *Genes Cells* **3,** 145–156
15. Mortensen, U. H., Bendixen, C., Sunjevaric, I., and Rothstein, R. (1996) *Proc. Natl. Acad. Sci. U. S. A.* **93,** 10729–10734
16. Sherman, F. (1991) in *Guide to Yeast Genetics and Molecular Biology*, (Guthrie, C., and Fink, G. R., eds) pp. 3–21, Academic Press, San Diego, CA
17. Thomas, B. J., and Rothstein, R. (1989) *Cell* **56,** 619–630
18. Fan, H. Y., Cheng, K. K., and Klein, H. L. (1996) *Genetics* **142,** 749–759
19. Zou, H., and Rothstein, R. (1997) *Cell* **90,** 87–96
20. Sherman, F., Fink, G. R., and Hicks, J. B. (1986) *Methods in Yeast Genetics*, Cold Spring Harbor Laboratory Press, Cold Spring Harbor, NY
21. Erdeniz, N., Mortensen, U. H., and Rothstein, R. (1997) *Genome Res.* **7,** 1174–1183
22. Trujillo, K. M., and Sung, P. (2001) *J. Biol. Chem.* **276,** 35458–35464
23. Song, B., and Sung, P. (2000) *J. Biol. Chem.* **275,** 15895–15904
24. Petukhova, G., Stratton, S., and Sung, P. (1998) *Nature* **393,** 91–94
25. Jiang, H., Xie, Y., Houston, P., Stemke-Hale, K., Mortensen, U. H., Rothstein, R., and Kodadek, T. (1996) *J. Biol. Chem.* **271,** 33181–33186
26. Smith, J., and Rothstein, R. (1999) *Genetics* **151,** 447–458
27. Lisby, M., Rothstein, R., and Mortensen, U. H. (2001) *Proc. Natl. Acad. Sci. U. S. A.* **98,** 8276–8282
28. Adzuma, K., Ogawa, T., and Ogawa, H. (1984) *Mol. Cell. Biol.* **4,** 2735–2744
29. Milne, G. T., and Weaver, D. T. (1993) *Genes Dev.* **7,** 1755–1765
30. Passy, S. I., Yu, X., Li, Z., Radding, C. M., and Egelman, E. H. (1999) *Proc. Natl. Acad. Sci. U. S. A.* **96,** 4279–4284
31. Kaytor, M. D., and Livingston, D. M. (1996) *Curr. Genet.* **29,** 203–210
32. Boundy-Mills, K. L., and Livingston, D. M. (1993) *Genetics* **133,** 39–49
33. Hays, S. L., Firmenich, A. A., Massey, P., Banerjee, R., and Berg, P. (1998) *Mol. Cell. Biol.* **18,** 4400–4406
34. Bai, Y., and Symington, L. S. (1996) *Genes Dev.* **10,** 2025–2037
35. Bai, Y., Davis, A. P., and Symington, L. S. (1999) *Genetics* **153,** 1117–1130
36. Asleson, E. N., Okagaki, R. J., and Livingston, D. M. (1999) *Genetics* **153,** 681–692

Attachment 3

Seong, C., Sehorn, M.G., Plate, I., Shi, I., Song, B., Chi, P., Mortensen, U., Sung, P., and Krejci, L.

Molecular anatomy of the recombination mediator function of Saccharomyces cerevisiae Rad52. The Journal of biological chemistry.

J Biol Chem. 283(18):12166-74. 2008

Molecular Anatomy of the Recombination Mediator Function of *Saccharomyces cerevisiae* Rad52*[S]

Changhyun Seong[‡1], Michael G. Sehorn[‡2], Iben Plate[§], Idina Shi[‡], Binwei Song[¶3], Peter Chi[‡], Uffe Mortensen[§], Patrick Sung[‡||], and Lumir Krejci[‡||1,4]

From the [‡]Department of Molecular Biophysics and Biochemistry, Yale University School of Medicine, New Haven, Connecticut 06520, the [§]Center for Microbial Biotechnology, BioCentrum-DTU, Technical University of Denmark, DK-2800 Lyngby, Denmark, the [¶]Institute of Biotechnology and Department of Molecular Medicine, University of Texas Health Science Center at San Antonio, San Antonio, Texac 78245, and the [||]National Center for Biomolecular Research, Masaryk University, Brno 62500, Czech Republic

A helical filament of Rad51 on single-strand DNA (ssDNA), called the presynaptic filament, catalyzes DNA joint formation during homologous recombination. Rad52 facilitates presynaptic filament assembly, and this recombination mediator activity is thought to rely on the interactions of Rad52 with Rad51, the ssDNA-binding protein RPA, and ssDNA. The N-terminal region of Rad52, which has DNA binding activity and an oligomeric structure, is thought to be crucial for mediator activity and recombination. Unexpectedly, we find that the C-terminal region of Rad52 also harbors a DNA binding function. Importantly, the Rad52 C-terminal portion alone can promote Rad51 presynaptic filament assembly. The middle portion of Rad52 associates with DNA-bound RPA and contributes to the recombination mediator activity. Accordingly, expression of a protein species that harbors the middle and C-terminal regions of Rad52 in the *rad52 Δ327* background enhances the association of Rad51 protein with a HO-made DNA double-strand break and partially complements the methyl-methane sulfonate sensitivity of the mutant cells. Our results provide a mechanistic framework for rationalizing the multi-faceted role of Rad52 in recombination and DNA repair.

In eukaryotes, homologous recombination (HR)[5] is mediated by genes of the *RAD52* epistasis group. HR plays a prominent role in chromosome damage repair and helps restart stalled DNA replication forks (1–3). In addition, meiotic recombination mediated by the *RAD52* group genes ensures the proper segregation of homologous chromosomes at meiosis I. Accordingly, mutants of the *RAD52* group are sensitive to genotoxic agents, bear a strong mutator phenotype, and exhibit severe meiotic abnormalities (2). In mammals, a deficiency in HR causes cell inviability and can lead to the cancer phenotype (4, 5).

The mechanistic aspects of HR are best understood in the yeast *Saccharomyces cerevisiae*, within the context of DNA double-strand break (DSB) repair (6, 7). In *S. cerevisiae*, the *RAD51*, *RAD52*, *RAD54*, *RAD55*, *RAD57*, *RAD59*, and *RDH54* genes are the core members of the *RAD52* epistasis group. The *RAD51*-encoded product, an orthologue of the *Escherichia coli* RecA recombinase (8), mediates the formation of DNA joints that link the recombining DNA molecules (8, 9). In the presence of ATP, Rad51 polymerizes onto ssDNA to form a right-handed filament called the presynaptic filament. The presynaptic filament also harbors a binding site for duplex DNA (8, 10). Once engaged, the duplex DNA is sampled for homology, leading to DNA joint formation with the ssDNA (8, 10). The nascent DNA joint is extended by DNA strand exchange (10, 11). Thus, assembly of the presynaptic filament and its maintenance represent a most critical event in HR (10); see below).

Because nucleation of Rad51 onto ssDNA is slow, presynaptic filament assembly is prone to interference by RPA, the single-strand DNA binding protein in eukaryotes. RPA was first recognized as an accessory factor in the assembly of the presynaptic filament (9) via DNA secondary structure removal (12). Later, it was shown that RPA also possesses a post-synaptic function through sequestering the ssDNA generated during DNA strand exchange (13, 14). However, because RPA has high affinity for ssDNA, it can prevent Rad51 from binding ssDNA and thus strongly inhibit presynaptic filament assembly (12, 15). Inclusion of Rad52 efficiently overcomes this inhibitory effect of RPA (15–17). This recombination mediator function of Rad52 stems from its ability to nucleate Rad51 onto RPA-coated ssDNA to seed the assembly of the presynaptic filament (7, 11).

Cell-based studies have validated the significance of the biochemical data as summarized above. Specifically, in chromatin immunoprecipitation and cytological experiments designed to examine the association of RPA and HR factors with DSBs, loading of RPA onto the DNA substrate occurs first, and then it is gradually replaced by Rad51 (18–22). This replacement of

RPA by Rad51 is dependent on Rad52. Aside from its recombination mediator role, Rad52 also functions in a pathway of HR between direct DNA repeats known as single-strand annealing. Herein, Rad52 is thought to anneal RPA-coated complementary single DNA strands (23–25) to form deletion recombinants (7).

Understanding the mechanistic basis of the Rad52 recombination mediator activity is of great importance, because an inability to shepherd Rad51 to DNA damage is a hallmark of cells deficient in the tumor suppressor BRCA2 (4). Several properties of Rad52 are believed to be germane for its recombination mediator function (2, 11). As first recognized by Mortensen *et al.* (23) and subsequently confirmed by others (16, 17, 26), Rad52 binds both ssDNA and dsDNA, showing a preference for the former. In addition, Rad52 exists as homo-oligomer (24) of seven or more subunits (27). The N-terminal third of Rad52 harbors the oligomerization domain and a Rad59 interaction domain and also exhibits DNA binding activity (23, 28–30). Rad52 also physically associates with Rad51 through its C terminus (31, 32) and is thought to bind RPA as well (16, 33, 34).

Disruption of the Rad51-binding domain in Rad52, as in the *rad52 Δ327* and *rad52 Δ409–412* alleles (16, 35), compromises its recombination mediator function. Although not yet formally proven, it seems reasonable to propose that Rad52 DNA binding function is important for the loading of Rad51 onto RPA-coated ssDNA. In this regard, it has been generally assumed that the N-terminal third of Rad52 is critical. In addition, the oligomeric structure of Rad52 may promote cooperative DNA binding that could be relevant for the recombination mediator activity (11).

In our continuing effort to dissect the Rad52 recombination mediator function, we unexpectedly find a robust DNA binding activity within the C-terminal third of the protein. We demonstrate that the Rad52 C terminus alone has recombination mediator activity. Importantly, we show that the middle portion of Rad52 interacts with DNA-bound RPA and makes a contribution to the recombination mediator function. Accordingly, a polypeptide harboring the middle and C-terminal portions of Rad52 partially complements the DNA damage sensitivity of the *rad52 Δ327* mutant strain and enhances the ability of these cells to target Rad51 to a DSB site. These results provide new molecular details into the role of Rad52 in HR.

EXPERIMENTAL PROCEDURES

Yeast Strains—The yeast strains are derivatives of JKM179 (*MATα Δho Δhml::ADE1 Δhmr::ADE1 ade1-110 leu2,3-112 lys5 trp1::hisG ura3-52 ade3::GAL10:HO*) (36). The *rad52-Δ327* strain was generated by inserting a stop codon and KanMX right after codon 327 of the chromosomal *RAD52* gene, and the *rad52Δ* strain was made by replacing the chromosomal *RAD52* gene by NatMX.

Construction of Plasmids—His$_6$-RAD52 harboring codons 34–504 of *RAD52* was ligated into the NcoI site of the pET11d vector. His$_6$-RAD52-C was ligated into BamHI or EcoRI sites of the pRSETc vector. His$_6$-RAD52-N/C was generated by inserting the C-terminal fragment of *RAD52* (codons 327–504) into the BamHI site of His$_6$-RAD52-N::pRSETc. His$_6$-RAD52-M/C was constructed by ligating the BamHI/BglII fragment of

GST-RAD52::*pGEX* (35) into the BamHI site of pRSETc. For the expression of the Rad52 species in yeast cells, the various alleles were inserted into the SmaI site of the 2μ vector *pRS426 ADH* (37) to place them under the control of the *ADH* promoter. The nuclear localization signal GGPKKKRKVG, derived from the SV40 large T antigen, was inserted at the end of the opening reading frame of the *RAD52-M/C* and *RAD52-C* genes.

Purification of Rad52 Species—The His$_6$-tagged Rad52 species were expressed in *E. coli* strain BL21 (DE3). Overnight cultures grown in Luria broth at 37 °C were diluted 1000-fold with fresh medium and incubated at 37 °C until the A_{600} reached 1.2. At that time, isopropyl-D-thiogalactopyranoside was added to 0.1 mM, and the culture was incubated at 16 °C for 24 h. The cells were harvested by centrifugation and stored at −80 °C. All of the protein purification steps were carried out at 4 °C. Lysate was prepared from 20 g of *E. coli* cell paste using a French press in 100 ml of buffer G (50 mM Tris-HCl, pH 7.4, 0.5 mM EDTA, 0.01% Igepal, 1 mM 2-mercaptoethanol, 10% sucrose, and 100 mM KCl that also contained aprotinin, chymostatin, leupeptin, and pepstatin A at 5 μg/ml each). The crude lysate was clarified by centrifugation (100,000 $\times$ g, 90 min).

For His$_6$-tagged Rad52-N/C—The clarified lysate was applied onto a SP Sepharose column (20 ml), which was developed with a 160-ml gradient from 100 to 400 mM KCl in K buffer (20 mM K$_2$HPO$_4$, pH 7.4, 1 mM 2-mercaptoethanol, 0.01% Igepal, and 10% glycerol). The fractions containing the His$_6$-tagged protein (12 ml total; 220 mM KCl) were mixed with 1 ml of nickel-nitrilotriacetic acid-agarose (Qiagen) for 3 h at 4 °C. The beads were washed three times with 20 ml of buffer K containing 400 mM KCl, and the bound His$_6$-Rad52-N/C was eluted with 5 ml of 10, 50, 100, and 200 mM imidazole in buffer K, respectively. The 100 and 200 mM imidazole eluates were combined, diluted with 10 ml 10% glycerol, and applied onto a 1-ml Macro-HAP (Bio-Rad) column, which was eluted with a 20-ml gradient from 0 to 300 mM KH$_2$PO$_4$ in buffer K. The Macro-HAP fractions (3 ml total; 120 mM KH$_2$PO$_4$) that contained the peak of Rad52-N/C were dialyzed, concentrated to 10 mg/ml, and stored at −80° C. The overall yield of highly purified Rad52-N/C was ~2 mg.

For His$_6$-tagged Rad52-C and Rad52-M/C—The clarified lysate was fractionated in a SP Sepharose column (20 ml) as above. The fractions containing the His$_6$-tagged proteins (12 ml total; 250 mM KCl) were subjected to affinity purification in nickel-nitrilotriacetic acid-agarose and chromatographic fractionation in Macro-HAP as above. The Macro-HAP fractions (3 ml total; 140 mM KH$_2$PO$_4$) that contained the peak of the Rad52 species were dialyzed, concentrated to 10 mg/ml, and stored as above. We could obtain ~5 mg of Rad52-C and ~2.5 mg of Rad52-M/C.

Purification of Other Proteins—The procedures for the expression and purification of the various GST-Rad52 species have been described elsewhere (35). Rad51 and RPA were expressed and purified as described previously (9).

DNA Substrates—The ϕX 174 viral (+) strand and replicative form I DNA were purchased from New England Biolabs and Invitrogen, respectively. The sequences of the oligonucleotides (oligonucleotides 1 and 2) used in ssDNA annealing and

Dissection of Rad52 Mediator Activity

DNA binding experiments and their ^{32}P labeling have been described (35).

DNA Binding Assay—Varying amounts of the Rad52 species were incubated with ^{32}P-labeled Oligo-1 (1.36 μM nucleotides) or dsDNA (1.36 μM base pairs; obtained by hybridizing oligonucleotide 1 to oligonucleotide 2) at 37 °C in 10 μl of buffer D (40 mM Tris-HCl, pH 7.8, 50 mM KCl, 1 mM dithiothreitol, and 100 μg/ml bovine serum albumin) for 10 min. After the addition of gel loading buffer (50% glycerol, 20 mM Tris-HCl, pH 7.4, 0.5 mM EDTA, 0.05% orange G), the reaction mixtures were resolved in 12% native polyacrylamide gels in TAE buffer (40 mM Tris-HCl, pH 7.4, 0.5 mM EDTA) at 4 °C. The gels were dried, and the DNA species were quantified using the *Quantity One* software in the Personal Molecular Imager FX (Bio-Rad). To show that the DNA substrate remained intact, we treated a reaction mixture containing the highest concentration of the Rad52 species with 0.5% SDS and 0.5 mg/ml proteinase K at 37 °C for 5 min before the analysis.

DNA Strand Exchange Assay—The DNA strand exchange reaction was performed according to our published procedure (26). Rad51 (10 μM) was incubated with ssDNA (30 μM nucleotides) in 10 μl of buffer R (35 mM 3-morpholinopropanesulfonic acid potassium salt, pH 7.2, 1 mM dithiothreitol, 50 mM KCl, 2.5 mM ATP, and 3 mM MgCl$_2$) for 5 min. After the addition of RPA (1.2 μM) in 0.5 μl, the reaction mixture was incubated for another 5 min, before the incorporation of dsDNA (25 μM nucleotides added in 1 μl) and 1 μl of 50 mM spermidine hydrochloride (final concentration, 4 mM). At the indicated times, a 4.5-μl portion of the reaction mixture was withdrawn, processed, and analyzed by agarose gel electrophoresis with ethidium bromide staining (9). Gel images were recorded in a NucleoTech gel documentation system and analyzed with the *GelExpert* software. To examine the Rad52 recombination mediator function, reaction mixtures (12.5 μl final volume) containing Rad51 (10 μM), RPA (2 μM), and the indicated amounts of the various Rad52 species were incubated on ice for 10 min in 9.5 μl of buffer R, followed by the addition of ssDNA in 1 μl and a 10-min incubation. After the incorporation of linear duplex and spermidine, the completed reactions were incubated and analyzed as before. For the time course experiments, the reactions were scaled up four times to 50 μl but were otherwise assembled in the same fashion.

GST Pulldown Assay—RPA or *E. coli* SSB (2 μM) was incubated with or without either ϕX174 ssDNA or dsDNA (30 μM nucleotides or base pairs) in 29 μl of buffer T (20 mM Tris-HCl, pH 7.5, 150 mM KCl, 1 mM dithiothreitol, 0.5 mM EDTA, and 0.01% Igepal) at 37 °C for 10 min before GST-Rad52-M (6 μM) was added in 1 μl. Following a 30-min incubation at 4 °C, the reactions were mixed with 10 μl of glutathione-Sepharose-4B beads at 4 °C for 30 min. After washing the beads twice with 150 μl of buffer T, the bound proteins were eluted with 30 μl of 3% SDS. The supernatants and SDS eluates, 10 μl each, were subjected to SDS-PAGE analysis.

Magnetic Bead-based Pulldown Assay—Purified RPA (2 μM) was incubated with 15 μl of magnetic beads containing ϕX174 ssDNA (30 μM nucleotides) immobilized on the beads through an annealed biotinylated oligonucleotide (38) in 43.5 μl of buffer T at 37 °C for 10 min. The magnetic beads in one-third of the slurry were captured with a magnetic particle separator and treated with 15 μl 1% SDS to elute the bound RPA, and 10 μl of the eluate (beads) was analyzed by SDS-PAGE. GST-Rad52-M (6 μM) was added to two-thirds of the slurry in 1 μl, followed by mixing for 30 min at 4 °C. The beads were captured with the magnetic particle separator and washed with 30 μl of the same buffer, and the bound proteins were eluted with 30 μl 1% SDS. The supernatant and SDS eluate, 10 μl each, were analyzed by SDS-PAGE.

Chromatin Immunoprecipitation—The yeast strains harbor a plasmid of the HO endonuclease gene under the control of the *GAL10* promoter, which permits the galactose induction of HO expression. Chromatin immunoprecipitation (ChIP) was carried out essentially as described (21). The cells were grown in YEP supplemented with 3% glycerol for 6 h until the mid-log phase, and 2% galactose was added to induce HO expression. At the designated times, the cells were harvested from 45 ml of the cultures, cross-linked with 1% formaldehyde for 20 min, and then quenched with 125 mM glycine for 5 min. After lysing the cells with glass beads and sonication to shear the chromatin, the cell lysates were incubated with anti-Rad51 antibodies (our own stock) or anti-Rad52 antibodies raised against the C terminus of the protein (Santa Cruz Biotechnology) and Dynabeads Protein G (Invitrogen). After a series of washes, the immunoprecipitates were incubated at 65 °C to reverse protein-DNA cross-link. Radioactive semi-quantitative PCR was performed to amplify the precipitated DNA. The primers used for amplifying *PHO5* and *MAT Z* were as described (21). The PCR products were resolved on 6% native polyacrylamide gels and quantified in a phosphorimaging device (Bio-Rad) using the Quantity One software (Bio-Rad).

Immunoblot Analysis—Cells grown in SC-Ura media at 30 °C were lysed with glass beads in buffer (50 mM HEPES-KOH, pH 7.5, 500 mM NaCl, 1 mM EDTA, 1% Triton X-100, 0.1% sodium deoxycholate, and the following protease inhibitors: aprotinin, chymostatin, leupeptin, and pepstatin A at 5 μg/ml each) and cleared by centrifugation at 15,000 × g and 4 °C for 15 min. Clarified lysates (10 μg of total protein) were subjected to immunoblot analysis with affinity-purified anti-Rad52 antibodies raised against amino acid residues 168–456 of Rad52 (15) and anti-rabbit secondary antibodies conjugated with horseradish peroxidase. The blots were developed with the SuperSignal Substrate (Pierce).

Electron Microscopy—Reactions containing Rad51 (10 μM), RPA (2 μM), and ssDNA (30 μM nucleotides) were assembled in the buffer used for DNA strand exchange and incubated for 15 min either in the absence or presence of Rad52 (1.2 μM) or Rad52-M/C (3 μM). After dilution, the samples were applied onto freshly glow discharged carbon-coated Mesh 400 copper grids, stained with uranyl acetate, and examined with a Technai-12 electron microscope (39).

MMS Survival Assay—*rad52Δ* and *rad52-Δ327* cells harboring plasmids that express Rad52, Rad52-C, and Rad52-M/C tagged with the SV40 nuclear localization signal were grown to the stationary phase in SC-Ura media at 30 °C and diluted 20-fold with fresh medium. When the cultures reached a density of $\sim$1 × 10^8 cells/ml, they were serially 10-fold diluted and then spotted on SC-Ura plates containing 0.005% MMS. The plates were incubated at 30 °C for 4 days and then photographed.
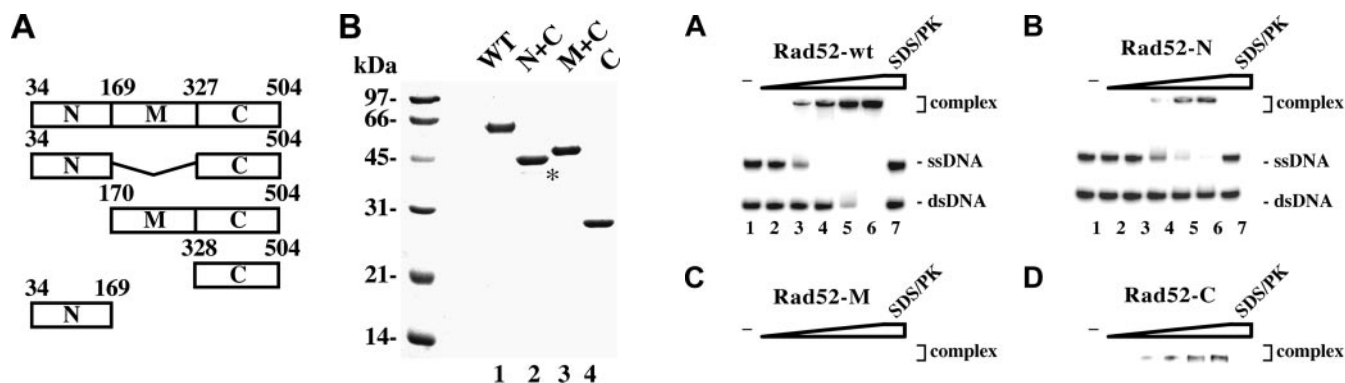
FIGURE 1. **Purification of Rad52 species.** *A*, schematic representation of the Rad52 species used. *B*, purified His$_6$-tagged proteins: Rad52, Rad52-N/C, Rad52-M/C, and Rad52-C (1 μg each) were run on a 10% denaturing SDS-PAGE and stained with Coomassie Blue. The *asterisk* designates a proteolytic fragment of Rad52-N/C.

RESULTS

Purification of Rad52 Domains—We previously expressed Rad52 and also the N-terminal third (designated as N), middle third (designated as M), and C-terminal third (designated as C) of this protein as GST fusions (35). We have since expressed and purified His$_6$-tagged Rad52, Rad52-C, and fusions of the M and C regions (Rad52-M/C) and the N and C regions (Rad52-N/C) (Fig. 1). The Rad52 species that contain the N-terminal region of this protein were made from the third ATG codon (corresponding to residue 34) in the *RAD52* protein coding frame, because this represents the first start codon that is used in Rad52 protein synthesis in yeast cells (40). At least two independent preparations of each of the Rad52 species were used in our study, and they all gave the same results.

Rad52-C Harbors DNA Binding Activity—Rad52 binds ssDNA and shows a weaker affinity for dsDNA (Ref. 23 and Fig. 2*A*), and the DNA binding activity is thought to reside within the N terminus (23). This region of Rad52 forms a ring-shaped oligomer that possesses an outer groove (24, 27, 29, 30) lined with basic and aromatic residues that are involved in binding DNA (29).

Even though GST-Rad52-N bound ^{32}P-labeled ssDNA and dsDNA, it was not nearly as proficient as GST-tagged Rad52 (Fig. 2*B*). This prompted us to investigate whether other parts of Rad52 could also be involved in DNA binding. GST-Rad52-M is devoid of any ability to bind DNA (Fig. 2*C*), but we were surprised to find a DNA binding activity in GST-Rad52-C (Fig. 2*D*). In fact, Rad52-C appears to be more adept at binding both ssDNA and dsDNA than Rad52-N (Fig. 2, *E* and *F*). The same conclusions were reached when the oligonucleotide substrates were replaced with ϕX174 ssDNA and dsDNA molecules (data not shown). Taken together, the results confirmed that the N terminus of Rad52 harbors a DNA binding function and, rather unexpectedly, revealed a DNA binding activity in the C-terminal third of the protein.

Rad52-C Has Recombination Mediator Activity—We used the His$_6$-tagged form of the Rad52 variants and a well established DNA strand exchange assay to test for recombination mediator activity (Fig. 3*A* and Refs. 15–17 and 41). In this assay, efficient DNA strand exchange is seen when the ϕX174 ssDNA is preincubated with Rad51 before the addition of RPA (Fig. 3*B*, *lanes 2*), whereas incubation of the ssDNA with Rad51 and RPA
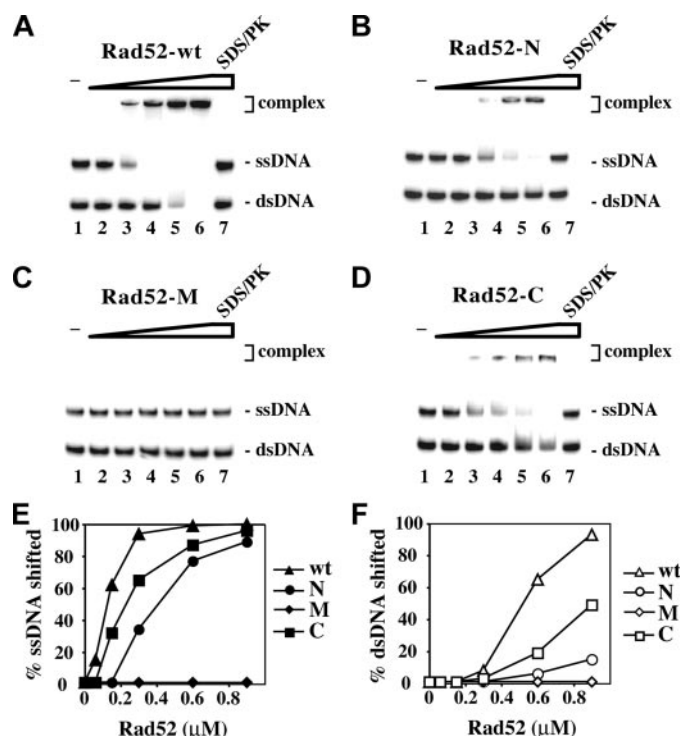
FIGURE 2. **The C-terminal region of Rad52 harbors a DNA binding activity.** *A–D*, Radiolabeled ssDNA and dsDNA were incubated without protein (*lane 1*) and with 60, 135, 270, and 400 nM of Rad52 (*A*), Rad52-N (*B*), Rad52-M (*C*), and Rad52-C (*D*). In *lane 7*, a reaction mixture containing the highest amount of each of the Rad52 species was treated with SDS and proteinase K before analysis. The results from *A–D* were plotted in *E* and *F*. Note that the ssDNA migrated more slowly than the dsDNA. *wt*, wild type.

simultaneously leads to a pronounced attenuation of the reaction because of interference of presynaptic filament assembly by RPA (Fig. 3*B*, *lanes 3*).

As expected, the inclusion of Rad52 effectively alleviated the suppressive effect of RPA on DNA strand exchange (Fig. 3*B*, *panel I*, *lanes 4–9*). Under the conditions used (10 μM Rad51, 30 μM ssDNA, and 2 μM RPA), the optimal concentration of Rad52 to see full restoration of DNA strand exchange was 1.2 μM. Reproducibly, Rad52-C could also restore a significant level of DNA strand exchange with RPA co-addition, although, when compared with Rad52, a higher amount (2–8 μM) was needed (Fig. 3*C*). The maximal extent of restoration that could be achieved with Rad52-C was, however, significantly lower, about one-third of that obtained with Rad52 (Fig. 3*C*). Full time course experiments demonstrating DNA strand exchange restoration by Rad52 and Rad52-C are presented in supplemental Fig. S1. We also found that neither GST-tagged Rad52-N nor GST-tagged Rad52-M is capable of restoring DNA strand exchange over a wide concentration range of these protein species (data not shown). In contrast, GST-Rad52 and GST-Rad52-C possess mediator activity comparable with that of the His$_6$-tagged version of these Rad52 species (data not shown). As anticipated, neither Rad52 nor any of the Rad52 domains (N, M, and C) exhibited any DNA strand exchange activity with or without RPA (data not shown).

Both Rad52 N and M Contribute to Recombination Mediator Function—Because Rad52 is considerably more effective than Rad52-C in DNA strand exchange restoration (Fig. 3*C*), we
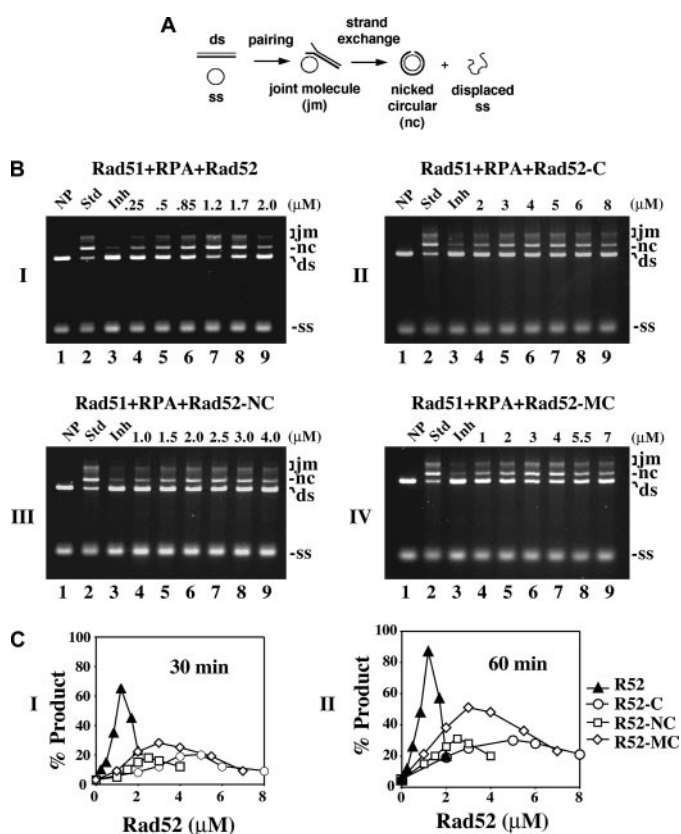
FIGURE 3. **The C terminus of Rad52 possesses recombination mediator activity.** *A*, schematic representation of the homologous DNA pairing and strand exchange reaction. Homologous pairing between the circular ssDNA (*ss*) and linear duplex DNA (*ds*) substrates yields a DNA joint molecule (*jm*), which is converted into a nicked circular duplex molecule (*nc*) by DNA strand exchange. *B*, DNA strand exchange reactions conducted to examine the recombination mediator activity of the Rad52 species: Rad52 in *panel I*, Rad52-C in *panel II*, Rad52-N/C in *panel III*, and Rad52-M/C in *panel IV*. The standard reaction (*Std, lane 2*) involved preincubating the ssDNA with Rad51 to allow for the formation of the presynaptic filament before RPA was added. Co-incubating the ssDNA with Rad51 and RPA resulted in severe inhibition of the DNA strand exchange reaction (*Inh, lane 3*). The inclusion of the various Rad52 species during the incubation of ssDNA with Rad51 and RPA led to restoration of DNA strand exchange. *NP* indicates no protein added. *C*, the results of the 30- and 60-min time points in *B* were plotted in *panels I* and *II*, respectively.

asked whether the N and M portions contribute toward the recombination mediator function. To address this, we fused either Rad52 N or M to the C portion. When expressed in *E. coli*, the Rad52-N/C and Rad52-M/C species are soluble, and we were able to devise procedures for their purification (Fig. 1). Relative to Rad52-C, significant restoration of DNA strand exchange was seen with a lower concentration of Rad52-N/C, but the maximal level of restoration was not higher than what could be achieved with Rad52-C (Fig. 3, *B* and *C*). Interestingly, Rad52-M/C was more effective than Rad52-C in restoring DNA strand exchange (Fig. 3*B*). Although restoration of DNA strand exchange by Rad52-M/C occurred over the same concentration range as Rad52-C, the final level was significantly higher. Full time course experiments involving Rad52-N/C and Rad52-M/C are presented in supplemental Fig. S1. As expected, neither Rad52-N/C nor Rad52-M/C has any DNA strand exchange activity with or without RPA (data not shown).

Rad52-M Interacts with DNA-bound RPA—Because the M portion of Rad52 has no DNA binding activity (Fig. 2) and does

not interact with Rad51 (32, 35), we wondered whether its enhancement of the Rad52-C recombination mediator activity (Fig. 3*B* and supplemental Fig. S1) could be due to an ability to associate with RPA. However, only a very weak interaction between GST-Rad52-M and RPA was observed in an affinity pulldown assay (Fig. 4*D*, compare *lanes 4* and *10*). The result, although negative, is entirely consistent with the observation that Rad52 does not associate strongly with RPA in solution (data not shown). We next considered the possibility that interaction between Rad52-M and RPA occurs when RPA is DNA-bound. Two separate affinity pulldown assays were employed to address this possibility. In the first assay, RPA was incubated with biotinylated ssDNA immobilized on streptavidin magnetic beads to produce a RPA-ssDNA affinity matrix, which was then used to test for a possible interaction with GST-Rad52-M (Fig. 4*A*). A significant amount of Rad52-M was retained on the RPA-ssDNA beads (Fig. 4*B*). As expected, Rad52-M did not associate with DNA magnetic beads without RPA (Fig. 4*B, lane 7*). In the second pulldown assay, Rad52-M was first incubated with RPA or *E. coli* SSB without DNA or with ssDNA or dsDNA, and then the reactions were mixed with glutathione-Sepharose beads to capture GST-Rad52-M and associated RPA or SSB (Fig. 4*C*). In agreement with the results from the first pulldown assay (Fig. 4*B*), a stoichiometric amount of RPA was found associated with Rad52-M upon inclusion of ssDNA, whereas no retention of RPA occurred without DNA (Fig. 4*D*, compare *lanes 8* and *10*). We also verified that GST-Rad52-M does not associate with *E. coli* SSB (Fig. 4*D*) and that dsDNA is ineffective in mediating complex formation of RPA with Rad52-M (Fig. 4*D*). Taken together, the results revealed an ability of Rad52-M to associate avidly with DNA-bound RPA, and it does so in a species-specific manner. As anticipated, Rad52-M does not interact with free or ssDNA-bound Rad51 (data not shown).

Examination of Recombination Mediator Activity by Electron Microscopy—We incubated ϕX174 circular ssDNA with Rad51 and RPA in the presence or absence of His$_6$-tagged Rad52 or Rad52-M/C. These reactions were then examined by electron microscopy. We analyzed over 100 randomly picked nucleoprotein complexes in each case and classified these complexes according to the extent of the Rad51 presynaptic filament. In the reaction that had Rad51 and RPA only, ~40% of the nucleoprotein complexes contained mostly or entirely RPA, and only very few (~10% of the total) of the DNA molecules had 60% or higher coverage by Rad51 (Fig. 5 and supplemental Fig. S2). As expected, the addition of Rad52 effectively restored presynaptic filament formation, with almost all of the nucleoprotein complexes possessing 60% or higher Rad51 coverage (Fig. 5 and supplemental Fig. S2). The inclusion of Rad52-MC had a strong impact on Rad51 presynaptic filament assembly, with a significant fraction (>35%) of the nucleoprotein complexes having ≥60% Rad51 coverage. Overall, the results from the electron microscopy analysis provided independent verification of Rad52-M/C possessing a recombination mediator activity. However, like for DNA strand exchange, Rad52-M/C is not as effective as Rad52 in the promotion of Rad51 presynaptic filament assembly (Fig. 5*B*).
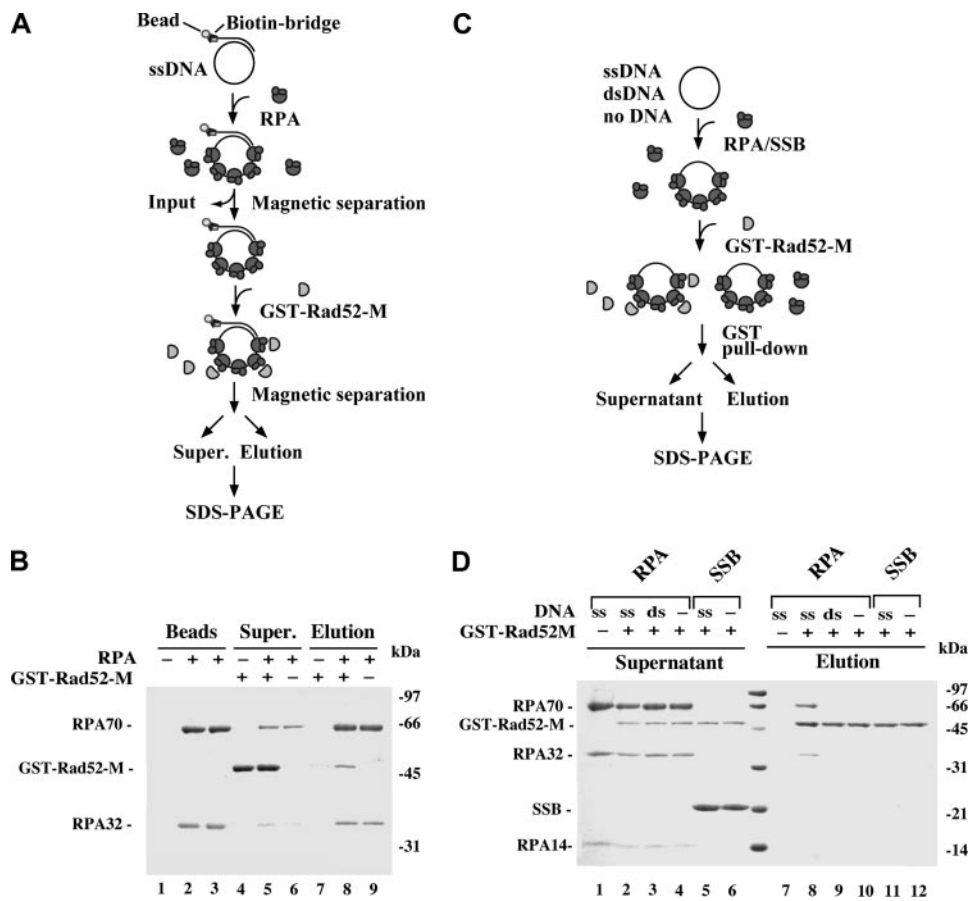
FIGURE 4. **Rad52-M interacts with DNA-bound RPA.** *A*, in this affinity pulldown assay, RPA is incubated with streptavidin magnetic beads harboring φX174 ssDNA, and the resulting RPA-containing beads are used to bind Rad52-M. *B*, three reactions were set up. In the first reaction, ssDNA magnetic beads that did not harbor RPA (*lane 1*) were mixed with GST-Rad52-M (*lanes 4* and *7*); in the second reaction, ssDNA magnetic beads harboring RPA (*lane 2*) were mixed with GST-Rad52-M (*lanes 5* and *8*); and in the third reaction, ssDNA magnetic beads harboring RPA (*lane 3*) were mixed in buffer without GST-Rad52-M (*lanes 6* and *9*). After mixing, the beads were captured with a magnet, and associated proteins were eluted with SDS. The supernatants (*Super.*) that contained unbound proteins and the SDS eluates (*Elution*) were analyzed by SDS-PAGE with Coomassie Blue staining. The RPA content of the magnetic beads (*Beads*) used in the three reactions is also shown. *C*, in this affinity pulldown assay, GST-Rad52-M is incubated with RPA or *E. coli* SSB either in the absence of DNA or in the presence of ssDNA or dsDNA before being mixed with glutathione-Sepharose to capture GST-Rad52-M and any associated RPA. *D*, the various supernatants containing unbound proteins and the SDS eluates harboring the captured proteins were analyzed by SDS-PAGE with Coomassie Blue staining. GST-Rad52-M was omitted from the control reaction in *lane 1*.

Rad52-M/C Is Biologically Efficacious in the rad52Δ327 Mutant—The above results indicated that the C portion of Rad52 has a recombination mediator activity that is augmented by the RPA-binding domain located within the M portion of the protein. To ask whether Rad52-M/C has biological activity *in vivo*, we examined the ability of plasmids containing either *RAD52* or *RAD52-M/C* inserted downstream of the *ADH* promoter for their ability to complement the sensitivity of *rad52* mutant strains to the genotoxin MMS. To ensure that Rad52-M/C is transported into the nucleus, its C terminus was joined to the nuclear localization signal sequence derived from the SV40 large T antigen. Protein expression was verified by immunoblot analysis of cell extracts using anti-Rad52 antibodies (Fig. 6*B* and supplemental Fig. S3). In addition to the *rad52Δ* mutant, we included the *rad52-Δ327* mutant, which does not express the C-terminal third of Rad52, in the analysis, because it is known that the N-terminal portion of the Rad52 contributes to HR in a Rad51-independent fashion (42, 43). *RAD52-M/C*

partially complemented the MMS sensitivity of the *rad52-Δ327* mutant (Fig. 6*A*), but little or no complementation of the MMS sensitivity of the *rad52Δ* mutant was seen (data not shown). In addition, we did not observe any complementation of the *rad52-Δ327* or *rad52Δ* strain transformed with a similar plasmid expressing *RAD52-C* (Fig. 6*A* and data not shown). This result is likely due to a lack of Rad52-C protein expression as revealed by immunoblot analysis (Fig. 6*B*). Finally, the presence of a His$_6$ tag at either the N or the C terminus of Rad52 has no effect on protein expression in yeast cells or on the complementation of the *rad52-Δ327* mutant (supplemental Fig. S3). Likewise, attaching a His$_6$ tag to the N terminus of Rad52-M/C does not affect its expression or biological efficacy (supplemental Fig. S3).

Rad52-M/C Targets Rad51 to DNA Double-strand Breaks in Cells—The recruitment of Rad51 to DSBs in cells is strongly dependent on Rad52 (18–21). We employed ChIP to examine the targeting of Rad51 to a site-specific HO-induced break in *rad52Δ* and *rad52-Δ327* mutant cells that expressed either Rad52, Rad52-C, or Rad52-M/C from the plasmids described in the previous section. We used yeast strains where the DSB is engaged by the HR machinery but cannot be repaired because of the absence of the homologous donor sequence (20).

The expression of the HO-endonuclease was induced with galactose, and DSB formation was monitored by PCR (Fig. 7*A*). At various times after DSB induction, cell extracts were prepared and subjected to immunoprecipitation with anti-Rad51 or anti-Rad52 antibodies. The target sequence (*MAT-Z*) and an internal control sequence (*PHO5*) were amplified from the precipitated DNA by PCR. In agreement with published work (20, 21), we observed rapid recruitment of Rad51 upon DSB formation in wild-type cells, reaching a maximum of 40-fold by 3 h (data not shown). In contrast, the amount of Rad51 at the DSB increased only about 2–3-fold in *rad52Δ* cells (data not shown). In *rad52-Δ327* cells, Rad51 recruitment was diminished, but not ablated, because there was a 12-fold enrichment by 3 h (Fig. 7*B*). Importantly, expression of Rad52-M/C and Rad52 in *rad52-Δ327* cells led to a 40-fold and >100-fold enrichment of Rad51 at the DSB site by 3 h, respectively (Fig. 7*B*). Moreover, Rad51 recruitment to the DSB was enhanced more then 10-fold in *rad52Δ* cells expressing Rad52-M/C (data not shown). We
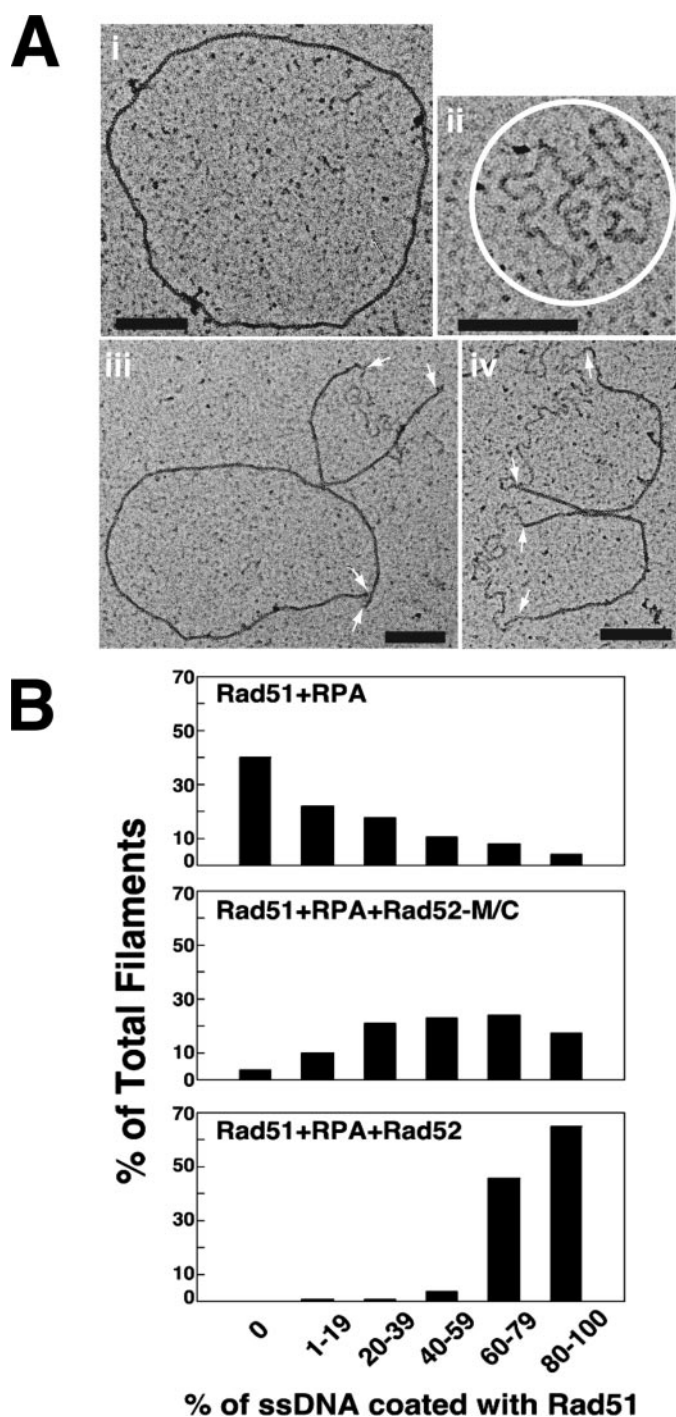
FIGURE 5. **Electron microscopy analysis of recombination mediator action.** *A*, micrographs showing an example of full Rad51 filament (*panel i*), a RPA-ssDNA nucleoprotein complex (*panel ii*), and ssDNA molecules covered partly by Rad51 and partly by RPA (*panels iii* and *iv*). The RPA-ssDNA complexes in *panel ii* are circled, and the *arrows* in *panels iii* and *iv* mark the junctions of Rad51-coated DNA and RPA-coated DNA. The *black scale bars* in the panels denote 200 nm. *B*, quantification of Rad51 presynaptic filament formation in the three reactions: Rad51+RPA, Rad51+RPA+ Rad52-M/C, and Rad51+RPA+Rad52.

did not find any Rad51 or Rad52-C enrichment at the HO-induced break in *rad52-Δ327* cells that harbor *ADH-RAD52-C* (Figs. 7*B* and 8). This was very likely due to a lack of Rad51-C protein expression (Fig. 6*B*). Lastly, as expected, both full-length Rad52 and Rad52-M/C are enriched at the DSB site (Fig.
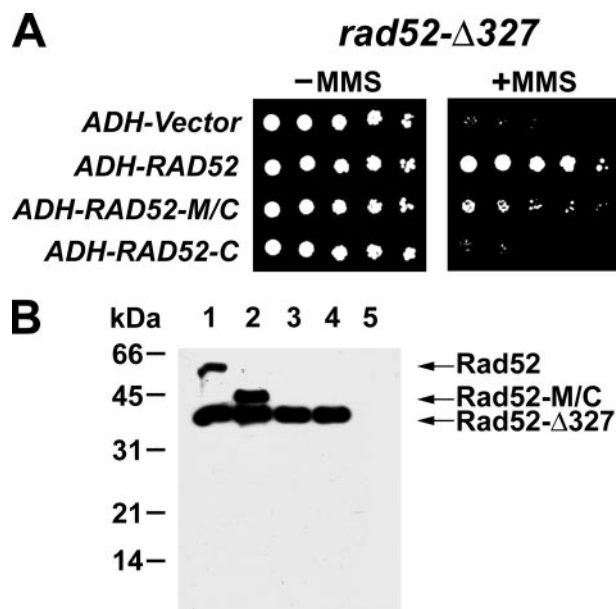
FIGURE 6. **Complementation of the *rad52-Δ327* mutant by Rad52-M/C.** *A*, *rad52-Δ327* strains harboring the empty *ADH* vector, *ADH-RAD52*, *ADH-RAD52-M/C*, or *ADH-RAD52-C* were serially diluted and spotted onto SC-Ura medium with or without 0. 005% MMS. *B*, extracts of *rad52-Δ327* cells harboring *ADH* plasmids expressing Rad52 (*lane 1*), Rad52-M/C (*lane 2*), Rad52-C (*lane 3*), or empty *ADH* vector (*lane 4*) or *rad52Δ* cells harboring empty *ADH* vector (*lane 5*) were subjected to immunoblot analysis with anti-Rad52 antibodies.

8). Taken together, the ChIP data are also indicative of the presence of a recombination mediator activity in Rad52-M/C. We note that the recruitment of Rad52-M/C to the HO breaks site is less robust than that of Rad52 (Fig. 8), which could be a contributing factor as to why this Rad52 species is not as biologically efficacious as the full-length protein.

DISCUSSION

New Insights Concerning the Role of Rad52 in HR—Rad52 plays a central role in various HR processes, including Rad51-dependent and Rad51-independent reactions (6, 7). Biochemical and cell-based analyses have unveiled a recombination mediator activity in Rad52 (15–17, 19–21). These studies have served as the model for understanding the function of this class of HR factors, including the human tumor suppressor BRCA2. Several properties of Rad52 are likely germane for its recombination mediator function, including the abilities to bind DNA, assemble into an oligomeric structure, and associate with Rad51 and RPA. Previous work has established that complex formation with Rad51 is critical for the recombination mediator function of Rad52 (16, 35). Here we have provided evidence that in addition to binding Rad51 (32, 35), the C-terminal third of Rad52 possesses a DNA binding activity and can also nucleate Rad51 onto a RPA-coated DNA template. Moreover, we have shown that the middle portion of Rad52 mediates an interaction with ssDNA-bound RPA and enhances the recombination mediator activity of the C-terminal portion. Consistent with these results, expression of Rad52-M/C partially complements the DNA damage sensitivity of *rad52-Δ327* mutant cells.

Genetic experiments by the Livingston group (42, 44) have demonstrated intragenic complementation involving expres-
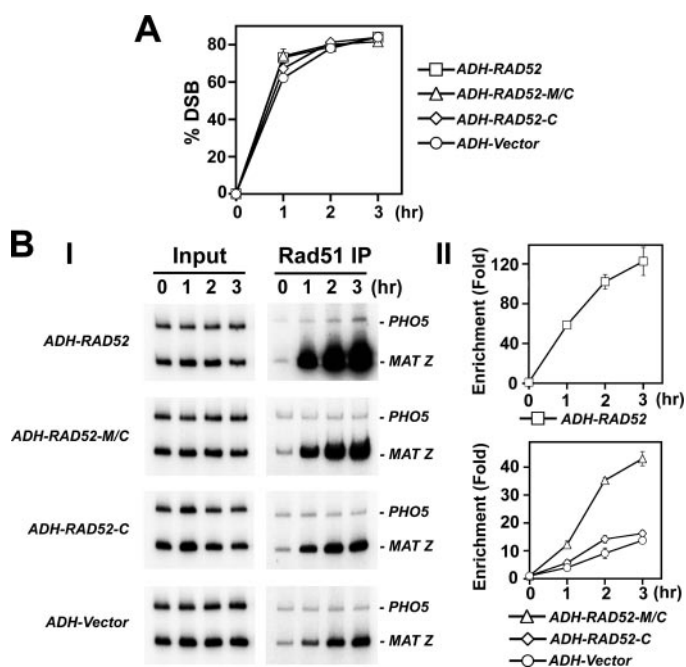
FIGURE 7. **Rad52-M/C promotes DSB recruitment of Rad51.** *A*, kinetics of DSB induction. Donorless *rad52-Δ327* cells harboring *GAL10-HO* and also the empty *ADH* vector or a *ADH* plasmid expressing Rad52, Rad52-M/C, or Rad52-C were grown in the presence of galactose to induce HO-expression and a DSB at *MAT*. The induction of the HO break was quantified by PCR (20, 21). *B*, recruitment of Rad51 to the HO-induced break in *rad52-Δ327* cells harboring the *ADH* vector or *ADH-RAD52*, *ADH-RAD52-M/C*, or *RAD52-C*. These cells were subjected to ChIP with anti-Rad51 antibodies. The *MAT Z* target sequence and control *PHO5* sequence were amplified using the appropriate primer sets (21). *Panels I* and *II* show the PCR products and the quantification of the results, respectively. Enrichment was determined by dividing the PCR signal of *MAT Z* by the *PHO5* PCR signal and normalizing to time zero value.
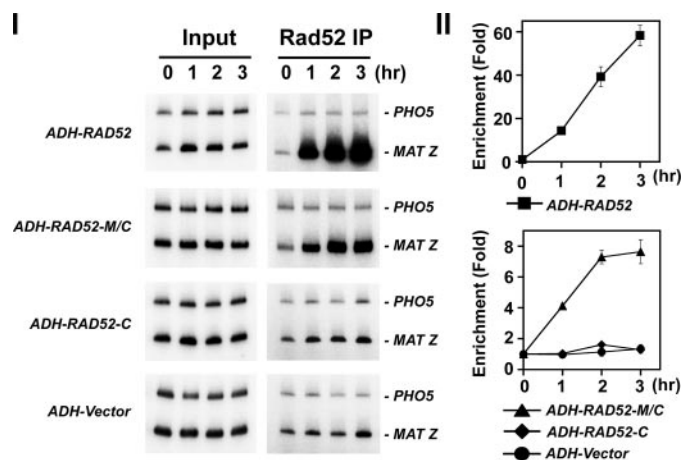
FIGURE 8. **DSB recruitment of Rad52 species in *rad52-Δ327* cells.** Recruitment of Rad52 to the HO breaks in *rad52-Δ327* cells harboring the *ADH* vector or *ADH-RAD52*, *ADH-RAD52-M/C*, or *ADH-RAD52-C*. These cells were subjected to ChIP with anti-Rad52 antibodies. The *MAT Z* target sequence and control *PHO5* sequence were amplified using the appropriate primer sets (21). *Panels I* and *II* show the PCR products and the quantification of the results, respectively. Enrichment was determined by dividing the PCR signal of *MAT Z* by the *PHO5* PCR signal and normalizing to time zero value.

sion of Rad52 fragments in the same cell. This is reminiscent of the complementation of the DNA repair and Rad51 recruitment deficiency by Rad52-M/C in the *rad52-Δ327* mutant seen here. Our biochemical analyses have further provided molecular information to explain this intragenic complementation phenomenon.

Biological Role of the Rad52 N Terminus—It is intriguing that the N terminus of Rad52 is in fact not absolutely required for the recombination mediator function *in vitro*. This finding clearly indicates that functional interactions with Rad51 and RPA can occur without the DNA binding activity and protein oligomerization domain that reside within this region. However, cells that lack the Rad51 interaction domain (as in *rad52-Δ327*) are still partially capable of Rad51 recruitment to a DSB. Accordingly, these cells are not as sensitive to DNA-damaging treatment as *rad52Δ* cells (this study and Ref. 32). This observation points to a key function of Rad52 in HR that does not entail a direct interaction with Rad51 but yet has an important impact upon the ability of cells to assemble or maintain the Rad51 presynaptic filament. Furthermore, the inability of the Rad52-M/C species to complement the *rad52Δ* mutation is also indicative of a vital HR function of the Rad52 N-terminal region.

The Rad55-Rad57 heterodimer also possesses a recombination mediator activity (18, 41, 45), and Rad54 is capable of stabilizing the Rad51 presynaptic filament (21, 46). In addition, the Rad59 protein binds DNA (47) and associates with Rad51, Rad52, and RPA in a complex (48). It remains to be determined whether Rad52, through its N-terminal and middle portions, functionally synergizes with these other HR factors to promote the assembly or stabilization of the Rad51 presynaptic filament. Likewise, the Rdh54 protein, which is structurally and functionally related to Rad54, might act in conjunction with Rad52 in reactions that either directly or indirectly (*e.g.* in chromatin remodeling) influence Rad51 presynaptic filament assembly or maintenance. It will be interesting to examine whether the Rad51 recruitment ability of the *rad52-Δ327* mutant is dependent on any of the aforementioned HR factors.

An amount of Rad52-N/C less than that of Rad52-C can achieve the same level of DNA strand exchange restoration (Fig. 3*C*), indicating that the N terminus makes a significant contribution toward the recombination mediator efficacy of Rad52. Because Rad52-N does not enhance the recombination mediator activity of Rad52-M/C (supplemental Fig. S4), these two Rad52 parts do not functionally cooperate *in trans*. Rad52 protein oligomerization that is mediated by the N terminus could confer the ability to bind ssDNA in a cooperative fashion. However, future studies will be needed to determine whether the protein oligomerization or the DNA binding activity of the N terminus is critical for the enhancement of recombination mediator activity. The available collection of N-terminal *rad52* mutants predicted to be compromised for DNA binding will be valuable in this regard (49).

Role of RPA Binding in Rad52 Function—*S. cerevisiae* Rad52 was previously shown to interact with RPA in the yeast two-hybrid system and in an affinity pulldown assay (24, 33). Moreover, human Rad52 and RPA readily form a complex in the absence of DNA (50). Taken together, the available evidence points to RPA interaction as an evolutionarily conserved property of Rad52. We have presented data showing the ability of the Rad52 middle portion to interact with RPA. This interaction is strongly dependent on ssDNA and is also species-specific. In addition, we have shown that the middle portion of Rad52 is able to enhance the mediator activity of Rad52-C.

Dissection of Rad52 Mediator Activity

Rad52 appears to make contacts with all three subunits of RPA (24, 33). Because the C terminus of Rad52 alone exhibits recombination mediator activity and can anneal RPA-coated complementary DNA strands, it too may harbor an ability to bind RPA. Future studies involving protein interaction domain mapping and mutant isolation will ascertain whether different surfaces of Rad52 contact the individual subunits of RPA and will delineate the functional significance of these contacts.

Implications for the Recombination Mediator Function of BRCA2—Cells harboring mutations in the tumor suppressor BRCA2 are profoundly deficient in the homology-directed repair of damaged chromosomes (51, 52). Several lines of evidence are consistent with the premise that BRCA2, like Rad52 in *S. cerevisiae*, regulates Rad51 activity by providing a recombination mediator function: 1) it physically interacts with Rad51 through several copies of the BRC repeat (53, 54) and also through its C terminus (55), 2) it binds ssDNA (56), 3) it interacts with RPA (57), and 4) *BRCA2* mutant cells are deficient in assembling DNA damage-induced Rad51 foci (52). Direct demonstration of the BRCA2 recombination mediator activity has been achieved in recent studies using a polypeptide derived from this protein (39) and also the *Ustilago maydis* BRCA2 orthologue Brh2 (58). The molecular dissection of Rad52 being conducted in our laboratory and by others should continue to provide useful information and complement parallel studies on related HR factors such as BRCA2.

REFERENCES

1. Cox, M. M., Goodman, M. F., Kreuzer, K. N., Sherratt, D. J., Sandler, S. J., and Marians, K. J. (2000) *Nature* **404,** 37–41
2. Symington, L. S. (2002) *Microbiol. Mol. Biol. Rev.* **66,** 630–670
3. Heller, R. C., and Marians, K. J. (2006) *Nat. Rev. Mol. Cell Biol.* **7,** 932–943
4. Jasin, M. (2002) *Oncogene* **21,** 8981–8993
5. D'Andrea, A. D. (2003) *Genes Dev.* **17,** 1933–1936
6. Paques, F., and Haber, J. E. (1999) *Microbiol. Mol. Biol. Rev.* **63,** 349–404
7. Krogh, B. O., and Symington, L. S. (2004) *Annu. Rev. Genet.* **38,** 233–271
8. Sung, P., and Klein, H. (2006) *Nat. Rev. Mol. Cell Biol.* **7,** 739–750
9. Sung, P. (1994) *Science* **265,** 1241–1243
10. Bianco, P. R., Tracy, R. B., and Kowalczykowski, S. C. (1998) *Front. Biosci.* **3,** D570–D603
11. Sung, P., Krejci, L., Van Komen, S., and Sehorn, M. G. (2003) *J. Biol. Chem.* **278,** 42729–42732
12. Sugiyama, T., Zaitseva, E. M., and Kowalczykowski, S. C. (1997) *J. Biol. Chem.* **272,** 7940–7945
13. Van Komen, S., Petukhova, G., Sigurdsson, S., and Sung, P. (2002) *J. Biol. Chem.* **277,** 43578–43587
14. Eggler, A. L., Inman, R. B., and Cox, M. M. (2002) *J. Biol. Chem.* **277,** 39280–39288
15. Sung, P. (1997) *J. Biol. Chem.* **272,** 28194–28197
16. Shinohara, A., and Ogawa, T. (1998) *Nature* **391,** 404–407
17. New, J. H., Sugiyama, T., Zaitseva, E., and Kowalczykowski, S. C. (1998) *Nature* **391,** 407–410
18. Gasior, S. L., Wong, A. K., Kora, Y., Shinohara, A., and Bishop, D. K. (1998) *Genes Dev.* **12,** 2208–2221
19. Lisby, M., Barlow, J. H., Burgess, R. C., and Rothstein, R. (2004) *Cell* **118,** 699–713
20. Sugawara, N., Wang, X., and Haber, J. E. (2003) *Mol Cell* **12,** 209–219
21. Wolner, B., van Komen, S., Sung, P., and Peterson, C. L. (2003) *Mol. Cell* **12,** 221–232
22. Wang, X., and Haber, J. E. (2004) *PLoS Biol.* **2,** 105–112
23. Mortensen, U. H., Bendixen, C., Sunjevaric, I., and Rothstein, R. (1996) *Proc. Natl. Acad. Sci. U. S. A.* **93,** 10729–10734
24. Shinohara, A., Shinohara, M., Ohta, T., Matsuda, S., and Ogawa, T. (1998) *Genes Cells* **3,** 145–156
25. Sugiyama, T., Kantake, N., Wu, Y., and Kowalczykowski, S. C. (2006) *EMBO J.* **25,** 5539–5548
26. Song, B., and Sung, P. (2000) *J. Biol. Chem.* **275,** 15895–15904
27. Stasiak, A. Z., Larquet, E., Stasiak, A., Muller, S., Engel, A., Van Dyck, E., West, S. C., and Egelman, E. H. (2000) *Curr. Biol.* **10,** 337–340
28. Cortes-Ledesma, F., Malagon, F., and Aguilera, A. (2004) *Genetics* **168,** 553–557
29. Kagawa, W., Kurumizaka, H., Ishitani, R., Fukai, S., Nureki, O., Shibata, T., and Yokoyama, S. (2002) *Mol. Cell* **10,** 359–371
30. Singleton, M. R., Wentzell, L. M., Liu, Y., West, S. C., and Wigley, D. B. (2002) *Proc. Natl. Acad. Sci. U. S. A.* **99,** 13492–13497
31. Shinohara, A., Ogawa, H., and Ogawa, T. (1992) *Cell* **69,** 457–470
32. Milne, G. T., and Weaver, D. T. (1993) *Genes Dev.* **7,** 1755–1765
33. Hays, S. L., Firmenich, A. A., Massey, P., Banerjee, R., and Berg, P. (1998) *Mol. Cell. Biol.* **18,** 4400–4406
34. Sugiyama, T., New, J. H., and Kowalczykowski, S. C. (1998) *Proc. Natl. Acad. Sci. U. S. A.* **95,** 6049–6054
35. Krejci, L., Song, B., Bussen, W., Rothstein, R., Mortensen, U. H., and Sung, P. (2002) *J. Biol. Chem.* **277,** 40132–40141
36. Lee, S. E., Moore, J. K., Holmes, A., Umezu, K., Kolodner, R. D., and Haber, J. E. (1998) *Cell* **94,** 399–409
37. Mumberg, D., Muller, R., and Funk, M. (1995) *Gene (Amst.)* **156,** 119–122
38. Krejci, L., Van Komen, S., Li, Y., Villemain, J., Reddy, M. S., Klein, H., Ellenberger, T., and Sung, P. (2003) *Nature* **423,** 305–309
39. San Filippo, J., Chi, P., Sehorn, M. G., Etchin, J., Krejci, L., and Sung, P. (2006) *J. Biol. Chem.* **281,** 11649–11657
40. Antunez de Mayolo, A., Lisby, M., Erdeniz, N., Thybo, T., Mortensen, U. H., and Rothstein, R. (2006) *Nucleic Acids Res.* **34,** 2587–2597
41. Sung, P. (1997) *Genes Dev.* **11,** 1111–1121
42. Asleson, E. N., Okagaki, R. J., and Livingston, D. M. (1999) *Genetics* **153,** 681–692
43. Tsukamoto, M., Yamashita, K., Miyazaki, T., Shinohara, M., and Shinohara, A. (2003) *Genetics* **165,** 1703–1715
44. Boundy-Mills, K. L., and Livingston, D. M. (1993) *Genetics* **133,** 39–49
45. Fortin, G. S., and Symington, L. S. (2002) *EMBO J.* **21,** 3160–3170
46. Mazin, A. V., Alexeev, A. A., and Kowalczykowski, S. C. (2003) *J. Biol. Chem.* **278,** 14029–14036
47. Petukhova, G., Stratton, S. A., and Sung, P. (1999) *J. Biol. Chem.* **274,** 33839–33842
48. Davis, A. P., and Symington, L. S. (2003) *DNA Repair (Amst.)* **2,** 1127–1134
49. Lettier, G., Feng, Q., de Mayolo, A. A., Erdeniz, N., Reid, R. J., Lisby, M., Mortensen, U. H., and Rothstein, R. (2006) *PLoS Genet.* **2,** 1773–1786
50. Park, M. S., Ludwig, D. L., Stigger, E., and Lee, S. H. (1996) *J. Biol. Chem.* **271,** 18996–19000
51. Xia, F., Taghian, D. G., DeFrank, J. S., Zeng, Z. C., Willers, H., Iliakis, G., and Powell, S. N. (2001) *Proc. Natl. Acad. Sci. U. S. A.* **98,** 8644–8649
52. Moynahan, M. E., Cui, T. Y., and Jasin, M. (2001) *Cancer Res.* **61,** 4842–4850
53. Wong, A. K., Pero, R., Ormonde, P. A., Tavtigian, S. V., and Bartel, P. L. (1997) *J. Biol. Chem.* **272,** 31941–31944
54. Chen, P. L., Chen, C. F., Chen, Y., Xiao, J., Sharp, Z. D., and Lee, W. H. (1998) *Proc. Natl. Acad. Sci. U. S. A.* **95,** 5287–5292
55. Sharan, S. K., Morimatsu, M., Albrecht, U., Lim, D. S., Regel, E., Dinh, C., Sands, A., Eichele, G., Hasty, P., and Bradley, A. (1997) *Nature* **386,** 804–810
56. Yang, H., Jeffrey, P. D., Miller, J., Kinnucan, E., Sun, Y., Thoma, N. H., Zheng, N., Chen, P. L., Lee, W. H., and Pavletich, N. P. (2002) *Science* **297,** 1837–1848
57. Wong, J. M., Ionescu, D., and Ingles, C. J. (2003) *Oncogene* **22,** 28–33
58. Yang, H., Li, Q., Fan, J., Holloman, W. K., and Pavletich, N. P. (2005) *Nature* **433,** 653–657

Attachment 4

Krejci, L., Van Komen, S., Li, Y., Villemain, J., Reddy, M. S., Klein, H., Ellenberger, T., Sung, P

DNA helicase Srs2 disrupts the Rad51 presynaptic filament.

Nature 423:305-9. 2003

mice with or without the C57Bl/Ka-Ly5.2 recipient bone marrow cells[1]. Reconstitution of donor (Ly5.1) myeloid and lymphoid cells was monitored by staining blood cells with antibodies against Ly5.1, CD3, B220, Mac-1 and Gr-1. The secondary bone marrow transplant was performed with 10^7 whole bone marrow cells from mice reconstituted with $Bmi\text{-}1^{+/+}$ or $Bmi\text{-}1^{-/-}$ fetal liver cells.

Retroviral gene transfer of HSCs

Mouse stem cell viruses expressing mouse $p16^{Ink4a}$ or $p19^{Arf}$ cDNAs together with GFP were produced using Phoenix ecotropic packaging cells[28]. Infection of HSCs was done as described[29] except that three cycles of infections were performed. After 48 h, single GFP-positive cells were sorted into a 96-well plate containing 100 μl HSC medium[29] and grown for 7 days. Each well was scored for the presence of GFP-positive cells by observation with a fluorescence microscope.

1. Morrison, S. J. & Weissman, I. L. The long-term repopulating subset of hematopoietic stem cells is deterministic and isolatable by phenotype. *Immunity* **1,** 661–673 (1994).
2. van der Lugt, N. M. *et al.* Posterior transformation, neurological abnormalities, and severe hematopoietic defects in mice with a targeted deletion of the *bmi-1* proto-oncogene. *Genes Dev.* **8,** 757–769 (1994).
3. Ramalho-Santos, M. *et al.* 'Stemness': transcriptional profiling of embryonic and adult stem cells. *Science* **298,** 597–600 (2002).
4. Park, I.-K. Molecular cloning and characterization of a novel regulator of G-protein signaling from mouse hematopoietic stem cells. *J. Biol. Chem.* **276,** 915–923 (2001).
5. Park, I. K. *et al.* Differential gene expression profiling of adult murine hematopoietic stem cells. *Blood* **99,** 488–498 (2002).
6. Lessard, J., Baban, S. & Sauvageau, G. Stage-specific expression of Polycomb group genes in human bone marrow cells. *Blood* **91,** 1216–1224 (1999).
7. Kiyono, T. *et al.* Both Rb/p16^{INK4a} inactivation and telomerase activity are required to immortalize human epithelial cells. *Nature* **396,** 84–88 (1998).
8. van der Lugt, N. M. T., Alkema, M., Berns, A. & Deschamps, J. The Polycomb-group homolog Bmi-1 is a regulator of murine Hox gene expression. *Mech. Dev.* **58,** 153–164 (1996).
9. Akashi, K. *et al.* Transcriptional accessibility for genes of multiple tissues and hematopoietic lineages is hierarchically controlled during early hematopoiesis. *Blood* **101,** 383–389 (2003).
10. Morrison, S., Hemmati, H., Wandycz, A. & Weissman, I. The purification and characterization of fetal liver hematopoietic stem cells. *Proc. Natl Acad. Sci. USA* **92,** 10302–10306 (1995).
11. Wright, D. E. *et al.* Hematopoietic stem cells are uniquely selective in their migratory reponse to chemokines. *J. Exp. Med.* **195,** 1145–1154 (2002).
12. Mahmoudi, T. & Verrijzer, C. P. Chromatin silencing and activation by Polycomb and trithorax group proteins. *Oncogene* **20,** 3055–3066 (2001).
13. Weber, J. D. *et al.* Nucleolar Arf sequesters Mdm2 and activates p53. *Nature Cell Biol.* **1,** 20–26 (1999).
14. Jacob, J. *et al.* The oncogene and Polycomb-group gene *bmi-1* regulates cell proliferation and senescence through the *ink4a* locus. *Nature* **397,** 164–168 (1999).
15. Quelle, D. E., Zindy, F., Ashmun, R. A. & Sherr, C. J. Alternative reading frames of the INK4a tumour suppressor gene encode two unrelated proteins capable of inducing cell cycle arrest. *Cell* **84,** 993–1000 (1995).
16. Antonchuk, J., Sauvageau, G. & Humphries, R. K. HOXB4 overexpression mediates very rapid stem cell regeneration and competitive hematopoietic repopulation. *Exp. Hematol.* **29,** 1125–1134 (2002).
17. Lawrence, H. J. *et al.* Mice bearing a targeted interruption of the homeobox gene HOXA9 have defects in myeloid, erythroid, and lymphoid hematopoiesis. *Blood* **89,** 1922–1930 (1997).
18. Christensen, J. L. & Weissman, I. L. Flk-2 is a marker in hematopoietic stem cell differentiation: a simple method to isolate long-term stem cells. *Proc. Natl Acad. Sci. USA* **98,** 14541–14546 (2001).
19. Zhang, Y., Xiong, Y. & Yarbrough, W. G. ARF promotes MDM2 degradation and stabilizes p53: ARF-INK4a locus deletion impairs both the Rb and p53 tumour suppression pathways. *Cell* **92,** 725–734 (1998).
20. Shivdasani, R., Mayer, E. & Orkin, S. Absence of blood formation in mice lacking the T-cell leukaemia oncoprotein tal-1/SCL. *Nature* **432,** 432–434 (1995).
21. Porcher, C. *et al.* The T cell leukemia oncoprotein SCL/tal-1 is essential for development of all hematopoietic lineages. *Cell* **86,** 47–57 (1996).
22. Antonchuk, J., Sauvageau, G. & Humphries, R. K. HOXB4-induced expansion of adult hematopoietic stem cells *ex vivo. Cell* **109,** 39–45 (2002).
23. Domen, J., Cheshier, S. H. & Weissman, I. L. The role of apoptosis in the regulation of hematopoietic stem cells: overexpression of BCL-2 increases both their number and repopulation potential. *J. Exp. Med.* **191,** 253–264 (2000).
24. Nichogiannopoulou, A. *et al.* Defects in hemopoietic stem cell activity in Ikaros mutant mice. *J. Exp. Med.* **190,** 1201–1214 (1999).
25. Fisher, R. C., Lovelock, J. D. & Scott, E. W. A critical role for PU.1 in homing and long-term engraftment by hematopoietic stem cells in the bone marrow. *Blood* **94,** 1283–1290 (1999).
26. Cheng, T. *et al.* Hematopoietic stem cell quiescence maintained by p21$^{cip1/waf1}$. *Science* **287,** 1804–1808 (2000).
27. Ohta, H. *et al.* Polycomb group gene rae28 is required for sustaining activity of hematopoietic stem cells. *J. Exp. Med.* **195,** 759–770 (2002).
28. Pear, W., Nolan, G., Scott, M. & Baltimore, D. Production of high-titer helper-free retroviruses by transient transfection. *Proc. Natl Acad. Sci. U.S.A.* **90,** 8392–8396 (1993).
29. Cotta, C., Swindle, C., Weissman, I. L. & Klug, C. A. *Retroviral Transduction of FACS-Purified Hematopoietic Stem Cells* (eds Klug, C. A. & Jordan, C. T.) 243–252 (Humana Press, Totowa, New Jersey, 2001).
30. Lessard, J. & Sauvageau, G. *Bmi-1* determines the proliferative capacity of normal and leukaemic stem cells. *Nature* advance online publication, 20 April 2003 (doi: 10.1038/nature01572).

....

DNA helicase Srs2 disrupts the Rad51 presynaptic filament

Lumir Krejci*†, **Stephen Van Komen***†, **Ying Li**‡, **Jana Villemain***,
Mothe Sreedhar Reddy*, **Hannah Klein**§, **Thomas Ellenberger**‡
& Patrick Sung*

* *Institute of Biotechnology and Department of Molecular Medicine, University of Texas Health Science Center at San Antonio, 15355 Lambda Drive, San Antonio, Texas 78245, USA*
‡ *Department of Biological Chemistry and Molecular Pharmacology, Harvard Medical School, Boston, Massachusetts 02115, USA*
§ *Department of Biochemistry, New York University School of Medicine, New York, New York 10016, USA*
† *These authors contributed equally to the work*

Mutations in the *Saccharomyces cerevisiae* gene *SRS2* result in the yeast's sensitivity to genotoxic agents, failure to recover or adapt from DNA damage checkpoint-mediated cell cycle arrest, slow growth, chromosome loss, and hyper-recombination[1,2]. Furthermore, double mutant strains, with mutations in DNA helicase genes *SRS2* and *SGS1*, show low viability that can be overcome by inactivating recombination, implying that untimely recombination is the cause of growth impairment[1,3,4]. Here we clarify the role of *SRS2* in recombination modulation by purifying its encoded product and examining its interactions with the Rad51 recombinase. Srs2 has a robust ATPase activity that is dependent on single-stranded DNA (ssDNA) and binds Rad51, but the addition of a catalytic quantity of Srs2 to Rad51-mediated recombination reactions causes severe inhibition of these reactions. We show that Srs2 acts by dislodging Rad51 from ssDNA. Thus, the attenuation of recombination efficiency by Srs2 stems primarily from its ability to dismantle the Rad51 presynaptic filament efficiently. Our findings have implications for the basis of Bloom's and Werner's syndromes, which are caused by mutations in DNA helicases and are characterized by increased frequencies of recombination and a predisposition to cancers and accelerated ageing[5].

We have been unable to overexpress Srs2 protein significantly in yeast, suggesting that this protein is unstable in, and/or toxic to, yeast cells. We therefore turned to *Escherichia coli* and an inducible T7 promoter as vehicle for Srs2 expression. Srs2 could be revealed by Coomassie Blue staining of *E. coli* extracts and by immunoblotting with antibodies against Srs2 (Fig. 1a). We subjected *E. coli* lysate to precipitation with ammonium sulphate and a five-step chromatographic fractionation scheme to purify Srs2 to near-homogeneity (Fig. 1b). Purified Srs2 has a robust ssDNA-dependent ATPase activity ($k_{cat} \geq 2,500$ min^{-1}) and a DNA helicase activity[6] that is fuelled by ATP hydrolysis (Fig. 1c).
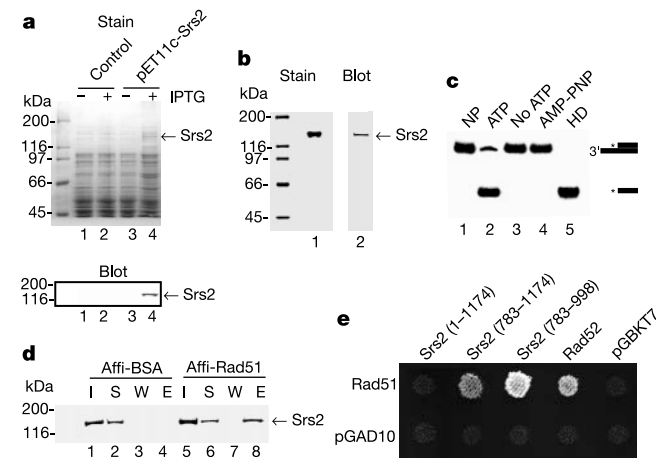
Previous studies have unveiled an anti-recombination function in *SRS2* and a genetic interaction with *RAD51* (refs 7–9). We investigated whether Srs2 protein interacts physically with Rad51 protein, and also tested its effect on the Rad51 recombinase activity[10]. To

examine whether Srs2 associates with Rad51, we coupled the latter to Affi-gel 15 beads and used the resulting matrix to bind Srs2. As shown in Fig. 1d, Srs2 was retained on the Affi-Rad51 beads, but no binding of Srs2 to bovine serum albumin (BSA) immobilized on Affi-beads (Affi-BSA) was detected. An interaction between Rad51 and two carboxy-terminal fragments of Srs2 was seen in the two-hybrid assay in yeast (Fig. 1e). We were unable to detect significant interaction between Rad51 and full-length Srs2 in this assay, which could be the result of low expression of full-length Srs2.

We next tested the effect of Srs2 on the Rad51-mediated homologous pairing and strand exchange reaction that serves to join recombining DNA molecules[10,11]. For this, we employed a commonly used assay in which Rad51 and the heterotrimeric ssDNA-binding factor RPA are incubated with ssDNA and ATP to form a Rad51–ssDNA nucleoprotein filament[11–13]. Such a filament, often called the presynaptic filament[11–13], is then incubated with the homologous linear duplex (Fig. 2Aa). Pairing between the DNA substrates yields a joint molecule, which is further processed by DNA strand exchange to nicked circular duplex (Fig. 2Aa, b). As shown in Fig. 2Ac, d, the addition of a catalytic quantity of Srs2 strongly suppressed the homologous pairing and strand exchange reaction.

To characterize its anti-recombination activity further, Srs2 was added to D-loop reactions in which pairing of a ^{32}P-labelled 90-mer oligonucleotide with a homologous duplex target is mediated by the combination of Rad51 and Rad54 proteins[14,15] (Fig. 2Ba). As reported previously[14–16], efficient D-loop formation was catalysed by Rad51 and Rad54 (Fig. 2Bb, d). As expected, the inclusion of Srs2 decreased the level of D-loop formation (Fig. 2Bb, d). RPA enhanced D-loop formation in the absence of Srs2 (Fig. 2Bc, d), but the inhibitory effect of Srs2 became much more pronounced when RPA was present. We provide an explanation below for this observation.

We considered the possibility that suppression of recombination by Srs2 might result from the dissociation of DNA joints by its helicase activity. To address this, D-loop was formed with Rad51/Rad54 and then Srs2 was added. Srs2 was incapable of dissociating the preformed D-loop, regardless of the presence or absence of RPA

(Fig. 3A), suggesting that suppression of the recombination reaction does not stem from the unwinding of DNA by Srs2.
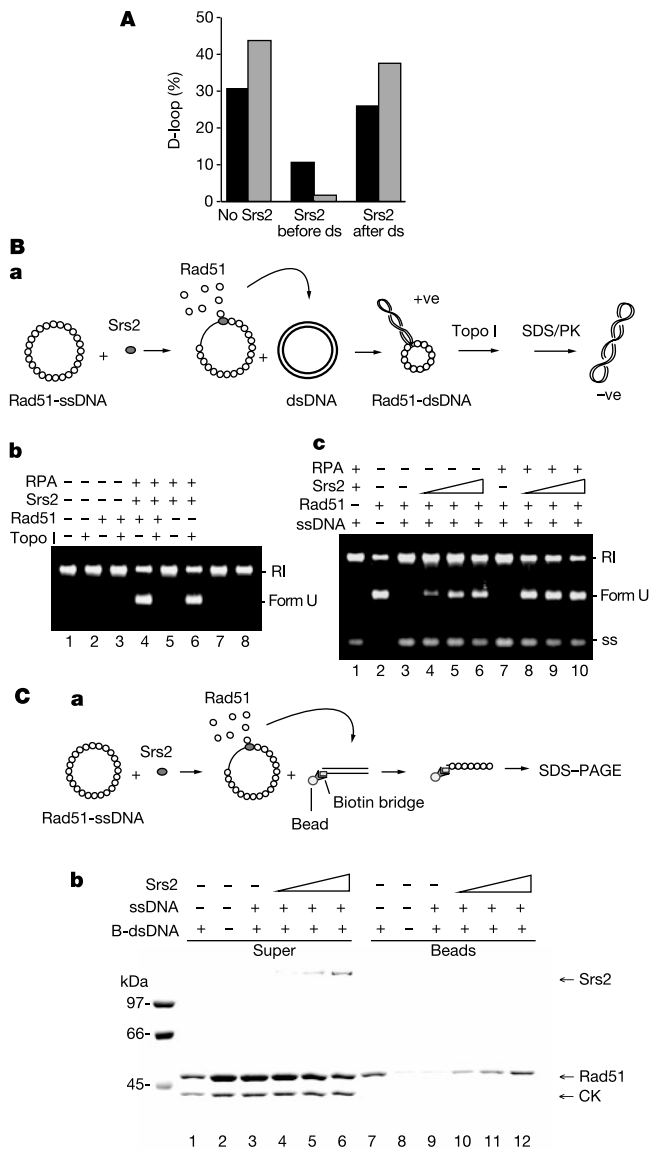
Several approaches were used to test the idea that Srs2 inhibits Rad51 recombinase function by disrupting the presynaptic filament. In doing so, we reasoned that disruption of the presynaptic filament would yield free Rad51 molecules that could be trapped on duplex DNA (dsDNA). The binding of Rad51 to topologically relaxed dsDNA induces lengthening of the DNA[17,18] that can be monitored as a change in the DNA linking number on treatment with topoisomerase I (Fig. 3Ba). The product of this reaction is an underwound species referred to as form U (Fig. 3Bb, lane 4). RPA and Srs2 do not catalyse the formation of form U (Fig. 3Bb, lane 8), and these proteins have no effect on the formation of form U by Rad51 (Fig. 3Bb, compare lanes 6 and 4). The presynaptic filament consisting of Rad51–ssDNA does not make form U (Fig. 3Bc, lane 3). The addition of Srs2 to the Rad51–ssDNA presynaptic filament causes the generation of form U (Fig. 3Bc, lanes 4–6), indicating the transfer of Rad51 from the presynaptic filament to the dsDNA. The addition of RPA further stimulates the Srs2-mediated release of Rad51 from the presynaptic filament and the formation of form U (Fig. 3Bc, lanes 8–10). RPA has high affinity for ssDNA and it can compete with Rad51 for binding to ssDNA[10,19,20]. The enhanced production of form U was therefore probably due to the sequestering of ssDNA by RPA after Srs2 had released Rad51, thereby preventing the renucleation of Rad51 on the ssDNA. This premise was verified by electron microscopy and explains the

Figure 1 Purification and characterization of Srs2. **a**, Extracts from *E. coli* cells harbouring pET11c::Srs2 and the control vector pET11c grown with or without isopropyl β-D-thiogalactoside (IPTG) were analysed by SDS–PAGE and immunoblotting. **b**, Purified Srs2 was analysed by SDS–PAGE (2 μg) and immunoblotting (20 ng). **c**, DNA unwinding by Srs2 occurs with ATP but not without it or with AMP-PNP. The substrate was also incubated alone (NP) or boiled (HD) for 1 min. **d**, Srs2 was mixed with Affi-Rad51 and Affi-BSA beads. The input (I), supernatant (S), wash (W) and SDS eluate (E) were immunoblotted. **e**, Full-length and truncated versions of Srs2 were tested for two-hybrid interaction with Rad51. Empty vectors and Rad52 were included as controls.

Figure 2 Srs2 inhibits Rad51-mediated DNA pairing and strand exchange. **A, a**, The DNA strand exchange scheme. In **b**, the DNA substrates were incubated with Rad51 and RPA. In **c**, Srs2 was also included. The results from **b** and **c** and from reactions with other Srs2 amounts are plotted in **d**. **B, a**, The D-loop reaction scheme. In **b**, Rad51, Srs2 and Rad54 were incubated with the DNA substrates. In **c**, RPA was also included. The results from **b** and **c** and from reactions with other Srs2 amounts are plotted in **d**. Filled symbols, reactions without RPA; open symbols, reactions with RPA.

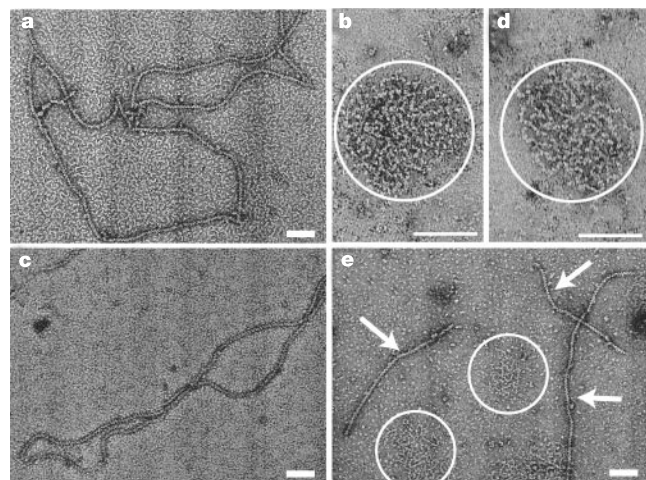RPA-mediated enhancement of the inhibitory effect of Srs2 in the D-loop reaction (Fig. 2B).

The Srs2-mediated disruption of the Rad51 presynaptic filament was examined by a second approach. Here, Rad51 that had been dissociated from ssDNA by Srs2 was trapped on a DNA duplex bound to magnetic beads through a biotin–streptavidin linkage (Fig. 3Ca). Rad51 was eluted from the bead-bound DNA duplex by treatment with SDS and then analysed in a denaturing polyacrylamide gel. Consistent with results from the topoisomerase I-linked assay (Fig. 3B) was the observation that there was an Srs2-concentration-dependent transfer of Rad51 from the presynaptic filament to the bead-bound DNA duplex (Fig. 3Cb).

Last, we used electron microscopy to characterize the action of Srs2 on the Rad51 presynaptic filament. After incubation of Rad51 with circular ssDNA, abundant presynaptic filaments[17,18] were seen (Fig. 4a). Under the same conditions, RPA formed complexes with ssDNA that appeared as compact structures with distinctive protein bulges (Fig. 4b). Although RPA alone was unable to disrupt the Rad51 presynaptic filaments (Fig. 4c), the addition of Srs2 with RPA to the presynaptic filaments caused a complete loss of the filaments, and the concomitant formation of RPA–ssDNA complexes (Fig. 4d). Previous biochemical experiments had shown transfer of Rad51 from the presynaptic filament to dsDNA promoted by Srs2 (Fig. 3B and C). This Srs2-mediated transfer of Rad51 to dsDNA could be observed directly by electron microscopy (Fig. 4e). The data from the electron microscopic analyses agree with results from the biochemical experiments (Figs 2 and 3), because they show that Srs2 disrupts the Rad51 presynaptic filament.

Even though homologous recombination is important for repairing DNA strand breaks induced by ionizing radiation and endogenous agents, and for restarting delinquent DNA replication forks, it can also generate deleterious genomic rearrangements and create DNA structures that cannot be properly resolved[1]. Cells have therefore evolved mechanisms to avoid untimely recombination[1,5]. Our studies provide evidence that Srs2 does this by disrupting the Rad51 presynaptic filament. The same conclusion has been reached independently[21]. Furthermore, even though RPA can function as a cofactor in the assembly of the Rad51 presynaptic filament[10,20], it might also promote the anti-recombination function of Srs2 by preventing reassembly of the presynaptic filament (Figs 3 and 4). That Srs2 uses the free energy from ATP hydrolysis to dislodge Rad51 from the presynaptic filament has been verified with mutant variants of Srs2 (srs2 K41A and srs2 K41R) defective for ATP hydrolysis. The physical interaction noted between Rad51 and Srs2 further suggests a mechanism for targeting the latter to the presynaptic filament. Taken together, the results presented here indicate that the motor activity of Srs2 driven by ATP hydrolysis is capable of dissociating not only DNA structures[6] but also DNA–protein complexes.

Figure 3 Srs2 disrupts the Rad51 presynaptic filament. **A**, D-loop reactions without and with Srs2 added before or after the duplex substrate were performed. The reactions were repeated with RPA present. Black bars, reactions without RPA; grey bars, reactions with RPA. **B**, **a**, The reaction scheme. PK, proteinase K. **b**, Only Rad51 makes form U. In **c**, Rad51 presynaptic filaments, assembled with or without RPA, were treated with Srs2 and topoisomerase. Lane 2 contained form U marker. RI, relaxed duplex; ss, single-stranded DNA. **C**, **a**, The reaction scheme. In **b**, Rad51 presynaptic filaments were incubated with Srs2 and then with beads containing dsDNA. Rad51 was also incubated with beads containing dsDNA (lanes 1 and 7) and beads without DNA (lanes 2 and 8). The supernatant and bead fractions were analysed. CK, creatine kinase.

Figure 4 EM analysis of Rad51 filament disruption by Srs2. **a**, **b**, Rad51 (**a**) and RPA (**b**) were each incubated with ssDNA; examples of the nucleoprotein complexes that formed are shown. **c**, RPA was not able to disrupt preformed Rad51 filaments; an example of the Rad51 filaments present is shown. **d**, Incubation of preformed Rad51 filaments with Srs2 and RPA caused the loss of filaments and concomitant formation of RPA–ssDNA complexes, an example of which is shown. **e**, When preformed Rad51–ssDNA filaments were incubated with Srs2, RPA and linear duplex, RPA–ssDNA complexes were formed (circled) and transfer of Rad51 onto the linear duplex was visualized (arrows). Scale bars, 100 nm.

The inhibitory effect of Srs2 on Rad51-mediated DNA strand exchange can be partly overcome by the inclusion of Rad52 protein, a recombination mediator that promotes Rad51 presynaptic filament assembly[11,12]. However, the Rad55–Rad57 complex, which also has recombination mediator activity[11,12], is much less effective in alleviating the inhibitory effect of Srs2. Furthermore, Rad52 and the Rad55–Rad57 complex do not seem to act synergistically. Interestingly, we have found that Srs2 can also dismantle presynaptic filaments of RecA and human Rad51 proteins. It therefore seems that the presynaptic filaments formed by the RecA/Rad51 class of general recombinases share a conserved feature that is recognized by Srs2, making them prone to disruption by the motor activity of Srs2.

The sensitivity of *srs2* mutants to DNA-damaging agents[6,22] is alleviated by deleting *RAD51* (ref. 23), and the inability to remove Rad51 from DNA in the *srs2* mutants most probably accounts for the hyper-recombination phenotype of these mutants[1]. Similarly, the cell cycle checkpoint recovery and adaptation defect in *srs2* mutants might be related to an inability to evict Rad51 from damaged DNA[2]. Cells mutated for *SRS2* grow slowly, exhibit an extended late S and/or G2 phase, and are defective in meiosis[25]. These defects could result from the generation of unresolvable recombination intermediates that trigger checkpoint activation and thereby compromise cell cycle progression. In addition to functioning as an anti-recombinase, Srs2 could conceivably prevent D-loop reversal by removing Rad51 bound to the displaced ssDNA strand. The various activities of Srs2 might be subject to modulation by phosphorylation[24].

Other DNA helicase enzymes are known to suppress recombination in eukaryotic cells, including the *S. cerevisiae* Sgs1 protein and the human BLM and WRN proteins, mutated in Bloom's syndrome and Werner's syndrome, respectively. Untimely and aberrant recombination events in Bloom's syndrome and Werner's syndrome cells could contribute to the genomic instability in these cells[26]. It has been suggested that BLM and WRN proteins control the level of recombination by dissociating recombination intermediates[5,27]. It will be of interest to test whether Sgs1, BLM and WRN proteins affect the integrity of the hRad51 presynaptic filament, as overexpression of Sgs1 protein can partly suppress some of the defects of *srs2* mutants[28]. □

Methods

Antibodies and Srs2 purification

Polyclonal antiserum was raised against residues 177–646 of Srs2 fused to glutathione *S* transferase. Antibodies were purified from the rabbit anti-serum by affinity chromatography on a column containing the antigen crosslinked to cyanogen bromide-activated sepharose 4B matrix (Amersham Biosciences). *SRS2* gene was placed under the T7 promoter in the vector pET11c to yield plasmid pET11c::Srs2, which was introduced into *E. coli* BL21 (DE3). Srs2 expression was induced by isopropyl β-D-thiogalactoside, and extract from 70 l of culture was subjected to precipitation with ammonium sulphate and chromatographic fractionation in columns of Q Sepharose, SP Sepharose, hydroxyapatite and Mono Q. The final Srs2 pool (300 μg at 2 mg ml^{-1}) was nearly homogeneous and stored in small portions at $-80\,°C$.

DNA substrates

The φX circular (+) strand was from New England Biolabs. The φX replicative form I DNA (Gibco-BRL) was linearized by digestion with *Apa*LI. The pBluescript SK(−) replicative form I DNA was prepared as described[29]. Oligonucleotide D1 has the sequence: 5′-AAATCAATCTAAAGTATATATGAGTAAACTTGGTCTGACAGTTACCAATGCTTAA TCAGTGAGGCACCTATCTCAGCGATCTGTCTATTT-3′, being complementary to positions 1932–2022 of the pBluescript replicative form I DNA. Oligonucleotide H2 has the sequence: 5′-GTAACTGTCAGACCAAGTTTACTCATATATACTTTAGATTGATTT-3′, being complementary to the first 45 residues of oligonucleotide D1. The two oligonucleotides were 5′ end-labelled with [γ-^{32}P]ATP and purified as described[29]. The DNA helicase substrate was obtained by hybridizing D1 to radiolabelled H2, as described[14].

Biotinylated dsDNA coupled to magnetic beads

The ends of a 769-base pair fragment derived from digesting φX174 replicative form I DNA with *Apa*LI and *Xho*I were filled in with the Klenow polymerase, using a mixture of dGTP, dTTP, Bio-7-dATP and Bio-11-dCTP (Enzo Diagnostics). The biotinylated DNA

fragment was immobilized on streptavidin-coated magnetic beads (Roche Molecular Biochemicals) to give biotinylated DNA at 40 ng μl^{-1} packed volume.

Binding of Srs2 to beads containing Rad51

Rad51 and BSA were coupled to Affi-Gel 15 beads (Bio-Rad) at 5 and 12 mg ml^{-1}, respectively[14]. To examine Srs2 binding, 3 μg Srs2 was mixed with 7 μl Affi-Rad 51 or Affi-BSA beads in 30 μl PBS (10 mM KH$_2$PO$_4$ pH 7.2, 150 mM KCl, 1 mM dithiothreitol (DTT) and 0.01% Igepal) at 4 °C for 30 min. The beads were collected by centrifugation; after the supernatant had been decanted off, the beads were washed twice with 100 μl buffer, then treated for 5 min with 30 μl 2% SDS at 37 °C to elute bound Srs2. The various fractions—10 μl each—were analysed by immunoblotting to determine their Srs2 content.

Yeast two-hybrid assay

RAD51 was cloned into pGAD10, which contains the *GAL4* transcription activation domain, and the resulting plasmid was introduced into the haploid yeast strain PJ69-4a (ref. 30). *SRS2* (residues 1–1174), two C-terminal fragments of *SRS2* (residues 783–1174 and residues 738–998), and *RAD52* were cloned into pGBKT7, which contains the *GAL4* DNA-binding domain; the resulting plasmids were introduced into the haploid yeast strain PJ69-4α (ref. 30). Diploid strains obtained by mating plasmid-bearing PJ69-4a and PJ69-4α haploids were grown on synthetic medium lacking tryptophan and leucine. To select for two-hybrid interactions, which would result in the activation of the *ADE2* and *HIS3* reporter genes, diploid cells were replica-plated on synthetic medium lacking tryptophan, leucine and adenine, and also on synthetic medium lacking tryptophan, leucine and histidine[30]. Both platings gave identical results. Only the plating on the tryptophan, leucine and adenine dropout medium is shown in Fig. 1e.

DNA helicase assay

Srs2 (35 nM) was incubated at 30 °C for 10 min with the DNA substrate (300 nM nucleotides) in 10 μl buffer H (25 mM Tris-HCl pH 7.5, 2.5 mM MgCl$_2$, 1 mM DTT, 100 μg ml^{-1} BSA) containing 2 mM ATP or β-γ-imidoadenosine 5′-phosphate (AMP-PNP) and then analysed[14].

Homologous DNA pairing and strand exchange reaction

Buffer R (35 mM Tris-HCl pH 7.4, 2.0 mM ATP, 2.5 mM MgCl$_2$, 50 mM KCl, 1 mM DTT, containing an ATP-regenerating system consisting of 20 mM creatine phosphate and 20 μg ml^{-1} creatine kinase) was used for the reactions, and all the incubation steps were performed at 37 °C. Rad51 (10 μM) was mixed with φX circular (+) strand (30 μM nucleotides) in 30 μl for 5 min, followed by the incorporation of RPA (2 μM) in 1.5 μl and a 3 min incubation. The reaction was completed by adding 3 μl 50 mM spermidine hydrochloride and linear φX dsDNA (30 μM nucleotides) in 3 μl. Portions (4.5 μl) of the reaction mixtures were taken at the indicated times, deproteinized and resolved in agarose gels followed by ethidium bromide staining of the DNA species, as described previously[18]. Srs2 was added to the reactions in 0.9 μl at the time of RPA incorporation.

D-loop reaction

Buffer R was used for the D-loop reactions. The radiolabelled oligonucleotide D1 (3 μM nucleotides) was incubated with Rad51 (1 μM) in 22 μl for 5 min at 37 °C, followed by the incorporation of Rad54 (150 nM) in 1 μl and a 2-min incubation at 23 °C. The reaction was initiated by adding pBluescript replicative form I DNA (50 μM base pairs) in 2 μl. The reaction mixtures were incubated at 30 °C, and 5-μl aliquots were withdrawn at the indicated times and processed for electrophoresis as described above. The gels were dried and subjected to phosphorimaging analysis. The percentage of D-loop refers to the quantity of the replicative form substrate that had been converted into D-loop. When present, RPA (200 nM) and Srs2 (40–70 nM) were added to the preassembled Rad51 filament, followed by a 4-min incubation at 37 °C before Rad54 was incorporated. In Fig. 3A, Srs2 (45 nM) was added to the D-loop reactions before Rad54 as above, or 1 min after the incorporation of the duplex substrate. The reactions were terminated after 4 min of incubation.

Topoisomerase-I-linked DNA unwinding assay

Buffer R was used for the reactions and all the incubation steps were performed at 37 °C. Rad51 (4 μM) was incubated for 4 min with pBluescript (−) strand (20 μM nucleotides) in 7.8 μl. Srs2 (40, 60 or 80 nM) and RPA (1 μM) were added in 1 μl, followed by a 4-min incubation. Topologically relaxed φX174 DNA (12.5 μM nucleotides) in 0.8 μl and 2.5 U calf thymus topoisomerase I (Invitrogen) in 0.4 μl storage buffer were then incorporated to complete the reaction. The reaction mixtures were incubated for 8 min and then stopped by adding SDS to 0.5%. In reactions that did not contain the (−) strand, Rad51, with or without RPA (1 μM) and Srs2 (80 nM), was incubated for 8 min with topologically relaxed φX174 DNA and topoisomerase I in a final volume of 10 μl. The reaction mixtures were treated for 10 min with proteinase K (0.5 mg ml^{-1}) before being analysed in 0.9% agarose gels.

Transfer of Rad51 to bead-bound biotinylated dsDNA

M13mp18 circular (+) strand (7.2 μM nucleotides) was incubated for 5 min with Rad51 (2.4 μM) at 37 °C, followed by the addition of Srs2 (30, 60 or 90 nM) in a final volume of 20 μl buffer R containing 50 mM KCl and 0.01% Igepal. After 3 min at 37 °C, 4 μl magnetic beads containing dsDNA were added to the reaction, followed by constant mixing for 5 min at 23 °C. The beads were captured with the Magnetic Particle Separator (Boehringer Mannheim), washed twice with 50 μl buffer, and the bound Rad51 was eluted with 20 μl 1% SDS. The supernatant, which contained unbound Rad51, and the SDS eluate (10 μl each) were analysed by SDS–polyacrylamide-gel electrophoresis (SDS–PAGE).

Electron microscopy

The reactions were performed in buffer R at 37 °C and had a final volume of 12.5 µl. To assemble the Rad51 presynaptic filament, M13mp18 (+) strand (7.2 µM nucleotides) and 1.3 µg Rad51 (2.4 µM) were incubated for 5 min. To test the effects of Srs2 and RPA, these proteins were added to the reaction mixtures containing the preassembled Rad51 presynaptic filament to final concentrations of 60 nM (Srs2) and 350 nM (RPA), followed by a 3-min incubation. In some cases, linear dsDNA (a 5.2-kilobase fragment derived from the pET24 vector) was also added with Srs2 and RPA to 7.2 µM base pairs, followed by a 5-min incubation. For electron microscopy, 3 µl of each reaction mixture was applied to copper grids coated with thin carbon film after glow-discharging the coated grids for 2 min. The grids were washed twice with buffer R and stained for 30 s with 0.75% uranyl formate. After air-drying, the grids were examined with a Philips Tecnai12 electron microscope under low-dose conditions. Images were recorded either with a charge-coupled device camera (Gatan) or on Kodak SO-163 films at × 30,000 magnification and then scanned on a SCAI scanner (Zeiss). The experiments shown in Fig. 4 were each independently repeated three or more times and at least 100 nucleoprotein complexes were examined in each experiment.

1. Klein, H. L. A radical solution to death. *Nature Genet.* **25,** 132–134 (2000).
2. Vaze, M. B. *et al.* Recovery from checkpoint-mediated arrest after repair of a double-strand break requires Srs2 helicase. *Mol. Cell* **10,** 373–385 (2002).
3. Lee, S. K., Johnson, R. E., Yu, S. L., Prakash, L. & Prakash, S. Requirement of yeast SGS1 and SRS2 genes for replication and transcription. *Science* **286,** 2339–2342 (1999).
4. Gangloff, S., Soustelle, C. & Fabre, F. Homologous recombination is responsible for cell death in the absence of the Sgs1 and Srs2 helicases. *Nature Genet.* **25,** 192–194 (2000).
5. Oakley, T. J. & Hickson, I. D. Defending genome integrity during S-phase: putative roles for RecQ helicases and topoisomerase III. *DNA Repair* **1,** 175–207 (2002).
6. Rong, L. & Klein, H. L. Purification and characterization of the SRS2 DNA helicase of the yeast *Saccharomyces cerevisiae*. *J. Biol. Chem.* **268,** 1252–1259 (1993).
7. Milne, G. T., Ho, T. & Weaver, D. T. Modulation of *Saccharomyces cerevisiae* DNA double-strand break repair by SRS2 and RAD51. *Genetics* **139,** 1189–1199 (1995).
8. Chanet, R., Heude, M., Adjiri, A., Maloisel, L. & Fabre, F. Semidominant mutations in the yeast Rad51 protein and their relationships with the Srs2 helicase. *Mol. Cell. Biol.* **16,** 4782–4789 (1996).
9. Schild, D. Suppression of a new allele of the yeast RAD52 gene by overexpression of RAD51, mutations in srs2 and ccr4, or mating-type heterozygosity. *Genetics* **140,** 115–127 (1995).
10. Sung, P. Catalysis of ATP-dependent homologous DNA pairing and strand exchange by yeast RAD51 protein. *Science* **265,** 1241–1243 (1994).
11. Sung, P., Trujillo, K. M. & Van Komen, S. Recombination factors of *Saccharomyces cerevisiae*. *Mutat. Res.* **451,** 257–275 (2000).
12. Cox, M. M. Recombinational DNA repair of damaged replication forks in *Escherichia coli*: questions. *Annu. Rev. Genet.* **35,** 53–82 (2001).
13. Bianco, P. R., Tracy, R. B. & Kowalczykowski, S. C. DNA strand exchange proteins: a biochemical and physical comparison. *Front. Biosci.* **3,** 570–603 (1998).
14. Petukhova, G., Stratton, S. & Sung, P. Catalysis of homologous DNA pairing by yeast Rad51 and Rad54 proteins. *Nature* **393,** 91–94 (1998).
15. Mazin, A. V., Zaitseva, E., Sung, P. & Kowalczykowski, S. C. Tailed duplex DNA is the preferred substrate for Rad51 protein-mediated homologous pairing. *EMBO J.* **19,** 1148–1156 (2000).
16. Van Komen, S., Petukhova, G., Sigurdsson, S. & Sung, P. Functional cross-talk among Rad51, Rad54, and replication protein A in heteroduplex DNA joint formation. *J. Biol. Chem.* **277,** 43578–43587 (2002).
17. Ogawa, T., Yu, X., Shinohara, A. & Egelman, E. H. Similarity of the yeast RAD51 filament to the bacterial RecA filament. *Science* **259,** 1896–1899 (1993).
18. Sung, P. & Robberson, D. L. DNA strand exchange mediated by a RAD51-ssDNA nucleoprotein filament with polarity opposite to that of RecA. *Cell* **82,** 453–461 (1995).
19. Sung, P. Yeast Rad55 and Rad57 proteins form a heterodimer that functions with replication protein A to promote DNA strand exchange by Rad51 recombinase. *Genes Dev.* **11,** 1111–1121 (1997).
20. Sugiyama, T., Zaitseva, E. M. & Kowalczykowski, S. C. A single-stranded DNA-binding protein is needed for efficient presynaptic complex formation by the *Saccharomyces cerevisiae* Rad51 protein. *J. Biol. Chem.* **272,** 7940–7945 (1997).
21. Veaute, X. *et al.* The Srs2 helicase prevents recombination by disrupting Rad51 nucleoprotein filaments. *Nature* **423,** 309–312 (2003).
22. Aboussekhra, A. *et al.* RADH, a gene of *Saccharomyces cerevisiae* encoding a putative DNA helicase involved in DNA repair. Characteristics of radH mutants and sequence of the gene. *Nucleic Acids Res.* **17,** 7211–7219 (1989).
23. Aboussekhra, A., Chanet, R., Adjiri, A. & Fabre, F. Semidominant suppressors of Srs2 helicase mutations of *Saccharomyces cerevisiae* map in the RAD51 gene, whose sequence predicts a protein with similarities to procaryotic RecA proteins. *Mol. Cell. Biol.* **12,** 3224–3234 (1992).
24. Liberi, G. *et al.* Srs2 DNA helicase is involved in checkpoint response and its regulation requires a functional Mec1-dependent pathway and Cdk1 activity. *EMBO J.* **19,** 5027–5038 (2000).
25. Palladino, F. & Klein, H. L. Analysis of mitotic and meiotic defects in *Saccharomyces cerevisiae* SRS2 DNA helicase mutants. *Genetics* **132,** 23–37 (1992).
26. Adams, M. D., McVey, M. & Sekelsky, J. J. *Drosophila* BLM in double-strand break repair by synthesis-dependent strand annealing. *Science* **299,** 265–267 (2003).
27. Wu, L., Davies, S. L., Levitt, N. C. & Hickson, I. D. Potential role for the BLM helicase in recombinational repair via a conserved interaction with RAD51. *J. Biol. Chem.* **276,** 19375–19381 (2001).
28. Mankouri, H. W., Craig, T. J. & Morgan, A. SGS1 is a multicopy suppressor of srs2: functional overlap between DNA helicases. *Nucleic Acids Res.* **30,** 1103–1113 (2002).
29. Petukhova, G., Stratton, S. A. & Sung, P. Single strand DNA binding and annealing activities in the yeast recombination factor Rad59. *J. Biol. Chem.* **274,** 33839–33842 (1999).
30. Krejci, L., Damborsky, J., Thomsen, B., Duno, M. & Bendixen, C. Molecular dissection of interactions between Rad51 and members of the recombination-repair group. *Mol. Cell. Biol.* **21,** 966–976 (2001).

....

The Srs2 helicase prevents recombination by disrupting Rad51 nucleoprotein filaments

Xavier Veaute*, Josette Jeusset†, Christine Soustelle*‡, Stephen C. Kowalczykowski§, Eric Le Cam† & Francis Fabre*

* *CEA, DSV, Département de Radiobiologie et Radiopathologie, UMR217 CNRS/CEA, BP6, 92265 Fontenay aux Roses Cedex, France*
† *Interactions Moléculaires et Cancer, UMR 81126 CNRS/IGR/UPS, Institut Gustave Roussy, Rue Camille Desmoulins, 94805 Villejuif Cedex, France*
§ *Sections of Microbiology and of Molecular and Cellular Biology, Center for Genetics and Development, University of California, Davis, California 95616-8665, USA*

....

Homologous recombination is a ubiquitous process with key functions in meiotic and vegetative cells for the repair of DNA breaks. It is initiated by the formation of single-stranded DNA on which recombination proteins bind to form a nucleoprotein filament that is active in searching for homology, in the formation of joint molecules and in the exchange of DNA strands[1]. This process contributes to genome stability but it is also potentially dangerous to cells if intermediates are formed that cannot be processed normally and thus are toxic or generate genomic rearrangements. Cells must therefore have developed strategies to survey recombination and to prevent the occurrence of such deleterious events. In *Saccharomyces cerevisiae*, genetic data have shown that the Srs2 helicase negatively modulates recombination[2,3], and later experiments suggested that it reverses intermediate recombination structures[4–7]. Here we show that DNA strand exchange mediated *in vitro* by Rad51 is inhibited by Srs2, and that Srs2 disrupts Rad51 filaments formed on single-stranded DNA. These data provide an explanation for the anti-recombinogenic role of Srs2 *in vivo* and highlight a previously unknown mechanism for recombination control.

Several phenotypes (discussed below) conferred by the *srs2* deletion are suppressed by mutations that prevent formation of the Rad51 nucleofilaments[8,9]. Two hypotheses could explain this suppression: either Srs2 functions in replication and repair to prevent the formation of toxic recombination structures, or Srs2 disrupts dead-end recombination intermediates, possibly formed after the arrest of the replication fork, to allow repair through alternative pathways. This second proposition led us to ask whether purified Srs2 acts on preformed recombination structures.

Srs2 was expressed from a baculovirus vector in which *SRS2* was cloned in frame with a histidine tag at its amino terminus. We showed that the protein fusion expressed in yeast fully complements the sensitivity of *srs2*-deleted cells to radiation (data not shown).

‡ Present address: UMR2167 CNRS Centre de Génétique Moléculaire, Bâtiment 26, avenue de la Terrasse, 91198 Gif-sur-Yvette Cedex, France.

Attachment 5

Krejci L, Macris M, Li Y, Van Komen S, Villemain J, Ellenberger T, Klein H, Sung P

Role of ATP hydrolysis in the antirecombinase function of *S. cerevisiae* Srs2 protein.

J Biol Chem., 279(22): 23193-9. 2004

Role of ATP Hydrolysis in the Antirecombinase Function of *Saccharomyces cerevisiae* Srs2 Protein*

Lumir Krejci‡, Margaret Macris‡, Ying Li§, Stephen Van Komen‡, Jana Villemain¶, Thomas Ellenberger§, Hannah Klein‖, and Patrick Sung‡**

From the ‡Department of Molecular Biophysics and Biochemistry, Yale University School of Medicine, New Haven, Connecticut 06520, the §Department of Biological Chemistry and Molecular Pharmacology, Harvard Medical School, Boston, Massachusetts 02115, the ¶Institute of Biotechnology and Department of Molecular Medicine, University of Texas Health Science Center at San Antonio, San Antonio, Texas 78245, and the ‖Department of Biochemistry, New York University School of Medicine, New York, New York 10016

Mutants of the *Saccharomyces cerevisiae SRS2* gene are hyperrecombinogenic and sensitive to genotoxic agents, and they exhibit a synthetic lethality with mutations that compromise DNA repair or other chromosomal processes. In addition, *srs2* mutants fail to adapt or recover from DNA damage checkpoint-imposed G_2/M arrest. These phenotypic consequences of ablating *SRS2* function are effectively overcome by deleting genes of the *RAD52* epistasis group that promote homologous recombination, implicating an untimely recombination as the underlying cause of the *srs2* mutant phenotypes. The *SRS2*-encoded protein has a single-stranded (ss) DNA-dependent ATPase activity, a DNA helicase activity, and an ability to disassemble the Rad51-ssDNA nucleoprotein filament, which is the key catalytic intermediate in Rad51-mediated recombination reactions. To address the role of ATP hydrolysis in Srs2 protein function, we have constructed two mutant variants that are altered in the Walker type A sequence involved in the binding and hydrolysis of ATP. The srs2 K41A and srs2 K41R mutant proteins are both devoid of ATPase and helicase activities and the ability to displace Rad51 from ssDNA. Accordingly, yeast strains harboring these *srs2* mutations are hyperrecombinogenic and sensitive to methylmethane sulfonate, and they become inviable upon introducing either the *sgs1Δ* or *rad54Δ* mutation. These results highlight the importance of the ATP hydrolysis-fueled DNA motor activity in *SRS2* functions.

DNA helicases perform important functions in various chromosomal transactions, including replication, repair, recombination, and transcription (1, 2). These proteins utilize the chemical energy from the hydrolysis of a nucleoside triphosphate to dissociate DNA structures and nucleoprotein complexes. Interestingly, mutations in several DNA helicases are involved in the pathogenesis of human diseases. For instance, mutations in the XPB and XPD helicases, which constitute subunits of the transcription factor TFIIH that has a dual role in nucleotide excision repair, lead to the cancer prone syndrome xeroderma pigmentosum (3). Furthermore, mutations in the BLM, WRN, and RecQ4 proteins, members of the RecQ helicase family, cause the cancer-prone Bloom, Werner, and Rothmund-Thomson syndromes, respectively (4, 5).

We are interested in the biology of various DNA helicases that influence homologous recombination and DNA repair processes. One such helicase is encoded by the *Saccharomyces cerevisiae SRS2* gene, altered forms of which were first described as either suppressors of the DNA damage sensitivity of *rad6* and *rad18* mutants (6) or as hyperrecombination mutants (7). Detailed genetic analyses have shown that a major function of *SRS2* is to attenuate homologous recombination activity to allow for the channeling of certain DNA lesions into the *RAD6/RAD18*-mediated postreplication repair pathway (8, 9). Accordingly, *srs2* mutants are sensitive to DNA damaging agents and show a hyperrecombination phenotype. Genetic deletion of the *RAD51* or *RAD52*, key members of the *RAD52* epistasis group functioning in homologous recombination, alleviates the DNA damage sensitivity and hyperrecombination phenotypes of *srs2* mutants (8), implicating untimely recombination events as the progenitor of these *srs2* phenotypes. *Srs2* mutations are lethal when combined with mutations in a variety of genes needed for DNA repair and other chromosomal processes, *e.g.* with mutations in the DNA repair and recombination gene *RAD54* and also with mutations in *SGS1*, which codes for the sole RecQ helicase in *S. cerevisiae* (10, 11). The synthetic lethality encountered in the *srs2 sgs1* and *srs2 rad54* double mutants is suppressed by inactivating key recombination genes (11). The available genetic evidence therefore implicates Srs2 protein in the attenuation of recombination events that produce toxic DNA structures or nucleoprotein intermediates (12, 13).

In congruence with the genetic data, biochemical assays have shown that the Srs2 protein strongly suppresses the recombinase activity of Rad51. Interestingly, although Srs2 has the ability to unwind DNA (14, 15) and had been predicted to dissociate DNA intermediates in recombination reactions, its antirecombinase function can be attributed to an ability to disassemble the Rad51-single-stranded DNA (ssDNA)[1] nucleoprotein filament (14, 15), the key catalytic intermediate in recombination reactions (16). Likewise, the failure of *srs2* mu-

** To whom correspondence should be addressed: Molecular Biophysics and Biochemistry, Yale University School of Medicine, 333 Cedar St., SHM C130A, New Haven, CT 06520. Tel.: 203-785-4553; Fax: 203-785-6037; E-mail: Patrick.Sung@yale.edu.
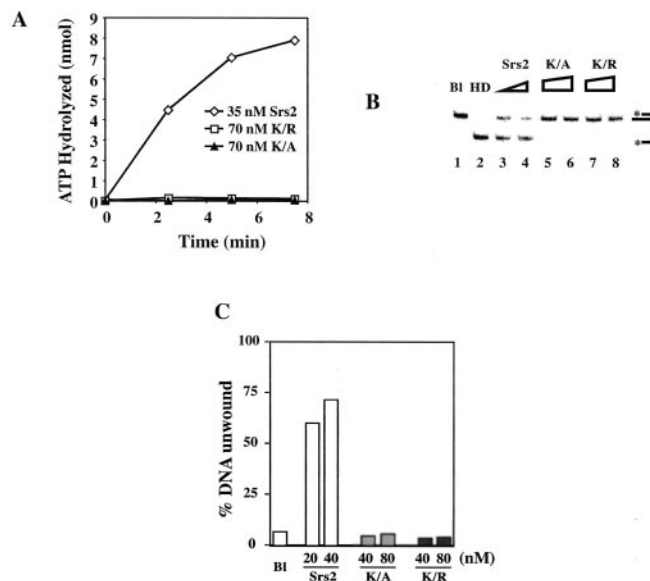
[1] The abbreviations used are: ssDNA, single-stranded DNA; MMS, methylmethane sulfonate; BSA, bovine serum albumin; dsDNA, double-stranded DNA; RPA, replicative protein A.
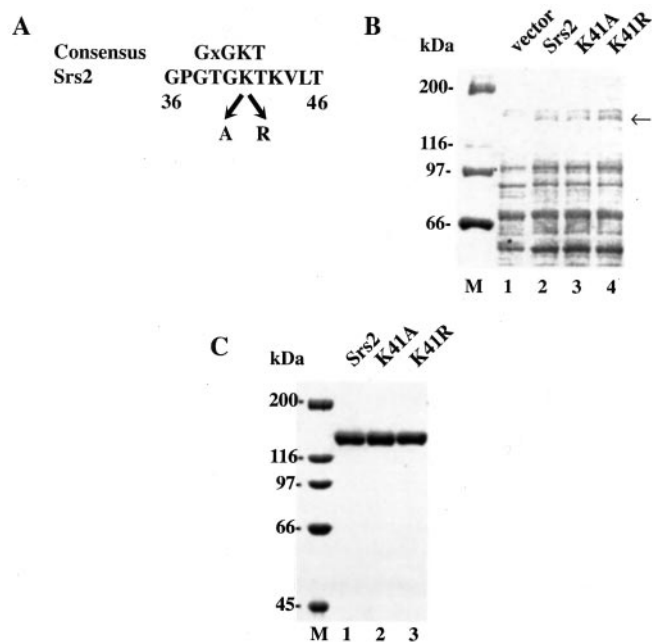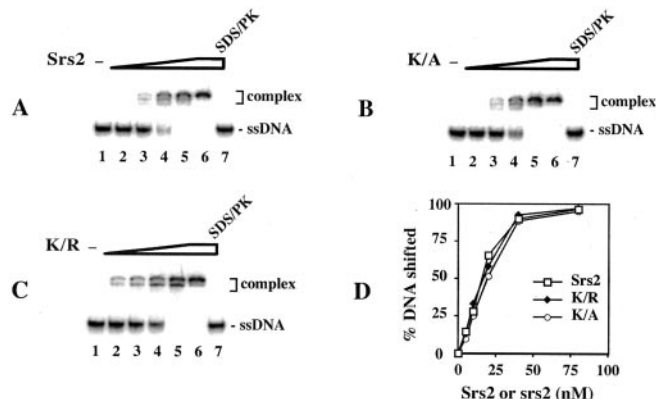
FIG. 1. **Expression and purification of srs2 K41A and srs2 K41R mutant proteins.** *A*, sequence of the Walker type A motif in Srs2 and the two mutant alleles, K41A (*A*) and K41R (*R*), constructed for this study. *B*, extracts from *E. coli* cells harboring the empty protein expression vector pET11c (*vector*, *lane 1*) and plasmids that express wild-type Srs2 (*lane 2*), srs2 K41A (*K41A*, *lane 3*) and srs2 K41R (*K41R*, *lane 4*) proteins were subjected to SDS-PAGE in a 7.5% gel and stained with Coomassie Blue. The *arrow* marks the position of the wild-type Srs2 and mutant srs2 proteins. *C*, purified Srs2 (*lane 1*), srs2 K41A (*K41A*, *lane 2*), and srs2 K41R (*K41R*, *lane 3*) proteins, 2 μg of each, were run in a 7.5% SDS-PAGE and then stained with Coomassie Blue.

FIG. 2. **Biochemical properties of srs2 Walker mutants.** *A*, the ssDNA-dependent ATP hydrolysis activities of Srs2 (35 nM), srs2 K41A (*K/A*, 70 nM), and srs2 K41R (*K/R*, 70 nM) proteins were measured as described under "Materials and Methods." *B*, the DNA unwinding activities of Srs2 (20 and 40 nM in *lanes 3* and *4*), srs2 K41A (*K/A*, 40 and 80 nM in *lanes 5* and *6*), and srs2 K41R (*K/R*, 40 and 80 nM in *lanes 7* and *8*) proteins were assayed using a 3'-tailed DNA helicase substrate. The reaction mixtures were deproteinized and resolved in a native 12% polyacrylamide gel. *HD*, heat-denatured substrate; *Bl*, reaction mixture that did not contain any protein. *C*, quantification of the data in *B*.

tants to recover from or adapt to DNA damage checkpoint-imposed G_2/M cell cycle arrest has been linked to a failure to remove Rad51 from DNA (17). These results imply that, in addition to its ability to unwind double-stranded DNA, Srs2 has a motor activity that clears proteins from single-stranded DNA. Srs2 physically interacts with Rad51 in the yeast two-hybrid system and *in vitro* (14), and it has been suggested that complex formation between Srs2 and Rad51 helps target the former to DNA sites where Rad51 nucleoprotein filaments have assembled (14). In addition to the recombination-related phenotypes, the *srs2Δ* mutant is partially deficient in the activation of the intra-S DNA damage checkpoint in response to treatment with methylmethane sulfonate (MMS) (18). Additionally, two independent studies (19, 20) have implicated *SRS2* in DNA double-strand break repair by the synthesis-dependent single-strand annealing mechanism as well. Srs2 also appears to influence the efficiency of single-strand annealing (17).

As summarized above, Srs2 appears to have a multifunctional role in nuclear processes including an ability to unwind DNA and disassemble the Rad51-ssDNA nucleoprotein filament. Here, we address the role of ATP in Srs2 protein functions by mutating the highly conserved lysine residue in the Walker type A motif expected to be involved in ATP binding and hydrolysis. We show that the resulting srs2 K41A and srs2 K41R mutant proteins are devoid of ATPase and helicase activities and are unable to dislodge Rad51 from DNA. Genetic analyses reveal that the *srs2 K41A* and *srs2 K41R* mutations cause hyperrecombination, sensitivity to MMS, and synthetic lethality with the *sgs1Δ* or *rad54Δ* mutation. Our results thus reveal a requirement for the Srs2 DNA motor activity in recombination attenuation. However, the *srs2 K41A* and *srs2 K41R* mutants are less sensitive to MMS than *srs2* null cells

FIG. 3. **srs2 K41A and srs2 K41R proteins have normal DNA binding activity.** Increasing concentrations (5, 10, 20, 40, and 80 nM in *lanes 2–6*, respectively) of Srs2 (*A*), srs2 K41A (*K/A* in *B*), and srs2 K41R (*K/R* in *C*) were incubated with a ^{32}P-labeled ssDNA oligonucleotide, and the reaction mixtures were analyzed in 12% native polyacrylamide gels. In *lane 7*, the highest concentration (80 nM) of Srs2 or srs2 mutant was incubated with the oligonucleotide substrate, but the reaction mixture was treated with SDS and proteinase K (*SDS/PK*) prior to gel analysis. In *lane 1*, the oligonucleotide substrate was incubated without protein. The percent DNA substrate shifted by Srs2, srs2 K41A, and srs2 K41R was determined by phosphorimaging analysis of the dried gels, and the data points are plotted in *D*.

and exhibit a more pronounced hyperrecombinational phenotype than the latter. It therefore seems possible that Srs2 has additional functions that are not strictly linked to ATP hydrolysis and Rad51 removal from DNA.

MATERIALS AND METHODS

Yeast Media and Strains—Yeast extract-peptone-dextrose (YPD) medium, synthetic complete (SC) medium, and synthetic complete media without leucine (SC-Leu), without uracil (SC-Ura), and without leucine and uracil (SC-Leu-Ura) were prepared as described (21). Media containing 5-fluoro-orotic acid were prepared as described (21). Except where noted, all strains are *RAD5* derivatives of W303 (22). The re-
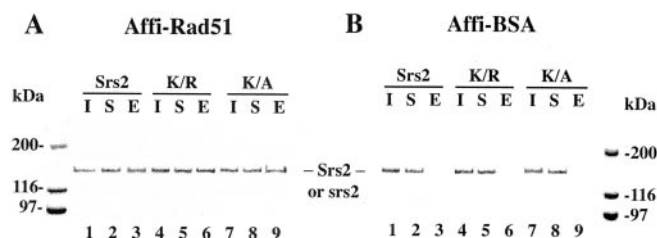
FIG. 4. **Interaction of mutant srs2 proteins with Rad51.** Srs2, srs2 K41A (*K/A*), and srs2 K41R (*K/R*) proteins were mixed with Affi-Rad51 beads (*A*) and Affi-BSA beads (*B*). The starting material (*I*), supernatant that contained unbound Srs2, srs2 K41A, or srs2 K41R (*S*), and the SDS eluate (*E*) were resolved by SDS-PAGE in a 10% gel and then stained with Coomassie Blue.
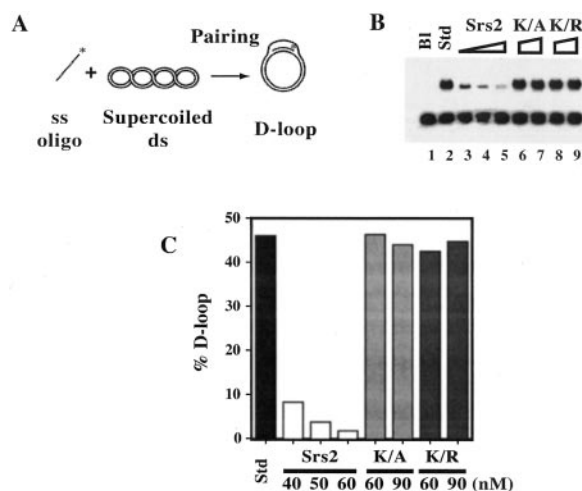

FIG. 5. **Mutant srs2 proteins fail to attenuate Rad51/Rad54/ RPA-mediated D-loop reaction.** *A*, D-loop reaction scheme. The radiolabeled 90-mer oligonucleotide D1 is paired with homologous pBluescript form I DNA to yield a D-loop. *B*, in *lanes 2–9*, radiolabeled D1 was incubated with Rad51, Rad54, RPA, and with or without Srs2 (40, 50, and 60 nM in *lanes 3–5*), srs2 K41A (*K/A*, 60 and 90 nM in *lanes 6 and 7*), or srs2 K41R (*K/R*, 60 and 90 nM in *lanes 8 and 9*) and then pBluescript form I DNA was incorporated. The reaction (*lane 2*) without Srs2 or mutant srs2 is designated as *Std*. *Lane 1* contained the DNA substrates but no protein (*Bl*). The reaction mixtures were incubated for 4 min, deproteinized, and then subject to electrophoresis in a 1% agarose gel. The gel was dried and analyzed in the PhosphorImager. *C*, the data points from phosphorimaging analysis of the gel in *B* are plotted.
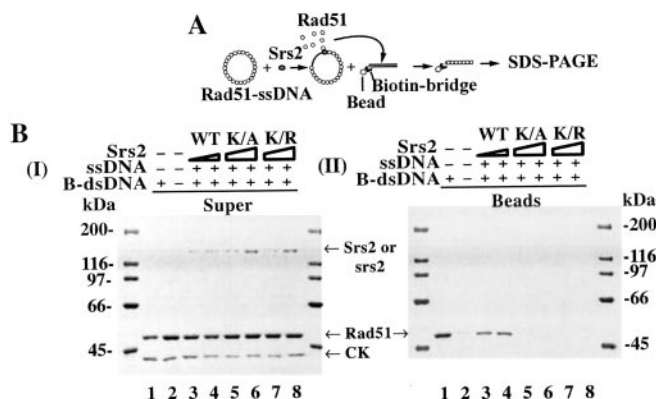

FIG. 6. **Disassembly of Rad51-ssDNA nucleoprotein filaments is coupled to ATP hydrolysis by Srs2.** *A*, Rad51 molecules displaced by Srs2 can be trapped on immobilized DNA duplex attached to streptavidin magnetic beads. Rad51 associated with the magnetic bead-bound duplex is eluted by SDS followed by SDS-PAGE analysis. *B*, pre-assembled Rad51-ssDNA nucleoprotein filaments (*lanes 2–8*) were incubated with Srs2 (*WT*, 60 and 90 nM in *lanes 3* and *4*), srs2 K41A (*K/A*, 90 and 180 nM in *lanes 5* and *6*), or srs2 K41R (*K/R*, 90 and 180 nM in *lanes 7* and *8*), and the reaction mixtures mixed with streptavidin magnetic beads containing biotinylated dsDNA (*lanes 3–8*). In *lane 1*, free Rad51 was mixed with streptavidin magnetic beads that contained biotinylated dsDNA, and in *lane 2*, free Rad51 was mixed with streptavidin magnetic beads that did not contain any dsDNA. The supernatant (*Super*, *panel I*) and bead-bound (*Beads*, *panel II*) fractions were subjected to SDS-PAGE in a 7.5% gel and stained with Coomassie Blue. *CK* denotes creatine kinase in the buffer.
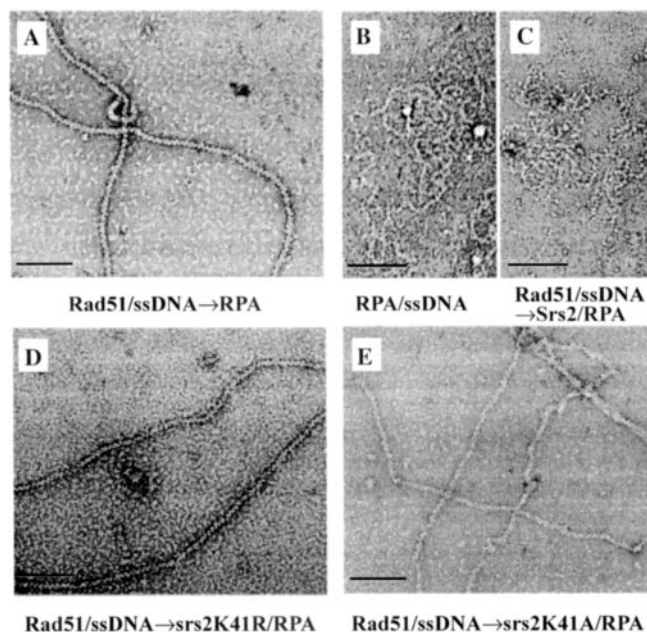

FIG. 7. **Electron micrographs showing effects of Srs2 and mutant srs2 proteins on Rad51-ssDNA filaments.** *A*, Rad51 was incubated with ssDNA before RPA was added, and an example of the resulting Rad51-ssDNA nucleoprotein filaments is shown. *B*, RPA was incubated with ssDNA, and an example of the RPA-ssDNA nucleoprotein complex that formed is shown. *C*, incubation of preformed Rad51-ssDNA nucleoprotein filaments with Srs2 caused the displacement of Rad51 from DNA and the formation of RPA-ssDNA nucleoprotein complexes, an example of which is shown. *D* and *E*, srs2 K41R and srs2 K41A were incapable of disrupting the Rad51-ssDNA nucleoprotein filaments. The *dark bar* represents 100 nm.

maining strains were derived from HKY344-27C and carry *leu2-112*::*URA3*::*leu2-k* and *his3-513*::*TRP1*::*his3-537* recombination reporters (7).

Plasmid Construction—To generate the *SRS2*::pUC18 plasmid, the ORF of *SRS2* was amplified using the following primers: C*GGGATCC*CA<u>CATATG</u>TCGTCGAACAATGATCTTTGGTTGC (sense, BamHI site italic, NdeI underline) and CG*GGATCC*<u>GGAATTC</u>CCTACTAATCGATGACTATGATTTCACCG (antisense, BamHI site italic, EcoRI site underline). The PCR product was digested with BamHI and ligated into the BamHI-digested pUC18. The mutations in the Walker A site in Srs2, K41A, and K41R, were introduced by using mutagenic DNA primers and QuikChange site-directed mutagenesis kit (Stratagene). The mutations were confirmed by DNA sequencing. For protein purification, the *srs2 K41R* and *srs2 K41A* mutant genes were introduced into the pET11c vector. pBS::SRS2 and YIpLac211-srs2 were constructed as follows. The 3.1-kb NdeI-BglII fragments containing the K41R or K41A segments of the mutated *SRS2* gene were used to replace the wild-type *SRS2* segment in plasmid pRL101 (9). Next, a 6.4-kb EcoRI-SalI fragment containing all of the *SRS2* coding region plus 927 bp upstream of the ATG start codon and 1602 bp downstream of the stop codon was inserted into the EcoRI and SalI sites of the polylinker of YIpLac211, which carries the *URA3* selectable marker, to form pHK284 (*srs2 K41A*) and pHK286 (*srs2 K41R*). These plasmids were linearized with BglII and then used to transform W303 and HKY344–27C strains. After selecting for Ura⁺ transformants, cells were grown non-selectively and then streaked on 5-fluoro-orotic acid plates. Fluoro-orotic acid-resistant colonies were tested for MMS sensitivity. MMS-sensitive colonies were examined for the presence of the *srs2* mutations by PCR amplification of the genomic region surrounding the *SRS2 K41* site. Primers used were CTTTTTCTTTTGCGCTGTAT and TCCCGAACTAAAGAAGGTGC. The mutant *srs2 K41A* and *K41R* sites carry an adjacent StyI

TABLE I
Gene conversion in srs2 K41A and srs2 K41R strains

Strains used for the gene conversion tests are derived from HKY344-27C and are of the genotype *leu2-112::URA3::leu2-k his3-513::TRP1::his3-537 ura3-52 trp1 ade1-101*. Strains used are HKY344-27C, HKY344-109D, and HKY1355-7B for *SRS2*, HKY1355-8B, HKY1355-12C, and HKY1355-16C for *srs2 K41A*, HKY1439-5C, HKY1439-9C, and HKY1439-10A for *srs2 K41R*, and F103-2A56, F126-1C, and F121-8C for *srs2Δ*.

Genotype	Leu + Ura + rate	Increase	His + Trp + rate	Increase
		-fold		*-fold*
SRS2	$5.65 \times 10^{-6} \pm 1.24 \times 10^{-6}$		$3.92 \times 10^{-6} \pm 1.65 \times 10^{-6}$	
srs2 K41A	$5.22 \times 10^{-5} \pm 3.63 \times 10^{-5}$	9.24	$6.15 \times 10^{-5} \pm 1.14 \times 10^{-5}$	15.69
srs2 K41R	$6.96 \times 10^{-5} \pm 3.75 \times 10^{-5}$	12.32	$6.77 \times 10^{-5} \pm 3.11 \times 10^{-5}$	17.27
srs2Δ	$1.93 \times 10^{-5} \pm 3.06 \times 10^{-6}$	3.42	Not done	

site that is not present in the wild-type sequence. PCR products were tested for the StyI site by restriction digestion and agarose gel electrophoresis.

Srs2 Expression and Purification—srs2 K41A and srs2 K41R proteins were overexpressed in *Escherichia coli* cells and purified to near homogeneity as described previously for wild-type Srs2 (14, 23). Rad51 was overexpressed in yeast and purified to near homogeneity as described (16). The concentration of the wild-type Srs2 and mutant srs2 proteins was determined by densitometric scanning of SDS-polyacrylamide gels containing multiple loadings of purified proteins against known quantities of bovine serum albumin. The concentrations of Rad51 and RPA were determined using extinction coefficients of 1.29×10^4 and 8.8×10^4 at 280 nm, respectively (24).

DNA Substrates—The H2 and D1 oligonucleotides used in the construction of the helicase substrate have been described (23). Oligo-1 used in the DNA binding experiments has also been described (25). The oligonucleotides were purified from 12% polyacrylamide gels and 5′-end-labeled with [γ-^{32}P] ATP using T4 polynucleotide kinase. The unincorporated nucleotide was removed from the oligonucleotides using Spin30 columns (Bio-Rad). The DNA helicase substrate was obtained by heating equimolar amounts of H2 and radiolabeled D1 oligonucleotides to 95 °C for 10 min in buffer B (50 mM Tris-HCl, pH 7.5, 10 mM MgCl$_2$, 100 mM NaCl), followed by slow cooling to room temperature. The annealed substrate was purified from a 12% non-denaturing polyacrylamide gel, as described (23). The φX174 (+) strand was purchased from New England Biolabs.

ATPase Assay—Srs2 (35 nM) was incubated with viral ssDNA (25 μM nucleotides) in 10 μl of buffer A (30 mM Tris-HCl, pH 7.2, 2.5 mM MgCl$_2$, 1 mM dithiothreitol, 150 mM KCl, and 100 μg/ml BSA) and 1 mM [γ-^{32}P] ATP for the indicated times at 37 °C. The released phosphate was separated from unhydrolyzed ATP by thin layer chromatography, as described (26). The levels of hydrolysis were determined by phosphorimaging analysis of the thin layer chromatography plates in a Personal Molecular Imager FX (Bio-Rad).

DNA Helicase Assay—Srs2 (20 and 40 nM), srs2 K41R (40 and 80 nM), or srs2 K41A (40 and 80 nM) was incubated at 30 °C for 5 min with the helicase substrate (300 nM nucleotides) in 10 μl of buffer H (30 mM Tris-HCl, pH 7.5, 2.5 mM MgCl$_2$, 1 mM dithiothreitol, 100 mM KCl, 2 mM ATP, and 100 μg/ml BSA). The reaction mixtures were resolved by electrophoresis in a 12% non-denaturing polyacrylamide gel run in TAE buffer (40 mM Tris-HCl, pH 7.4, 0.5 mM EDTA) at 4 °C. The gel was dried onto Whatman DE81 paper and analyzed in the PhosphorImager.

DNA Mobility Shift—Varying amounts of Srs2, srs2 K41A or srs2 K41R (0–80 nM) was incubated with ^{32}P-labeled oligo-1 (1.36 μM nucleotides) at 37 °C in 10 μl of buffer D (40 mM Tris-HCl, pH 7.8, 50 mM KCl, 1 mM dithiothreitol, and 100 μg/ml BSA) for 10 min. After the addition of gel loading buffer (50% glycerol, 20 mM Tris-HCl, pH 7.4, 2 mM EDTA, 0.05% orange G), the reaction mixtures were resolved in 12% native polyacrylamide gels in TAE buffer (40 mM Tris acetate, 1 mM EDTA) at 4 °C, and the DNA species were quantified using Quantity One software (Bio-Rad). To release the DNA substrate from bound Srs2 and srs2 mutants, the reaction mixtures were treated with 0.5% SDS and 0.5 mg/ml proteinase K at 37 °C for 10 min before being subject to electrophoresis.

Binding of Srs2 to Rad51 Affi-beads—Affi-gel 15 beads containing Rad51 (Affi-Rad51; 5 mg/ml) and bovine serum albumin (Affi-BSA, 12 mg/ml) were prepared as described previously (26). Purified Srs2, srs2 K41A, or srs2 K41R, 5 μg of each, was mixed with 5 μl of Affi-Rad51 or Affi-BSA in 60 μl of phosphate-buffered saline (10 mM Na$_2$HPO$_4$, 1.8 mM KH$_2$PO$_4$, pH 7.4, and 150 mM NaCl) for 30 min on ice. The beads were washed twice with 150 μl of the same buffer before being treated with 25 μl of 2% SDS to elute bound protein. The starting material, a supernatant that contained unbound Srs2, srs2 K41A, or srs2 K41R,

TABLE II
Mutation rates in srs2 K41A and srs2 K41R strains

Strains used for the *CAN1* mutation rate determinations are derived from *CAN1* versions of W303 and are of the genotype *leu2-3, 112 his3-11, 15 ADE2 ura3-1 trp1-1 RAD5 CAN1*. Strains used are HKY1025-47D for *SRS2*, HKY1434-4A for *srs2 K41A*, HKY1433-8A for *srs2 K41R*, and HKY1303-1B for *srs2Δ*.

| Genotype	Can^r rate	Increase
		-fold
SRS2	9.30×10^{-8}	
srs2 K41A	9.33×10^{-8}	1.0
srs2 K41R	4.66×10^{-8}	0.5
srs2Δ	1.41×10^{-7}	1.5

and the SDS eluate, 10 μl of each, were analyzed by 10% SDS-PAGE and staining with Coomassie Blue.

D-loop Reaction—The reactions were carried out in Buffer R (35 mM Tris-HCl, pH 7.4, 2.0 mM ATP, 2.5 mM MgCl$_2$, 50 mM KCl, 1 mM dithiothreitol, containing an ATP-regenerating system consisting of 20 mM creatine phosphate, 20 μg/ml creatine kinase) and had a final volume of 12.5 μl. The radiolabeled oligonucleotide D1 (3 μM nucleotides) was incubated with Rad51 (1 μM) for 5 min at 37 °C to assemble Rad51-ssDNA nucleoprotein filaments, followed by the incorporation of Rad54 (150 nM) and RPA (200 nM) and a 2 min incubation at 23 °C. The D-loop reaction was initiated by the addition of pBluescript replicative form I DNA (50 μM base pairs). The reaction mixtures were incubated at 30 °C for 4 min, deproteinized by treatment with SDS (0.5%) and proteinase K (0.5 mg/ml) at 37 °C for 10 min, and then run in a 1% agarose gel in TAE buffer. The gel was dried and subject to phosphorimaging analysis. The percentage D-loop refers to the quantity of the replicative form I substrate that had been converted into D-loop. When present, Srs2 (40, 50, and 60 nM), srs2 K41A (60 and 90 nM), and srs2 K41R (60 and 90 nM) were added to the pre-assembled Rad51-ssDNA nucleoprotein filaments, followed by a 4-min incubation at 37 °C before Rad54 and RPA were incorporated.

Transfer of Rad51 to Bead-bound Biotinylated dsDNA—M13mp18 circular (+) strand (7.2 μM nucleotides) was incubated for 5 min with Rad51 (2.4 μM) at 37 °C, followed by the addition of Srs2 (60 and 90 nM), srs2 K41A (90 and 180 nM), or srs2 K41R (90 and 180 nM) in a final volume of 20 μl of buffer R containing 0.01% igepal. After 3 min at 37 °C, 4 μl of magnetic beads containing dsDNA (14) were added to the reaction mixture, followed by constant mixing for 5 min at 23 °C. The beads were captured with the Magnetic Particle Separator (Roche Molecular Biochemicals), washed twice with the same buffer, and the bound Rad51 was eluted with 20 μl of 1% SDS. The supernatant, which contained unbound Rad51, and the SDS eluate (10 μl of each) were analyzed by SDS-PAGE.

Electron Microscopy—The reactions were carried out in buffer R and had a final volume of 12.5 μl. To assemble the Rad51 presynaptic filament, M13mp18(+) strand (7.2 μM nucleotides) and Rad51 (2.4 μM) were incubated at 37 °C for 5 min, followed by the addition of RPA (350 nM) and a 3 min incubation. To test the effects of Srs2 and mutant srs2 proteins, 60 nM of these proteins were incubated with the pre-assembled Rad51-ssDNA nucleoprotein filaments at 37 °C for 3 min. For electron microscopy, 2.5 μl of each reaction mixture was applied to copper grids coated with thin carbon film, after glow-discharging the grids for 2 min. The grids were washed twice with buffer R and stained for 30 s with 0.75% uranyl formate. After air-drying, the grids were examined with a Philips Tecnai 12 electron microscope under low-dose conditions. Images were recorded with a charge-coupled device camera (Gatan).

FIG. 8. **MMS sensitivity of the *srs2 K41A* and *srs2 K41R* mutants.** srs2 mutant strains grow normally on YPD plates but are sensitive when grown on plates containing MMS. Overnight cultures were serially diluted, and 3-μl aliquots were dropped on the plates. The pictures were taken after two and three days of incubation at 30 °C.
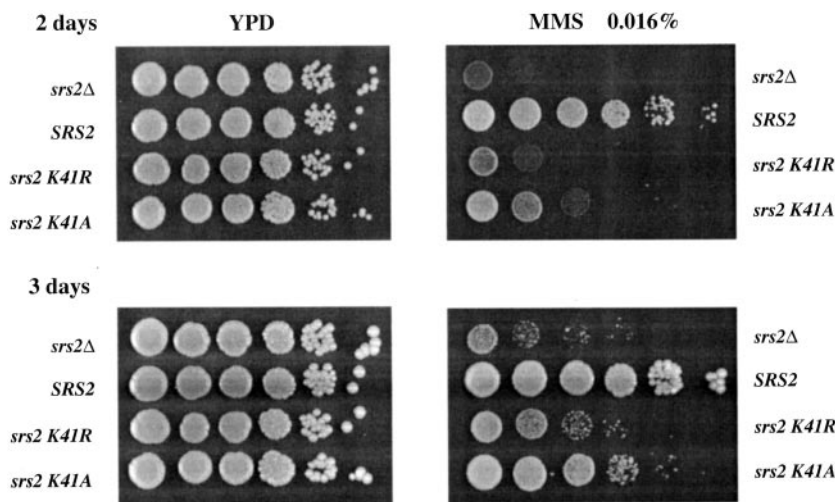
Genetic Studies—MMS sensitivity was determined using freshly made YPD plates containing 0.016% MMS. Overnight cultures of strains to be tested were serially diluted, and 3-μl aliquots of each dilution were applied onto YPD and YPD+MMS plates. Growth was assessed after 2 and 3 days at 30 °C. Forward mutation rates of *CAN1* were determined in haploid *CAN1* strains by fluctuation tests. These tests were conducted according to the median method (27) and were repeated three to five times for each genotype. Gene conversion between intrachromosomal *leu2-112* and *leu2-k* as well as between *his3-513* and *his3-537* heteroalleles was measured in haploid strain HKY344-27C and its isogenic derivatives.

RESULTS

srs2 Variants Mutated for the Walker Type A ATP Binding Motif—Srs2 contains canonical Walker-type ATP binding motifs. For addressing the role of ATP binding and hydrolysis in Srs2 functions, we have substituted the highly conserved lysine residue (lysine 41) in the Walker type A motif with either alanine or arginine using site-directed mutagenesis (Fig. 1*A*). The *srs2 K41A* and *srs2 K41R* mutant genes were sequenced to ensure that no unintended change had been introduced during the mutagenesis procedure. To express the srs2 K41A and srs2 K41R proteins, the mutant genes were placed under the isopropyl-1-thio-β-D-galactopyranoside-inducible T7 promoter in the *E. coli* expression vector pET11c, which we previously used for the expression and purification of wild-type Srs2 (14). Expression of the srs2 K41A and srs2 K41R mutant proteins in *E. coli* was verified by SDS-PAGE analysis of cell extracts (Fig. 1*B*) and by immunoblot analysis of these extracts with affinity-purified anti-Srs2 polyclonal antibodies (14). The srs2 K41A and srs2 K41R mutant proteins were purified to near homogeneity (Fig. 1*C*) using the chromatographic procedure that we have developed for wild-type Srs2 (14).

Biochemical Properties of srs2 K41A and srs2 K41R Mutant Proteins—Based on studies with the equivalent Walker mutations in other DNA-dependent ATPases (28, 29), the srs2 K41A and srs2 K41R mutant proteins were expected to be defective in ATP hydrolysis. This expectation was confirmed by examining the ATPase activity of purified proteins with [α-^{32}P] ATP and thin layer chromatography (14, 23). We showed previously that ATP hydrolysis by Srs2 occurs only in the presence of DNA with ssDNA being much more effective than dsDNA in this regard (9, 23). As summarized in Fig. 2*A*, although robust ATPase activity was observed with wild-type Srs2 in the presence of ssDNA (14, 23), the two srs2 mutant proteins showed less than 1% of the wild-type level of ATP hydrolysis. Likewise, no significant ATP hydrolysis by either of the srs2 mutants was seen when the ssDNA was omitted or substituted with dsDNA (data not shown). We next examined the two srs2 mutant

proteins for DNA helicase activity using a ^{32}P-labeled substrate that contained a 40-bp duplex region adjacent to a 40-nucleotide 3'-ssDNA overhang (Fig. 2*B* and Ref. 23). As shown in Fig. 2*B*, although wild-type Srs2 at 40 nM unwound greater than 70% of the substrate after 5 min of incubation, neither of the srs2 mutants, even at the increased concentration of 80 nM, showed a significant helicase activity under the same conditions (Fig. 2*B*) or even after a prolonged incubation (data not shown).

Even though the results presented in Fig. 2 were consistent with the premise that the K41A and K41R mutations abolish the ATPase activity of Srs2, there existed the possible caveat that this defect had originated from a loss of DNA binding by the mutant proteins. For this reason, we compared the DNA binding ability of the two Walker mutants to that of the wild-type protein by a DNA mobility shift assay. To do this, increasing amounts of wild-type Srs2 and the two mutant proteins were incubated with a ^{32}P-labeled 83-mer oligonucleotide, followed by resolution of the reaction mixtures in non-denaturing polyacrylamide gels and phosphorimaging analysis of the dried gels to detect and quantify the DNA mobility shift. As shown in Fig. 3, both srs2 mutant proteins were just as proficient as wild-type Srs2 in DNA binding. Consistent with this result, using the same DNA substrate, we found that DNA binding by wild-type Srs2 and the two srs2 mutant proteins is not influenced by ATP (data not shown).

Attenuation of Rad51-mediated Homologous DNA Pairing and Strand Exchange by Srs2 Requires ATP Hydrolysis—Recently, we (14) and Fabre and co-workers (15) demonstrated that Srs2 is highly adept at attenuating Rad51-mediated homologous DNA pairing and strand exchange, the biochemical reaction that serves to link recombining chromosomes (30). In addition, a physical interaction between Rad51 and Srs2 was demonstrated by us (14). Before examining the srs2 K41A and srs2 K41R mutant proteins for their ability to suppress the Rad51 recombinase activity, we first verified that the srs2 mutant proteins retain the ability to interact with Rad51. For this, purified Srs2, srs2 K41A, and srs2 K41R proteins were each mixed with Affi-Gel beads that contained covalently conjugated Rad51 protein (Affi-Rad51) or Affi-Gel beads that contained conjugated bovine serum albumin (Affi-BSA). After being washed with buffer, the Affi-Rad51 and Affi-BSA beads were treated with SDS to elute bound Srs2 and srs2 mutant proteins. As shown in Fig. 4*A*, the two srs2 mutant proteins interacted with Rad51 just as avidly as wild-type Srs2 did. As expected, neither the wild-type Srs2 protein nor either of the srs2 mutants was retained on the Affi-BSA control beads (Fig. 4*B*).

Dependence of Srs2 Functions on ATP Hydrolysis

We employed the D-loop assay (Fig. 5*A*) for testing the proficiency of the srs2 K41A and srs2 K41R mutant proteins in recombination attenuation. As reported in our published work, the addition of a catalytic quantity of Srs2 (40–60 nM) to the D-loop reaction containing Rad51 (1 μM), Rad54 (150 nM), and RPA (200 nM) caused pronounced inhibition (Fig. 5, *B* and *C*). For instance, at 50 nM Srs2, the level of D-loop was suppressed by greater than 10-fold (Fig. 5, *B* and *C*). Importantly, as much as 90 nM of srs2 K41A and srs2 K41R did not exert any inhibitory effect on the D-loop reaction (Fig. 5, *B* and *C*), thus revealing a requirement for the Srs2 ATPase activity in the attenuation of the Rad51 recombinase activity. We independently verified this conclusion by using a homologous DNA pairing and strand exchange system that employs ϕX174 (+) strand DNA and linear duplex as substrates (Refs. 14 and 16, data not shown).

Disassembly of Rad51-ssDNA Nucleoprotein Filament by Srs2 Requires ATP Hydrolysis—The results above have verified that the ATPase activity of Srs2 protein is indispensable for attenuating Rad51-mediated recombination reactions *in vitro*. We have devised previously a bead-based biochemical assay to monitor the Srs2-mediated dissociation of Rad51 from ssDNA. Briefly, Rad51 molecules displaced by Srs2 from the presynaptic filament are trapped on a biotinylated duplex DNA fragment tethered to streptavidin-conjugated magnetic beads, followed by elution of Rad51 from the beads and SDS-PAGE analysis (Fig. 6*A*, and Ref. 14). As reported previously, incubation of Rad51 nucleoprotein filaments with Srs2 protein (60–90 nM) resulted in the release of Rad51 from the filaments as indicated by Rad51 being trapped on the streptavidin-magnetic beads that contained duplex DNA (Fig. 6*B*). Importantly, neither of the srs2 mutants, even in an amount twice that of Srs2 (180 nM), was capable of releasing Rad51 protein from the nucleoprotein filaments (Fig. 6*B*).

We also used electron microscopy to examine the ability of the two srs2 mutant proteins to catalyze the disassembly of the presynaptic filament, following the guidelines described in Krejci *et al.* (14). Briefly, the Rad51 presynaptic filament, which is extended and has a striated appearance (Fig. 7*A*), was incubated with Srs2 or the srs2 mutant proteins in the presence of RPA, and the dissociation of the Rad51 filament was gauged by the disappearance of the filament and the concomitant appearance of RPA-ssDNA nucleoprotein complexes, which appear as compact structures with bulges of bound protein molecules (14) (Fig. 7*B*). As expected, incubation of the Rad51 presynaptic filament with Srs2 led to its replacement by the RPA-ssDNA complex (Fig. 7*C*). However, the Rad51 filament was completely stable in the presence of either srs2 K41R (Fig. 7*D*) or srs2 K41A (Fig. 7*E*). Taken together, the results from the biochemical and electron microscopy analyses (Figs. 6 and 7) clearly indicated that disassembly of the Rad51 presynaptic filament by Srs2 requires the ATPase activity of the latter.

Genetic Characterization of the srs2 K41A and srs2 K41R Mutant Alleles—Previous studies (8, 9) of *SRS2* have highlighted the role of *SRS2* in attenuating Rad51-mediated recombination. We determined the effect of loss of Srs2 ATP hydrolysis on mitotic gene conversion, using two reporters that measure intra-chromosomal gene conversion between heteroalleles. As shown in Table I, both *srs2 K41A* and *srs2 K41R* elevated the gene conversion rates with both reporters. Interestingly, the hyperrecombination phenotype of two *srs2* mutants was even more pronounced than that of the *srs2* deletion mutant. Thus, the results show clearly that the antirecombination function of Srs2 requires the ATPase activity of this protein. Although the rate of gene conversion is increased in
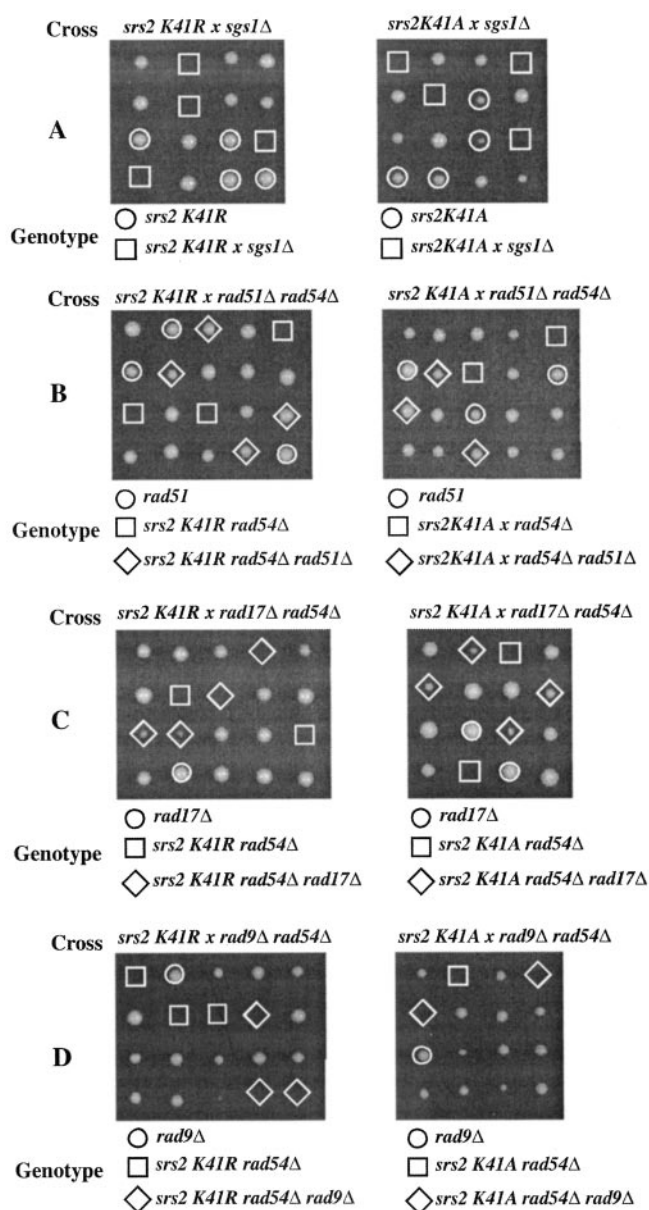

FIG. 9. **Synthetic lethal behavior of the *srs2 K41A* and *srs2 K41R* mutants.** Four or five tetrads from crosses indicated above each picture are shown. Synthetic lethality with the *sgs1Δ* mutation is shown in *A*. Synthetic lethality with the *rad54Δ* mutation is suppressed by loss of *RAD51* (*B*), partially suppressed by loss of the DNA damage checkpoint gene *RAD17* (*C*), and not suppressed by loss of the DNA damage checkpoint gene *RAD9* (*D*).

the *srs2* mutants, the spontaneous mutation rate measured for forward mutations at *CAN1* remains unchanged (Table II).

Mutants of *SRS2* are sensitive to MMS and other DNA damaging agents (8), and MMS sensitivity was actually used in our study to select transplacement segregants harboring the two *srs2* Walker mutant alleles (see "Materials and Methods"). The MMS sensitivity of the *srs2 K41A* and *srs2 K41R* strains is shown in Fig. 8. Both *srs2* mutants were sensitive in this assay, but the *srs2Δ* strain was significantly more sensitive than either of the two point mutants.

The *srs2Δ* mutation by itself is not lethal, but *srs2Δ* cells become inviable when *SGS1* or *RAD54* is also ablated (9, 11, 12). To determine the role of the Srs2 ATPase activity in these genetic interactions, we combined the *srs2 K41A* and *srs2 K41R* mutations with *sgs1Δ* or *rad54Δ*. The *srs2 K41A sgs1Δ* and *srs2 K41R sgs1Δ* double mutants are inviable or grow extremely

poorly (Fig. 9*A*), whereas the *srs2 K41A rad54Δ* and *srs2 K41R rad54Δ* double mutants are inviable (Fig. 9*B*). We checked the possible suppression of the *srs2 rad54Δ* lethality by *rad51Δ*, rad9Δ, or *rad17Δ* (8) by constructing the respective triple mutants. The lethality of *srs2 rad54Δ* is fully overcome by *rad51Δ* (Fig. 9*B*) and partially suppressed by *rad17Δ* (Fig. 9*C*), but *rad9Δ* was ineffective in this regard (Fig. 9*D*).

DISCUSSION

To assess the role of ATP hydrolysis in Srs2 protein functions, we have constructed variants of this protein that harbor mutations in the Walker type A motif involved in ATP binding and hydrolysis. We have overexpressed the srs2 K41A and srs2 K41R proteins in *E. coli* and purified them to near homogeneity. Our biochemical analyses show that both of these mutant proteins retain DNA binding activity and the ability to interact with Rad51, but they are defective in ATP hydrolysis and lack DNA helicase activity. Both srs2 mutant proteins are unable to dissociate the Rad51 presynaptic filament and, accordingly, do not exert any inhibitory effect on Rad51-mediated homologous DNA pairing and strand exchange. The biochemical studies reported here thus establish the requirement for ATP hydrolysis in Srs2-mediated DNA unwinding and disassembly of the Rad51 presynaptic filament.

The results from our genetic studies provide support for the premise that ATP hydrolysis by Srs2 is needed to prevent untimely recombination, as the *srs2 K41A* and *srs2 K41R* mutants both exhibit a hyperrecombinational phenotype. Interestingly, the degree of hyperrecombination (measured as intrachromosomal gene conversion between heteroalleles) is even more pronounced in the srs2 point mutants than in the *srs2Δ* strain. In this regard, the two *srs2* Walker mutants resemble the *srs2–101* mutant described previously, which harbors the amino acid change of P39L, that is also significantly more hyperrecombinogenic than the *srs2Δ* mutant (9). These observations (Ref. 9 and this study) suggest that when Srs2 is absent, other non-recombinational pathways are used to repair spontaneous DNA damage, but when Srs2 protein is present but defective, it can interfere with these DNA repair pathways. Alternatively, or in addition, the *srs2* Walker mutants and the *srs2–101* mutant could induce DNA damage that is channeled into the homologous recombination pathway for repair, convert non-recombinogenic DNA lesions into recombinogenic ones, or enhance the activities of homologous recombination proteins. Because Srs2 is also important for the maximal activation of the S phase DNA damage checkpoint (18), it remains possible that the two *srs2* Walker mutants exert a positive influence on homologous recombination efficiency through its effect on checkpoint pathways (18). Further studies are needed to distinguish among these possibilities. That the *srs2 K41A* and *srs2 K41R* mutants do not behave exactly like the *srs2Δ* mutant is further attested by the observation that they are less sensitive to MMS than the latter. Just as in the case of *srs2Δ* (8, 9), we observed synthetic lethality of both *srs2* Walker mutants with either *rad54Δ* or *sgs1Δ*. We have also shown that the lethality of *srs2 K41A rad54Δ* and *srs2 K41R rad54Δ* can be overcome by deleting *RAD51* or *RAD17*.

Recently, reports from Haber and co-workers (20) and Kupiec and co-workers (19) showed that Srs2 is also needed for the repair of a site-specific double-strand break by synthesis-dependent single-strand annealing or double-ended synthesis-dependent single-strand annealing, the major pathway of gene conversion in mitotic yeast cells. In one of these published studies, the *srs2 K41A* allele was found to be defective in synthesis-dependent single-strand annealing (20). Likewise, the function of Srs2 in promoting adaptation or recovery from DNA damage checkpoint-mediated G_2/M arrest is reliant on its ATPase activity, as the *srs2 K41A* mutant is defective in this regard (17). We similarly expect the *srs2 K41R* mutant to be impaired in synthesis-dependent single-strand annealing and recovery/adaptation from DNA damage checkpoint-mediated G_2/M arrest. However, as alluded to above, whether or not the two srs2 Walker mutants retain S phase checkpoint function (18) will have to be determined experimentally.

We have demonstrated a physical interaction between Srs2 and Rad51 by the yeast two-hybrid system and also by biochemical means with purified proteins (14). We have suggested that the physical interaction between Rad51 and Srs2 may be germane for targeting the latter to chromosomal sites, *e.g.* ssDNA gaps created at stalled DNA replication forks, where Rad51 molecules are bound. However, it remains possible that the physical interaction noted (14) enables Srs2 to specifically displace Rad51 from ssDNA. The isolation of Rad51 and Srs2 mutants defective in complex formation will be necessary to address this issue.

REFERENCES

1. Schmid, S. R., and Linder, P. (1992) *Mol. Microbiol.* **6,** 283–291
2. Howard, M. T., Neece, S. H., Matson, S. W., and Kreuzer, K. N. (1994) *Proc. Natl. Acad. Sci. U. S. A.* **91,** 12031–12035
3. Berneburg, M., and Lehmann, A. R. (2001) *Adv. Genet.* **43,** 71–102
4. Ellis, N. A., Groden, J., Ye, T. Z., Straughen, J., Lennon, D. J., Ciocci, S., Proytcheva, M., and German, J. (1995) *Cell* **83,** 655–666
5. Yu, C. E., Oshima, J., Fu, Y. H., Hisama, F., Alisch, R., Matthews, S., Nakura, J., Miki, T., Ouais, S., Martin, G. M., Mulligan, J., and Schellenberg, G. D. (1996) *Science* **272,** 258–262
6. Lawrence, C. W., and Christensen, R. B. (1979) *J. Bacteriol.* **139,** 866–876
7. Aguilera, A., and Klein, H. L. (1988) *Genetics* **119,** 779–790
8. Chanet, R., Heude, M., Adjiri, A., Maloisel, L., and Fabre, F. (1996) *Mol. Cell. Biol.* **16,** 4782–4789
9. Rong, L., Palladino, F., Aguilera, A., and Klein, H. L. (1991) *Genetics* **127,** 75–85
10. Lee, S. K., Johnson, R. E., Yu, S. L., Prakash, L., and Prakash, S. (1999) *Science* **286,** 2339–2342
11. Gangloff, S., Soustelle, C., and Fabre, F. (2000) *Nat. Genet.* **25,** 192–194
12. Klein, H. L. (2001) *Genetics* **157,** 557–565
13. Klein, H. L. (2000) *Nat. Genet.* **25,** 132–134
14. Krejci, L., Van Komen, S., Li, Y., Villemain, J., Reddy, M. S., Klein, H., Ellenberger, T., and Sung, P. (2003) *Nature* **423,** 305–309
15. Veaute, X., Jeusset, J., Soustelle, C., Kowalczykowski, S. C., Le Cam, E., and Fabre, F. (2003) *Nature* **423,** 309–312
16. Sung, P. (1994) *Science* **265,** 1241–1243
17. Vaze, M. B., Pellicioli, A., Lee, S. E., Ira, G., Liberi, G., Arbel-Eden, A., Foiani, M., and Haber, J. E. (2002) *Mol. Cell* **10,** 373–385
18. Liberi, G., Chiolo, I., Pellicioli, A., Lopes, M., Plevani, P., Muzi-Falconi, M., and Foiani, M. (2000) *EMBO J.* **19,** 5027–5038
19. Aylon, Y., Liefshitz, B., Bitan-Banin, G., and Kupiec, M. (2003) *Mol. Cell. Biol.* **23,** 1403–1417
20. Ira, G., Malkova, A., Liberi, G., Foiani, M., and Haber, J. E. (2003) *Cell* **115,** 401–411
21. Sherman, F. (1991) in *Guide to Yeast Genetics and Molecular Biology* (Guthrie, C., and Fink, G. R., eds) pp. 3–21, Academic Press, San Diego, CA
22. Thomas, B. J., and Rothstein, R. (1989) *Genetics* **123,** 725–738
23. Van Komen, S., Reddy, M. S., Krejci, L., Klein, H., and Sung, P. (2003) *J. Biol. Chem.* **278,** 44331–44337
24. Sugiyama, T., Zaitseva, E. M., and Kowalczykowski, S. C. (1997) *J. Biol. Chem.* **272,** 7940–7945
25. Krejci, L., Song, B., Bussen, W., Rothstein, R., Mortensen, U. H., and Sung, P. (2002) *J. Biol. Chem.* **277,** 40132–40141
26. Petukhova, G., Stratton, S., and Sung, P. (1998) *Nature* **393,** 91–94
27. Lea, D. E., and Coulson, C. A. (1949) *J. Genet.* **119,** 264–284
28. Sung, P., Higgins, D., Prakash, L., and Prakash, S. (1988) *EMBO J.* **7,** 3263–3269
29. Sung, P., and Stratton, S. A. (1996) *J. Biol. Chem.* **271,** 27983–27986
30. Sung, P., Krejci, L., Van Komen, S., and Sehorn, M. G. (2003) *J. Biol. Chem.* **278,** 42729–42732

Attachment 6

55

Colavito S, Macris-Kiss M, Seong C, Gleeson O, Greene EC, Klein HL, Krejci L, Sung P

Functional significance of the Rad51-Srs2 complex in Rad51 presynaptic filament disruption.

Functional significance of the Rad51-Srs2 complex in Rad51 presynaptic filament disruption

Sierra Colavito[1], Margaret Macris-Kiss[1], Changhyun Seong[1], Olive Gleeson[2], Eric C. Greene[3], Hannah L. Klein[2], Lumir Krejci[1,4,*] and Patrick Sung[1,*]

[1]Department of Molecular Biophysics and Biochemistry, Yale University School of Medicine, New Haven, CT 06520, [2]Department of Biochemistry and Kaplan Cancer Center, New York University, School of Medicine, New York, NY 10016, [3]Department of Biochemistry and Molecular Biophysics, Columbia University College of Physicians and Surgeons, New York, NY 10032, USA and [4]Department of Biology and National Center for Biomolecular Research, Masaryk University, Brno 62500, Czech Republic

ABSTRACT

The *SRS2* (Suppressor of RAD Six screen mutant 2) gene encodes an ATP-dependent DNA helicase that regulates homologous recombination in *Saccharomyces cerevisiae*. Mutations in *SRS2* result in a hyper-recombination phenotype, sensitivity to DNA damaging agents and synthetic lethality with mutations that affect DNA metabolism. Several of these phenotypes can be suppressed by inactivating genes of the *RAD52* epistasis group that promote homologous recombination, implicating inappropriate recombination as the underlying cause of the mutant phenotype. Consistent with the genetic data, purified Srs2 strongly inhibits Rad51-mediated recombination reactions by disrupting the Rad51-ssDNA presynaptic filament. Srs2 interacts with Rad51 in the yeast two-hybrid assay and also *in vitro*. To investigate the functional relevance of the Srs2-Rad51 complex, we have generated srs2 truncation mutants that retain full ATPase and helicase activities, but differ in their ability to interact with Rad51. Importantly, the srs2 mutant proteins attenuated for Rad51 interaction are much less capable of Rad51 presynaptic filament disruption. An internal deletion in Srs2 likewise diminishes Rad51 interaction and anti-recombinase activity. We also present evidence that deleting the Srs2 C-terminus engenders a hyper-recombination phenotype. These results highlight the importance of Rad51 interaction in the anti-recombinase function of Srs2, and provide evidence that this Srs2 function can be uncoupled from its helicase activity.

INTRODUCTION

Homologous recombination (HR) is a major pathway for the elimination of DNA double-strand breaks (DSBs) induced by genotoxic agents or that arise from endogenous damage and replication fork demise. As such, HR is critical for maintaining genome integrity and important for cancer avoidance in humans (1–3). Paradoxically, intermediates generated by the HR machinery can trigger prolonged arrest of the cell cycle (4), and the aberrant resolution of these intermediates can lead to gross chromosomal rearrangements, such as translocations (5,6). Moreover, the HR machinery can interfere with other DNA repair pathways, such as *RAD6/RAD18*-mediated post-replicative repair (PRR) (4,7). For these reasons, cells possess multiple mechanisms to prevent untimely and deleterious HR events. One such mechanism is mediated by the *SRS2* (Suppressor of RAD Six screen mutant 2) gene in *Saccharomyces cerevisiae*.

A mutant variant of *SRS2* was first recognized as a suppressor of the DNA damage sensitivity of *rad6* or *rad18* mutants (8). Suppression of the *rad6* or *rad18* DNA repair defect by the *srs2* mutation requires that HR be functional (9), suggesting that *SRS2* negatively regulates HR. By attenuating HR, it is thought that *SRS2* helps ensure the channeling of DNA lesions encountered by the DNA replication machinery into the Rad6/Rad18-mediated PRR pathway. Yeast strains harboring certain *SRS2* mutations also exhibit a

hyper-recombination phenotype, failure to recover from DNA damage checkpoint-mediated G2/M arrest, and synthetic lethality with a variety of other mutations, such as *sgs1,* that affect DNA metabolism (10). The synthetic lethality of these double mutants often can be overcome by eliminating HR (11,12), implicating inappropriate HR events as the cause of lethality.

As a member of the SF1 family of nucleic acid unwinding enzymes (13), Srs2 possesses ssDNA-dependent ATPase and DNA helicase activities (14,15). In concordance with the genetic data, Srs2 strongly inhibits the formation of DNA joints in *in vitro* recombination reactions that are mediated by the Rad51 recombinase (16,17). Extensive biochemical and electron microscopic analyses have shown that Srs2 accomplishes this feat by disrupting the Rad51 presynaptic filament, comprised of a right-handed Rad51 helical polymer assembled on ssDNA (16,17), that catalyzes recombination reactions (18). The Rad51 presynaptic filament dissociative function and HR attenuating role of Srs2 require its ATPase activity (19). Srs2 interacts with the sumoylated form of the proliferating cell nuclear antigen (PCNA) at DNA replication forks (20,21). This serves to target Srs2 to DNA replication forks to prevent Rad51 presynaptic filament assembly, thereby avoiding unwanted recombination during DNA replication (20,21). Interestingly, when PCNA is not able to be sumoylated, Srs2 recruitment to S phase replication fork foci is decreased, while its recruitment to recombination foci is unaffected (22). This reveals that recruitment of Srs2 to replication forks or sites of recombination are independent processes.

Interestingly, even though Srs2 suppresses spontaneous recombination events, it facilitates DSB repair by the synthesis-dependent single-strand annealing (SDSA) pathway of HR (23–25). In addition to its DSB repair function, Srs2 has been shown to have a role in DNA damage checkpoint activation during S phase (26) and to act with DNA polymerase δ to suppress DNA triplet repeat expansion, possibly by unwinding DNA stem-loop structures formed by the repeats (27,28).

By yeast two hybrid and biochemical analyses, Srs2 was found to physically interact with Rad51 (16). However, the significance of the Rad51-Srs2 complex with regards to the anti-recombinase function of Srs2 is not clear. Here, we finely map the Rad51 interaction domain in Srs2 and generate mutant srs2 forms that retain ATP hydrolysis and helicase activities, but differ in their ability to interact with Rad51. We show that the Rad51 interaction-deficient mutant srs2 proteins are attenuated for the Rad51 presynaptic filament dissociative function. Our results thus reveal a requirement for complex formation with Rad51 in the anti-recombinase function of Srs2.

MATERIALS AND METHODS

Yeast two-hybrid assay

RAD51 was fused to the *GAL4* transcription activation domain in the vector pGAD10, and a C-terminal *SRS2* fragment encompassing residues 783–1174 harboring the Rad51 interaction domain (16) was fused to the *GAL4* DNA-binding domain in pGBKT7. The pGAD10-*RAD51* and pGBKT7-srs2 plasmids were introduced into haploid yeast strains PJ69-4a (*MATa trp1-901 leu2-3,112 ura3-52 his3-200 gal4Δ gal80Δ LYS2::GAL1-HIS3 GAL2-ADE2 met2::GAL7-lacZ*) and PJ69-4α (*MATα trp1-901 leu2-3,112 ura3-52 his3-200 gal4Δ gal80Δ LYS2::GAL1-HIS3 GAL2-ADE2 met2::GAL7-lacZ*), respectively (29,30). Diploid strains obtained by mating plasmid-bearing PJ69-4a and PJ69-4α haploids were grown on synthetic medium lacking tryptophan and leucine (30). To select for two-hybrid interactions, which would result in the activation of the *ADE2* or *HIS3* reporter genes, diploid cells were replica-plated on synthetic medium lacking tryptophan, leucine and adenine, or on synthetic medium lacking tryptophan, leucine and histidine, respectively. Both plating gave the same results. Only the plating on the tryptophan, leucine and adenine dropout medium is shown in Figure 1A. Additional pGBKT7-based plasmids containing Srs2 residues 783–998, 783–914 and 783–862 were also tested for interaction with Rad51.

Plasmid construction

The pET11c-(His)₉-*SRS2* plasmid was generated by site-directed mutagenesis (Stratagene) of pET11c-*SRS2*, resulting in the addition of an N-terminal 9-histidine tag to the open reading frame of Srs2 (21). The srs2 variants were generated by site-directed mutagenesis (Stratagene) using the pET11c-(His)₉-*SRS2* plasmid as template. The srs2 783–998 and srs2 783–1174 cloned in pGBKT7 were described elsewhere (16). The other two constructs, srs2 783–862 and srs2 783–914 in pGBKT7 were generated by site-directed mutagenic insertion of a stop codon in srs2 783–998/pGBKT7.

Protein purification

The purification of the (His)₉-tagged Srs2 and mutant srs2 proteins from *Escherichia coli* cells (50 g of cell paste, from 10 L of culture) was conducted as previously described (15), except that an affinity step on nickel NTA agarose was included to exploit the (His)₉ tag. Peak fractions from the SP Sepharose column were combined and incubated with 2 ml of nickel-NTA agarose (Qiagen) for 2 h at 4°C with gentle mixing. The beads were washed with 50 ml of K buffer (20 mM K_2HPO_4, pH 7.4, 10% glycerol, 0.5 mM DTT and 0.5 mM EDTA) containing 300 mM KCl and 10 mM imidazole. Srs2 or mutant was eluted with 12 ml (8 fractions of 1.5 ml each) of 300 mM imidazole in K buffer containing 300 mM KCl. The peak fractions were diluted with 2.5 volumes of T buffer (20 mM Tris–HCl, pH 7.5, 10% glycerol, 0.5 mM DTT and 0.5 mM EDTA), before being fractionated in a 1 ml Mono S column, as described (16). The nearly homogeneous Srs2 and mutant protein preparations were concentrated to ∼5 mg/ml and stored in small aliquots at −80°C.

Rad51 and RPA were over-expressed in yeast and purified to near homogeneity, as described (31). Rad54 and PCNA were expressed in *E. coli* and purified to near homogeneity, as described (32,33).

DNA substrates

The DNA helicase substrate was constructed using the unlabeled H3 oligonucleotide and ^{32}P-labeled H1 oligonucleotide, as previously described (15). The ϕX174 (+) strand DNA was purchased from New England Biolabs. The D1 oligonucleotide used in the D-loop assay and the 150-mer E oligonucleotide used in electron microscopy have been described (16,34).

Affinity pulldown assays

Affi-gel 15 beads containing Rad51 (Affi-Rad51; 5 mg/ml) and bovine serum albumin (Affi-BSA; 12 mg/ml) were prepared as described previously (35). (His)$_9$-tagged Srs2 or the indicated mutant variant (5 µg) was incubated with 5 µl of Affi-Rad51 or Affi-BSA in 30 µl of K buffer (20 mM K$_2$HPO$_4$, 10% glycerol, 0.5 mM EDTA, 0.01% Igepal and 1 mM DTT) containing 150 mM KCl for 1 hr on ice, with gentle mixing. The beads were washed twice with 150 µl of the same buffer before being treated with 30 µl of 2% SDS to elute the bound protein. The supernatant that contained unbound Srs2 or mutant, the second wash, and the SDS eluate, 10 µl of each, were analyzed by 7.5% SDS-PAGE and staining with Coomassie Blue. For the pull-down with srs2 Δ875–902 and Rad51, purified (His)$_9$-tagged Srs2 or srs2 Δ875–902 (5 µg) was mixed with purified Rad51 (5 µg) in buffer K containing 150 mM KCl for 1 hr on ice, before adding 10 µl Ni-NTA agarose beads (Qiagen) and continuing the incubation for 30 min on ice with gentle mixing. The beads were washed twice with 150 µl of the same buffer before being treated with 30 µl of 2% SDS to elute the bound protein. The supernatant that contained unbound proteins, the second wash and the SDS eluate, 10 µl each, were analyzed by 7.5% SDS-PAGE and staining with Coomassie Blue. For examining Srs2-PCNA complex formation, nickel pull-downs were conducted as described above for srs2 Δ875–902 and Rad51, however purified PCNA (5 µg) was used in place of Rad51.

ATPase assay

Purified Srs2 or truncated srs2 (35 nM) was incubated with 1 mM (γ-^{32}P) ATP and ϕX174 (+) strand DNA (25 µM nucleotides) in 10 µl of buffer A (30 mM Tris–HCl, pH 7.5, 2.5 mM MgCl$_2$, 1 mM DTT, 150 mM KCl and 100 µg/ml BSA) for 7.5 min at 37°C. The level of ATP hydrolysis was determined by thin layer chromatography with phosphorimaging analysis in a Personal Molecular Imager FX (Bio-Rad), as described (35).

DNA helicase assay

Purified Srs2 or mutant srs2 (40 nM) was incubated at 30°C for 5 min with the helicase substrate (300 nM nucleotides) in 10 µl of buffer H (30 mM Tris–HCl, pH 7.5, 2.5 mM MgCl$_2$, 1 mM DTT, 100 mM KCl, 2 mM ATP and 100 µg/ml BSA). The reaction mixtures were stopped, deproteinized and resolved in a 10% nondenaturing polyacrylamide gel run in TAE buffer (40 mM Tris–HCl, pH 7.4, 0.5 mM EDTA) at 4°C.

The gel was dried onto Whatman DE81 paper and subjected to phosphorimaging analysis.

D-loop reaction

Reactions were carried out in Buffer D (35 mM Tris–HCl, pH 7.5, 2 mM ATP, 2.5 mM MgCl$_2$, 1 mM DTT, including an ATP-regenerating system consisting of 20 mM creatine phosphate and 20 µg/ml creatine kinase) and 50, 100 or 150 mM KCl in a final volume of 12.5 µl, as described previously (16). The ^{32}P-labeled D1 oligonucleotide (3 µM nucleotides) was incubated with Rad51 (1 µM) for 5 min at 37°C to assemble the Rad51-ssDNA nucleoprotein filaments, followed by the incorporation of RPA (200 nM) and a 4 min incubation. Then, Rad54 (150 nM) was added, and following a 3 min incubation at 23°C, the reaction was initiated by adding pBluescript replicative form I DNA (50 µM base pairs), followed by a 6 min incubation at 30°C. The reaction was stopped by treatment with SDS (0.5%) and proteinase K (0.5 mg/ml) at 37°C for 5 min and resolved in a 1% agarose gel in TAE buffer. The gel was dried and subjected to phosphorimaging analysis. The percentage D-loop refers to the quantity of the D1 oligonucleotide substrate that has been converted into D-loop. When present, Srs2 or mutant srs2 (7.5 or 15 nM, as indicated) was added to the reaction with RPA.

DNA strand exchange reaction

Reactions were conducted at 37°C in Buffer R (35 mM Tris–HCl, pH 7.4, 2 mM ATP, 2.5 mM MgCl$_2$, 50 mM KCl, 1 mM DTT and an ATP-regenerating system) in a final volume of 12.5 µl, as described previously (36). Rad51 (10 µM) was incubated with ϕX174 circular (+) strand (30 µM nucleotides) for 4 min, followed by a 6 min incubation with RPA (2 µM). The reaction was completed by adding spermidine hydrochloride (4 mM) and linear ϕX dsDNA (30 µM nucleotides). After an 80 min incubation, the reaction mixtures were deproteinized and resolved in 0.9% agarose gels, followed by ethidium bromide staining of the DNA species. When present, Srs2 or srs2 mutant (30–60 nM, as indicated) was added to the reaction with RPA.

Topoisomerase I-linked assay

Reactions were carried out in 10 µl of Buffer R at 37°C. Rad51 (4 µM) was incubated for 5 min with ϕX174 circular (+) strand DNA (20 µM nucleotides). Srs2 or mutant srs2 (60 or 80 nM, as indicated) and RPA (1 µM) were added, followed by a 4 min incubation. Topologically relaxed ϕX174 DNA (12.5 µM nucleotides) and 2.5 U calf thymus topoisomerase I (Invitrogen) were then incorporated to complete the reaction. After 8 min of incubation, the reaction mixtures were deproteinized and then subject to electrophoresis in 0.9% agarose gels. The DNA species were stained with ethidium bromide.

Electron microscopy

Reaction mixtures were assembled as described for the DNA strand exchange reaction except that the 150-mer

E oligonucleotide (34) (7.2 µM nucleotides), Rad51 (2.4 µM), RPA (0.5 µM), Srs2 or mutant srs2 (100 nM) were used. After a 3 min incubation, the reaction mixtures were diluted 10 times with buffer R lacking the ATP regenerating system, and a 3 µl aliquot was applied to 400-mesh grids coated with carbon film and which had been glow-discharged in air. The grids were stained with 2% uranyl acetate for 30 sec and rinsed with water before being examined with a Tecnai 12 Biotwin electron microscope (FEI company) equipped with a tungsten filament at 100 keV. Digital images were captured with a Morada (Olympus Soft Imaging Solutions) charge-coupled device camera at a nominal magnification of 87 000X.

Yeast strains

All yeast strains were in the W303 background (*leu2-3, 112 his3-11,15 ade2-1 ura3-1 trp1-1 can1-100 RAD5*). All constructs were verified by DNA sequencing. The strains were: HKY2070-4 (*srs2 1–860*), HKY2082-4 (*srs2 Δ875– 902*), HKY590-1D (*srs2Δ*), HKY579-10A (*SRS2*), and F28-1A (*rad18Δ*).

Methyl methane sulfonate sensitivity

Methyl methane sulfonate (MMS) sensitivity was determined using freshly made plates containing 0.005% MMS. Overnight cultures of strains were serially diluted and 4 µl aliquots of each dilution were applied onto YPD and YPD + MMS plates. Growth was assessed after 2 and 3 days at 30°C. The *rad18Δ* strain used has been described (37).

Determination of recombination rates

Recombination rates were calculated by the median method of Lea and Coulson (38) using the *leu2-ecoRI::URA3::leu2-bstEII* recombination system as described previously (39). Three different strains derived from the same parental strains were analyzed for each genotype studied. For each strain, nine independent colonies were analyzed for each fluctuation test.

RESULTS

Mapping the Srs2-Rad51 interaction in the yeast two-hybrid assay

In previously published work, we and others demonstrated an interaction between Rad51 and the carboxy-terminal region of Srs2 in the yeast two-hybrid assay, such that Srs2 fragments encompassing residues 783–1174 or residues 783–998 are capable of Rad51 association (16,40) (Figure 1A). Based on these two-hybrid data, additional constructs harboring two other portions of the Srs2 C-terminus were created and tested for Rad51 interaction. As shown in Figure 1A, while the 783–914 fragment showed robust interaction with Rad51, no signal could be detected with the 783–862 fragment (Figure 1A). Based on these results, we suspected the Rad51 interaction domain in Srs2 to lie between amino acid residues 862 and 914.
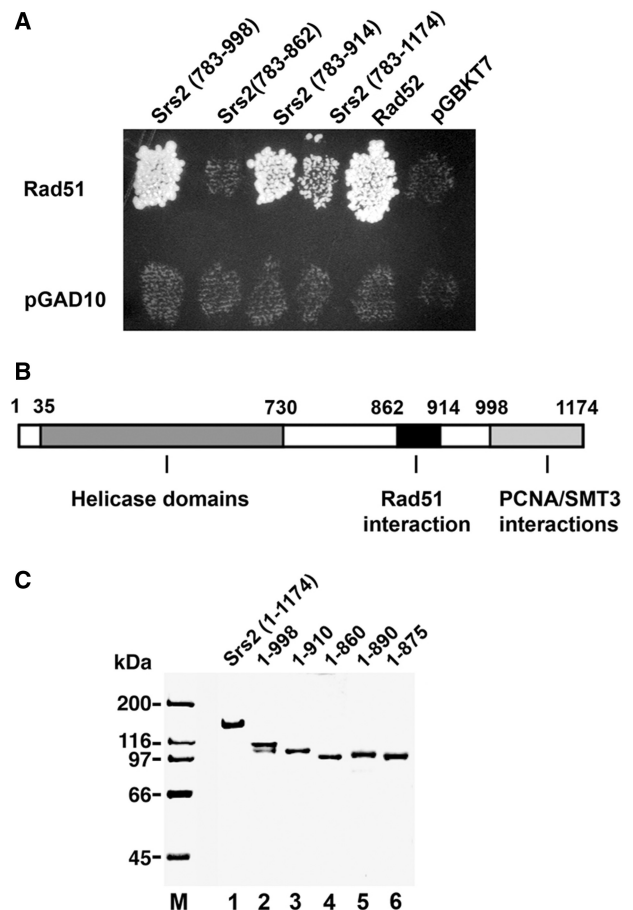

Figure 1. Two-hybrid interactions of Rad51 with Srs2. (**A**) Fragments of Srs2 were tested for two-hybrid interaction with Rad51 by plating on medium lacking leucine, tryptophan and adenine. The empty vector (pGBKT7) and plasmid harboring *RAD52* were included as negative and positive controls, respectively. (**B**) A schematic of the helicase and protein-protein interaction domains in Srs2. (**C**) Purified Srs2, srs2 1–998, srs2 1–910, srs2 1–860, srs2 1–890 and srs2 1–875, 1 µg each, were analyzed by SDS-PAGE and stained with Coomassie Blue.

C-terminally truncated variants of Srs2 deficient for Rad51 interaction

To verify the yeast two-hybrid data *in vitro* and for additional biochemical analyses, we constructed various C-terminally truncated Srs2 variants—1–998, 1–910, 1–890, 1–875 and 1–860—by introducing stop codons within the pET11c-(His)₉-SRS2 plasmid. The tagged full length Srs2 and the truncated variants were expressed in *E. coli* by the use of the IPTG-inducible T7 promoter. The chromatographic procedure for purification of the (His)₉-tagged proteins was modified from the original protocol (16) to include a nickel affinity step. By this method, we were able to purify full length Srs2 and the truncated srs2 variants to near homogeneity (Figure 1C).

To test for interaction with Rad51, purified Srs2 and the five srs2 truncation mutant proteins were each mixed with Affi-gel beads that contained covalently conjugated Rad51 protein (Affi-Rad51) or bovine serum albumin (Affi-BSA). The beads were washed with buffer before being treated with SDS to elute the bound Srs2 or srs2
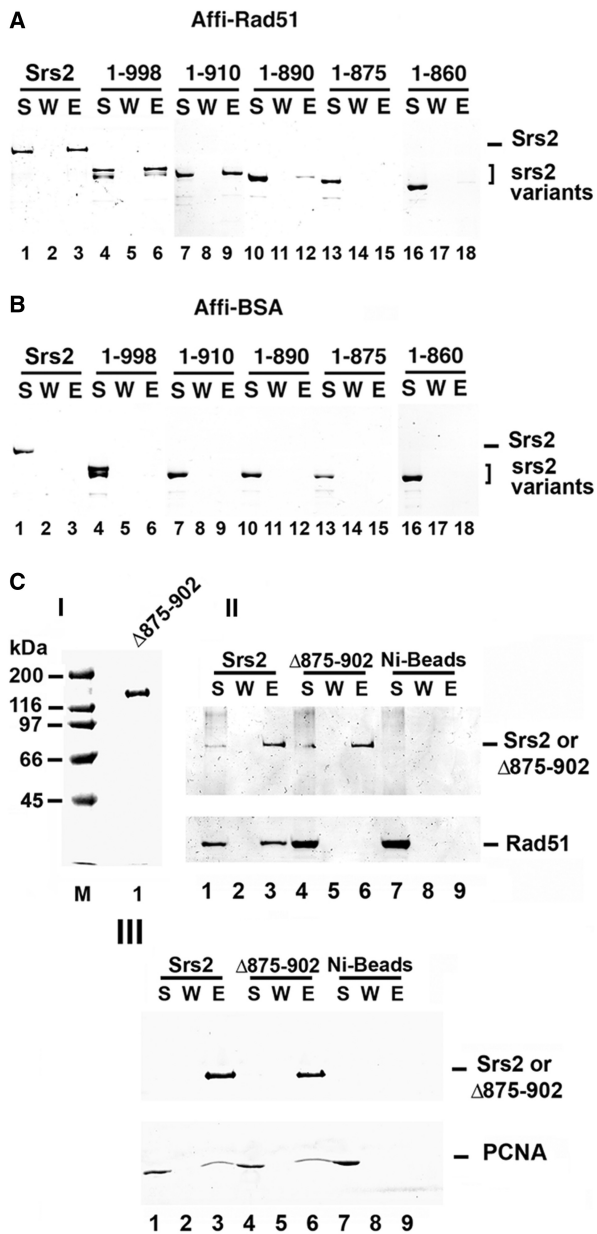
Figure 2. Mapping of Rad51 interaction by *in vitro* pull-down assay. Purified Srs2, srs2 1–998, srs2 1–910, srs2 1–890, srs2 1–875 and srs2 1–860 were mixed with Affi-Rad51 beads (**A**) or Affi-BSA beads (**B**) The supernatant that contained unbound protein (S), wash (W) and the SDS eluate (E) were resolved by SDS-PAGE and stained with Coomassie Blue. (**C**) In panel I, Purified srs2 Δ875–902, 1 μg, analyzed by SDS-PAGE and stained with Coomassie Blue. In panel II, Srs2 and srs2 Δ875–902 were combined with purified Rad51 and mixed with nickel NTA agarose beads. The supernatant that contained unbound protein (S), wash (W) and the SDS eluate (E) were resolved by SDS-PAGE and stained with Coomassie Blue (lanes 1–6). As control, Rad51 alone was incubated with nickel NTA agarose beads (lanes 7–9). In panel III, Srs2 and srs2 Δ875–902 were examined for PCNA interaction (lanes 1–9) following the same procedure in panel II.

mutant protein, followed by SDS-PAGE analysis. Consistent with results from the yeast two-hybrid analysis, full length Srs2, srs2 1–998, and srs2 1–910 were retained on the Affi-Rad51 beads but not on the Affi-BSA beads (Figure 2A and B). Importantly, and

consistent with the yeast two-hybrid results, srs2 1–860 did not bind the Affi-Rad51 beads (Figure 2A), indicating that it is defective for Rad51 interaction. Moreover, while srs2 1–890 showed only a slightly attenuated affinity for Affi-Rad51, little or no srs2 1–875 was retained on the Affi-Rad51 beads (Figure 2A). These results indicated that the region between amino acid residues 875 and 910 in Srs2 is likely critical for Rad51 interaction.

Based on the above domain mapping results, we created a form of Srs2 that lacks amino acid residues 875–902, but is otherwise full length. The srs2 Δ875–902 mutant was expressed and purified to near homogeneity following the strategy used for other Srs2 forms (Figure 2C, panel I) and examined for interaction with Rad51. The internal deletion mutant exhibited some non-specific binding to Affi-BSA beads, thus the pulldown analysis was conducted using nickel NTA affinity beads to isolate the protein complex via the $(His)_9$-tag on Srs2. Full-length Srs2 was able to bind Rad51 as expected, but little or no Rad51 associated with srs2 Δ875–902 (Figure 2C, panel II). This provides evidence that the region between residues 875–902 of Srs2 is needed for Rad51 interaction. Additionally, we tested the ability of the internal deletion mutant to bind PCNA. The PCNA interaction domain is known to lie in the far C-terminus of Srs2 (20,41), and consistent with this, we found that srs2 Δ875–902 is just as adept as Srs2 in PCNA interaction (Figure 2C, panel III).

C-terminal truncations do not affect ATPase and helicase activities

The deduced Rad51 interaction domain in Srs2 resides distally to the catalytic domains that are concerned with ATP hydrolysis and helicase activity (Figure 1B), so we expected even the shortest of our srs2 truncation variants, i.e. srs2 1–860, to retain the ability to hydrolyze ATP and unwind DNA. To verify this expectation, the purified srs2 mutant proteins were first tested for their ability to hydrolyze ATP. We showed previously that ATP hydrolysis by Srs2 is ssDNA-dependent (15), and, as summarized in Figure 3A, all of the srs2 truncation variants show a level of ssDNA-dependent ATPase activity comparable to that of the wild-type protein. We next examined the various srs2 truncation mutant proteins for DNA helicase activity using a ^{32}P-labeled substrate that contained a 40 bp duplex region with a 40-nucleotide 3′-ssDNA overhang [Figure 3B and (15)]. As shown in Figure 3B, the srs2 mutants were as adept as the full length Srs2 protein in unwinding the DNA substrate. Based on the above results, we can conclude that all of the truncated forms of srs2 that we have generated possess ATP hydrolysis and DNA helicase activities comparable to those of the wild-type counterpart.

Interaction of Srs2 with Rad51 is critical for its anti-recombinase function

We (16) and others (17) demonstrated previously that Srs2 inhibits the recombinase activity of Rad51 (42). We used the D-loop assay to test the anti-recombinase activity of our srs2 truncation mutants (Figure 4A).
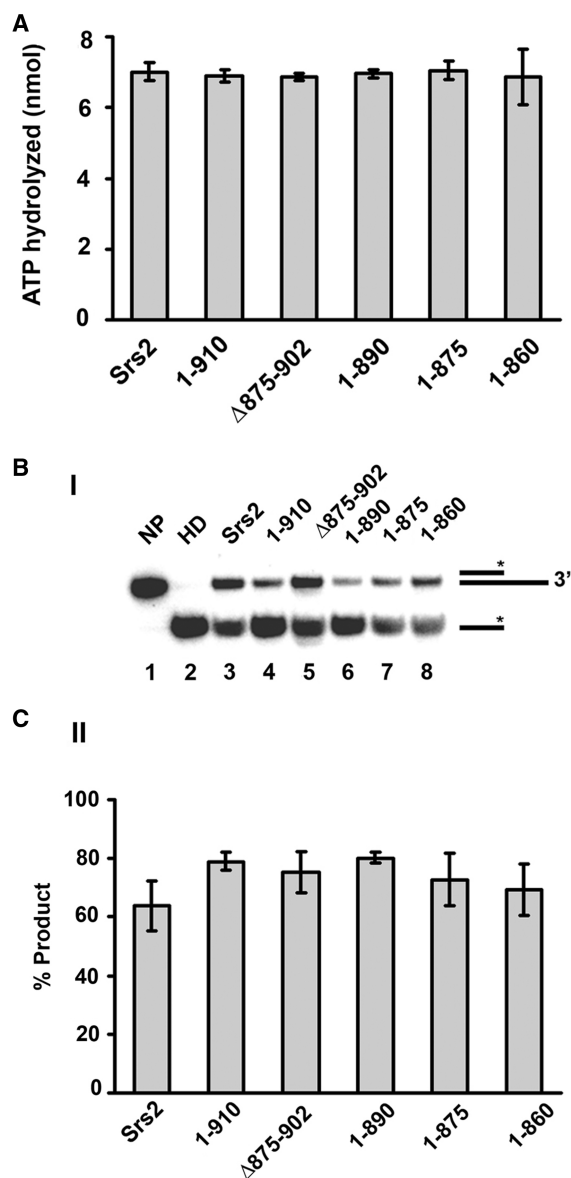
Figure 3. Proficiency of the srs2 mutants in ATP hydrolysis and DNA unwinding. (**A**) Graphical representation of the ssDNA-dependent ATPase activity of Srs2 and srs2 mutants. (**B**) The DNA helicase activity of Srs2 and srs2 mutants was assayed using a 3′-tailed duplex substrate (panel I) and the results quantified (panel II). NP, no protein control; HD, heat-denatured substrate. In all cases, error bars represent the standard deviations derived from three independent experiments.

As we reported previously, the addition of a small amount of Srs2 (7.5–15 nM) to the D-loop reaction containing Rad51, Rad54 and the heterotrimeric ssDNA-binding factor RPA led to pronounced inhibition of the reaction (Figure 4B). The two srs2 truncation mutants, srs2 1–998 and srs2 1–910, that are able to interact with Rad51 also inhibited the D-loop reaction to a comparable degree as Srs2 (Figure 4B). However, the srs2 1–875 and srs2 1–860 mutants, which are deficient in Rad51 interaction, exerted only a slight inhibitory effect on the D-loop reaction (Figure 4B). The slight inhibition observed with increasing amounts of srs2 1–875 or srs2 1–860 could be due to

a residual interaction with Rad51. Likewise, the srs2 Δ875–902 mutant that is also deficient in Rad51 interaction is again significantly impaired for the ability to suppress the D-loop reaction (Figure 4C). Interestingly, the srs2 1–890 truncation mutation that is partially attenuated for Rad51 interaction showed an intermediate level of inhibition of the D-loop reaction, with the defect being much more obvious at higher concentrations of KCl (Figure 4B, panel III), which very likely weakened the residual interaction between Rad51 and this srs2 mutant. Altogether, these results revealed interaction with Rad51 as important for the anti-recombinase activity of Srs2.

Examination of Rad51-interaction defective srs2 mutants in the DNA strand exchange reaction

We applied a DNA strand exchange system that uses plasmid length DNA substrates to seek independent verification that interaction with Rad51 is critical for the anti-recombinase attribute of Srs2. In this system, Rad51-made DNA joint molecules are processed by DNA strand exchange to yield nicked circular duplex as the final reaction product (16,18) (Figure 5A). As expected (16), the addition of a catalytic quantity of Srs2 (30 and 60 nM) strongly suppressed the DNA strand exchange reaction (Figure 5B). In contrast, little or no attenuation of DNA strand exchange efficiency was seen when srs2 1–860 or srs2 Δ875–902 was tested (Figure 5B). The above results support our conclusion that the efficacy of Srs2's anti-recombinase activity is contingent upon Rad51 interaction.

Relevance of protein–protein interaction in Rad51 presynaptic filament disruption

The above results obtained using C-terminally truncated srs2 mutant proteins helped establish that interaction with Rad51 is critical for Srs2's ability to attenuate Rad51-mediated HR homologous DNA pairing and strand exchange. We employed a biochemical assay to provide evidence that the impairment of anti-recombinase activity in the truncated srs2 mutants stems from an inability to disrupt the Rad51 presynaptic filament. In this biochemical test, pre-assembled presynaptic filaments are incubated with Srs2 or one of the srs2 mutants together with RPA, and then topologically relaxed duplex DNA is added to trap the Rad51 molecules freed from ssDNA as a result of anti-recombinase function. Since Rad51 binding induces lengthening of the DNA trap, the level of anti-recombination function can be conveniently monitored as a DNA linking number change upon treatment of the duplex with topoisomerase I [Figure 6A, (16)]. The product of this reaction, an underwound DNA species called form U (Figure 6B, lane 2), is resolved from other DNA species by agarose gel electrophoresis and then revealed by ethidium bromide staining.

As expected, the addition of Srs2 to the presynaptic filaments led to the generation of form U, indicative of the release of Rad51 from the ssDNA [Figure 6B, (15)]. Abundant Form U DNA was also seen when the Rad51 interaction proficient srs2 1–910 mutant, which we
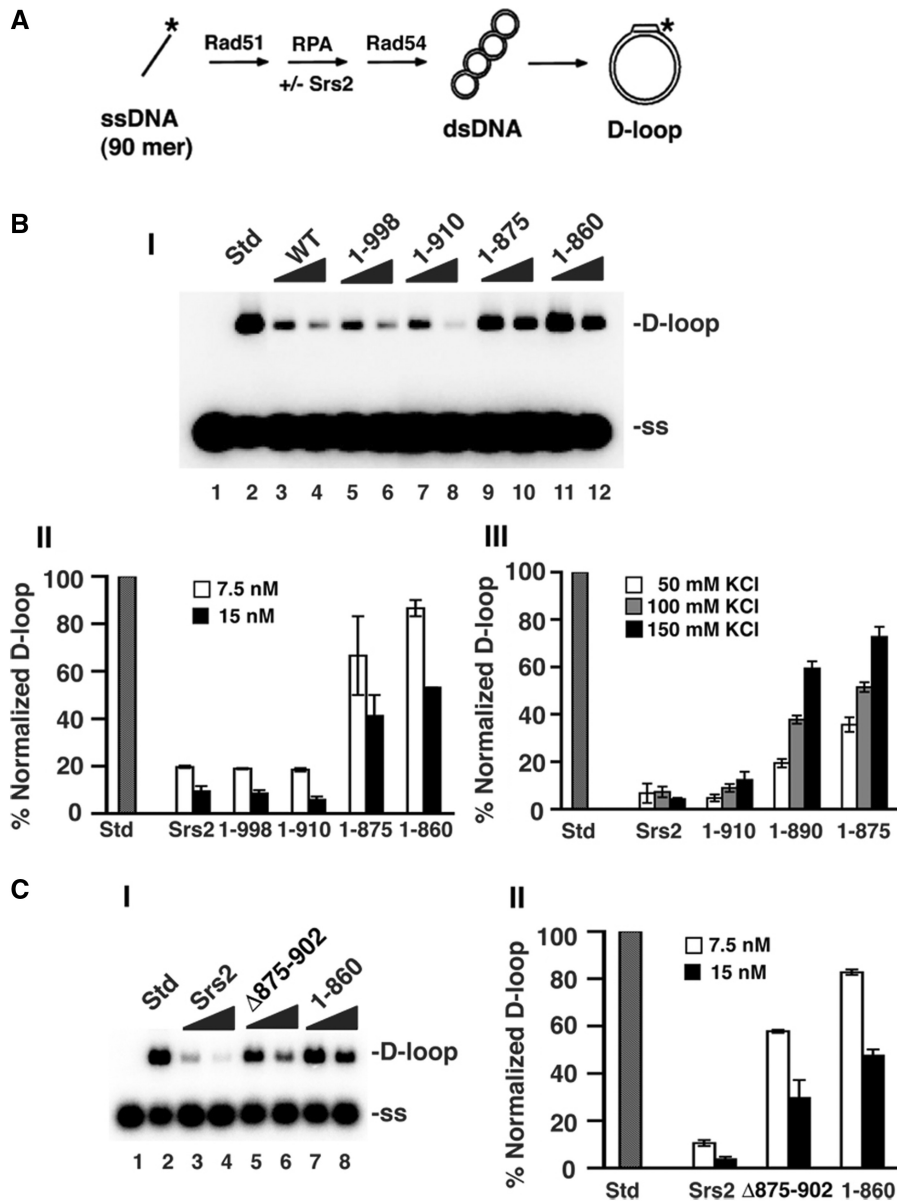
Figure 4. Relevance of the Srs2-Rad51 complex in the attenuation of the D-loop reaction. (**A**) D-loop reaction scheme. (**B**) In panel I, the radiolabeled D1 oligonucleotide was incubated with Rad51, Rad54, RPA (lanes 2–12) and with or without Srs2, srs2 1–998, srs2 1–910, srs2 1–875 or srs2 1–860 (7.5 or 15 nM) and then pBluescript form I DNA was incorporated. The reaction (lane 2) without Srs2 or mutant srs2 is designated as standard (Std) and corresponded to conversion of 43% of the input D1 oligonucleotide into the D-loop product. Lane 1 contained the DNA substrates but no protein. The KCl concentration was 50 mM KCl in these reactions and the results were quantified and plotted in panel II. In panel III, the results from D-loop reactions carried out at 50, 100, and 150 mM KCl with 15 nM of Srs2 or srs2 mutant were quantified and plotted. The D-loop product in the standard (Std) was 58%, 61% and 66% at 50, 100 and 150 mM KCl, respectively. (**C**) Panel I shows D-loop reactions with 7.5 and 15 nM Srs2, srs2 Δ875–902 or srs2 1–860 at 50 mM KCl. The D-loop in the standard (Std) was 54%. The results were quantified and plotted in panel II. In all cases, error bars represent the standard deviations derived from three independent experiments.

showed earlier to possess the wild-type level of anti-recombinase activity (e.g. Figure 4B), was incubated with the presynaptic filaments (Figure 6B). Importantly, the Rad51-interaction deficient srs2 1–860, srs2 1–875 and srs2 Δ875–902 mutants, which we found to be impaired for anti-recombinase activity, were incapable of producing a significant amount of Form U DNA (Figure 6B). These results thus provide direct evidence that dissociation of the Rad51 presynaptic filament by Srs2 is reliant upon the interaction between Srs2 and Rad51.

Analysis by electron microscopy

We also employed electron microscopy to examine and quantify the disruption of Rad51 presynaptic filaments by Srs2 and several of the srs2 truncation mutants. For this purpose, we assembled Rad51 presynaptic filaments on a 150-mer oligonucleotide (43) and then incubated these filaments with Srs2 or one of several srs2 mutants in conjunction with RPA. The reaction mixtures were diluted with buffer, applied onto carbon grids, and then examined by electron microscopy to quantify the levels of
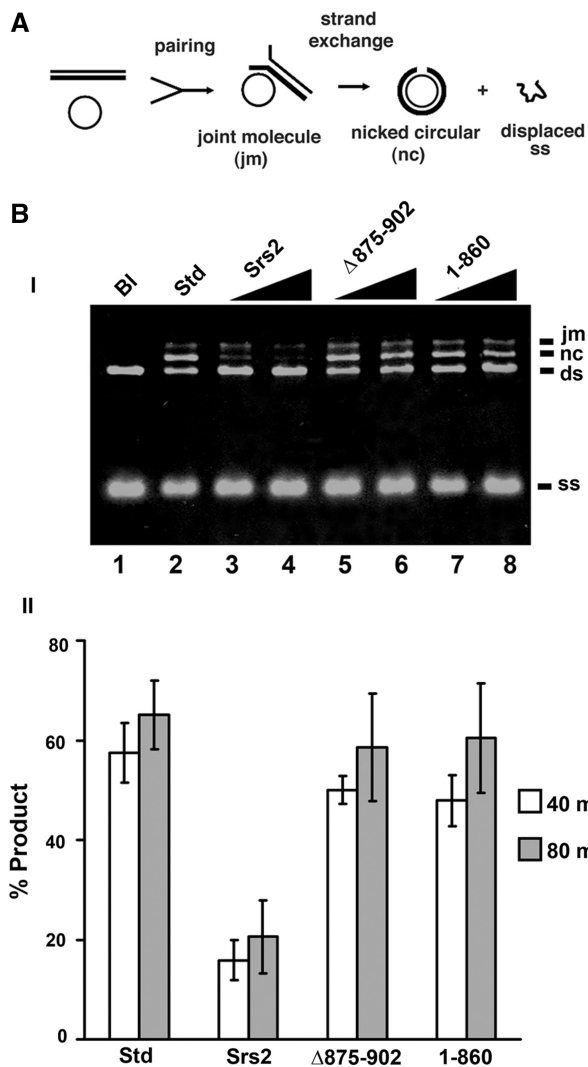
Figure 5. Anti-recombinase activity examined by DNA strand exchange. (**A**) The DNA strand exchange scheme. (**B**) In panel I, circular φX174 (+) strand DNA was incubated with Rad51, RPA, and in the absence or presence of Srs2, srs2 Δ875–902 or srs2 1–860 (30 and 60 nM), and then spermidine and linear φX dsDNA were added and the reaction incubated for either 40 or 80 min. A reaction without Srs2 or mutant srs2, designated as standard (Std; lane 2) served as a control. The DNA substrates were also incubated without any protein (Bl; lane 1). Only the results from the 80 min time-point are shown. In panel II, the sum of joint molecules and nicked circular duplex from the 40 min and 80 min time-points of reactions that contained 30 nM Srs2 or srs2 mutant was plotted. In all cases, error bars represent the standard deviations derived from the results of three independent experiments.

Rad51 presynaptic filament and RPA–ssDNA complex in each case. As summarized in Figure 7, Rad51 presynaptic filaments accounted for ~80% of the nucleoprotein complexes in Srs2's absence, whereas these filaments represented only a little over 20% of the nucleoprotein complexes upon the addition of Srs2. As we had anticipated, srs2 1–910 was just as adept as the full-length protein in Rad51 presynaptic filament dissociation, but, importantly, srs2 1–875 or srs2 Δ875–902 was much less effective in this regard (Figure 7). Overall, the results
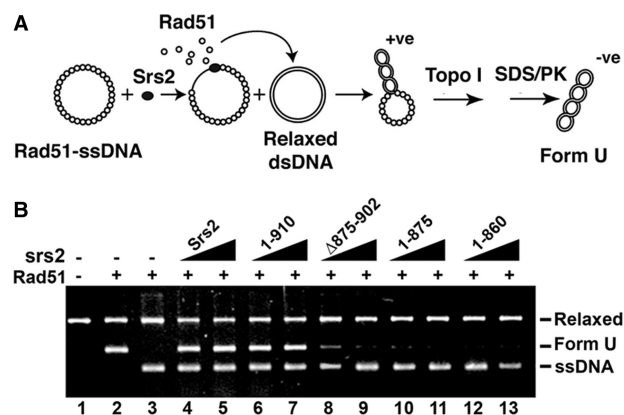
Figure 6. Rad51 presynaptic filament disruption as measured by a topoisomerase-linked assay. (**A**) Reaction scheme for detecting Rad51 presynaptic filament disruption. (**B**) Rad51 presynaptic filaments were incubated without or with Srs2, srs2 1–910, srs2 Δ875–902, srs2 1–875 or srs2 1–860 (60 and 80 nM) before the addition of relaxed DNA and topoisomerase I (lanes 3–13). Lane 2 contains Form U DNA made by incubating topologically relaxed DNA with Rad51 and topoisomerase I. Lane 1 contains topologically relaxed DNA.

from the EM analysis provided independent support for Rad51 interaction as a key determinant in the efficacy of Srs2 as an anti-recombinase.

Phenotypic analysis of *srs2* mutants

We wished to examine the genetic behavior of some of our srs2 mutants. Yeast strains were created which lacked Srs2 (*srs2Δ*), or that lacked amino acid residues 861–1174 (the *1–860* allele) or 875–902 (the *Δ875–902* allele) of Srs2. As expected (8), the deletion of *SRS2* suppressed the DNA damage sensitivity of the *rad18Δ* mutation (Figure 8A). DNA damage sensitivity of *rad18Δ* mutants can be suppressed by nonfunctional *srs2* mutations in a *RAD51*-dependent manner (13). Suppression of the *rad18Δ* MMS sensitivity was seen with the *srs2 1–860* but not the *srs2 Δ875–902* allele (Figure 8A).

We next examined the *srs2* mutant strains for a hyper-recombination phenotype. Consistent with published results (10), we observed a 4-fold increase in the rate of gene conversion events in *srs2Δ* cells (Figure 8B). A similarly elevated gene conversion rate, one that was three-fold that of wild-type (Figure 8B), was found for the *srs2 1–860* mutant. In contrast, the *srs2 Δ875–902* gave a gene conversion rate that is only slightly higher than the wild-type control (Figure 8B). These findings fit with our observations that the srs2 1–860 mutant protein is quite defective in Rad51 interaction and in the inhibition of Rad51-mediated reactions, while the srs2 Δ875–902 mutant protein retains some ability to interact with Rad51 and possesses residual anti-recombinase activity.
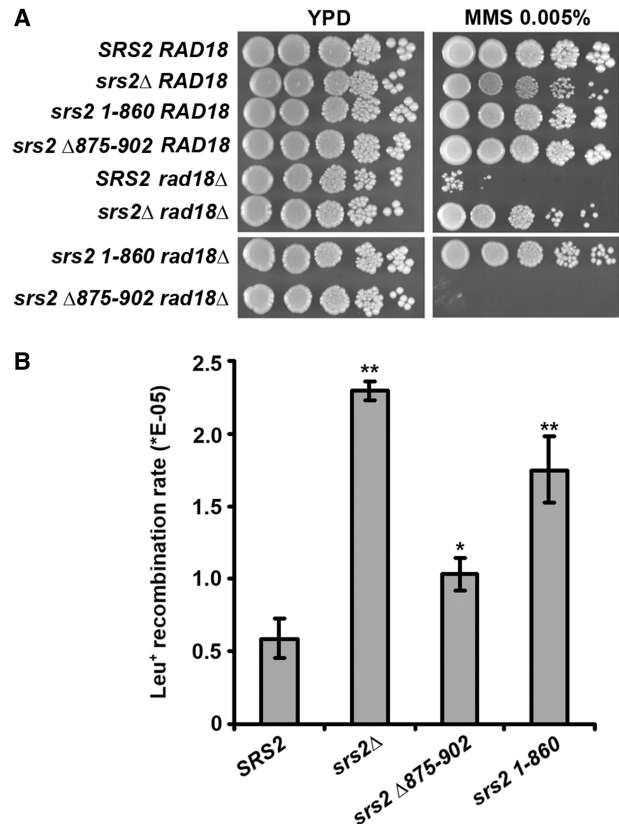
DISCUSSION

Despite the important contributions that HR makes to the elimination of deleterious DNA lesions and the re-establishment of injured DNA replication forks, it must be tightly regulated so as to prevent untimely

A

B
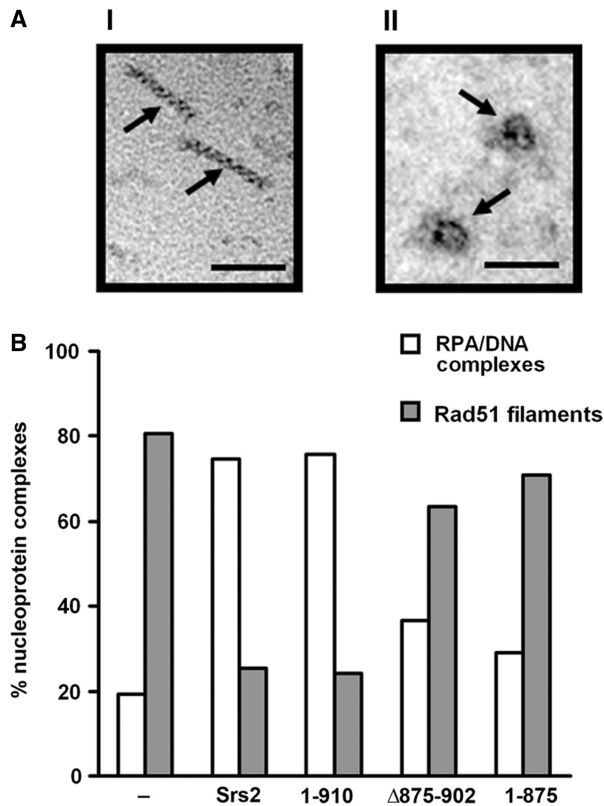
Figure 7. Quantification of Rad51 presynaptic filament disruption by electron microscopy. (**A**) Representative Rad51 nucleoprotein filaments (I) or RPA-ssDNA complexes (II) assembled on 150-mer ssDNA. The scale bar represents 50 nm. (**B**) Distribution of Rad51 presynaptic filaments and RPA-ssDNA complexes observed following incubation without or with 100 nM Srs2, srs2 1–910, srs2 Δ875–902 or srs2 1–875.

A

B

Figure 8. Phenotypic analysis of srs2 1-860 and srs2 Δ875-902. (**A**) The ability of the *srs2 1–860* and *srs2 Δ875–902* alleles to suppress the MMS sensitivity of *rad18Δ* cells was examined. Platings on both YPD and YPD containing 0.005% MMS are shown. (**B**) Rates of recombination between the *leu2-RI* and *leu2-bsteII* alleles were determined and the results graphed. The rates shown represent the mean from three independent fluctuation tests performed for each strain. Error bars are the standard deviations derived from this mean of three independent rate determinations. Asterisks denote significant results, as determined by *t*-tests: ** $P < 0.005$; * $P < 0.05$. Specifically, the rates for *SRS2* and *srs2Δ875–902* are significantly different ($P = 0.00004$), the rates for *SRS2* and *srs2 Δ875–902* are marginally different ($P = 0.0117$), and the rates for *SRS2* and *srs2 1–860* are significantly different ($P = 0.0016$).

events that interfere with other DNA and replication fork repair processes, or to avoid the generation of toxic nucleoprotein intermediates that trigger prolonged cell cycle arrest (6,7,11,44). Moreover, crossover HR events are disfavored in mitotic cells, as they can give rise to undesirable chromosome rearrangements, such as translocations. Genetic and other companion analyses have found several pathways able to attenuate undesirable HR events or promote the usage of the conservative SDSA pathway that does not entail the generation of crossovers. Importantly, all of these HR regulatory pathways are dependent on a DNA helicase. Specifically, the human BLM helicase, and likely its *S. cerevisiae* counterpart Sgs1, functions with Topo IIIα (Top 3 in yeast), a type 1A topoisomerase, and other associated factors to resolve key HR DNA intermediates, such as the double Holliday structure, to non-crossover recombinants in a process termed double Holliday junction dissolution (45). Interestingly, the Srs2 helicase suppresses spurious HR events and also prevents crossover formation via a unique ability to disrupt the Rad51 presynaptic filament (16,17). Genetic and biochemical evidence has been presented to implicate the mammalian RECQ5 helicase in HR regulation via the same general mechanism as Srs2 (43). More recently, a separate means of HR regulation has

been documented for the *S. cerevisiae* Mph1 helicase and its orthologues human FANCM and *Schizosaccharomyces pombe* Fml1; these orthologous helicases have been suggested to promote the use of the SDSA pathway of HR by disrupting the D-loop intermediate made by the Rad51 recombinase protein (34,46). Finally, the human RTEL1 helicase has also been shown to disrupt Rad51-made D-loops, but this novel attribute of RETL1 is thought to exert a general suppressive effect on HR frequency rather than fulfilling a regulatory role. Importantly, mutations in all the above helicases compromise genome instability and in some cases are associated with the tumor phenotype (43,47,48).

Several of the aforementioned helicases, including Srs2, RECQ5 and BLM/Sgs1 are known to physically interact with Rad51 (16,43,49), although the functional significance of these protein-protein interactions has not been addressed. In this study, we have strived to address the

functional relevance of the Srs2-Rad51 complex at the biochemical level. Specifically, by a combination of yeast two-hybrid analysis and biochemical mapping, we have narrowed the Rad51 interaction domain to a short region within the Srs2 C-terminus, and have taken advantage of this information to generate several truncation mutants of Srs2 that retain wild-type levels of ATPase and helicase activities but are specifically compromised for Rad51 interaction. Importantly, with both biochemical means and electron microscopy, we have demonstrated a diminished ability of these srs2 mutants to attenuate Rad51-mediated HR reactions and to dismantle the Rad51 presynaptic filament, in concordance with the degree of Rad51 interaction deficiency. We note that, by employing a kinetic assay involving the use of a fluorescently labeled DNA substrate, Antony *et al*. (50) also showed recently that the srs2 1–860 mutant is deficient in anti-recombinase activity. Thus, in aggregate, our findings and those of Antony *et al*. (50) reveal that the efficacy of Srs2 as an anti-recombinase is dependent on its physical interaction with Rad51. Consistent with our biochemical results, we found that the *srs2 1–860* mutant displays a hyper-recombination phenotype. Since the srs2 1–860 mutant protein retains wild-type levels of ATPase and helicase activities, our results thus provide evidence that the Srs2 helicase domain alone is insufficient for anti-recombinase function in cells. We have shown that the srs2 Δ875–902 mutant protein is less impaired for Rad51 interaction or for the ability to inhibit Rad51-mediated reactions *in vitro*. The phenotype of *srs2 Δ875–902* cells is accordingly mild or near wild-type.

Like Srs2, the human RECQ5 helicase associated with Rad51 physically, inhibits the Rad51-mediated D-loop reaction, and catalyzes the removal of Rad51 from ssDNA in a manner that is dependent on its ATPase activity (43). Based on these functional similarities between Srs2 and RECQ5, it seems reasonable to suggest that Rad51 interaction is also a determinant of the anti-recombinase activity of RECQ5. The results of Antony *et al*. have suggested that Srs2 enhances ATP hydrolysis by Rad51 within the presynaptic filament, thereby hastening Rad51 dissociation from DNA (50). It will be interesting to test whether RECQ5 also acts by a similar mechanism.

We note that Srs2 becomes phosphorylated on multiple sites in response to intra-S phase DNA damage (26), and several of these phosphorylation sites are located within the C-terminus of the protein, including two such sites in the region spanning residues 875–902 (51) that we know are important for complex formation with Rad51 (this work). It will be particularly interesting to ascertain how C-terminal phosphorylation of Srs2 in response to DNA damage regulates its anti-recombinase function via an influence on complex formation with Rad51.

REFERENCES

1. Richards,R.I. (2001) Fragile and unstable chromosomes in cancer: causes and consequences. *Trends Genet*., **17**, 339–345.
2. Popescu,N.C. (2003) Genetic alterations in cancer as a result of breakage at fragile sites. *Cancer Lett*., **192**, 1–17.
3. Kennedy,R.D. and D'Andrea,A.D. (2005) The Fanconi Anemia/ BRCA pathway: new faces in the crowd. *Genes Dev*., **19**, 2925–2940.
4. Smirnova,M. and Klein,H.L. (2003) Role of the error-free damage bypass postreplication repair pathway in the maintenance of genomic stability. *Mutat. Res*., **532**, 117–135.
5. Hickson,I.D. (2003) RecQ helicases: caretakers of the genome. *Nat. Rev. Cancer*, **3**, 169–178.
6. Sung,P. and Klein,H. (2006) Mechanism of homologous recombination: mediators and helicases take on regulatory functions. *Nat. Rev. Mol. Cell Biol*., **7**, 739–750.
7. Fabre,F., Chan,A., Heyer,W.D. and Gangloff,S. (2002) Alternate pathways involving Sgs1/Top3, Mus81/Mms4, and Srs2 prevent formation of toxic recombination intermediates from single-stranded gaps created by DNA replication. *Proc. Natl Acad. Sci. USA*, **99**, 16887–16892.
8. Lawrence,C.W. and Christensen,R.B. (1979) Metabolic suppressors of trimethoprim and ultraviolet light sensitivities of Saccharomyces cerevisiae rad6 mutants. *J. Bacteriol*., **139**, 866–876.
9. Schiestl,R.H., Prakash,S. and Prakash,L. (1990) The SRS2 suppressor of rad6 mutations of Saccharomyces cerevisiae acts by channeling DNA lesions into the RAD52 DNA repair pathway. *Genetics*, **124**, 817–831.
10. Krogh,B.O. and Symington,L.S. (2004) Recombination proteins in yeast. *Annu. Rev. Genet*., **38**, 233–271.
11. Gangloff,S., Soustelle,C. and Fabre,F. (2000) Homologous recombination is responsible for cell death in the absence of the Sgs1 and Srs2 helicases. *Nat. Genet*., **25**, 192–194.
12. Klein,H.L. (2001) Spontaneous chromosome loss in Saccharomyces cerevisiae is suppressed by DNA damage checkpoint functions. *Genetics*, **159**, 1501–1509.
13. Aboussekhra,A., Chanet,R., Adjiri,A. and Fabre,F. (1992) Semidominant suppressors of Srs2 helicase mutations of Saccharomyces cerevisiae map in the RAD51 gene, whose sequence predicts a protein with similarities to procaryotic RecA proteins. *Mol. Cell Biol*., **12**, 3224–3234.
14. Rong,L. and Klein,H.L. (1993) Purification and characterization of the SRS2 DNA helicase of the yeast Saccharomyces cerevisiae. *J. Biol. Chem*., **268**, 1252–1259.
15. Van Komen,S., Reddy,M.S., Krejci,L., Klein,H. and Sung,P. (2003) ATPase and DNA helicase activities of the Saccharomyces cerevisiae anti-recombinase Srs2. *J. Biol. Chem*., **278**, 44331–44337.
16. Krejci,L., Van Komen,S., Li,Y., Villemain,J., Reddy,M.S., Klein,H., Ellenberger,T. and Sung,P. (2003) DNA helicase Srs2 disrupts the Rad51 presynaptic filament. *Nature*, **423**, 305–309.
17. Veaute,X., Jeusset,J., Soustelle,C., Kowalczykowski,S.C., Le Cam,E. and Fabre,F. (2003) The Srs2 helicase prevents recombination by disrupting Rad51 nucleoprotein filaments. *Nature*, **423**, 309–312.
18. Sung,P. (1994) Catalysis of ATP-dependent homologous DNA pairing and strand exchange by yeast RAD51 protein. *Science*, **265**, 1241–1243.
19. Krejci,L., Macris,M., Li,Y., Van Komen,S., Villemain,J., Ellenberger,T., Klein,H. and Sung,P. (2004) Role of ATP hydrolysis in the antirecombinase function of Saccharomyces cerevisiae Srs2 protein. *J. Biol. Chem*., **279**, 23193–23199.

20. Pfander,B., Moldovan,G.L., Sacher,M., Hoege,C. and Jentsch,S. (2005) SUMO-modified PCNA recruits Srs2 to prevent recombination during S phase. *Nature*, **436**, 428–433.

21. Papouli,E., Chen,S., Davies,A.A., Huttner,D., Krejci,L., Sung,P. and Ulrich,H.D. (2005) Crosstalk between SUMO and ubiquitin on PCNA is mediated by recruitment of the helicase Srs2p. *Mol. Cell*, **19**, 123–133.

22. Burgess,R.C., Lisby,M., Altmannova,V., Krejci,L., Sung,P. and Rothstein,R. (2009) Localization of recombination proteins and Srs2 reveals anti-recombinase function in vivo. *J. Cell Biol.*, **185**, 969–981.

23. Ira,G., Malkova,A., Liberi,G., Foiani,M. and Haber,J.E. (2003) Srs2 and Sgs1-Top3 suppress crossovers during double-strand break repair in yeast. *Cell*, **115**, 401–411.

24. Aylon,Y., Liefshitz,B., Bitan-Banin,G. and Kupiec,M. (2003) Molecular dissection of mitotic recombination in the yeast Saccharomyces cerevisiae. *Mol. Cell Biol.*, **23**, 1403–1417.

25. Ira,G. and Haber,J.E. (2002) Characterization of RAD51-independent break-induced replication that acts preferentially with short homologous sequences. *Mol. Cell Biol.*, **22**, 6384–6392.

26. Liberi,G., Chiolo,I., Pellicioli,A., Lopes,M., Plevani,P., Muzi-Falconi,M. and Foiani,M. (2000) Srs2 DNA helicase is involved in checkpoint response and its regulation requires a functional Mec1-dependent pathway and Cdk1 activity. *EMBO J.*, **19**, 5027–5038.

27. Huang,M. and Elledge,S.J. (2000) The FHA domain, a phosphoamino acid binding domain involved in the DNA damage response pathway. *Cold Spring Harb. Symp. Quant. Biol.*, **65**, 413–421.

28. Bhattacharyya,S. and Lahue,R.S. (2004) Saccharomyces cerevisiae Srs2 DNA helicase selectively blocks expansions of trinucleotide repeats. *Mol. Cell Biol.*, **24**, 7324–7330.

29. James,P., Halladay,J. and Craig,E.A. (1996) Genomic libraries and a host strain designed for highly efficient two-hybrid selection in yeast. *Genetics*, **144**, 1425–1436.

30. Krejci,L., Damborsky,J., Thomsen,B., Duno,M. and Bendixen,C. (2001) Molecular dissection of interactions between Rad51 and members of the recombination-repair group. *Mol. Cell Biol.*, **21**, 966–976.

31. Sung,P. (1997) Yeast Rad55 and Rad57 proteins form a heterodimer that functions with replication protein A to promote DNA strand exchange by Rad51 recombinase. *Genes Dev.*, **11**, 1111–1121.

32. Raschle,M., Van Komen,S., Chi,P., Ellenberger,T. and Sung,P. (2004) Multiple interactions with the Rad51 recombinase govern the homologous recombination function of Rad54. *J. Biol. Chem.*, **279**, 51973–51980.

33. Ayyagari,R., Impellizzeri,K.J., Yoder,B.L., Gary,S.L. and Burgers,P.M. (1995) A mutational analysis of the yeast proliferating cell nuclear antigen indicates distinct roles in DNA replication and DNA repair. *Mol. Cell Biol.*, **15**, 4420–4429.

34. Prakash,R., Satory,D., Dray,E., Papusha,A., Scheller,J., Kramer,W., Krejci,L., Klein,H., Haber,J.E., Sung,P. *et al.* (2009) Yeast Mph1 helicase dissociates Rad51-made D-loops: implications for crossover control in mitotic recombination. *Genes Dev.*, **23**, 67–79.

35. Petukhova,G., Stratton,S. and Sung,P. (1998) Catalysis of homologous DNA pairing by yeast Rad51 and Rad54 proteins. *Nature*, **393**, 91–94.

36. Sung,P. and Robberson,D.L. (1995) DNA strand exchange mediated by a RAD51-ssDNA nucleoprotein filament with polarity opposite to that of RecA. *Cell*, **82**, 453–461.

37. Palladino,F. and Klein,H.L. (1992) Analysis of mitotic and meiotic defects in Saccharomyces cerevisiae SRS2 DNA helicase mutants. *Genetics*, **132**, 23–37.

38. Lea,D.E. and Coulson,C.A. (1949) The distribution of the numbers of mutants in bacterial populations. *J. Genet.*, **49**, 264–285.

39. Aguilera,A. and Klein,H.L. (1988) Genetic control of intrachromosomal recombination in Saccharomyces cerevisiae. I. Isolation and genetic characterization of hyper-recombination mutations. *Genetics*, **119**, 779–790.

40. Jentsch,S., McGrath,J.P. and Varshavsky,A. (1987) The yeast DNA repair gene RAD6 encodes a ubiquitin-conjugating enzyme. *Nature*, **329**, 131–134.

41. Le Breton,C., Dupaigne,P., Robert,T., Le Cam,E., Gangloff,S., Fabre,F. and Veaute,X. (2008) Srs2 removes deadly recombination intermediates independently of its interaction with SUMO-modified PCNA. *Nucleic Acids Res.*, **36**, 4964–4974.

42. Sung,P., Krejci,L., Van Komen,S. and Sehorn,M.G. (2003) Rad51 recombinase and recombination mediators. *J. Biol. Chem.*, **278**, 42729–42732.

43. Hu,Y., Raynard,S., Sehorn,M.G., Lu,X., Bussen,W., Zheng,L., Stark,J.M., Barnes,E.L., Chi,P., Janscak,P. *et al.* (2007) RECQL5/Recql5 helicase regulates homologous recombination and suppresses tumor formation via disruption of Rad51 presynaptic filaments. *Genes Dev.*, **21**, 3073–3084.

44. Magner,D.B., Blankschien,M.D., Lee,J.A., Pennington,J.M., Lupski,J.R. and Rosenberg,S.M. (2007) RecQ promotes toxic recombination in cells lacking recombination intermediate-removal proteins. *Mol. Cell*, **26**, 273–286.

45. Bussen,W., Raynard,S., Busygina,V., Singh,A.K. and Sung,P. (2007) Holliday junction processing activity of the BLM-Topo IIIalpha-BLAP75 complex. *J. Biol. Chem.*, **282**, 31484–31492.

46. Sun,W., Nandi,S., Osman,F., Ahn,J.S., Jakovleska,J., Lorenz,A. and Whitby,M.C. (2008) The FANCM ortholog Fml1 promotes recombination at stalled replication forks and limits crossing over during DNA double-strand break repair. *Mol. Cell*, **32**, 118–128.

47. Ellis,N.A., Groden,J., Ye,T.Z., Straughen,J., Lennon,D.J., Ciocci,S., Proytcheva,M. and German,J. (1995) The Bloom's syndrome gene product is homologous to RecQ helicases. *Cell*, **83**, 655–666.

48. Barber,L.J., Youds,J.L., Ward,J.D., McIlwraith,M.J., O'Neil,N.J., Petalcorin,M.I., Martin,J.S., Collis,S.J., Cantor,S.B., Auclair,M. *et al.* (2008) RTEL1 maintains genomic stability by suppressing homologous recombination. *Cell*, **135**, 261–271.

49. Wu,L., Davies,S.L., Levitt,N.C. and Hickson,I.D. (2001) Potential role for the BLM helicase in recombinational repair via a conserved interaction with RAD51. *J. Biol. Chem.*, **276**, 19375–19381.

50. Antony,E., Tomko,E.J., Xiao,Q., Krejci,L., Lohman,T.M. and Ellenberger,T. (2009) Srs2 disassembles Rad51 filaments by a protein-protein interaction triggering ATP turnover and dissociation of Rad51 from DNA. *Mol. Cell*, **35**, 105–115.

51. Chiolo,I., Carotenuto,W., Maffioletti,G., Petrini,J.H., Foiani,M. and Liberi,G. (2005) Srs2 and Sgs1 DNA helicases associate with Mre11 in different subcomplexes following checkpoint activation and CDK1-mediated Srs2 phosphorylation. *Mol. Cell Biol.*, **25**, 5738–5751.

Attachment 7

Seong C, Colavito S, Kwon Y, Sung P, Krejci L

Regulation of Rad51 Recombinase Presynaptic Filament Assembly via Interactions with the Rad52 Mediator and the Srs2 Anti-recombinase.

Regulation of Rad51 Recombinase Presynaptic Filament Assembly via Interactions with the Rad52 Mediator and the Srs2 Anti-recombinase[*]

Changhyun Seong[‡], Sierra Colavito[‡], Youngho Kwon[‡], Patrick Sung[‡1], and Lumir Krejci[‡§2]

From the [‡]Department of Molecular Biophysics and Biochemistry, Yale University School of Medicine, New Haven, Connecticut 06520 and the [§]Department of Biology, National Center for Biomolecular Research, Masaryk University, Kamenice S/A4, Brno 62500, Czech Republic

Homologous recombination represents an important means for the error-free elimination of DNA double-strand breaks and other deleterious DNA lesions from chromosomes. The Rad51 recombinase, a member of the *RAD52* group of recombination proteins, catalyzes the homologous recombination reaction in the context of a helical protein polymer assembled on single-stranded DNA (ssDNA) that is derived from the nucleolytic processing of a primary lesion. The assembly of the Rad51-ssDNA nucleoprotein filament, often referred to as the presynaptic filament, is prone to interference by the single-strand DNA-binding factor replication protein A (RPA). The *Saccharomyces cerevisiae* Rad52 protein facilitates presynaptic filament assembly by helping to mediate the displacement of RPA from ssDNA. On the other hand, disruption of the presynaptic filament by the Srs2 helicase leads to a net exchange of Rad51 for RPA. To understand the significance of protein-protein interactions in the control of Rad52- or Srs2-mediated presynaptic filament assembly or disassembly, we have examined two rad51 mutants, rad51 Y388H and rad51 G393D, that are simultaneously ablated for Rad52 and Srs2 interactions and one, rad51 A320V, that is differentially inactivated for Rad52 binding for their biochemical properties and also for functional interactions with Rad52 or Srs2. We show that these mutant rad51 proteins are impervious to the mediator activity of Rad52 or the disruptive function of Srs2 in concordance with their protein interaction defects. Our results thus provide insights into the functional significance of the Rad51-Rad52 and Rad51-Srs2 complexes in the control of presynaptic filament assembly and disassembly. Moreover, our biochemical studies have helped identify A320V as a separation-of-function mutation in Rad51 with regards to a differential ablation of Rad52 interaction.

Homologous recombination (HR)[3] helps maintain genomic stability by eliminating DNA double-strand breaks induced by ionizing radiation and chemical reagents, by restarting damaged or collapsed DNA replication forks, and by elongating shortened telomeres especially when telomerase is dysfunctional (1–3). Accordingly, defects in HR invariably lead to enhanced sensitivity to genotoxic agents, chromosome aberrations, and tumor development (4, 5). In meiosis also, HR helps mediate the linkage of homologous chromosome pairs via arm cross-overs, thus ensuring the proper segregation of chromosomes at the first meiotic division (6). Accordingly, HR mutants exhibit a plethora of meiotic defects, including early meiotic cell cycle arrest, aneuploidy, and inviability.

Much of the knowledge regarding the mechanistic basis of HR has been derived from studies of model organisms, such as the budding yeast *Saccharomyces cerevisiae*. Genetic analyses in *S. cerevisiae* have led to the identification of the *RAD52* group of genes, namely, *RAD50*, *RAD51*, *RAD52*, *RAD54*, *RAD55*, *RAD57*, *RAD59*, *RDH54*, *MRE11*, and *XRS2* (1), that are needed for the successful execution of HR. Each member of the *RAD52* group of genes has an orthologue in higher eukaryotes, including humans, and mutations in any of these genes cause defects in HR and repair of double-strand breaks.

The DNA pairing and strand invasion step of the HR reaction is mediated by *RAD51*-encoded protein, which is orthologous to the *Escherichia coli* recombinase RecA (2). Like RecA, Rad51 polymerizes on ssDNA, derived from the nucleolytic processing of a primary lesion such as a double-strand break, to form a right-handed nucleoprotein filament, often referred to as the presynaptic filament (3, 7). The presynaptic filament engages dsDNA, conducts a search for homology in the latter, and catalyzes DNA joint formation between the recombining ssDNA and dsDNA partners upon the location of homology (1, 3). As such, the timely and efficient assembly of the presynaptic filament is indispensable for the successful execution of HR.

Because the nucleation of Rad51 onto ssDNA is a rate-limiting process, presynaptic filament assembly is prone to interference by the single-strand DNA-binding protein replication protein A (RPA) (1, 3, 7). In reconstituted biochemical systems, the addition of Rad52 counteracts the inhibitory action of RPA

[3] The abbreviations used are: HR, homologous recombination; RPA, replication protein A; ss, single-stranded; ds, double-stranded; Ni-NTA, nickel-nitrilotriacetic acid; DTT, dithiothreitol.

(8, 9). Consistent with the biochemical results, in both mitotic and meiotic cells, the recruitment of Rad51 to double-strand breaks is strongly dependent on Rad52 (10–12). This effect of Rad52 on Rad51 presynaptic filament assembly has been termed a "recombination mediator" function (13).

Interestingly, genetic studies have shown that the Srs2 helicase fulfills the role of an anti-recombinase. Specifically, mutations in Srs2 often engender a hyper-recombinational phenotype and can also help suppress the DNA damage sensitivity of *rad6* and *rad18* mutants, because of the heightened HR proficiency being able to substitute for the post-replicative DNA repair defects of these mutant cells (2, 14). Importantly, in reconstituted systems, Srs2 exerts a strong inhibitory effect on Rad51-mediated reactions in a manner that is potentiated by RPA. Biochemical and electron microscopic analyses have provided compelling evidence that Srs2 acts by disassembling the presynaptic filament, to effect the replacement of Rad51 by RPA (15, 16). The ability of Srs2 to dissociate the presynaptic filament relies on its ATPase activity, revealed using mutant variants, K41A and K41R, that harbor changes in the Walker type A motif involved in ATP engagement. Accordingly, the *srs2 K41A* and *srs2 K41R* mutants are biologically inactive (17).

In both yeast two-hybrid and biochemical analyses, a complex of Rad51 with either Rad52 or Srs2 can be captured (1, 16). Using yeast two-hybrid-based mutagenesis, several *rad51* mutant alleles, *A320V*, *Y388H*, and *G393D*, that engender a defect in the yeast two-hybrid association with Rad52 have been found (18). Here we document our biochemical studies demonstrating the inability of these rad51 mutant proteins to physically and functionally interact with Rad52. Interestingly, we find that two of these rad51 mutants, namely, Y388H and G393D, are also defective in Srs2 interaction. Accordingly, these mutant rad51 proteins form presynaptic filaments that are resistant to the disruptive action of Srs2. Our results thus emphasize the role of Rad51-Rad52 and Rad51-Srs2 interactions in the regulation of Rad51 presynaptic filament assembly and maintenance, and they also reveal the presence of overlapping Rad52 and Srs2 interaction motifs in Rad51. In these regards, our biochemical studies have identified the A320V change as a separation-of-function mutation in Rad51.

EXPERIMENTAL PROCEDURES

Purification of Proteins—All of the chromatographic steps in protein purification were carried out at 4 °C. The rad51 A320V, rad51 Y388H, and rad51 G393D proteins were expressed in yeast cells and purified to near homogeneity, as described for the wild type counterpart (19). Rad52 with a His_6 tag at its C terminus and Srs2 with a His_9 tag at its N terminus were expressed in *E. coli* Rosetta strains (Novagen) and purified to near homogeneity, as described (16, 20). Rad54 and Rdh54 containing a thioredoxin-His_6 double tag at its N terminus were purified from Rosetta cells, as described (21, 22).

For the expression and purification of Rad52-C, a DNA fragment harboring amino acid residues 327–504 of Rad52 was introduced into pET-11d. Rosetta cells harboring this plasmid were grown at 37 °C to A_{600} 0.6–0.8, at which time 0.4 mM isopropyl D-thiogalactopyranoside was added. The culture was incubated for another 3 h at 37 °C, and the cells were harvested by centrifugation. Cell lysate from 20 g of cells (being equivalent to 10 liters of culture) was prepared by sonicating the cell suspension in 50 ml of cell breakage buffer (50 mM Tris-HCl, pH 7.4, 50 mM KCl, 2 mM EDTA, 1 mM DTT, 10% sucrose, 0.01% Igepal, 5 μg/ml leupeptin, pepstatin A, aprotinin, chymostatin, and 0.4 mM phenylmethylsulfonyl fluoride) and ultracentrifugation (100,000 × *g* for 90 min). The clarified lysate was applied onto a Q Sepharose column (20 ml), and the flow-through fraction was collected and applied onto a SP Sepharose column (20 ml). The proteins were fractionated with a 160-ml gradient from 50 to 300 mM KCl in K buffer (10 mM K_2HPO_4, pH 7.4, 10% glycerol, 1 mM DDT, and 0.5 mM EDTA). The fractions containing Rad52-C (8 ml total, 200 mM KCl) were applied onto a Macro-Hydroxyapatite column (1 ml; Bio-Rad) and then eluted with a 40-ml gradient from 0 to 200 mM KH_2PO_4 in K buffer. The Macro-Hydroxyapatite fractions (6 ml total, 60 mM KH_2PO_4) were applied onto 1-ml Mono S column and eluted with a 40-ml gradient from 50 to 300 mM KCl in K buffer. The peak fractions (5 ml total, 150 mM KCl) were collected and concentrated to 10 mg/ml with Amicon Ultra-4 concentrator (Millipore). The overall yield of highly purified Rad52-C was ~1.5 mg.

In Vitro Pulldown Assay—Rad51 or rad51 mutant (5.0 μM) was mixed with Rad52 (5.0 μM), Rad54 (5.0 μM), or Srs2 (5.0 μM) at 4 °C for 30 min in 30 μl of buffer (25 mM Tris-HCl, pH 7.5, 150 mM KCl, 10 mM imidazole, 1 mM β-mercaptoethanol, 0.01% Igepal). To examine the effect of Rad52 on Rad51-Srs2 complex formation, Rad51 or rad51 A320V (5.0 μM) was mixed with Rad52-C (3.3, 5.0, or 6.7 μM) and Srs2 (5.0 μM), as above. The reactions were gently mixed at 4 °C for 30 min with 20 μl of Ni-NTA resin (Qiagen), which binds the polyhistidine tag on Rad52, Rad54, or Srs2, to capture protein complexes. After washing the resin three times with 20 μl of the same buffer, the bound proteins were eluted with 2% SDS. The supernatant (S), wash (W), and SDS eluate (E) fractions, 10 μl each, were resolved by SDS-PAGE and stained with Coomassie Blue.

DNA Substrates—The ϕX174 replicative form I DNA and viral (+) strand DNA were purchased from New England Biolabs. The linear ϕX174 dsDNA was prepared by digesting the replicative form I DNA with the restriction enzyme ApaLI. Topologically relaxed ϕX174 DNA was prepared by treating the replicative form I DNA with calf thymus topoisomerase I (Invitrogen) as described previously (23). For the DNA mobility shift assay, the 83-mer oligonucleotide (5'-TTTATATCCTTTT-ACTTTATTTTCTATGTTTATTCATTTACTTATTTTGTA-TTATCCTTATACTTTTTACTTTATGTTCATTT-3') was 5' end-labeled with T4 polynucleotide kinase (Roche Applied Science) and [γ-^{32}P]ATP (Amersham Biosciences). The radiolabeled oligonucleotides were annealed to its exact complement by heating the two oligonucleotides at 85 °C for 3 min followed by slow cooling to 23 °C. The resulting duplex DNA was purified from a 10% polyacrylamide gel, as described (22). For the D-loop assay, a 5' end-labeled 90-mer oligonucleotide complementary to positions 1932–2022 of pBluescript SK DNA was used (24). The 150-mer oligonucleotide (5'-TCTTATTTATG-TCTCTTTTATTTCATTTCCTATATTTATTCCTATTATG-TTTTATTCATTTACTTATTCTTTATGTTCATTTTTTAT-ATCCTTTACTTTATTTTCTCTGTTTATTCATTTACTTA-TTTTGTATTATCCTTATCTTATTTA-3') was used as DNA

substrate in the electron microscopic analysis of presynaptic filament formation.

ATPase Assay—Rad51 or rad51 mutant (3.5 μM) was incubated with ϕX174 circular (+) strand DNA (30 μM nucleotides) in 10 μl of buffer (35 mM Tris-HCl, pH 7.2, 50 mM KCl, 5 mM MgCl$_2$, 1 mM DTT, 0.1 mM [γ-^{32}P]ATP) at 37 °C. A 2-μl aliquot of the reaction mixtures was removed at the indicated times and mixed with an equal volume of 500 mM EDTA to halt the reaction. Thin layer chromatography and phosphorimaging analysis were used to determine the level of ATP hydrolysis, as described (25).

DNA Mobility Shift Assay—The ^{32}P-labeled 83-mer ssDNA or dsDNA (4.5 μM nucleotides) was mixed with the indicated amounts of Rad51 or rad51 mutant in 10 μl of buffer (35 mM Tris-HCl, pH 7.2, 50 mM KCl, 1 mM DTT, 1 mM ATP, 5 mM MgCl$_2$, 0.1 mg/ml bovine serum albumin) for 10 min at 37 °C. The reaction mixtures were resolved in 10% polyacrylamide gels in TA buffer (30 mM Tris acetate, pH 7.4) containing 5 mM magnesium acetate. The gels were dried on a sheet of DEAE paper (Whatman) and subjected to phosphorimaging analysis.

Assays for Rad51-induced DNA Topology Change—To measure DNA topology change induced by Rad51 or the rad51 mutants, the indicated amount of the wild type or mutant protein was incubated with topologically relaxed ϕX174 dsDNA (15 μM nucleotides) for 5 min at 37 °C in 8.1 μl of buffer (35 mM Tris-HCl, pH 7.2, 100 mM KCl, 1 mM DTT, 2 mM ATP, 5 mM MgCl$_2$, 0.1 mg/ml bovine serum albumin), followed by the incorporation of 3 units of calf thymus topoisomerase I (Invitrogen; added in 0.4 μl) and a 20-min incubation. To measure the disruption of the presynaptic filament by Srs2, Rad51 or rad51 mutant (2 μM) was incubated with ϕX174 ssDNA (8.5 μM nucleotides) for 5 min with an ATP regenerating system (20 mM creatine phosphate and 20 μg/ml creatine kinase) in 8.1 μl of buffer, followed by the incorporation of RPA (1 μM, added in 0.5 μl) and Srs2 (35 or 50 nM, added in 0.7 μl) and a 5-min incubation. Topologically relaxed ϕX174 dsDNA (15 μM nucleotides) and 3 units of calf thymus topoisomerase I (Invitrogen) were then added in 0.7 and 0.4 μl, respectively, followed by an 8-min incubation. The reaction mixtures were deproteinized with SDS (0.5%) and proteinase K (0.5 mg/ml) for 5 min at 37 °C, before being resolved on 0.9% agarose gel run in TAE buffer (30 mM Tris acetate, pH 7.4, 0.5 mM EDTA). DNA species were stained with ethidium bromide, and the results were recorded in a gel documentation station (Bio-Rad).

DNA Strand Exchange Assay—All of the reaction steps were carried out at 37 °C. For the standard reaction, the indicated amount of Rad51 or rad51 mutant was incubated with ϕX174 ssDNA (30 μM nucleotides) in 10.3 μl of buffer (35 mM Tris-HCl, pH 7.2, 50 mM KCl, 1 mM DTT, 2.5 mM ATP, 3 mM MgCl$_2$) at 37 °C for 5 min. Following the addition of RPA (1.2 μM, added in 0.5 μl), linearized ϕX174 dsDNA (25 μM nucleotides, added in 0.7 μl) and spermidine hydrochloride (final concentration, 4 mM added in 1 μl) were incorporated into the reaction, followed by a 60-min incubation. After deproteinizing treatment, the reaction mixtures were resolved by agarose gel electrophoresis and analyzed as before. To examine the effects of the *rad51* mutations, Rad51 or rad51 mutant (10 μM), RPA (2 μM), and the indicated amounts of Rad52 were mixed on ice for 10 min in

buffer before adding ssDNA and a 10-min incubation. Otherwise, these reactions were treated and processed in the same manner as above.

D-loop Reaction—The radiolabeled 90-mer oligonucleotide (3 μM nucleotides) was incubated with Rad51 or rad51 mutant (1 μM) for 5 min at 37 °C in 10 μl of buffer (35 mM Tris-HCl, pH 7.2, 140 mM KCl, 2 mM ATP, 5 mM MgCl$_2$, 1 mM DTT, and the ATP-regenerating system) to assemble the Rad51-ssDNA nucleoprotein filament, followed by the incorporation of RPA (200 nM, added in 0.5 μl) and Srs2 (17 or 24 nM, added in 0.5 μl) and a 4-min incubation at 37 °C. Then Rad54 (150 nM) was added in 0.5 μl, and the reaction mixtures were incubated for 3 min at 23 °C. DNA pairing was initiated by adding pBluescript replicative form I DNA (50 μM base pairs) in 1 μl, and the reaction mixtures were incubated at 30 °C for 7 min. The reaction mixtures were deproteinized and subjected to agarose gel electrophoresis, as above, and the gels were dried and subjected to phosphorimaging analysis.

Electron Microscopy—To assemble the presynaptic filament, the 150-mer oligonucleotide (7.2 μM nucleotides) and Rad51 or rad51 G393D (2.4 μM) were incubated for 5 min in 12 μl of buffer containing 2 mM ATP, 2.5 mM MgCl$_2$, 50 mM KCl, and an ATP-regenerating system at 37 °C. Following the addition of RPA (240 nM, in 0.5 μl) and Srs2 (100 nM, in 0.4 μl), the reaction mixture was incubated for 3 min at 37 °C. After a 10-fold dilution with buffer, a 3-μl aliquot of the reaction was applied to a 400-mesh grid coated with carbon film, which had been glow-discharged in air. The grid was stained with 2% uranyl acetate for 30 s and rinsed with water. The samples were examined with a Tecnai 12 Biotwin electron microscope (FEI) equipped with a tungsten filament at 100 keV. Digital images were captured with a Morada (Olympus Soft Imaging Solutions) charge-coupled device camera at a nominal magnification of 87,000–135,000×.

RESULTS

Purification of rad51 Mutants—A mutagenic screen conducted previously identified three *RAD51* mutations, namely, *A320V*, *Y388H*, and *G393D*, that ablate the interaction of Rad51 with Rad52 but not with Rad54 or Rad55 in the yeast two-hybrid system (18). For their biochemical analyses, we expressed the three rad51 mutant proteins alongside the wild type counterpart in yeast cells deleted for the endogenous *RAD51* gene and purified these proteins to near homogeneity (Fig. 1) using the procedure devised for the wild type protein (19). The mutants were expressed to the same level as the wild type protein, and during purification, all three mutants behaved like the wild type protein chromatographically. Moreover, a yield of these mutants similar to that of the wild type protein was obtained.

The rad51 Mutants Retain the Basic Biochemical Attributes of Rad51—Before evaluating the rad51 mutants for their physical and functional interactions with Rad52 and Srs2, we wished to first establish that they possess the biochemical attributes of the wild type protein with regards to ATP hydrolysis, DNA binding, and the ability to mediate homologous DNA pairing and strand exchange in conjunction with RPA. First, the ATPase activity was measured with ϕX174 (+) DNA as co-
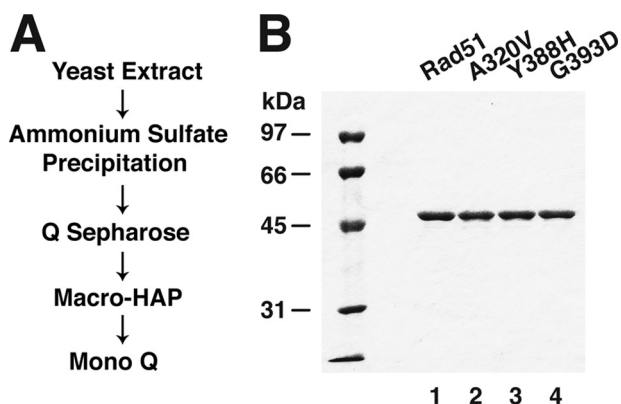
FIGURE 1. **Purification of rad51 mutants.** *A*, scheme of protein purification. *B*, purified Rad51, rad51 A320V, rad51 Y388H, and rad51 G393D (2 μg each) were analyzed by 10% SDS-PAGE and staining with Coomassie Blue.
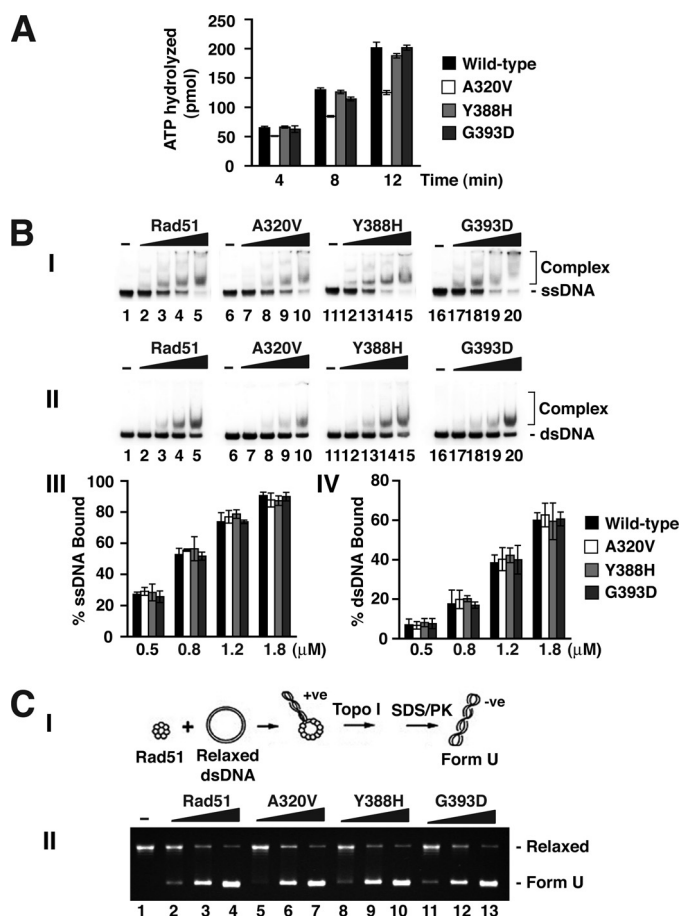

FIGURE 2. **Biochemical properties of the rad51 mutants.** *A*, the ATPase activity of Rad51, rad51 A320V, rad51 Y388H, or rad51 G393D was examined. *B*, the ssDNA (*panel I*) or dsDNA (*panel II*) binding activity of Rad51 and rad51 mutants was examined. The amounts of these proteins used were 0.5, 0.8, 1.2, and 1.8 μM. The results from these DNA binding experiments are plotted in *panels III* and *IV*. *C*, DNA topology change induced by Rad51 and mutants. *Panel I* depicts the basis of the topoisomerase I-linked assay. In *panel II*, 0.5, 1.0, and 2.0 μM of Rad51 and the three rad51 mutants were examined for their ability to induce Form U.
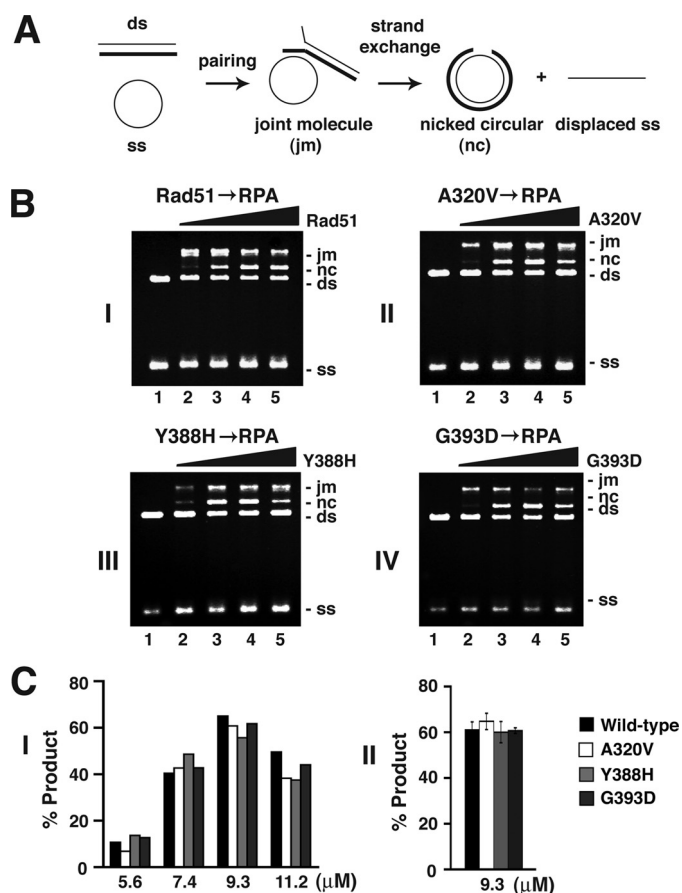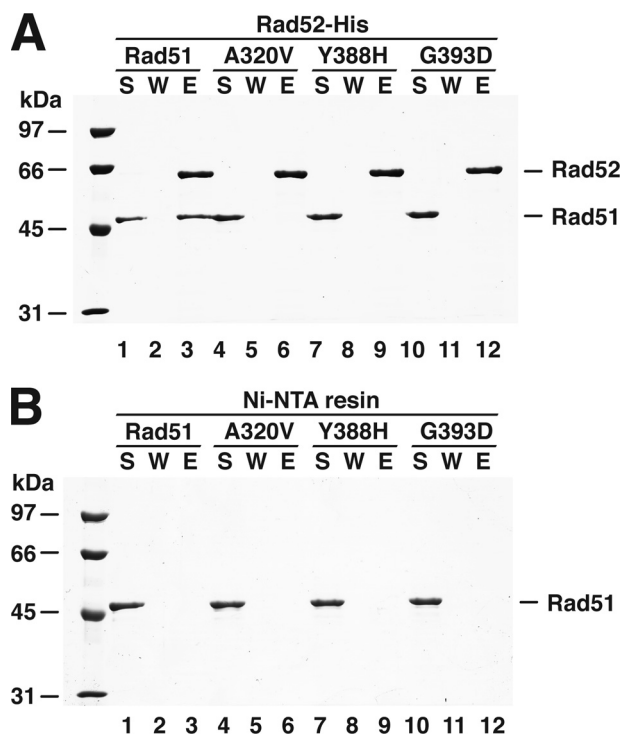

FIGURE 3. **Homologous DNA pairing and strand exchange by rad51 mutants.** *A*, scheme of the homologous DNA pairing and strand exchange reaction. Pairing between the circular φX174 (+) ssDNA and linear φX174 dsDNA yields a joint molecule (*jm*), which can be further processed by strand exchange to produce a nicked circular duplex (*nc*). *B*, Rad51, rad51 A320V, rad51 Y388H, or rad51 G393D (5.6, 7.4, 9.3, and 11.2 μM) was pre incubated with ssDNA to assemble presynaptic filaments before RPA and dsDNA addition. *C*, total products (joint molecule plus nicked circular duplex) catalyzed by the optimal level of Rad51 or rad51 mutant (9.3 μM) were quantified and plotted in the histogram.

any noticeable DNA binding deficiency. One of the key characteristic of Rad51 is the ability to form extended helical nucleoprotein filaments on DNA. The extent of nucleoprotein filament formation can be conveniently monitored by a topoisomerase I-linked assay (Fig. 2*C*). The resulting products are negatively supercoiled species called Form U (underwound). Fig. 2*C* showed that all three rad51 mutants are just as adept as the wild type protein in inducing the formation of Form U DNA.

We next tested the three rad51 mutant proteins for their ability to catalyze the homologous DNA pairing and DNA strand exchange reaction. In the *in vitro* system used, φX174 circular ssDNA is first incubated with Rad51 to allow for presynaptic filament assembly, and then RPA followed by homologous linear dsDNA are added to complete the reaction. Under these prescribed conditions, RPA enhances the efficiency of the reaction, by helping remove secondary structure in the ssDNA and also sequestering the displaced ssDNA generated as a result of DNA strand exchange. As shown in Fig. 3, all three rad51 mutants generated the same level of reaction products as wild type Rad51. Thus, all three rad51 mutants are just as capable as

factor, and the results showed that all three rad51 mutant proteins possess a level of ATPase activity comparable with that of the wild type protein (Fig. 2*A*). By a DNA mobility shift assay conducted with radiolabeled ssDNA or dsDNA as substrate (Fig. 2*B*), we also verified that none of the rad51 mutants has

FIGURE 4. **Interaction of rad51 mutants with Rad52.** Rad51, rad51 A320V, rad51 Y388H, or rad51 G393D was incubated with His$_6$-tagged Rad52. The reaction mixtures were mixed with Ni-NTA resin to capture any protein complex that had formed. Bound proteins were eluted from the resin with SDS. The supernatant (*S*), wash (*W*), and SDS eluate (*E*) were analyzed by 10% SDS-PAGE with Coomassie Blue staining (*A*). Neither Rad51 nor any of the three rad51 mutants bound the Ni-NTA resin in the absence of Rad52 (*B*).

wild type Rad51 in the catalysis of homologous DNA pairing and strand exchange. Altogether, the results from the four independent analyses as summarized above allowed us to conclude that the rad51 A320V, Y388H, and G393D mutants possess biochemical activities comparable with that of wild type Rad51.

The rad51 Mutants Are Defective in Rad52 Interaction—We used affinity pulldown to test whether the rad51 mutants are defective in physical interaction with Rad52 tagged with a His$_6$ epitope at its C terminus. For this, the purified rad51 mutants and wild type Rad51 were individually mixed with purified Rad52, and any protein complex that formed was captured on Ni-NTA resin, which recognized the His$_6$ affinity tag on Rad52. Bound proteins were eluted with SDS and then analyzed. None of three rad51 mutants interacted with Rad52, whereas, as expected, a complex of wild type Rad51 with Rad52 was seen (Fig. 4*A*). Neither wild type Rad51 nor any of the rad51 mutants bound the Ni-NTA resin in the absence of Rad52 (Fig. 4*B*). Thus, all three rad51 mutants are defective in complex formation with Rad52. In contrast, all three rad51 mutants retain the wild type level of ability to interact with Rad54 (see later), Rdh54, and Rad59 (data not shown).

Reliance of Rad52 Recombination Mediator Function on Rad51 Interaction—Because of the ability of RPA to compete with Rad51 for sites on ssDNA, co-addition of RPA with Rad51 to the ssDNA template strongly inhibits the homologous DNA pairing and strand exchange reaction. Importantly, the reaction efficiency can be fully restored by the inclusion of an amount of Rad52 substoichiometric to that of Rad51 (20). We used the

RPA/Rad51 co-addition protocol (RPA, 1°) to test for the responsiveness of the three rad51 mutant proteins to Rad52. As expected, RPA strongly suppressed the efficiency of homologous pairing and strand exchange mediated by wild type Rad51 or any of the three mutants (Fig. 5, *A*, compare *lanes 3* with *lanes 2*, and *B*). Importantly, although Rad52 was able to help overcome the inhibitory action of RPA with wild type Rad51 (Fig. 5, *A*, *panel I*, *lanes 4–8*, and *B*), with maximal restoration occurring at a Rad51 to Rad52 ratio of ∼10 (Fig. 5, *A*, *panel I*, and *B*), the inhibition posed by RPA was not at all relieved by Rad52 when any of the rad51 mutant proteins was examined (Fig. 5, *A*, *panels II–IV*, *lanes 4–8*, and *B*). These results thus provide evidence that interaction with Rad51 is critical for the efficacy of Rad52 recombination mediator activity.

rad51 Y388H and rad51 G393D Are Impaired for Srs2 Interaction—As described above and elsewhere (18), the rad51 A320V, rad51 Y388H, and rad51 G393D mutants are proficient in interaction with Rad54, Rdh54, and Rad59 but are specifically defective in Rad52 binding. We wondered whether these rad51 mutants retain the ability to interact with Srs2. To address this question, purified Rad51 and rad51 mutants were each mixed with His$_9$-tagged Srs2 and subsequently with Ni-NTA affinity resin to capture protein complexes, which were eluted from the resin with SDS and analyzed. Rad51 associated with Srs2 as previously described (Fig. 6*A*) (16). Interestingly, whereas rad51 A320V also bound Srs2, much less rad51 Y388H or rad51 G393D was found associated with Srs2 (Fig. 6*A*). Specifically, whereas nearly 80% of the input Rad51 or rad51 A320V associated with Srs2, only 15% of rad51 Y388H or 17% of rad51 G393D was pulled down by Srs2 under the same conditions (Fig. 6*A*). As expected, neither Rad51 nor any of the rad51 mutants was retained on the Ni-NTA affinity resin without Srs2 (Fig. 6*B*). These affinity pulldown data thus revealed an Srs2 interaction defect in the rad51 Y388H and rad51 G393D proteins and provide evidence that the *rad51 A320V* mutation differentially inactivates Rad52 interaction.

Effect of Srs2 on the D-loop Reaction Mediated by rad51 Mutants—As an anti-recombinase, Srs2 interferes with Rad51-mediated homologous DNA pairing and strand exchange by disrupting the presynaptic filament (16). The availability of the rad51 Y388H and rad51 G393D mutant proteins that retain the basic functional attributes of Rad51 but are defective in Srs2 interaction provides the opportunity to verify the functional significance of the Rad51-Srs2 complex in the anti-recombinase function of Srs2. Because Srs2 exerts a strong suppressive effect on the D-loop reaction mediated by the Rad51-Rad54 protein pair (16), we asked whether the D-loop reaction mediated by rad51 A320V, rad51 Y388H, or rad51 G393D in conjunction with Rad54 is also prone to the inhibitory action of Srs2. Consistent with their proficiency in Rad54 interaction (Fig. 7*A*), all three rad51 mutants gave a level of D-loop product comparable with that obtained with wild type Rad51 (Fig. 7*B*). However, whereas the rad51 A320V-mediated D-loop reaction was suppressed to a similar degree as in the case of wild type Rad51, much less inhibition was seen with either rad51 Y388H or rad51 G393D (Fig. 7*B*). These results thus revealed a dependence of Srs2 anti-recombinase function on its ability to interact with Rad51 protein.

A

B
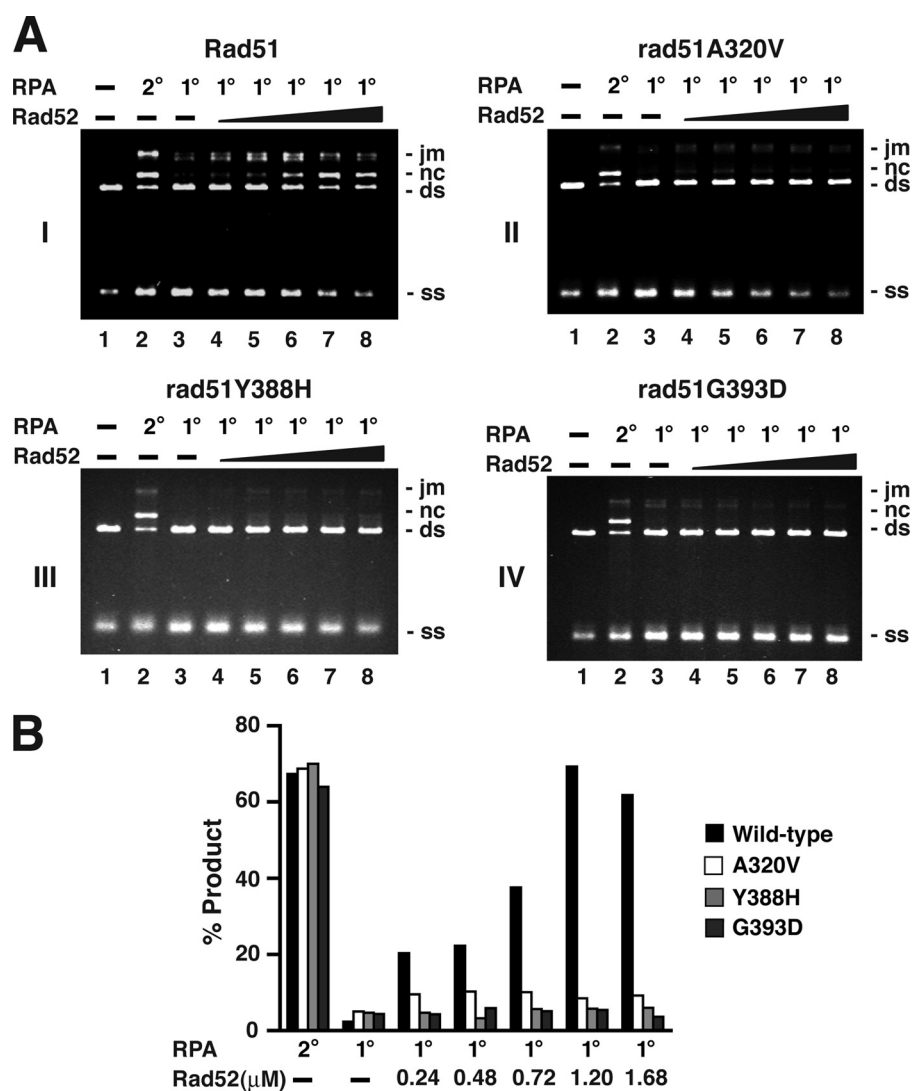
FIGURE 5. **rad51 mutants are refractory to Rad52 mediator activity.** *A*, DNA strand exchange reactions were conducted as described in Fig. 3, with RPA added after Rad51, rad51 A320V, rad51 Y388H, or rad51 G393D was allowed to bind the ssDNA (RPA 2°) or with RPA added together with Rad51 or rad51 mutant to the ssDNA (RPA 1°). Rad52 (0.24, 0.48, 0.72, 1.2, or 1.68 μM) was added together with Rad51 and RPA, as indicated. *B*, the results from *A* were plotted. *jm*, joint molecule; *nc*, nicked circular duplex.

Resistance of rad51 Y388H or rad51 G393D Presynaptic Filaments to Srs2 Action—We employed a topoisomerase-linked assay to test the susceptibility of presynaptic filaments of the rad51 A320V, rad51 Y388H, and rad51 G393D mutants to Srs2. In this assay, Rad51 displaced from ssDNA by Srs2 is trapped on topologically relaxed dsDNA, leading to lengthening of the latter DNA species that can be monitored as a DNA linking number change upon treatment with calf thymus topoisomerase I (Fig. 8*A*, *panel I*). The underwound dsDNA species, called Form U, is visualized by ethidium bromide staining after agarose gel electrophoresis (16). We had already established that the three rad51 mutants are just as effective as the wild type protein in inducing the Form U species when allowed to bind to dsDNA (Figs. 2*C* and 8*A*, *panel II, lanes 2, 6, 10, and 14*). In addition, the presynaptic filaments made by the mutant proteins are stable in the absence of Srs2 (Fig. 8*A*, *panel II, lanes 3, 7, 11, and 15*).

The addition of Srs2 to the Rad51 presynaptic filament induced the generation of Form U (Fig. 8*A*, *panel II, lanes 4 and*
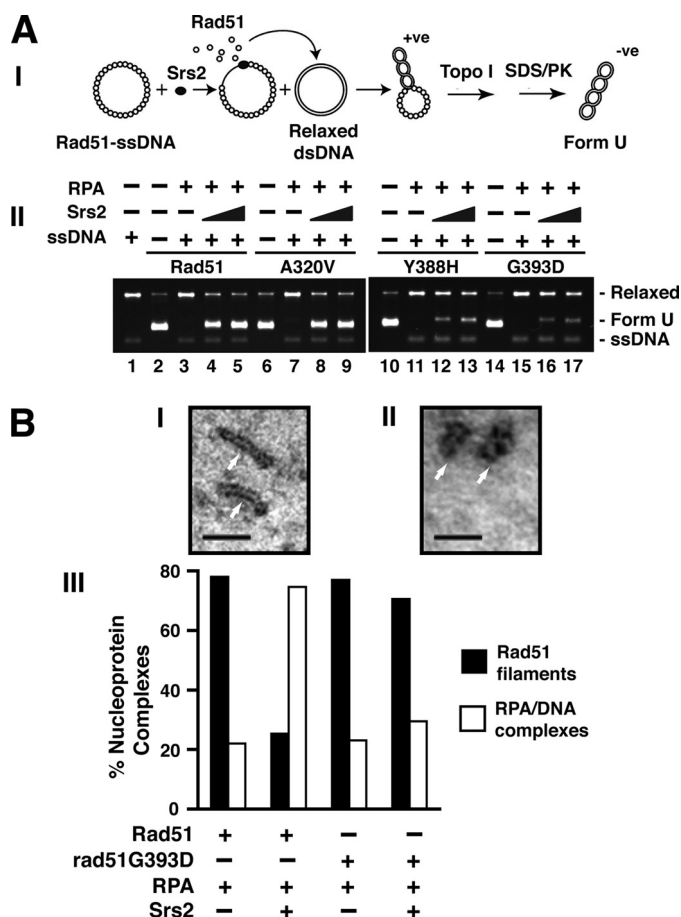
5), indicating the displacement of Rad51 from the ssDNA and trapping of the dissociated Rad51 molecules on the dsDNA. Similarly, Form U was efficiently generated when Srs2 was mixed with presynaptic filaments that harbored rad51 A320V (Fig. 8*A*, *panel II, lanes 8 and 9*). In sharp contrast, only a trace of Form U DNA was evident when presynaptic filaments of rad51 Y388H or rad51 G393D were incubated with Srs2 (Fig. 8*A*, *panel II, lanes 12, 13, 16, and 17*). These results provide clear evidence that disruption of Rad51 nucleoprotein filament by Srs2 requires the interaction of Rad51 with Srs2.

Characterization of Presynaptic Filaments by Electron Microscopy—Electron microscopy was employed to further characterize the effect of Srs2 on the Rad51 or rad51 G393D presynaptic filaments, with the prediction that the latter filaments would be more resistant to Srs2. Incubation of Rad51 or rad51 G393D with a 150-mer oligonucleotide produced abundant presynaptic filaments with the characteristic striations (Fig. 8*B*, *panels I and III*; data not shown) and few RPA-ssDNA complexes with a nondescript appearance (Fig. 8*B*, *panels II and III*). As reported previously, the addition of Srs2 to Rad51 presynaptic filaments led to their dissociation, such that the RPA-ssDNA complexes now comprised the majority of nucleoprotein species

(Fig. 8*B*, *panel III*). Importantly, the presynaptic filaments of rad51 G393D were much less sensitive to the disruptive action of Srs2, because only a slight reduction in their level was observed upon the inclusion of Srs2 (Fig. 8*B*, *panel III*). Thus, these results also support the notion that the disassembly of presynaptic filament by Srs2 is dependent on the interaction between Rad51 and Srs2.

Rad52 Inhibits Rad51-Srs2 Complex Formation—Because rad51 Y388H and rad51 G393D are simultaneously impaired for Rad52 and Srs2 interaction, it seems possible that the domains in Rad51 that mediate its interaction with Rad52 and Srs2 might overlap. If this were the case, then Rad52 should compete with Srs2 for Rad51 binding. To address this, His$_9$-tagged Srs2 immobilized on Ni-NTA-agarose beads was mixed with Rad51 and an increasing concentration of a Rad52 fragment (residues 327–504, termed Rad52-C) harboring the Rad51-binding domain (26, 27). After washing the beads with buffer, bound proteins were eluted with SDS and analyzed, to

FIGURE 6. **Interaction of rad51 mutants with Srs2.** Rad51, rad51 A320V, rad51 Y388H, or rad51 G393D was incubated with His$_9$-tagged Srs2, and the reaction mixtures were mixed with Ni-NTA resin to capture any protein complex that had formed. The proteins were eluted from the resin with SDS. The supernatant (*S*), wash (*W*), and SDS eluate (*E*) were analyzed by 8% SDS-PAGE with Coomassie Blue staining (*A*). Neither Rad51 nor any of the three rad51 mutants bound the Ni-NTA in the absence of Srs2 (*B*).

quantify the amount of Srs2-Rad51 complex. As shown in Fig. 9*A*, less Srs2-Rad51 complex was captured on the Ni-NTA-agarose beads upon the inclusion of Rad52-C, and this effect was clearly dependent on the concentration of Rad52-C. Importantly, under the same reaction conditions, the complex made with Srs2 and rad51 A320V mutant, which we have shown earlier to be defective only in Rad52 interaction (Fig. 4), was resistant to even the highest concentration of Rad52-C tested. Thus, the results from the above pulldown experiments validate the premise that the Rad52 and Srs2 interaction domains in Rad51 overlap. They also provide further support that the change of alanine 320 in Rad51 to valine represents a separation-of-function mutation with regards to the differential impairment of Rad52 interaction.

DISCUSSION

The inhibitory effect of RPA on Rad51 presynaptic filament assembly can be effectively overcome by Rad52 (3). By multiple criteria, including co-immunoprecipitation, yeast two-hybrid analysis, and biochemical means, yeast Rad51 and Rad52 have been shown to form a stable complex (1, 3). The Rad51 interaction domain resides within the C terminus of Rad52 (27), and previously, using variants of Rad52 that lack the C-terminal Rad51 interaction domain, we and others have provided evidence for a role of the Rad51-Rad52 complex in the delivery of Rad51 to RPA-coated ssDNA to seed the assembly of the presynaptic filament (9, 26).

FIGURE 7. **Resistance of the rad51 Y388H and rad51 G393D mutants to Srs2.** *A*, Rad51, rad51 A320V, rad51 Y388H, or rad51 G393D was incubated with His$_6$-tagged Rad54. The reaction mixtures were mixed with Ni-NTA resin to capture any protein complex that had formed. Bound proteins were eluted from the resin with SDS. The supernatant (*S*), wash (*W*), and SDS eluate (*E*) were analyzed by 8% SDS-PAGE with Coomassie Blue staining (*panel I*). Neither Rad51 nor any of the three rad51 mutants bound the Ni-NTA resin in the absence of Rad54 (*panel II*). *B*, scheme of the D-loop assay is shown in *panel I*. *Panel II* shows D-loop reactions that were mediated by Rad51, rad51 A320V, rad51 Y388H, or rad51 G393D in conjunction with Rad54 and RPA (*lanes 2–13*). Srs2 was added to 17 or 24 nM, where indicated. The results from *panel II* were quantified and plotted in *panel III*.

To further define the importance of the Rad51-Rad52 complex in presynaptic filament assembly, we have expressed and purified three rad51 mutants that each harbor a single amino acid change, namely, rad51 A320V, rad51 Y388H, and rad51 G393D, shown previously to be impaired for Rad52 interaction by the yeast two-hybrid assay (18). We have provided herein several lines of evidence that these rad51 mutants possess nor-

FIGURE 8. **Resistance of the rad51 Y388H and rad51 G393D presynaptic filaments to Srs2.** *A*, the schematic of the topoisomerase I-linked assay is shown in *panel I*. *Panel II* shows the results obtained when presynaptic filaments of Rad51, rad51 A320V, rad51 Y388H, or rad51 G393D were incubated with or without Srs2. The appropriate controls were included. *B*, electron microscopic analysis. Representative Rad51 nucleoprotein filaments (*panel I*) or RPA-ssDNA complexes (*panel II*) assembled on 150-mer ssDNA and imaged at 87,000× magnification. The *scale bars* represent 50 nm. *Panel III* shows the distributions of presynaptic filaments and RPA-ssDNA complexes upon incubation of Rad51 or rad51 G393D presynaptic filaments with RPA alone or with RPA and Srs2, as indicated.

mal biochemical attributes with regards to DNA binding, ATP hydrolysis, and the ability to conduct homologous DNA pairing and strand exchange. Importantly we have verified that all three rad51 mutants are indeed defective in complex formation with Rad52, even though they retain the ability to interact with other recombination factors including Rad54, Rad59, and Rdh54. Consistent with their deficiency in Rad52 interaction, none of the three rad51 mutants is responsive to the recombination mediator activity of Rad52. Thus, our analyses with these rad51 mutants along with previous studies involving the use of Rad51 interaction defective variants of Rad52 (9, 26) provide unequivocal support for the notion that physical interaction with Rad51 is indispensable for the recombination mediator attribute of Rad52.

Ablation of *SRS2* leads to elevated levels of recombination including cross-over recombination, cell cycle arrest, and synthetic impairment of growth fitness in combination with other mutations (17, 28–30). Studies in the past several years have indicated that Srs2 serves the role of an anti-recombinase, act-
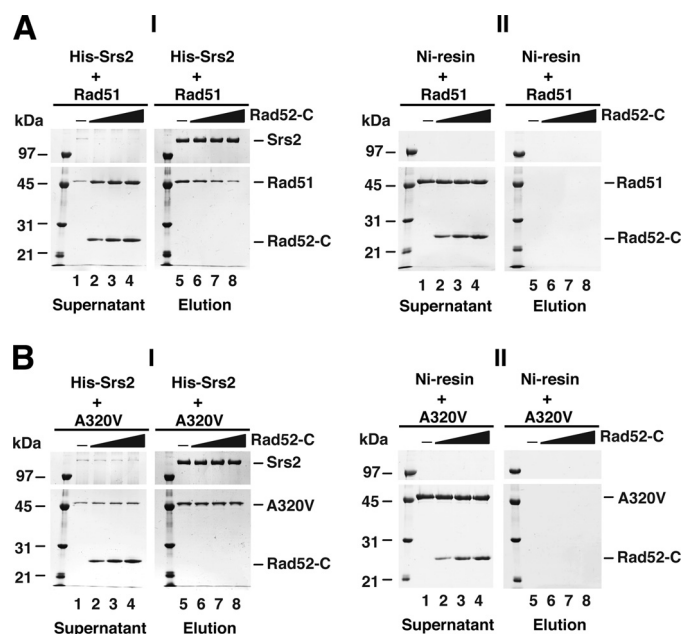
FIGURE 9. **Rad52 interferes with Rad51-Srs2 complex assembly.** Rad51 (*A*) or rad51 A320V (*B*), 5.0 μM each, was incubated with (*panels I*) or without (*panels II*) His₉-tagged Srs2 (5.0 μM) in the absence or presence of 3.3, 5.0, or 6.7 μM Rad52-C. The reaction mixtures were mixed with Ni-NTA resin to capture any protein complex that had formed. After washing with buffer, the resin was treated with SDS to elute bound proteins, and the supernatant (*left panels*) and SDS eluate fractions (*right panels*) were analyzed by 12% SDS-PAGE with Coomassie Blue staining.

ing to prevent untimely or undesirable HR events via the disruption of the Rad51 presynaptic filaments (15, 16). The ssDNA freed of Rad51 molecules via Srs2 action becomes occupied by RPA, thus making the DNA inaccessible for Rad51 reloading (16). In yeast two-hybrid and biochemical analyses, Srs2 forms a complex with Rad51, and we have mapped the Rad51 interaction domain to the C-terminal region of Srs2 (16). Unexpectedly we found that rad51 Y388H and rad51 G393D, but not rad51 A320V, are impaired for Srs2 interaction. With these rad51 mutant proteins, we have presented evidence derived from biochemical and electron microscopic analyses to validate the premise that the "disruptase" activity of Srs2 relies on complex formation with the Rad51 recombinase. The interaction defective rad51 Y388H and rad51 G393D mutants are much more resistant to the anti-recombinase activity of Srs2 than is either wild type Rad51 or the interaction proficient mutant rad51 A320V. Consistent with the premise that the Rad52 and Srs2 interactions motifs overlap in Rad51, we have furnished biochemical results that Srs2 is precluded from interacting with Rad51 when an excess of Rad52 is present. However, the fact that the rad51 A320V mutation differentially inactivates the ability to interact with Rad52 suggests that the Rad52 makes an additional contact with Rad51 protein that is not shared by Srs2. Alternatively, the rad51 A320V mutation alters the conformation of Rad51 in such a fashion as to ablate Rad52 interaction without affecting Srs2 binding.

Fig. 10 maps the locations of the three *rad51* mutations onto the known three-dimensional structure of the yeast Rad51 filament (Fig. 10*A*). We note that Tyr[388] and Gly[393] are located on the outer surface of the Rad51 helical polymer, whereas Ala[320] is situated in the interior of the polymer. We
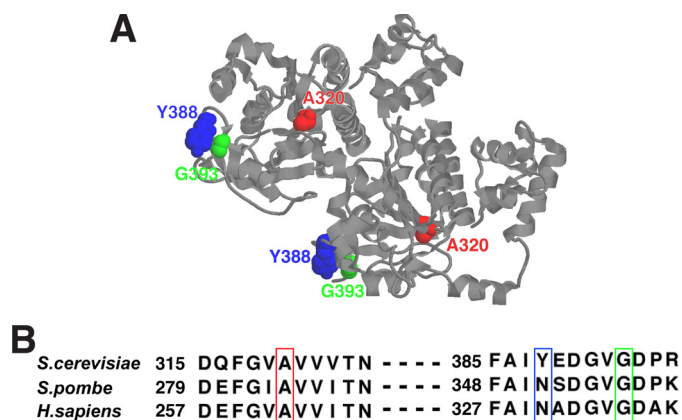
FIGURE 10. **Locations of the rad51 mutations in the Rad51 polymer.** *A*, the positions of the amino acid residues Ala[320], Tyr[388], and Gly[393] in the Rad51 filament, colored in *red*, *blue*, and *green*, respectively, adapted from Ref. 33. *B*, sequence alignment of the Rad51 orthologues from budding, fission yeast, and humans. Positions of amino acid residues explored in this study are boxed in *red*, *blue*, or *green* as in *A*.

also note that Ala[320] and Gly[393] are conserved among various Rad51 orthologues, including human Rad51 (Fig. 10*B*). It will be interesting to ask whether these residues contribute to the association of Rad51 proteins from other species with their cognate mediator proteins, such as the BRCA2 protein in human cells, and toward the association of the Rad51 orthologues with anti-recombinase proteins, such as the RECQ5 helicase in human cells (31, 32).

REFERENCES

1. Symington, L. S. (2002) *Microbiol. Mol. Biol. Rev.* **66,** 630–670
2. Sung, P., and Klein, H. (2006) *Nat. Rev. Mol. Cell Biol.* **7,** 739–750
3. San Filippo, J., Sung, P., and Klein, H. (2008) *Annu. Rev. Biochem.* **77,** 229–257
4. Jasin, M. (2002) *Oncogene* **21,** 8981–8993
5. D'Andrea, A. D., and Grompe, M. (2003) *Nat. Rev. Cancer* **3,** 23–34
6. Bishop, D. K., and Zickler, D. (2004) *Cell* **117,** 9–15
7. Bianco, P. R., Tracy, R. B., and Kowalczykowski, S. C. (1998) *Front. Biosci.* **3,** D570–D603
8. New, J. H., Sugiyama, T., Zaitseva, E., and Kowalczykowski, S. C. (1998) *Nature* **391,** 407–410
9. Shinohara, A., and Ogawa, T. (1998) *Nature* **391,** 404–407
10. Sugawara, N., Wang, X., and Haber, J. E. (2003) *Mol. Cell* **12,** 209–219
11. Wolner, B., van Komen, S., Sung, P., and Peterson, C. L. (2003) *Mol. Cell* **12,** 221–232
12. Lisby, M., Barlow, J. H., Burgess, R. C., and Rothstein, R. (2004) *Cell* **118,** 699–713
13. Sung, P., Krejci, L., Van Komen, S., and Sehorn, M. G. (2003) *J. Biol. Chem.* **278,** 42729–42732
14. Schiestl, R. H., Prakash, S., and Prakash, L. (1990) *Genetics* **124,** 817–831
15. Veaute, X., Jeusset, J., Soustelle, C., Kowalczykowski, S. C., Le Cam, E., and Fabre, F. (2003) *Nature* **423,** 309–312
16. Krejci, L., Van Komen, S., Li, Y., Villemain, J., Reddy, M. S., Klein, H., Ellenberger, T., and Sung, P. (2003) *Nature* **423,** 305–309
17. Krejci, L., Macris, M., Li, Y., Van Komen, S., Villemain, J., Ellenberger, T., Klein, H., and Sung, P. (2004) *J. Biol. Chem.* **279,** 23193–23199
18. Krejci, L., Damborsky, J., Thomsen, B., Duno, M., and Bendixen, C. (2001) *Mol. Cell. Biol.* **21,** 966–976
19. Sung, P., and Robberson, D. L. (1995) *Cell* **82,** 453–461
20. Seong, C., Sehorn, M. G., Plate, I., Shi, I., Song, B., Chi, P., Mortensen, U., Sung, P., and Krejci, L. (2008) *J. Biol. Chem.* **283,** 12166–12174
21. Raschle, M., Van Komen, S., Chi, P., Ellenberger, T., and Sung, P. (2004) *J. Biol. Chem.* **279,** 51973–51980
22. Chi, P., Kwon, Y., Seong, C., Epshtein, A., Lam, I., Sung, P., and Klein, H. L. (2006) *J. Biol. Chem.* **281,** 26268–26279
23. Petukhova, G., Van Komen, S., Vergano, S., Klein, H., and Sung, P. (1999) *J. Biol. Chem.* **274,** 29453–29462
24. Van Komen, S., Petukhova, G., Sigurdsson, S., Stratton, S., and Sung, P. (2000) *Mol. Cell* **6,** 563–572
25. Petukhova, G., Stratton, S., and Sung, P. (1998) *Nature* **393,** 91–94
26. Krejci, L., Song, B., Bussen, W., Rothstein, R., Mortensen, U. H., and Sung, P. (2002) *J. Biol. Chem.* **277,** 40132–40141
27. Milne, G. T., and Weaver, D. T. (1993) *Genes Dev.* **7,** 1755–1765
28. Aguilera, A., and Klein, H. L. (1988) *Genetics* **119,** 779–790
29. Schild, D. (1995) *Genetics* **140,** 115–127
30. Gangloff, S., Soustelle, C., and Fabre, F. (2000) *Nat. Genet.* **25,** 192–194
31. Yang, H., Li, Q., Fan, J., Holloman, W. K., and Pavletich, N. P. (2005) *Nature* **433,** 653–657
32. San Filippo, J., Chi, P., Sehorn, M. G., Etchin, J., Krejci, L., and Sung, P. (2006) *J. Biol. Chem.* **281,** 11649–11657
33. Conway, A. B., Lynch, T. W., Zhang, Y., Fortin, G. S., Fung, C. W., Symington, L. S., and Rice, P. A. (2004) *Nat. Struct. Mol. Biol.* **11,** 791–796

ADDITIONS AND CORRECTIONS

Regulation of Rad51 recombinase presynaptic filament assembly via interactions with the Rad52 mediator and the Srs2 anti-recombinase.

Changhyun Seong, Sierra Colavito, Youngho Kwon, Patrick Sung, and Lumir Krejci

Authors are urged to introduce these corrections into any reprints they distribute. Secondary (abstract) services are urged to carry notice of these corrections as prominently as they carried the original abstracts.

Attachment 8

Marini V, and Krejci L

Srs2: the "Odd-Job Man".

DNA Repair, 9(3):268-75. 2010

ARTICLE IN PRESS

Mini-review

Srs2: The "Odd-Job Man" in DNA repair

Victoria Marini[a], Lumir Krejci[a,b,*]

[a] Department of Biology, Faculty of Medicine, Masaryk University, Brno CZ-625 00, Czech Republic
[b] National Centre for Biomolecular Research, Faculty of Science, Masaryk University, Brno CZ-625 00, Czech Republic

ARTICLE INFO

Article history:
Available online xxx

Keywords:
DNA repair
Recombination
Helicases
Srs2

ABSTRACT

Homologous recombination plays a key role in the maintenance of genome integrity, especially during DNA replication and the repair of double-stranded DNA breaks (DSBs). Just a single un-repaired break can lead to aneuploidy, genetic aberrations or cell death. DSBs are caused by a vast number of both endogenous and exogenous agents including genotoxic chemicals or ionizing radiation, as well as through replication of a damaged template DNA or the replication fork collapse. It is essential for cell survival to recognise and process DSBs as well as other toxic intermediates and launch most appropriate repair mechanism. Many helicases have been implicated to play role in these processes, however their detail roles, specificities and co-operativity in the complex protein-protein interaction networks remain unclear. In this review we summarize the current knowledge about Saccharomyces cerevisiae helicase Srs2 and its effect on multiple DNA metabolic processes that generally affect genome stability. It would appear that Srs2 functions as an "Odd-Job Man" in these processes to make sure that the jobs proceed when and where they are needed.

© 2010 Elsevier B.V. All rights reserved.

Contents

1. Introduction

The genome is constantly threatened by various damaging agents and maintaining its integrity is crucial in all organisms. Several repair pathways have been implicated in the removal of different types of lesions from DNA. Among them, homologous recombination (HR) plays a key role in repair of double-strand breaks (DSBs). Although HR is a highly important repair mechanism, it has to be regulated to prevent it from interfering with other DNA repair pathways, generating toxic intermediates, or blocking the progression of the replication fork. Therefore, it is not surprising that cells have evolved mechanisms that counteract untimely HR events. In the yeast *Saccharomyces cerevisiae*, one of the pathways responsible for regulation of HR requires the action of the *SRS2* gene product. Mutations in the *SRS2* gene exhibit pleiotropic recombination phenotypes ranging from anti-recombinogenic in one aspect to pro-recombinogenic in another. In addition to its role in HR, Srs2 is also involved in other DNA metabolism processes, including post-replication repair (PRR), preservation of replication fork integrity, DNA-damage checkpoint responses, DNA triplet maintenance and non-homologous end joining (NHEJ).
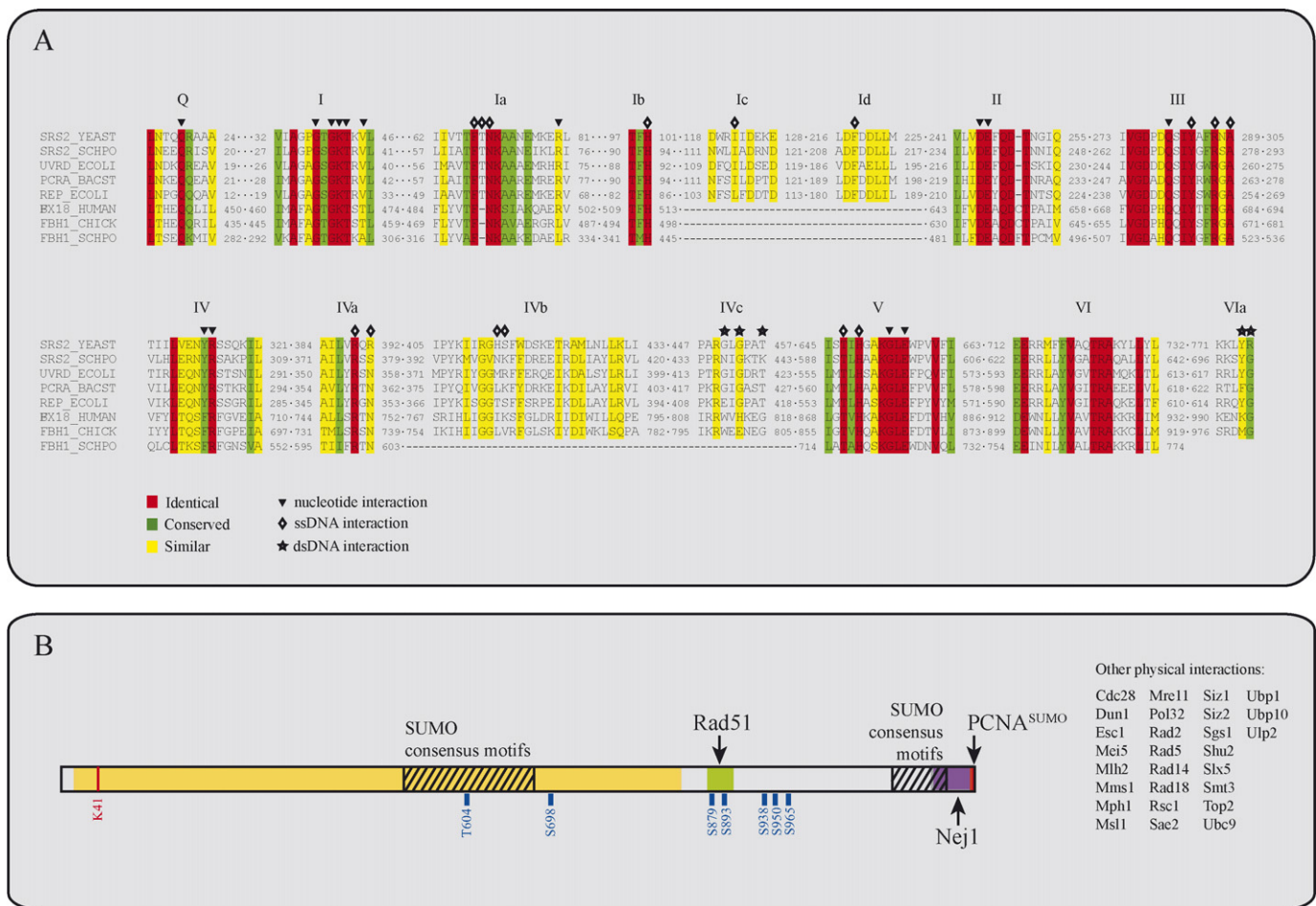
Fig. 1. Homology of Srs2 with other known helicases. (A) Several members of the SF-I family helicases and their alignment to Srs2 using CLUSTALW. Helicase motifs are indicated above the sequences. Color-coding is based on amino acid conservation. Symbols indicate important interaction amino acids within UvrD. (B) Schematic representation of Srs2. The helicase domain is colored in yellow, the Rad51 interaction domain in green and the PCNA^{SUMO} interaction domain in red. Striped areas contain SUMO consensus motifs. The marked amino acids in blue are phosphorylation sites. K41 represents the Walker type A motif.

2. Biochemical properties

The *SRS2* gene encodes a superfamily I DNA helicase with homologies to the bacterial helicases Rep, PcrA and UvrD [1–3] (Fig. 1). In contrast to these prokaryotic helicases, Srs2 contains an additional C-terminal region that mediates many protein–protein interactions and is also a target for post-translational modification. Interestingly, a previously performed large scale 2-hybrid screen using Srs2 as bait identified 166 potential interacting proteins and some of which are shown in Fig. 1 [4]. Biochemically, Srs2 possesses strong ssDNA-dependent ATPase activity with a kcat $\geq$3000 min^{-1} unwinds DNA with 3–5′ polarity [5,6], and the Walker A motif is absolutely required for both ATPase and helicase activities [7]. DNA with a 3′ overhang containing at least 10 nucleotides is the preferred substrate for its helicase activity. Srs2 is also able to unwind substrates containing forks, flaps, D-loops as well as 5′ ssDNA overhangs and blunt end dsDNA substrates ([6]; Marini and Krejci, unpublished data). Srs2 is also able to unwind *in vitro* structures that resemble D-loops recombination intermediates and this activity is stimulated by Rad51 bound to dsDNA [8]. However, recent experiments have shown that the helicase Mph1 is more efficient than Srs2 in dissociating D-loops formed by Rad51 [9]. In addition, the single-strand DNA binding proteins, RPA or SSB, enhance Srs2 unwinding of long substrates, by preventing the reannealing of the separated strands [6]. Srs2 is able to translocate on ssDNA as a monomer, with an average processivity of almost 1600 nt with a

rate of 300 nt/s, as revealed by analytical centrifugation [10]. Interestingly, it has been proposed for other helicases that translocase and helicase activities are separate functions and oligomerization might be required for the latter [11]. Further mechanistic analysis of the helicase and translocase activities of Srs2, investigation of the roles of Srs2 interacting partners, and structural characterization of Srs2 will help to understand its biological roles.

3. Anti-recombinase activity

HR contributes to genomic integrity and the repair of DSBs as well as acting during the recovery of damaged replication forks. However, HR must be also tightly regulated to prevent untimely events that could interfere with other DNA repair mechanisms as well as during replication fork progression. It has been noted that damaged DNA, blocked replication forks, or nucleoprotein complexes generated by the HR machinery can trigger cell cycle arrest and even cause cell death in certain genetic backgrounds [12–15]. Several pathways are involved in the elimination of undesirable HR intermediates. Interestingly, they all include the action of a helicase but use different mechanisms and act at different stages. One pathway involves the activity of the Srs2 helicase, which allegedly suppresses HR events at an early stage by dismantling the Rad51-presynaptic filament. A second mechanism involves the action of Mph1 or human RTEL that have been suggested to influence the efficiency of HR by disrupting the D-loop intermediate produced by the
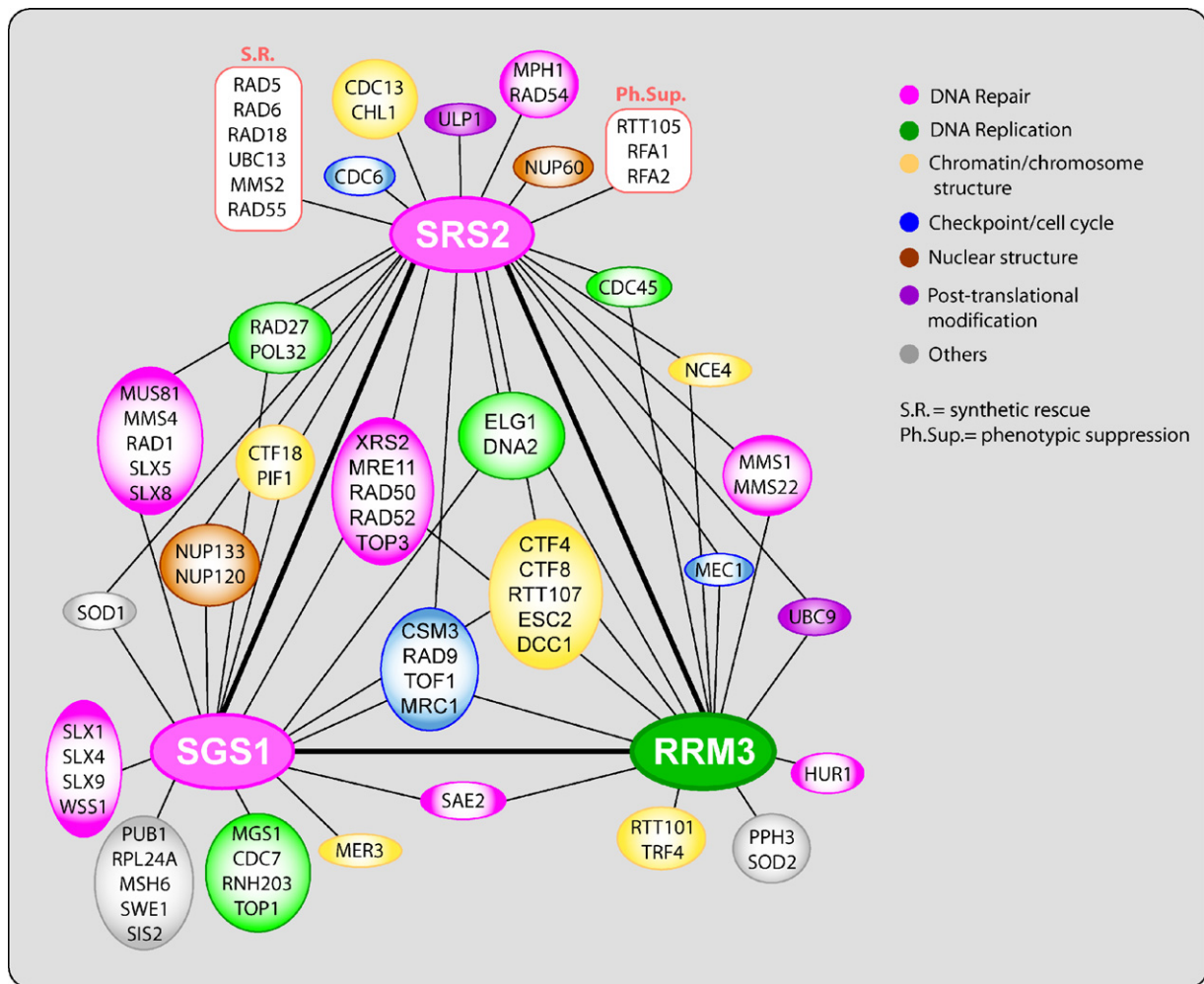
Fig. 2. Complexity of genetic interactions between *SRS2*, *SGS1*, and *RRM3* helicases as well as other genes as a part of a genome integrity network.

Rad51 recombinase [9,16]. Finally, BLM/Sgs1 together with Top3 is required for dissolution of dHJ or other recombination intermediates [17–19]. Here, we will describe in detail the anti-recombinase activity of Srs2 protein. The role of other helicases during HR will be the focus of other accompanying reviews.

Genetic studies were the first to suggest a possible role for Srs2 as an anti-recombinase. Mutations in the *SRS2* gene lead to a hyper-recombination phenotype due to inappropriate channeling of the lesions into the homologous recombination pathway [20–23]. The need for appropriate regulation of HR is most clearly illustrated by the near lethal phenotype of the *srs2 sgs1* double mutant. Deletion of recombination genes can efficiently suppress the severe phenotype of this double mutant as well as the *srs2* mutant [12,20,24–26]. These genetic data suggest that *sgs1 srs2* cells accumulate toxic recombination intermediates that cannot be resolved in the absence of the Srs2 and Sgs1 helicases.

To directly demonstrate the effect of Srs2 on the efficiency of recombination, biochemical studies have shown that catalytic amounts of Srs2 protein can dramatically inhibit the formation of Rad51-mediated joint molecules and D-loop formation [27,28]. Additional biochemical and electron microscopy analysis revealed that Srs2 efficiently dismantles the presynaptic filament formed by Rad51, an early HR intermediate. This is further enhanced in the presence of RPA that prevents re-nucleation of Rad51 on cleared ssDNA [27,28]. The helicase activity does not appear to be responsible for the dissociation of these intermediate molecules due to its modest processivity as well as lower activities on these struc-

tures [6,9,27]. Rather, ATP hydrolysis-fueled translocase activity is necessary for Srs2 to dismantle Rad51 filaments; mutants that cannot bind or hydrolyze ATP fail to disrupt Rad51-presynaptic filaments [7]. In agreement with the biochemical data, these ATPase dead mutants also show similar sensitivities to genotoxic agents, a hyper-recombination phenotype and synthetic interactions when compared to the *srs2* deletion mutant [7]. It has been suggested that Srs2 activity might be guided to the Rad51-filament via its direct physical interaction with Rad51 [27]. In agreement with this view, mutants of Rad51 that fail to interact with Srs2 are resistant to its anti-recombinase activity [29]. Accordingly, a mutant version of Srs2 that retains wild type levels of ATPase and helicase activities, but fails to interact with Rad51 is compromised for its anti-recombinase function [30]. The mechanism by which Srs2 dismantles Rad51 seems to be the result of ATP-driven motor activities of Srs2 that are capable of dissociating not only DNA structures but also protein–DNA complexes. Recent evidence suggests that the direct interaction between Srs2 and Rad51 is used both to target Srs2 to HR intermediates and to trigger ATP hydrolysis within the Rad51 filament, causing Rad51 to dissociate from DNA [10]. In line with this, the crystal structures of Rad51 and RecA reveal the importance of adjacent monomers in the coordination of ATP binding [31–33]. It is therefore intriguing to hypothesize that Rad51 filaments could actually sense/coordinate the Srs2 translocase activity through its own ATP hydrolysis-mediated affinity towards ssDNA, thus allowing more efficient clearing of the nucleoprotein filament by Srs2.

4. Role of Srs2 in replication fork maintenance and post-replication repair (PRR)

During replication, a damaged DNA template frequently blocks the progression of the replication fork. Unless stalled forks are able to restart, the cells cannot complete replication, which leads to cell cycle arrest and cell death. Several checkpoint-related proteins have been implicated in reducing the frequency of HR, that otherwise could lead to destabilization of replication forks and generation of toxic HR intermediates [34,35]. Srs2 is directly implicated in the replication checkpoint. This is based on the fact that *srs2* mutants fail to fully activate a Rad53-dependent DNA damage response, which is required to slow DNA replication [36]. Srs2 is also required for recovery and adaptation in response to checkpoint-mediated cell cycle arrest [14,36]. It still needs to be addressed whether the role for Srs2 during DNA-damage checkpoint activation requires its anti-recombinase activity or if this is dependent on its role in determining the fate of the replication fork.

Several mechanisms have been described that would provide multiple options for cells to counteract damage while replicating their DNA. Mechanisms that control recombination and other DNA repair processes during replication are again distinguished by the action of several helicases. Among them, *SRS2*, *SGS1* and *RRM3* genes show overlapping roles in genome maintenance as demonstrated by growth impairments or lethal phenotypes when mutations in these genes are combined [22,37–41]. It has been established that these helicases perform specific functions that cannot be executed by any another helicase (Fig. 2). As mentioned above, the inhibition of these alternative pathways in Srs2 mutants leads to synthetic lethal phenotypes, which can be suppressed by preventing recombination. This suggests that the helicase double mutants accumulate toxic HR intermediates, further supporting the need for tight regulation of recombination during DNA replication [22,39]. Rrm3, together with other components of the replication fork machinery ensures fork progression in the presence of replication blockages and prevents extended fork pausing that may occasionally lead to fork collapse [39,42–44]. The Sgs1 helicase seems to promote fork restart using HR via generation of recombination intermediates, as well as mediating their resolution [22]. The second mechanism involved in the restart of collapsed replication forks requires the action of the Srs2 helicase and other members of the *RAD6* epistasis group, which are required for PRR. This pathway may also lead to the formation of repair intermediates that require processing by the activity of the Sgs1 helicase [45]. Alternatively, another yeast helicase Mph1 has been implicated in an error-free DNA damage bypass pathway that requires genes from HR [46].

The *SRS2* gene was first identified as a suppressor of DNA damage sensitivity of both *rad6* and *rad18* mutants (Suppressor of *RAD* Six mutant 2) and this suppression requires functional HR [3,47–49]. Accordingly, Srs2 is also actively recruited to replication forks via its interaction with SUMOylated PCNA and this recruitment favors the use of PRR [50–52]. At the replication fork, Srs2 acts as a molecular switch between PRR and HR by channeling DNA lesions into the *RAD6* pathway while preventing the use of an alternative recombination repair [21,26,53]. Little is known about the molecular details of PRR, but genetic studies have revealed an intricate system of several independent pathways, comprising error-free and error-prone sub-pathways that allow the bypass of replication-blocking lesions [54]. It is possible that Srs2 could act at several stages of PRR, involving both early as well as late roles. It could prevent substrates assigned for PRR to be repaired by recombinational mechanisms by directly disrupting Rad51-filaments. It could also prevent or reverse Rad51 binding to repair intermediates, which could be important for preventing the nascent strand from pairing to generate chicken-foot structures that occur at stalled replication forks [55]. It is also possible that Srs2 could facilitate the generation of substrates needed for the error-prone or error free sub-pathways of PRR [45,54]. Such ability would help to explain the increased UV-sensitivity of *rad6/rad18* strain in the *srs2* mutant [23,56]. It has been noted that Srs2 is required for some or all branches of PRR where it could play an important role in the decision between error-free or error-prone PRR pathways [57–59]. However, further studies are needed to elucidate the mechanistic role of Srs2 in PPR pathways.

5. Srs2 as part of a recombination "quality control" mechanism

Recently, the cellular role of Srs2 at replication forks and in the regulation of HR was addressed. A decreased requirement for Rad52 activity during Rad51 focus formation in the *srs2Δ* mutant was observed, suggesting that Srs2 antagonizes Rad52 in the formation of Rad51 filaments [60]. This idea was further supported, by the ability of Rad52 protein to suppress the inhibitory effect of Srs2 on Rad51-mediated strand exchange [60]. Furthermore, Rad51 mutants, originally isolated as Rad52-interaction deficient mutants [61], also appeared defective for the interaction with Srs2, suggesting that these proteins compete for the same interaction region on Rad51 [29]. As expected, these Rad51 mutants show resistance to the action of Srs2 as well as an inability of Rad52 to overcome the RPA inhibition during Rad51-mediated strand exchange [29]. Accordingly, an Srs2 mutant protein that fails to interact with Rad51 is compromised for anti-recombinase function *in vitro* as well as *in vivo* [10,30]. However, additional mechanisms could still exist that restrict the recruitment of HR proteins to replication forks even in the absence of Srs2.

Based on our current knowledge, a model for a recombination "quality control" mechanism for the repair of DSBs and damaged replication forks can be proposed (Fig. 3). In one pathway of this model, Srs2 scans the chromosomes for inappropriate Rad51-filaments. This is in agreement with recent observations showing that deletion of *SRS2* results in an increase in the number of Rad51 and Rad54 foci even at genomic locations that are not relevant to HR, confirming the loading of HR proteins at inappropriate sites [60]. Srs2 anti-recombinase activity is able to remove Rad51 molecules from ssDNA that are subsequently occupied by RPA, thus making the DNA inaccessible for Rad51 reloading. In addition, the RPA-coated ssDNA, as a common structure generated at the sites of DNA damage or as a result of Srs2 anti-recombinase activity, is a target for modification as well as responsible for recruitment of the checkpoint machinery [15,62,63] and/or Rad18 [64]. The damage checkpoint once recruited may participate in the choice of repair pathways. If required, Srs2 could also channel substrates derived from other repair processes into the PRR pathway. When the cell favors HR, the second pathway of this model (Fig. 3) involving Rad52 mediator activity will antagonize Srs2 by nucleating Rad51-filaments [65–67]. Therefore, an equilibrium between these pathways might exist allowing cells to quickly and appropriately react to the incoming signal. Perhaps post-translational modifications or additional factors could shift this equilibrium accordingly as a part of a quality control mechanism. Future studies should provide details of how such regulation determines the fate of DNA repair at replication forks. Interestingly, the C-terminal region of Srs2 can be envisioned as a control node that integrates motor activity of Srs2 with protein interactions (Fig. 1). Similarly, Rad52 is also modified by phosphorylation and SUMOylation [68,69]. In summary, it is attractive to speculate that a cooperative or coordinated regulatory mechanism exists that determines the outcome of repair events at common HR intermediates.
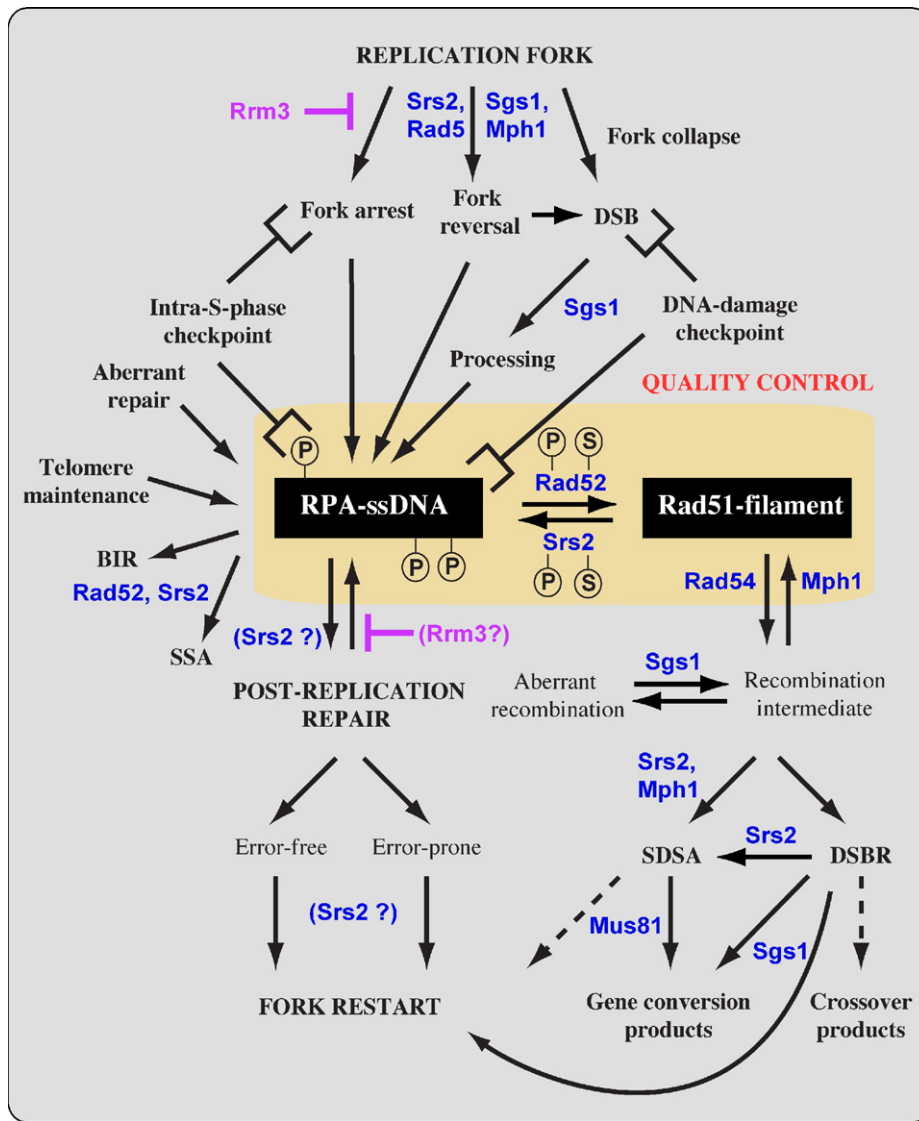
Fig. 3. Multifunctional role of Srs2 and other helicases during DNA repair and homologous recombination. RRM3 prevents the replication fork from stalling and collapsing. However, when this happens stalled or broken forks activate the intra-S-phase or DNA damage checkpoints, respectively. Also the RPA–ssDNA complex triggers a checkpoint response. Srs2 and Sgs1 serve distinct as well as overlapping functions in the regulation of recombination bypass of replication forks. Collapsed or broken forks are channeled either to Rad51-mediated recombination or Rad51-independent PRR. Sgs1 is involved in processing DSBs to generate 3′ tails for Rad51 filament formation and together with other helicases facilitate fork reversal. Srs2 and Rad52 are part of a "quality control" mechanism that influences the efficiency of repair via alternative routes. The quality control mechanism allows the cell to regulate the outcome of the intermediate, RPA–ssDNA or Rad51-filament, formed during repair. Srs2 and Mph1 or Sgs1 also play a downstream role in SDSA and DSBR, respectively. A synthetic lethal interaction between these helicases is due to the generation of toxic recombination intermediates, as deletion of recombination genes suppresses the lethality. The only difference is that deletion of the *RAD52* gene that does not alleviate the synthetic phenotype, arguing for a role of a Rad52-mediated and Rad51-independent process (BIR or SSA) as an alternative repair pathways. However, it should also be noted that Rad51 could be required for a specific role at blocked forks as suggested for bacterial RecA. It was proposed that RecA binds to the ssDNA region on the blocked lagging strand, and that this RecA filament invades the homologous leading strand, thus forming a reversed fork [103,104]. Also in yeast, recombination and template switching had previously been considered as separate mechanisms. Recent studies suggest that Rad51 and Rad18 have overlapping functions in the formation of sister-chromatid joint molecules after MMS treatment [45].

6. Srs2 and additional roles in DNA repair

Interestingly, even though Srs2 suppresses spontaneous recombination events via its anti-recombinase activity, the same activity also facilitates DSB repair by the synthesis-dependent single-strand annealing (SDSA) pathway [70,71]. Srs2 channels recombination intermediates into non-crossover pathways to minimize crossing over. During SDSA, Srs2 could facilitate strand displacement and/or displacement of Rad51 from non-invading ssDNA in the D-loop structure, thus preventing second-end capture. A role of Srs2 downstream of the strand invasion step and possibly in promoting double-strand break repair is further supported by the failure

to detect accumulation of recombination intermediates in *srs2* or *pol30* mutants in contrast to *sgs1* and *ubc9* mutants [72,73]. In addition, the Srs2 mutants defective in ATP binding and hydrolysis display a hyper-recombination phenotype that is even more pronounced than in a *srs2* deletion strain, suggesting that when Srs2 is absent, recombination is used to repair spontaneous DNA damage, but when a defective Srs2 protein is present, it might impede alternative pathways of repair [7]. The ability of Srs2 to remove Rad51 from ssDNA might also be required during other alternative repair pathways, including break-induced replication (BIR) and single-strand annealing (SSA) [74–77]. It has been recently observed that Srs2 is recruited to DSBs by Nej1 to promote NHEJ via SSA-like

repair [75]. In this pathway, Rad52-dependent strand annealing and subsequent repair are probably achieved by Srs2-mediated removal of Rad51 from ssDNA overhangs. This mechanism could help to explain why Srs2 is recruited to HR foci independent of Rad51 [60].

Srs2 has also been implicated in maintaining the stability of trinucleotide repeats, which are known to be responsible for a series of hereditary neurological disorders. Mutation in *srs2* leads to triplet repeat expansion. The function of Srs2 in preventing expansion is dependent on its helicase activity, requires connection with polymerase δ, but it is not dependent on recombination [78]. Srs2 is more efficient than Sgs1 and UvrD in unwinding substrates that mimic the triplet repeat hairpin, which is believed to be the relevant intermediate during expansions *in vivo* [79,80]. However, a recent study of long trinucleotide repeats established dependency, but to different degrees, on *RAD52* and *RAD51*, in both *srs2* and *sgs1* mutants [81]. This discrepancy could reflect a possible repeat size threshold that triggers HR [81]. In general, Srs2 seems to be responsible for prevention of repeat expansions that could arise via hairpin formation on the nascent lagging strand. In contrast, mutation in *SGS1* leads to contractions, suggestive of a role in unwinding hairpins that form on the lagging-strand template [81]. Nevertheless, other data point towards a role for Sgs1 in large-scale repeat expansions, possibly via a template switching mechanism [82].

7. Regulation of Srs2 activities

The roles of Srs2 in a number of different repair processes necessitate the proper regulation of its activity. Regulation and communication of Srs2 with cell cycle checkpoint pathways may provide a means to chose the most appropriate method to overcome stalled replication forks and other types of DNA damage. The post-translational modification of Srs2 could regulate the availability of specific DNA substrates that either favor homologous recombination or promote the use of alternate pathway to bypass the damage, such as template switching. In general, *SRS2* is expressed at low levels and its expression is coordinated with DNA synthesis genes, which are induced at the G1-S transition. In addition, Srs2 expression is induced by UV irradiation, but this is restricted to G2 cells [83].

Srs2 is also regulated by phosphorylation, which occurs following activation of the intra-S-phase checkpoint and this requires Dun1, Mec1 and Rad53 kinases [36]. Several studies have suggested that regulation of Srs2 can also be achieved through its recruitment to replication forks via its interaction with SUMOylated PCNA [50,51]. Accordingly, Srs2 was shown to form S-phase foci in a PCNA-SUMO dependent fashion; mutants deficient for PCNA SUMOylation or Srs2 lacking the SUMO interaction domain failed to form replication foci [60]. Conversely, recruitment of Srs2 to DSB foci is independent of PCNA interaction and also does not require interaction with Rad51. Instead, SUMOylation of Srs2 and the protein Siz1 plays a role in Srs2 recruitment to these foci [60]. Thus, recruitment of Srs2 to replication forks and other sites of recombination are genetically distinct processes. Perhaps SUMOylation of Srs2 itself is involved in its recruitment, as Srs2 was shown to interact with Smt3 (SUMO) and is SUMOylated both *in vitro* and *in vivo* ([84,85]; Krejci and Zhao, unpublished data). It is also possible that Srs2 regulation is under the direct control of components of the PRR pathway. For example, ubiquitination of Srs2 mediated by either Rad6 or Mms2/Ubc13 ubiquitin-conjugating activities could regulate its activities or recruitment. Understanding the nature of Srs2 regulation will help to clarify the complex relationships between DNA replication, repair and recombination and will be a key challenge for the future.

8. The search for human homologs

Srs2 shares a core architecture with other members of the SF-1 family of helicases, including UvrD, PcrA, and Rep [86–88]. UvrD appears to be both structural and functional homolog of Srs2 as it also disrupts formation of RecA filaments and has a role in replication fork maintenance [89,90]. Importantly, Srs2 also contains an additional C-terminal region that possesses many interaction as well as regulatory domains that may be responsible for its other specialized functions (Fig. 1). Fission yeast contains a sequence homolog of Srs2 that shares a number of phenotypes with its budding yeast Srs2 homolog, including hyper-sensitivity to DNA damaging agents, hyper-recombination, and several synthetic lethal interactions [91,92]. However, unlike in budding yeast, the fission yeast homolog is not required for channeling lesions to the PRR pathway [92,93] and can act on stalled or collapsed replication forks independently of PRR [93]. Interestingly, *S. pombe* (unlike *S. cerevisiae*) contains an additional Srs2-like protein, the F-box helicase Fbh1 that appears to serve in an overlapping manner with Srs2 to alleviate stress caused by DNA damage [94,95]. Mutation in the fission yeast *FBH1* gene leads to a phenotype and genetic interactions that resemble those of *srs2* mutant, suggesting that spFbh1 does indeed act as an anti-recombinase [95–97]. In addition, the expression of hFBH1 can partly complement the *srs2* phenotypes in *S. cerevisiae* [98] and mutation of chicken *FBH1* in DT40 cells leads to a slight increase in SCE [94]. Despite their functional similarities, spFbh1 and spSrs2 likely target different HR intermediates [95]. In contrast to Srs2, spFbh1 does not seem to interact with Rad51 and the deletion mutant does not affect spontaneous recombination at direct repeats [95]. The duplication of the *SRS2* locus in certain species suggests that gene duplication might have facilitated their rapid evolution towards specialized functions [99]. It also remains possible that some of the RecQ helicases also possess one or more of the activities of the Srs2 protein (see accompanying reviews). For example, similar to Srs2, RecQL5 was shown to displace Rad51 from ssDNA and acts to suppress recombination in human cells [100]. In addition, BLM and RTEL1 were also shown to inhibit Rad51-mediated SDSA reactions by dissociating D-loops [16,101], this however might reflect an alternative pathway, similar to yeast Mph1 [9].

It is apparent that cells possess a number of over-lapping and compensating anti- and pro-recombination activities associated with Srs2, Fbh1, RecQ helicases, and other helicases (FML1, RTEL1 and others). Each of these helicases contributes to genome stability without strict functional conservation among species. It is likely that the distinct roles played by these helicases are a direct consequence of their association with other cofactors. However, functional redundancy clearly exists between this group of helicases, which illustrates the importance of regulating recombination reactions. Despite the apparent functional overlap, mutants in these helicases clear exhibit distinct cellular phenotypes as well as characteristics indicative of specific functions alone or in combination with other factors. Understanding how these activities cooperate and compensation for each other will continue to provide valuable insights for understanding genome maintenance.

Conflict of Interest

None.

References

[1] A.E. Gorbalenya, E.V. Koonin, A.P. Donchenko, V.M. Blinov, A novel super-family of nucleoside triphosphate-binding motif containing proteins which are probably involved in duplex unwinding in DNA and RNA replication and recombination, FEBS Lett. 235 (1988) 16–24.

[2] M.C. Hall, S.W. Matson, Helicase motifs: the engine that powers DNA unwinding, Mol. Microbiol. 34 (1999) 867–877.

[3] A. Aboussekhra, R. Chanet, Z. Zgaga, C. Cassier-Chauvat, M. Heude, F. Fabre, RADH, a gene of *Saccharomyces cerevisiae* encoding a putative DNA helicase involved in DNA repair. Characteristics of radH mutants and sequence of the gene, Nucleic Acids Res. 17 (1989) 7211–7219.

[4] I. Chiolo, W. Carotenuto, G. Maffioletti, J.H. Petrini, M. Foiani, G. Liberi, Srs2 and Sgs1 DNA helicases associate with Mre11 in different subcomplexes following checkpoint activation and CDK1-mediated Srs2 phosphorylation, Mol. Cell. Biol. 25 (2005) 5738–5751.

[5] L. Rong, H.L. Klein, Purification and characterization of the SRS2 DNA helicase of the yeast *Saccharomyces cerevisiae*, J. Biol. Chem. 268 (1993) 1252–1259.

[6] S. Van Komen, M.S. Reddy, L. Krejci, H. Klein, P. Sung, ATPase and DNA helicase activities of the *Saccharomyces cerevisiae* anti-recombinase Srs2, J. Biol. Chem. 278 (2003) 44331–44337.

[7] L. Krejci, M. Macris, Y. Li, S. Van Komen, J. Villemain, T. Ellenberger, H. Klein, P. Sung, Role of ATP hydrolysis in the anti-recombinase function of *Saccharomyces cerevisiae* Srs2 protein, J. Biol. Chem. 279 (2004) 23193–23199.

[8] P. Dupaigne, C. Le Breton, F. Fabre, S. Gangloff, E. Le Cam, X. Veaute, The Srs2 helicase activity is stimulated by Rad51 filaments on dsDNA: implications for crossover incidence during mitotic recombination, Mol. Cell 29 (2008) 243–254.

[9] R. Prakash, D. Satory, E. Dray, A. Papusha, J. Scheller, W. Kramer, L. Krejci, H. Klein, J.E. Haber, P. Sung, G. Ira, Yeast Mph1 helicase dissociates Rad51-made D-loops: implications for crossover control in mitotic recombination, Genes Dev. 23 (2009) 67–79.

[10] E. Antony, E.J. Tomko, Q. Xiao, L. Krejci, T.M. Lohman, T. Ellenberger, Srs2 disassembles Rad51 filaments by a protein–protein interaction triggering ATP turnover and dissociation of Rad51 from DNA, Mol. Cell 35 (2009) 105–115.

[11] T.M. Lohman, E.J. Tomko, C.G. Wu, Non-hexameric DNA helicases and translocases: mechanisms and regulation, Nat. Rev. Mol. Cell Biol. 9 (2008) 391–401.

[12] S. Gangloff, C. Soustelle, F. Fabre, Homologous recombination is responsible for cell death in the absence of the Sgs1 and Srs2 helicases, Nat. Genet. 25 (2000) 192–194.

[13] A. Pellicioli, S.E. Lee, C. Lucca, M. Foiani, J.E. Haber, Regulation of *Saccharomyces* Rad53 checkpoint kinase during adaptation from DNA damage-induced G2/M arrest, Mol. Cell 7 (2001) 293–300.

[14] M.B. Vaze, A. Pellicioli, S.E. Lee, G. Ira, G. Liberi, A. Arbel-Eden, M. Foiani, J.E. Haber, Recovery from checkpoint-mediated arrest after repair of a double-strand break requires Srs2 helicase, Mol. Cell 10 (2002) 373–385.

[15] L. Zou, S.J. Elledge, Sensing DNA damage through ATRIP recognition of RPA–ssDNA complexes, Science 300 (2003) 1542–1548.

[16] L.J. Barber, J.L. Youds, J.D. Ward, M.J. McIlwraith, N.J. O'Neil, M.I. Petalcorin, J.S. Martin, S.J. Collis, S.B. Cantor, M. Auclair, H. Tissenbaum, S.C. West, A.M. Rose, S.J. Boulton, RTEL1 maintains genomic stability by suppressing homologous recombination, Cell 135 (2008) 261–271.

[17] W. Bussen, S. Raynard, V. Busygina, A.K. Singh, P. Sung, Holliday junction processing activity of the BLM-Topo IIIalpha–BLAP75 complex, J. Biol. Chem. 282 (2007) 31484–31492.

[18] L. Wu, C.Z. Bachrati, J. Ou, C. Xu, J. Yin, M. Chang, W. Wang, L. Li, G.W. Brown, I.D. Hickson, BLAP75/RMI1 promotes the BLM-dependent dissolution of homologous recombination intermediates, Proc. Natl. Acad. Sci. U.S.A. 103 (2006) 4068–4073.

[19] L. Wu, I.D. Hickson, The Bloom's syndrome helicase suppresses crossing over during homologous recombination, Nature 426 (2003) 870–874.

[20] A. Aboussekhra, R. Chanet, A. Adjiri, F. Fabre, Semidominant suppressors of Srs2 helicase mutations of *Saccharomyces cerevisiae* map in the *RAD51* gene, whose sequence predicts a protein with similarities to procaryotic RecA proteins, Mol. Cell. Biol. 12 (1992) 3224–3234.

[21] R. Chanet, M. Heude, A. Adjiri, L. Maloisel, F. Fabre, Semidominant mutations in the yeast Rad51 protein and their relationships with the Srs2 helicase, Mol. Cell. Biol. 16 (1996) 4782–4789.

[22] F. Fabre, A. Chan, W.D. Heyer, S. Gangloff, Alternate pathways involving Sgs1/Top3, Mus81/Mms4, and Srs2 prevent formation of toxic recombination intermediates from single-stranded gaps created by DNA replication, Proc. Natl. Acad. Sci. U.S.A. 99 (2002) 16887–16892.

[23] L. Rong, F. Palladino, A. Aguilera, H.L. Klein, The hyper-gene conversion hpr5-1 mutation of *Saccharomyces cerevisiae* is an allele of the SRS2/RADH gene, Genetics 127 (1991) 75–85.

[24] H.L. Klein, RDH54, a RAD54 homologue in *Saccharomyces cerevisiae*, is required for mitotic diploid-specific recombination and repair and for meiosis, Genetics 147 (1997) 1533–1543.

[25] M. McVey, M. Kaeberlein, H.A. Tissenbaum, L. Guarente, The short life span of *Saccharomyces cerevisiae* sgs1 and srs2 mutants is a composite of normal aging processes and mitotic arrest due to defective recombination, Genetics 157 (2001) 1531–1542.

[26] D. Schild, Suppression of a new allele of the yeast RAD52 gene by overexpression of RAD51, mutations in srs2 and ccr4, or mating-type heterozygosity, Genetics 140 (1995) 115–127.

[27] L Krejci, S. Van Komen, Y. Li, J. Villemain, M.S. Reddy, H. Klein, T. Ellenberger, P. Sung, DNA helicase Srs2 disrupts the Rad51 presynaptic filament, Nature 423 (2003) 305–309.

[28] X. Veaute, J. Jeusset, C. Soustelle, S.C. Kowalczykowski, E. Le Cam, F. Fabre, The Srs2 helicase prevents recombination by disrupting Rad51 nucleoprotein filaments, Nature 423 (2003) 309–312.

[29] C. Seong, S. Colavito, Y. Kwon, P. Sung, L. Krejci, Regulation of Rad51 recombinase presynaptic filament assembly via interactions with the Rad52 mediator and the Srs2 anti-recombinase, J. Biol. Chem. 284 (2009) 24363–24371.

[30] S. Colavito, M. Macris-Kiss, C. Seong, O. Gleeson, E.C. Greene, H.L. Klein, L. Krejci, P. Sung, Functional significance of the Rad51–Srs2 complex in Rad51 presynaptic filament disruption, Nucleic Acids Res. 37 (2009) 6754–6764.

[31] Z. Chen, H. Yang, N.P. Pavletich, Mechanism of homologous recombination from the RecA–ssDNA/dsDNA structures, Nature 453 (2008) 489–494.

[32] A.B. Conway, T.W. Lynch, Y. Zhang, G.S. Fortin, C.W. Fung, L.S. Symington, P.A. Rice, Crystal structure of a Rad51 filament, Nat. Struct. Mol. Biol. 11 (2004) 791–796.

[33] X. Qian, Y. He, Y. Wu, Y. Luo, Asp302 determines potassium dependence of a RadA recombinase from *Methanococcus voltae*, J. Mol. Biol. 360 (2006) 537–547.

[34] D. Branzei, M. Foiani, The Rad53 signal transduction pathway: replication fork stabilization, DNA repair, and adaptation, Exp. Cell Res. 312 (2006) 2654–2659.

[35] D. Branzei, M. Foiani, The checkpoint response to replication stress, DNA Repair (Amst.) 8 (2009) 1038–1046.

[36] G. Liberi, I. Chiolo, A. Pellicioli, M. Lopes, P. Plevani, M. Muzi-Falconi, M. Foiani, Srs2 DNA helicase is involved in checkpoint response and its regulation requires a functional Mec1-dependent pathway and Cdk1 activity, EMBO J. 19 (2000) 5027–5038.

[37] S.L. Ooi, D.D. Shoemaker, J.D. Boeke, DNA helicase gene interaction network defined using synthetic lethality analyzed by microarray, Nat. Genet. 35 (2003) 277–286.

[38] X. Pan, P. Ye, D.S. Yuan, X. Wang, J.S. Bader, J.D. Boeke, A DNA integrity network in the yeast *Saccharomyces cerevisiae*, Cell 124 (2006) 1069–1081.

[39] K.H. Schmidt, R.D. Kolodner, Requirement of Rrm3 helicase for repair of spontaneous DNA lesions in cells lacking Srs2 or Sgs1 helicase, Mol. Cell. Biol. 24 (2004) 3213–3226.

[40] K.H. Schmidt, R.D. Kolodner, Suppression of spontaneous genome rearrangements in yeast DNA helicase mutants, Proc. Natl. Acad. Sci. U.S.A. 103 (2006) 18196–18201.

[41] P. Ye, B.D. Peyser, X. Pan, J.D. Boeke, F.A. Spencer, J.S. Bader, Gene function prediction from congruent synthetic lethal interactions in yeast, Mol. Syst. Biol. 1 (2005) 2005 0026.

[42] A. Azvolinsky, S. Dunaway, J.Z. Torres, J.B. Bessler, V.A. Zakian, The *S. cerevisiae* Rrm3p DNA helicase moves with the replication fork and affects replication of all yeast chromosomes, Genes Dev. 20 (2006) 3104–3116.

[43] A.S. Ivessa, J.Q. Zhou, V.P. Schulz, E.K. Monson, V.A. Zakian, *Saccharomyces* Rrm3p, a 5′ to 3′ DNA helicase that promotes replication fork progression through telomeric and subtelomeric DNA, Genes Dev. 16 (2002) 1383–1396.

[44] J.Z. Torres, S.L. Schnakenberg, V.A. Zakian, *Saccharomyces cerevisiae* Rrm3p DNA helicase promotes genome integrity by preventing replication fork stalling: viability of rrm3 cells requires the intra-S-phase checkpoint and fork restart activities, Mol. Cell. Biol. 24 (2004) 3198–3212.

[45] D. Branzei, F. Vanoli, M. Foiani, SUMOylation regulates Rad18-mediated template switch, Nature 456 (2008) 915–920.

[46] K.A. Schurer, C. Rudolph, H.D. Ulrich, W. Kramer, Yeast MPH1 gene functions in an error-free DNA damage bypass pathway that requires genes from homologous recombination, but not from postreplicative repair, Genetics 166 (2004) 1673–1686.

[47] A. Aguilera, H.L. Klein, Genetic control of intrachromosomal recombination in *Saccharomyces cerevisiae*. I. Isolation and genetic characterization of hyper-recombination mutations, Genetics 119 (1988) 779–790.

[48] C.W. Lawrence, R.B. Christensen, Metabolic suppressors of trimethoprim and ultraviolet light sensitivities of *Saccharomyces cerevisiae* rad6 mutants, J. Bacteriol. 139 (1979) 866–876.

[49] R.H. Schiestl, J. Zhu, T.D. Petes, Effect of mutations in genes affecting homologous recombination on restriction enzyme-mediated and illegitimate recombination in *Saccharomyces cerevisiae*, Mol. Cell. Biol. 14 (1994) 4493–4500.

[50] E. Papouli, S. Chen, A.A. Davies, D. Huttner, L. Krejci, P. Sung, H.D. Ulrich, Crosstalk between SUMO and ubiquitin on PCNA is mediated by recruitment of the helicase Srs2p, Mol. Cell 19 (2005) 123–133.

[51] B. Pfander, G.L. Moldovan, M. Sacher, C. Hoege, S. Jentsch, SUMO-modified PCNA recruits Srs2 to prevent recombination during S phase, Nature 436 (2005) 428–433.

[52] P. Stelter, H.D. Ulrich, Control of spontaneous and damage-induced mutagenesis by SUMO and ubiquitin conjugation, Nature 425 (2003) 188–191.

[53] G.T. Milne, T. Ho, D.T. Weaver, Modulation of *Saccharomyces cerevisiae* DNA double-strand break repair by SRS2 and RAD51, Genetics 139 (1995) 1189–1199.

[54] L. Barbour, W. Xiao, Regulation of alternative replication bypass pathways at stalled replication forks and its effects on genome stability: a yeast model, Mutat. Res. 532 (2003) 137–155.

[55] J.M. Sogo, M. Lopes, M. Foiani, Fork reversal and ssDNA accumulation at stalled replication forks owing to checkpoint defects, Science 297 (2002) 599–602.

[56] R.H. Schiestl, S. Prakash, L. Prakash, The SRS2 suppressor of rad6 mutations of *Saccharomyces cerevisiae* acts by channeling DNA lesions into the RAD52 DNA repair pathway, Genetics 124 (1990) 817–831.

[57] S. Broomfield, W. Xiao, Suppression of genetic defects within the RAD6 pathway by srs2 is specific for error-free post-replication repair but not for damage-induced mutagenesis, Nucleic Acids Res. 30 (2002) 732–739.

[58] M. Smirnova, H.L. Klein, Role of the error-free damage bypass postreplication repair pathway in the maintenance of genomic stability, Mutat. Res. 532 (2003) 117–135.

[59] H.D. Ulrich, The srs2 suppressor of UV sensitivity acts specifically on the RAD5- and MMS2-dependent branch of the RAD6 pathway, Nucleic Acids Res. 29 (2001) 3487–3494.

[60] R.C. Burgess, M. Lisby, V. Altmannova, L. Krejci, P. Sung, R. Rothstein, Localization of recombination proteins and Srs2 reveals anti-recombinase function *in vivo*, J. Cell Biol. 185 (2009) 969–981.

[61] L. Krejci, J. Damborsky, B. Thomsen, M. Duno, C. Bendixen, Molecular dissection of interactions between Rad51 and members of the recombination-repair group, Mol. Cell. Biol. 21 (2001) 966–976.

[62] C. Lucca, F. Vanoli, C. Cotta-Ramusino, A. Pellicioli, G. Liberi, J. Haber, M. Foiani, Checkpoint-mediated control of replisome–fork association and signalling in response to replication pausing, Oncogene 23 (2004) 1206–1213.

[63] L. Zou, D. Liu, S.J. Elledge, Replication protein A-mediated recruitment and activation of Rad17 complexes, Proc. Natl. Acad. Sci. U.S.A. 100 (2003) 13827–13832.

[64] A.A. Davies, D. Huttner, Y. Daigaku, S. Chen, H.D. Ulrich, Activation of ubiquitin-dependent DNA damage bypass is mediated by replication protein A, Mol. Cell 29 (2008) 625–636.

[65] J.H. New, T. Sugiyama, E. Zaitseva, S.C. Kowalczykowski, Rad52 protein stimulates DNA strand exchange by Rad51 and replication protein A, Nature 391 (1998) 407–410.

[66] A. Shinohara, T. Ogawa, Stimulation by Rad52 of yeast Rad51-mediated recombination, Nature 391 (1998) 404–407.

[67] P. Sung, Function of yeast Rad52 protein as a mediator between replication protein A and the Rad51 recombinase, J. Biol. Chem. 272 (1997) 28194–28197.

[68] A. Antunez de Mayolo, M. Lisby, N. Erdeniz, T. Thybo, U.H. Mortensen, R. Rothstein, Multiple start codons and phosphorylation result in discrete Rad52 protein species, Nucleic Acids Res. 34 (2006) 2587–2597.

[69] M. Sacher, B. Pfander, C. Hoege, S. Jentsch, Control of Rad52 recombination activity by double-strand break-induced SUMO modification, Nat. Cell Biol. 8 (2006) 1284–1290.

[70] Y. Aylon, B. Liefshitz, G. Bitan-Banin, M. Kupiec, Molecular dissection of mitotic recombination in the yeast *Saccharomyces cerevisiae*, Mol. Cell. Biol. 23 (2003) 1403–1417.

[71] G. Ira, A. Malkova, G. Liberi, M. Foiani, J.E. Haber, Srs2 and Sgs1-Top3 suppress crossovers during double-strand break repair in yeast, Cell 115 (2003) 401–411.

[72] D. Branzei, J. Sollier, G. Liberi, X. Zhao, D. Maeda, M. Seki, T. Enomoto, K. Ohta, M. Foiani, Ubc9- and mms21-mediated sumoylation counteracts recombinogenic events at damaged replication forks, Cell 127 (2006) 509–522.

[73] G. Liberi, G. Maffioletti, C. Lucca, I. Chiolo, A. Baryshnikova, C. Cotta-Ramusino, M. Lopes, A. Pellicioli, J.E. Haber, M. Foiani, Rad51-dependent DNA structures accumulate at damaged replication forks in sgs1 mutants defective in the yeast ortholog of BLM RecQ helicase, Genes Dev. 19 (2005) 339–350.

[74] N. Sugawara, G. Ira, J.E. Haber, DNA length dependence of the single-strand annealing pathway and the role of *Saccharomyces cerevisiae* RAD59 in double-strand break repair, Mol. Cell. Biol. 20 (2000) 5300–5309.

[75] S.D. Carter, D. Vigasova, J. Chen, M. Chovanec, S.U. Astrom, Nej1 recruits the Srs2 helicase to DNA double-strand breaks and supports repair by a single-strand annealing-like mechanism, Proc. Natl. Acad. Sci. U.S.A. 106 (2009) 12037–12042.

[76] T.E. Wilson, A genomics-based screen for yeast mutants with an altered recombination/end-joining repair ratio, Genetics 162 (2002) 677–688.

[77] J.F. Ruiz, B. Gomez-Gonzalez, A. Aguilera, Chromosomal translocations caused by either pol32-dependent or -independent triparental break-induced replication, Mol. Cell. Biol. (2009).

[78] S. Bhattacharyya, R.S. Lahue, *Saccharomyces cerevisiae* Srs2 DNA helicase selectively blocks expansions of trinucleotide repeats, Mol. Cell. Biol. 24 (2004) 7324–7330.

[79] S. Bhattacharyya, R.S. Lahue, Srs2 helicase of *Saccharomyces cerevisiae* selectively unwinds triplet repeat DNA, J. Biol. Chem. 280 (2005) 33311–33317.

[80] A. Dhar, R.S. Lahue, Rapid unwinding of triplet repeat hairpins by Srs2 helicase of *Saccharomyces cerevisiae*, Nucleic Acids Res. 36 (2008) 3366–3373.

[81] A. Kerrest, R.P. Anand, R. Sundararajan, R. Bermejo, G. Liberi, B. Dujon, C.H. Freudenreich, G.F. Richard, SRS2 and SGS1 prevent chromosomal breaks and stabilize triplet repeats by restraining recombination, Nat. Struct. Mol. Biol. 16 (2009) 159–167.

[82] A.A. Shishkin, I. Voineagu, R. Matera, N. Cherng, B.T. Chernet, M.M. Krasilnikova, V. Narayanan, K.S. Lobachev, S.M. Mirkin, Large-scale expansions of Friedreich's ataxia GAA repeats in yeast, Mol. Cell 35 (2009) 82–92.

[83] M. Heude, R. Chanet, F. Fabre, Regulation of the *Saccharomyces cerevisiae* Srs2 helicase during the mitotic cell cycle, meiosis and after irradiation, Mol. Gen. Genet. 248 (1995) 59–68.

[84] J.T. Hannich, A. Lewis, M.B. Kroetz, S.J. Li, H. Heide, A. Emili, M. Hochstrasser, Defining the SUMO-modified proteome by multiple approaches in *Saccharomyces cerevisiae*, J. Biol. Chem. 280 (2005) 4102–4110.

[85] C. Hoege, B. Pfander, G.L. Moldovan, G. Pyrowolakis, S. Jentsch, RAD6-dependent DNA repair is linked to modification of PCNA by ubiquitin and SUMO, Nature 419 (2002) 135–141.

[86] S. Korolev, J. Hsieh, G.H. Gauss, T.M. Lohman, G. Waksman, Major domain swiveling revealed by the crystal structures of complexes of *E. coli* Rep helicase bound to single-stranded DNA and ADP, Cell 90 (1997) 635–647.

[87] J.Y. Lee, W. Yang, UvrD helicase unwinds DNA one base pair at a time by a two-part power stroke, Cell 127 (2006) 1349–1360.

[88] S.S. Velankar, P. Soultanas, M.S. Dillingham, H.S. Subramanya, D.B. Wigley, Crystal structures of complexes of PcrA DNA helicase with a DNA substrate indicate an inchworm mechanism, Cell 97 (1999) 75–84.

[89] M.J. Flores, V. Bidnenko, B. Michel, The DNA repair helicase UvrD is essential for replication fork reversal in replication mutants, EMBO Rep. 5 (2004) 983–988.

[90] X. Veaute, S. Delmas, M. Selva, J. Jeusset, E. Le Cam, I. Matic, F. Fabre, M.A. Petit, UvrD helicase, unlike rep helicase, dismantles RecA nucleoprotein filaments in *Escherichia coli*, EMBO J. 24 (2005) 180–189.

[91] M. Maftahi, J.C. Hope, L. Delgado-Cruzata, C.S. Han, G.A. Freyer, The severe slow growth of Deltasrs2 Deltarqh1 in *Schizosaccharomyces pombe* is suppressed by loss of recombination and checkpoint genes, Nucleic Acids Res. 30 (2002) 4781–4792.

[92] S.W. Wang, A. Goodwin, I.D. Hickson, C.J. Norbury, Involvement of *Schizosaccharomyces pombe* Srs2 in cellular responses to DNA damage, Nucleic Acids Res. 29 (2001) 2963–2972.

[93] C.L. Doe, M.C. Whitby, The involvement of Srs2 in post-replication repair and homologous recombination in fission yeast, Nucleic Acids Res. 32 (2004) 1480–1491.

[94] M. Kohzaki, A. Hatanaka, E. Sonoda, M. Yamazoe, K. Kikuchi, N. Vu Trung, D. Szuts, J.E. Sale, H. Shinagawa, M. Watanabe, S. Takeda, Cooperative roles of vertebrate Fbh1 and Blm DNA helicases in avoidance of crossovers during recombination initiated by replication fork collapse, Mol. Cell. Biol. 27 (2007) 2812–2820.

[95] A. Lorenz, F. Osman, V. Folkyte, S. Sofueva, M.C. Whitby, Fbh1 limits Rad51-dependent recombination at blocked replication forks, Mol. Cell. Biol. 29 (2009) 4742–4756.

[96] T. Morishita, F. Furukawa, C. Sakaguchi, T. Toda, A.M. Carr, H. Iwasaki, H. Shinagawa, Role of the *Schizosaccharomyces pombe* F-box DNA helicase in processing recombination intermediates, Mol. Cell. Biol. 25 (2005) 8074–8083.

[97] F. Osman, J. Dixon, A.R. Barr, M.C. Whitby, The F-box DNA helicase Fbh1 prevents Rhp51-dependent recombination without mediator proteins, Mol. Cell. Biol. 25 (2005) 8084–8096.

[98] I. Chiolo, M. Saponaro, A. Baryshnikova, J.H. Kim, Y.S. Seo, G. Liberi, The human F-box DNA helicase FBH1 faces *Saccharomyces cerevisiae* Srs2 and postreplication repair pathway roles, Mol. Cell. Biol. 27 (2007) 7439–7450.

[99] G.F. Richard, A. Kerrest, I. Lafontaine, B. Dujon, Comparative genomics of hemiascomycete yeasts: genes involved in DNA replication, repair, and recombination, Mol. Biol. Evol. 22 (2005) 1011–1023.

[100] Y. Hu, S. Raynard, M.G. Sehorn, X. Lu, W. Bussen, L. Zheng, J.M. Stark, E.L. Barnes, P. Chi, P. Janscak, M. Jasin, H. Vogel, P. Sung, G. Luo, RECQL5/Recql5 helicase regulates homologous recombination and suppresses tumor formation via disruption of Rad51 presynaptic filaments, Genes Dev. 21 (2007) 3073–3084.

[101] D.V. Bugreev, X. Yu, E.H. Egelman, A.V. Mazin, Novel pro- and anti-recombination activities of the Bloom's syndrome helicase, Genes Dev. 21 (2007) 3085–3094.

[103] M.E. Robu, R.B. Inman, M.M. Cox, RecA protein promotes the regression of stalled replication forks *in vitro*, Proc. Natl. Acad. Sci. U.S.A. 98 (2001) 8211–8218.

[104] M. Seigneur, S.D. Ehrlich, B. Michel, RuvABC-dependent double-strand breaks in dnaBts mutants require recA, Mol. Microbiol. 38 (2000) 565–574.

Attachment 9

Altmannova V, Eckert-Boulet N, Arneric M, Kolesar P, Chaloupkova R, Damborsky J, Sung P, Zhao X, Lisby M and Krejci L

Rad52 SUMOylation affects the efficiency of the DNA repair.

Nucleic Acids Res. 38 (14): 4708-21. 2010

Rad52 SUMOylation affects the efficiency of the DNA repair

Veronika Altmannova[1,2], Nadine Eckert-Boulet[3], Milica Arneric[4], Peter Kolesar[1,2], Radka Chaloupkova[2,5], Jiri Damborsky[2,5], Patrick Sung[6], Xiaolan Zhao[4], Michael Lisby[3] and Lumir Krejci[1,2,*]

[1]Department of Biology, Masaryk University, Kamenice 5/A7, 625 00 Brno, [2]National Centre for Biomolecular Research, Masaryk University, Kamenice 5/A4, 625 00 Brno, Czech Republic, [3]Department of Biology, University of Copenhagen, DK-2200 Copenhagen N, Denmark, [4]Molecular Biology Program, Memorial Sloan-Kettering Cancer Center, New York, NY 10065, USA, [5]Loschmidt Laboratories, Institute of Experimental Biology, Masaryk University, Kamenice 5/A4, 625 00 Brno, Czech Republic and [6]Department of Molecular Biophysics and Biochemistry, Yale University School of Medicine, New Haven, CT 06520, USA

ABSTRACT

Homologous recombination (HR) plays a vital role in DNA metabolic processes including meiosis, DNA repair, DNA replication and rDNA homeostasis. HR defects can lead to pathological outcomes, including genetic diseases and cancer. Recent studies suggest that the post-translational modification by the small ubiquitin-like modifier (SUMO) protein plays an important role in mitotic and meiotic recombination. However, the precise role of SUMOylation during recombination is still unclear. Here, we characterize the effect of SUMOylation on the biochemical properties of the *Saccharomyces cerevisiae* recombination mediator protein Rad52. Interestingly, Rad52 SUMOylation is enhanced by single-stranded DNA, and we show that SUMOylation of Rad52 also inhibits its DNA binding and annealing activities. The biochemical effects of SUMO modification *in vitro* are accompanied by a shorter duration of spontaneous Rad52 foci *in vivo* and a shift in spontaneous mitotic recombination from single-strand annealing to gene conversion events in the SUMO-deficient Rad52 mutants. Taken together, our results highlight the importance of Rad52 SUMOylation as part of a 'quality control' mechanism regulating the efficiency of recombination and DNA repair.

INTRODUCTION

DNA double-strand breaks (DSBs) are one of the most toxic kinds of chromosome damage that are implicated in cancer and many other diseases. A single unrepaired break can lead to aneuploidy, genetic aberrations or cell death. DSBs are caused by a vast number of endogenous and exogenous agents including genotoxic chemicals or ionizing radiation, as well as through replication of a damaged DNA template or replication fork collapse. In the yeast *Saccharomyces cerevisiae*, homologous recombination (HR) is the major pathway for repair of DSBs (1).

Genes of the *RAD52* epistasis group mediate HR. The members of this gene group were identified by mutants' sensitivity to ionizing radiation or their deficiency in DSB repair, and they include *RAD50, RAD51, RAD52, RAD54, RAD55, RAD57, RAD59, RDH54/TID1, MRE11* and *XRS2*. These genes are also needed for HR and chromosome segregation in meiosis I and are in general highly conserved among eukaryotes (2,3).

HR involves DNA homology search and DNA strand invasion to form a joint between the recombining DNA molecules. These reaction steps are mediated by the Rad51 recombinase, an orthologue of the *Escherichia coli* RecA recombinase (4). In the presence of ATP, Rad51 binds single-stranded DNA (ssDNA) and forms a right-handed filament called the presynaptic filament. Since the assembly of the presynaptic filament proceeds rather slowly, it is prone to interference by other competing factors such as replication protein A (RPA)

---

*To whom correspondence should be addressed. Tel: +420 549493767; Fax: +420 549492556; Email: lkrejci@chemi.muni.cz

(5,6). RPA is a heterotrimeric ssDNA-binding protein with a complex role in HR. *In vitro*, it was shown that RPA stimulates recombination by eliminating secondary structures in ssDNA and stabilizing the displaced strand of the D-loop. However, due to its very high affinity for ssDNA, it can prevent Rad51 from binding ssDNA, thus leading to the inhibition of presynaptic filament formation (7). This inhibitory effect can be overcome by the recombination mediator activity of Rad52 (1).

Rad52 multimerizes and forms a ring structure (8). The assembly of a ring structure requires sequences in the evolutionary conserved N-terminal domain of Rad52, which also possesses a DNA binding activity with a preference for ssDNA (9). Yeast Rad52 can interact with Rad51 as well as with RPA to help ensure the efficient displacement of RPA from ssDNA by Rad51 (10–12). The interaction with RPA is mediated by a domain within the middle portion of Rad52, while the carboxyl terminus harbours the Rad51 interaction domain (13,14). Moreover, the C-terminal domain also possesses a DNA binding activity and alone has recombination mediator activity (5). A robust DNA annealing activity has been described for Rad52 as well (9).

Many proteins participating in HR can be post-translationally modified by the small ubiquitin-like modifier (SUMO) protein, and this modification can potentially influence the biochemical activity and function of the target protein. Recently, Sacher *et al.* (15) identified the residues that serve as SUMO acceptor sites in Rad52. In addition to the SUMO-conjugating enzyme Ubc9, Rad52 modification is stimulated by the SUMO ligase Siz2 (15). SUMO was shown to protect Rad52 from proteasomal degradation and to facilitate the exclusion of Rad52 recombination foci from the nucleolus to maintain a low level of recombinational repair at the ribosomal gene locus (16).

Here, we show that the SUMOylation of Rad52 is significantly stimulated in the presence of ssDNA *in vitro*. We find that enhanced SUMOylation is mediated via the C-terminal DNA binding domain of Rad52 and requires lysine K253. Moreover, we demonstrate that SUMOylated Rad52 exhibits lower affinity towards ssDNA and dsDNA, and also has reduced single-strand annealing activity. These data provide mechanistic information regarding the role of SUMOylation in the regulation of the biochemical activities of Rad52.

MATERIALS AND METHODS

Genetic methods, yeast strains and plasmids

Yeast strains were manipulated using standard genetic techniques, and media were prepared as previously described (17). All strains used in this study are *RAD5* derivatives of W303 (Supplementary Table S1) (18,19). To generate the $(His)_6$-*RAD52(N+M)::pET11d* plasmid, the $(His)_6$-*RAD52::pET11d* plasmid was digested with *BamHI*. The resulting DNA product was isolated from agarose gel, ligated and sequenced. The plasmids expressing the *rad52 (K43,44R)*, *rad52 (K253R)* and *rad52 (K43,44,253R)* mutants were constructed by site-directed mutagenesis using specific primers (Supplementary Table S2). The amino acid numbering corresponds to translation from first ATG of GenBank accession number CAA86623 for Rad52 protein.

DNA substrates

Oligonucleotides were purchased from VBC Biotech. The sequences of the oligonucleotides are shown in Supplementary Table S2. Oligo-1 and Oligo-3 were modified with fluorescein at the 5′ end. The DNA substrates were prepared by mixing an equimolar amount of the constituent oligonucleotides in the hybridization buffer H (50 mM Tris–HCl, pH 7.5, 100 mM NaCl, 10 mM $MgCl_2$), heated at 90°C for 3 min, and cooled slowly to room temperature to allow DNA annealing. The annealed DNA substrates were purified by fractionation in a 1-ml Mono Q column (GE Healthcare Life Sciences) with a 20-ml gradient of 50–1000 mM NaCl in 10 mM Tris–HCl, pH 7.5. Peak fractions were filtered, dialysed into 50 mM Tris–HCl, pH 7.5, containing 5 mM $MgCl_2$ and concentrated in a Vivaspin concentrator with a 5 kDa cutoff. The concentration of the DNA substrates was determined by absorbance measurement at 260 nm.

Recombinant protein expression and purification

The various Rad52 species were expressed and purified with modifications as described (5). Rad51 and RPA proteins were purified as described (4,20).

Purification of Aos1/Uba2 complex (E1 protein). The *Escherichia coli* strain BL21(DE3) transformed with plasmid for expression of E1 (Aos1/Uba2 complex) protein (a kind gift from Dr B. Schulman) containing GST-tagged Aos1 was induced with 0.5 mM IPTG for 3 h at 37°C. The cells were pelleted and stored at −80°C. The cell pellet (7 g) was resuspended in 25 ml of cell breakage buffer (CBB) (50 mM Tris–HCl, pH 7.5, 10% sucrose, 2 mM EDTA) containing 150 mM KCl, 0.01% NP40, 1 mM β-mercaptoethanol, sonicated and centrifuged (100 000*g*, 90 min). Clarified supernatant was loaded onto 7-ml SP-sepharose column with its outlet connected to a 7-ml Q-sepharose column (Amersham Biosciences). Both columns were pre-equilibrated with buffer K (20 mM K_2HPO_4, 10% glycerol, 0.5 mM EDTA) containing 100 mM KCl. The Q-sepharose column was subsequently eluted with a 70-ml gradient of 100–800 mM KCl in buffer K. Peak E1 protein fractions eluting around 330–470 mM KCl were pooled and mixed with 800 µl of GTH-sepharose (Amersham Biosciences) washed in buffer K containing 100 mM KCl for 1 h at 4°C. The GTH-sepharose with bound proteins was washed with 8 ml of 100 mM KCl in buffer K and eluted in steps with 800 µl of 10, 50, 100 or 200 mM glutathione (GTH) in buffer K containing 100 mM KCl. The peak fractions eluting within the range of 10–100 mM GTH were loaded onto a 0.5-ml Mono Q column followed by elution using 5-ml gradient of 100–700 mM KCl in buffer K. The main fractions of E1 protein eluting from the Mono Q column at ∼560 mM KCl were concentrated in

a Centricon-30 to 5 µg/µl and stored in small aliquots at −80°C.

Purification of Ubc9 (E2 protein). The plasmid (a kind gift from Dr Erica Johnson) expressing E2 (Ubc9) protein containing (His)6-affinity tag was introduced into *E. coli* strain BL21(DE3). Overnight culture grown at 37°C in 2×TY medium was diluted 100-fold into fresh 2×TY medium and incubated at 37°C. The overexpression of E2 was induced by addition of 0.1 mM IPTG followed by an incubation at 25°C overnight. To prepare cell extract, 13g of cell pellet was thawed in 20 ml of CBB containing 150 mM KCl, 0.01% NP40, 1 mM β-mercaptoethanol and protease inhibitor cocktail (pepstatin, leupeptin, aprotinin, chymostatin, benzamidine and phenylmethylsulfonyl fluoride). The cells were disrupted by sonication and the crude extract was clarified by centrifugation (100 000g, 4°C, 90 min). The supernatant was passed through a 7-ml column of Q-sepharose and the flow-through fraction was applied directly to a 7-ml SP-sepharose column that was eluted with 70-ml gradient of 100–750 mM KCl in buffer K. E2 protein eluted from SP-column at 290–370 mM KCl. The peak fractions were mixed with 750 µl of Ni–NTA agarose (Qiagen) for 75 min at 4°C. The beads were washed with 7.5 ml of buffer K containing 100 mM KCl followed by a 7.5 ml wash with buffer K containing 100 mM KCl and 10 mM imidazole. E2 protein was then eluted with buffer K containing 100 mM KCl and 50, 150 or 300 mM imidazole, respectively. The fractions eluted from Ni–NTA agarose column from 50 to 150 mM imidazole were pooled, applied onto a 1-ml Mono S column, and eluted using a 10-ml gradient of 100–750 mM KCl in buffer K. E2 protein eluted at 360–510 mM KCl was concentrated to 20 µg/µl in a Centricon-30 and stored in small aliquots at −80°C.

Purification of SUMO protein. The plasmid containing the SUMO (Smt3) gene containing both (His)6-affinity and FLAG tags (a kind gift from Dr Erica Johnson) was introduced into *E. coli* strain BL21(DE3). Overnight culture grown in 2×TY medium at 37°C was diluted 100-fold into fresh medium and incubated at 37°C until OD600 reached 0.8. At that time, IPTG was added to 0.5 mM, and the culture was incubated at 37°C for 3 h. The cells were harvested by centrifugation and stored at −80°C. Extract from 5 g of cell paste was prepared by sonication in 25 ml of CBB containing 150 mM KCl, 0.01% NP40, 1 mM β-mercaptoethanol and protease inhibitor cocktail. The lysate was clarified by ultracentrifugation and the resulting supernatant was passed in tandem over SP- and Q-sepharose columns (7 ml each). The Q-column was then eluted with a 70-ml gradient of 100–750 mM KCl in buffer K. The SUMO-containing fractions (370–470 mM KCl) were pooled and mixed with 600 µl Ni–NTA agarose. The bead-bound proteins were washed with 6 ml of buffer K containing 100 mM KCl, followed by 6-ml of buffer K containing 100 mM KCl and 10 mM imidazole. The bound proteins were eluted with buffer K containing 50, 150, or 300 mM imidazole and 100 mM KCl. The fractions with SUMO protein

eluting from 50 to 300 mM imidazole were pooled and loaded onto a 0.5-ml Mono Q column and then eluted with a 5-ml gradient of 100–900 mM KCl in buffer K. The peak fractions (400–700 mM KCl) were pooled, concentrated in a Centricon-30 to 10 µg/µl and stored at −80°C.

In vitro SUMOylation assay

The assay was performed in a 20 µl reaction volume containing 5.6 µM of purified SUMO protein (Smt3), 400 nM E1 protein (Aos1/Uba2), 2.8 µM E2 protein (Ubc9), 2.5 mM ATP, buffer S (50 mM HEPES, 100 mM NaCl, 10 mM MgCl$_2$, 0.1 mM DTT) and 2.7–4.1 µM of various Rad52 proteins. Reactions were incubated at 30°C for 3 h, stopped by addition of 30 µl of SDS Laemmli buffer (62.5 mM Tris–HCl, 2% SDS, 5% β-mercaptoethanol, 10% glycerol, 0.002% bromphenol blue) and analysed by SDS–PAGE and western blotting. The quantification of Rad52 SUMOylation was done using Quantity One software (Bio-Rad) and is presented as a ratio of mono-SUMOylated versus non-modified Rad52.

Circular dichroism spectroscopy

Circular dichroism (CD) spectra were recorded at 10°C using a Jasco J-810 spectrometer (Jasco, Tokyo, Japan) coupled with Peltier temperature controller. Data were collected from 195 to 340 nm, at 100 nm/min, 1 s response time and 2 nm bandwidth using a 0.1 cm quartz cuvette containing studied protein/DNA in 20 mM phosphate buffer and 50 mM KCl (pH 7.5). CD difference spectrum was calculated by subtracting spectrum of DNA from that of protein–DNA complex. Each spectrum represents an average of 10 individual scans and is corrected for absorbance caused by the buffer. CD data were expressed in millidegrees (instrument units of CD).

Electrophoretic mobility shift assay

Indicated amounts of various forms of Rad52 protein were incubated with fluorescently-labelled DNA substrates (0.44 µM nucleotides) at 37°C in 10 µl of buffer B (50 mM Tris–HCl, pH 7.8, 5 mM MgCl$_2$ and 1 mM DTT) for 10 min. After the addition of gel loading buffer (60% glycerol, 10 mM Tris–HCl, pH 7.4 and 60 mM EDTA), the reaction mixtures were resolved in 7.5% native polyacrylamide gels in TBE buffer (40 mM Tris–HCl, 20 mM boric acid, 2 mM EDTA, pH 7.5) at 4°C, and the DNA species were quantified using Quantity One software (Bio-Rad).

Single-strand annealing assay

The assay was essentially done as described previously (14). Oligo-2 and fluorescently labelled Oligo-1 (0.26 µM nucleotides) were incubated in separate tubes at 37°C for 3 min in the absence or presence of RPA (20 nM) in 20 µl of buffer D (40 mM Tris–HCl, pH 7.5, 50 mM KCl, 1 mM DTT and 100 µg/ml bovine serum albumin (BSA)). Varying amounts of Rad52 or Smt3-Rad52 were added to the tube containing Oligo-2 and then mixed with

Oligo-1. The completed reactions were incubated at 37°C for 8 min. At the indicated times, 9 μl of the annealing reactions was removed and treated with 0.5% SDS, and 500 μg/ml proteinase K at 37°C for 10 min in a total volume of 10 μl. The individual samples were resolved in 12% native polyacrylamide gels run in TBE buffer. DNA annealing was quantified as the portion of the fluorescently-labelled Oligo-1 that had been converted into the double-stranded form.

Binding of Rad52 to Rad51 and RPA immobilized on Affi-gels

Affi-gel 15 beads containing either Rad51 (Affi-Rad51; 300 ng/μl) or RPA (Affi-RPA; 350 ng/μl) were prepared as described previously (21). Purified Rad52 or Smt3-Rad52 were mixed with 30 μl of Affi-Rad51 or Affi-RPA in 25 μl of buffer T (20 mM Tris–HCl, pH 7.5, 150 mM KCl, 1 mM DTT, 0.5 mM EDTA and 0.01% NP40) for 30 min at 4°C. The beads were washed twice with 100 μl of buffer T before being treated with 30 μl of SDS Laemmli buffer to elute bound proteins. The supernatant that contained unbound Rad52 or Smt3-Rad52 protein, and the SDS eluate (10 μl each) were analysed by SDS–PAGE in 10% gel.

Gel filtration

A Sephacryl S400 column (25 ml total) was used to monitor the oligomeric status of Rad52 and SUMOylated Rad52 proteins. The proteins were filtered through the sizing column at 0.1 ml/min in buffer K containing 200 mM KCl, collecting 0.5 ml fractions. The indicated column fractions were separated by SDS–PAGE electrophoresis to determine contents of the Rad52, or SUMOylated Rad52 proteins, respectively.

Determination of mitotic recombination rates

Interchromosomal and direct-repeat recombination between non-functional *leu2* heteroalleles was measured as described (22), except that the single colonies were inoculated into liquid SC medium containing 100 μg/ml adenine. The plating efficiency and the number of recombinants were determined by plating an appropriate number of cells on SC and SC-Leu medium. After 3 days at 30°C, the number of colonies was counted. The Leu$^+$ colonies were replica-plated to SC-Leu-Ura in order to distinguish between gene conversion (Ura$^+$) and single-strand annealing (Ura$^-$) events in the direct-repeat assay. For each strain, 15–19 independent trials were carried out. The corresponding recombination rates and their standard deviations were calculated according to the median method (23). The rate of *ADE2* marker loss at the rDNA was determined as described (24). In brief, single colonies were grown overnight in liquid YPD medium at 30°C. Then, cultures grown to exponential phase were diluted before plating an appropriate number of cells on YPD. After 3 days at 30°C, the number of half-sectored red–white colonies was counted as a direct measure of the rDNA recombination rate.

Analysis of meiotic recombination

Sporulation was induced by replica-plating of the fresh patch of cells from solid YPD to SPO medium and followed by incubation at 30°C for 3 days. Next, cells were resuspended in H$_2$O and inspected microscopically to determine the sporulation efficiency. For each strain, 18 four-spore tetrads were dissected to determine the germination efficiency. To determine the meiotic recombination frequency and relative viability, OD$_{600}$ was measured and cells were sonicated before plating an appropriate number of cells on SC and SC-Leu medium.

Analysis of inverted-repeat substrate recombination and break-induced replication

Recombination between inverted repeats was assayed using the ade2-5′Δ::TRP1::ade2-n system (provided by L. Symington, Columbia University, New York, NY, USA). The experiments were essentially performed as described (23). A chromosome fragmentation assay was used to measure the efficiency of break-induced replication (BIR) in Rad52 SUMOylation-defective mutant. The experiments were performed as previously described (25).

Microscopy

Cells were processed for fluorescence microscopy as described previously (26). Yellow fluorescent protein (YFP) was visualized using a band-pass YFP (Cat. no. 41028) filter set from Chroma (Brattleboro, VT, USA). Images were acquired with a 10% neutral density filter in place to reduce photobleaching and phototoxicity. Fluorescence intensities were measured in arbitrary units (AU) using Volocity software (Improvision).

Results

Enhancement of Rad52 SUMOylation by ssDNA

Previous studies have shown that Rad52 protein is SUMOylated at lysines K43, K44 and K253 in response to DNA damage [Figure 1A, (15)]. To define the biochemical requirements of this reaction, we have established an *in vitro* SUMOylation assay using purified yeast Ubc9, Aos1, Uba2 and Smt3 (SUMO in yeast) proteins (Figure 1B and Supplementary Figure S3). Addition of Rad52 protein to this reaction resulted in its modification (Figure 2A). We have also confirmed that lysines K43, 44 and 253 are the major *in vitro* SUMO conjugation sites as observed *in vivo* [(15), Supplementary Table S3)]. Since Rad52 is known to bind both ssDNA and dsDNA, we decided to assess the effect of DNA on Rad52 SUMOylation. Importantly, when the SUMOylation of Rad52 was performed in the presence of ssDNA cofactor, we noticed a significant stimulation of the SUMO modification (~3-fold, Figure 2A). That Rad52 was modified by SUMO conjugation was confirmed by immunoblotting with anti–Smt3 and anti–Rad52 antibodies (Figure 2B and C). In contrast, the addition of dsDNA did not enhance the level of SUMOylated Rad52 species (Figure 2A), suggesting that only ssDNA binding confers this stimulation. Interestingly,
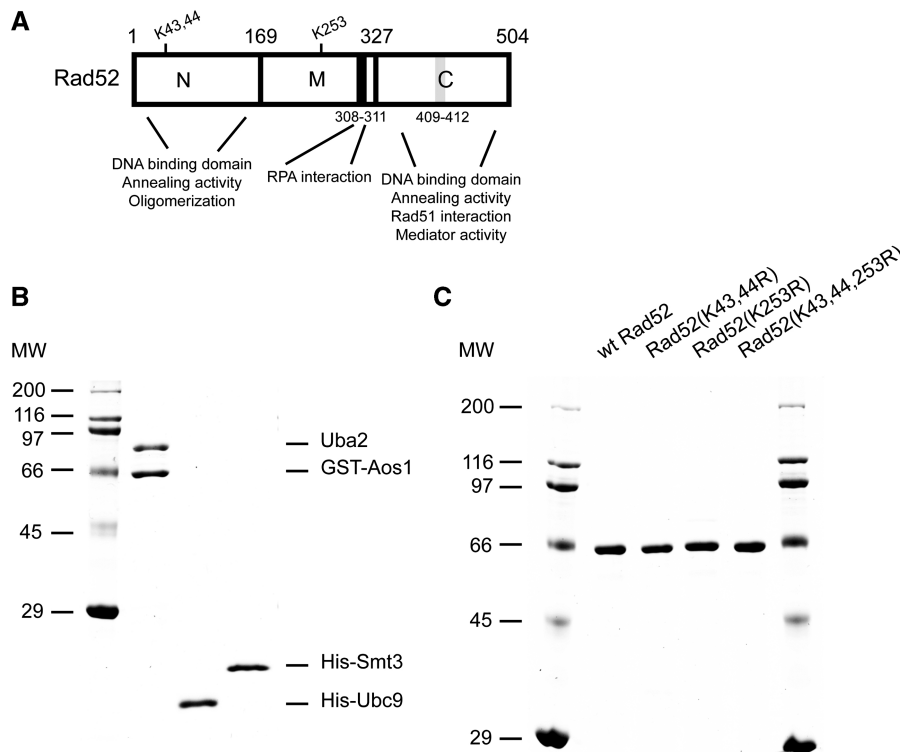
Figure 1. Purification of Rad52 species and SUMO machinery proteins. (**A**) Schematic representation of functional domain within *S. cerevisiae* Rad52 protein, including the positions of known SUMO acceptor lysines. The RPA interaction domain (black box, residues 308–311) and Rad51 interaction domain (grey box, residues 409–412) are indicated. (**B**) Purified SUMO machinery proteins: GST-tagged Aos1/Uba2 heterodimer (1 μg), (His)$_6$-tagged Ubc9 and Smt3 proteins (1 μg each) were run on a 15% SDS–PAGE and stained with Coomassie blue. (**C**) Purified (His)$_6$-tagged Rad52 species (1 μg each): Rad52, Rad52 (K43,44R), Rad52 (K253R) and Rad52 (K43,44,253R) were run on a 10% SDS–PAGE and stained with Coomassie blue.

experiments with titration of ssDNA showed that stimulation of Rad52 SUMOylation was optimal when the ratio of Rad52 to nucleotides reached approximate ratio 1:37 (Figure 2D and E). This is in good correlation with previously published data indicating that Rad52 protein binds ~36 nt of ssDNA (27). Maximum stimulation corresponded up to 25% of modified Rad52 protein. Altogether these data show that: (i) Rad52 can be SUMOylated *in vitro*, (ii) the pattern of SUMOylation is identical to that observed *in vivo* and (iii) Rad52 binding to ssDNA stimulates its SUMOylation.

Binding of ssDNA causes a conformational change in Rad52

Stimulation of Rad52 SUMOylation by ssDNA prompted us to test whether ssDNA binding could cause conformational changes in the Rad52 protein. Therefore, we measured and compared CD spectrum of Rad52 alone and difference spectrum of Rad52 in the presence of DNA (Figure 2F; red and green squares, respectively). The results provided evidence that interaction of Rad52 protein with ssDNA induced a conformational change in the protein. This conformational change takes place without any alteration in the structure of the DNA, since the DNA spectrum did not change above 240 nm. We attribute the increased magnitude of the negative bands to an increase in the α-helicity of Rad52 (28). In

summary, binding of ssDNA results in a conformational change within Rad52 equivalent to an increase in the α-helicity.

ssDNA bound by RPA but not by Rad51 can stimulate SUMOylation of Rad52

The ssDNA generated during DSB repair is often protected by interaction with other ssDNA binding proteins, namely RPA and Rad51. Therefore, we tested if RPA- or Rad51-bound ssDNA is still accessible for interaction with Rad52 and whether it enhances Rad52 SUMOylation. We pre-incubated ssDNA with increasing amounts of RPA protein and examined the effect of RPA on Rad52 SUMOylation *in vitro*. Under the experimental conditions, RPA bound efficiently to ssDNA (Supplementary Figure S4) with stoichiometry of one RPA trimer per up to 30 nt. As shown in Figure 3A and B, the level of stimulation was similar to that without RPA, suggesting that ssDNA coated with RPA can enhance Rad52 SUMOylation. Even with a 2-fold molar excess of RPA over the ssDNA (Figure 3A, lane 8), stimulation of Rad52 SUMOylation is comparable to that observed with ssDNA (Figure 3A, lane 3). Next, we pre-incubated ssDNA with increasing amounts of Rad51 protein to form presynaptic filaments. Notably, this DNA was no longer accessible for Rad52 and resulted in decreased Rad52 SUMOylation to the basal level observed in the absence of ssDNA (Figure 3C and D).
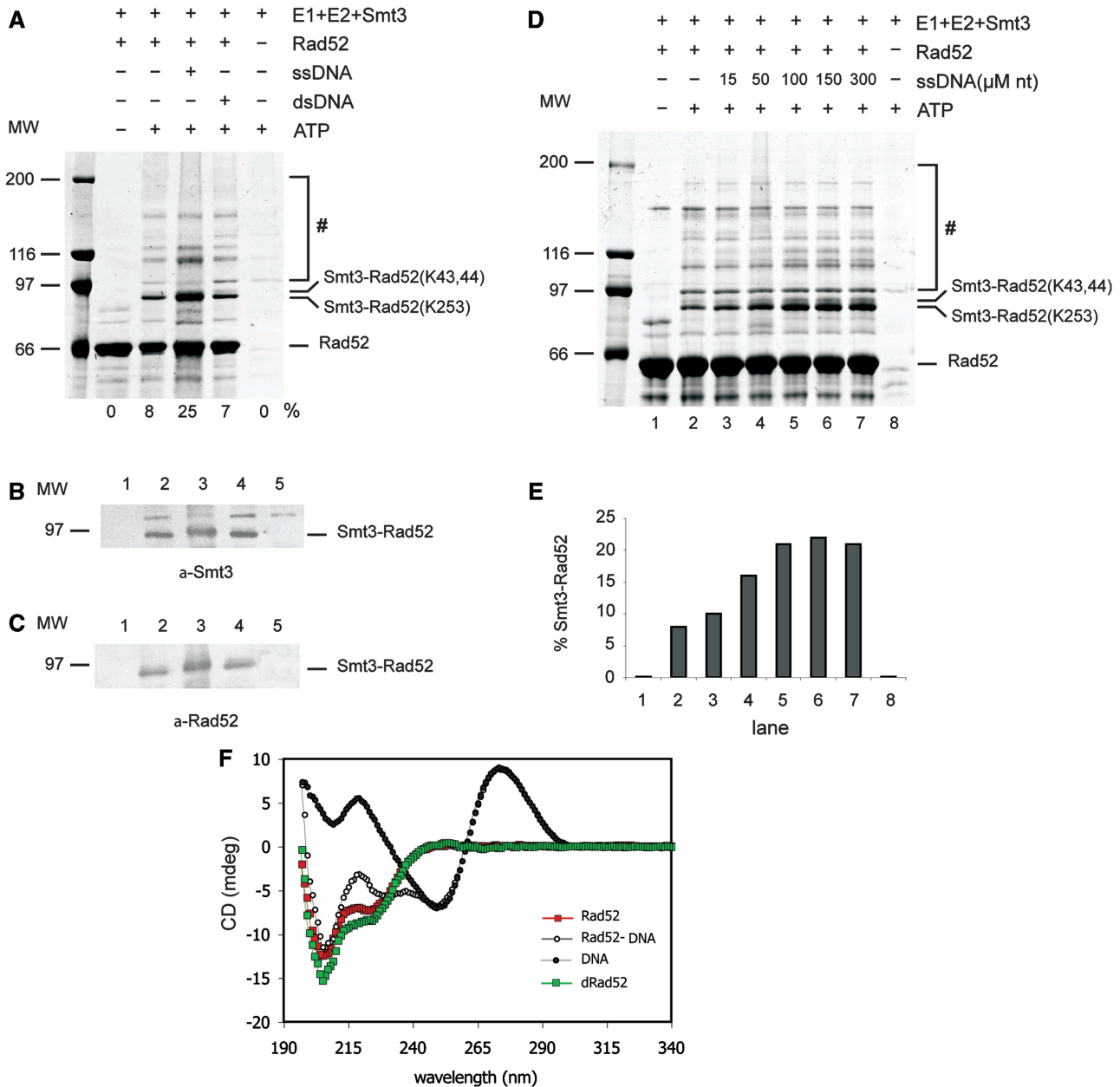
Figure 2. *In vitro* SUMOylation of Rad52 is stimulated by ssDNA. (**A**) The effect of ssDNA and dsDNA on Rad52 SUMOylation. *In vitro* SUMOylation assays were performed with recombinant Aos1/Uba2 (400 nM), Ubc9 (2.8 μM) and Smt3 (5.6 μM) in the presence or absence of ATP (2.5 mM), Rad52 (2.7 μM), 83-mer ss-DNA (100 μM nucleotides) or dsDNA as indicated. The reaction mixtures were incubated for 3 h at 30°C, stopped by adding 30 μl of SDS Laemmli buffer and analysed on 7% SDS–PAGE followed by silver staining. The hash symbol indicates high molecular poly-SUMOylated species of Rad52 and E1. The number at the bottom of the gel represents the ratio of modified and unmodified Rad52. SUMOylated Rad52 protein was confirmed by western blotting using anti-Smt3 (**B**) or anti-Rad52 (**C**) antibodies. (**D**) *In vitro* SUMOylation assay on Rad52 protein carried out without DNA (lanes 1 and 2) or with increasing amount of 83-mer ssDNA (15, 50, 100, 150, 300 μM nucleotides; lanes 3–7). The hash symbol indicates high molecular weight SUMOylated species. (**E**) Graphical representation of the gel in panel D, as a ratio of mono-SUMOylated versus non-modified Rad52. (**F**) The CD spectrum of 83-mer ssDNA (black), Rad52 (red) and the Rad52-ssDNA complex (white). The difference spectrum (green) represents values for Rad52 in the complex with DNA from which the spectrum of DNA has been subtracted. To form the complex, protein and DNA were incubated together for 10 min at 37°C prior to the analysis. The concentration of the protein was 3.87 μM and the concentration of DNA was 2.24 μM. The samples were measured at 10°C in 20 mM phosphate buffer containing 50 mM KCl, pH 7.5.

Specifically, the maximum inhibition of Rad52 SUMOylation occurred at 3 nt of ssDNA per Rad51 monomer, corresponding to the ssDNA binding site size of Rad51 and ensuring fully coated DNA (20). Further increasing the Rad51 amount did not have any additional effect on Rad52 SUMOylation (Figure 3C, lane 10 and data not shown). Taken together, these data indicate that ssDNA bound by RPA is fully accessible for binding by Rad52, whereas the DNA in a Rad51 nucleoprotein filament is not.
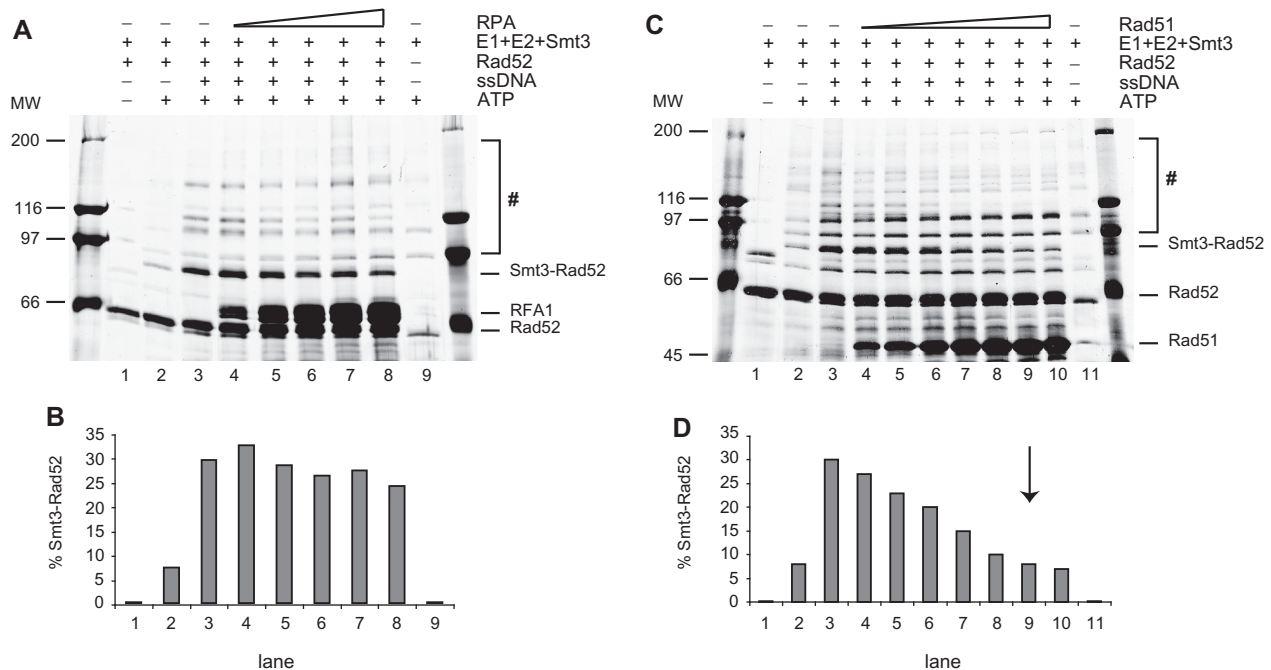
Figure 3. Effect of accessibility of RPA- or Rad51-coated ssDNA on Rad52 SUMOylation. (**A**) RPA bound to ssDNA does not affect Rad52 SUMOylation. Increasing amounts of RPA protein (1.2, 3.5, 4.6, 5.9 and 8.3 μM) were pre-incubated with 83-mer ssDNA (100 μM nucleotides) for 10 min at 37°C and then mixed with E1 (400 nM), E2 (2.8 μM), Smt3 (5.6 μM), Rad52 (2.7 μM) and 2.5 mM ATP. After 3 h incubation at 30°C, the reactions were analysed by 7.5% SDS–PAGE and silver-stained. (**B**) The ratio of mono-SUMOylated versus non-modified Rad52 is presented by quantifying the corresponding bands in (A). (**C**) Rad51-coated ssDNA does not stimulate Rad52 SUMOylation. The reactions were carried out as in (A) except increasing amounts of Rad51 were used (3, 7, 14, 21, 27, 34, 41 μM). The reaction mixtures were stopped and analysed by 10% SDS–PAGE followed by silver staining. (**D**) Quantification of Rad52-Smt3 conjugate from C, as a ratio of mono-SUMOylated versus non-modified Rad52. The arrow indicates amount of Rad51 that fully coats ssDNA. The hash symbol indicates high molecular poly-SUMO chains of Rad52 and E1 proteins.

The enhancement of Rad52 SUMOylation at residue K253 is mediated via the C-terminal DNA binding domain

Rad52 SUMOylation occurs at three lysine residues: K43, K44 and K253 (15), so we constructed and purified Rad52 mutant proteins lacking one or more of these SUMO-conjugation sites for the *in vitro* studies (Figure 1C). Interestingly, the Rad52 (K43,44R) mutant showed a pattern of SUMOylation similar to wild-type Rad52 both in the absence and presence of ssDNA (Figure 4A), suggesting that ssDNA-enhanced SUMOylation can occur at K253 alone. The other two Rad52 mutant proteins containing the K253R mutation [Rad52 (K253R) and Rad52 (K43,44,253R)] are strongly impaired for Rad52 SUMOylation (Figure 4A), indicating that residues K43 and K44 are modified as a consequence of SUMOylation at lysine 253 (Figure 4A). This is different to previously published data which could reflect the presence of E3 ligase in the *in vivo* situation (15). To help eliminate the possibility that the individual mutations could affect the protein folding, we tested all our mutant proteins for DNA binding and DNA strand annealing, and found no difference between wild-type and mutant proteins (Supplementary Figure S1).

Rad52 was shown to harbour two DNA binding domains, one at the amino-terminus and the other at its carboxyl-terminus [Figure 1A, (5)]. We wished to examine which of these domains are responsible for enhancement of Rad52 SUMOylation. Since this stimulation is mediated via K253, located at the middle region of Rad52, we checked the SUMOylation status and its enhancement after ssDNA binding using three Rad52 fragments that harbour either the amino-terminus and the middle portion of the protein (N+M), the middle portion only (M) or both the middle portion and carboxyl-terminus (M+C). Even though all three fragments can be SUMOylated *in vitro*, only the reaction involving Rad52 (M+C) was stimulated by ssDNA (Figure 4B), suggesting that the C-terminal binding region is responsible for the SUMOylation enhancement.

SUMOylation attenuates DNA binding and strand annealing

The effect of ssDNA on SUMOylation efficiency prompted us to test the biochemical properties of SUMOylated Rad52 protein. The oligomeric status of Rad52 prevents purification of the SUMOylated fraction from the *in vitro* SUMOylation reaction. Therefore, the SUMOylation reaction was performed in the presence or absence of ATP to ensure the same quantity of Rad52 for individual experiments, leading to up to 10% of modified Rad52. First, we tested both free and SUMOylated Rad52 for its ability to bind DNA using a well-established electrophoretic mobility shift assay. The SUMOylated Rad52 showed a significant decrease in DNA binding efficiency
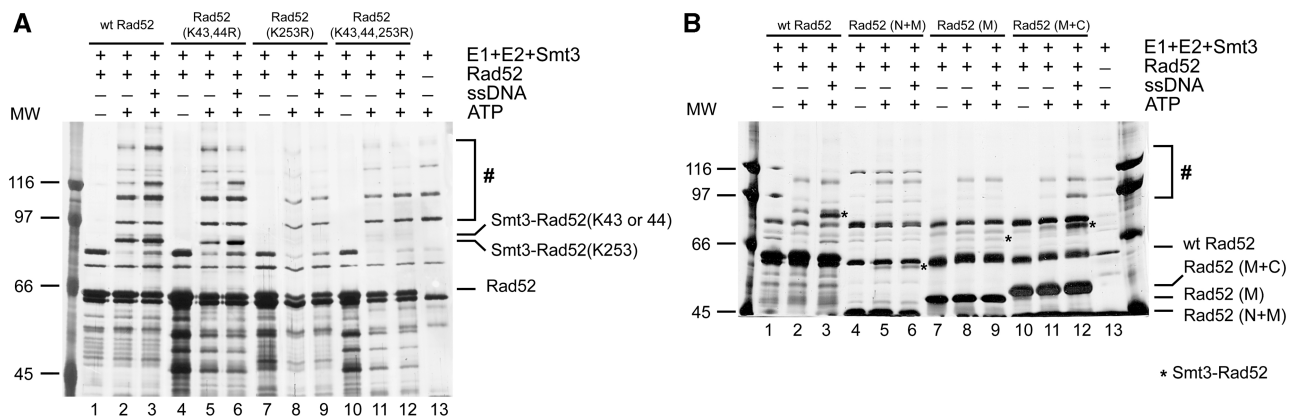
Figure 4. Binding of Rad52 to ssDNA via C-terminal domain enhances the SUMOylation of lysine K253. (**A**) SUMOylation at lysine K253 is stimulated by ssDNA. The standard *in vitro* SUMOylation reaction was done with wild-type Rad52 (2.7 μM) or SUMO-deficient acceptor lysine Rad52 mutants: Rad52 (K43,44R), Rad52 (K253R) and Rad52 (K43,44,253R). (**B**) The C-terminal DNA binding domain of Rad52 is responsible for stimulation of SUMOylation. Rad52 protein and its fragments: Rad52 (N+M) (4.13 μM), Rad52 (M) containing GST-tag (3.52 μM) and Rad52 (M+C) (4.03 μM) were SUMOylated *in vitro* in the presence or absence of 83-mer ssDNA (100 μM nucleotides) and analysed. The asterisks indicate main SUMOylated Rad52 species. The hash symbol indicates high molecular poly-SUMO chains of Rad52 and E1 proteins.
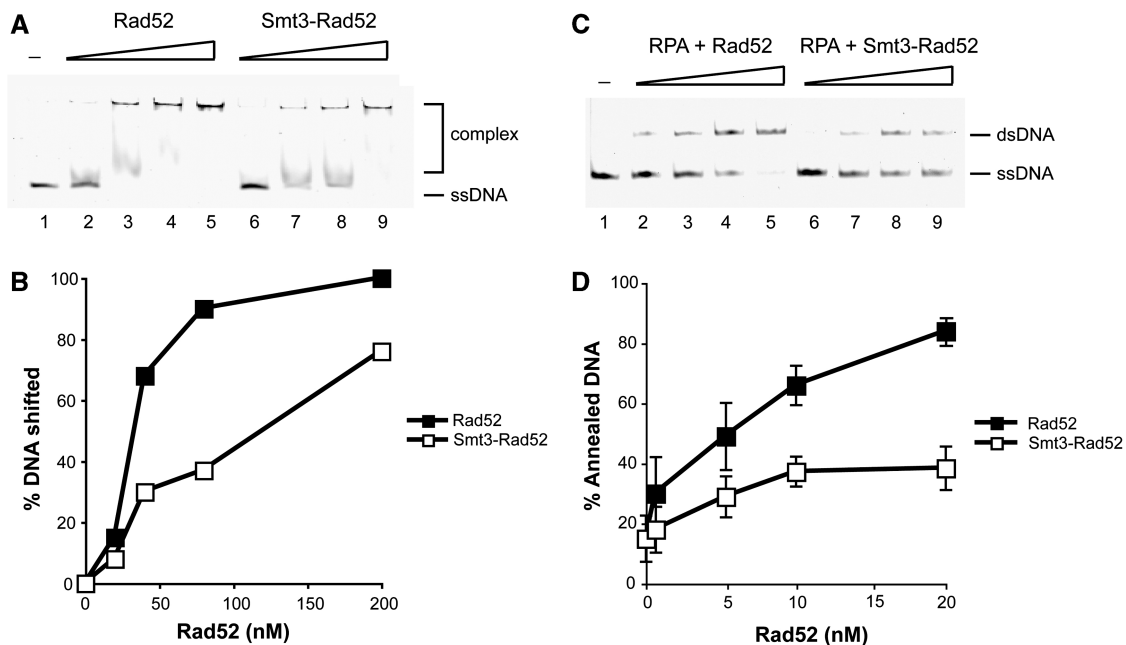
Figure 5. Rad52 SUMOylation affects its biochemical activities. (**A**) SUMOylation of Rad52 inhibits its binding to DNA. Increasing amounts of Rad52 or Smt3-Rad52 (20, 40, 80, 200 nM) were incubated with fluorescently labelled 49-mer ssDNA (0.49 μM nucleotides) at 37°C for 10 min. The reaction mixtures were resolved in 7.5% native polyacrylamide gels, and the DNA species were quantified using Quantity One software (Bio-Rad). (**B**) The results from (A) plotted. (**C**) SUMOylation of Rad52 inhibits its strand annealing activity. Labelled Oligo-1 (0.25 μM nucleotides) and Oligo-2 (0.25 μM nucleotides) were incubated separately with RPA (20 nM) for 3 min at 37°C. The annealing reactions were initiated by mixing RPA-coated oligonucleotides and Rad52 or Smt3-Rad52 proteins (0.7, 5, 10, 20 nM) and incubated at 37°C. After 8 min of incubation, 9 μl of the annealing reactions was removed and treated with 0.5% SDS, and 500 μg/ml proteinase K at 37°C for 10 min. The reaction mixtures were resolved in 12% native polyacrylamide gels. (**D**) The averaged values of results from three independent experiments are plotted.

towards both ssDNA and dsDNA (Figure 5A and B, and data not shown). Next, we addressed whether the lower affinity towards DNA can also affect the annealing activity of Rad52 protein. Both unmodified and SUMOylated Rad52 were incubated with complementary ssDNA strands, and their annealing ability was monitored. Importantly, SUMOylated Rad52 showed a lower activity in the annealing reaction (Supplementary Figure S2). This has been further confirmed in the reaction when ssDNA is coated by RPA to reflect the *in vivo* conditions and to prevent the effect of possible DNA self-annealing (Figure 5C and D). No effect of components of the SUMOylation reaction or ATP alone on DNA binding or single-strand annealing activity was observed (data not shown). In summary, SUMOylation of as little as 10% of the total Rad52 protein is sufficient

to significantly decrease Rad52 affinity towards both ssDNA and dsDNA and decrease single-strand annealing activity.

SUMOylation of Rad52 does not affect its interactions with Rad51 and RPA

Rad52 is known to self-associate (8) and interact with other HR proteins including Rad51 (10,11) and RPA proteins (12,29,30). We have tested the effect of Rad52 SUMOylation on these interactions. Since Smt3 protein in this experiment contains the FLAG tag, we first

assayed the Rad52 oligomerization status on anti-FLAG agarose beads. As shown in Figure 6A, the ratio of modified versus unmodified Rad52 protein does not change after anti-FLAG pull-down. This was further confirmed by size exclusion chromatography (Sephacryl S400, see 'Materials and Methods' section), which showed that SUMOylation has little or no effect on the oligomeric state of Rad52 (Figure 6B). In summary, the oligomeric state of Rad52 is not affected upon SUMOylation. Moreover, SUMO conjugation occurs to the same degree among the individual Rad52 oligomers (Figure 6A and B).
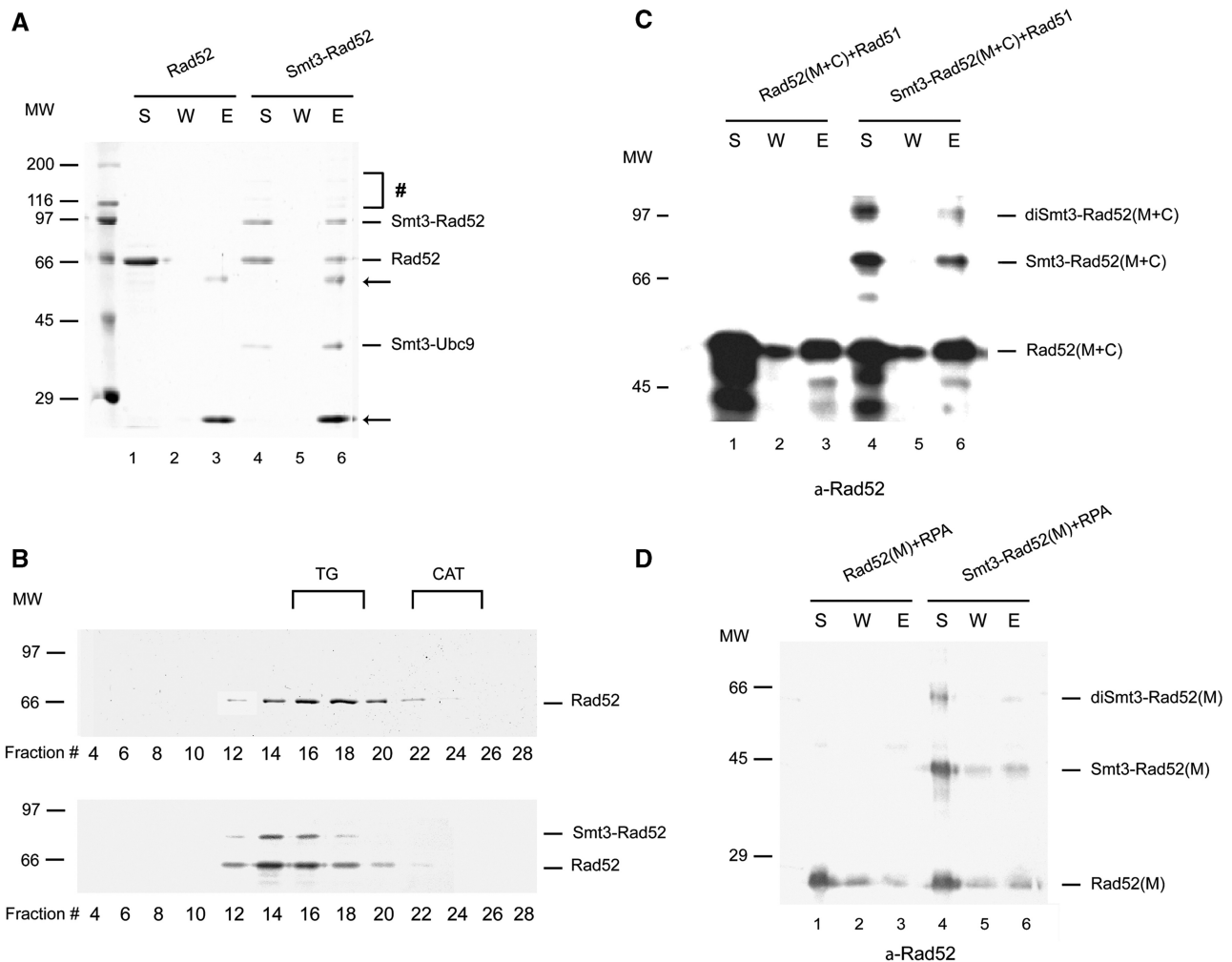
Figure 6. Rad52 oligomerization and interaction with RPA and Rad51 are not affected by its SUMOylation. (**A**) SUMOylation of Rad52 does not influence its oligomerization status. Rad52 and Smt3-Rad52 (2.3 μM) in 40 μl of buffer S were incubated with 4 μl of anti-FLAG agarose in 10 μl of buffer T containing 200 mM KCl for 30 min at 4°C. The beads were washed and treated with 25 μl of SDS Laemmli buffer to elute bound proteins. The supernatant (S) that contained unbound Rad52 or Smt3-Rad52 protein, wash (W) and the SDS eluate (E) (10 μl each) were analysed on 12% gel SDS–PAGE followed by staining with Coomassie Blue. The arrows and symbol hash denote anti-FLAG IgG and higher order SUMOylated species, respectively. (**B**) Analysis of Rad52 oligomerization status by gel filtration. Purified Rad52 or Smt3-Rad52 proteins (9 μM) in 200 μl of buffer S were filtered through a sephacryl S400 column. The indicated fractions were run on 10% SDS–PAGE followed by staining with Coomassie blue. The elution positions of the size markers are indicated: TG, thyroglobulin (669 kDa) and CAT, catalase (223 kDa). (**C**) SUMOylation of Rad52 does not affect its interaction with Rad51. Purified Rad52(M + C) or Smt3-Rad52(M + C) (22 μM) were mixed with Affi-Rad51 beads (4,6 μM Rad51) in 25 μl of buffer K and incubated for 30 min at 4°C. The beads were washed and treated with 25 μl of SDS Laemmli buffer to elute bound proteins. The supernatant that contained unbound Rad52 or Smt3-Rad52 protein, wash, and the SDS eluate (5 μl each) were analysed by SDS–PAGE in 12% gel followed by western blotting using anti-Rad52 antibody. (**D**) SUMOylation of Rad52 does not affect its interaction with RPA. The interaction with RPA was tested using purified Rad52 (M) or Smt3-Rad52 (M) (230 pmol) and Affi-RPA (1 μM RPA) beads pre-incubated with ssDNA (1 μg of ΦX174) for 10 min at 37°C. Both mixtures were combined in 45 μl of buffer T followed by an incubation for 30 min at 4°C and then analysed as in panel C.

However, we cannot exclude the possibility that SUMOylated and unmodified subunits re-distributed during the SUMOylation and pull-down assays. Electron microscopy of unmodified and SUMOylated Rad52 also revealed no difference in the oligomeric status of Rad52 (data not shown).

Next, we checked the ability of SUMOylated Rad52 to interact with Rad51. For this purpose, we generated Affi-Rad51 beads to use as affinity matrix for testing inter-action with unmodified and modified Rad52. We used a Rad52 fragment without the N-terminal oligomerization domain [Rad52 (M + C)] to minimize its effect on the role of SUMOylation on Rad51 interaction. The result from this experiment showed SUMOylated Rad52 is just as capable of Rad51 association as the unmodified protein (Figure 6C). To test the interaction with RPA, we generated Affi-RPA beads and performed a pull-down assay as described previously (5). Rad52 (M) fragment missing the N- and C-terminal DNA binding domains was used to monitor its ability to interact with DNA-bound RPA (5). Little or no change could be observed between Rad52 (M) and SUMOylated Rad52 (M) for RPA association (Figure 6D). Taken together, the above results allowed us to conclude that

SUMOylation does not affect Rad52 self-association or its interaction with Rad51 and RPA.

Rad52 SUMOylation regulates recombination *in vivo*

To address the effects of Rad52 SUMOylation *in vivo*, we examined the SUMO-deficient mutants (*rad52-K43,44R, -K253R* or *-K43,44,253R*) using several recombination assays. In agreement with previous work (15), we found that these mutations did not dramatically affect the rate of intra- or inter-chromosomal recombination during mitosis (Tables 1 and 2), but caused a shift from single-stranded annealing to gene conversion events (Table 1). In addition, these mutations resulted in slight hyper-recombination phenotype in rDNA recombination [Table 3, (16)].

We also expanded the previous studies and examined the effect of *rad52* SUMOylation mutants in additional mitotic and meiotic recombination assays. We found that *rad52-K43,44,253R* exhibited 60% of a wild-type level of BIR (Table 4), suggesting that Rad52 SUMOylation contributes positively to this type of recombination. In meiosis, although all three *rad52* SUMO mutants exhibited wild-type levels of recombination at the *leu2* locus (Table 5), *rad52-K43,44,253R*, but not *rad52-K43,44R* and *rad52-K253R* cells exhibited

Table 1. Effect of *rad52* SUMOylation-defective mutants on mitotic heteroallelic and direct-repeat recombination

| Genotype	Heteroallelic recombination rate ($\times 10^{-8}$)[a]	Fold change relative to wild-type[b]	Direct-repeat recombination ($\times 10^{-6}$)[a]	Fold change relative to wild-type	P-value (direct-repeat)[c]	Fraction Ura$^+$ GC	P-value (Ura$^+$)[d]
RAD52	219 ± 29	1	51 ± 8	1	n.a.	0.33	n.a.
rad52Δ	0.7 ± 0.4	0.005	2.3 ± 0.5	0.03	<0.001	0.0004	<0.001
K43,44R	253 ± 48	1.2	107 ± 15	2.1	0.06	0.45	<0.001
K253R	179 ± 30	0.8	70 ± 11	1.4	0.13	0.37	0.075
K43,44,253R	216 ± 36	1.0	74 ± 11	1.4	0.16	0.40	<0.001

[a]Recombination rate is presented as events per cell per generation as described previously (37). For each strain, 15–19 trials were performed. Strains ML412 (wild-type), ML414 (*rad52Δ*), ML466 (*rad52-K43,44R*), ML467 (*rad52-K253R*), ML480 (*rad52-K43,44,253R*).
[b]There is no significant difference in mitotic heteroallelic recombination between wild-type and the SUMOylation defective *rad52* mutants.
[c]P-value for *t*-test applied to the direct-repeat recombination rate relative to wild-type.
[d]P-value for Pearson's χ^2 test relative to wild-type.
Schematic of the assays for spontaneous heteroallelic (i) and direct-repeat (ii) recombination between *leu2-ΔEcoRI* and *leu2-ΔBstEII* heteroalleles.
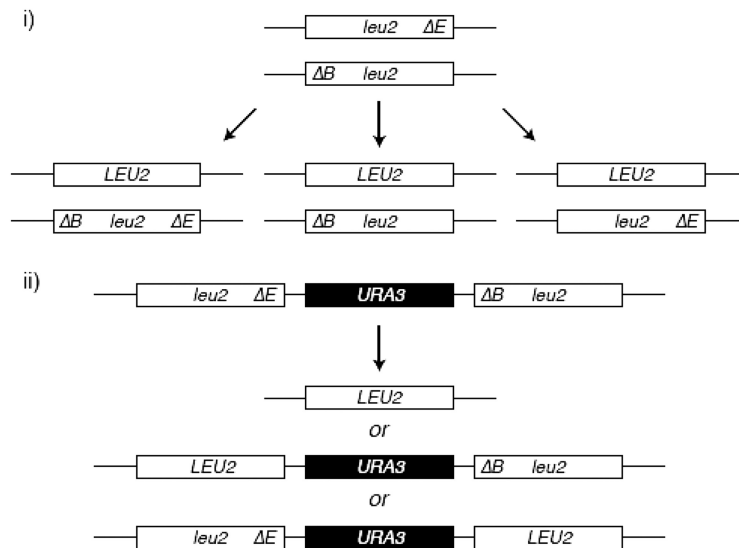
Table 2. Effect of *rad52-K43,44,253R* on recombination rates of the inverted-repeat substrate[a]

Genotype	Rates (10^{-8})[a]	P-value (χ^2)[b]	Fold change relative to wild-type
WT	$28\,432 \pm 4982$	n.a.	1.00
rad52Δ	5 ± 1.4	n.d	0.0002
rad51Δ	5631 ± 1358	n.a.	0.20
rad51Δ, rad52Δ	0	0.002	<0.00004
rad51Δ, rad52K43,44,253R	4986 ± 1617	0.31	0.18

[a]Rates are per cell per generation as described previously (38). Results presented are a mean of 3–5 independent isolates for each genotype, out of a single representative experiments.
[b]The χ^2-test was applied to compare the recombination rates with that of *rad51Δ* strain.
Schematic of the assay for spontaneous inverted-repeat recombination between *ade2-5′Δ* and *ade2-ΔNdeI* heteroalleles.
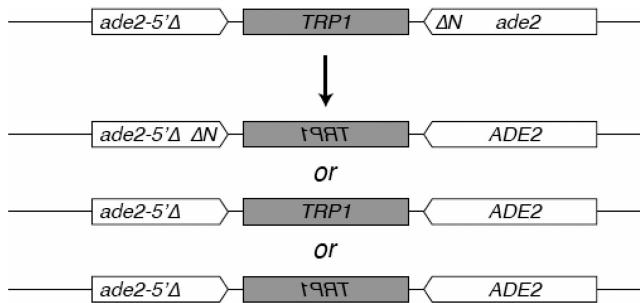
Table 3. Effect of *rad52* SUMOylation-defective mutants on rDNA recombination

Genotype	*ADE2* loss[a]			Fold change relative to wild-type
	Rate of loss $(\times 10^{-3})$	P-value[b]	Half-sectored/ total	
RAD52	2.89	n.a.	112/38 700	1
rad52Δ	0.85	<0.001	17/20 029	0.29
K43,44R	3.71	0.095	79/21 279	1.28
K253R	3.95	0.036	84/21 271	1.36
K43,44,253R	9.51	<0.001	380/39 939	3.29

[a]rDNA recombination in the first generation after plating was assayed by counting half-sectored colonies as described previously (24). Recombination was assayed in strains RMY180-5A (wild-type), NEB136-2B (*rad52Δ*), NEB187-10A (*rad52-K43,44R*), NEB168-11B (*rad52-K253R*), NEB63-2B (*rad52-K43,44,253R*).
[b]Fisher's exact test was applied to compare the recombination rate with that of the wild-type strain.
Schematic of the assay for spontaneous rDNA recombination resulting in *ADE2* marker loss.
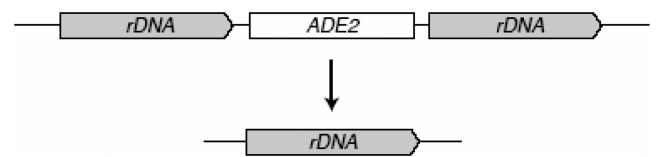
Table 4. Effect of *rad52-K43,44,253R* mutation on the frequency of break-induced replication[a]

Genotype	Frequency of stable Ura+ $(\times 10^{-2})$ with CFV/D8B-tg	P-value (χ^2)[b]	Fold change relative to wild-type
RAD52	3.94 ± 0.75	n.a.	1
rad52Δ	<0.0002	n.d.	<0.0039
K43,44,253R	2.39 ± 0.44	0.0044	0.60

[a]The frequency of break-induced replication is the number of stable Ura+ transformants per microgram with cut DNA divided by the number of transformants per microgram with uncut DNA transformed, as described previously (25). For each genotype, five to seven trials were performed.
[b]The χ^2-test was applied to compare the recombination rate with that of the wild-type strain.
Schematic of the assay for BIR resulting in a stable Ura+ recombinant strain with the CFV/D8B-tg fragment.
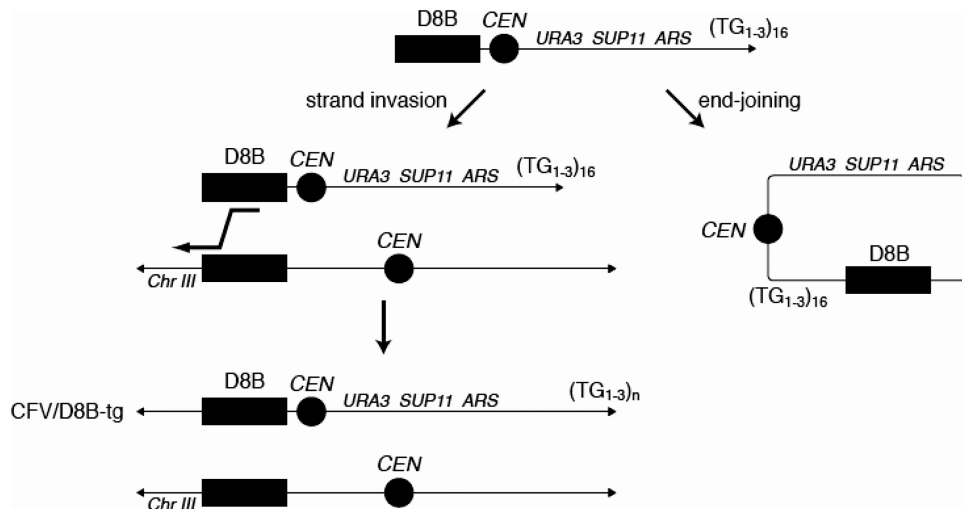
**Table 5.** Effect of *rad52* SUMOylation-defective mutants on meiotic recombination

Genotype	Meiotic recombination frequency $(\times 10^{-4})$ [a]	Fold change relative to wild-type	Sporulation efficiency[b], %	Germination efficiency[c], %	Relative viability[d]
RAD52	118 ± 31	1	41	96	1
rad52Δ	0.06 ± 0.06	0.001	1	n.a.	0.10
K43,44R	144 ± 38	1.2	58	69	0.95
K253R	77 ± 24	0.7	55	88	0.84
K43,44,253R	109 ± 27	0.9	53	96	2.39

[a]Recombination frequency is presented as events per colony forming unit. For each strain, three trials were performed. Strains ML412 (wild type), ML414 (*rad52Δ*), ML466 (*rad52-K43,44R*), ML467 (*rad52-K253R*), ML480 (*rad52-K43,44,253R*) were sporulated on solid medium at 30°C essentially as described previously (39). [See schematic in Table 1(i)].
[b]Sporulation efficiency was determined as the fraction of three to four spore tetrads out of all cells after 3 days on solid SPO medium at 30°C.
[c]Germination efficiency was determined by tetrad dissection of four-spore tetrads after 3 days on solid SPO medium at 30°C.
[d]Viability is the number of colony forming units per milliliter per OD_{600} after sporulated on solid medium at 30°C.
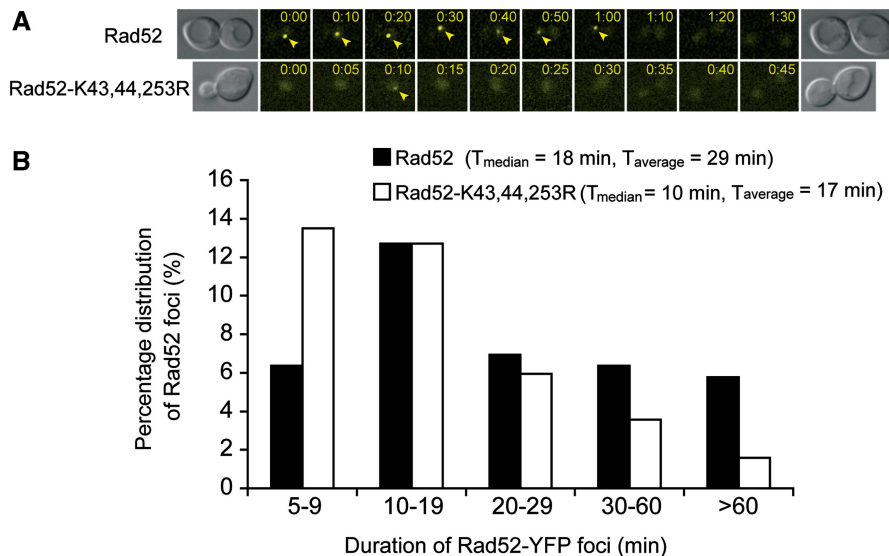
Figure 7. Rad52-K43,44,253R foci exhibits shorter duration than wild-type. Time-lapse of spontaneous wild-type Rad52 and mutant Rad52-K43,44,253R foci. Strains W5094-1C (*RAD52-YFP*) and ML228 (*rad52-K43,44,253R-YFP*) were examined by fluorescence microscopy at 5 min intervals as described in the 'Materials and Methods' section. (**A**) Representative examples of time-lapse image sequences. Arrowheads mark Rad52 foci. (**B**) Quantitative analysis of time-lapse analysis. The number of cell cycles analysed is $n = 173$ for wild-type Rad52 and $n = 252$ for the Rad52-K43,44,253R mutant protein. The class of cells for which no foci were observed amounted to 62 and 63% for *RAD52* and *rad52-K43,44,253R*, respectively (not shown in the graph).

increased spore viability. This effect is not due to an alteration of the ability of these mutant proteins to bind ssDNA or dsDNA or to anneal complementary DNA, because Rad52-K43,44,253R, Rad52-K43,44R and Rad52-K253R proteins exhibit wild-type levels of activities in these reactions *in vitro* (Supplementary Figure S1). Thus, the effect on spore viability could be due to the fact that SUMOylation of Rad52 affects other meiotic events. Taken together, these results suggest that Rad52 SUMOylation facilitates certain recombination sub-pathways and disfavours the others and may contribute to meiotic processes that determine spore viability.

Finally, we also tested the *in vivo* localization of a Rad52 SUMO-deficient mutant by cytological analysis. The fusion of wild-type as well as the Rad52-K43,44,253R proteins to YFP revealed that the mutant protein forms foci similarly to wild-type, but the duration of the foci is significantly shorter ($P = 0.01$, *t*-test) (Figure 7A and B). The average intensity of the YFP signal for wild-type and the SUMO-deficient mutant foci is similar, suggesting that the difference in duration of foci is not due to a difference in the amount of proteins (data not shown).

DISCUSSION

HR is essential for genome maintenance and must be tightly controlled to avoid of loss of heterozygosity, chromosome translocations and gene deletions (1,3). Recent studies have documented several examples of HR proteins and associated factors being post-translationally modified by the SUMO protein. In particular, defects in SUMOylation of Rad52, Rad59 and RPA result in genomic context-dependent changes in HR and chromosomal rearrangements (31). Also, during S-phase, Srs2

(a helicase that blocks recombinational repair by disrupting Rad51 nucleoprotein filaments) is recruited to replication forks via interaction with SUMOylated PCNA (proliferating cell nuclear antigen), thereby preventing assembly of Rad51 nucleoprotein filaments on ssDNA associated with the replication forks (32).

In this study we have strived to determine the effects of SUMOylation on the Rad52 protein. Using *in vitro* biochemical assays, we have found that Rad52 is SUMOylated in a manner that is stimulated by ssDNA and dependent on the carboxyl-terminal DNA binding domain. The stimulation is specific for ssDNA, as dsDNA has no effect on the level of SUMOylation. In addition, the CD analysis revealed that binding of ssDNA by Rad52 is accompanied by a conformational change. By replacing each of the SUMOylation-targeted lysines with arginine, we observed that increasing SUMOylation in the presence of ssDNA is directed to residue K253. In addition, we have found that RPA-bound, but not Rad51-bound, ssDNA promotes Rad52 SUMOylation, suggesting that Rad52 SUMOylation is favoured prior to the formation of Rad51 nucleoprotein filament during HR in cells. Significantly, while Rad52 SUMOylation has no effect on its oligomerization and interaction with RPA and Rad51, a small percentage (<10%) of SUMOylated Rad52 markedly decreases its affinity to ssDNA and dsDNA, and causes a reduction of its DNA annealing activity.

Collectively, our biochemical results suggest that upon binding to resected ssDNA tails coated with RPA, Rad52 undergoes conformational change that can promote its efficient SUMOylation. Because SUMOylation does not affect Rad52 interaction with RPA and Rad51 or its oligomerization, this modification does not appear to function by altering protein–protein interactions. Instead, our results suggest that SUMOylation attenuates Rad52 strand annealing activity and prompts its disassociation from DNA. This can provide a mechanism either for favouring appropriate pathways over others or for dynamic exchange of Rad52 on DNA. Consistently with previous reports (15,16), we find that SUMOylation of Rad52 *in vivo* suppresses rDNA recombination and favours single-strand annealing over gene conversion in direct repeat recombination at the *LEU2* locus. In addition, we show that both the N-terminal (K43,44) and central (K253) SUMOylation sites contribute to these effects. Further, we show in this study that Rad52 SUMOylation reduces meiotic spore viability and appears to favour BIR events. While the mechanism for these effects remains to be determined, it may reflect a requirement of Rad52 dynamics in these pathways or a role of SUMO in facilitating events unique to these pathways.

Finally, it is noteworthy that the effects of SUMO on Rad52 activity are somewhat reminiscent of that on thymine-DNA glycosylase, SUMOylation of which induce its dissociation from the abasic site (33). However, different from thymine-DNA glycosylase, Rad52 functions in concert with several additional mediator and recombination proteins, such that its regulation is more complex and defects in any single form of regulation can be buffered by other mechanisms. Our *in vivo* results suggest that this is likely the case, as the lack of Rad52 SUMOylation does not dramatically affect several mitotic or meiotic recombination processes examined here. However, the observed alteration of recombination pathway usage as well as the changes of duration times of recombination foci in *rad52* SUMOylation defective mutants indicate the modification of Rad52 can indeed influence recombination pathway choice or efficiency. An intriguing possibility is that SUMOylation, in conjunction with other Rad52 functions such as antagonizing Srs2 (34,35), helps to fine-tune the efficiency of recombinational repair. In addition, as other recombination proteins and Rad52-interacting factors are also subject to SUMOylation, the presence and modification of these factors may collectively provide a quality control mechanism to direct HR pathway choice depending on substrate types and the chromosomal environment (36). This work brings initial characterization of the role of SUMOylation during HR; additional studies will need to further our understanding of the underlying molecular mechanism.

SUPPLEMENTARY DATA

Supplementary Data are available at NAR Online.

ACKNOWLEDGEMENTS

FUNDING

REFERENCES

1. Krogh,B.O. and Symington,L.S. (2004) Recombination proteins in yeast. *Ann. Rev. Genet.*, **38**, 233–271.
2. Symington,L.S. (2002) Role of RAD52 epistasis group genes in homologous recombination and double-strand break repair. *Microbiol. Mol. Biol. Rev.*, **66**, 630–670.
3. Sung,P. and Klein,H. (2006) Mechanism of homologous recombination: mediators and helicases take on regulatory functions. *Nat. Rev. Mol. Cell Biol.*, **7**, 739–750.

4. Sung,P. (1997) Function of yeast Rad52 protein as a mediator between replication protein A and the Rad51 recombinase. *J. Biol. Chem.*, **272**, 28194–28197.

5. Seong,C., Sehorn,M.G., Plate,I., Shi,I., Song,B., Chi,P., Mortensen,U., Sung,P. and Krejci,L. (2008) Molecular anatomy of the recombination mediator function of Saccharomyces cerevisiae Rad52. *J. Biol. Chem.*, **283**, 12166–12174.

6. Sung,P., Krejci,L., Van Komen,S. and Sehorn,M.G. (2003) Rad51 recombinase and recombination mediators. *J. Biol. Chem.*, **278**, 42729–42732.

7. Li,X. and Heyer,W.D. (2008) Homologous recombination in DNA repair and DNA damage tolerance. *Cell Res.*, **18**, 99–113.

8. Shinohara,A., Shinohara,M., Ohta,T., Matsuda,S. and Ogawa,T. (1998) Rad52 forms ring structures and co-operates with RPA in single-strand DNA annealing. *Genes Cells*, **3**, 145–156.

9. Mortensen,U.H., Bendixen,C., Sunjevaric,I. and Rothstein,R. (1996) DNA strand annealing is promoted by the yeast Rad52 protein. *Proc. Natl Acad. Sci. USA*, **93**, 10729–10734.

10. Shinohara,A., Ogawa,H. and Ogawa,T. (1992) Rad51 protein involved in repair and recombination in S. cerevisiae is a RecA-like protein. *Cell*, **69**, 457–470.

11. Milne,G.T. and Weaver,D.T. (1993) Dominant negative alleles of RAD52 reveal a DNA repair/recombination complex including Rad51 and Rad52. *Genes Dev*, **7**, 1755–1765.

12. Hays,S.L., Firmenich,A.A., Massey,P., Banerjee,R. and Berg,P. (1998) Studies of the interaction between Rad52 protein and the yeast single-stranded DNA binding protein RPA. *Mol. Cell Biol.*, **18**, 4400–4406.

13. Plate,I., Hallwyl,S.C., Shi,I., Krejci,L., Muller,C., Albertsen,L., Sung,P. and Mortensen,U.H. (2008) Interaction with RPA is necessary for Rad52 repair center formation and for its mediator activity. *J. Biol. Chem.*, **283**, 29077–29085.

14. Krejci,L., Song,B., Bussen,W., Rothstein,R., Mortensen,U.H. and Sung,P. (2002) Interaction with Rad51 is indispensable for recombination mediator function of Rad52. *J. Biol. Chem.*, **277**, 40132–40141.

15. Sacher,M., Pfander,B., Hoege,C. and Jentsch,S. (2006) Control of Rad52 recombination activity by double-strand break-induced SUMO modification. *Nat. Cell Biol.*, **8**, 1284–1290.

16. Torres-Rosell,J., Sunjevaric,I., De Piccoli,G., Sacher,M., Eckert-Boulet,N., Reid,R., Jentsch,S., Rothstein,R., Aragon,L. and Lisby,M. (2007) The Smc5-Smc6 complex and SUMO modification of Rad52 regulates recombinational repair at the ribosomal gene locus. *Nat. Cell Biol.*, **9**, 923–931.

17. Sherman,F., Fink,G.R. and Hicks,J.B. (1986) *Methods in Yeast Genetics*. Cold Spring Harbor, NY.

18. Thomas,B.J. and Rothstein,R. (1989) Elevated recombination rates in transcriptionally active DNA. *Cell*, **56**, 619–630.

19. Zhao,X., Muller,E.G. and Rothstein,R. (1998) A suppressor of two essential checkpoint genes identifies a novel protein that negatively affects dNTP pools. *Mol. Cell*, **2**, 329–340.

20. Sung,P. (1994) Catalysis of ATP-dependent homologous DNA pairing and strand exchange by yeast RAD51 protein. *Science*, **265**, 1241–1243.

21. Petukhova,G., Stratton,S. and Sung,P. (1998) Catalysis of homologous DNA pairing by yeast Rad51 and Rad54 proteins. *Nature*, **393**, 91–94.

22. Smith,J. and Rothstein,R. (1995) A mutation in the gene encoding the Saccharomyces cerevisiae single-stranded DNA-binding protein Rfa1 stimulates a RAD52-independent pathway for direct-repeat recombination. *Mol. Cell Biol.*, **15**, 1632–1641.

23. Lea,D.E. and Coulson,C.A. (1949) The distribution in the numbers of mutants in bacterial populations. *J. Genetics*, **49**, 264–285.

24. Merker,R.J. and Klein,H.L. (2002) hpr1Delta affects ribosomal DNA recombination and cell life span in Saccharomyces cerevisiae. *Mol. Cell Biol.*, **22**, 421–429.

25. Davis,A.P. and Symington,L.S. (2004) RAD51-dependent break-induced replication in yeast. *Mol. Cell Biol.*, **24**, 2344–2351.

26. Lisby,M., Rothstein,R. and Mortensen,U.H. (2001) Rad52 forms DNA repair and recombination centers during S phase. *Proc. Natl Acad. Sci. USA*, **98**, 8276–8282.

27. Parsons,C.A., Baumann,P., Van Dyck,E. and West,S.C. (2000) Precise binding of single-stranded DNA termini by human RAD52 protein. *Embo J.*, **19**, 4175–4181.

28. Johnson,N.P., Lindstrom,J., Baase,W.A. and von Hippel,P.H. (1994) Double-stranded DNA templates can induce alpha-helical conformation in peptides containing lysine and alanine: functional implications for leucine zipper and helix-loop-helix transcription factors. *Proc. Natl Acad. Sci. USA*, **91**, 4840–4844.

29. Shinohara,A. and Ogawa,T. (1998) Stimulation by Rad52 of yeast Rad51-mediated recombination. *Nature*, **391**, 404–407.

30. Sugiyama,T., New,J.H. and Kowalczykowski,S.C. (1998) DNA annealing by RAD52 protein is stimulated by specific interaction with the complex of replication protein A and single-stranded DNA. *Proc. Natl Acad. Sci. USA*, **95**, 6049–6054.

31. Burgess,R.C., Rahman,S., Lisby,M., Rothstein,R. and Zhao,X. (2007) The Slx5-Slx8 complex affects sumoylation of DNA repair proteins and negatively regulates recombination. *Mol. Cell Biol.*, **27**, 6153–6162.

32. Papouli,E., Chen,S., Davies,A.A., Huttner,D., Krejci,L., Sung,P. and Ulrich,H.D. (2005) Crosstalk between SUMO and ubiquitin on PCNA is mediated by recruitment of the helicase Srs2p. *Mol. Cell*, **19**, 123–133.

33. Steinacher,R. and Schar,P. (2005) Functionality of human thymine DNA glycosylase requires SUMO-regulated changes in protein conformation. *Curr. Biol.*, **15**, 616–623.

34. Burgess,R.C., Lisby,M., Altmannova,V., Krejci,L., Sung,P. and Rothstein,R. (2009) Localization of recombination proteins and Srs2 reveals anti-recombinase function in vivo. *J. Cell Biol.*, **185**, 969–981.

35. Seong,C., Colavito,S., Kwon,Y., Sung,P. and Krejci,L. (2009) Regulation of Rad51 recombinase presynaptic filament assembly via interactions with the Rad52 mediator and the Srs2 anti-recombinase. *J. Biol. Chem.*, **284**, 24363–24371.

36. Marini,V. and Krejci,L. (2010) Srs2: the "Odd-Job Man" in DNA repair. *DNA repair*, **9**, 268–275.

37. Mortensen,U.H., Erdeniz,N., Feng,Q. and Rothstein,R. (2002) A molecular genetic dissection of the evolutionarily conserved N terminus of yeast Rad52. *Genetics*, **161**, 549–562.

38. Rattray,A.J. and Symington,L.S. (1994) Use of a chromosomal inverted repeat to demonstrate that the RAD51 and RAD52 genes of Saccharomyces cerevisiae have different roles in mitotic recombination. *Genetics*, **138**, 587–595.

39. Lisby,M., Rothstein,R. and Mortensen,U.H. (2001) Rad52 forms DNA repair and recombination centers during S phase. *Proc. Natl Acad. Sci. USA*, **98**, 8276–8282.

Attachment 10

Matulova P, Marini V, Burgess RC, Sisakova A, Kwon Y, Rothstein R, Sung P, Krejci L

Co-operativity of Mus81-Mms4 with Rad54 in the resolution of recombination and replication intermediates.

J Biol Chem. 284 (12):7733-7745. 2009.

⌘ *Author's Choice*

Cooperativity of Mus81·Mms4 with Rad54 in the Resolution of Recombination and Replication Intermediates*⑤

Petra Matulova[‡], **Victoria Marini**[‡], **Rebecca C. Burgess**[§], **Alexandra Sisakova**[‡], **Youngho Kwon**[¶], **Rodney Rothstein**[§], **Patrick Sung**[¶], and **Lumir Krejci**[‡1]

From the [‡]National Centre for Biomolecular Research, Masaryk University, Brno 62500, Czech Republic, [¶]Department of Molecular Biophysics and Biochemistry, Yale University School of Medicine, New Haven, Connecticut 06520, and [§]Department of Genetics and Development, Columbia University Medical Center, New York, New York 10032-2704

The *Saccharomyces cerevisiae* Mus81·Mms4 protein complex, a DNA structure-specific endonuclease, helps preserve genomic integrity by resolving pathological DNA structures that arise from damaged or aborted replication forks and may also play a role in the resolution of DNA intermediates arising through homologous recombination. Previous yeast two-hybrid studies have found an interaction of the Mus81 protein with Rad54, a Swi2/Snf2-like factor that serves multiple roles in homologous recombination processes. However, the functional significance of this novel interaction remains unknown. Here, using highly purified *S. cerevisiae* proteins, we show that Rad54 strongly stimulates the Mus81·Mms4 nuclease activity on a broad range of DNA substrates. This nuclease enhancement does not require ATP binding nor its hydrolysis by Rad54. We present evidence that Rad54 acts by targeting the Mus81·Mms4 complex to its DNA substrates. In addition, we demonstrate that the Rad54-mediated enhancement of the Mus81·Mms4 (Eme1) nuclease function is evolutionarily conserved. We propose that Mus81·Mms4 together with Rad54 efficiently process perturbed replication forks to promote recovery and may constitute an alternative mechanism to the resolution/dissolution of the recombination intermediates by Sgs1·Top3. These findings provide functional insights into the biological importance of the higher order complex of Mus81·Mms4 or its orthologue with Rad54.

Barriers arising from DNA structures or lesions caused by endogenous and exogenous genotoxic agents are frequently encountered during DNA replication. Because of this, the suc-cessful completion of DNA replication relies on its coordination with a variety of replication fork repair and restart mechanisms. Several such mechanisms have been described. Depending on the circumstance, a mechanism that employs end tail repriming, template switch, fork regression and recovery, or translesion DNA synthesis may be used (1–4). Alternatively, the perturbed fork can be cleaved, creating a DNA double-strand break that is repaired by the homologous recombination machinery in a manner that leads to fork restart (5, 6).

Mounting evidence has implicated the Mus81 protein in the processing of stalled DNA replication forks (7–9). The *mus81* mutant exhibits hypersensitivity to methyl methanesulfonate, camptothecin (CPT),[2] UV, and hydroxyurea (HU), reagents that in general cause replication fork stalling or collapse, and it also shows synthetic interactions with mutations in DNA replication proteins (6, 10). Mus81 inactivation results in elevated levels of genomic instability, elicits checkpoint activation, and also leads to checkpoint-dependent cell cycle arrest (11–13). Mus81 is a member of the XPF family of endonucleases that play crucial roles in various DNA repair processes, including nucleotide excision repair, DNA interstrand cross-link repair, and homology-directed repair (14). XPF and its homologs function in the context of a heterodimeric complex with a partner protein. Mms4 (Eme1 in fission yeast and human) is the partner protein for Mus81, and the Mus81·Mms4 complex shows a preference for branched DNA structures that are believed to arise during the processing of stalled or collapsed replication forks as well as during recombination (4, 6, 10).

In general, Mus81·Mms4 prefers to cleave substrates with three- and four-way junctions containing a 5′ end at the junction, which serves to direct the cleavage reaction (8, 15, 16). Mus81 in complex with Mms4 or Eme1 also cleaves nicked Holliday junctions (HJ), and to a much lesser degree, intact HJs as well (6, 10). Whether the HJ represents a physiological substrate for the Mus81·Mms4 (Eme1) complex remains unclear. It has been also suggested that the activity of the Mus81 complex on intact HJ may be enhanced by a cellular factor (17). Nevertheless, *mus81/mms4/eme1* mutants show severe meiotic phenotypes, indicating an essential role of this complex in processing recombination intermediates during meiotic recombination (6, 10).

⌘ *Author's Choice*—Final version full access.

⑤ The on-line version of this article (available at http://www.jbc.org) contains supplemental Figs. 1–4.

1 To whom correspondence should be addressed: National Centre for Biomolecular Research, Masaryk University, Kamenice 5/A4, Brno 62500, Czech Republic. Tel.: 420-549493767; Fax: 420-549492556; E-mail: lkrejci@chemi.muni.cz.

2 The abbreviations used are: CPT, camptothecin; HU, hydroxyurea; HJ, Holliday junction; SC, synthetic complete; nt, nucleotide(s); dsDNA and ssDNA, double-stranded and single-stranded DNA, respectively; FITC, fluorescein isothiocyanate.

Several models have been postulated in regard to the role of homologous recombination in processing stalled, blocked, and collapsed replication forks as well as their restart (3, 5, 6, 10). Furthermore, Mus81 was suggested to be required for processing recombination intermediates that form downstream of collapsed replication forks (18). In these models recombinational processing or repair of the damaged or collapsed forks is initiated via the assembly of the Rad51 nucleoprotein filament on single-stranded DNA to mediate the invasion of the sister chromatid. The product of this DNA strand invasion reaction is a structure called a D-loop, and this step appears to be enhanced by the Swi2/Snf2-like factor Rad54 (19, 20). Interestingly, Mus81 was initially identified in a two-hybrid screen for Rad54 interaction partners (14). Here, using purified proteins, we show a direct association between Rad54 and Mus81 and present data to reveal a dramatic stimulation of the Mus81·Mms4 nuclease activity by Rad54. In addition, we demonstrate that the ATP binding and hydrolysis by Rad54 is not required for Mus81·Mms4 enhancement and that Rad54 acts by targeting the Mus81·Mms4 complex to its substrates. We discuss the biological significance of the physical and functional interactions between Rad54 and Mus81·Mms4 (Eme1).

EXPERIMENTAL PROCEDURES

Purification of Rad54 Protein and Mutants—The expression and purification of Rad54 was carried out as described by Raschle *et al.* (21) with slight modifications. The cells (30 g) were resuspended in 200 ml of lysis buffer C (50 mM Tris-HCl, pH 7.5, 10% sucrose, 10 mM EDTA, 1 mM dithiothreitol, 0.01% Nonidet P-40, protease inhibitors) containing 0.6 M KCl and lysed by sonication. All subsequent steps were performed at 4 °C. The lysate was clarified by centrifugation for 50 min at $100,000 \times g$ and applied sequentially onto a 20-ml Q-Sepharose (Amersham Biosciences) column and a 20-ml SP-Sepharose (Amersham Biosciences) column. The SP-Sepharose column was developed with a 210-ml gradient of 150–1000 mM KCl in buffer K (20 mM K_2HPO_4, pH 7.5, 20% glycerol and 0.5 mM EDTA, 0.01% Nonidet P-40, and 1 mM β-mercaptoethanol). *Saccharomyces cerevisiae* Rad54 protein was eluted at 400 mM KCl, and the peak fractions were mixed with 1 ml of His-Select nickel affinity gel (Sigma) for 30 min. The beads were washed with buffer K containing 10 mM imidazole and 600 mM KCl and eluted with a step-gradient using 50, 150, and 270 mM imidazole in buffer K. The 50 and 150 mM imidazole fractions were concentrated in a Vivaspin concentrator (Sigma) and stored in small portions at −80 °C. The human Rad54 protein and *S. cerevisiae* rad54-K341A and rad54-K341R mutant proteins were expressed and purified according to published procedures (22, 23). The concentration of all these proteins was determined by densitometric scanning of SDS-polyacrylamide gels containing multiple loadings of purified proteins against known quantities of bovine serum albumin.

Purification of Mus81 and Mus81·Mms4—The *Escherichia coli* protein expression constructs were generous gifts from Steven Brill (Rutgers University). Protein expression and purification was based on a previously described procedure (18). *E. coli* cells (21 g of cell paste) were resuspended in 80 ml of cell lysis buffer C containing 150 mM KCl. After sonication, the crude lysate was clarified by centrifugation ($100,000 \times g$, 90 min). The clarified lysate was applied sequentially onto Q-Sepharose (20 ml) and then SP-Sepharose (20 ml). Proteins were eluted from SP-Sepharose with a 200-ml gradient of 150–1000 mM KCl in buffer K. Mus81 or Mms4-Mus81 fractions were pooled and mixed with 1 ml of His-Select nickel affinity gel for 1 h at 4 °C. After extensive washing with buffer K containing 150 mM KCl and 10 mM imidazole, the bound proteins were eluted using 50, 150, and 300 mM imidazole in buffer K containing 150 mM KCl. The 150 and 300 mM imidazole fractions were pooled and loaded on a 1 ml hydroxyapatite column (Bio-Rad), and proteins were eluted with a 10-ml gradient from 0 to 500 mM KH_2PO_4 in buffer K. Peak fractions were pooled, loaded onto a 1-ml Mono S column (GE Healthcare), and eluted with a 10-ml gradient from 150 to 1000 mM KCl in buffer K. Pooled fractions were and stored in small portions at −80 °C.

Purification of Mus81·Eme1—The Mus81·Eme1 expression construct was a kind gift from Stephen West (Cancer Research UK), and protein complex was expressed as described (24). Lysate was prepared from 10 g of *E. coli* cell paste using sonication in 50 ml of buffer C containing 150 mM KCl. The cleared lysate was applied sequentially onto a 7-ml Q-Sepharose column and a 7-ml SP-Sepharose column. Proteins were eluted from the SP-Sepharose column with a 70-ml gradient from 150 to 800 mM KCl in buffer K. The peak fractions were pooled and mixed with 1 ml of His-Select nickel affinity gel for 2 h at 4 °C. The column was washed with 10 ml of buffer K containing 150 mM KCl and 10 mM imidazole, and the bound proteins were eluted using 50, 150, 300, and 500 mM imidazole in buffer K containing 150 mM KCl. The 150, 300, and 500 mM imidazole fractions were loaded onto a 1-ml hydroxyapatite column which was eluted with a 10-ml gradient from 0 to 500 mM KH_2PO_4 in buffer K. The peak fractions were concentrated and stored in 5-μl aliquots at −80 °C.

Expression and Purification of Fen1—The plasmid for expression of Fen1 in *E. coli* was a generous gift from Binghui Shen (City of Hope National Medical Center). Fen1 protein was expressed and purified by a method modified from that described for the human FEN-1 protein (25). Lysate was prepared from 6 g of *E. coli* cell paste using sonication in 30 ml of buffer C containing 150 mM KCl. The crude lysate was clarified by centrifugation ($100,000 \times g$, 90 min). The clarified lysate was applied sequentially onto a 7-ml Q-Sepharose column and a 7-ml SP-Sepharose column. The SP-Sepharose column was developed with a 70-ml gradient from 0 to 800 mM KCl in buffer K. The peak fractions were pooled and mixed with 0.5 ml of His-Select nickel affinity gel. The beads were washed with 10 column volumes of buffer K containing 150 mM KCl and 5 mM imidazole. The bound proteins were eluted from the affinity beads using 50, 150, 300, and 500 mM imidazole in buffer K containing 150 mM KCl. The 150, 300, and 500 mM imidazole fractions were pooled and further fractionated in a 0.5-ml Mono S column with a 5-ml gradient of 220 to 700 mM KCl in buffer K. Fractions with purified Fen1 were pooled, concentrated in a Vivaspin concentrator, and then stored in 5-μl aliquots at −80 °C.

DNA Substrates—Oligonucleotides were purchased from VBC Biotech. The sequences of the oligonucleotides and the

structures of DNA substrates made from these oligonucleotides are shown in Table 1. The asterisk in the substrates denotes end modification by a fluorescent dye (fluorescein or Cy3). The substrates were prepared by mixing an equimolar amount of the constituent oligonucleotides in the hybridization buffer (50 mM Tris-HCl, pH 7.5, 100 mM NaCl, 10 mM MgCl$_2$) heated at 90 °C for 3 min and cooled slowly to room temperature to allow DNA annealing. The substrates were purified by fractionation in a 1-ml Mono Q column (GE Healthcare) with a 20-ml gradient of 50–1000 mM NaCl in 10 mM Tris-HCl, pH 7.5. Peak fractions were filtered dialyzed into 50 mM Tris-HCl, pH 7.5, containing 5 mM MgCl$_2$ and concentrated in a Vivaspin concentrator with a 5-kDa cutoff. The concentration of the DNA substrates was determined by absorbance measurement at 260 nm.

Affinity Pulldown Studies—*S. cerevisiae* Rad54-containing protein complexes were captured using S-protein-agarose (Novagen), specific for the S-tag on Rad54. Purified Rad54 (4 μg in Fig. 1*B* and 3 μg in Fig. 1*C*) was incubated with Mus81 (4 μg), Mus81·Mms4 (3 μg), Rad51 (4 μg), or Fen1 (3 μg) in 30 μl of buffer T (20 mM Tris-HCl, pH 7.5, 150 mM KCl, 1 mM dithiothreitol, 0.5 mM EDTA, and 0.01% Nonidet P-40) for 30 min at 4 °C. The reactions were mixed with 15 μl of S-Protein-agarose at 4 °C for 30 min and then treated with DNase I (2 units, New England Biolabs) for 10 min at 37 °C. After washing the beads twice with 150 μl of buffer T, the bound proteins were eluted with 30 μl of 5% SDS. The supernatant, wash, and SDS eluate, 10 μl each, were subject to SDS-PAGE analysis.

Nuclease Assay—The nuclease assay with Mus81·Mms4 was performed essentially as described (18). Reaction mixtures containing the indicated amount of Mus81·Mms4 and 6 nM DNA substrate in 20 μl of buffer N (20 mM Tris, pH 8.0, 100 mM NaCl, 100 μg/ml bovine serum albumin, 0.2 mM dithiothreitol, 5% glycerol, and 10 mM MgCl$_2$) were incubated at 37 °C for the indicated times. After deproteinization by incubation with 0.1% SDS and 500 μg/ml of proteinase K at 37 °C for 10 min, the reactions were mixed with ⅕ volume of loading buffer (60% glycerol, 10 mM Tris-HCl, pH 7.4, 60 mM EDTA, 0.10% Orange G) and resolved in a 10% polyacrylamide gel in TAE buffer (40 mM Tris-HCl, 20 mM sodium acetate, 2 mM EDTA, pH 7.5). The fluorescent DNA species were visualized and quantified in the PharosFX Plus imager with the QuantityOne software (Bio-Rad). The experiment addressing the effect of rad54-K341A and rad54-K341R mutants was done in the presence of 2 mM ATP and ATP-regenerating system (10 μg/ml creatine phosphokinase and 20 mM creatine phosphate). In the Mus81·Mms4 targeting assay (Fig. 7), preincubation of the indicated DNA substrate with Rad54 was for 5 min at 25 °C. The nuclease assay with Mus81·Eme1 or Fen1 was carried out as described (24, 25).

DNA Mobility Shift Assay—Purified *S. cerevisiae* Rad54 (50 or 100 nM) was incubated with the indicated fluorescently labeled substrate (12 nM) at 37 °C in 10 μl of buffer D (40 mM Tris-HCl, pH 7.8, 50 mM KCl, 1 mM dithiothreitol, and 100 μg/ml bovine serum albumin) for 10 min. After the addition of gel loading buffer, the reaction mixtures were resolved in 10% native polyacrylamide gels in TAE buffer at 4 °C and analyzed as above.
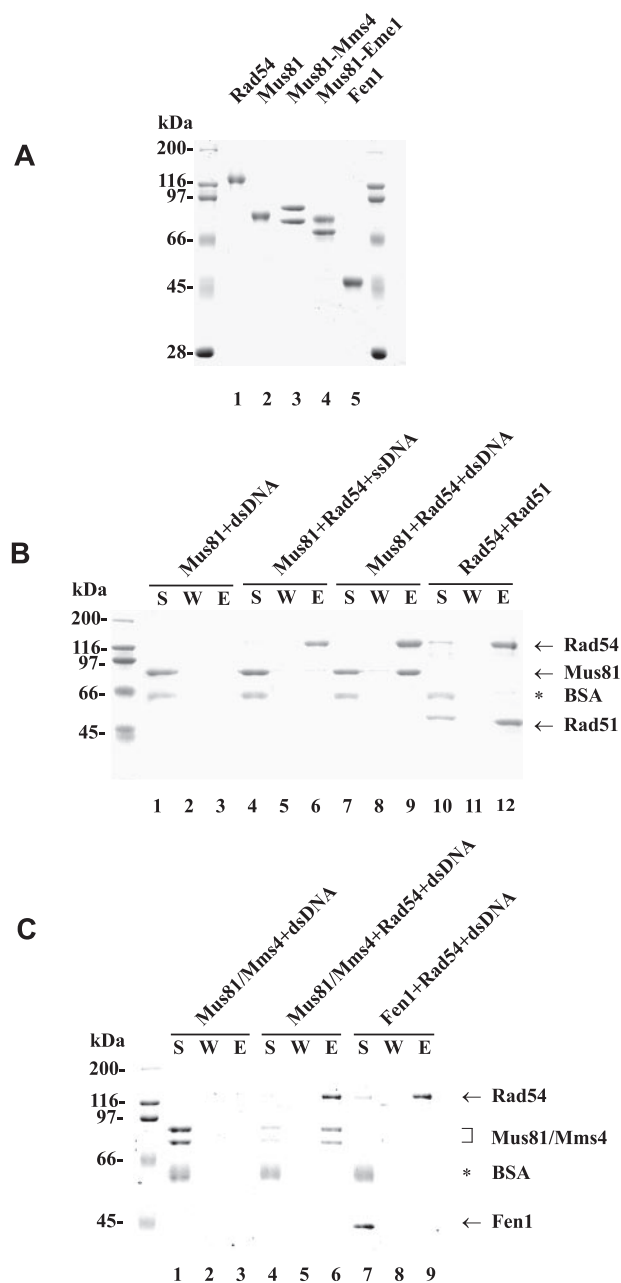
FIGURE 1. **Physical interaction of Rad54 with Mus81 and Mus81·Mms4.** *A*, purified Rad54 (*lane 1*), Mus81 (*lane 2*), Mus81·Mms4 (*lane 3*), Mus81·Eme1 (*lane 4*), and Fen1 (*lane 5*) were resolved by SDS-PAGE and stained with Coomassie Blue. *B*, Mus81 (4 μg) was mixed with S-protein-agarose in the presence of dsDNA (*lane 1–3*) or with S-protein-agarose beads coated with Rad54 (4 μg) in the presence of ssDNA (*lanes 4–6*) or dsDNA (*lanes 7–9*). The beads were incubated with DNase I (2 units), washed, and treated with SDS to elute bound proteins. The supernatant that contained unbound proteins (*S*), the wash (*W*), and the SDS eluate (*E*) were analyzed by SDS-PAGE. As a positive control, Rad51 (4 μg) was mixed with S-protein-agarose beads coated with Rad54 (4 μg) in the absence of DNA (*lanes 10–12*) and then analyzed. *C*, Mus81·Mms4 (3 μg) was mixed with S-protein-agarose beads (*lanes 1–3*) or S-protein-agarose beads coated with Rad54 (3 μg; *lanes 4–6*) in the presence of dsDNA. As a negative control, Fen1 (3 μg) was mixed with S-protein-agarose beads coated with Rad54 (3 μg) in the presence of dsDNA (*lanes 7–9*) and then analyzed. *BSA*, bovine serum albumin.
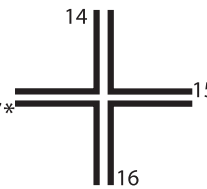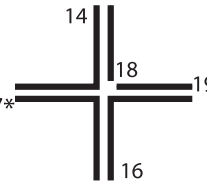
Camptothecin Sensitivity Spot Assays—Cells were grown to mid- to late-log phase and diluted in water to A_{600} of ~0.2. 10-Fold serial dilutions were made in water such that the most

TABLE 1

DNA substrates used in this study

The list includes oligonucleotides used in substrate construction. In each substrate schematic, the numbers denote the constituent oligonucleotides and are positioned at the 5′ end of these oligonucleotides. The asterisk denotes the position of the fluorescent dye (FITC or Cy3).

```
Oligo1:  5′-AGCTACCATGCCTGCACGAATTAAGCAATTCGTAATCATGGTCATAGCT-3′

Oligo2:  5′-AGCTATGACCATGATTACGAATTGCTTAATTCGTGCAGGCATGGTAGCT-3′

Oligo3:  5′-CTACAGTTCGTCAGGATTCC-3′

Oligo4:  5′-AATTCGTGCAGGCATGGTAGCT-3′

Oligo5:  5′-AGCTATGACCATGATTACGAATTGCTT-3′

Oligo6:  5′-AGCTATGACCATGATTACGAATTGCTTGGAATCCTGACGAACTGTAG-3′

Oligo7:  5′-GATGTCAAGCAGTCCTAAGGAATTCGTGCAGGCATGGTAGCT-3′

Oligo8:  5′-GGCATGGTAGCT-3′

Oligo9:  5′-GTGCAGGCATGGTAGCT-3′

Oligo10: 5′-ATTCGTGCAGGCATGGTAGCT-3′

Oligo11: 5′-AGCTATGACCATGATTACGAATTGCTTG-3′

Oligo12: 5′-AGCTATGACCATGATTACGAATTGCTTGGAAT-3′

Oligo13: 5′-AGCTATGACCATGATTACGAATTGCTTGGAATCCTGA-3′

Oligo14: 5′-TGGGTCAACGTGGGCAAAGATGTCCTAGCAATGTAATCGTCTATGACGTT-3′

Oligo15: 5′-TGCCGAATTCTACCAGTGCCAGTGATGGACATCTTTGCCCACGTTGACCC-3′

Oligo16: 5′-GTCGGATCCTCTAGACAGCTCCATGATCACTGGCACTGGTAGAATTCGGC-3′

Oligo17: 5′-CAACGTCATAGACGATTACATTGCTACATGGAGCTGTCTAGAGGATCCGA-3′

Oligo18: 5′-GGACATCTTTGCCCACGTTGACCC-3′

Oligo19: 5′-TGCCGAATTCTACCAGTGCCAGTGAT-3′

Oligo20: 5′-TATAGAACATCTTGCTCTTA-3′

Oligo21: 5′-TAAGAGCAAGATGTTCTATAAAAGATGTCCTAGCAAGGCAC-3′

Oligo22: 5′-GGGTGAACCTGCAGGTGGGCGGCTGCTCATCGTAGGTTAGTTGGTAGAATTCGGCAGCGTC-3′

Oligo23: 5′-GACGCTGCCGAATTCTACCAGTGCCTTGCTAGGACATCTTTGCCCACCTGCAGGTTCACCC-3′
```

concentrated spot contained ~10^5 cells, and the dilutions were spotted on synthetic complete plates (SC), SC + DMSO, or SC + 1 μg/ml CPT (from a stock of 2 mg/ml in DMSO). In all experiments, the SC + DMSO plate mirrored the SC alone plate and, therefore, are not shown. For HU, dilutions were spotted on yeast extract/peptone/dextrose (YPD) or YPD + 200 mM HU. Drugs were added to the agar medium just before pouring the plates.

Live Cell Fluorescent Microscopy—Cells for microscopic analysis were grown and processed as detailed previously (26) with the following changes; cells were harvested by brief centrifugation (3800 × *g*) and resuspended in approximately 10 times the cell pellet volume of growth media. Immobilization of cells was carried out by mixing equal volumes of cell suspension and 1.4% low-melt-agarose (Nu-Sieve 3:1, FMC) plus growth medium solution (held at 42 °C before mixing) on a glass slide. When applicable, cells were treated with γ-irradiation (40 Gy

from a Gammacell-220 ^{60}Co source, Atomic Energy, Ottawa, Canada) or CPT (5 μg/ml) during mid-log phase growth and harvested for microscopy as above at the indicated times.

Images were acquired identically as in Lisby *et al.* (26) on the microscope apparatus described therein. For Mus81-yellow fluorescent protein detection, an exposure time of 3000 ms was used. Images were false-colored and overlaid in Openlab (Improvision, Lexington, MA), then transferred to Adobe Photoshop for scaling.

RESULTS

Association of Rad54 with Mus81 and Mus81·Mms4 Complex Occurs on dsDNA—Results from a yeast two-hybrid screen for Rad54 partner proteins have identified a fragment of Mus81 protein as capable of Rad54 interaction (14). We used purified proteins (Fig. 1*A*) to ascertain Rad54·Mus81 interaction. For this purpose we mixed S- and His$_6$-tagged Rad54 with His$_6$-
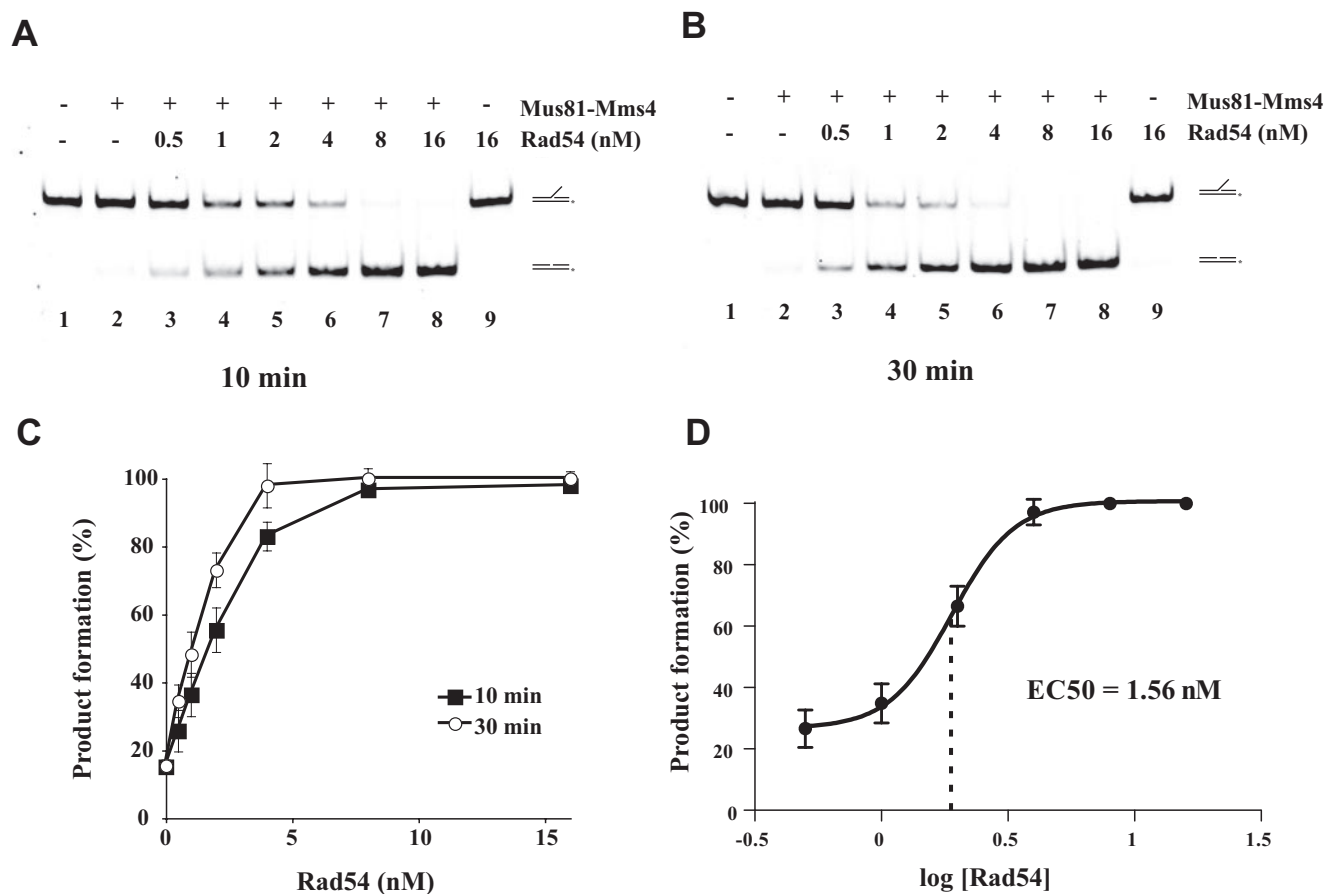
FIGURE 2. **Rad54 concentration-dependent enhancement of Mus81·Mms4-mediated 3′ DNA flap cleavage.** Reaction mixtures containing 3′ DNA flap (6 nM), Mus81·Mms4 (0.25 nM), and the indicated amount of Rad54 (0.5, 1, 2, 4, 8, or 16 nM) were incubated at 37 °C for 10 min (*A*) and 30 min (*B*) and then analyzed. *C*, quantification of the data in *A* and *B* with S.D. based on three independent experiments. *D*, plot of percent of product formation as a logarithm of Rad54 concentration with indicated median effective concentration (EC_{50}).
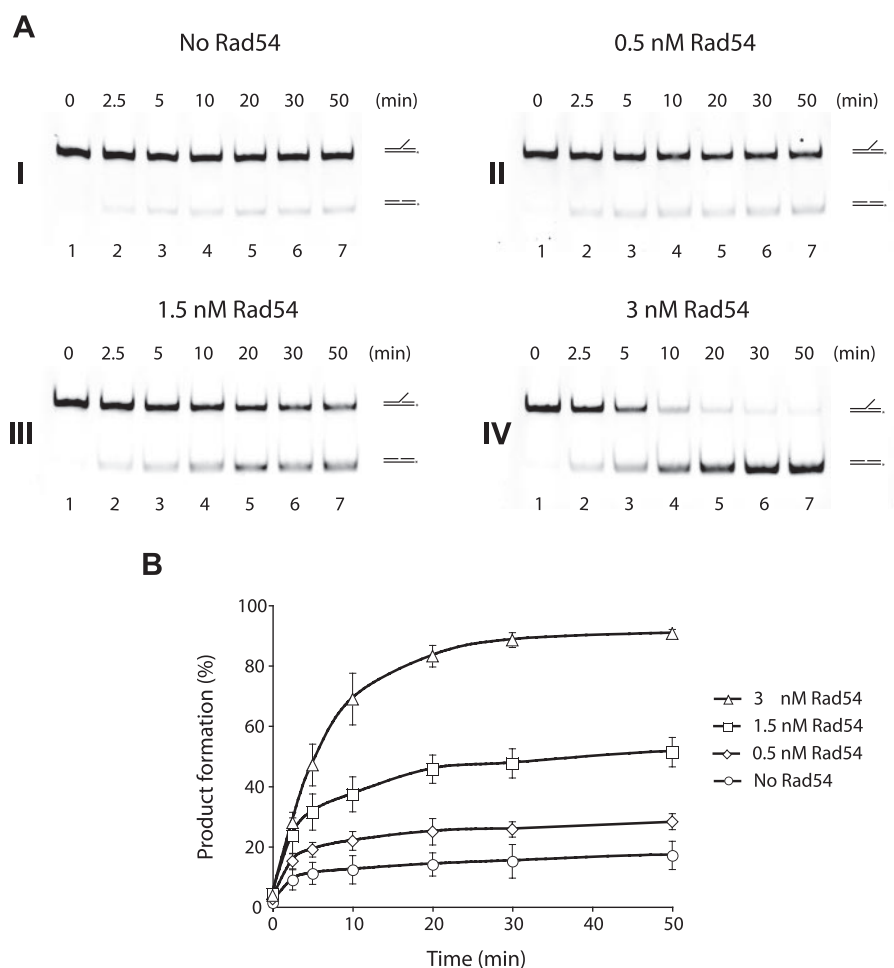
tagged Mus81 or His_6-Mus81·Mms4 and then incubated the reaction mixtures with S-protein conjugated agarose to capture any Rad54 protein complex that might have formed. We eluted the bound proteins from the S-protein-agarose beads with SDS and then analyzed them by SDS-PAGE. However, we were not able to detect any significant association of Rad54 with either Mus81 or Mus81·Mms4 (data not shown). We note that, as determined by co-immunoprecipitation, Interthal and Heyer found only weak or transient interaction between Rad54 and overexpressed Mus81 (14). One strong possibility is that complex formation between Mus81 and Rad54 occurs on DNA. Therefore, we examined this possibility by incubating Rad54 with Mus81 or Mus81·Mms4 in the presence of 49-mer ss- or dsDNA. We used an amount of Rad54 in excess over DNA as determined by binding experiments (supplemental Fig. 1). Furthermore, the mixture was treated with DNase I to ensure that the association was not due to direct bridging of the interaction via free DNA. As shown in Fig. 1, *B* and *C*, only reactions containing dsDNA retained a stoichiometric amount of Mus81 or Mus81·Mms4 on the Rad54-S-protein beads. As expected, Mus81 or Mus81·Mms4 was not retained on the S-protein beads in the absence of Rad54 (Fig. 1, *B* and *C*). The interaction of Mus81 with Rad54 is specific, as Fen1, also a DNA structure-specific endonuclease, did not show any association with Rad54 in the presence of dsDNA (Fig. 1*C*). As reported before (19, 27),

Rad54 forms a complex with Rad51 in the absence of DNA (Fig. 1*B*). Taken together, the results show an ability of Mus81 and Mus81·Mms4 to associate with Rad54 protein in a dsDNA-dependent manner.

Rad54 Binds Branched DNA Substrates Preferentially—The requirement for dsDNA in the Rad54·Mus81 interaction prompted us to test the affinity of yeast Rad54 for DNA structures that Mus81·Mms4 complex is able to cleave. Specifically, we examined the affinity of yeast Rad54 protein toward ssDNA, dsDNA, 3′ flap (3Fl), fork, Y form DNA (Y), intact HJ, and also a nicked HJ (Table 1). To do this increasing amounts of Rad54 protein was incubated with the fluorescently labeled substrates followed by resolution of the reaction mixtures on native polyacrylamide gels. Fluorescence imaging analysis of the gels allowed us to detect and quantify the extent of DNA mobility shift. As shown in supplemental Fig. 1, Rad54 protein bound all these DNA substrates with higher affinity for the branched structures. We note that human Rad54 also prefers to bind similar types of DNA molecules (28).

Rad54 Stimulates Cleavage of 3′ DNA Flap—The physical interaction between Rad54 and Mus81 together with the demonstrated binding preference of Rad54 for substrates that Mus81·Mms4 acts on prompted us to test whether Rad54 might modulate the nuclease activity of the Mus81·Mms4 complex. We first used the 3′ DNA flap substrate, as it is bound by Rad54

A

No Rad54

0   2.5   5   10   20   30   50   (min)

I

1   2   3   4   5   6   7

0.5 nM Rad54

0   2.5   5   10   20   30   50   (min)

II

1   2   3   4   5   6   7

1.5 nM Rad54

0   2.5   5   10   20   30   50   (min)

III

1   2   3   4   5   6   7

3 nM Rad54

0   2.5   5   10   20   30   50   (min)

IV

1   2   3   4   5   6   7

B

FIGURE 3. **Time course of the enhancement of Mus81·Mms4-mediated 3′ DNA flap cleavage by Rad54.** *A*, Mus81·Mms4 (0.25 nM) was incubated with the 3′ DNA flap (6 nM) at 37 °C in the absence (*panel I*) or presence of 0.5, 1.5, or 3 nM Rad54 (*panels II, III*, and *IV*). Aliquots of the reactions were taken at the indicated times and analyzed. *B*, quantification of the data with S.D. based on three independent experiments.

His$_6$ affinity tag on Mms4 does not have any significant effect on the nuclease activity of Mus81·Mms4 or on the enhancement of substrate cleavage by Rad54 (supplemental Fig. 3). Taken together, the results demonstrate that Rad54 can strongly stimulate the ability of Mus81·Mms4 to cleave the 3′ DNA flap structure and also suggest that optimal enhancement is contingent upon oligomerization of Rad54.

Enhancement of Gapped 3′ DNA Flap Cleavage by Rad54—It has been suggested that a crucial determinant for Mus81·Mms4 endonuclease activity is recognition of the 5′ end at the flap junction as the DNA cleavage efficiency declines with increasing DNA gap size in the flap (18). Mus81·Mms4-mediated cleavage of the 3′ DNA flap substrate that harbors a 1-nt gap occurred with a similar efficiency as that of the 3′ DNA flap without any gap (data not shown). However, the cleavage efficiency decreased as the gap size increased to 5 nt and was much lower with a 10-nt gap (Fig. 4*A*). Under the conditions used, the Y substrate was resistant to Mus81·Mms4 cleavage (Fig. 4*A*). Then we tested the ability of Rad54 to stimulate Mus81·Mms4 activity on the gapped 3′ DNA flap struc-

with higher affinity and represents a relevant DNA intermediate that arises during DNA repair or replication. We performed a Rad54 protein titration with 0.25 nM Mus81·Mms4, an amount that could cleave only a small fraction of the substrate (supplemental Fig. 2, *A* and *C*). Importantly, strong enhancement of the Mus81·Mms4 DNA cleavage activity occurred in a Rad54 protein concentration-dependent manner. Flap cleavage was stimulated 3-fold by 1 nM Rad54 and 5-fold by 2 nM Rad54, and complete incision of the substrate was seen when 8 nM Rad54 was added (Fig. 2, *A–C*). The plot of the percent product formed as a logarithmic function of Rad54 concentration yields a sigmoid curve for stimulation, with the median effective concentration EC$_{50}$ = 1.56 nM (Fig. 2*D*). This Rad54 amount corresponds to 6 times that of Mus81·Mms4 heterodimer. Because Rad54 forms oligomeric complexes on DNA (22, 29, 30), our results are consistent with the premise that optimal stimulation of Mus81·Mms4 occurs upon assembly of a Rad54 oligomer. As expected, Rad54 alone was devoid of nucleolytic activity (Fig. 2, *A* and *B, lane 9*). Time course experiments provided further details on the effect of Rad54 on the rate of Mus81·Mms4-mediated DNA cleavage (Fig. 3). We note that the presence of Rad54 does not affect the position of the cleavage site within the flap structure (data not shown). In addition, the presence of

tures. The addition of Rad54 (from 0.5 to 16 nM) resulted in the up-regulation of Mus81·Mms4 (0.25 nM) activity on flaps containing a 1- or 5-nt gap (Fig. 4*B*) without effecting significant cleavage of the flap with the 10-nt gap. Interestingly, at 2 nM Mus81·Mms4 that could afford an ~10% incision of the flap with the 10-nt gap, the addition of Rad54 (from 0.5 to 16 nM) also enhanced DNA cleavage (Fig. 4*C*). In the case of the Y substrate, cleavage was not seen with as high as 10 nM Mus81·Mms4 regardless of whether Rad54 (up to 40 nM) was added or not (Fig. 4*C*).

Cleavage of Nicked HJ and D-loop Structures Is Also Stimulated by Rad54—Next we wanted to test substrates that are known to arise during homologous recombination, including the D-loop, nicked HJ, and intact HJ. As stated elsewhere (8, 18, 24, 31–33) and confirmed here, Mus81·Mms4 has only a limited ability to cleave an intact HJ. Specifically, as much as 65 nM Mus81·Mms4 cleaved only 6% of the HJ after 30 min of incubation (Fig. 4*D*). The addition of up to 400 nM Rad54 had only a slight stimulatory effect (Fig. 4*D*). As reported before (8, 17, 34) and in our hands also, the cleavage of nicked HJs by Mus81·Mms4 was very efficient and was greatly stimulated by Rad54 to the same extent as when the 3′ DNA flap substrate was used (Fig. 4, *E* and *F*). In addition, we also tested the ability of Rad54
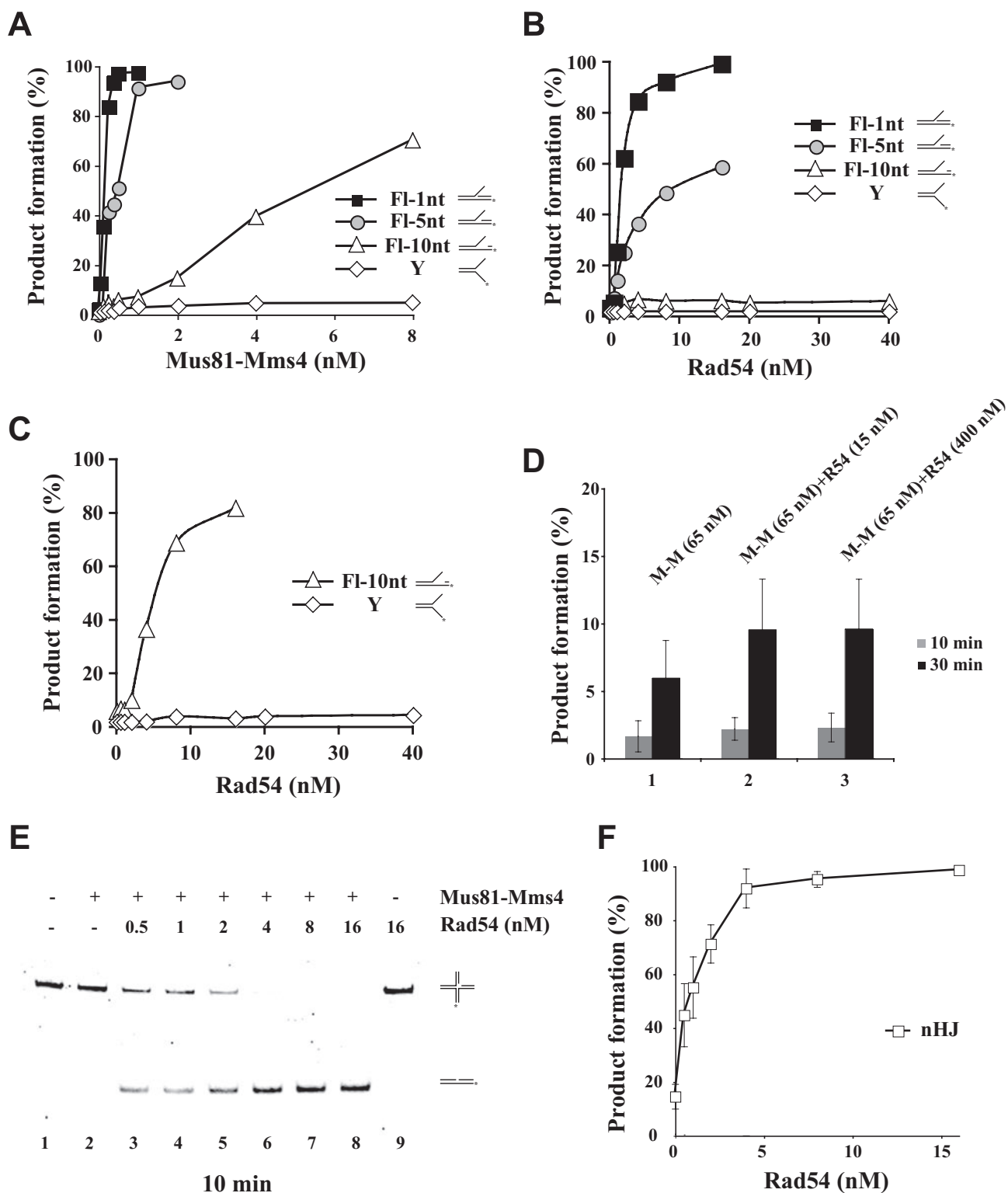
FIGURE 4. **Effect of Rad54 on Mus81·Mms4 cleavage of 3′ DNA flap substrates with varying gap sizes.** *A*, cleavage of 3′ DNA flap (*Fl*) substrates with increasing gap size (1, 5, or 10 nt) and of Y form DNA. Each of these substrates (6 nM) was incubated with Mus81·Mms4 (0.13, 0.25, 0.5, 1, 2, 4, or 8 nM) at 37 °C for 30 min and then analyzed. *B*, reaction mixtures containing gapped 3′ DNA flaps or Y form DNA (6 nM each), Mus81·Mms4 (0.25 nM), and the indicated amounts of Rad54 (0.5, 1, 2, 4, 8, or 16 nM) were incubated at 37 °C for 30 min and then analyzed. *C*, Mus81·Mms4 (2 nM) was incubated with the 3′ DNA flap containing a 10-nt gap and Rad54 (0.5, 1, 2, 4, 8, 16, 20, or 40 nM) at 37 °C for 30 min and then analyzed. For the Y form DNA substrate, 10% of cleavage could not be achieved; therefore, 10 nM Mus81·Mms4 was incubated with the indicated amounts of Rad54 (0.5, 1, 2, 4, 8, 16, 20, or 40 nM) at 37 °C for 30 min and then analyzed. *D*, Rad54 has little effect on the cleavage of an intact HJ. The HJ substrate (2 nM) was incubated with Mus81·Mms4 (65 nM) and with or without Rad54 (15 or 400 nM) at 37 °C for 30 min and then analyzed. Quantification of the data with S.D. was based on three independent experiments. *E*, cleavage of a nicked HJ (2 nM) by Mus81·Mms4 (0.05 nM) is greatly stimulated by Rad54 (0.5, 1, 2, 4, 8, or 16 nM) in a dose-dependent manner. *F*, graphical representation of the data shown in *panel E* with S.D. based on three independent experiments.
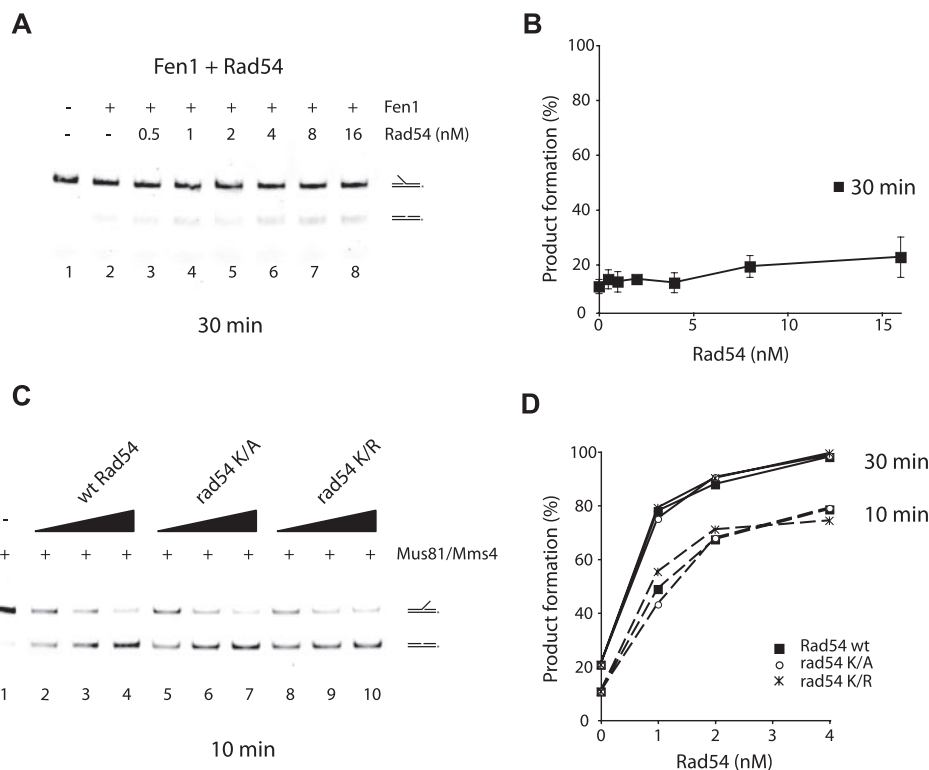
A

B

C

D
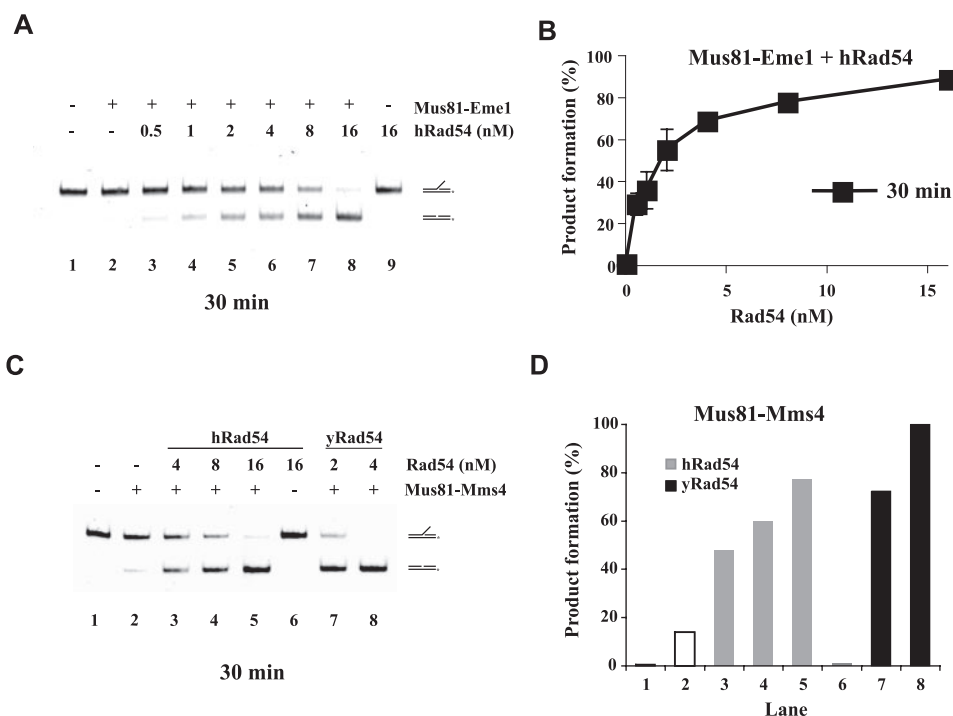
FIGURE 5. **Enhancement of the human Mus81·Eme1 nuclease function by human Rad54.** *A*, the 3′ DNA flap substrate (6 nM) was incubated with human Mus81·Eme1 (0.13 nM) and without or with human Rad54 (*hRad54*) (0.5, 1, 2, 4, 8, or 16 nM) at 37 °C for 30 min and then analyzed. *B*, quantification of the data shown in *panel A*. *C*, human Rad54 enhances the nuclease activity of Mus81·Mms4. The 3′ DNA flap (6 nM) was incubated with Mus81·Mms4 (0.25 nM) and the indicated amounts of human Rad54 (4, 8, or 16 nM) or yeast Rad54 (*yRad54*, 2 or 4 nM) at 37 °C for 30 min and then analyzed. *D*, quantification of the data shown in *C*.

A

B

C

D

FIGURE 6. **ATP binding and hydrolysis by Rad54 is dispensable for Mus81·Mms4 enhancement.** *A*, the nuclease activity of Fen1 is unresponsive to Rad54. The 5′ DNA flap (6 nM) was incubated with Fen1 (2 nM) without or with Rad54 (0.5, 1, 2, 4, 8, or 16 nM) at 37 °C for 30 min and then analyzed. *B*, quantification of the data shown in *panel A* with S.D. based on three independent experiments. *C*, the 3′ DNA flap (6 nM) was incubated in buffer containing ATP with Mus81·Mms4 (0.25 nM) and Rad54, rad54-K341A, or rad54-K341R (1, 2, or 4 nM concentrations of each protein) at 37 °C for 10 min and then analyzed. *wt*, wild type. *D*, the data from the 10- and 30-min time points of the experiment in *C* were plotted.

to activate the cleavage of a D-loop substrate by Mus81·Mms4, and a similar level of stimulation was observed (supplemental Fig. 4). In summary, Rad54 is able to dramatically increase the DNA cleavage activity of Mus81·Mms4 on the D-loop and nicked HJ but has little or no effect on the cleavage of the intact HJ.

Stimulation of Mus81 Activity by Rad54 Is Evolutionarily Conserved—To determine whether the functional interaction of Rad54 with Mus81 is evolutionarily conserved, we examined the effect of human Rad54 on the nuclease activity of the human Mus81·Eme1 complex. We used the 3′ DNA flap substrate and demonstrated that the addition of human Rad54 (0.5–16 nM) to the reaction containing 0.13 nM Mus81·Eme1 resulted in a robust enhancement of nuclease activity (Fig. 5, *A* and *B*). The extent of stimulation was similar to that obtained with the equivalent yeast proteins.
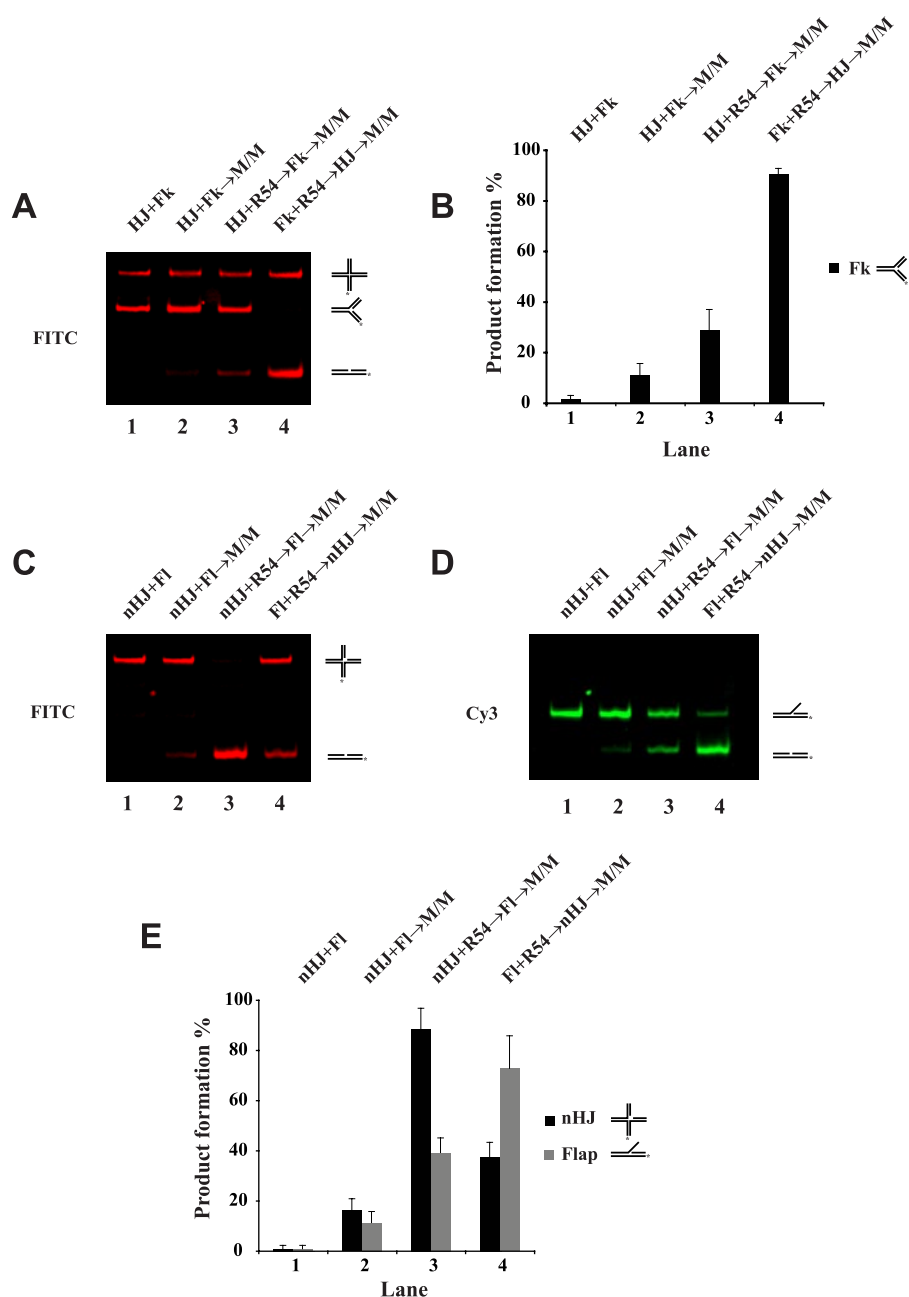
We next asked whether human and yeast Rad54 proteins are interchangeable with regard to the enhancement of the Mus81·Mms4 (Eme1) nuclease function. As shown in Fig. 5, *C* and *D*, hRad54, at the relatively higher concentration of 4–16 nM, exerted a 2.5–5-fold stimulatory effect on the Mus81·Mms4 (0.25 nM) activity. Similarly, yeast Rad54, at the relatively high concentration of 4–16 nM, was also able to stimulate Mus81·Eme1 (0.13 nM) by about 3-fold (data not shown). On the other hand, yeast Rad54 does not have any effect on the activity of another DNA structure-specific nuclease, Fen1 (Fig. 6, *A* and *B*). Overall, the results in this section provide evidence that the Rad54-mediated enhancement of the Mus81·Mms4 (Eme1) nuclease function is specific and evolutionarily conserved.

ATP Binding and Hydrolysis by Rad54 Is Dispensable for Mus81· Mms4 Nuclease Enhancement—Rad54 possesses a dsDNA-dependent ATPase activity (19, 35). We sought to establish the role of ATP

FIGURE 7. **Substrate targeting of Mus81·Mms4 by Rad54.** The DNA substrate pairs (the HJ and the DNA fork (*Fk*) in *A*; the nicked Holliday junction (*nHJ*) and 3′ DNA flap (*Fl*) in *C* and *D*), 3 nM each, were incubated with Mus81·Mms4 (*M/M*; 0.25 nM) and Rad54 (*R54*; 2 nM) in the indicated orders at 37 °C for 20 min and then analyzed. The reaction mixtures that contained FITC-labeled HJ and Fk are shown in *A*, and the results with S.D. based on three independent experiments are presented in the histogram in *B*. The reactions that contained FITC-labeled nicked HJ and Cy3-labeled Fl are shown in *C* and *D*, and the results with S.D. based on three independent experiments are presented in the histogram in *E*.

Rad54 Targets Mus81·Mms4 Complex to the DNA Substrate— Because our results have suggested that physical interaction between Rad54 and Mus81 or Mus81·Mms4 occurs when these protein species are DNA-bound (Fig. 1), we asked whether Rad54 serves to target Mus81·Mms4 to various DNA substrates. We set up two experiments using mixtures of different substrates to address this possibility. In one reaction Rad54 (2 nM) was pre-incubated with a non-cleavable intact HJ before the cleavable DNA fork substrate was added together with Mus81·Mms4 (0.25 nM). This resulted in a modest stimulation of DNA fork cleavage compared with the control reaction without Rad54 (Fig. 7, *A* and *B*, compare *lanes 2* and *3*). On the other hand, preincubation of Rad54 with the fork substrate resulted in strong stimulation of its cleavage (~9-fold) (Fig. 7, *A* and *B*, *lane 4*). In the other assay we used two cleavable substrates, a nicked HJ and a 3′ DNA flap, labeled with FITC and Cy3 fluorescent dyes, respectively, to allow us to distinguish the products resulting from the cleavage of these substrates. Preincubation with Rad54 again led to a greater enhancement of substrate cleavage (Fig. 7, *C–E*, compare *lanes 3* and *4*). Altogether these results suggest that Rad54 acts by targeting the Mus81·Mms4 complex to its cleavage substrate, and it does not seem to function in *trans*.

Epistatic Relationship of Rad54 and Mus81— Previous genetic analysis showed that Rad54 and Mus81 act together in the recombination pathway for the repair of γ-ray induced DNA damage (14). We wanted to investigate their relationship in regard to the removal of replication-blocking damage. Therefore, we tested sensitivities of *rad54*, *mus81*, or the double mutant to CPT and HU, which impede DNA replication by poisoning topoisomerase I and ribonucleotide reductase, respectively. As shown in Fig. 8, *A* and *B*, the *mus81 rad54* double mutant was no more sensitive to CPT or HU than the *rad54* single mutant. Thus, *RAD54* and *MUS81* likely act in the same pathway for the repair of injured DNA replication forks.

This observation together with our biochemical data prompted us to test whether Rad54 and Mus81 co-localize *in vivo* with or without DNA damaging treatment. Only about 5%
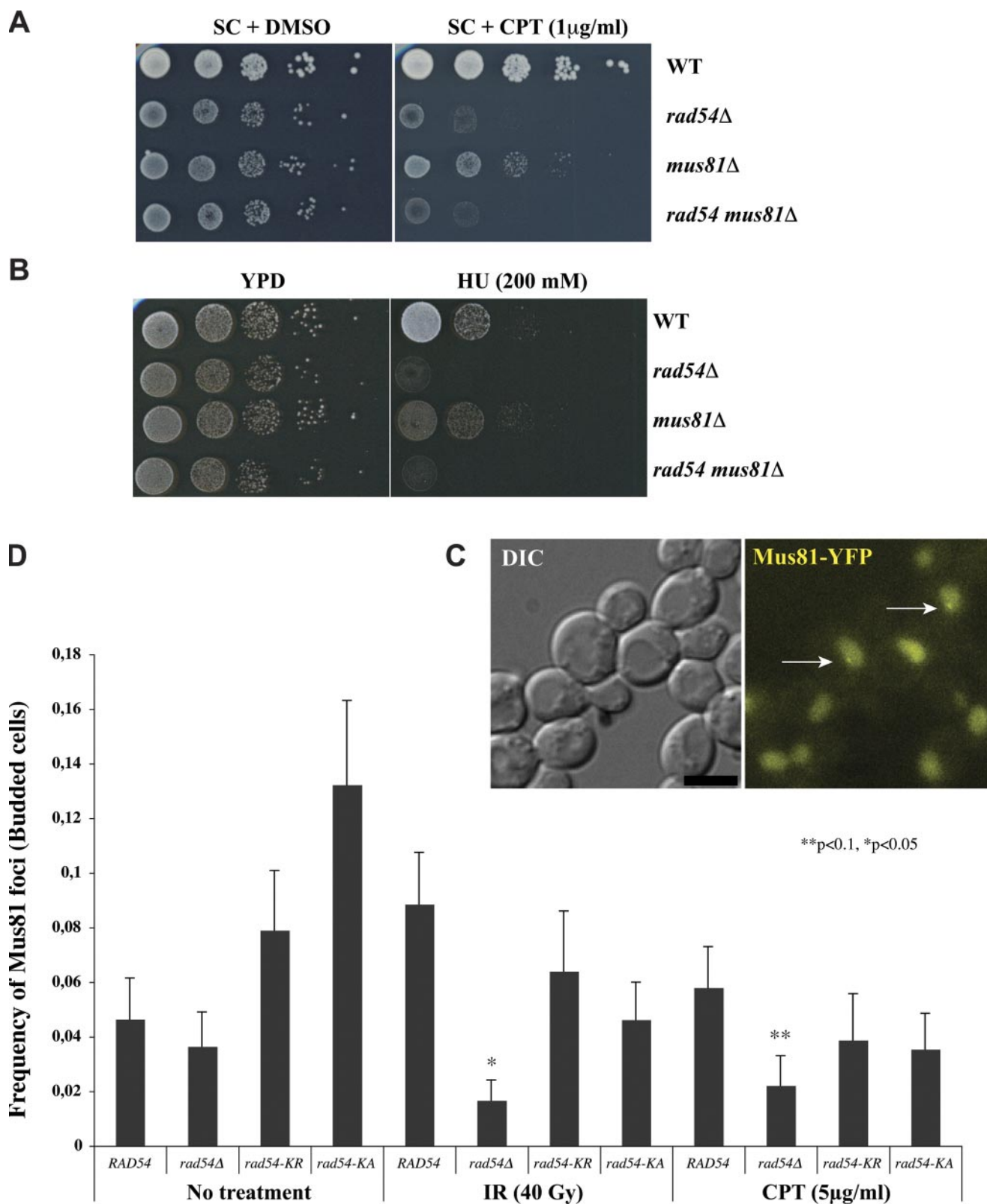
binding and hydrolysis in the Rad54-mediated stimulation of the Mus81·Mms4 nuclease activity. For this purpose we used two mutants, rad54-K341A and rad54-K341R, that are expected to be defective in interaction with ATP and to retain the ability to bind but not hydrolyze ATP, respectively (22). As shown in Fig. 6, *C* and *D*, rad54-K341A and rad54-K341R were just as proficient as the wild type protein in enhancing the cleavage of the 3′ flap DNA by Mus81·Mms4 in the presence of ATP, thus formally establishing that the up-regulation of the Mus81·Mms4 nuclease function does not require binding or hydrolysis of ATP by Rad54.

FIGURE 8. **Epistatic relationship of Rad54 and Mus81.** Sensitivity of wild type (*WT*), *mus81Δ*, *rad54Δ*, and double mutant cells to DNA-damaging agents was assayed by growth on plates containing the indicated concentrations of CPT (*A*) or HU (*B*). *YPD*, yeast extract/peptone/dextrose. *C*, representative maximum intensity projection image of CPT-induced Mus81-yellow fluorescent protein (YFP) foci (indicated by *arrows*). Images were captured 5 h after treatment. *Scale bar*, 3 μm. *DIC*, differential interference contrast. *D*, quantification of Mus81 foci in *RAD54*, *rad54Δ*, *rad54-K341A* (*rad54-K/A*), and *rad54-K341R* (*rad54-K/R*) genetic backgrounds. IR-treated cells were examined for foci 3 h after treatment. CPT-treated cells were examined 5 h post-treatment. *Bars* indicate the frequency of Mus81 foci observed in S phase or G_2/M cells (*Budded cells*). *Error bars* depict the binomial S.E. Significance from the wild type was determined by a χ^2 test.

of the budded cells contained spontaneous Mus81 foci, and this formation was induced to 9% by DNA damage treatment. In contrast to frequent and bright Rad54 foci (~70% of budded cells after DNA damage treatment, data not shown), Mus81 foci were quite dim (Fig. 8*C*), suggesting that these foci contain only very few Mus81·Mms4 molecules. Interestingly, we noticed only transient co-localization of both proteins (data not shown), which is in agreement with the nature of this protein-protein interaction seen in a biochemical pulldown. Importantly, deletion of the *RAD54* gene causes a significant reduction of Mus81 focus formation especially in the presence of DNA damage (Fig. 8*D*). However, Mus81 focus formation is decreased only by the absence of Rad54 but not by the lack of Rad54 ATPase activity, as both the *rad54-K341R* and *rad54-K341A* mutants are still able to assemble DNA damage-induced Mus81 foci (Fig. 8*D*). Taken together, our results suggest that Rad54 and Mus81 function together in the repair of chromosome damage caused by γ-rays as well as replication blocking agents and that the ATPase activity of Rad54 is dispensable in this regard.

DISCUSSION

The Mus81·Mms4 (Eme1) complex is believed to be responsible for processing intermediates of homologous recombination as well as those derived from stalled, blocked, and broken replication forks. However, the manner in which the activities of Mus81·Mms4 are connected to these cellular processes is still not clear. Interestingly, Mus81 was first identified in a two-hybrid screen for Rad54 interacting partners, and this interaction seems to be evolutionary conserved from yeast to humans (14, 36, 37). Rad54 is one of the key proteins involved in homologous recombination. It interacts with the Rad51 recombinase, promotes the assembly and stability of Rad51 filament, stimulates D-loop formation, and could allow Rad51 filament to engage in homology search. In addition, Rad54 removes Rad51 from dsDNA, remodels chromatin structure, and also promotes the migration of branched DNA structures (38, 39).

We have presented data showing a direct physical interaction of Rad54 with Mus81 and the Mus81·Mms4 complex when dsDNA is present. It is possible that the two-hybrid signal of Mus81·Rad54 interaction reflects a transient association of these proteins or that it stems from an interaction of these proteins on DNA (14). We note that even though yeast Rad52 binds RPA in the yeast two-hybrid assay (40), significant complex formation between the two purified proteins requires ssDNA (41). We also show that the association of Rad54 with Mus81·Mms4 leads to a strong stimulation of the nuclease activity of the latter on a variety of substrates and that cleavage by human Mus81·Eme1 is similarly enhanced by human Rad54, indicating evolutionary conservation of the functional interaction between these two protein species. We note that while our work was undergoing peer review, a paper by Mazina and Mazin (42) showing enhancement of the Mus81·Eme1 nuclease activity by human Rad54 had appeared. Rad54 possesses ATP-dependent branch migration activity on Holliday junctions (43, 44). Our results and those of Mazina and Mazin (42) provide biochemical and biological insights linking the ability of Rad54 to promote D-loop formation (19) and branch migration of late

recombination intermediates (43, 44) with the nucleolytic processing of replication and/or recombination intermediates by Mus81·Mms4 (Eme1).

Interestingly, neither ATP binding nor its hydrolysis by Rad54 is needed for the stimulation of Mus81·Mms4 nuclease activity *in vitro*. Genetic results presented here and elsewhere (14) establish that Rad54 and Mus81 function together in the same pathways of DNA damage and replication fork repair and that the assembly of DNA damage-induced Mus81 foci is dependent on Rad54. Both the *rad54-K341R* and *rad54-K341A* mutants are still able to assemble DNA damage-induced Mus81 foci. This observation is in congruence with a less severe defect in recombination rates for both mutants compared with the *rad54Δ* mutant (22). However, we expect the dsDNA translocase and DNA branch migration activities of Rad54 (30, 43–46) to facilitate the formation of substrates that are resolved by the Mus81·Mms4 complex *in vivo*. The yeast *mus81* and *rad54* mutants fall into the same epistasis group regarding γ-ray sensitivity (14), and we have presented data showing epistasis of these mutants in the repair of damaged replication forks as well. We note that homologous recombination mediated by Mus81·Eme1 and Rad54 is needed for the DNA replication-dependent interstrand DNA cross-link repair pathway in human cells, with Mus81 contributing to replication restart by generating double-strand breaks (13, 47, 48). In addition, the yeast *mus81* and *mms4* mutants are inviable in the absence of the Sgs1 helicase, which is thought to act in conjunction with Top3 and Rmi1 to resolve late recombination intermediates, such as the double Holliday junction, to generate non-crossover recombinants (18, 49). Thus, Rad54 together with Mus81·Mms4 (Eme1) comprises an alternative mechanism for the resolution of DNA intermediates parallel to the Sgs1·Top3 (BLM·Top3) pathway. Both *mus81* and *mms4* mutants show severe meiotic phenotypes as a result of unprocessed recombination intermediates that activate a meiotic checkpoint (50, 51). Importantly, defects in the initiation of recombination are able to overcome the *sgs1* synthetic lethality in both budding and fission yeasts (8, 15, 51). Overall, the available evidence is consistent with the premise that Mus81·Mms4 (Eme1) helps to resolve otherwise toxic recombination intermediates in mitotic and meiotic cells, and our biochemical data reveal an involvement of Rad54 in the enhancement of these Mus81·Mms4 (Eme1) activities.

There has been much discussion regarding the possible role of Mus81·Mms4 in the nucleolytic resolution of intact HJs. We have confirmed that a nicked HJ is more efficiently cleaved by Mus81·Mms4 than an intact HJ. Although Rad54 renders the Mus81·Mms4-mediated cleavage of flap substrates efficiently, it has only minimal stimulatory effect on the cleavage of an intact HJ. This result argues against Mus81·Mms4 acting to resolve HJ structures in cells and is consistent with the suggestion that the cleavage of intact HJs reflects a secondary effect of Mus81·Mms4 flap cleavage activity (24). Furthermore, the efficient cleavage of nicked HJ structure supports a mechanism by which Mus81·Mms4 could act on the nascent D-loop before it is converted into an intact HJ. As discussed by others previously, Mus81·Mms4-mediated D-loop cleavage may favor crossover production during meiosis and could account for the

decrease in crossovers observed for *mus81* mutants (10). However, one cannot exclude the possibility that there is another partner of Mus81·Mms4 that allows the latter to act on intact HJs in cells (52–54).

The successful assembly of a Rad51 nucleoprotein filament is a prerequisite for Rad54 recruitment to recombination substrates in cells (26, 27, 55, 56) placing Rad54 in temporal and spatial arrangement to mediate later steps in recombination. During these steps, via its ability to stimulate the recombinase activity of Rad51 and to migrate branched DNA structures (43, 44), Rad54 is expected to mediate the formation of certain DNA structures, such as the D-loop or nicked Holliday junction, that are subject to nucleolytic processing by the Mus81·Mms4 complex. In this regard, Rad54 likely targets Mus81·Mms4 to these structures to affect their processing. However, from genetic experiments (6, 39), it seems clear that Mus81·Mms4 and Rad54 also possess additional functions during meiotic or damage-induced double-strand break repair.

Recently, the human BLM helicase was also shown to stimulate the nuclease activity of the Mus81·Eme1 complex, albeit to a lesser degree than what we have documented for Rad54 (57). Interestingly, both BLM and Rad54 are capable of mediating the migration of branched DNA structures. The lesser ability of BLM to activate Mus81·Eme1 could reflect a role of BLM as a backup to the Rad54-mediated up-regulation of the Mus81·Eme1 nuclease function.

REFERENCES

1. Heller, R. C., and Marians, K. J. (2006) *Nature* **439,** 557–562
2. Lehmann, A. R. (2003) *Cell Cycle* **2,** 300–302
3. McGlynn, P., and Lloyd, R. G. (2002) *Nat. Rev. Mol. Cell Biol.* **3,** 859–870
4. Michel, B., Flores, M. J., Viguera, E., Grompone, G., Seigneur, M., and Bidnenko, V. (2001) *Proc. Natl. Acad. Sci. U. S. A.* **98,** 8181–8188
5. Higgins, N. P., Kato, K., and Strauss, B. (1976) *J. Mol. Biol.* **101,** 417–425
6. Osman, F., and Whitby, M. C. (2007) *DNA Repair* **6,** 1004–1017
7. Haber, J. E., and Heyer, W. D. (2001) *Cell* **107,** 551–554
8. Kaliraman, V., Mullen, J. R., Fricke, W. M., Bastin-Shanower, S. A., and Brill, S. J. (2001) *Genes Dev.* **15,** 2730–2740
9. Mullen, J. R., Kaliraman, V., Ibrahim, S. S., and Brill, S. J. (2001) *Genetics* **157,** 103–118
10. Hollingsworth, N. M., and Brill, S. J. (2004) *Genes Dev.* **18,** 117–125
11. Boddy, M. N., Lopez-Girona, A., Shanahan, P., Interthal, H., Heyer, W. D., and Russell, P. (2000) *Mol. Cell. Biol.* **20,** 8758–8766
12. Chen, C., and Kolodner, R. D. (1999) *Nat. Genet.* **23,** 81–85
13. Hiyama, T., Katsura, M., Yoshihara, T., Ishida, M., Kinomura, A., Tonda, T., Asahara, T., and Miyagawa, K. (2006) *Nucleic Acids Res.* **34,** 880–892
14. Interthal, H., and Heyer, W. D. (2000) *Mol. Gen. Genet.* **263,** 812–827
15. Boddy, M. N., Gaillard, P. H., McDonald, W. H., Shanahan, P., Yates, J. R., III, and Russell, P. (2001) *Cell* **107,** 537–548
16. Chen, X. B., Melchionna, R., Denis, C. M., Gaillard, P. H., Blasina, A., Van de Weyer, I., Boddy, M. N., Russell, P., Vialard, J., and McGowan, C. H. (2001) *Mol. Cell* **8,** 1117–1127
17. Gaillard, P. H., Noguchi, E., Shanahan, P., and Russell, P. (2003) *Mol. Cell* **12,** 747–759
18. Bastin-Shanower, S. A., Fricke, W. M., Mullen, J. R., and Brill, S. J. (2003) *Mol. Cell. Biol.* **23,** 3487–3496
19. Petukhova, G., Stratton, S., and Sung, P. (1998) *Nature* **393,** 91–94
20. Sung, P., Krejci, L., Van Komen, S., and Sehorn, M. G. (2003) *J. Biol. Chem.* **278,** 42729–42732
21. Raschle, M., Van Komen, S., Chi, P., Ellenberger, T., and Sung, P. (2004) *J. Biol. Chem.* **279,** 51973–51980
22. Petukhova, G., Van Komen, S., Vergano, S., Klein, H., and Sung, P. (1999) *J. Biol. Chem.* **274,** 29453–29462
23. Sigurdsson, S., Van Komen, S., Petukhova, G., and Sung, P. (2002) *J. Biol. Chem.* **277,** 42790–42794
24. Ciccia, A., Constantinou, A., and West, S. C. (2003) *J. Biol. Chem.* **278,** 25172–25178
25. Qiu, J., Qian, Y., Frank, P., Wintersberger, U., and Shen, B. (1999) *Mol. Cell. Biol.* **19,** 8361–8371
26. Lisby, M., Barlow, J. H., Burgess, R. C., and Rothstein, R. (2004) *Cell* **118,** 699–713
27. Clever, B., Interthal, H., Schmuckli-Maurer, J., King, J., Sigrist, M., and Heyer, W. D. (1997) *EMBO J.* **16,** 2535–2544
28. Mazina, O. M., Rossi, M. J., Thomaa, N. H., and Mazin, A. V. (2007) *J. Biol. Chem.* **282,** 21068–21080
29. Kiianitsa, K., Solinger, J. A., and Heyer, W. D. (2006) *Proc. Natl. Acad. Sci. U. S. A.* **103,** 9767–9772
30. Ristic, D., Wyman, C., Paulusma, C., and Kanaar, R. (2001) *Proc. Natl. Acad. Sci. U. S. A.* **98,** 8454–8460
31. Constantinou, A., Chen, X. B., McGowan, C. H., and West, S. C. (2002) *EMBO J.* **21,** 5577–5585
32. Fricke, W. M., Bastin-Shanower, S. A., and Brill, S. J. (2005) *DNA Repair* **4,** 243–251
33. Whitby, M. C., Osman, F., and Dixon, J. (2003) *J. Biol. Chem.* **278,** 6928–6935
34. Osman, F., Dixon, J., Doe, C. L., and Whitby, M. C. (2003) *Mol. Cell* **12,** 761–774
35. Swagemakers, S. M., Essers, J., de Wit, J., Hoeijmakers, J. H., and Kanaar, R. (1998) *J. Biol. Chem.* **273,** 28292–28297
36. Hanada, K., Budzowska, M., Modesti, M., Maas, A., Wyman, C., Essers, J., and Kanaar, R. (2006) *EMBO J.* **25,** 4921–4932
37. Mimida, N., Kitamoto, H., Osakabe, K., Nakashima, M., Ito, Y., Heyer, W. D., Toki, S., and Ichikawa, H. (2007) *Plant Cell Physiol.* **48,** 648–654
38. San Filippo, J., Sung, P., and Klein, H. (2008) *Annu. Rev. Biochem.* **77,** 229–257
39. Tan, T. L., Kanaar, R., and Wyman, C. (2003) *DNA Repair* **2,** 787–794
40. Hays, S. L., Firmenich, A. A., Massey, P., Banerjee, R., and Berg, P. (1998) *Mol. Cell. Biol.* **18,** 4400–4406
41. Seong, C., Sehorn, M. G., Plate, I., Shi, I., Song, B., Chi, P., Mortensen, U., Sung, P., and Krejci, L. (2008) *J. Biol. Chem.* **283,** 12166–12174
42. Mazina, O. M., and Mazin, A. V. (2008) *Proc. Natl. Acad. Sci. U. S. A.* **105,** 18249–18254
43. Bugreev, D. V., Hanaoka, F., and Mazin, A. V. (2007) *Nat. Struct. Mol. Biol.* **14,** 746–753
44. Bugreev, D. V., Mazina, O. M., and Mazin, A. V. (2006) *Nature* **442,** 590–593
45. Amitani, I., Baskin, R. J., and Kowalczykowski, S. C. (2006) *Mol. Cell* **23,** 143–148
46. Van Komen, S., Petukhova, G., Sigurdsson, S., Stratton, S., and Sung, P. (2000) *Mol. Cell* **6,** 563–572
47. Abraham, J., Lemmers, B., Hande, M. P., Moynahan, M. E., Chahwan, C., Ciccia, A., Essers, J., Hanada, K., Chahwan, R., Khaw, A. K., McPherson, P., Shehabeldin, A., Laister, R., Arrowsmith, C., Kanaar, R., West, S. C., Jasin, M., and Hakem, R. (2003) *EMBO J.* **22,** 6137–6147
48. Hanada, K., Budzowska, M., Davies, S. L., van Drunen, E., Onizawa, H., Beverloo, H. B., Maas, A., Essers, J., Hickson, I. D., and Kanaar, R. (2007) *Nat. Struct. Mol. Biol.* **14,** 1096–1104
49. Fabre, F., Chan, A., Heyer, W. D., and Gangloff, S. (2002) *Proc. Natl. Acad. Sci. U. S. A.* **99,** 16887–16892
50. de los Santos, T., Hunter, N., Lee, C., Larkin, B., Loidl, J., and Hollingsworth, N. M. (2003) *Genetics* **164,** 81–94
51. de los Santos, T., Loidl, J., Larkin, B., and Hollingsworth, N. M. (2001) *Genetics* **159,** 1511–1525
52. Gaskell, L. J., Osman, F., Gilbert, R. J., and Whitby, M. C. (2007) *EMBO J.*

26, 1891–1901

53. Ehmsen, K. T., and Heyer, W. D. (2008) *Nucleic Acids Res.* **36,** 2182–2195

54. Taylor, E. R., and McGowan, C. H. (2008) *Proc. Natl. Acad. Sci. U. S. A.* **105,** 3757–3762

55. Jiang, H., Xie, Y., Houston, P., Stemke-Hale, K., Mortensen, U. H., Roth-stein, R., and Kodadek, T. (1996) *J. Biol. Chem.* **271,** 33181–33186

56. Krejci, L., Damborsky, J., Thomsen, B., Duno, M., and Bendixen, C. (2001) *Mol. Cell. Biol.* **21,** 966 –976

57. Zhang, R., Sengupta, S., Yang, Q., Linke, S. P., Yanaihara, N., Bradsher, J., Blais, V., McGowan, C. H., and Harris, C. C. (2005) *Cancer Res.* **65,** 2526 –2531

Attachment 11

Sebesta M, Burkovics P, Haracska L and Krejci L

Reconstitution of DNA repair synthesis in vitro and the role of polymerase and helicase activities.

DNA Repair (Amst). 10(6):567-76. 2011

Reconstitution of DNA repair synthesis *in vitro* and the role of polymerase and helicase activities

Marek Sebesta [a,b], Peter Burkovics [b,c], Lajos Haracska [c], Lumir Krejci [a,b,d,*]

[a] *Department of Biology, Masaryk University, Kamenice 5/A7, 625 00 Brno, Czech Republic*
[b] *National Centre for Biomolecular Research, Masaryk University, Kamenice 5/A4, 625 00 Brno, Czech Republic*
[c] *Institute of Genetics, Biological Research Center, Hungarian Academy of Sciences, Temesvari krt. 62, 6726 Szeged, Hungary*
[d] *International Clinical Research Center, St. Anne's University Hospital Brno, Pekarska 53, 656 91 Brno, Czech Republic*

ABSTRACT

The error-free repair of double-strand DNA breaks by homologous recombination (HR) ensures genomic stability using undamaged homologous sequence to copy genetic information. While some of the aspects of the initial steps of HR are understood, the molecular mechanisms underlying events downstream of the D-loop formation remain unclear. Therefore, we have reconstituted D-loop-based *in vitro* recombination-associated DNA repair synthesis assay and tested the efficacy of polymerases Pol δ and Pol η to extend invaded primer, and the ability of three helicases (Mph1, Srs2 and Sgs1) to displace this extended primer. Both Pol δ and Pol η extended up to 50% of the D-loop substrate, but differed in product length and dependency on proliferating cell nuclear antigen (PCNA). Mph1, but not Srs2 or Sgs1, displaced the extended primer very efficiently, supporting putative role of Mph1 in promoting the synthesis-dependent strand-annealing pathway. The experimental system described here can be employed to increase our understanding of HR events following D-loop formation, as well as the regulatory mechanisms involved.

© 2011 Elsevier B.V. All rights reserved.

1. Introduction

Damage to DNA in cells continuously arises either endogenously (*e.g.* from exposure to metabolically generated oxidants or replication of damaged template) or exogenously (*e.g.* from exposure to ionizing radiation or xenochemicals). Among these DNA lesions, the double-stranded breaks (DSBs) represent the most toxic form, which once left unrepaired can lead to cell cycle arrest and cell death [1].

There are two major pathways for the repair of DSBs: a non-homologous end joining (NHEJ) pathway, and a homologous recombination (HR) pathway [2]. NHEJ occurs predominantly in higher eukaryotes, or in cases where a cell lacks a homologous sequence. In this pathway the broken arms of DNA are simply rejoined, with or without processing or micro-homology-mediation, often accompanied by deletions or insertions [3]. In contrast, in HR a homologous sequence is used as a donor from which the damaged or lost sequence of the broken molecule is copied in an error-free manner.

In the early steps of HR, DSBs are resected to generate a 3′ single-stranded DNA (ssDNA) tail. This 5′ resection at the site of the break associates with the Rad50-Mre11-Xrs2 (RMX) nuclease complex, together with Sae2, Exo1 and Dna2/Sgs1 proteins [4,5]. The ssDNA tail is protected by replication protein A (RPA), and is transformed into a Rad51 nucleoprotein filament (also known as a pre-synaptic filament) with the help of recombination mediators (Rad52, Rad59 and Rad55/Rad57) [6–8], which is then capable of searching for homologous sequences [9]. However, in the case of "unscheduled" recombination, Srs2 helicase can counteract filament formation by disassociating Rad51 from ssDNA and directly competing with Rad52 [10–13]. Thus, Srs2 and Rad52 serve as HR quality controllers, ensuring normal course of recombination [14,15].

As HR proceeds, the Rad51 pre-synaptic filament invades donor duplex DNA to form a stable intermediate known as the D-loop [16,17]. This process is promoted by Rad54, a molecular motor protein that not only stabilizes the nucleoprotein filament, but also allows the search for homologous sequences in normal and chromatinized templates [18–20]. The invading strand in the D-loop structure is then extended using several components of the replication machinery, namely: DNA polymerase δ or ε; the proliferating cell nuclear antigen (PCNA); and its loader, replication factor C (RFC) [21–23].

HR can then proceed by either of two sub-pathways. The first of these is double-strand break repair (DSBR), in which the second

* Corresponding author at: Department of Biology & National Centre for Biomolecular Research, Masaryk University, Kamenice 5/A7, Brno 62500, Czech Republic. Tel.: +420 549493767; fax: +420 549492556.
E-mail address: lkrejci@chemi.muni.cz (L. Krejci).

end of the broken DNA is captured and stabilized by D-loop, then a second round of DNA synthesis occurs, followed by the formation of a double Holliday junction. This structure can then be resolved or dissolved, generating crossover or non-crossover products. In the alternative sub-pathway, synthesis-dependent strand-annealing (SDSA), the newly extended strand is displaced from the D-loop and annealed with its original complementary strand to generate a non-crossover product. *In vitro* and *in vivo* data suggest that the actions of helicases Mph1, Srs2, and Sgs1 are required for the displacement of the extended primer [24–27].

In contrast to the initial phases of HR, the steps occurring after D-loop formation are poorly understood. Hence, our aim in the present study was to reconstitute recombination-associated DNA repair synthesis machinery *in vitro*, capable of mimicking the *in vivo* events downstream of D-loop formation, in order to study the primer extension step during the repair of DSBs and the role of specific helicases in promoting the SDSA pathway of HR. The results both provide new information on the events downstream of D-loop formation during DSB repair, and demonstrate that the reconstituted system provides a means to explore these events (and the regulatory mechanisms involved) in detail.

2. Materials and methods

2.1. DNA substrates

Oligonucleotides were purchased from VBC Biotech with sequences shown in Table 1. Substrates were prepared as described by [28].

2.2. PCNA purification

PCNA was expressed in *E. coli* and purified essentially using the procedure described by Ayyagari et al. [29]. Briefly, 6 g of *E. coli* cell paste was sonicated in 30 ml lysis buffer C, consisting of 50 mM Tris–HCl (pH 7.5), 10% sucrose (w/v), the protease inhibitors EDTA (10 mM), dithiothreitol (1 mM), nonidet (0.01%, v/v), and KCl (750 mM). The crude lysate was clarified by centrifugation (100,000 × g for 90 min). A fraction of the proteins within the supernatant was then harvested by adding 0.21 g solid ammonium sulfate per ml, stirring for 1 h, centrifuging at 15,000 × g for 20 min, adding another 0.32 g/ml solid ammonium sulfate to the supernatant, stirring for 1 h, then centrifuging at 15,000 × g for 1 h. The resulting pellet was dissolved in 35 ml of buffer K – 20 mM K$_2$HPO$_4$, 20% (v/v) glycerol, 0.5 mM EDTA (pH 7.5), 0.01% (v/v) NP40, and 1 mM β-mercaptoethanol – then the mixture was applied to a 7-ml SP sepharose column (GE Healthcare Life Sciences). The flow-through was immediately loaded onto a 7 ml Q sepharose column (GE Healthcare Life Sciences), and eluted with a 70 ml linear gradient of 50–900 mM KCl in buffer K. The peak fractions were pooled and loaded onto a 1 ml hydroxyapatite column (BioRad), and proteins were eluted with a 15 ml gradient from 50 to 1000 mM KH$_2$PO$_4$ in buffer K. Peak fractions were again pooled, and loaded onto a 1 ml Mono Q column (GE Healthcare Life Sciences), and eluted with a 15 ml gradient of 50–900 mM KCl in buffer K. Fractions containing nearly homogenous PCNA were concentrated in a Vivaspin concentrator and stored in 5 μl aliquots at −80 °C.

2.3. Srs2 and Srs2$^{1–860}$ purification

E. coli Rosseta cells were transformed with plasmids harboring sequences encoding Srs2 and Srs2$^{1–860}$ fused with a His$_9$ tag at the N-terminus, then the proteins were expressed and purified essentially as described by [12]. Nearly homogeneous

Srs2 polypeptides were flash-frozen in liquid nitrogen in 2 μl aliquots and stored at −80 °C.

2.4. Polymerase δ purification

The polymerase δ complex was expressed and purified according to the method of [30] with modifications. Briefly, 100 g of cell paste was lysed in a cryo-mill, the resulting powder was re-suspended in 200 ml lysis buffer C containing 175 mM (NH$_4$)$_2$SO$_4$ and centrifuged (100,000 × g for 60 min at 4 °C). The volume of cleared supernatant was measured and 40 μl of 10% (v/v) Polymin P was added per ml of lysate. After 5 min the suspension was centrifuged at 15,000 × g for 45 min and solid (NH$_4$)$_2$SO$_4$ was added to the supernatant to a final concentration 0.28 g/ml. Precipitated proteins were collected by centrifugation (15,000 × g for 20 min at 4 °C), and the pellet was re-suspended in buffer K to yield conductivity equivalent to that of buffer K containing 25 mM KCl. The suspension was loaded onto a 25 ml SP-sepharose column, and proteins were eluted with 100 ml of buffer K containing 750 mM KCl. Protein fractions were pooled and dialyzed against buffer K containing 25 mM KCl and loaded onto a 1 ml Mono Q column. Proteins were then eluted with a 15 ml gradient of 25–500 mM KCl in buffer K. Peak fractions were pooled, diluted 3-fold, loaded onto a 1 ml Mono S column and proteins were eluted with a 15 ml gradient of 50–500 mM KCl in buffer K. The eluted proteins were pooled, concentrated to 300 μl and loaded onto a 25-ml Superdex 400 column (GE Healthcare Life Sciences), which was eluted with 25 ml buffer K containing 300 mM KCl. Nearly homogeneous polymerase δ was concentrated, flash-frozen in 2 μl aliquots, and stored at −80 °C.

2.5. Purification of other proteins

Rad51, Rad54 and RPA were purified according to the procedure of [31], while RFC complex, Mph1 and Pol η were purified according to [32–34], respectively.

2.6. D-loop and primer extension assays

Essentially, the D-loop assay was performed as described by [10]. Briefly, fluorescently labeled, radioactively labeled or unlabeled 90-mers (3 μM nucleotides) were incubated for 5 min at 37 °C with Rad51 (1 μM) in 10 μl of buffer R (35 mM Tris–HCl pH 7.4, 2 mM ATP, 2.5 mM MgCl$_2$, 50 mM KCl, 1 mM DTT and an ATP-regenerating system consisting of 20 mM creatine phosphate and 20 μg/ml creatine kinase) then 1 μl of Rad54 (150 nM) was added and the mixture was incubated for a further 3 min at 23 °C. The reaction was initiated by adding pBluescript replicative form I (50 μM base pairs) in 1.5 μl, and the mixture was incubated for 5 min at 23 °C.

Next, RPA (660 nM), PCNA (6.66 nM), RFC (10 nM) and either Pol δ or Pol η (15 nM) in buffer O (20 mM Tris–HCl pH 7.5, 5 mM DTT, 0.1 mM EDTA, 150 mM KCl, 40 μg/ml BSA, 8 mM MgCl$_2$, 5% (v/v) glycerol, 0.5 mM ATP and 75 μM each of dGTP and dCTP) were added, and the mixture was incubated for 5 min at 30 °C. DNA synthesis was initiated by adding start buffer (75 μM dTTP and either unlabeled dATP at 75 μM or 0.375 μCi [α-^{32}P]dATP in buffer O) to a 30 μl final reaction volume. Equal amounts of all dNTPs was not necessary to use to monitor the reaction as lower amounts of [α-^{32}P]dATP did not have any effect on the extension reaction. After 10 min at 30 °C, reactions were stopped with SDS (0.5% final) and proteinase K (0.5 mg/ml) at 37 °C for 3 min, and loaded onto an agarose gel (0.8%, w/v). After electrophoresis the gel was dried on DE81 paper and either exposed to a phosphorimager screen, or directly scanned for fluorescent DNA with a Fuji FLA 9000 imager, followed by analysis with Multi Gauge software (Fuji).

2.7. 2D gel electrophoresis

D-loop formation and primer extension reactions were performed as described above, the resulting mixtures were split into two parts and electrophoretically separated in 0.8% (w/v) agarose gel in 1× TAE buffer, then lanes were excised from the gel. The lane displaying D-loops and products from one aliquot of each reaction mixture was dried, and the rest of the gel was soaked for 60 min in denaturing buffer (50 mM NaOH, 1 mM EDTA). The excised lane was loaded onto a denaturing agarose gel (1% (w/v) in 50 mM NaOH and 1 mM EDTA) and run for 6 h. The dried gel was exposed to a phosphorimager screen and visualized using a Fuji FLA 9000 imager with Multi Gauge software (Fuji).

2.8. Dissociation of extended primer by helicases

Primer extension reactions using Pol δ were performed as described above. When the reactions were complete, serial concentrations (1, 7, 33 and 167 nM) of Srs2, Srs2$^{1–860}$ or Mph1 were added and the mixtures were incubated for a further 5 min at 30 °C. The reactions were stopped with SDS (0.5% final) and proteinase K (0.5 mg/ml) and loaded onto a 0.8% (w/v) agarose gel. After electrophoresis the gel was dried on DE81 paper, exposed to a phosphorimager screen, and analyzed using a Fuji FLA 9000 imager with Multi Gauge software (Fuji).

Table 1
Oligonucleotides used in this study.

Name	Sequence
D1	5′AAATCAATCTAAAGTATATATGAGTAAACTTGGTCTGACAG TTACCAATGCTTAATCAGTGAGGCACCTATCTCAGCGATCTGT CTATTT3′
49N	FITC 5′AGCTACCATGCCTGCACGAATTAAGCAATTCGTAATCATGGT CATAGCT3′
22mer	5′AATTCGTGCAGGCATGGTAGCT3′
27mer	FITC 5′AGCTATGACCATGATTACGAATTGCTT3′

3. Results

3.1. Proteins required for extending the D-loop substrate

The D-loop represents one of the first intermediates of HR, therefore we used it as a substrate to confirm the functionality and explore the roles of components of our reconstituted DNA repair synthesis machinery. The initial part of the *in vitro* process consisted of a standard D-loop assay involving formation of the Rad51 nucleoprotein filament assembled on 90-mer oligo D1, followed by invasion of homologous super-coiled plasmid dsDNA aided by Rad54 (Fig. 1A). After the D-loop formation several factors expected to play a role in the subsequent DNA synthesis reactions were added (Pol δ, RFC and PCNA at 15 nM, 10 nM and 6.6 nM, respectively). Strong incorporation of radiolabeled dATP was only observed when all of these components were added (Fig. 1B, lane 7). However, some unspecific extension was observed in the absence of a Rad51/Rad54-mediated D-loop (Fig. 1, lanes 5 and 6). Addition of the single-strand binding protein, RPA (666 nM), enhanced the extension of the D-loop substrate, indicating that secondary structures might abrogate the synthesis of long extension products (Fig. 1, lane 4). Thus, Pol δ, RFC, PCNA and RPA are essential for primer extension (Fig. 1, lane 7), and all D-loop mediating factors (including Rad51 and Rad54) are also required for maximal and specific extension.

Next, we titrated individual components to determine the optimal reaction conditions (Supplementary Fig. 1). Addition of various concentrations of PCNA (up to 6.6 nM), at sub-equimolar concentrations (compared to Pol δ), resulted in more efficient extension (Supplementary Fig. 1, lanes 5–8). Further increase of PCNA concentration did not significantly affect the extent of DNA synthesis, but resulted in the accumulation of shorter extension products (lanes 6 and 7). Conversely, increasing RPA concentrations from 0.66 through 6.6 and 66 to 666 nM (lanes 9–12) improved the efficiency of D-loop extension. Addition of Pol δ at concentrations of 0.15, 1.5 and 15 nM resulted not only in strong stimulation of primer extension activity, but also generated fully extended products (Supplementary Fig. 1A, lanes 13–15). In contrast, the addition of 150 nM Pol δ resulted in a dramatic reduction in the efficiency of DNA synthesis (Supplementary Fig. 1, lane 16). To test the specificity of our extension assay we also used a bacterial polymerase (Klenow fragment). As shown in Supplementary Fig. 1B, Klenow fragment (500 nM) was only able to extend the D-loop substrate at concentrations 30-times higher compare to Pol δ indicating the specificity of the reaction.

To further analyze the role of RPA in the process, we performed an order of addition experiment (Supplementary Fig. 2), in which RPA was added at various points and the reaction was monitored using [32P]-dATP. Predictably, adding RPA before the formation of the nucleoprotein filament inhibited the process (lane 2). When RPA was added after Rad51 nucleation of ssDNA, it had no effect (lanes 3–6), irrespective of whether it was added together with Rad54, dsDNA, or either before or after loading PCNA (Supplementary Fig. 1, lanes 3–6).

3.2. Pol δ–PCNA interaction is essential for repair synthesis

To corroborate the finding that PCNA must be loaded on DNA for primer extension to occur, we performed another order of addition experiment, again using [32P]-dATP to follow the reaction, taking samples 0, 1, 2.5, 5 and 10 min after its addition (Fig. 2A). When PCNA was added together with Pol δ (lanes 3–6), 65% of the [32P]-dATP was incorporated in reaction products within 2.5 min, but only 49% was incorporated within this time when PCNA was loaded before addition of Pol δ (lanes 7–10). A further delay was observed when Pol δ was incubated first with the D-loop, followed by addi-

tion of PCNA/RFC complex (lanes 11–14); these conditions led to 26% incorporation within 2.5 min (Fig. 2A). The effects of the salt concentration on PCNA requirements were also studied by varying the concentration of KCl in reaction mixtures (Fig. 2B) both lacking PCNA (lanes 1–5) and containing PCNA (lanes 6–10). In the absence of PCNA at 40 mM KCl, 95% less [32P]-dATP was incorporated than in the presence of PCNA (lanes 1 and 6). Furthermore, in the presence of PCNA, incorporation of the [32P]-dATP decreased with increasing salt concentrations, and only 38% incorporation was detected in mixtures with 190 mM KCl, suggesting that high salt concentrations adversely affect the Pol δ/PCNA interaction. Almost identical results were obtained from order of addition and salt dependency experiments using the φX DNA-based extension assay (Supplementary Fig. 3A and B). Overall, these findings suggest that for efficient extension PCNA must be actively loaded onto the substrate together with Pol δ and that this efficiency is salt dependent. At low salt concentrations some PCNA-independent extension was also observed.

3.3. The efficiency and length of D-loop extension

To probe the kinetics of D-loop conversion, and the length of the products formed, we performed time-course experiments using radioactively labeled oligonucleotide D1 as a substrate in the D-loop assay. Aliquots were withdrawn from the standard reaction mixture after 1, 2.5, 5 and 10 min and quantities of D-loop and extension products were analyzed. At the start of the extension, the reaction mixture contained over 35% of D-loop substrate. After 1 min around 10% of the D-loops were extended. The elongated products were gradually formed with up to 50% of the D-loops being extended after 10 min (Fig. 3A and B), indicating that they were rapidly and efficiently extended by Pol δ.

To estimate the length of the extension products we again used radioactively labeled oligonucleotide D1 and resolved the reaction mixtures by 2D gel electrophoresis. Fig. 3C (left panel) shows a radiogram of products of a reaction with a physiological salt concentration (150 mM KCl). Under these conditions most of the extended primer (74%) migrated as a population of molecules with estimated lengths ~200 nt (>100 nt extension of the 90-mer primer), and a small proportion had apparent lengths reaching ca. 700 nt. When the reaction was performed in the presence of 50 mM KCl, most (68%) of the products were extended to >1000 nt (Fig. 3C, right panel). Thus, extension product lengths varied from 200 nt to 1000 nt, depending on the salt concentration.

## 3.4. Comparison of Rad51-mediated D-loop extension by Pol δ and Pol η

Next, we compared the basic properties of two polymerases associated with DNA synthesis repair, Pol δ and Pol η. For this purpose, we expressed and purified both polymerases to near-homogeneity and analyzed their ability to extend the D-loop substrate in a time-course experiment (Fig. 4A and B). In reaction mixtures containing Pol δ (lanes 1–5) products appeared within 1 min, while in mixtures with Pol η (lanes 6–10) no detectable products formed within 5 min, indicating that Pol δ is more efficient (Fig. 4B). Interestingly, however, after 10 min Pol η yielded a similar proportion of extended products (>45%) to Pol δ (Fig. 4B). The activity of the two polymerases was further compared in the presence of serial concentrations of PCNA and at two salt concentrations (50 mM and 150 mM KCl) (Fig. 4C). At the low salt concentration (50 mM KCl), Pol δ (lanes 1–6) was able to extend the primer in a PCNA concentration-dependent manner. Pol η was able to extend the primer more efficiently than Pol δ, but its activity was PCNA independent (Fig. 4C, lanes 7–12). At the high salt concentration (150 mM KCl, lanes 13–24), both polymerases showed

similar PCNA-dependent D-loop extension efficiency (Fig. 4C and D). The only observed difference was that Pol δ (but not Pol η) yielded an additional, slowly migrating band representing longer extension products (Fig. 4C, lanes 4–6 and 16–18). Using 2D gel analysis to determine the length of products extended by Pol η in the D-loop extension reaction, we found that, in contrast to Pol δ, products extended by Pol η reached on average 150 nt in length in the presence of both low (50 mM) (data not shown) and high (150 mM) salt concentrations (Fig. 4E).

3.5. Unwinding of the extension products by Mph1 and Srs2

The SDSA sub-pathway of DSB repair involves displacement of the newly extended strand from the D-loop followed by annealing with its original complementary strand. The actions of Srs2, Mph1 and Sgs1 helicases are implicated in SDSA [24–27], therefore we expressed and purified these helicases and tested their ability to unwind newly extended D-loops. In a first experiment (Fig. 5A) we assembled the D-loop and monitored products using [α³²P]-dATP during 10 min extension. Serial concentrations (1, 7, 33 or 167 nM) of either Mph1 (lanes 3–6) or Srs2 (lanes 7–10) were then added and the resulting mixtures were incubated for an additional 5 min at 30 °C. The addition of 1 nM Mph1 resulted in the

displacement of 15% of the extended primer. At the highest Mph1 concentration tested (167 nM) almost 90% of the extended primers were displaced (Fig. 5, lanes 3–6). In contrast, Srs2 was not able to displace the primers even at 167 nM, if anything it resulted in slight stimulation of D-loop extension (Fig. 5A and B). Similar extensions and kinetics of strand displacement were observed when the reaction was monitored using radioactively labeled oligonucleotide D1 (Fig. 5C and D). To confirm that the difference between the helicases is not due to the inability of Srs2 to unwind DNA substrates, their helicase activities were compared using a DNA substrate with a 3′ overhang. Incubation of Srs2 with such a DNA substrate resulted in the normal generation of unwound product (Supplementary Fig. 5). Furthermore, to exclude the possibility that interactions with other proteins present could inhibit unwinding of the extended primer by Srs2, we used a truncated fragment (Srs2¹⁻⁸⁶⁰), which lacks the domain required for interactions with Rad51 and PCNA. Similarly to wild-type Srs2, this fragment was not capable of unwinding the extended primer (Supplementary Fig. 6, compare lanes 7–10 to lanes 11–14). Finally, Sgs1, another helicase implicated in promoting SDSA, did not have any effect on strand displacement (Supplementary Fig. 7). Taken together, these findings suggest that Mph1, but none of Srs2 or Sgs1, is fully capable of dissociating the extended primer.
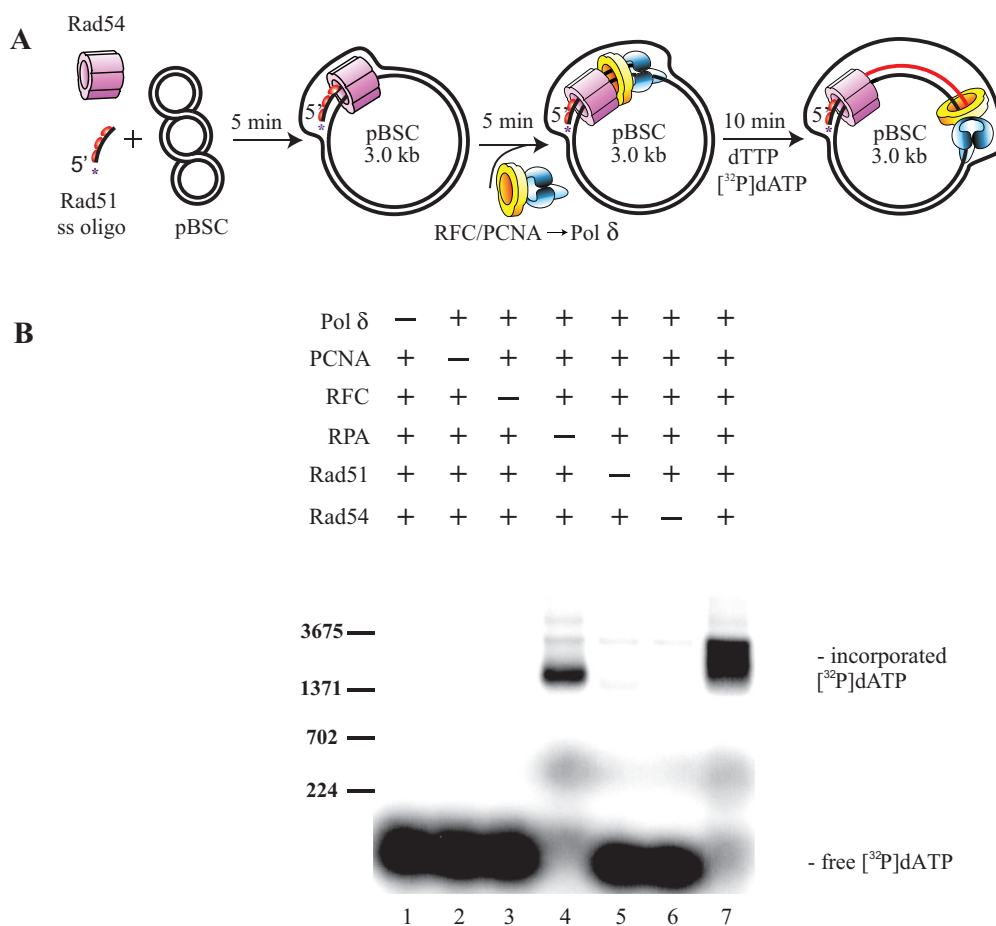
Fig. 1. Reconstitution of recombination-associated DNA synthesis. (A) Schematic diagram of the reaction. Rad51 protein (1 μM) was mixed with ssDNA oligonucleotide D1 (3 μM nucleotides) and incubated at 37 °C for 5 min in the presence of ATP (2.5 mM). Rad54 (150 nM), depicted as oligomer [57,58] was added to the mixture and incubated for a further 3 min at RT. D-loop formation was initiated by adding supercoiled pBluescript dsDNA (50 μM as nucleotides). Next, PCNA (6.66 nM) was loaded onto the primer by RFC complex (10 nM) during 5 min incubation at 30 °C in the presence of Pol δ (15 nM), dGTP and dCTP (75 μM each). Primer extension was initiated by adding dTTP (75 μM) and [α-³²P] dATP, followed by incubation for 10 min at 30 °C. Reactions were stopped, then the mixtures were deproteinized and analyzed. (B) Proteins required for recombination-associated DNA synthesis. The reaction was performed as described in (A) except that indicated proteins were omitted from the reaction mixtures. Labeled lambda digested with BstEI was used as marker (only a subset of bands is depicted in the figure).

A

B
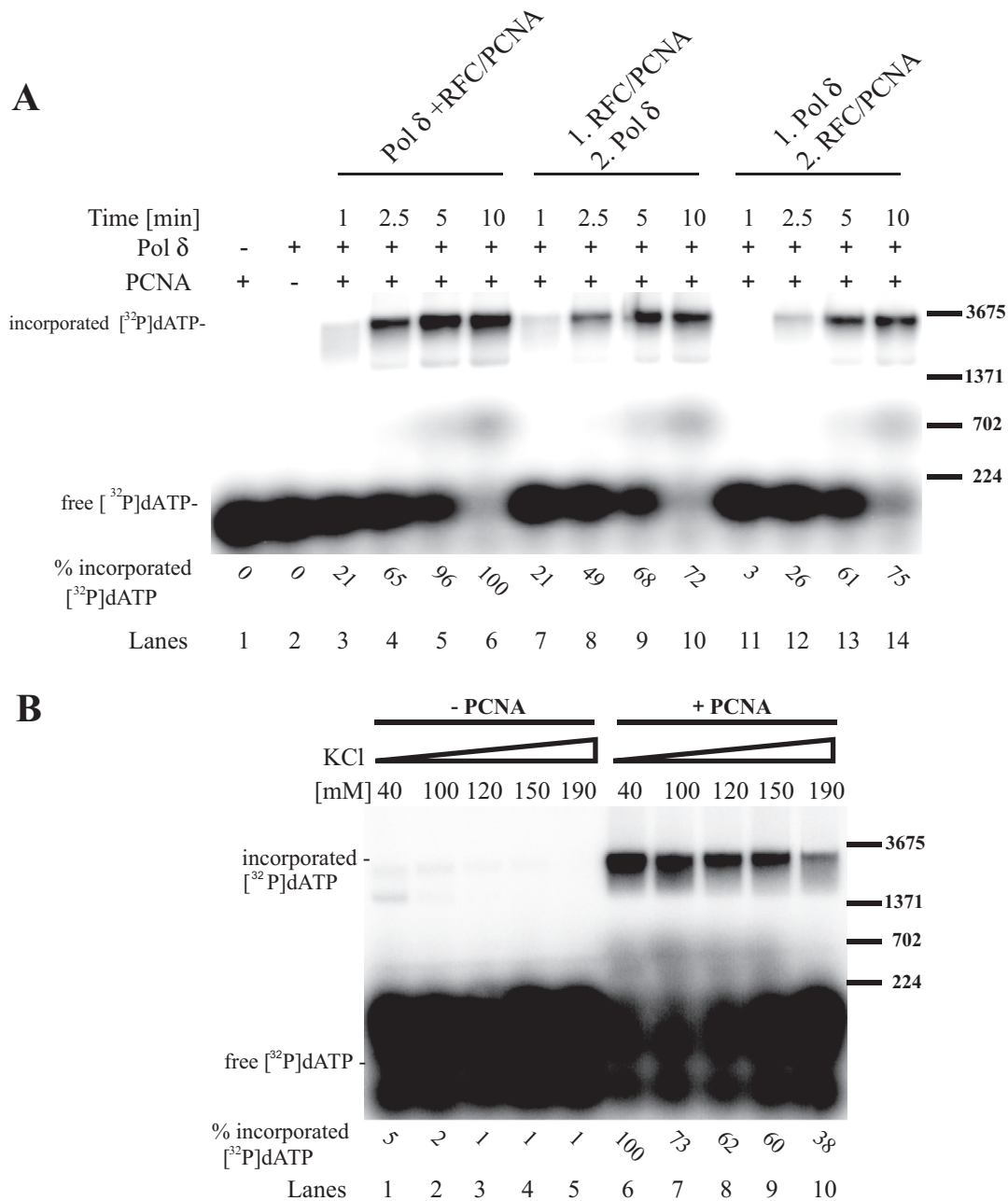
Fig. 2. Loaded PCNA is crucial for DNA repair synthesis. (A) PCNA needs to be loaded to stimulate DNA repair synthesis. An order of addition experiment was performed in which Pol δ (15 nM) was added at the same time as (lanes 3–6), after (lanes 7–10), or before (lanes 11–14) PCNA (6.66 nM)/RFC (10 nM). Samples were withdrawn after 1, 2.5, 5 and 10 min. In control experiments indicated factors were omitted (lanes 1 and 2). (B) PCNA was required at every salt concentration. Gel showing results of D-loop assays using oligonucleotide D1 and [^{32}P]-dATP in the presence of 40, 100, 120, 150 and 190 mM KCl in both the absence (lanes 1–5) and presence of PCNA (lanes 6–10). Labeled lambda digested with *Bst*EI was used as marker (only a subset of bands is depicted in the figure).

4. Discussion

Homologous recombination is one of the major pathways for the repair of DSBs. During this process the broken DNA is sealed with a copy of an undamaged homologous sequence. The D-loop is one of the first intermediates of HR, and here we aimed to reconstitute DNA repair synthesis and strand displacement machinery *in vitro*, utilizing this substrate, to elucidate downstream events in HR. In our system, polymerase δ, PCNA and RFC were found to be absolutely required for the extension of the primer from the D-loop substrate (Fig. 1), in good agreement with previous biochemical and genetic studies [21,35,36]. The extension reaction seems to be also highly specific as *E. coli* Klenow fragment of DNA

polymerase I is able to extend the D-loop only at very high concentrations (Supplementary Fig. 1B). In addition, the specificity of the reaction is supported by the ratio of substrate to protein (1:5), estimated based on the concentration of D1 oligo (8 nM) with average 35% efficiency of D-loop formation and concentration of Pol δ (15 nM), is very similar to DNA replication assay [37] and much lower to previously reported D-loop extension [21]. In comparison to the efficiency of Klenow fragment the extension by Pol δ thus should result from physiological number of polymerization cycles. Furthermore, most of the extension products were approximately 0.2 kb long, much shorter than conversion tracts observed *in vivo* [38–40], probably due to topological constraints of DNA synthesis in the plasmid system.
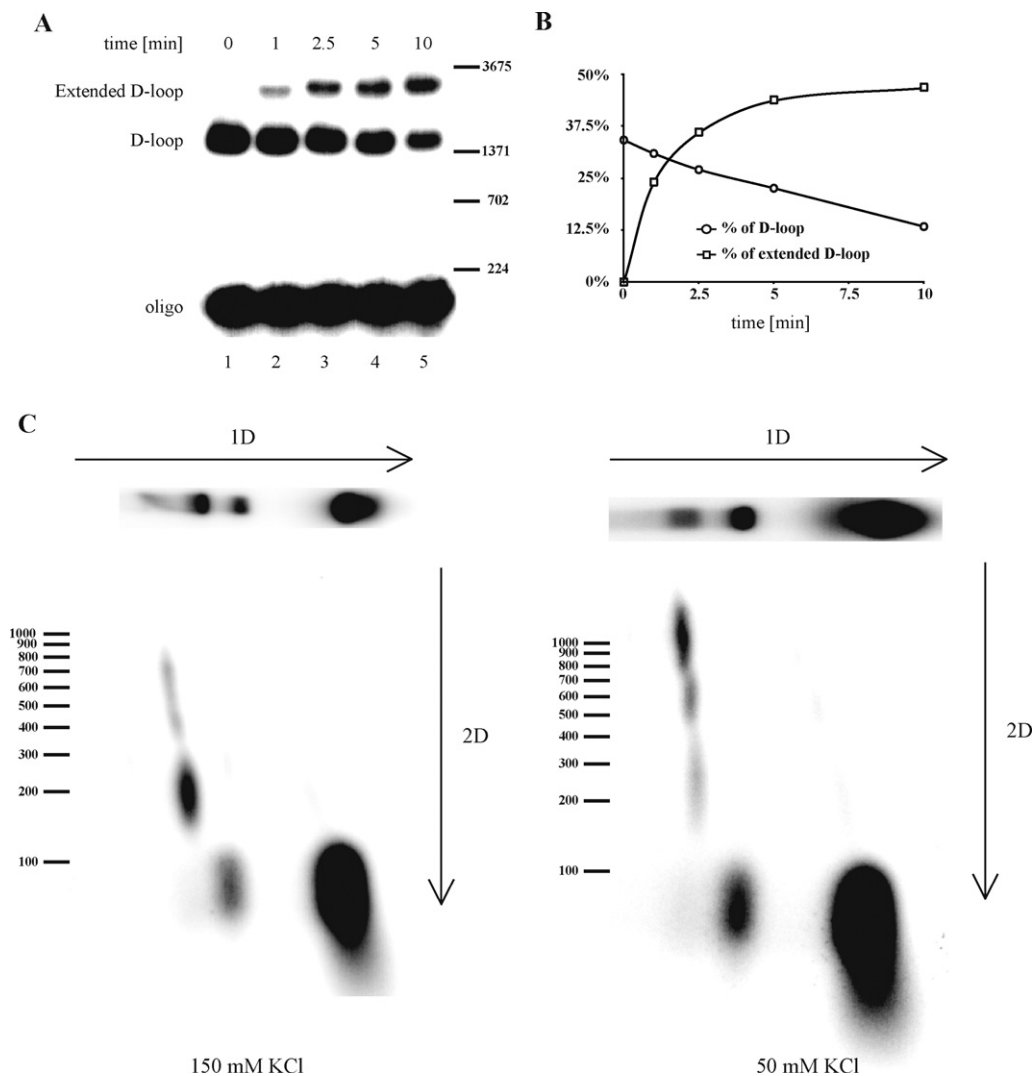
Fig. 3. Characterization of DNA repair synthesis. (A) Extent of D-loop synthesis monitored in a time course experiment. Gel showing electrophoretically separated D-loops and products in samples withdrawn at 0, 1, 2.5, 5 and 10 min after PCNA addition. Labeled oligonucleotide was used to monitor the rate of the extension. (B) Plots showing the accumulation of extended products (percentage of extended products versus D-loops, squares) and D-loops (percentage of D-loops versus oligo, circles) presented in (A). (C) The extension length is salt dependent. The reaction was set up as described in Section 2, in the presence in the presence of 50 mM KCl (right panel) or 150 mM KCl (left panel). Radioactively labeled oligonucleotide was used to monitor the process. Each reaction mixture was loaded into two lanes and separated in neutral agarose gel. One lane was dried and analyzed, while the other was excised from the gel, soaked for 60 min in denaturing buffer (50 mM NaOH, 1 mM EDTA), and run in a second dimension under denaturing conditions, then the products were examined by phosphorimaging analysis. Labeled lambda digested with *Bst*EI was used as marker (only a subset of bands is depicted in the figure).

In addition to corroborating previously published findings, our results show that the length of extension products strongly depends on the salt concentration, as increasing it to physiological concentrations resulted in a 5-fold reduction in the size of the products (Fig. 3C). This could be due to a higher dissociation rate of the Pol δ/PCNA complex or inhibition of its ability to bind DNA, which can be overcome by using PCNA in excess of Pol δ (Fig. 4C, other data not shown). Increasing the concentration of the single-strand binding protein RPA also improved the efficiency of DNA extension, probably due to stabilization of the displaced ssDNA during the extension reaction. In addition, the data using standard model system containing singly primed ΦX-174 circular ssDNA (Supplementary Fig. 3) indicates that D-loop structure and its progression *per se* does not hinder the activities of replication proteins and also confirm the requirement of PCNA for Pol δ activity at every salt concentration tested. Alternatively, under *in vivo* conditions, additional factors might be required to overcome topological constraints or other processivity obstacles for efficient DNA extension under physiological conditions.

It has been suggested that the replicative Pol δ plays a major role in DNA repair synthesis, and it is considered to be the main polymerase associated with DNA repair extension [23,40]. *In vitro* as well as *in vivo* data indicate that a translesion polymerase, Pol η, is also capable of mediating D-loop extensions [41,42], however, further genetic studies are needed to verify the role of Pol η in repair synthesis. Here we provide a detailed comparison of the activities of these two polymerases. While Pol δ extended the primer to more than 1 kb, Pol η produced (as expected) short extension products (Fig. 4E), reflecting the differences in the biochemical properties of these polymerases, including their processivity or strand-displacement activity (Supplementary Fig. 4 [30,43,44]). DNA extension mediated by Pol η was also observed by Li et al. [21], however, our data indicate that at the reported salt concentration the DNA extension is PCNA-independent (Fig. 4C), in accordance with previous analyses of human Pol η activity using synthetic D-loop substrate [41]. The extension is only fully dependent on PCNA at physiological salt concentration, suggesting that higher salt levels could effect processivity by destabilizing the association
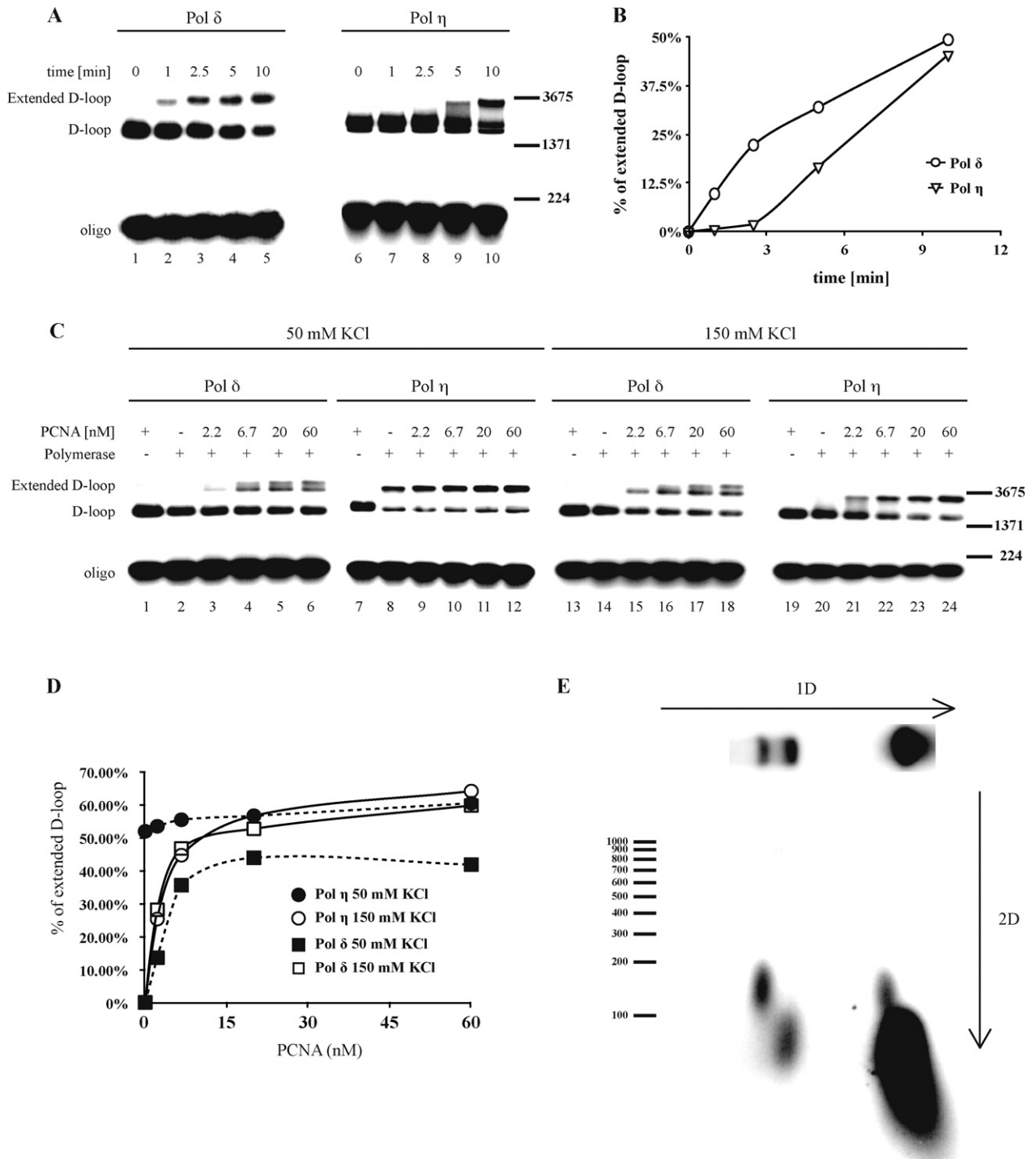
Fig. 4. D-loop extension by Pol η and Pol δ differs due to lower processivity of the former. (A) The two polymerases exhibit different time-dependent kinetics. A time-course experiment was performed with radioactively labeled oligonucleotide to monitor the extension, in which samples were withdrawn 0, 1, 2.5, 5 and 10 min after start of the reaction. Lanes 1–5 and 6–10 represent results of experiments with Pol δ and Pol η (15 nM in both cases), respectively. (B) Quantification of the reaction described in (A). (C) Polymerases differ in PCNA requirements under low salt concentrations. Results of reactions with serial concentrations of PCNA (2.22, 6.66, 20 and 60 nM) in the presence of Pol δ (15 nM, lanes 1–6 and 13–18) or Pol η (15 nM, lanes 7–12 and 19–24) and either 50 mM KCl (lanes 1–12) or 150 mM KCl (lanes 13–24). (D) Quantification of the reaction described in (C). (E) The length of Pol η extensions was determined by 2D electrophoresis, in the presence of 150 mM KCl, using radioactively labeled oligonucleotide to monitor the extension. Labeled lambda digested with *Bst*EI was used as marker (only a subset of bands is depicted in the figure).

of Pol η with DNA template. Interestingly, despite differences in the length of the extension products and rate of product formation, we observed very similar repair extension efficiencies for both polymerases, indicating that Pol η probably mediates multiple rounds of primer extension.

After successful primer extension step of HR, repair can proceed by either the SDSA or DSBR sub-pathways. The SDSA pathway is characterized by displacement of the extended primer from the D-loop, supposedly due to helicase action. *In vivo* studies have identified several helicases (including Sgs1, Mph1 and Srs2)
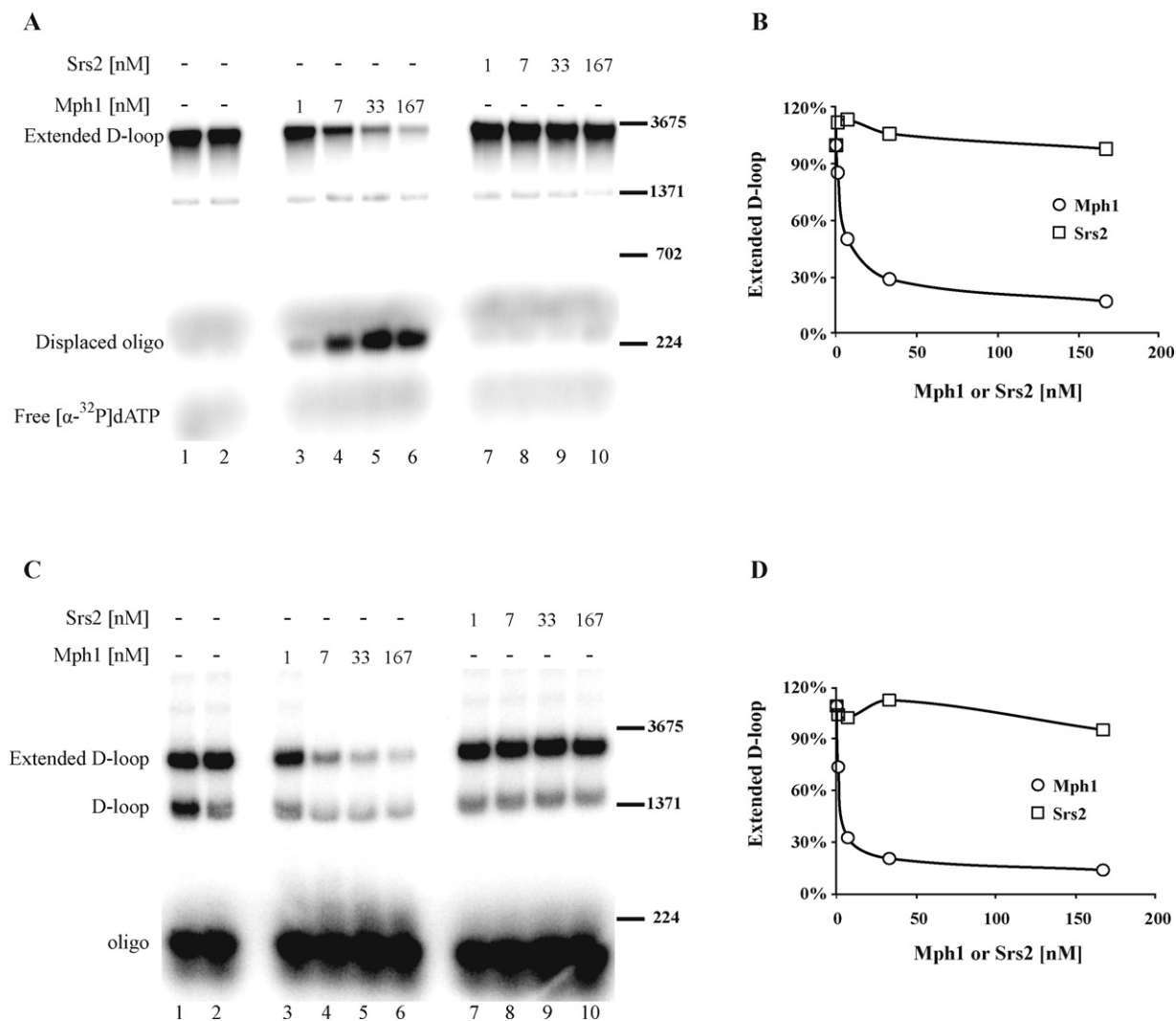
Fig. 5. Mph1 preferably dissociates extended products. (A) A reaction mixture containing extended D-loop was incubated for 5 min at 30 °C in the presence of Mph1 (1, 7, 33 and 167 nM, lanes 3–6) or Srs2 (1, 7, 33 and 167 nM, lanes 7–10). D-loop extension was monitored by measuring the incorporation of α-[32P]dATP. As controls, reactions were stopped at the point when either Mph1 or Srs2 was added (lane 1) or after an additional 5 min incubation (lane 2). (B) Quantification of the reaction described in (A). (C) Results of the reaction described in (A), except that D-loop extension was monitored using radioactively labeled oligonucleotide. (D) Quantification of the reaction described in (C). Labeled lambda digested with *Bst*EI was used as marker (only a subset of bands is depicted in the figure).

that reduce the generation of crossover products and promote SDSA [24,27,45,46]. Sgs1 suppresses crossovers by dissolving the double Holliday junctions formed via second-end capture into non-crossovers [47–49], but is not capable of dissociating extended D-loops in our system. However, Srs2 might promote the SDSA pathway by unwinding the invading strand from the D-loop [10,11]. While Srs2 is able to unwind synthetic D-loop structures [26 and our unpublished data], we observed no effects of Srs2 on the unwinding of Rad51-mediated D-loops [24] or on products of D-loop extension (Fig. 5). In fact, we observed a slight stabilization of extension products at low Srs2 concentrations (Fig. 5). Thus, the role of Srs2 in promoting SDSA appears to be removal of Rad51 protein from the second end of the DSB, thus preventing formation of a double Holliday Junction intermediate. Alternatively, it could influence D-loop extension by interacting with Pol32 and sumoylated PCNA [15,50–53]. Post-translational modification may also be an important factor as phosphorylation and sumoylation of Srs2 influence SDSA promotion [25]. Our data clearly demonstrate that Mph1 is fully capable of dissociating the extended strand after DNA repair synthesis, in accordance with its observed ability to unwind invading strands from D-loops [24]. Mechanisms that regulate Mph1 activity during meiosis, or whenever exchange of

genetic information occurs, remain to be determined. It is possible that Mph1 transcription is down-regulated, as seen during sporulation and after alpha factor arrest, processes that precede meiosis in which transcription of Mph1 decreases 2-fold [54,55]. Post-translational modifications and/or sub-cellular re-localization might also be important regulatory processes. Other factors, such as MutSα, that have been shown to participate in the Mph1-dependent promotion of SDSA, may also modulate Mph1 activity [56]. Taken together, these findings suggest that Mph1 displaces the extended primer, whereas Srs2 and Sgs1 promote SDSA by other mechanisms.

In summary, we have described an in vitro system that offers the opportunity to unravel the molecular mechanisms and regulation of HR downstream of D-loop formation. While it has been shown that the invasion step occurs with almost equal efficiency and kinetics to those observed in gene conversion (GC), break-induced replication (BIR) and single-strand annealing (SSA) [46,56], new DNA synthesis is regulated differently in these processes. It will, therefore, be enlightening to study further the differences between these processes, and thus elucidate their specific regulatory elements, including the roles of post-translational modifications and protein–protein interactions.

Conflict of interest statement

Appendix A. Supplementary data

Supplementary data associated with this article can be found, in the online version, at doi:10.1016/j.dnarep.2011.03.003.

References

[1] F. Paques, J.E. Haber, Multiple pathways of recombination induced by double-strand breaks in Saccharomyces cerevisiae, Microbiol. Mol. Biol. Rev. 63 (1999) 349–404.
[2] P. Sung, H. Klein, Mechanism of homologous recombination: mediators and helicases take on regulatory functions, Nat. Rev. Mol. Cell Biol. 7 (2006) 739–750.
[3] M.R. Lieber, The mechanism of double-strand DNA break repair by the nonhomologous DNA end-joining pathway, Annu. Rev. Biochem. 79 (2010) 181–211.
[4] E.P. Mimitou, L.S. Symington, Sae2, Exo1 and Sgs1 collaborate in DNA double-strand break processing, Nature 455 (2008) 770–774.
[5] Z. Zhu, W.H. Chung, E.Y. Shim, S.E. Lee, G. Ira, Sgs1 helicase and two nucleases Dna2 and Exo1 resect DNA double-strand break ends, Cell 134 (2008) 981–994.
[6] G. Petukhova, S.A. Stratton, P. Sung, Single strand DNA binding and annealing activities in the yeast recombination factor Rad59, J. Biol. Chem. 274 (1999) 33839–33842.
[7] P. Sung, Function of yeast Rad52 protein as a mediator between replication protein A and the Rad51 recombinase, J. Biol. Chem. 272 (1997) 28194–28197.
[8] P. Sung, Yeast Rad55 and Rad57 proteins form a heterodimer that functions with replication protein A to promote DNA strand exchange by Rad51 recombinase, Genes Dev. 11 (1997) 1111–1121.
[9] P. Sung, L. Krejci, S. Van Komen, M.G. Sehorn, Rad51 recombinase and recombination mediators, J. Biol. Chem. 278 (2003) 42729–42732.
[10] L. Krejci, S. Van Komen, Y. Li, J. Villemain, M.S. Reddy, H. Klein, T. Ellenberger, P. Sung, DNA helicase Srs2 disrupts the Rad51 presynaptic filament, Nature 423 (2003) 305–309.
[11] X. Veaute, J. Jeusset, C. Soustelle, S.C. Kowalczykowski, E. Le Cam, F. Fabre, The Srs2 helicase prevents recombination by disrupting Rad51 nucleoprotein filaments, Nature 423 (2003) 309–312.
[12] S. Colavito, M. Macris-Kiss, C. Seong, O. Gleeson, E.C. Greene, H.L. Klein, L. Krejci, P. Sung, Functional significance of the Rad51-Srs2 complex in Rad51 presynaptic filament disruption, Nucleic Acids Res. 37 (2009) 6754–6764.
[13] C. Seong, S. Colavito, Y. Kwon, P. Sung, L. Krejci, Regulation of Rad51 recombinase presynaptic filament assembly via interactions with the Rad52 mediator and the Srs2 anti-recombinase, J. Biol. Chem. 284 (2009) 24363–24371.
[14] V. Marini, L. Krejci, Srs2: the "Odd-Job Man" in DNA repair, DNA Repair (Amst.) 9 (2010) 268–275.
[15] R.C. Burgess, M. Lisby, V. Altmannova, L. Krejci, P. Sung, R. Rothstein, Localization of recombination proteins and Srs2 reveals anti-recombinase function in vivo, J. Cell Biol. 185 (2009) 969–981.
[16] P. Sung, Catalysis of ATP-dependent homologous DNA pairing and strand exchange by yeast RAD51 protein, Science 265 (1994) 1241–1243.
[17] P. Sung, D.L. Robberson, DNA strand exchange mediated by a RAD51-ssDNA nucleoprotein filament with polarity opposite to that of RecA, Cell 82 (1995) 453–461.
[18] G. Petukhova, S. Stratton, P. Sung, Catalysis of homologous DNA pairing by yeast Rad51 and Rad54 proteins, Nature 393 (1998) 91–94.
[19] M. Jaskelioff, S. Van Komen, J.E. Krebs, P. Sung, C.L. Peterson, Rad54p is a chromatin remodeling enzyme required for heteroduplex DNA joint formation with chromatin, J. Biol. Chem. 278 (2003) 9212–9218.
[20] B. Wolner, C.L. Peterson, ATP-dependent and ATP-independent roles for the Rad54 chromatin remodeling enzyme during recombinational repair of a DNA double strand break, J. Biol. Chem. 280 (2005) 10855–10860.
[21] X. Li, C.M. Stith, P.M. Burgers, W.D. Heyer, PCNA is required for initiation of recombination-associated DNA synthesis by DNA polymerase delta, Mol. Cell 36 (2009) 704–713.
[22] A.M. Holmes, J.E. Haber, Double-strand break repair in yeast requires both leading and lagging strand DNA polymerases, Cell 96 (1999) 415–424.
[23] X. Wang, G. Ira, J.A. Tercero, A.M. Holmes, J.F. Diffley, J.E. Haber, Role of DNA replication proteins in double-strand break-induced recombination in Saccharomyces cerevisiae, Mol. Cell Biol. 24 (2004) 6891–6899.
[24] R. Prakash, D. Satory, E. Dray, A. Papusha, J. Scheller, W. Kramer, L. Krejci, H. Klein, J.E. Haber, P. Sung, G. Ira, Yeast Mph1 helicase dissociates Rad51-made D-loops: implications for crossover control in mitotic recombination, Genes Dev. 23 (2009) 67–79.
[25] M. Saponaro, D. Callahan, X. Zheng, L. Krejci, J.E. Haber, H.L. Klein, G. Liberi, Cdk1 targets Srs2 to complete synthesis-dependent strand annealing and to promote recombinational repair, PLoS Genet. 6 (2010) e1000858.
[26] P. Dupaigne, C. Le Breton, F. Fabre, S. Gangloff, E. Le Cam, X. Veaute, The Srs2 helicase activity is stimulated by Rad51 filaments on dsDNA: implications for crossover incidence during mitotic recombination, Mol. Cell 29 (2008) 243–254.
[27] G. Ira, A. Malkova, G. Liberi, M. Foiani, J.E. Haber, Srs2 and Sgs1-Top3 suppress crossovers during double-strand break repair in yeast, Cell 115 (2003) 401–411.
[28] P. Matulova, V. Marini, R.C. Burgess, A. Sisakova, Y. Kwon, R. Rothstein, P. Sung, L. Krejci, Cooperativity of Mus81.Mms4 with Rad54 in the resolution of recombination and replication intermediates, J. Biol. Chem. 284 (2009) 7733–7745.
[29] R. Ayyagari, K.J. Impellizzeri, B.L. Yoder, S.L. Gary, P.M. Burgers, A mutational analysis of the yeast proliferating cell nuclear antigen indicates distinct roles in DNA replication and DNA repair, Mol. Cell. Biol. 15 (1995) 4420–4429.
[30] P.M. Burgers, K.J. Gerik, Structure and processivity of two forms of Saccharomyces cerevisiae DNA polymerase delta, J. Biol. Chem. 273 (1998) 19756–19762.
[31] S. Van Komen, M. Macris, M.G. Sehorn, P. Sung, Purification and assays of Saccharomyces cerevisiae homologous recombination proteins, Methods Enzymol. 408 (2006) 445–463.
[32] J. Finkelstein, E. Antony, M.M. Hingorani, M. O'Donnell, Overproduction and analysis of eukaryotic multiprotein complexes in Escherichia coli using a dual-vector strategy, Anal. Biochem. 319 (2003) 78–87.
[33] R. Prakash, L. Krejci, S. Van Komen, K. Anke Schurer, W. Kramer, P. Sung, Saccharomyces cerevisiae MPH1 gene, required for homologous recombination-mediated mutation avoidance, encodes a 3′ to 5′ DNA helicase, J. Biol. Chem. 280 (2005) 7854–7860.
[34] R.E. Johnson, S. Prakash, L. Prakash, Efficient bypass of a thymine–thymine dimer by yeast DNA polymerase, Poleta, Science 283 (1999) 1001–1004.
[35] J.R. Lydeard, S. Jain, M. Yamaguchi, J.E. Haber, Break-induced replication and telomerase-independent telomere maintenance require Pol32, Nature 448 (2007) 820–823.
[36] J.A. Nickoloff, D.B. Sweetser, J.A. Clikeman, G.J. Khalsa, S.L. Wheeler, Multiple heterologies increase mitotic double-strand break-induced allelic gene conversion tract lengths in yeast, Genetics 153 (1999) 665–679.
[37] L.D. Langston, M. O'Donnell, DNA polymerase delta is highly processive with proliferating cell nuclear antigen and undergoes collision release upon completing DNA, J. Biol. Chem. 283 (2006) 29522–29531.
[38] S.R. Judd, T.D. Petes, Physical lengths of meiotic and mitotic gene conversion tracts in Saccharomyces cerevisiae, Genetics 118 (1988) 401–410.
[39] R.H. Borts, J.E. Haber, Length and distribution of meiotic gene conversion tracts and crossovers in Saccharomyces cerevisiae, Genetics 123 (1989) 69–80.
[40] W.M. Hicks, M. Kim, J.E. Haber, Increased mutagenesis and unique mutation signature associated with mitotic gene conversion, Science 329 (2010) 82–85.
[41] M.J. McIlwraith, A. Vaisman, Y. Liu, E. Fanning, R. Woodgate, S.C. West, Human DNA polymerase eta promotes DNA synthesis from strand invasion intermediates of homologous recombination, Mol. Cell 20 (2005) 783–792.
[42] M.J. McIlwraith, S.C. West, DNA repair synthesis facilitates RAD52-mediated second-end capture during DSB repair, Mol. Cell 29 (2008) 510–516.
[43] Y.H. Jin, R. Ayyagari, M.A. Resnick, D.A. Gordenin, P.M. Burgers, Okazaki fragment maturation in yeast. II. Cooperation between the polymerase and 3′–5′-exonuclease activities of Pol delta in the creation of a ligatable nick, J. Biol. Chem. 278 (2003) 1626–1633.
[44] M.T. Washington, R.E. Johnson, S. Prakash, L. Prakash, Fidelity and processivity of Saccharomyces cerevisiae DNA polymerase eta, J. Biol. Chem. 274 (1999) 36835–36838.
[45] Y.C. Lo, K.S. Paffett, O. Amit, J.A. Clikeman, R. Sterk, M.A. Brenneman, J.A. Nickoloff, Sgs1 regulates gene conversion tract lengths and crossovers independently of its helicase activity, Mol. Cell Biol. 26 (2006) 4086–4094.
[46] S. Jain, N. Sugawara, J. Lydeard, M. Vaze, N. Tanguy Le Gac, J.E. Haber, A recombination execution checkpoint regulates the choice of homologous recombination pathway during DNA double-strand break repair, Genes Dev. 23 (2009) 291–303.
[47] L. Wu, I.D. Hickson, The Bloom's syndrome helicase suppresses crossing over during homologous recombination, Nature 426 (2003) 870–874.
[48] L. Wu, C.Z. Bachrati, J. Ou, C. Xu, J. Yin, M. Chang, W. Wang, L. Li, G.W. Brown, I.D. Hickson, BLAP75/RMI1 promotes the BLM-dependent dissolution of homologous recombination intermediates, Proc. Natl. Acad. Sci. U. S. A. 103 (2006) 4068–4073.

[49] S. Raynard, W. Bussen, P. Sung, A double Holliday junction dissolvasome comprising BLM, topoisomerase IIIalpha, and BLAP75, J. Biol. Chem. 281 (2006) 13861–13864.
[50] M.E. Huang, A.G. Rio, M.D. Galibert, F. Galibert, Pol32, a subunit of Saccharomyces cerevisiae DNA polymerase delta, suppresses genomic deletions and is involved in the mutagenic bypass pathway, Genetics 160 (2002) 1409–1422.
[51] E Papouli, S. Chen, A.A. Davies, D. Huttner, L. Krejci, P. Sung, H.D. Ulrich, Crosstalk between SUMO and ubiquitin on PCNA is mediated by recruitment of the helicase Srs2p, Mol. Cell 19 (2005) 123–133.
[52] B. Pfander, G.L. Moldovan, M. Sacher, C. Hoege, S. Jentsch, SUMO-modified PCNA recruits Srs2 to prevent recombination during S phase, Nature 436 (2005) 428–433.
[53] C. Le Breton, P. Dupaigne, T. Robert, E. Le Cam, S. Gangloff, F. Fabre, X. Veaute, Srs2 removes deadly recombination intermediates independently of its interaction with SUMO-modified PCNA, Nucleic Acids Res. 36 (2008) 243–254.

[54] S. Chu, J. DeRisi, M. Eisen, J. Mulholland, D. Botstein, P.O. Brown, I. Herskowitz, The transcriptional program of sporulation in budding yeast, Science 282 (1998) 699–705.
[55] C.J. Roberts, B. Nelson, M.J. Marton, R. Stoughton, M.R. Meyer, H.A. Bennett, Y.D. He, H. Dai, H.W.L. Walker, T.R. Hughes, et al., Signaling and circuitry of multiple MAPK pathways revealed by a matrix of global gene expression profiles, Science 287 (2000) 873–880.
[56] Y.D. Tay, J.M. Sidebotham, L. Wu, Mph1 requires mismatch repair-independent and -dependent functions of MutSalpha to regulate crossover formation during homologous recombination repair, Nucleic Acids Res. 38 (2010) 1889–1901.
[57] K. Kiianits, J.A. Solinger, W.D. Heyer, Terminal association of Rad54 protein with the Rad51–dsDNA filament, Proc. Natl. Acad. Sci. U. S. A. 103 (2006) 9767–9772.
[58] D. Ristic, C. Wyman, C. Paulusma, R. Kanaar, The architecture of the human Rad54–DNA complex provides evidence for protein translocation along DNA, Proc. Natl. Acad. Sci. U. S. A. 98 (2001) 8454–8460.